November 2018

Control of Uncertain Dynamical Systems with Spatial and Temporal Constraints

Ehsan Arabi
University of South Florida, arabi.ehsan@gmail.com

Control of Uncertain Dynamical Systems with Spatial and Temporal Constraints

by

Ehsan Arabi

A dissertation submitted in partial fulfillment
of the requirements for the degree of
Doctor of Philosophy in Mechanical Engineering
Department of Mechanical Engineering
College of Engineering
University of South Florida

Major Professor: Tansel Yucelen, Ph.D.
Nhan T. Nguyen, Ph.D.
Rajiv Dubey, Ph.D.
Kyle Reed, Ph.D.
Yasin Yilmaz, Ph.D.

Date of Approval:
October 11, 2018

Keywords: Model reference adaptive control, Stability and performance guarantees, Distributed control, Finite-time control, Multiagent systems

DEDICATION

This dissertation is dedicated to my parents, Hossein and Mahin Arabi, who have always been an unlimited source of love, support, and encouragement for me. This dissertation is also dedicated to my lovely wife, Bahareh Niati, for her kindness, devotion, and unconditional support as well as to my wonderful sister, Azar Arabi.

ACKNOWLEDGMENTS

I would like to take this opportunity to thank the people who helped me through the completion of this dissertation in any form. First of all, I would like to express my sincere gratitude to my advisor, Dr. Tansel Yucelen, for his continuous support, motivation, and immense knowledge. He has been a true mentor and an inspiring figure for me through every step of my Ph.D. study. His enthusiasm and joy in doing research were extremely contagious and motivational for me, which helped me overcome the tough times in my research. I would also like to thank Dr. Nhan Nguyen with NASA Ames Research Center for his valuable insights and suggestions during the course of my study. I gratefully acknowledge the other members of my Ph.D. committee, Dr. Rajiv Dubey, Dr. Kyle Reed, and Dr. Yasin Yilmaz, for their time and helpful comments. I would also wish to thank Dr. Rasim Guldiken for his extensive academic guidance.

I would also like to thank Dr. Sivasubramanya N. Balakrishnan from Missouri University of Science and Technology, Dr. Eric A. Butcher from the University of Arizona, Dr. Animesh Chakravarthy from Wichita State University, Dr. Mario L. Fravolini from the University of Pergia, Dr. Keqin Gu from Southern Illinois University Edwardsville, Dr. Wassim M. Haddad from Georgia Institute of Technology, Dr. Kelly E. Hashemi from NASA Intelligent Systems Division, Dr. Ali T. Kutay from Middle East Technical University, Dr. Morad Nazari from Embry-Riddle Aeronautical University, Dr. John R. Singler from Missouri University of Science and Technology, Dr. Rifat Sipahi from Northeastern University, Dr. James Steck from Wichita State University, Metehan Yayla from Middle East Technical University, and Dr. Yildiray Yildiz from Bilkent University, for the opportunities to collaborate. In addition, I would like to acknowledge the support from National Aeronautics and Space Administration under grants, for example, NNX15AM51A and NNX15AN04A.

My sincere thanks also goes to my fellow labmates at the University of South Florida and the Missouri University of Science and Technology. I would like to thank Merve Dogan, Dr. Ali Albattat, Dr. Benjamin Gruenwald, Dr. Ahmet Koru, Mehdi Madani, Daniel Peterson, Stefan Ristevski, Burak Sarsilmaz,

Dzung Tran, and Emre Yildrim. I am very grateful for all the personal and professional discussions, and all the fun we had in the last four years. I wish to also thank my wonderful friends Babak Baghi and Dr. Reza Abiri, who despite being thousands miles away, have always been motivating me to move forward in whatever I pursue.

Last but not the least, I would like to thank my parents, my sister, and my wife. Words fail me to thank them enough, for their everlasting love, support and encouragement. I would like to specially thank my dear wife Bahareh, who has been very caring, patient, and supportive during the past four years and has made them the best years of my life.

"*A human being is a part of the whole, called by us "Universe," a part limited in time and space*"

— Albert Einstein

TABLE OF CONTENTS

LIST OF TABLES

LIST OF FIGURES

ABSTRACT

The overarching objective of this dissertation is the development of feedback control frameworks for uncertain dynamical systems that are subject to spatial and/or temporal constraints. These spatiotemporal constraints usually arise from the physical and/or performance characteristics associated with a considered dynamical system in safety-critical applications, where synthesis and analysis of feedback control laws are not trivial. Specifically, the proposed control architectures in this dissertation mainly contribute to the model reference adaptive control and finite-time control literature. In particular, unlike existing model reference adaptive control approaches that are not capable of enforcing user-defined performance guarantees without an ad-hoc tuning process, the proposed control architectures utilize an error-dependent learning rate that enables a control designer to assign a user-defined performance bound to the system trajectories. In addition, the convergence time of the existing finite-time controllers either depends on the initial conditions of the system or the upper bound on the system uncertainties; hence, this convergence time cannot be strictly assigned by the control designer. The proposed finite-time control algorithms in this dissertation utilize a time transformation technique to address this challenge, where the resulting convergence time is independent of the initial conditions and the knowledge of upper bound of the system uncertainties.

Research in adaptive control theory has demonstrated the capabilities of these feedback algorithms in suppressing the effects of adverse conditions resulting from exogenous disturbances, imperfect system modeling, degraded modes of operation, and changes in system dynamics. Yet, not only standard adaptive controllers usually yield to conservative performance bound on the system error signal, but also they require the knowledge of the upper bound on the system uncertainties to specify such a bound. Therefore, a major challenge in standard adaptive control algorithms is their inability to address control problems with a-priori given spatial constraints. In this dissertation, this critical issue is addressed by introducing the set-theoretic model reference adaptive control architecture. This approach utilizes so-called generalized restricted potential functions by incorporating a system error-dependent learning rate in the adaptation process. The resulting control architecture ensures that the system error signal evolves in a user-defined compact set for

all time without the requirement of the knowledge of the upper bound on the system uncertainties. For the case where the system uncertainty is unstructured, a new neuroadaptive control architecture predicated on a set-theoretic treatment is then studied such that the closed-loop system trajectories are guaranteed to stay within the compact set without violating the universal function approximation property. As another contribution in this dissertation, the set-theoretic model reference is generalized to enforce a time-varying performance bound on the norm of system error vector. This gives a control designer the flexibility to control the closed-loop system performance as desired on different time intervals separately. In practice, a subset of system trajectories can be more critical than the others. Hence, it is desired not only to enforce a performance bound on the entire norm of the system error, but also to be able to adjust the resulting performance bound specifically for that critical subset. To address this problem, a command governor approach is embedded in the set-theoretic model reference adaptive control architecture. Actuator dynamics and actuator failures are two of the most important considerations for implementing any control algorithm. To this end, extensions of the set-theoretic model reference adaptive control architecture are proposed, where it ensures the system stability as well as the user-defined performance guarantee despite the presence of actuator dynamics or actuator failures during an operation.

The applications of the proposed set-theoretic model reference adaptive control is also studied within the context of this dissertation. Specifically, this framework is implemented on a generic transport model developed by NASA on both longitudinal and lateral-directional dynamics. In addition, the proposed set-theoretic model reference adaptive control is evaluated on an aerospace testbed, which is configured as a conventional dual-rotor helicopter for enforcing constant and time-varying performance bounds. Practical implementation considerations for the set-theoretic model reference adaptive control architecture is also studied. In particular, a generalization of this control architecture with dead-zone effect is proposed where it stops the adaptation process inside the dead-zone, but it still ensures that the norm of the system error is evolving inside a user-defined performance bound. The set-theoretic model reference adaptive control is also augmented at the inner-loop control structure of human-in-the-loop control architectures to provide a sufficient stability condition for the overall physical system.

Another major contribution of this dissertation is to address control problems with temporal constraints. This problem is considered in the context of networked multiagent systems, where the control objective is to drive the agents to a time-varying leader within a user-defined finite time interval. To this end, using a time transformation approach, the desired user-defined finite-time interval of interest is converted

into a stretched infinite-time interval. The robustness properties of the proposed control algorithm, as well as the finite-time convergence guarantees is established in this new infinite-time interval. One can then readily transfer back the results into the original finite time interval of interest. The effects of sensor uncertainties are also studied in this dissertation, where they can significantly deteriorate the achievable closed-loop system performance in networked multiagent systems. These uncertainties may arise due to low sensor quality, sensor failure, sensor bias, or detrimental environmental conditions. To tackle this challenge, a resilient distributed control algorithm is designed to mitigate the effect of sensor uncertainties.

Finally, a unified control architecture is proposed to simultaneously address the problem of spatiotemporal constraints for uncertain dynamical systems. The proposed control architecture, ensures that the agents converge to a time-varying leader at a user-defined finite time of interest, while guaranteeing user-defined performance bounds on the system error trajectories.

The stability and performance properties for all of the aforementioned control architectures are rigorously established using system-theoretic methods and their efficacy are demonstrated through illustrative numerical examples.

CHAPTER 1: INTRODUCTION

This chapter presents a summary of the developments made throughout this dissertation. Building on the model reference adaptive control literature, the proposed control architectures seek to improve the overall system stability, robustness, and performance characteristics of uncertain physical systems. In particular, the primary goal in this dissertation is to develop control architectures for physical systems subject to constraints to achieve user-defined system performance guarantees, where these constraints can be associated with space or time (i.e., spatiotemporal constraints).

The spatial constraints usually result from the structural and/or operational limitations in safety-critical applications. In such applications, unpredictable deviations from an ideal system response, which is characterized to obey certain spatial limits, is not desired and needs to be avoided in practice. Therefore, a feedback control design must have the ability to keep the system trajectories close enough to the ideal reference trajectories to ensure that the system operates within a safe operating zone. In the light of recent developments in adaptive control algorithms, current practice relies heavily on either excessive vehicle testing for verification purposes or development of the tools to validate adaptive control algorithms. However, the excessive vehicle testing only provides limited performance guarantees for the specific tested conditions such as the fixed set of initial conditions, user commands, and possible failure and adversary profiles [5–7]. In addition, the existing tools for validating adaptive control algorithms require a-priori and almost complete knowledge of upper and lower bounds on the system uncertainties; otherwise, they yield in conservative performance guarantees [8, 9]. Hence, these bounds are not necessarily always practical in establishing performance guarantees on the system errors denoting the distance between the uncertain system dynamics and a given reference model (see Section 1.1 for more details).

On the other hand, the temporal constraints are generally related to time-critical applications where it is necessary to accomplish a given task over a desired time interval. It should be noted that the convergence time achieved through classical finite-time control architectures depends on the initial conditions of the considered physical system (see for example, [10, 11]); hence, the convergence time cannot be assigned as

a user-defined parameter for all initial conditions of the system. To address this challenge in time-critical applications, fixed-time finite-time control architectures (see for example, [12, 13]) and predefined-time finite-time control architectures (see for example, [14, 15]) are proposed. Yet, in these results, either the calculated upper bound on the convergence time do not necessarily hold globally for all initial conditions and they can be conservative [12], or they can require a strict knowledge of the upper bounds of the considered class of system uncertainties in their design [13].

In what follows, first a concise overview of model reference adaptive control approach is presented. The contributions of this dissertation in developing feedback algorithms for dynamical systems subject to spatiotemporal constraints are then introduced.

1.1 Model Reference Adaptive Control Architecture

An adaptive controller is a nonlinear control system that utilizes a parameter adjustment mechanism (i.e., adaptation mechanism or adaptive law) for updating the parameters within the control structure (i.e., adaptive parameters). The adaptation characteristic of these controllers makes them a suitable candidate for controlling uncertain dynamical systems. In fact, decades of research in adaptive control systems has shown their capability to suppress the effects of adverse conditions resulting from exogenous disturbances, imperfect dynamical system modeling, degraded modes of operation, and changes in system dynamics.

Adaptive control systems can be broadly classified into two categories; namely, direct and indirect adaptive control systems. In direct adaptive control systems, the adaptive parameters are updated directly via an online adaptation mechanism. However, indirect adaptive control systems estimate the unknown system parameters and use these estimations within the control structure [16, 17]. In this dissertation, direct adaptive control schemes and in particular, model reference adaptive control systems serve as a base control system method. In particular, as depicted in Figure 1.1, a model reference adaptive control system consists of a reference model, an adaptive law, and a controller. Here, the ultimate objective is to design a control signal $u(t)$ to provide overall system stability and performance, such that the uncertain dynamical system state $x(t)$ follows an ideal system behavior captured by the reference model system state $x_{\mathrm{r}}(t)$ for tracking the desired command signal $c(t)$. In this control architecture, the controller contains a nominal portion as well as an adaptive portion. The adaptive parameter are then updated through the adaptive law based on the deviation of the uncertain system state and the reference model system state; that is, $e(t) \triangleq x(t) - x_{\mathrm{r}}(t)$. In

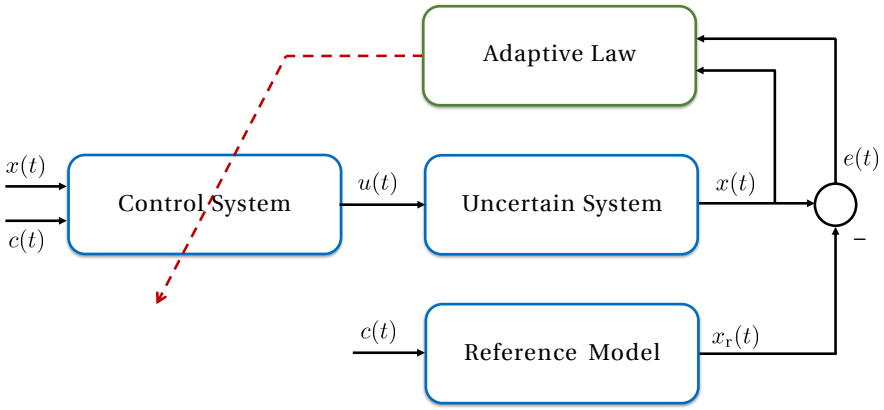

Figure 1.1: Block diagram of a standard model reference adaptive control approach.

addition, the adaptive law utilizes an adaptation gain for scaling the error signal that serves to control the adaptation rate.

Although model reference adaptive controllers are capable of guaranteeing closed-loop system stability in the presence of exogenous disturbances and system uncertainties, a crucial problem is their inability in providing a-priori given, user-defined performance guarantees. In fact, their calculated worst-case performance bounds based on Lyapunov or Lyapunov-like functions usually depend on the system uncertainties. Hence, their resulting performance bounds on the system error are often conservative and are not always practical for addressing control problems with spatial constraints [1].

1.2 Spatial Performance Guarantees

Enforcing performance guarantees on the system state or the system output is referred to as a spatial constraint problem, which has been the subject of several works in the adaptive control literature [18–27]. In particular, the authors of [18–20] use an error transformation approach to transform an uncertain dynamical system subject to spatial constraints into an equivalent form without constraints. However, the result in [18] is limited to the case where the control signals can access to every element of the state vector, the result in [19] uses a backstepping adaptive control approach under the assumption that a desired trajectory and its derivatives are available and all bounded, and the result in [20] utilizes a switching control approach and enforces constraints only on measurable output signals but not on state vector. Furthermore, [22–26] use restricted potential functions (i.e., barrier Lyapunov functions) for the systems in strict feedback form and

in the context of backstepping adaptive control to achieve strict performance guarantees. Finally, the result in [21] provides performance guarantees under the assumption that system uncertainties are constant.

In the light of above discussions, this dissertation presents a new set-theoretic model reference adaptive control architecture to enforce a-priori given, user-defined worst-case performance bounds on the error between the trajectories of an uncertain dynamical system and the desired reference model trajectories.

1.2.1 Set-Theoretic Model Reference Adaptive Control Architecture

This dissertation presents a fundamental contribution to the model reference adaptive control literature by proposing the set-theoretic model reference adaptive control architecture that has the ability to enforce a-priori given, user-defined performance guarantees. Unlike the standard model reference adaptive control architecture that utilizes a constant adaptation rate, an error-dependent adaptation rate is embedded in the proposed control system. This error-dependent adaptation rate is predicated on a generalized restricted potential function to auto-tune the adaptive control design. The key characteristic of this new adaptation mechanism increases the effective learning rate when the system error trajectories get close to the boundaries of a prescribed user-defined compact set that represents the spatial constraint. Consequently, the system trajectories are theoretically enforced to evolve in this compact set for all time, without requiring a strict knowledge of the upper bounds of the system uncertainties. As a byproduct, an upper bound can be also calculated directly for the adaptive control signals without inducing (excessive) conservatism that only depends on user-defined design parameters.

As another important contribution of this dissertation, a set-theoretic model reference neuroadaptive control architecture is proposed in which the well-known system uncertainty parameterization assumption, as used in, for example, [28–32], is no longer needed. In fact, using neural networks on a compact set of the real coordinate space, neuroadaptive control systems are able to approximate system uncertainties with an unknown structure and unknown parameters [33–36]. However, the challenge is to keep the system trajectories within this compact set such that the universal function approximation property is valid and the overall system stability is achieved. The proposed control framework ensures that the closed-loop system trajectories evolve within an a-priori given, user-defined compact set; hence, the universal function approximation property remains always valid.

1.2.2 Generalization of the Set-Theoretic Model Reference Adaptive Control Architecture

In practice, usually large magnitude of error signal can be tolerated at the beginning stage of an applied command, while guaranteeing the overall system stability. However, after the initial transient period, it is required to track the desired command signal more closely. Therefore, in order to cover a wider class of spatial constraint problems, two set-theoretic model reference adaptive control architectures are presented to address time-varying performance guarantees. Specifically, the key feature of this framework gives the control designer a flexibility to control the closed-loop system performance as desired on different time intervals (e.g., transient time interval and steady-state time interval).

As noted in Section 1.2.1, the proposed set-theoretic model reference adaptive control architecture is capable of enforcing user-defined strict performance guarantees on the entire norm of the system error vector. However, from a practical standpoint (especially when the number of system states gets large), a subset of system state trajectories can be more critical than the rest due to physical and/or performance characteristics associated with a problem of interest. As a consequence, it is often desired not only to have strict guarantees on the norm of the entire system error vector but also to be able to adjust the resulting worst-case performance bound specifically for that critical subset. To this end, a new model reference adaptive control architecture predicated on a set-theoretic treatment is developed for enforcing an a-priori given, user-defined performance bound on the selected subset of dynamical system trajectories.

As it is well-known, when the bandwidth of the system actuator dynamics is not sufficiently high, the stability of model reference adaptive controllers can be degraded drastically. The hedging method proposed in [37] is one of the effective approaches for addressing this challenge. In this study, the ideal reference model is modified by the hedge signal such that the adaptation process becomes independent from the actuator dynamics [37–39]. The result in [40, 41] generalizes this method and provides sufficient condition based on linear matrix inequalities such that the modified reference model trajectories, and hence, the overall closed-loop dynamical system, become stable in the presence of actuator dynamics. However, due to utilizing the standard model reference adaptive control framework in these studies, the performance bounds between the uncertain dynamical system trajectories and the ideal reference model trajectories are conservative and they depends on the system uncertainties (e.g., see Theorem 1.4.1 of [41]). As another contribution of this dissertation, unlike the results in [40, 41], the proposed set-theoretic model reference adaptive control architecture is able to enforce a-priori, user-defined performance bounds on the error

between the uncertain dynamical system trajectories and the modified reference model trajectories. In addition, it is shown that the error bounds between the ideal reference model trajectories and the uncertain dynamical system trajectories can be also characterized by this user-defined bound as well as the actuator bandwidth limit; hence, it is a-priori computable using a given set of adaptive control design parameters.

Actuator failures are another phenomena that can crucially degrade the control system performance and lead to instability [42–44]. A well-known class of actuator failures is when one or more control surfaces suddenly become inaccessible and remain at some unknown value. After an actuator failure, an adaptive control design can reconfigure the remaining control surfaces to recover the system stability and obtain a desired system performance. The authors of [45–52] propose approaches to deal with actuator failures in the context of adaptive control systems, among which only the result in [52] establishes strict guarantees on the closed-loop system performance. Yet, this result utilizes a backstepping procedure and hold under the assumption that a desired trajectory and its derivatives are available (and are all bounded). As another generalization to the set-theoretic model reference adaptive control architecture introduced in Section 1.2.1, a new control architecture is proposed to achieve strict closed-loop system performance guarantees in the presence of finite number of actuator failures. The actuators may fail based on a common failure model in which they can get stuck at some unknown values at some unknown time; hence, the actuator failure structure is unknown in terms of time, pattern, and value.

1.2.3 Applications of the Set-Theoretic Model Reference Adaptive Control Architecture

In this dissertation, four results are presented as applications of the proposed set-theoretic model reference adaptive control architecture introduced in Sections 1.2.1 and 1.2.2. First, an application of this control framework is illustrated on a generic transport model developed by NASA. Specifically, the set-theoretic adaptive controllers are designed for both longitudinal and lateral-directional dynamics that enforce the norm of system error vector to evolve within a user-defined compact set.

Second, experimental results of the set-theoretic model reference adaptive control architecture on an aerospace testbed that is configured as a conventional dual-rotor helicopter, is presented. In particular, this framework is implemented with a constant user-defined bound to enforce a uniform performance bound on the system error for all time. In addition, the set-theoretic model reference adaptive control architecture with time-varying performance bounds is applied that empowers a control designer to assign the closed-loop

system performance as desired on different time intervals (e.g. transient time interval and steady-state time interval) and also to handle a possible system initialization error that can happen in practice.

Third, from a practical stand point, since small system errors usually contain high-frequency residual content of exogenous disturbances and/or measurement noise, a new set-theoretic model reference adaptive control architecture with dead-zone effect is proposed. The key feature of this framework stops the adaptation process inside a dead-zone, while keeping the norm of the system error less than a-priori, user-defined worst-case performance bound. In addition, when this bound is time-varying, the dead-zone embedded in this control algorithm also scales its size automatically which provides flexibility to control the closed-loop system performance as desired on different time intervals. Experimental implementations on the aerospace testbed further demonstrate the efficacy of the proposed method.

Finally, the set-theoretic model reference adaptive control is also augmented at the inner-loop control structure of human-in-the-loop control architectures. Specifically, this is motivated by the fact that the inner loop system errors during the transient phase of adaptively suppressing system uncertainties can severely affect the human-outer loop interactions. Therefore, the augmented set-theoretic model reference adaptive control at the inner-loop structure provides sufficient stability condition for the overall physical system with human dynamics modeled as a linear time-invariant system with human reaction time-delay where unlike other approaches, this condition does not depend on the system uncertainties.

1.3 Temporal Performance Guarantees

As briefly discussed at the beginning of this chapter, the temporal constraints problems are studied in the literature in the context of finite-time control systems. Although the classical finite-time control approaches ensure achieving the control objective within a finite time, their convergence time depends on the initial conditions of the system [10, 11, 53–60]. This sensitivity can pose a serious limitation in control applications where the convergence time needs to be defined prior to the design. For these time-critical applications, fixed-time finite-time control architectures are studied to upper bound the convergence time independently from the initial conditions [12, 13, 61–65]. However, these calculated bounds do not necessarily hold globally and/or can be conservative. More importantly, some of these results that consider system uncertainties require a knowledge of uncertainty upper bounds for stability. To overcome this limitation, predefined-time finite-time control architectures [14, 15, 66–71] are proposed to guarantee convergence at a user-defined finite time. While they are promising, these results are limited to sole systems

or first-order multiagent systems, and more importantly, once again, some of these results that consider system uncertainties require a knowledge of uncertainty upper bounds for stability [4, 72, 73].

To address the aforementioned limitations, as another major contribution of this dissertation, a new distributed control algorithm is proposed based on a time transformation technique for uncertain multiagent systems. The key feature of this control algorithm is to link a user-defined finite-time interval of interest $t \in [0, T)$ to a stretched infinite-time interval $s \in [0, \infty)$. This enables a control designer to exploit any standard system-theoretic tools for synthesis and analysis purposes in this infinite horizon. After establishing the robustness and convergence properties in this new time domain, these results can be transferred back into the original finite time interval of interest. In contrast to existing finite-time approaches, it is shown that the proposed algorithms can preserve a-priori given, user-defined finite-time convergence property regardless of the initial conditions of the multiagent system and without requiring a knowledge of the upper bounds of the system uncertainties.

As a byproduct of the control design for uncertain multiagent systems, other type of system uncertainties are also investigated in this dissertation. Specifically, an important class of system uncertainties in control of multiagent systems is sensor uncertainties, where they can significantly deteriorate the achievable closed-loop system performance. These uncertainties may arise due to low sensor quality, sensor failure, sensor bias, or detrimental environmental conditions [74–77]. In addition, sensor uncertainties can be viewed as sensor measurements corrupted by malicious attacks, that is an important subject in controlling systems through large-scale, multi-layered communication networks such as cyber-physical systems. To this end, a new distributed adaptive control architecture is presented for multiagent systems to mitigate the effect of sensor uncertainties. Two classes of these uncertainties—namely, constant and time-varying sensor uncertainties—are considered. Asymptotic stability is guaranteed for the constant sensor uncertainties and uniform ultimate boundedness result is obtained for the case when the sensor uncertainties are time-varying.

1.4 Spatiotemporal Performance Guarantees

Finally, to answer the overall objective of this dissertation; that is, achieving the spatial and temporal performance guarantees, a unified and novel control architecture is presented to simultaneously address the problem of spatiotemporal constraints in uncertain dynamical systems. The proposed distributed control architecture not only ensures that the agents converge to a time-varying leader at a user-defined finite time of interest (temporal performance guarantee) but also it limits the distance between the state trajectories of

agents and their reference state trajectories to be less than the given bounds (spatial performance guarantee). Unlike other approaches in the literature, the important feature of the proposed distributed control architecture is that the obtained spatiotemporal performance guarantees are independent of the initial conditions of agents, and it does not require a strict knowledge of the upper bounds of the considered class of system uncertainties.

1.5 Organization

The organization of this dissertation is as follows. Chapter 2 presents a set-theoretic model reference adaptive control architecture for enforcing user-defined performance guarantees to address the spatial constraint problem. Chapter 3 generalizes this framework to neuroadaptive control of dynamical systems with unstructured system uncertainties such that the universal function approximation property is not violated. Chapter 4 then provides several key extensions of the set-theoretic model reference adaptive control architecture. Applications of the set-theoretic model reference adaptive control architecture are the introduced in Chapter 5. Chapter 6 addresses the temporal constraint problem by presenting a novel distributed control architecture with user-defined finite-time convergence guarantees. Chapter 7 provides further results on networked multiagent systems for mitigating the effect of sensor uncertainties. Simultaneous spatial and temporal constraint problem is addressed in Chapter 8. Finally, concluding remarks and future research directions are presented in Chapter 9.

CHAPTER 2: A SET-THEORETIC MODEL REFERENCE ADAPTIVE CONTROL ARCHITECTURE FOR DISTURBANCE REJECTION AND UNCERTAINTY SUPPRESSION WITH STRICT PERFORMANCE GUARANTEES[1]

Research in adaptive control algorithms for safety-critical applications is primarily motivated by the fact that these algorithms have the capability to suppress the effects of adverse conditions resulting from exogenous disturbances, imperfect dynamical system modeling, degraded modes of operation, and changes in system dynamics. Although government and industry agree on the potential of these algorithms in providing safety and reducing vehicle development costs, a major issue is the inability to achieve a-priori, user-defined performance guarantees with adaptive control algorithms. In this paper, a new model reference adaptive control architecture for uncertain dynamical systems is presented to address disturbance rejection and uncertainty suppression. The proposed framework is predicated on a set-theoretic adaptive controller construction using generalized restricted potential functions. The key feature of this framework allows the system error bound between the state of an uncertain dynamical system and the state of a reference model, which captures a desired closed-loop system performance, to be less than a-priori, user-defined worst-case performance bound, and hence, it has the capability to enforce strict performance guarantees. Examples are provided to demonstrate the efficacy of the proposed set-theoretic model reference adaptive control architecture.

2.1 Introduction

Research in adaptive control algorithms for safety-critical applications is primarily motivated by the fact that these algorithms have the capability to suppress the effects of adverse conditions resulting from exogenous disturbances, imperfect dynamical system modeling, degraded modes of operation, and changes in system dynamics. Although government and industry agree on the potential of these algorithms in providing safety and reducing vehicle development costs, *a major issue is the inability to achieve a-*

[1]This chapter is previously published in [1]. Permission is included in Appendix H.

priori, user-defined performance guarantees with adaptive control algorithms. To address this challenge, current practice relies heavily on either *excessive vehicle testing* as a means of performing verification or *development of the tools* to validate adaptive control algorithms.

The drawback of excessive vehicle testing is that it only provides *limited performance guarantees for what is tested*; the fixed set of initial conditions, user commands, and possible failure and adversary profiles (see, for example, [5–7]). In addition, the drawback of existing tools for validating adaptive control algorithms is that such tools can only provide guarantees *if there exists a-priori and almost complete knowledge of upper and lower bounds on the unknown gains* appearing in system uncertainty parameterizations and otherwise yield *conservative* performance guarantees (see, for example, [8, 9]). While these bounds may be available for some specific applications with low dynamical system complexity, the actual bounds on the unknown gains may change during operation, for example, when a vehicle undergoes a change in dynamics as a result of reconfiguration, deployment of a payload, docking, or structural damage [78, 79]. In such circumstances, the performance guarantees obtained from the existing tools can *no longer be true*. Therefore, it is important to achieve *strict performance guarantees* with adaptive control algorithms at the *pre-design stage*, instead of relying on excessive vehicle testing and tools to validate their performance during the *post-design stage*.

Notable contributions for achieving strict performance guarantees with adaptive control algorithms include [18–27]. Specifically, [18] use an error transformation approach such that an uncertain dynamical system subject to performance constraints is transformed into an equivalent form without constraints and analysis is performed for this equivalent form to show that the uncertain dynamical system satisfies given performance constraints. Even though the methodology documented in [18] is promising, it is assumed that the control signals can access to every element of the state vector. This limitation is avoided in [19] by considering a backstepping adaptive control approach under the assumption that a desired trajectory and its derivatives are available and all bounded. In addition, the same approach is extended to a generalized class of uncertain dynamical systems in [20] to enforce constraints on measurable output signals but not on measurable state vectors. [21] propose an adaptive control architecture with strict performance guarantees under the assumption that system uncertainties do not depend on time, where their approach do not directly generalize to time-varying case to handle exogenous disturbances and changes in system dynamics. Restricted potential functions (barrier Lyapunov functions) are employed in [22–26] in the context of backstepping adaptive control to construct a closed-loop dynamical system with strict performance guarantees. Finally, [27] uses

bounding functions to enforce performance constraints in the context of model reference adaptive control. Even though this is a promising approach, violation of the performance constraints may happen if the growth rate of the bounding functions is not sufficiently large.

2.1.1 Contribution

In this paper, we focus on the model reference adaptive control problem of uncertain dynamical systems in the presence of exogenous disturbances and system uncertainties, where both sources of system adversaries can depend on time to capture dynamic environment conditions (e.g., winds or turbulent flows) and changes in system dynamics (e.g., system reconfiguration, deployment of a payload, docking, or structural damage). For this problem, *the fundamental research contribution* of this paper is a new model reference adaptive control architecture, where its novel characteristic is *the capability to enforce strict performance guarantees* at the pre-design stage. Specifically:

i) The key feature of the proposed model reference adaptive controller allows *the system error bound* between the state of an uncertain dynamical system and the state of a reference model to be less than *a-priori, user-defined worst-case performance bound* (see Theorem 2.3.1). Since this bound is user-defined, it is *practical* in the sense that it does *not* depend on any unknown parameters. Therefore, a control engineer can establish a guaranteed worst-case performance using the proposed architecture at the *pre-design stage* to control uncertain dynamical systems (see Examples 1, 2, and 3). This is a *significant* departure from the existing, standard model reference adaptive control approaches, because their error bounds *do depend on unknown parameters*, and hence, they cannot provide strict guarantees. This is the reason why such approaches practically rely on *excessive* vehicle testing and tools to validate their performance during the *post-design stage* based on the collected system data (see Remarks 2.2.3 and 2.3.2 for additional details).

ii) As a byproduct, we show that an upper bound for the adaptive control signals can be directly calculated without inducing (excessive) conservatism, which only depends on user-defined design parameters (see Theorem 2.3.2). Once again, this is a *significant* departure from the existing, standard model reference adaptive control approaches, because their upper bounds for the adaptive control signals depend on not only the design parameters specified by control engineers but also initial conditions and *unknown parameters* (see Remarks 2.2.4 and 2.3.2 for additional details).

iii) In addition to the major contributions stated in *i)* and *ii)*, another contribution of this paper is the generalization of the proposed model reference adaptive control architecture to accommodate *nonlinear reference systems*, which are desired for several practical applications especially for those involving guidance and control of highly-maneuverable aircrafts, guided projectiles, and space launch vehicles (see Theorem 2.4.1).

To summarize, the proposed architecture is a unique contribution to the model reference adaptive control literature since it can be an effective control methodology for safety-critical applications to enforce the state of a given uncertain dynamical system to strictly evolve in a pre-defined state-space set; for example, for preserving safe flight envelope in aerospace applications (see Remark 2.4.2).

2.1.2 Organization and Notation

The organization of this paper is as follows. In Section 2.2, we present an overview on the (standard) model reference adaptive control problem. In Section 2.3, we develop and analyze the proposed set-theoretic adaptive control architecture for linear reference models, whereas Section 2.4 generalizes these results for a class of nonlinear reference models. Numerical examples are provided in Section 2.5 to demonstrate the efficacy of the proposed approach. Finally, we present conclusions and highlight some recommendations for future research in Section 2.6.

The notation used in this paper is fairly standard. Specifically, $\mathbb{N}$ denotes the set of natural numbers, $\mathbb{R}$ denotes the set of real numbers, $\mathbb{R}^n$ denotes the set of $n \times 1$ real column vectors, $\mathbb{R}^{n\times m}$ denotes the set of $n \times m$ real matrices, $\mathbb{R}_+$ (respectively, $\overline{\mathbb{R}}_+$) denotes the set of positive (respectively, nonnegative-definite) real numbers, $\mathbb{R}_+^{n\times n}$ (respectively, $\overline{\mathbb{R}}_+^{n\times n}$) denotes the set of $n \times n$ positive-definite (respectively, nonnegative-definite) real matrices, $\mathbb{D}^{n\times n}$ denotes the set of $n \times n$ real matrices with diagonal scalar entries, $0_{n\times n}$ denotes the $n \times n$ zero matrix, and "$\triangleq$" denotes equality by definition. In addition, we write $(\cdot)^{\mathrm{T}}$ for the transpose operator, $(\cdot)^{-1}$ for the inverse operator, $\det(\cdot)$ for the determinant operator, $\|\cdot\|_{\mathrm{F}}$ for the Frobenius norm, and $\|\cdot\|_2$ for the Euclidean norm. Furthermore, we write $\|x\|_{\mathrm{A}} \triangleq \sqrt{x^{\mathrm{T}}Ax}$ for the weighted Euclidean norm of $x \in \mathbb{R}^n$ with the matrix $A \in \mathbb{R}_+^{n\times n}$, $\|A\|_2 \triangleq \sqrt{\lambda_{\max}(A^{\mathrm{T}}A)}$ for the induced 2-norm of the matrix $A \in \mathbb{R}^{n\times m}$, $\lambda_{\min}(A)$ (resp., $\lambda_{\max}(A)$) for the minimum (resp., maximum) eigenvalue of the matrix $A \in \mathbb{R}^{n\times n}$, $\mathrm{tr}(\cdot)$ for the trace operator, and $\underline{x}$ (resp., $\overline{x}$) for the lower bound (resp., upper bound) of a bounded signal $x(t) \in \mathbb{R}^n$, $t \geq 0$, that is, $\underline{x} \leq \|x(t)\|_2$, $t \geq 0$ (resp., $\|x(t)\|_2 \leq \overline{x}$, $t \geq 0$).

2.2 Model Reference Adaptive Control Overview

In this section, we present an overview on the (standard) model reference adaptive control problem. Specifically, we begin with the definition of the projection operator.

Definition 2.2.1 *Let* $\psi : \mathbb{R}^n \longrightarrow \mathbb{R}$ *be a continuously differentiable convex function given by* $\psi(\theta) \triangleq \frac{(\varepsilon_\theta+1)\theta^{\mathrm{T}}\theta-\theta_{\max}^2}{\varepsilon_\theta\theta_{\max}^2}$, *where* $\theta_{\max} \in \mathbb{R}$ *is a projection norm bound imposed on* $\theta \in \mathbb{R}^n$ *and* $\varepsilon_\theta > 0$ *is a projection tolerance bound. Then, the projection operator* $\mathrm{Proj} : \mathbb{R}^n \times \mathbb{R}^n \to \mathbb{R}^n$ *is defined by*

$$\mathrm{Proj}(\theta, y) \triangleq \begin{cases} y, & \text{if } \psi(\theta) < 0, \\ y, & \text{if } \psi(\theta) \geq 0 \text{ and } \psi'(\theta)y \leq 0, \\ y - \frac{\psi'^{\mathrm{T}}(\theta)\psi'(\theta)y}{\psi'(\theta)\psi'^{\mathrm{T}}(\theta)}\psi(\theta), & \text{if } \psi(\theta) \geq 0 \text{ and } \psi'(\theta)y > 0, \end{cases} \tag{2.1}$$

where $y \in \mathbb{R}^n$.

It follows from Definition 2.2.1 that

$$(\theta - \theta^*)^{\mathrm{T}}\left[\mathrm{Proj}(\theta, y) - y\right] \leq 0, \tag{2.2}$$

holds [80]. The definition of the projection operator can be generalized to matrices as

$$\mathrm{Proj}_{\mathrm{m}}(\Theta, Y) = (\mathrm{Proj}(\mathrm{col}_1(\Theta), \mathrm{col}_1(Y)), \ldots, \mathrm{Proj}(\mathrm{col}_m(\Theta), \mathrm{col}_m(Y))), \tag{2.3}$$

where $\Theta \in \mathbb{R}^{n\times m}, Y \in \mathbb{R}^{n\times m}$, and $\mathrm{col}_i(\cdot)$ denotes i th column operator. In this case, for a given matrix Θ^*, it follows from (2.2) that

$$\mathrm{tr}\left[(\Theta - \Theta^*)^{\mathrm{T}}\left[\mathrm{Proj}_{\mathrm{m}}(\Theta, Y) - Y\right]\right] = \sum_{i=1}^{m}\left[\mathrm{col}_i(\Theta - \Theta^*)^{\mathrm{T}}\left[\mathrm{Proj}(\mathrm{col}_i(\Theta), \mathrm{col}_i(Y)) - \mathrm{col}_i(Y)\right]\right] \leq 0. \tag{2.4}$$

Throughout this paper, we assume without loss of generality that the projection norm bound imposed on each column of $\Theta \in \mathbb{R}^{n\times m}$ is $\theta_{\max}$.

Next, consider the uncertain dynamical system given by

$$\dot{x}_{\mathrm{p}}(t) = A_{\mathrm{p}}x_{\mathrm{p}}(t) + B_{\mathrm{p}}\Lambda u(t) + B_{\mathrm{p}}\delta_{\mathrm{p}}(t, x_{\mathrm{p}}(t)), \quad x_{\mathrm{p}}(0) = x_{\mathrm{p}0}, \quad t \geq 0, \tag{2.5}$$

where $x_{\rm p}(t) \in \mathbb{R}^{n_{\rm p}}$, $t \geq 0$, is the measurable state vector, $u(t) \in \mathbb{R}^m$, $t \geq 0$, is the control input, $A_{\rm p} \in \mathbb{R}^{n_{\rm p} \times n_{\rm p}}$ is a known system matrix, $B_{\rm p} \in \mathbb{R}^{n_{\rm p} \times m}$ is a known input matrix, $\delta_{\rm p} : \overline{\mathbb{R}}_+ \times \mathbb{R}^{n_{\rm p}} \to \mathbb{R}^m$ is a system uncertainty, $\Lambda \in \mathbb{R}_+^{m \times m} \cap \mathbb{D}^{m \times m}$ is an unknown control effectiveness matrix, and the pair $(A_{\rm p}, B_{\rm p})$ is controllable. We now introduce a standard assumption on system uncertainty parameterization (see, for example, [28–30]).

Assumption 2.2.1 *The system uncertainty given by* (2.5) *is parameterized as*

$$\delta_{\rm p}(t, x_{\rm p}) \quad = \quad W_{\rm p}^{\rm T}(t) \sigma_{\rm p}(x_{\rm p}), \tag{2.6}$$

where $W_{\rm p}(t) \in \mathbb{R}^{s \times m}$, $t \geq 0$, is a bounded unknown weight matrix (i.e., $\|W_{\rm p}(t)\|_{\rm F} \leq w_{\rm p}$, $t \geq 0$) with a bounded time rate of change (i.e., $\|\dot{W}_{\rm p}(t)\|_{\rm F} \leq \dot{w}_{\rm p}$, $t \geq 0$) and $\sigma_{\rm p} : \mathbb{R}^{n_{\rm p}} \to \mathbb{R}^s$ is a known basis function of the form $\sigma_{\rm p}(x_{\rm p}) = [\sigma_{\rm p1}(x_{\rm p}), \sigma_{\rm p2}(x_{\rm p}), \ \ldots, \sigma_{{\rm p}s}(x_{\rm p})]^{\rm T}$.

Remark 2.2.1 *The system uncertainty parameterization in (2.6) captures time-varying changes in system dynamics due to system reconfiguration, deployment of a payload, docking, or structural damage. By letting the first element of the basis function be a constant (i.e., $\sigma_{\rm p1}(x_{\rm p}) = b$), then this parameterization is also sufficient to capture exogenous disturbances depending on time, which can represent adversaries due to environment conditions such as winds or turbulent flows.*

To address command following, let $c(t) \in \mathbb{R}^{n_{\rm c}}$, $t \geq 0$, be a given bounded piecewise continuous command and $x_{\rm c}(t) \in \mathbb{R}^{n_{\rm c}}$, $t \geq 0$, be the integrator state satisfying

$$\dot{x}_{\rm c}(t) = E_{\rm p} x_{\rm p}(t) - c(t), \quad x_{\rm c}(0) = x_{\rm c0}, \quad t \geq 0, \tag{2.7}$$

where $E_{\rm p} \in \mathbb{R}^{n_{\rm c} \times n_{\rm p}}$ allows to choose a subset of $x_{\rm p}(t)$, $t \geq 0$, to follow $c(t)$, $t \geq 0$. Now, (2.5) can be augmented with (2.7) as

$$\dot{x}(t) \quad = \quad Ax(t) + B\Lambda u(t) + BW_{\rm p}^{\rm T}(t)\sigma_{\rm p}(x_{\rm p}(t)) + B_{\rm r}c(t), \quad x(0) = x_0, \quad t \geq 0, \tag{2.8}$$

where $x(t) \triangleq [x_{\rm p}^{\rm T}(t), \ x_{\rm c}^{\rm T}(t)]^{\rm T} \in \mathbb{R}^n$, $t \geq 0$, $n = n_{\rm p} + n_{\rm c}$, is the augmented state vector, $x_0 \triangleq [x_{\rm p0}^{\rm T}, x_{\rm c0}^{\rm T}]^{\rm T}$,

$$A \quad \triangleq \quad \begin{bmatrix} A_{\rm p} & 0_{n_{\rm p} \times n_{\rm c}} \\ E_{\rm p} & 0_{n_{\rm c} \times n_{\rm c}} \end{bmatrix} \in \mathbb{R}^{n \times n}, \tag{2.9}$$

$$B \triangleq \begin{bmatrix} B_{\mathrm{p}}^{\mathrm{T}} & 0_{n_{\mathrm{c}}\times m}^{\mathrm{T}} \end{bmatrix}^{\mathrm{T}} \in \mathbb{R}^{n\times m}, \tag{2.10}$$

$$B_{\mathrm{r}} \triangleq \begin{bmatrix} 0_{n_{\mathrm{p}}\times n_{\mathrm{c}}}^{\mathrm{T}} & -I_{n_{\mathrm{c}}\times n_{\mathrm{c}}} \end{bmatrix}^{\mathrm{T}} \in \mathbb{R}^{n\times n_{\mathrm{c}}}. \tag{2.11}$$

We now consider the feedback control law given by

$$u(t) = u_{\mathrm{n}}(t) + u_{\mathrm{a}}(t), \quad t \geq 0, \tag{2.12}$$

where $u_{\mathrm{n}}(t) \in \mathbb{R}^m$, $t \geq 0$, and $u_{\mathrm{a}}(t) \in \mathbb{R}^m$, $t \geq 0$, are the nominal and adaptive control laws, respectively. Furthermore, let the nominal control law be

$$u_{\mathrm{n}}(t) = -Kx(t), \quad t \geq 0, \tag{2.13}$$

such that $A_{\mathrm{r}} \triangleq A - BK$, $K \in \mathbb{R}^{m\times n}$, is Hurwitz. Using (2.12) and (2.13) in (2.8) yields

$$\dot{x}(t) = A_{\mathrm{r}}x(t) + B_{\mathrm{r}}c(t) + B\Lambda\left[u_{\mathrm{a}}(t) + W^{\mathrm{T}}(t)\sigma\big(x(t)\big)\right], \quad x(0) = x_0, \quad t \geq 0, \tag{2.14}$$

where $W(t) \triangleq \left[\Lambda^{-1}W_{\mathrm{p}}^{\mathrm{T}}(t),\ (\Lambda^{-1} - I_{m\times m})K\right]^{\mathrm{T}} \in \mathbb{R}^{(s+n)\times m}$, $t \geq 0$, is an unknown (aggregated) weight matrix and $\sigma\big(x(t)\big) \triangleq [\sigma_{\mathrm{p}}^{\mathrm{T}}\big(x_{\mathrm{p}}(t)\big), x^{\mathrm{T}}(t)]^{\mathrm{T}} \in \mathbb{R}^{s+n}$, $t \geq 0$, is a known (aggregated) basis function. Considering (2.14), in addition, let the adaptive control law be

$$u_{\mathrm{a}}(t) = -\hat{W}^{\mathrm{T}}(t)\sigma\big(x(t)\big), \quad t \geq 0, \tag{2.15}$$

where $\hat{W}(t) \in \mathbb{R}^{(s+n)\times m}$, $t \geq 0$, is the estimate of $W(t)$, $t \geq 0$, satisfying the update law

$$\dot{\hat{W}}(t) = \gamma\mathrm{Proj}_{\mathrm{m}}\Big(\hat{W}(t), \sigma\big(x(t)\big)e^{\mathrm{T}}(t)PB\Big), \quad t \geq 0, \tag{2.16}$$

with $\hat{W}_{\max}$ being the projection norm bound. In (2.16), $\gamma \in R_+$ is the learning rate (i.e., adaptation gain), $P \in \mathbb{R}_+^{n\times n}$ is a solution of the Lyapunov equation given by

$$0 = A_{\mathrm{r}}^{\mathrm{T}}P + PA_{\mathrm{r}} + R, \tag{2.17}$$

with $R \in \mathbb{R}_+^{n\times n}$, and $e(t) \triangleq x(t) - x_{\mathrm{r}}(t)$, $t \geq 0$, is the system error with $x_{\mathrm{r}}(t) \in \mathbb{R}^n$, $t \geq 0$, being the reference state vector, which satisfies the reference model given by

$$\dot{x}_{\mathrm{r}}(t) \quad = \quad A_{\mathrm{r}}x_{\mathrm{r}}(t) + B_{\mathrm{r}}c(t), \quad x_{\mathrm{r}}(0) = x_{\mathrm{r}0}, \quad t \geq 0. \tag{2.18}$$

Using (2.14), (2.15), and (2.18), the system error dynamics is given by

$$\dot{e}(t) \quad = \quad A_{\mathrm{r}}e(t) - B\Lambda\tilde{W}^{\mathrm{T}}(t)\sigma\big(x(t)\big), \quad e(0) = e_0, \quad t \geq 0, \tag{2.19}$$

where $\tilde{W}(t) \triangleq \hat{W}(t) - W(t) \in \mathbb{R}^{(s+n)\times m}$, $t \geq 0$, is the weight estimation error and $e_0 \triangleq x_0 - x_{\mathrm{r}0}$. Note that $\|W(t)\|_{\mathrm{F}} \leq w, t \geq 0$, and $\|\dot{W}(t)\|_{\mathrm{F}} \leq \dot{w}, t \geq 0$, automatically holds as a direct consequence of Assumption 2.2.1.

Remark 2.2.2 *The update law given by* (2.16) *for the (standard) model reference adaptive control problem can be derived by considering the following Lyapunov function candidate*

$$V(e,\tilde{W}) = e^{\mathrm{T}}Pe + \gamma^{-1}\mathrm{tr}\big[(\tilde{W}\Lambda^{1/2})^{\mathrm{T}}(\tilde{W}\Lambda^{1/2})\big]. \tag{2.20}$$

Specifically, the time derivative of (2.20) along the closed-loop system trajectories is given by

$$\begin{aligned}\dot{V}\big(e(t),\tilde{W}(t)\big) \quad &= \quad -e^{\mathrm{T}}(t)Re(t) - 2\gamma^{-1}\mathrm{tr}\tilde{W}^{\mathrm{T}}(t)\dot{W}(t)\Lambda \\ &\quad + 2\mathrm{tr}\tilde{W}^{\mathrm{T}}(t)\Big(\mathrm{Proj}_{\mathrm{m}}\big(\hat{W}(t),\sigma\big(x(t)\big)e^{\mathrm{T}}(t)PB\big) - \sigma\big(x(t)\big)e^{\mathrm{T}}(t)PB\Big)\Lambda \\ &\leq \quad -\lambda_{\min}(R)\|e(t)\|_2^2 + 2\gamma^{-1}\tilde{w}\,\dot{w}\|\Lambda\|_2,\end{aligned} \tag{2.21}$$

where $\tilde{w} = \hat{W}_{\max} + w$. *Hence,* $\dot{V}\big(e(t),\tilde{W}(t)\big) < 0$ *outside of the compact set*

$$\Omega \triangleq \big\{\big(e(t),\tilde{W}(t)\big) : \ \|e(t)\|_2 \leq \eta \ \ \textit{and} \ \ \|\tilde{W}(t)\| \leq \tilde{w}\big\}, \tag{2.22}$$

where $\eta \triangleq \sqrt{\gamma^{-1}\|\Lambda\|_2 \frac{2\tilde{w}\dot{w}+\tilde{w}^2}{\lambda_{\min}(R)}}$, *which proves the boundedness of the solution* $\big(e(t),\tilde{W}(t)\big)$.

Remark 2.2.3 *From a practical standpoint, it is important to calculate an upper bound on the norm of the system error for understanding the effect of design parameters on the system performance. Specifically, to find an ultimate bound of* $e(t)$ *for* $t \geq T$, *note from Remark 2.2.2 that* $\lambda_{\min}(P)\|e(t)\|_2^2 \leq V(e(t),\tilde{W}(t)) \leq$

$\lambda_{\max}(P)\eta^2+\gamma^{-1}\tilde{w}^2\|\Lambda\|_2$, *and hence,*

$$\|e(t)\|_2 \leq \sqrt{\frac{\lambda_{\max}(P)\eta^2+\gamma^{-1}\tilde{w}^2\|\Lambda\|_2}{\lambda_{\min}(P)}}, \quad t \geq T. \tag{2.23}$$

Since $\dot{V}\big(e(t),\tilde{W}(t)\big)<0$ *outside of the compact set (2.22) for* $t\in[0,T)$*, then*

$$V\big(e(t),\tilde{W}(t)\big)\leq V\big(e(0),\tilde{W}(0)\big), \tag{2.24}$$

and hence, it follows from (2.24) and $\lambda_{\min}(P)\|e(t)\|_2^2\leq V\big(e(t),\tilde{W}(t)\big)$ *that*

$$\|e(t)\|_2 \leq \sqrt{\frac{\lambda_{\max}(P)\|e(0)\|^2+\gamma^{-1}\|\tilde{W}(0)\|_2^2\|\Lambda\|_2}{\lambda_{\min}(P)}}, \quad t\in[0,T). \tag{2.25}$$

Note that if the solution $\big(e(t),\tilde{W}(t)\big)$ *is on the compact set (2.22) at* $t=0$*, then (2.23) holds for* $t\geq 0$ *since* $T=0$ *in this case.*

Remark 2.2.4 *On the upper bounds on the norm of the system error given by (2.23) and (2.25) in Remark 2.2.3, the following two observations are now immediate. First, we note that these upper bounds are conservative, and hence, they do not provide strict performance guarantees. Second, these upper bounds do not solely depend on user-defined design parameters due to the existence of the unknown matrices* W *and* Λ *appearing in these bounds, and hence, they are not a-priori verifiable at the pre-design stage. In addition, based on these upper bounds, one may be interested in calculating an upper bound on the control signal. To elucidate this point, assume* $\|\sigma(x)\|_2\leq\overline{\sigma}+\mathcal{L}\|x\|_2$, $\mathcal{L}\in\mathbb{R}_+$*, where it follows from* $\|u(t)\|_2\leq\|K\|_2\|x(t)\|_2+\hat{W}_{\max}\big(\mathcal{L}\|x(t)\|_2+\overline{\sigma}\big)\leq\big(\|K\|_2+\mathcal{L}\hat{W}_{\max}\big)\big(\|e(t)\|_2+\overline{x_{\mathrm{r}}}\big)+\overline{\sigma}\hat{W}_{\max}$*, (2.23), and (2.25) that*

$$\|u(t)\|_2 \leq \left(\|K\|_2+\mathcal{L}\hat{W}_{\max}\right)\left(\sqrt{\frac{\lambda_{\max}(P)\eta^2+\gamma^{-1}\tilde{w}^2\|\Lambda\|_2}{\lambda_{\min}(P)}}+\overline{x_{\mathrm{r}}}\right)+\overline{\sigma}\hat{W}_{\max}, \quad t\geq T, \tag{2.26}$$

$$\|u(t)\|_2 \leq \left(\|K\|_2+\mathcal{L}\hat{W}_{\max}\right)\left(\sqrt{\frac{\lambda_{\max}(P)\|e(0)\|_2^2+\gamma^{-1}\|\tilde{W}(0)\|_2^2\|\Lambda\|_2}{\lambda_{\min}(P)}}+\overline{x_{\mathrm{r}}}\right)+\overline{\sigma}\hat{W}_{\max}, \quad t\in[0,T). \tag{2.27}$$

Note that since (2.23) and (2.25) are conservative, then (2.26) and (2.27) are automatically conservative and they do not solely depend on user-defined design parameters as well, and hence, they may not be practical for controller design.

2.3 Set-Theoretic Model Reference Adaptive Control

In this section, we design and analyze a set-theoretic model reference adaptive control architecture that allows the system error bound between the state of an uncertain dynamical system and the state of a linear reference model to be less than a-priori, user-defined worst-case performance bound in the presence of time-varying exogenous disturbances and system uncertainties, wherein Section 2.4 generalizes these results for a class of nonlinear reference models. For this purpose, we introduce the following definition.

Definition 2.3.1 *Let $\|z\|_H = \sqrt{z^{\mathrm{T}}Hz}$ be a weighted Euclidean norm, where $z \in \mathbb{R}^p$ is a real column vector and $H \in \mathbb{R}_+^{p\times p}$. We define $\phi(\|z\|_{\mathrm{H}})$, $\phi : \mathbb{R} \to \mathbb{R}$, to be a generalized restricted potential function (generalized barrier Lyapunov function) on the set*

$$\mathcal{D}_\varepsilon \triangleq \{z : \|z\|_{\mathrm{H}} \in [0, \varepsilon)\}, \tag{2.28}$$

with $\varepsilon \in \mathbb{R}_+$ being a-priori, user-defined constant, if the following statements hold:

i) If $\|z\|_{\mathrm{H}} = 0$, then $\phi(\|z\|_{\mathrm{H}}) = 0$.

ii) If $z \in \mathcal{D}_\varepsilon$ and $\|z\|_{\mathrm{H}} \neq 0$, then $\phi(\|z\|_{\mathrm{H}}) > 0$.

iii) If $\|z\|_{\mathrm{H}} \to \varepsilon$, then $\phi(\|z\|_{\mathrm{H}}) \to \infty$.

iv) $\phi(\|z\|_{\mathrm{H}})$ is continuously differentiable on $\mathcal{D}_\varepsilon$.

v) If $z \in \mathcal{D}_\varepsilon$, then $\phi_d(\|z\|_{\mathrm{H}}) > 0$, where

$$\phi_d(\|z\|_{\mathrm{H}}) \triangleq \frac{\mathrm{d}\phi(\|z\|_{\mathrm{H}})}{\mathrm{d}\|z\|_{\mathrm{H}}^2}. \tag{2.29}$$

vi) If $z \in \mathcal{D}_\varepsilon$, then

$$2\phi_d(\|z\|_{\mathrm{H}})\|z\|_{\mathrm{H}}^2 - \phi(\|z\|_{\mathrm{H}}) > 0. \tag{2.30}$$

Remark 2.3.1 *Note that Definition 2.3.1 generalizes the definition of the restricted potential functions (barrier Lyapunov functions) used by the authors of [21–26]. A candidate generalized restricted potential function satisfying the conditions given in Definition 2.3.1 has the form*

$$\phi(\|z\|_{\mathrm{H}}) = \frac{\|z\|_{\mathrm{H}}^2}{\varepsilon - \|z\|_{\mathrm{H}}}, \quad z \in \mathcal{D}_\varepsilon, \tag{2.31}$$

which has the partial derivative

$$\phi_d(\|z\|_{\mathrm{H}}) = \frac{\varepsilon - \frac{1}{2}\|z\|_{\mathrm{H}}}{\left(\varepsilon - \|z\|_{\mathrm{H}}\right)^2} > 0, \quad z \in \mathcal{D}_\varepsilon, \tag{2.32}$$

with respect to $\|z\|_{\mathrm{H}}^2$ *and*

$$2\phi_d(\|z\|_{\mathrm{H}})\|z\|_{\mathrm{H}}^2 - \phi(\|z\|_{\mathrm{H}}) = \frac{\varepsilon\|z\|_{\mathrm{H}}^2}{\left(\varepsilon - \|z\|_{\mathrm{H}}\right)^2} > 0, \quad z \in \mathcal{D}_\varepsilon. \tag{2.33}$$

Next, consider the augmented uncertain dynamical system given by (2.8) with the feedback control law in (2.12), where the nominal and adaptive control laws satisfy (2.13) and (2.15), respectively. Here, we propose the (set-theoretic) update law constructed using generalized restricted potential functions given by

$$\dot{\hat{W}}(t) = \gamma \mathrm{Proj}_{\mathrm{m}}\Big(\hat{W}(t), \phi_d(\|e(t)\|_P)\sigma\big(x(t)\big)e^{\mathrm{T}}(t)PB\Big), \quad \hat{W}(0) = \hat{W}_0, \quad t \geq 0, \tag{2.34}$$

where $\gamma \in R_+$ is the learning rate, $P \in \mathbb{R}_+^{n\times n}$ is a solution of the Lyapunov equation given by (2.17) with $R \in \mathbb{R}_+^{n\times n}$, and $e(t) \triangleq x(t) - x_{\mathrm{r}}(t)$, $t \geq 0$, is the system error with $x_{\mathrm{r}}(t) \in \mathbb{R}^n$, $t \geq 0$, being the reference state vector, which satisfies the linear reference model given by (2.18). Note that $\phi_d(\|e(t)\|_P)$ in (2.34) can be viewed as an error dependent learning rate.

For the next theorem presenting the main result of this paper, one can write the system error dynamics and the weight estimation error dynamics respectively given by

$$\dot{e}(t) = A_{\mathrm{r}}e(t) - B\Lambda\tilde{W}^{\mathrm{T}}(t)\sigma\big(x(t)\big), \quad e(0) = e_0, \quad t \geq 0, \tag{2.35}$$

$$\dot{\tilde{W}}(t) = \gamma \mathrm{Proj}_{\mathrm{m}}\Big(\hat{W}(t), \phi_d(\|e(t)\|_P)\sigma\big(x(t)\big)e^{\mathrm{T}}(t)PB\Big) - \dot{W}(t), \quad \tilde{W}(0) = \tilde{W}_0, \quad t \geq 0, \tag{2.36}$$

where $\tilde{W}(t) \triangleq \hat{W}(t) - W(t)$, $t \geq 0$, is the weight estimation error.

Theorem 2.3.1 *Consider the uncertain dynamical system given by (2.5) subject to Assumption 2.2.1, the linear reference model given by (2.18), and the feedback control law given by (2.12) along with (2.13), (2.15), and (2.34). If* $\|e_0\|_P < \varepsilon$, *then the closed-loop dynamical system given by (2.35) and (2.36) are bounded, where the bound on the system error strictly satisfies a-priori given, user-defined worst-case performance*

$$\|e(t)\|_P < \varepsilon, \quad t \geq 0. \tag{2.37}$$

If, in addition, the unknown weight matrix in (2.6) is constant, then $\lim_{t\to\infty} e(t) = 0$.

Proof. To show boundedness of the closed-loop dynamical system given by (2.35) and (2.36), consider the energy function $V : \mathcal{D}_\varepsilon \times \mathbb{R}^{(n+s)\times m} \to \overline{\mathbb{R}}_+$ given by

$$V(e,\tilde{W}) = \phi(\|e\|_P) + \gamma^{-1}\mathrm{tr}\big[(\tilde{W}\Lambda^{1/2})^{\mathrm{T}}(\tilde{W}\Lambda^{1/2})\big], \tag{2.38}$$

where $\mathcal{D}_\varepsilon \triangleq \{e(t) : \|e(t)\|_P < \varepsilon\}$, and $P \in \mathbb{R}^{n\times n}_+$ is a solution of the Lyapunov equation in (2.17) with $R \in \mathbb{R}^{n\times n}_+$. Note that $V(0,0) = 0$, $V\big(e,\tilde{W}\big) > 0$ for all $\big(e,\tilde{W}\big) \neq (0,0)$, and

$$\frac{\mathrm{d}\phi(\|e(t)\|_P)}{\mathrm{d}t} = \frac{\mathrm{d}\phi(\|e(t)\|_P)}{\mathrm{d}\|e(t)\|_P^2}\,\frac{\mathrm{d}\|e(t)\|_P^2}{\mathrm{d}t} = 2\phi_d(\|e(t)\|_P)e^{\mathrm{T}}(t)P\dot{e}(t). \tag{2.39}$$

Specifically, the time derivative of (2.38) along the closed-loop system trajectories (2.35) and (2.36) is given by

$$\begin{aligned}
\dot{V}\big(e(t),\tilde{W}(t)\big) &= \frac{\mathrm{d}\phi(\|e(t)\|_P)}{\mathrm{d}t} + 2\gamma^{-1}\mathrm{tr}\tilde{W}^{\mathrm{T}}(t)\dot{\tilde{W}}(t)\Lambda \\
&= 2\phi_d(\|e(t)\|_P)e^{\mathrm{T}}(t)P\dot{e}(t) \\
&\quad +2\gamma^{-1}\mathrm{tr}\tilde{W}^{\mathrm{T}}(t)\Big(\gamma\mathrm{Proj}_{\mathrm{m}}\Big(\hat{W}(t),\phi_d(\|e(t)\|_P)\sigma\big(x(t)\big)e^{\mathrm{T}}(t)PB\Big) - \dot{W}(t)\Big)\Lambda \\
&= 2\phi_d(\|e(t)\|_P)e^{\mathrm{T}}(t)PA_{\mathrm{r}}e(t) - 2\phi_d(\|e(t)\|_P)e^{\mathrm{T}}(t)PB\Lambda\tilde{W}^{\mathrm{T}}(t)\sigma\big(x(t)\big) \\
&\quad +2\mathrm{tr}\tilde{W}^{\mathrm{T}}(t)\mathrm{Proj}_{\mathrm{m}}\Big(\hat{W}(t),\phi_d(\|e(t)\|_P)\sigma\big(x(t)\big)e^{\mathrm{T}}(t)PB\Big)\Lambda - 2\gamma^{-1}\mathrm{tr}\tilde{W}^{\mathrm{T}}(t)\dot{W}(t)\Lambda \\
&= 2\phi_d(\|e(t)\|_P)e^{\mathrm{T}}(t)PA_{\mathrm{r}}e(t) - 2\mathrm{tr}\big(\hat{W}^{\mathrm{T}}(t) - W^{\mathrm{T}}(t)\big)\Big(\phi_d(\|e(t)\|_P)\sigma\big(x(t)\big)e^{\mathrm{T}}(t)PB \\
&\quad -\mathrm{Proj}_{\mathrm{m}}\Big(\hat{W}(t),\phi_d(\|e(t)\|_P)\sigma\big(x(t)\big)e^{\mathrm{T}}(t)PB\Big)\Big)\Lambda - 2\gamma^{-1}\mathrm{tr}\tilde{W}^{\mathrm{T}}(t)\dot{W}(t)\Lambda.
\end{aligned} \tag{2.40}$$

Now, using the property of projection operator in (2.4), one can write

$$\begin{aligned}
\dot{V}\big(e(t),\tilde{W}(t)\big) &\leq -\phi_d(\|e(t)\|_P)e^{\mathrm{T}}(t)Re(t)+d \\
&\leq -\alpha\phi_d(\|e(t)\|_P)e^{\mathrm{T}}(t)Pe(t)+d+\frac{1}{2}\alpha\phi(\|e(t)\|_P)-\frac{1}{2}\alpha\phi(\|e(t)\|_P) \\
&\quad +\frac{1}{2}\alpha\gamma^{-1}\mathrm{tr}\big[(\tilde{W}(t)\Lambda^{1/2})^{\mathrm{T}}(\tilde{W}(t)\Lambda^{1/2})\big]-\frac{1}{2}\alpha\gamma^{-1}\mathrm{tr}\big[(\tilde{W}(t)\Lambda^{1/2})^{\mathrm{T}}(\tilde{W}(t)\Lambda^{1/2})\big] \\
&\leq -\frac{1}{2}\alpha\Big(\phi(\|e(t)\|_P)+\gamma^{-1}\mathrm{tr}\big[(\tilde{W}(t)\Lambda^{1/2})^{\mathrm{T}}(\tilde{W}(t)\Lambda^{1/2})\big]\Big) \\
&\quad -\alpha\Big[\phi_d(\|e(t)\|_P)e^{\mathrm{T}}(t)Pe(t)-\frac{1}{2}\phi(\|e(t)\|_P)\Big]+\frac{1}{2}\alpha\gamma^{-1}\mathrm{tr}\big[(\tilde{W}(t)\Lambda^{1/2})^{\mathrm{T}}(\tilde{W}(t)\Lambda^{1/2})\big]+d \\
&\leq -\frac{1}{2}\alpha V(e,\tilde{W})-\alpha\Big[\phi_d(\|e(t)\|_P)e^{\mathrm{T}}(t)Pe(t)-\frac{1}{2}\phi(\|e(t)\|_P)\Big]+\mu, \qquad (2.41)
\end{aligned}$$

and it follows from (2.30) in Definition 2.3.1 that

$$\dot{V}\big(e(t),\tilde{W}(t)\big) \leq -\frac{1}{2}\alpha V(e,\tilde{W})+\mu, \qquad (2.42)$$

where $\alpha \triangleq \frac{\lambda_{\min}(R)}{\lambda_{\max}(P)}$, $d \triangleq 2\gamma^{-1}\tilde{w}\,\dot{w}\|\Lambda\|_2$, and $\mu \triangleq \frac{1}{2}\alpha\gamma^{-1}\tilde{w}^2\|\Lambda\|_2+d$. The boundedness of the closed-loop dynamical system given by (2.35) and (2.36) as well as the strict performance bound on the system error given by (2.37) is now immediate by applying Lemma 1 of [25] and [23]. If, in addition, the unknown weight matrix in (2.6) is constant, then it follows from a simplified version of the above analysis and using the steps in the proof of Theorem 5.3 of [21] that $\lim_{t\to\infty} e(t)=0$. ■

For the next theorem, we assume without loss of generality that $\|\sigma(x)\|_2 \leq \overline{\sigma}+\mathcal{L}\|x\|_2$, $\mathcal{L}\in\mathbb{R}_+$, where it can be readily generalized to case $\|\sigma(x)\|_2 \leq \overline{\sigma}+\mathcal{L}\|x\|_2^l$ with $l\in\mathbb{N}$ and $l\geq 2$.

Theorem 2.3.2 *Consider the uncertain dynamical system given by (2.5) subject to Assumption 2.2.1, the linear reference model given by (2.18), and the feedback control law given by (2.12) along with (2.13), (2.15), and (2.34). If $\|e_0\|_P<\varepsilon$ and $\|\sigma(x)\|_2 \leq \overline{\sigma}+\mathcal{L}\|x\|_2$, then an upper bound for the control signal is given by*

$$\|u(t)\|_2 < \Big(\|K\|_2+\mathcal{L}\hat{W}_{\max}\Big)\Big(\frac{\varepsilon}{\sqrt{\lambda_{\min}(P)}}+\overline{x_{\mathrm{r}}}\Big)+\overline{\sigma}\hat{W}_{\max}, \quad t\geq 0. \qquad (2.43)$$

Proof. It follows from (2.12) that

$$\|u(t)\|_2 = \big\|-Kx(t)-\hat{W}^{\mathrm{T}}(t)\sigma\big(x(t)\big)\big\|_2$$

$$
\begin{aligned}
&\leq \|K\|_2\,\|x(t)\|_2 + \hat{W}_{\max}\left(\overline{\sigma} + \mathcal{L}\|x(t)\|_2\right)\\
&\leq \left(\|K\|_2 + \mathcal{L}\hat{W}_{\max}\right)\left(\|e(t)\|_2 + \|x_r(t)\|_2\right) + \overline{\sigma}\hat{W}_{\max}\\
&< \left(\|K\|_2 + \mathcal{L}\hat{W}_{\max}\right)\left(\frac{\varepsilon}{\sqrt{\lambda_{\min}(P)}} + \overline{x_{\mathrm{r}}}\right) + \overline{\sigma}\hat{W}_{\max}, \qquad (2.44)
\end{aligned}
$$

which gives the result. ■

Remark 2.3.2 *As compared with the upper bounds on the norm of the system error given by (2.23) and (2.25) for the (standard) model reference adaptive control problem, the worst-case performance bound given by (2.37) not only is strict but also solely depends on a-priori given, user-defined design parameter ε. That is, since (2.37) does not depend on the unknown matrices W and Λ unlike (2.23) and (2.25), this performance bound is a-priori computable at the pre-design stage, which yields to a guaranteed system performance. As a side note, (2.37) can be also written using the Euclidean norm of the system error as*

$$
\|e(t)\|_2 < \frac{\varepsilon}{\sqrt{\lambda_{\min}(P)}}, \quad t \geq 0. \qquad (2.45)
$$

Likewise, as compared with the upper bounds on the norm of the control signal given by (2.26) and (2.27) for the (standard) model reference adaptive control problem, the bound on the control signal given by (2.43) is less conservative for the proposed set-theoretic model reference adaptive control architecture and depends only on the controller design parameters.

Remark 2.3.3 *One can readily calculate the lower and upper bounds on the error dependent learning rate $\phi_d(\|e(t)\|_P)$, $t \geq 0$, by utilizing a specific generalized restricted potential function that satisfies Definition 2. To elucidate this point, consider the generalized restricted potential function in Remark 2.3.1. In particular, it follows from* (2.42) *that $V(e,\tilde{W})$ is upper bounded by $V_{\max} \triangleq \max\{V_0, \frac{2\mu}{\alpha}\}$, where $V_0 \triangleq V(e(0),\tilde{W}(0))$, $\alpha = \frac{\lambda_{\min}(R)}{\lambda_{\max}(P)}$, and $\mu = \frac{1}{2}\alpha\gamma^{-1}\tilde{w}^2\|\Lambda\|_2 + 2\gamma^{-1}\tilde{w}\,\dot{w}\|\Lambda\|_2$. Using* (2.38) *one can write $\phi(\|e(t)\|_P) + \gamma^{-1}\mathrm{tr}(\tilde{W}(t)\Lambda^{1/2})^{\mathrm{T}}(\tilde{W}(t)\Lambda^{1/2}) \leq V_{\max}$, $t \geq 0$, and hence, $\phi(\|e(t)\|_P) \leq V_{\max}$, $t \geq 0$. Now, utilizing (2.31), it follows from $\phi(\|e(t)\|_P) \leq V_{\max}$, $t \geq 0$, that*

$$
\|e\|_P \in \{\|e\|_P \in \mathbb{R} : \ 0 \leq \|e\|_P \leq \bar{e}\}, \quad \bar{e} \triangleq \frac{-V_{\max} + \sqrt{V_{\max}^2 + 4V_{\max}\,\varepsilon}}{2}, \qquad (2.46)
$$

and it can be readily shown that $\bar{e} < \varepsilon$. Since (2.32) is a strictly increasing function, one can calculate the lower and upper bound on the $\phi_d(\|e(t)\|_P)$, $t \geq 0$, as

$$\frac{1}{\varepsilon} \leq \phi_d(\|e(t)\|_P) \leq \phi_d(\bar{e}). \tag{2.47}$$

2.4 Generalizations to Nonlinear Reference Models

Reference models in adaptive control problems define how the closed-loop dynamical systems have to ideally behave in the presence of exogenous disturbances and system uncertainties. In particular, if one resorts to linear nominal control laws given by (2.13), then this nominal control law selection results in linear reference models given by (2.18) to capture the ideal closed-loop dynamical system performance. However, nonlinear nominal control laws are also desired for several practical applications especially for those involving guidance and control of highly-maneuverable aircrafts, guided projectiles, and space launch vehicles. Although [81–85] present notable contributions to allow adaptive control laws to augment nonlinear nominal control laws, these results do not yield to strict guarantees on the system performance. In this section, we generalize the results of Section 2.3 (and the results in [85]) such that the proposed set-theoretic adaptive control architecture augments nonlinear nominal control laws, and hence, the system error bound between the state of an uncertain dynamical system and the state of a class of nonlinear reference models is guaranteed to be less than a-priori, user-defined worst-case performance bound.

Consider the augmented uncertain dynamical system given by (2.8) with the feedback control law in (2.12). Let the nominal control law be

$$u_{\mathrm{n}}(t) = -k\big(x(t), c(t)\big), \quad t \geq 0, \tag{2.48}$$

where $k : \mathbb{R}^n \times \mathbb{R}^m \to \mathbb{R}^m$. Now, (2.8) can be identically rewritten as -.15cm

$$\dot{x}(t) = Ax(t) - Bk\big(x(t), c(t)\big) + B_{\mathrm{r}}c(t) + B\Lambda\Big[u_{\mathrm{a}}(t) + W^{\mathrm{T}}(t)\sigma\big(x(t)\big)\Big], \ x(0) = x_0, \ t \geq 0. \tag{2.49}$$

In addition, consider the nonlinear reference model given by

$$\dot{x}_{\mathrm{r}}(t) = Ax_{\mathrm{r}}(t) - Bk\big(x_{\mathrm{r}}(t), c(t)\big) + B_{\mathrm{r}}c(t), \quad t \geq 0, \tag{2.50}$$

such that $x_{\mathrm{r}}(t)$, $t \geq 0$, is bounded.

Next, the system error dynamics is given by using (2.50) and (2.49) as

$$\dot{e}(t) = Ae(t) - B\Big[k\big(x(t),c(t)\big) - k\big(x_{\mathrm{r}}(t),c(t)\big)\Big] + B\Lambda\Big[u_{\mathrm{a}}(t) + W^{\mathrm{T}}(t)\sigma\big(x(t)\big)\Big], \quad e(0) = e_0. \tag{2.51}$$

Note that there exists a known signal $v(x(t),x_{\mathrm{r}}(t),c(t)) \in \mathbb{R}^m$ [85] such that

$$A_{\mathrm{r}}e(t) = Ae(t) - B\Big[k\big(x(t),c(t)\big) - k\big(x_{\mathrm{r}}(t),c(t)\big)\Big] + Bv(\cdot), \quad t \geq 0, \tag{2.52}$$

holds, since $A_{\mathrm{r}} \triangleq A - BK$ (the matrix K is utilized here to make A_{r} Hurwitz, and hence, it should not be confused with the linear nominal controller gain matrix used in Section 2.3). Thus, we let

$$v(\cdot) = -Ke(t) + k\big(x(t),c(t)\big) - k\big(x_{\mathrm{r}}(t),c(t)\big), \quad t \geq 0, \tag{2.53}$$

which acts like a feedback linearization term. Using (2.52), (2.51) can be rewritten as

$$\dot{e}(t) = A_{\mathrm{r}}e(t) + B\Lambda\Big[u_{\mathrm{a}}(t) + W_0^{\mathrm{T}}(t)\sigma_0\big(x(t),c(t)\big)\Big], \quad e(0) = e_0, \quad t \geq 0, \tag{2.54}$$

where $W_0(t) \triangleq \big[W^{\mathrm{T}}(t), -\Lambda^{-1}\big]^{\mathrm{T}}$, $t \geq 0$, and $\sigma_0(x(t),c(t)) \triangleq \big[\sigma^{\mathrm{T}}(x(t)), v^{\mathrm{T}}(\cdot)\big]^{\mathrm{T}}$, $t \geq 0$.

Now, let the adaptive control law be

$$u_{\mathrm{a}}(t) = -\hat{W}_0^{\mathrm{T}}(t)\sigma_0\big(x(t),c(t)\big), \quad t \geq 0, \tag{2.55}$$

where $\hat{W}_0(t)$ is an estimate of $W_0(t)$ satisfying the (set-theoretic) update law constructed using generalized restricted potential functions given by

$$\dot{\hat{W}}_0(t) = \gamma \mathrm{Proj}_{\mathrm{m}}\Big(\hat{W}_0(t), \phi_d(\|e(t)\|_P)\sigma_0\big(x(t),c(t)\big)e^{\mathrm{T}}(t)PB\Big), \quad \hat{W}_0(0) = \hat{W}_{00}. \tag{2.56}$$

In (2.56), $\gamma \in R_+$ is the learning rate and $P \in \mathbb{R}_+^{n\times n}$ is a solution of the Lyapunov equation given by (2.17) with $R \in \mathbb{R}_+^{n\times n}$. Note that, once again, $\phi_d(\|e(t)\|_P)$ in (2.56) can be viewed as an error dependent learning rate.

For the next theorem, one can write the system error dynamics and the weight estimation error dynamics respectively given by

$$\dot{e}(t) = A_{\mathrm{r}}e(t) - B\Lambda\tilde{W}_0^{\mathrm{T}}(t)\sigma_0\big(x(t),c(t)\big), \quad e(0) = e_0, \quad t \geq 0, \tag{2.57}$$

$$\dot{\tilde{W}}_0(t) = \gamma\mathrm{Proj}_{\mathrm{m}}\Big(\hat{W}_0(t), \phi_d(\|e(t)\|_P)\sigma_0\big(x(t),c(t)\big)e^{\mathrm{T}}(t)PB\Big) - \dot{W}_0(t), \quad \tilde{W}_0(0) = \tilde{W}_{00}, \quad t \geq 0, \tag{2.58}$$

where $\tilde{W}_0(t) \triangleq \hat{W}_0(t) - W_0(t)$, $t \geq 0$, is the weight estimation error.

Theorem 2.4.1 *Consider the uncertain dynamical system given by (2.5) subject to Assumption 2.2.1, the nonlinear reference model given by (2.50), and the feedback control law given by (2.12) along with (2.48), (2.55), and (2.56). If $\|e_0\|_P < \varepsilon$, then the closed-loop dynamical system given by (2.57) and (2.58) are bounded, where the bound on the system error strictly satisfies a-priori given, user-defined worst-case performance*

$$\|e(t)\|_P < \varepsilon, \quad t \geq 0. \tag{2.59}$$

If, in addition, the unknown weight matrix in (2.6) is constant, then $\lim_{t\to\infty} e(t) = 0$.

Proof. The proof is similar to the proof of Theorem 2.3.1, and hence, is omitted. ■

Remark 2.4.1 *Similar to the discussion in Remark 2.3.2, one can conclude that the worst-case performance bound given by (2.59) not only is strict but also solely depends on a-priori given, user-defined design parameter ε. In addition, as it is done in Theorem 2.3.2, under certain set of assumptions on $\sigma_0\big(x(t),c(t)\big)$ and $k\big(x(t),c(t)\big)$, one can readily calculate an upper bound on the control signal that depends only on the controller design parameters.*

Remark 2.4.2 *The proposed set-theoretic model reference adaptive control architecture can be an effective control methodology for the state of an uncertain dynamical system to evolve in a safe state-space set (e.g., for preserving safe flight envelope in aerospace applications). To elucidate this point, let $\mathcal{S}_{\mathrm{F}}$ be a safe state-space set such that the state of an uncertain dynamical system has to evolve inside this set, i.e., $x(t) \in \mathcal{S}_{\mathrm{F}}$. In addition, let $\mathcal{S}_{\mathrm{R}} \subset \mathcal{S}_{\mathrm{F}}$ be a state-space set such that the state of a reference model evolves inside this set, i.e., $x_{\mathrm{r}}(t) \in \mathcal{S}_{\mathrm{R}}$. Then, the size of $\mathcal{D}_\varepsilon$ can be adjusted by judiciously choosing the user-defined parameter ε such that $\mathcal{S}_{\mathrm{R}} \cup \mathcal{D}_\varepsilon \in \mathcal{S}_{\mathrm{F}}$ holds and the state of an uncertain dynamical system does not violate the safe state-space set $\mathcal{S}_{\mathrm{F}}$. Illustration of the sets used in this remark is given in Figure 2.1. Finally, for instants when the trajectory of the reference model is not predetermined and controlled by a user (e.g., pilot), then the nonlinear reference models approach presented in this section can be used to constrain the reference*

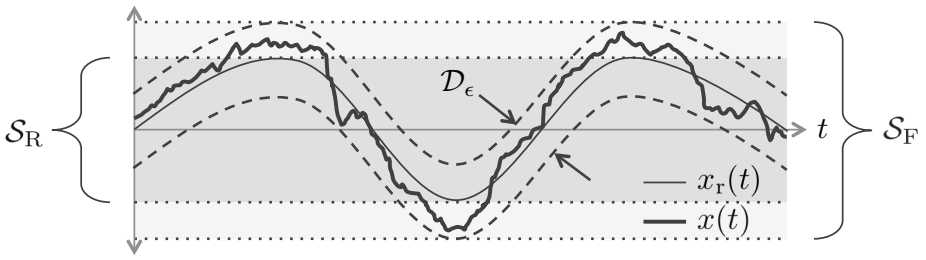

Figure 2.1: Illustration of the sets in Remark 2.4.2.

state to stay inside a predetermined state-space set $\mathcal{S}_{\mathrm{R}}$ by limiting the authority of this user (see Section 2.5 for an illustrative numerical example regarding this point).

2.5 Illustrative Numerical Examples

In this section, we present several numerical examples to demonstrate the efficacy of the proposed set-theoretic model reference adaptive control architecture.

2.5.1 Example 1

We begin with a scalar uncertain dynamical system given by

$$\dot{x}_{\mathrm{p}}(t) \quad = \quad x_{\mathrm{p}}(t)+\Lambda u(t)+W_{\mathrm{p}}(t), \quad x(0)=0, \quad t\geq 0, \tag{2.60}$$

with $\Lambda = 0.75$ and $W_{\mathrm{p}}(t) = 2\sin(0.5t)$. For command tracking, we let $E_{\mathrm{p}} = 1$ in (2.7) and choose a linear nominal controller gain matrix $K = \begin{bmatrix} 3.9, & 3.2 \end{bmatrix}$ in (2.13). For the proposed set-theoretic model reference adaptive control architecture in Theorem 2.3.1, we use the generalized restricted potential function given in Remark 2.3.1 with $\varepsilon = 0.1$ to strictly guarantee $\|x(t)-x_{\mathrm{r}}(t)\|_P < 0.1$, $t \geq 0$ (an upper bound on the control signal is calculated from Theorem 2.3.2 as $\|u(t)\|_2 < 4.97$ for this case). Finally, we set the projection norm bound imposed on each element of the parameter estimate to 3 and use $R = I$ to calculate P from (2.17) for the resulting A_{r} matrix.

Figure 2.2 shows the closed-loop dynamical system performance with the nominal controller, where it is evident from the system error phase portrait in Figure 2.3 that the nominal controller does not have the capability to achieve given strict performance guarantees. Next, we apply the proposed set-theoretic adaptive controller with $\gamma = 1$ in Figure 2.4, where Figures 2.5 and 2.6 clearly show that this controller

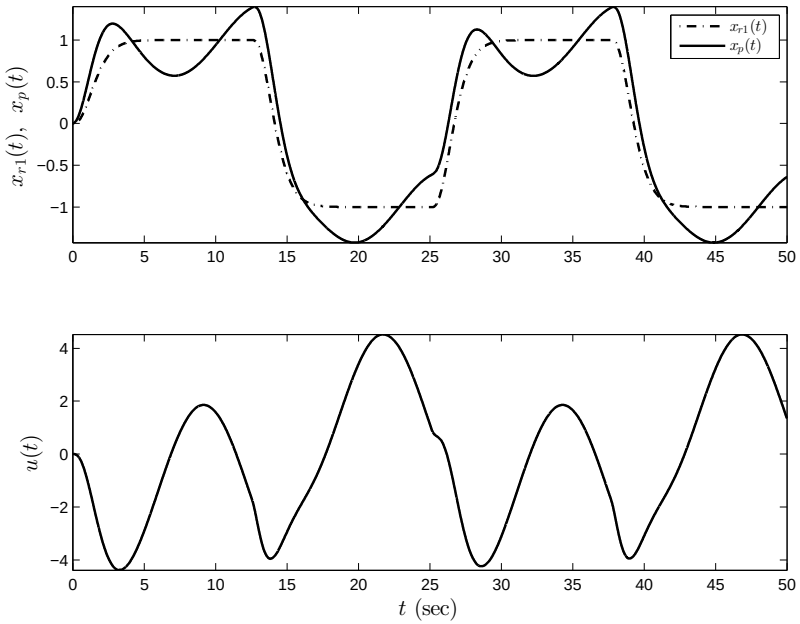

Figure 2.2: Command following performance with the nominal controller in Example 1.

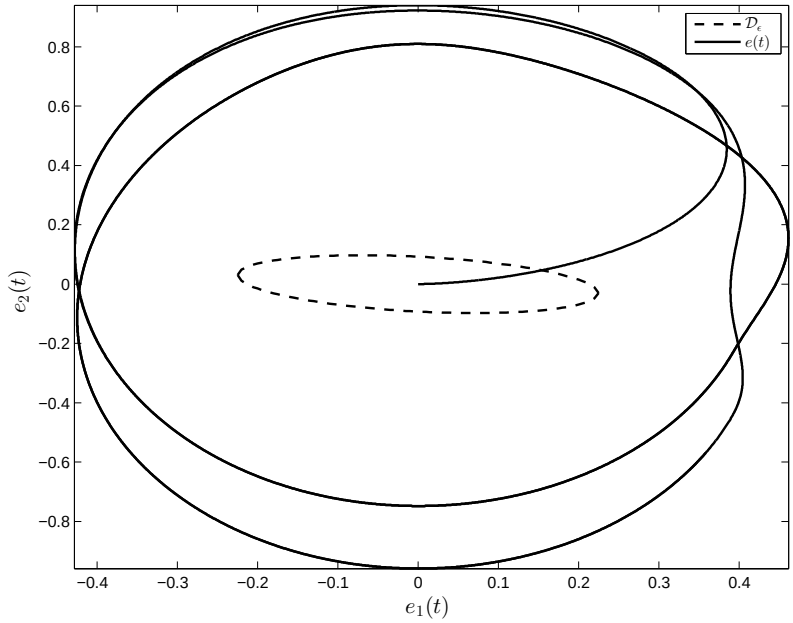

Figure 2.3: System error phase portrait with the nominal controller in Example 1.

strictly guarantees $\|x(t) - x_{\rm r}(t)\|_P < 0.1$. Note from Figure 2.5 that the proposed controller adjusts $\phi_{\rm d}(\cdot)$, and hence, its effective learning rate $\gamma\phi_{\rm d}(\cdot)$, in response to system error in order to keep the system error trajectories on $\mathcal{D}_\varepsilon$. Finally, Figure 2.7 shows the effect of the learning rate γ on the system error trajectory,

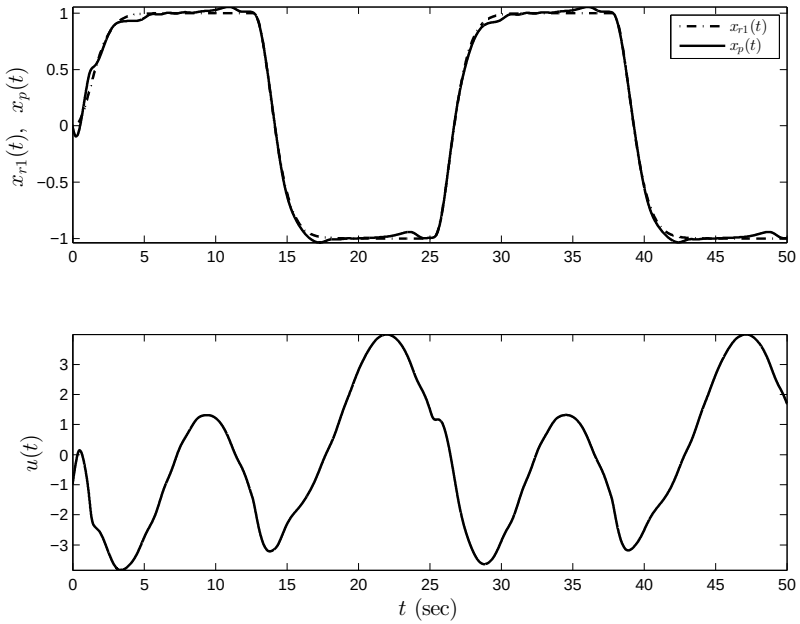

Figure 2.4: Command following performance with the proposed set-theoretic adaptive controller in Example 1.

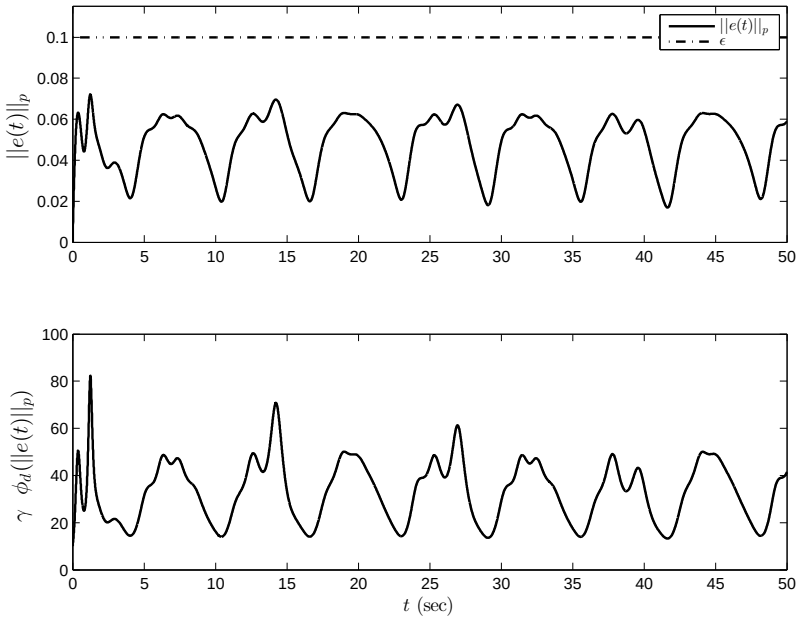

Figure 2.5: Norm of the system error trajectories with the proposed set-theoretic adaptive controller and the evolution of the effective learning rate $\gamma\phi_{\mathrm{d}}(\cdot)$ in Example 1.

where it can be seen regardless of the value of γ that the system error trajectory is bounded by the predefined set $\mathcal{D}_\varepsilon$. $\triangle$

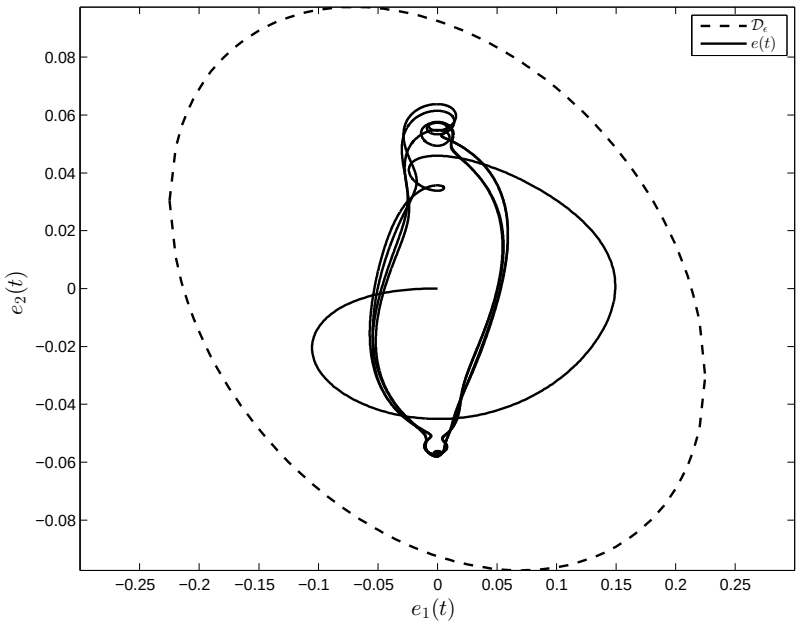

Figure 2.6: System error phase portrait with the proposed set-theoretic adaptive controller in Example 1.

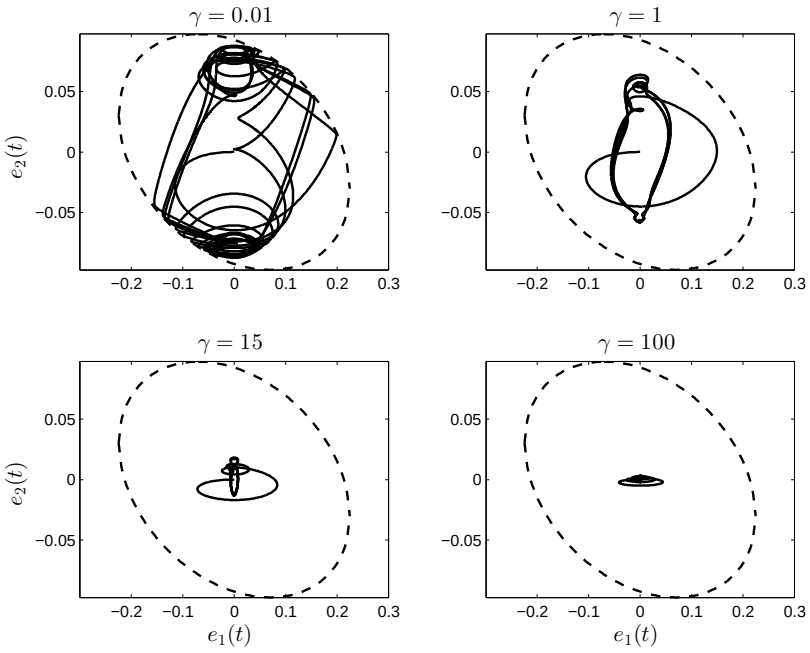

Figure 2.7: System error phase portraits with the proposed set-theoretic adaptive controller in Example 1 for different learning rates.

2.5.2 Example 2

Consider the controlled longitudinal motion of a Boeing 747 airplane linearized at an altitude of 40 kft and a velocity of 774 ft/sec with the dynamics given by [86]

$$\dot{x}_{\rm p}(t) = A_{\rm p}x_{\rm p}(t)+B_{\rm p}\Lambda u(t)+B_{\rm p}\delta_{\rm p}(t,x_{\rm p}(t)), \quad x_{\rm p}(0)=x_{\rm p0}, \quad t\geq 0, \tag{2.61}$$

with

$$A_{\rm p}=\begin{bmatrix} -0.0030 & 0.0390 & 0 & -0.3220 \\ -0.0650 & -0.3190 & 7.7400 & 0 \\ 0.0201 & -0.1010 & -0.4290 & 0 \\ 0 & 0 & 1.0000 & 0 \end{bmatrix}, \quad B_{\rm p}=\begin{bmatrix} 0.0100 \\ -0.1800 \\ -1.1600 \\ 0 \end{bmatrix}, \tag{2.62}$$

where $x_{\rm p}(t)=\begin{bmatrix} x_1(t), & x_2(t), & x_3(t), & x_4(t) \end{bmatrix}^{\rm T}\in\mathbb{R}^4$, is the state vector with $x_1(t)$ representing the component of the velocity along the x-axis of the aircraft with respect to the reference axes (in ft/sec), $x_2(t)$ representing the component of the velocity along the z-axis of the aircraft with respect to the reference axes (in ft/sec), $x_3(t)$ representing the component of the velocity along the y-axis of the aircraft (pitch rate) with respect to the reference axes (in crad/sec), $x_4(t)$ representing the pitch Euler angle of the aircraft body axes with respect to the reference axes (in crad), and $u(t)\in\mathbb{R}$ representing the elevator input (in crad). In (2.61), $\delta_{\rm p}(t,x_{\rm p}(t))$ represents an uncertainty of the form $\delta_{\rm p}(t,x_{\rm p}(t))=\sin(t)+1.5x_1(t)+x_2(t)+3x_1(t)x_2(t)$ and $\Lambda=1.75$ represents an uncertain control effectiveness matrix. For command tracking, we let $E_{\rm p}=\begin{bmatrix} 1, & 0, & 0, & 0 \end{bmatrix}$ in (2.7) and choose a linear nominal controller gain matrix $K=\begin{bmatrix} 23.49, & 1.35 & -2.54, & -15.27, & 5.77 \end{bmatrix}$ in (2.13). For the proposed set-theoretic model reference adaptive control architecture in Theorem 2.3.1, we use the generalized restricted potential function given in Remark 2.3.1 with $\varepsilon=1.5$ to strictly guarantee $\|x(t)-x_{\rm r}(t)\|_P<1.5$, $t\geq 0$. In addition, we choose the basis function as $\sigma(x(t))=\begin{bmatrix} 1, & x_1(t), & x_2(t), & x_1(t)x_2(t), & x^{\rm T}(t) \end{bmatrix}^{\rm T}$. Finally, we set the projection norm bound imposed on each element of the parameter estimate to 8 and use $R=I$ to calculate P from (2.17) for the resulting $A_{\rm r}$ matrix.

In this illustrative numerical example, we do not provide the closed-loop dynamical system performance with the nominal controller, because it is unstable. Next, we apply the proposed set-theoretic adaptive controller with $\gamma=0.01$ in Figure 2.8, where Figure 2.9 clearly shows that this controller strictly guarantees $\|x(t)-x_{\rm r}(t)\|_P<1.5$. △

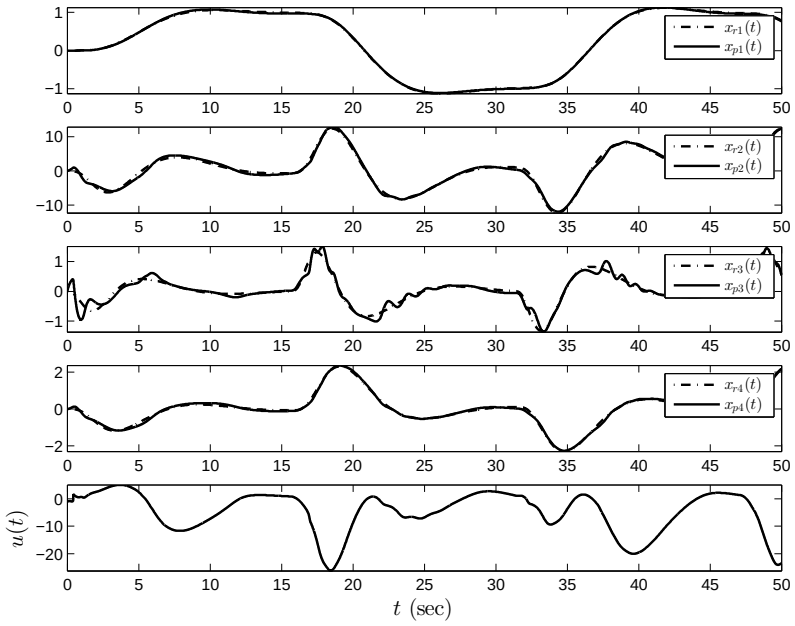

Figure 2.8: Command following performance with the proposed set-theoretic adaptive controller in Example 2.

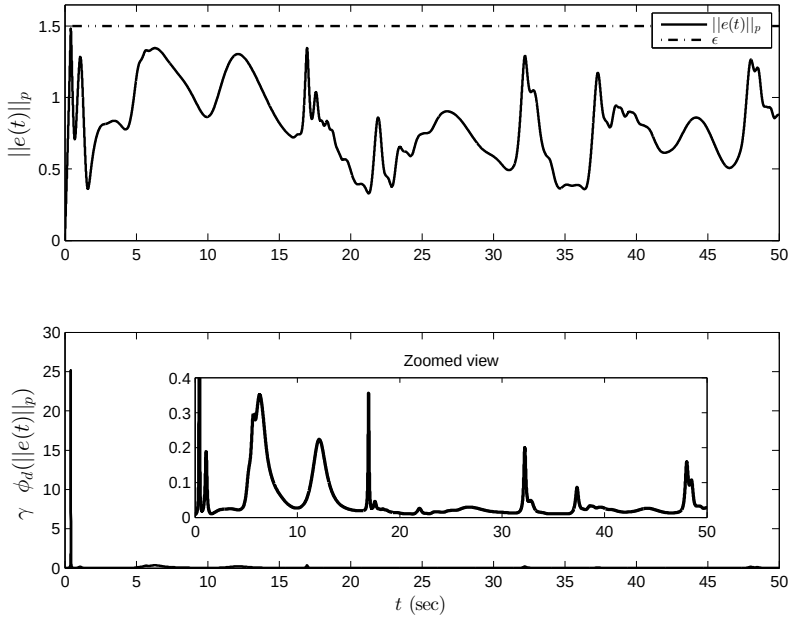

Figure 2.9: Norm of the system error trajectories with the proposed set-theoretic adaptive controller and the evolution of the effective learning rate $\gamma\phi_{\mathrm{d}}(\cdot)$ in Example 2.

2.5.3 Example 3

Consider the uncertain dynamical system representing a controlled wing rock dynamics model given by [32]

$$\dot{x}_{\rm p}(t) = \begin{bmatrix} 0 & 1 \\ 0 & 0 \end{bmatrix} x_{\rm p}(t) + \begin{bmatrix} 0 \\ 1 \end{bmatrix} \Big(\Lambda u(t) + \delta_{\rm p}(t, x_{\rm p}(t)) \Big), \quad x_{\rm p}(0) = 0 \quad t \geq 0, \tag{2.63}$$

where $x_{\rm p}(t) = \begin{bmatrix} x_{\rm p1}(t) & x_{\rm p2}(t) \end{bmatrix}^{\rm T}$ with $x_{\rm p1}(t)$ representing the roll angle (in rad) and $x_{\rm p2}(t)$ representing the roll rate (in rad/sec). In (2.63), $\delta_{\rm p}(t, x_{\rm p}(t))$ represents an uncertainty of the form

$$\delta_{\rm p}(t, x_{\rm p}(t)) = \alpha_1 \sin(t) + \alpha_2 x_{\rm p1} + \alpha_3 x_{\rm p2} + \alpha_4 |x_{\rm p1}| x_{\rm p2} + \alpha_5 |x_{\rm p2}| x_{\rm p2} + \alpha_6 x_{\rm p1}^3, \tag{2.64}$$

with $\alpha_1 = 0.25$, $\alpha_2 = 0.5$, $\alpha_3 = 1.0$, $\alpha_4 = -1.0$, $\alpha_5 = 1.0$, and $\alpha_6 = 1.0$, and $\Lambda = 0.75$ represents an uncertain control effectiveness matrix. For command tracking, we let $E_{\rm p} = \begin{bmatrix} 1, & 0 \end{bmatrix}$ in (2.7). Based on the proposed control architecture in Theorem 2.4.1, we select the nonlinear reference model as

$$\dot{x}_{\rm r}(t) = \begin{bmatrix} 0 & 1 & 0 \\ 0 & 0 & 0 \\ 1 & 0 & 0 \end{bmatrix} x_{\rm r}(t) - f \begin{bmatrix} 0 \\ 1 \\ 0 \end{bmatrix} k(x_{\rm r}(t), c(t)) + \begin{bmatrix} 0 \\ 0 \\ -1 \end{bmatrix} c(t), \quad x_{\rm r}(0) = 0 \quad t \geq 0, \tag{2.65}$$

where $k(x_{\rm r}(t), c(t)) = K_1 [x_{\rm r1}(t), \ x_{\rm r2}(t)]^{\rm T} + K_2 \Psi(x_{\rm r}(t)) x_{\rm r3}$ with $K_1 = [4.98, \ 3.31]$, $K_2 = 2.23$, $c(t) = c_d(t)$ $\cdot \Psi(x_{\rm r}(t))$, and $\Psi(x_{\rm r}(t)) = \tanh\big(5\big||x_{\rm r1}(t)| - 2\big|\big)$. Here, the purpose of the nonlinear function $\Psi(\cdot)$ is to constrain the absolute value of the roll angle state to stay less than or equal to 2, and hence, to enforce the roll angle state to stay inside a predetermined state-space set by limiting the authority of the pilot. For the proposed set-theoretic model reference adaptive control architecture, we use the generalized restricted potential function given in Remark 2.3.1 with $\varepsilon = 1.5$ to strictly guarantee $\|x(t) - x_{\rm r}(t)\|_P < 1.5$, $t \geq 0$. In addition, we choose the basis function as $\sigma(x) = \begin{bmatrix} 1, & x_{\rm p1}, & x_{\rm p2}, & |x_{\rm p1}| x_{\rm p2}, & |x_{\rm p2}| x_{\rm p2}, & x_{\rm p1}^3, & x^{\rm T} \end{bmatrix}^{\rm T}$. Finally, we set the projection norm bound imposed on each element of the parameter estimate to 22.5 and use $R = I$ to calculate P from (2.17) for the resulting $A_{\rm r}$ matrix.

In this illustrative numerical example, once again, we do not provide the closed-loop dynamical system performance with the nominal controller, because it is unstable. Next, we apply the proposed set-

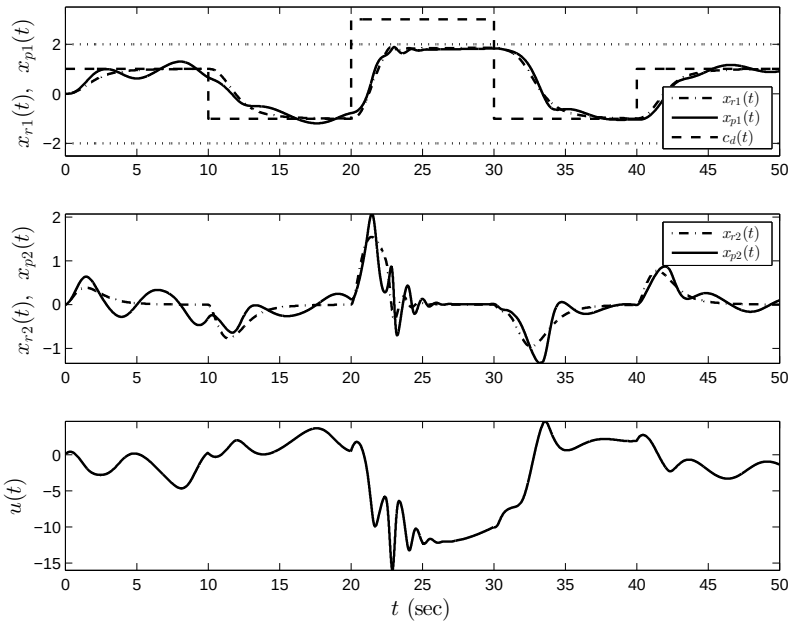

Figure 2.10: Command following performance with the proposed set-theoretic adaptive controller in Example 3.

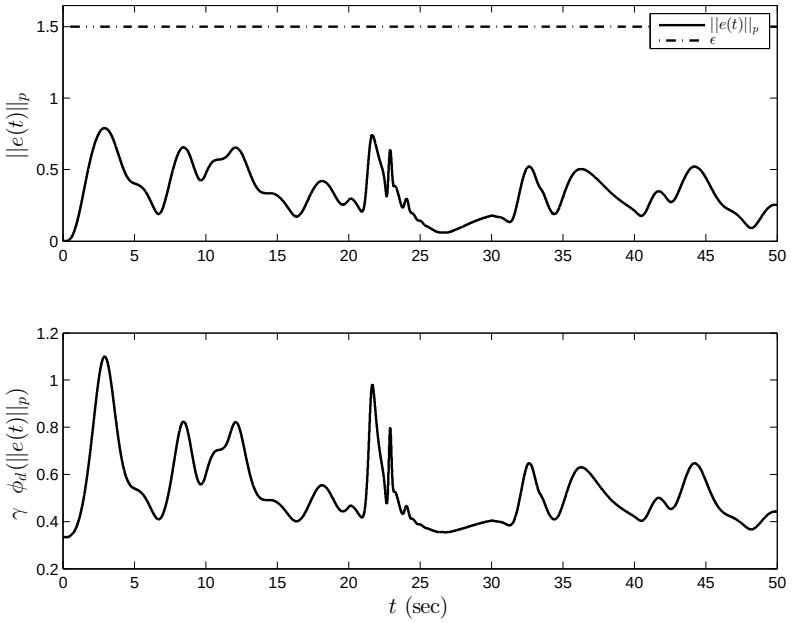

Figure 2.11: Norm of the system error trajectories with the proposed set-theoretic adaptive controller and the evolution of the effective learning rate $\gamma\phi_{\mathrm{d}}(\cdot)$ in Example 3.

theoretic adaptive controller with $\gamma = 0.5$ in Figure 2.10, where Figures 2.11 and 2.12 clearly show that this controller strictly guarantees $\|x(t) - x_{\mathrm{r}}(t)\|_P < 1.5$. Note from Figure 2.10 that during $t \in [20, 30]$ a command

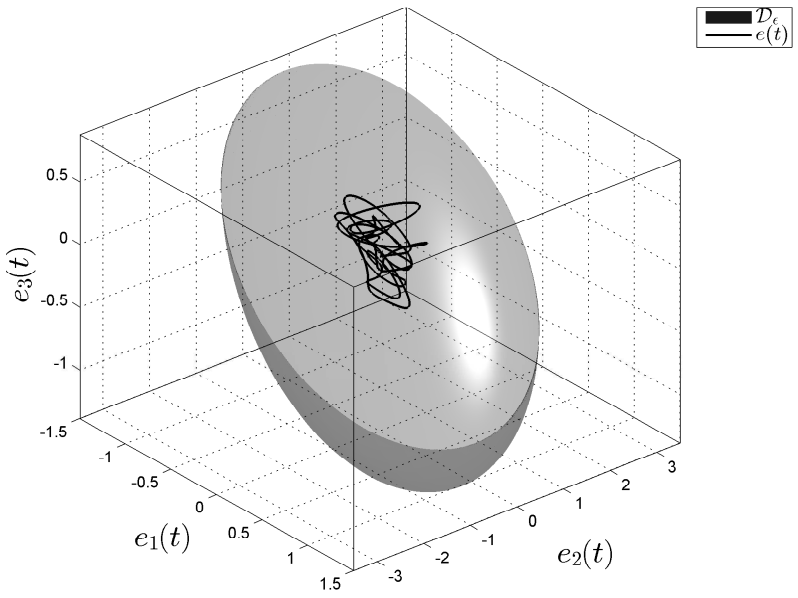

Figure 2.12: System error phase portrait with the proposed set-theoretic adaptive controller in Example 3.

larger than the maximum allowed value of 2 is applied and the nonlinear function $\Psi(\cdot)$ is smoothly activated to prevent the roll angle to exceed this maximum allowed value. $\triangle$

2.6 Conclusion

A challenge in the design of model reference adaptive controllers is to achieve a-priori, user-defined performance guarantees. Motivated from this standpoint, we proposed and analyzed a new model reference adaptive control architecture for uncertain dynamical systems to address disturbance rejection and uncertainty suppression. The proposed framework was predicated on a set-theoretic adaptive controller construction, which has the capability to enforce a-priori, user-defined worst-case performance bound on the system error bound between the state of an uncertain dynamical system and the state of a (linear or nonlinear) reference model. As a byproduct, we showed that an upper bound for the adaptive control signals can be directly calculated without inducing (excessive) conservatism, which only depends on user-defined design parameters and without dependence on initial conditions and unknown parameters in contrast to standard model reference adaptive controllers. The novel characteristic of our framework was the capability to enforce strict performance guarantees at the pre-design stage, instead of relying on excessive vehicle testing and tools to validate the performance of adaptive controllers during the post-design stage. Several

illustrative numerical examples demonstrated the efficacy of the proposed set-theoretic model reference adaptive control architecture.

Future research will include generalizations using universal function approximation techniques such as neural networks for instants when the basis function is not available for adaptive controller design. In addition, we will also extend the proposed architecture for adaptive controller design in the presence of loss of control as well as in the absence of measurable state vector by utilizing an output feedback adaptive control mechanism. Finally, experimental validation through flight tests and robotic system demonstrations will be considered as a future research.

2.7 Acknowledgment

The authors wish to thank Jonathan A. Muse from the Air Force Research Laboratory for his constructive suggestions.

CHAPTER 3: A NEUROADAPTIVE ARCHITECTURE FOR MODEL REFERENCE CONTROL OF UNCERTAIN DYNAMICAL SYSTEMS WITH PERFORMANCE GUARANTEES[1]

Neuroadaptive control systems have the capability to approximate unstructured system uncertainties on a given compact set using neural networks. Yet, a challenge in their design is to guarantee the closed-loop system trajectories stay in this set such that the universal function approximation property is satisfied and the overall system stability is achieved. To address this challenge, we present and analyze a new neuroadaptive architecture in this paper for model reference control of uncertain dynamical systems with strict performance guarantees. Specifically, the proposed architecture is predicated on a novel set-theoretic framework and has the capability to keep the closed-loop system trajectories within an a-priori, user-defined compact set without violating the universal function approximation property. A transport aircraft example is also given to complement the presented theoretical results.

3.1 Introduction

3.1.1 Literature Review

Both adaptive and neuroadaptive control systems have the capability to effectively handle the effects of adverse system conditions resulting from exogenous disturbances, imperfect system modeling, degraded modes of operation, and changes in system dynamics. Specifically, parameterized system uncertainty models with a known structure but unknown parameters are utilized in adaptive control systems (e.g., see [9, 28–32, 40, 59, 87, 88] and references therein). For applications involving system uncertainties with unknown structures and unknown parameters, neuroadaptive control systems are preferred since they are based on the universal function approximation property and can handle a larger class of system uncertainties that may not be tolerated by adaptive control systems (e.g., see [8, 33–36, 78, 89–92] and references therein). In particular, using neural networks on a compact set of the real coordinate space, neuroadaptive control systems have the capability to closely approximate system uncertainties with an unknown structure and unknown parameters (i.e., unstructured system uncertainties).

[1]This chapter has been submitted to the *Systems & Control Letters* for possible publication.

Yet, a challenge in the design of neuroadaptive control systems is to guarantee the closed-loop system trajectories stay in this compact set such that the universal function approximation property is satisfied and the overall system stability is achieved. This is due to the fact that approximation of a given system uncertainty may not be valid for time instants when the closed-loop system trajectories are outside of the considered compact set of the real coordinate space, where this can lead to instability of the closed-loop system trajectories. Current practice relies heavily on excessive simulations and vehicle testing to address this challenge as a means of developing guarantees on the closed-loop system performance. However, drawback of these approaches is that they only provide limited verification with respect to what is tested; fixed and finite set of initial conditions, user commands, and adverse system conditions [5–7].

Notable theoretical exceptions that do not rely on ad-hoc testing include [18–20, 25, 26, 30]. In particular, the authors of [18] use an error transformation approach to achieve constrained performance guarantees, where it is assumed that the control signals can access every element of the state vector. This limitation is avoided in [19] by considering a backstepping approach under the assumption that a desired trajectory and its derivatives are available and all bounded. In addition, the same approach is extended to a generalized class of uncertain dynamical systems in [20] in order to enforce constraints on output signals but not on state vectors. Restricted potential functions (barrier Lyapunov functions) are employed in the neuroadaptive control schemes of [25] and [26] in the context of a backstepping approach to construct a closed-loop dynamical system with strict performance guarantees. It should be also noted that the authors of [30] consider a model reference neuroadaptive control methodology under the assumption that the approximation tolerance resulting from the neural network approximation of the system uncertainty is known inside a compact set and upper bounded by a known function outside this set.

3.1.2 Contribution

In this paper, we focus on disturbance rejection and unstructured system uncertainty suppression for dynamical systems. Our contribution is to present and analyze a new neuroadaptive architecture for model reference control with strict performance guarantees, where it can be viewed as a significant and nontrivial generalization of the results presented in the previous work of authors in [1] that utilize parameterized system uncertainty models with a known structure but unknown parameters. Specifically, the proposed approach is predicated on a novel set-theoretic approach based on restricted potential functions, where the approximation tolerance resulting from the neural network approximation of the system uncertainty is generally treated as

unknown. It is shown that the proposed neuroadaptive framework has the capability to keep the closed-loop system trajectories within an a-priori, user-defined compact set of the real coordinate space without violating the universal function approximation property. This is achieved by proper selection of the user-defined performance bound within the proposed set-theoretic model reference neuroadaptive control architecture, in connection with the set in which the trajectories of the reference system evolves (see Remark 3.3.1).

Contents of the paper are as follows. In Section 3.2, we overview mathematical preliminaries. In Sections 3.3 and 3.4, we respectively present the problem formulation and the proposed set-theoretic model reference neuroadaptive control architecture, where its stability analysis and performance guarantees are established in Section 3.5. The efficacy of our theoretical results is demonstrated on a transport aircraft example in Section 3.6 and conclusions are drawn in Section 3.7. Note that a preliminary conference version of this paper appeared in [93], where the present paper considerably expands on [93] by providing new key theoretical results and detailed proofs of all the results with a new example.

3.2 Mathematical Preliminaries

The notation used throughout this paper is standard. In particular, $\mathbb{R}$ denotes the set of real numbers, $\mathbb{R}^n$ denotes the set of $n \times 1$ real column vectors, $\mathbb{R}^{n\times m}$ denotes the set of $n \times m$ real matrices, $\mathbb{R}_+$ (respectively, $\overline{\mathbb{R}}_+$) denotes the set of positive (respectively, nonnegative-definite) real numbers, $\mathbb{R}_+^{n\times n}$ (respectively, $\overline{\mathbb{R}}_+^{n\times n}$) denotes the set of $n \times n$ positive-definite (respectively, nonnegative-definite) real matrices, $\mathbb{D}^{n\times n}$ denotes the set of $n \times n$ real matrices with diagonal scalar entries, $0_{n\times n}$ denotes the $n \times n$ zero matrix, and "$\triangleq$" denotes equality by definition. We also write $\|\cdot\|_{\mathrm{F}}$ for the Frobenius norm, $\|\cdot\|_2$ for the Euclidean norm, $\|A\|_2 \triangleq \sqrt{\lambda_{\max}(A^{\mathrm{T}}A)}$ for the induced 2-norm of the matrix $A \in \mathbb{R}^{n\times m}$, and $\lambda_{\min}(A)$ (respectively, $\lambda_{\max}(A)$) for the minimum (respectively, maximum) eigenvalue of the Hermitian matrix A.

The following definitions are needed for the main results of this paper.

Definition 3.2.1 *Let* $\Omega = \left\{\theta \in \mathbb{R}^n : (\theta_i^{\min} \leq \theta_i \leq \theta_i^{\max})_{i=1,2,\cdots,n}\right\}$ *be a convex hypercube in* $\mathbb{R}^n$, *where* ($\theta_i^{\min}$, $\theta_i^{\max}$) *represent minimum and maximum bounds for the* i^{th} *component of n-dimensional parameter vector* θ. *For a sufficiently small positive constant* ν, *define second hypercube as* $\Omega_\nu = \left\{\theta \in \mathbb{R}^n : (\theta_i^{\min} + \nu \leq \theta_i \leq \theta_i^{\max} - \nu)_{i=1,2,\cdots,n}\right\}$, *where* $\Omega_\nu \subset \Omega$. *With* $y \in \mathbb{R}^n$, *projection operator* $\mathrm{Proj} : \mathbb{R}^n \times \mathbb{R}^n \to \mathbb{R}^n$ *is then defined componentwise by* $\mathrm{Proj}(\theta, y) \triangleq \left(\frac{\theta_i^{\max} - \theta_i}{\nu}\right) y_i$ *if* $\theta_i > \theta_i^{\max} - \nu$ *and* $y_i > 0$, $\mathrm{Proj}(\theta, y) \triangleq \left(\frac{\theta_i - \theta_i^{\min}}{\nu}\right) y_i$ *if* $\theta_i < \theta_i^{\min} + \nu$ *and* $y_i < 0$, *and* $\mathrm{Proj}(\theta, y) \triangleq y_i$ *otherwise.*

Based on the above formulation, note that $\left(\theta-\theta^*\right)^{\mathrm{T}}\left(\mathrm{Proj}\left(\theta,y\right)-y\right)\leq 0, \theta^*\in\Omega_\nu$ [30, 80], where this inequality can be also readily generalized to matrices using $\mathrm{Proj_m}(\Theta,Y)=\big(\mathrm{Proj}(\mathrm{col}_1(\Theta),\mathrm{col}_1(Y)),\ldots,$ $\mathrm{Proj}(\mathrm{col}_m(\Theta)\ ,\mathrm{col}_m(Y))\big)$ with $\Theta\in\mathbb{R}^{n\times m}$, $Y\in\mathbb{R}^{n\times m}$, and $\mathrm{col}_i(\cdot)$ denoting ith column operator.

Definition 3.2.2 *Let $\|z\|_H=\sqrt{z^{\mathrm{T}}Hz}$ be a weighted Euclidean norm, where $z\in\mathbb{R}^p$ is a real column vector and $H\in\mathbb{R}_+^{p\times p}$. We define $\phi(\|z\|_{\mathrm{H}})$, $\phi:\mathbb{R}\to\mathbb{R}$, to be a generalized restricted potential function (generalized barrier Lyapunov function) on the set $\mathcal{D}_\varepsilon\triangleq\{z:\|z\|_{\mathrm{H}}\in[0,\varepsilon)\}$, with $\varepsilon\in\mathbb{R}_+$ being a-priori, user-defined constant, if the following statements hold [1]: i) If $\|z\|_{\mathrm{H}}=0$, then $\phi(\|z\|_{\mathrm{H}})=0$. ii) If $z\in\mathcal{D}_\varepsilon$ and $\|z\|_{\mathrm{H}}\neq 0$, then $\phi(\|z\|_{\mathrm{H}})>0$. iii) If $\|z\|_{\mathrm{H}}\to\varepsilon$, then $\phi(\|z\|_{\mathrm{H}})\to\infty$. iv) $\phi(\|z\|_{\mathrm{H}})$ is continuously differentiable on $\mathcal{D}_\varepsilon$. v) If $z\in\mathcal{D}_\varepsilon$, then $\phi_d(\|z\|_{\mathrm{H}})>0$, where $\phi_d(\|z\|_{\mathrm{H}})\triangleq\frac{\mathrm{d}\phi(\|z\|_{\mathrm{H}})}{\mathrm{d}\|z\|_{\mathrm{H}}^2}$. vi) If $z\in\mathcal{D}_\varepsilon$, then $2\phi_d(\|z\|_{\mathrm{H}})\|z\|_{\mathrm{H}}^2-\phi(\|z\|_{\mathrm{H}})>0$.*

Remark 3.2.1 *A generalized restricted potential function satisfying above conditions has the form $\phi(\|z\|_{\mathrm{H}})=\|z\|_{\mathrm{H}}^2/\left(\varepsilon-\|z\|_{\mathrm{H}}\right)$, $z\in\mathcal{D}_\varepsilon$, which has partial derivative $\phi_d(\|z\|_{\mathrm{H}})=\left(\varepsilon-\frac{1}{2}\|z\|_{\mathrm{H}}\right)/\left(\varepsilon-\|z\|_{\mathrm{H}}\right)^2>0$, $z\in\mathcal{D}_\varepsilon$, with respect to $\|z\|_{\mathrm{H}}^2$, and $2\phi_d(\|z\|_{\mathrm{H}})\|z\|_{\mathrm{H}}^2-\phi(\|z\|_{\mathrm{H}})=\varepsilon\|z\|_{\mathrm{H}}^2/\left(\varepsilon-\|z\|_{\mathrm{H}}\right)^2>0$, $z\in\mathcal{D}_\varepsilon$ [1].*

Definition 3.2.3 *We define $\tanh(x)\triangleq\left[\tanh(x(1)),\tanh(x(2)),\ldots,\tanh(x(s))\right]^{\mathrm{T}}\in\mathbb{R}^s$ for any vector $x\in\mathbb{R}^s$.*

Remark 3.2.2 *For any scalar $\eta\in\mathbb{R}$, $|\eta|-\eta\tanh(\eta)\leq\mathcal{L}$ holds with $\mathcal{L}=0.2785$ [94]. This can be generalized for any vector $\eta\in\mathbb{R}^s$ as $\|\eta\|_2-\eta^{\mathrm{T}}\tanh(\eta)\leq\mathcal{L}$.*

3.3 Problem Formulation

This section introduces the problem formulation focused in this paper. Specifically, consider the uncertain dynamical system given by

$$\dot{x}(t)=Ax(t)+B\Lambda\big(u(t)+\delta(t,x(t))\big),\quad x(0)=x_0,\quad t\geq 0, \tag{3.1}$$

where $x(t)\in\mathbb{R}^n$, $t\geq 0$, is the measurable state vector, $u(t)\in\mathbb{R}^m$, $t\geq 0$, is the control input, $A\in\mathbb{R}^{n\times n}$ is a known system matrix, $B\in\mathbb{R}^{n\times m}$ is a known input matrix, $\delta:\overline{\mathbb{R}}_+\times\mathbb{R}^n\to\mathbb{R}^m$ is a system uncertainty, $\Lambda\in\mathbb{R}_+^{m\times m}\cap\mathbb{D}^{m\times m}$ is an unknown control effectiveness matrix, and the pair (A,B) is controllable. Note that a wide range of physical dynamical systems either explicitly or approximately satisfy the system model considered in (3.1). Specifically, these systems include but not limited to mass-spring-damper systems [95], pendulum systems linearized around an equilibrium point of interest subject to friction uncertainties [96], ground mobile robots [97], and flight control systems [30, 98].

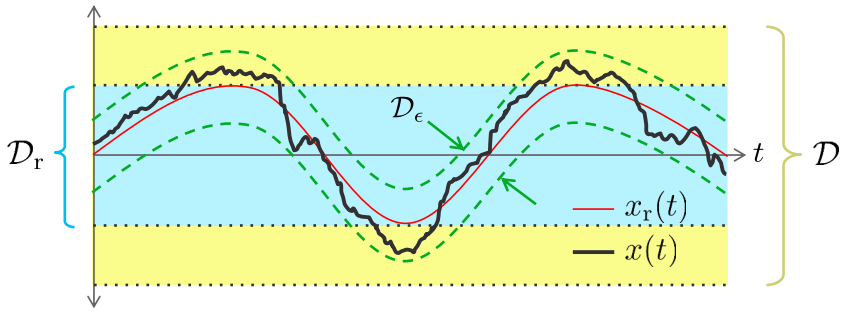

Figure 3.1: An illustration of the sets in Remark 3.3.1.

Assumption 3.3.1 *On a compact set $\mathcal{D}$ of the real coordinate space, the system uncertainty in* (3.1) *is parameterized as*[1]

$$\delta(t,x(t)) = W_{\mathrm{N}}^{\mathrm{T}}(t)\sigma_{\mathrm{N}}(x(t)) + \varepsilon_{\mathrm{N}}(x(t)), \quad x(t) \in \mathcal{D}, \tag{3.2}$$

where $W_{\mathrm{N}}(t) \in \mathbb{R}^{s\times m}$, $t \geq 0$, is a bounded unknown weight matrix (i.e., $\|W_{\mathrm{N}}(t)\|_{\mathrm{F}} \leq w_{\mathrm{N}}$, $t \geq 0$) with a bounded time rate of change (i.e., $\|\dot{W}_{\mathrm{N}}(t)\|_{\mathrm{F}} \leq \dot{w}_{\mathrm{N}}$, $t \geq 0$), $\sigma_N : \mathbb{R}^n \to \mathbb{R}^s$ is a basis function constructed using neural networks of the form $\sigma_{\mathrm{N}}(x(t)) = [\sigma_{\mathrm{N1}}(x(t)), \sigma_{\mathrm{N2}}(x(t)), \ldots, \sigma_{\mathrm{N}s}(x(t))]^{\mathrm{T}}$, and $\varepsilon_N : \mathbb{R}^n \to \mathbb{R}^m$ is the approximation tolerance upper bounded by an unknown constant ε^* such that[2]

$$\|\varepsilon_{\mathrm{N}}(x(t))\|_2 \leq \varepsilon^*, \quad \forall x(t) \in \mathcal{D}. \tag{3.3}$$

Remark 3.3.1 *The overall control objective considered in this paper is to have the state trajectory of the uncertain dynamical system given in* (3.1) *to evolve in a compact set such that the neural network approximation given in* (3.2) *is always valid. To elucidate this point and for illustration purposes, consider the case with scalar trajectories as shown in Figure 3.1. In addition, let $\mathcal{D}$ be a compact set of the real coordinate space in which the neural network approximation is valid, and let $\mathcal{D}_{\mathrm{r}} \subset \mathcal{D}$ be the set such that the state of a reference model evolves inside this set, i.e., $x_{\mathrm{r}}(t) \in \mathcal{D}_{\mathrm{r}}$. In what follows, we show that the distance between the trajectories of the uncertain dynamical system and the trajectories of the reference system can be adjusted by the size of a user-defined compact set $\mathcal{D}_{\varepsilon}$ by choosing a user-defined parameter ε such that $\mathcal{D}_{\mathrm{r}} \cup \mathcal{D}_{\varepsilon} \subset \mathcal{D}$ holds and the system uncertainty parameterization in* (3.2) *remains always valid.*

[1] As discussed in Section 3.1, the parameterization given by (3.2) is preferred for applications involving system uncertainties with unknown structures and unknown parameters. We refer to, for example, Section 12.4 in [30] for further reading.

[2] Note that the magnitude of parameter ε^* can be arbitrarily reduced within the compact set $\mathcal{D}$ by providing a sufficient large number of neurons to the considered neural network [99].

Now, consider the feedback control law given by

$$u(t) = u_{\mathrm{n}}(t) + u_{\mathrm{a}}(t), \quad t \geq 0, \tag{3.4}$$

where $u_{\mathrm{n}}(t) \in \mathbb{R}^m$, $t \geq 0$, and $u_{\mathrm{a}}(t) \in \mathbb{R}^m$, $t \geq 0$, are the nominal and adaptive control laws, respectively. Furthermore, let the nominal control law be

$$u_{\mathrm{n}}(t) = -K_1 x(t) + K_2 c(t), \quad t \geq 0, \tag{3.5}$$

where $c(t) \in \mathbb{R}^{n_c}$ is a bounded reference command such that $A_{\mathrm{r}} \triangleq A - BK_1$, $K_1 \in \mathbb{R}^{m \times n}$, is Hurwitz and $B_{\mathrm{r}} \triangleq BK_2$, $K_2 \in \mathbb{R}^{m \times n_c}$.

Next, consider the reference model capturing a desired closed-loop behavior

$$\dot{x}_{\mathrm{r}}(t) = A_{\mathrm{r}} x_{\mathrm{r}}(t) + B_{\mathrm{r}} c(t), \quad x_{\mathrm{r}}(t) \in \mathcal{D}_{\mathrm{r}}, \quad x_{\mathrm{r}}(0) = x_{\mathrm{r}0}, \quad t \geq 0, \tag{3.6}$$

where $x_r(t) \in \mathbb{R}^n$ is the reference model state vector, $A_r \in \mathbb{R}^{n \times n}$ is the desired Hurwitz system matrix, $B_r \in \mathbb{R}^{n \times n_c}$ is the command input matrix, and $\mathcal{D}_{\mathrm{r}}$ is a user-defined set (see Remark 3.3.1). Using (3.1), (3.4), (3.5) and (3.6), the system error dynamics is given by

$$\dot{e}(t) = A_{\mathrm{r}} e(t) + B\Lambda\big(\big(\Lambda^{-1} - I_{\mathrm{m}\times\mathrm{m}}\big)\big(K_1 x(t) - K_2 c(t)\big) + u_{\mathrm{a}}(t) + \delta(t, x(t))\big), \quad e(0) = e_0, \quad t \geq 0, \tag{3.7}$$

where $e(t) \triangleq x(t) - x_{\mathrm{r}}(t)$, $t \geq 0$, is the system error. Using (3.2) in (3.7) yields

$$\dot{e}(t) = A_{\mathrm{r}} e(t) + B\Lambda\big(W^{\mathrm{T}}(t)\sigma(x(t)) + u_{\mathrm{a}}(t) + \varepsilon_{\mathrm{N}}(x(t))\big), \quad e(0) = e_0, \quad t \geq 0, \tag{3.8}$$

where $W(t) \triangleq [W_{\mathrm{N}}^{\mathrm{T}}(t),\ (\Lambda^{-1} - I_{\mathrm{m}\times\mathrm{m}})K_1,\ -(\Lambda^{-1} - I_{\mathrm{m}\times\mathrm{m}})K_2]^{\mathrm{T}} \in \mathbb{R}^{(s+n+n_c)\times m}$, $t \geq 0$, is an unknown weight matrix and $\sigma\big(x(t), c(t)\big) \triangleq \big[\sigma_{\mathrm{N}}^{\mathrm{T}}\big(x(t)\big),\ x^{\mathrm{T}}(t),\ c^{\mathrm{T}}(t)\big]^{\mathrm{T}} \in \mathbb{R}^{s+n+n_c}$, $t \geq 0$, is a known function involving neural network-based basis functions, the system state vector, and the reference command.

The statement of the model reference neuroadaptive control objective of this paper is now given as follows. Consider the uncertain dynamical system given by (3.1) subject to Assumption 3.3.1. *Our aim is to design the adaptive control signal* $u_{\mathrm{a}}(t)$, $t \geq 0$, *to achieve stability of the overall closed-loop system and keep the system error trajectories inside an a-priori, user-defined compact set such that the parameterization in*

Assumption 3.3.1 remains valid for all time. To address this objective, the next section introduces the proposed set-theoretic neuroadaptive model reference adaptive control architecture.

3.4 Set-Theoretic Model Reference Neuroadaptive Control

We now present a set-theoretic model reference neuroadaptive control approach based on restricted potential functions with strict performance guarantees such that the closed-loop system trajectories stay inside the set $\mathcal{D}$, and hence, the universal function approximation remains valid for all time. For this purpose, let the adaptive control law be

$$u_{\mathrm{a}}(t) = -\hat{W}^{\mathrm{T}}(t)\sigma\big(x(t)\big) - v(t), \quad t \geq 0, \tag{3.9}$$

where $v(t) \in \mathbb{R}^m$ is a corrective signal and $\hat{W}(t) \in \mathbb{R}^{(s+n+n_c)\times m}$, $t \geq 0$, is the estimate of $W(t)$, $t \geq 0$, satisfying the update law

$$\dot{\hat{W}}(t) = \gamma_1 \mathrm{Proj}_{\mathrm{m}}\Big(\hat{W}(t), \phi_d(\|e(t)\|_P)\sigma\big(x(t)\big)e^{\mathrm{T}}(t)PB\Big), \quad \hat{W}(0) = \hat{W}_0, \quad t \geq 0, \tag{3.10}$$

with $\hat{W}_{\max}$ and $-\hat{W}_{\max}$ respectively being the maximum and minimum element-wise projection bounds, $\phi_d(\|e(t)\|_P) \in \mathbb{R}_+$ is an error dependent learning gain, $\gamma_1 \in \mathbb{R}_+$ is a design scalar, and $P \in \mathbb{R}_+^{n\times n}$ is a solution of the Lyapunov equation

$$0 = A_{\mathrm{r}}^{\mathrm{T}}P + PA_{\mathrm{r}} + R, \tag{3.11}$$

where $R \in \mathbb{R}_+^{n\times n}$.

Next, we design the corrective signal $v(t)$ in (3.9) as

$$v(t) = \tanh\big(\phi_d(\|e(t)\|_P)B^{\mathrm{T}}Pe(t)\big)\hat{q}(t), \quad t \geq 0, \tag{3.12}$$

where $\hat{q}(t) \in \mathbb{R}_+$, $t \geq 0$, is the estimate of $q \triangleq \frac{\lambda_{\max}(\Lambda)}{\lambda_{\min}(\Lambda)}\varepsilon^*$ satisfying the corrective update law

$$\dot{\hat{q}}(t) = \gamma_2 \mathrm{Proj}\Big(\hat{q}(t), \phi_d(\|e(t)\|_P)e^{\mathrm{T}}(t)PB\tanh\big(\phi_d(\|e(t)\|_P)B^{\mathrm{T}}Pe(t)\big) - \xi\hat{q}(t)\Big), \quad \hat{q}(0) = \hat{q}_0 \in \mathbb{R}_+, \quad t \geq 0, \tag{3.13}$$

with $\hat{q}_{\max}$ and 0 being the maximum and minimum projection bounds respectively, $\gamma_2 \in R_+$ is a design scalar, and $\xi \in R_+$ is the σ-modification gain.

Using (3.9) in (3.8), the system error dynamics now become

$$\dot{e}(t) = A_{\mathrm{r}}e(t) - B\Lambda\big(\tilde{W}^{\mathrm{T}}(t)\sigma\big(x(t)\big) - \varepsilon_{\mathrm{N}}(x(t)) + v(t)\big), \quad e(0) = e_0, \quad t \geq 0, \tag{3.14}$$

where $\tilde{W}(t) \triangleq \hat{W}(t) - W(t) \in \mathbb{R}^{(s+n+n_c)\times m}$, $t \geq 0$, is the weight estimation error and $e_0 \triangleq x_0 - x_{\mathrm{r}0}$. Note that $\|W(t)\|_{\mathrm{F}} \leq w, t \geq 0$, and $\|\dot{W}(t)\|_{\mathrm{F}} \leq \dot{w}, t \geq 0$, automatically hold as a direct consequence of Assumption 3.3.1. In addition, one can also write the weight estimation error dynamics and the residual bound estimation error dynamics respectively as

$$\dot{\hat{W}}(t) = \gamma_1 \mathrm{Proj}_{\mathrm{m}}\big(\hat{W}(t), \phi_d(\|e(t)\|_P)\sigma\big(x(t)\big)e^{\mathrm{T}}(t)PB\big) - \dot{W}(t), \ \tilde{W}(0) = \tilde{W}_0, \tag{3.15}$$

$$\dot{\hat{q}}(t) = \gamma_2 \mathrm{Proj}\big(\hat{q}(t), \phi_d(\|e(t)\|_P)e^{\mathrm{T}}(t)PB\tanh\big(\phi_d(\|e(t)\|_P)B^{\mathrm{T}}Pe(t)\big) - \xi\hat{q}(t)\big), \quad \tilde{q}(0) = \tilde{q}_0, \tag{3.16}$$

where $\tilde{q}(t) \triangleq \hat{q}(t) - q$ is the residual bound estimation error.

3.5 Analysis of the Proposed Neuroadaptive Control Architecture

The main purpose of this section is to present the stability analysis and establish strict performance guarantees of the proposed model reference neuroadaptive control architecture in Section 4 (see Section 5.1), where we also present a special case of the proposed algorithm (see Section 5.2).

3.5.1 Stability Analysis and Performance Guarantees

We start with the following first result of this paper.

Theorem 3.5.1 *Consider the uncertain dynamical system given by (3.1) subject to Assumption 3.3.1, the reference model given by (3.6), and the feedback control law given by (3.4) along with the update laws (3.5), (3.9), (3.10), (3.12), and (3.13). If $\|e_0\|_P < \varepsilon$, then the closed-loop dynamical system given by (3.14), (3.15) and (3.16) are bounded, where the bound on the system error strictly satisfies a-priori given, user-defined worst-case performance*

$$\|e(t)\|_P < \varepsilon, \quad t \geq 0. \tag{3.17}$$

Proof. See Appendix A for the proof of Theorem 3.5.1.

Similar to Remark 7 of [1], the next corollary is now immediate with the proposed set-theoretic model reference neuroadaptive control architecture. In particular, it shows that if one utilizes the error dependent learning rate defined in Remark 3.2.1, $\phi_d(\|e(t)\|_P) = \big(\varepsilon - \frac{1}{2}\|e(t)\|_P\big)/\big(\varepsilon - \|e(t)\|_P\big)^2$, then it does not exceed a finite bound when it is used in the update laws (3.10) and (3.13). Note that the same conclusion can be made for other selections of error dependent learning rates by following the steps outlined in the proof of the following corollary, and hence, there is not much loss of generality.

Corollary 3.5.1 *Consider the uncertain dynamical system given by (3.1) subject to Assumption 3.3.1, the reference model given by (3.6), and the feedback control law given by (3.4) along with the update laws (3.5), (3.9), (3.10), (3.12), and (3.13). If* $\|e_0\|_P < \varepsilon$ *and* $\phi(\|e(t)\|_P) = \|e(t)\|_P^2/\big(\varepsilon - \|e(t)\|_P\big)$, *then the error dependent learning rate* $\phi_d(\|e(t)\|_P) = \big(\varepsilon - \frac{1}{2}\|e(t)\|_P\big)/\big(\varepsilon - \|e(t)\|_P\big)^2$ *is lower and upper bounded by* $\frac{1}{\varepsilon} \leq \phi_d(\|e(t)\|_P) \leq \phi_d(\bar{e})$, $t \geq 0$, *where* $\bar{e} \triangleq (-V_{\max} + \sqrt{V_{\max}^2 + 4V_{\max}\,\varepsilon})/2$, $V_{\max} \triangleq \max\{V_0, \frac{2\mu}{\alpha}\}$, *and* $V_0 \triangleq V(e(0), \tilde{W}(0), \tilde{q}(0))$.

Proof. See Appendix B for the proof of Corollary 3.5.1.

3.5.2 A Special Case

For completeness, we now present a special case. Specifically, the next corollary shows a simplified version of the proposed set-theoretic model reference neuroadaptive control architecture for cases when the approximation tolerance in (3.3) has a known upper bound, as considered in (12.12) of [30].

Corollary 3.5.2 *Consider the uncertain dynamical system given by (3.1) subject to Assumption 3.3.1, the reference model given by (3.6), and the feedback control law given by (3.4) along with the update laws (3.5), (3.9), and (3.10). If* $\|e_0\|_P < \varepsilon$ *and there exist known constants* $c_1 \in \mathbb{R}_+$, $c_2 \in \mathbb{R}_+$, *and* $c_3 \in \mathbb{R}_+$ *such that*

$$\|\varepsilon_{\mathrm{N}}(x(t))\|_2 \leq \varepsilon^* \leq c_1, \quad \forall x(t) \in \mathcal{D}, \tag{3.18}$$

$$c_2 I \leq \lambda_{\min}(\Lambda) I \leq \Lambda \leq \lambda_{\max}(\Lambda) I \leq c_3 I, \tag{3.19}$$

hold, then the corrective signal $v(t)$ *given by*

$$v(t) = \tanh\big(\phi_d(\|e(t)\|_P) B^{\mathrm{T}} P e(t)\big) c_1 c_2^{-1} c_3, \quad t \geq 0, \tag{3.20}$$

results in a bounded closed-loop dynamical system given by (3.14) and (3.15), where the bound on the system error strictly satisfies a-priori given, user-defined worst-case performance

$$\|e(t)\|_P < \varepsilon, \quad t \geq 0. \tag{3.21}$$

Proof. See Appendix C for the proof of Corollary 3.5.2.

Remark 3.5.1 *Note that Theorem 3.5.1 and Corollaries 3.5.1 and 3.5.2 significantly generalize the results presented in the previous work of authors in Theorem 3.1 of [1] by considering an unstructured uncertainty for the dynamical system and using the universal function approximation property of neural networks. Specifically, Theorem 3.5.1 shows that the proposed neuroadaptive control framework has the capability to keep the closed-loop system trajectories within an a-priori, user-defined compact set of the real coordinate space such that the universal function approximation property is not violated.*

3.6 Illustrative Numerical Example

In this section, we present a numerical example to demonstrate the efficacy of the proposed set-theoretic model reference neuroadaptive control architecture. Specifically, an aircraft landing problem adopting from Section 12.4 of [30] is considered such that the aircraft experiences increase in its aerodynamic lift force when it approaches to the runway (i.e., the ground effect). To this end, a generic mid-size transport aircraft flying wings-level at an altitude of $h_0 = 300$ ft above ground is considered, with its landing gear down and with flaps/slats extended ([30, 100]). The vehicle true airspeed is $V_0 = 250$ ft/s. The corresponding longitudinal linear dynamics are of the form $\dot{x}(t) = Ax(t) + B\Lambda\big(u(t) + \theta_g \alpha_g(h(t))\big)$, $x(0) = x_0$, $t \geq 0$, with A, B and θ_g matrices as given in Example 12.3 of [30], and where $x(t) = \big[V(t),\ \alpha(t),\ q(t),\ \theta(t),\ h(t)\big]^{\mathrm{T}} \in \mathbb{R}^5$ is the state vector with $V(t)$ representing the true airspeed (in ft/s), $\alpha(t)$ representing the angle of attack (in rad), $q(t)$ representing the pitch rate (in deg/s), $\theta(t)$ representing the pitch angle (in deg), $h(t)$ representing the altitude above the runway (in ft), and $u(t) = [\delta_{\mathrm{th}}(t),\ \delta_{\mathrm{e}}(t)]^{\mathrm{T}} \in \mathbb{R}^2$ with $\delta_{\mathrm{th}}(t)$ representing the engine thrust (in %), and $\delta_{\mathrm{e}}(t)$ the elevator input (in deg). Here, $\alpha_g(h(t))$ represents the ground effect of the aircraft that is considered as an uncertainty of the form $\alpha_g(h(t)) = -0.0698(1 - \tanh(0.1(h(t) - 60)))$ and $\Lambda = I$ (i.e., control effectiveness matrix is not uncertain in this example).

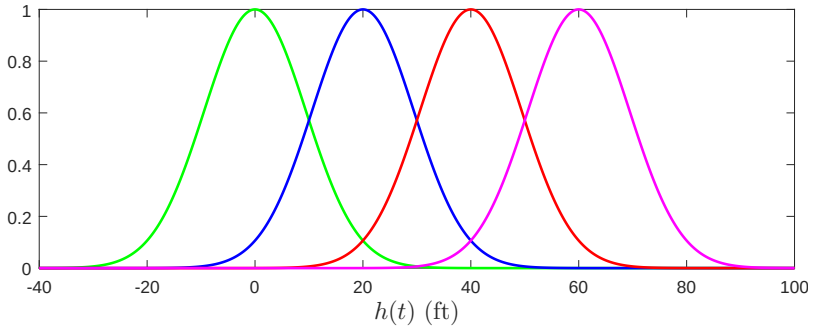

Figure 3.2: Distribution of the RBFs in (3.22) in transport aircraft example.

Linear quadratic regulator theory is used to design the nominal controller gain matrices as $K_1 = \begin{bmatrix} 0.147 & -89.216 & 53.147 & 139.971 & 0.173 \\ 0.009 & -28.197 & 3.832 & 42.774 & 0.142 \end{bmatrix}$ and $K_2 = \begin{bmatrix} -0.721 & 0.173 \\ 0.879 & 0.142 \end{bmatrix}$. Furthermore, we choose the command signal $c = [V_c,\ h_c]^T$ with $V_c = 250$ ft/s and h_c being the desired altitude profile shown in Figures 3.3 and 3.4. In order to approximate the uncertain term due to the ground effect ($\theta_g \alpha_g(h(t))$), we utilize a neural network with the altitude-dependent regressor vector as

$$\sigma(h) = [\sigma_1(h),\ \sigma_2(h),\ \sigma_3(h),\ \sigma_4(h),\ 1]^T, \quad t \geq 0, \tag{3.22}$$

with $\sigma_i(h) = \exp(-0.0056(h-h_i)^2), i = 1,\ldots,4$, for uniform distribution of RBFs on the altitude interval (0, 60) ft to provide a homogeneous coverage of the altitude range in which the ground effect is active as depicted in Figure 3.2. For the proposed set-theoretic model reference adaptive control architecture in Theorem 3.5.1, we use the generalized restricted potential function given in Remark 3.2.1 with $\varepsilon = 2$ to strictly guarantee $\|x(t) - x_r(t)\|_P < 2$, $t \geq 0$. Finally, we set the projection norm bound imposed on the parameter estimate to $\hat{W}_{\max} = 10$ and $\hat{q}_{\max} = 15$ and use $R = I$ to calculate P from (3.11) for the resulting A_r matrix.

Figure 3.3 shows the closed-loop dynamical system performance with the nominal controller. One can see from this figure that the airspeed deviated from the command signal and the aircraft cannot reach the ground due to the ground effect. Next, we apply the proposed set-theoretic adaptive controller with $\gamma_1 = \gamma_2 = 5$ and $\xi = 0.2$. It can be seen in Figure 3.4 that desired performance is obtained and the control surfaces do not exceed practical limitations, and Figure 3.5 clearly shows that this controller strictly guarantees $\|x(t) - x_r(t)\|_P < 2$. Note that since the error trajectory is contained within $\mathcal{D}_\varepsilon$, and both ε and radial basis functions in (3.22) are selected such that the system trajectory remains within the compact set $\mathcal{D}$, the neural network approximation is always valid on the compact set $\mathcal{D}$ with the bounded approximation error in (3.3).

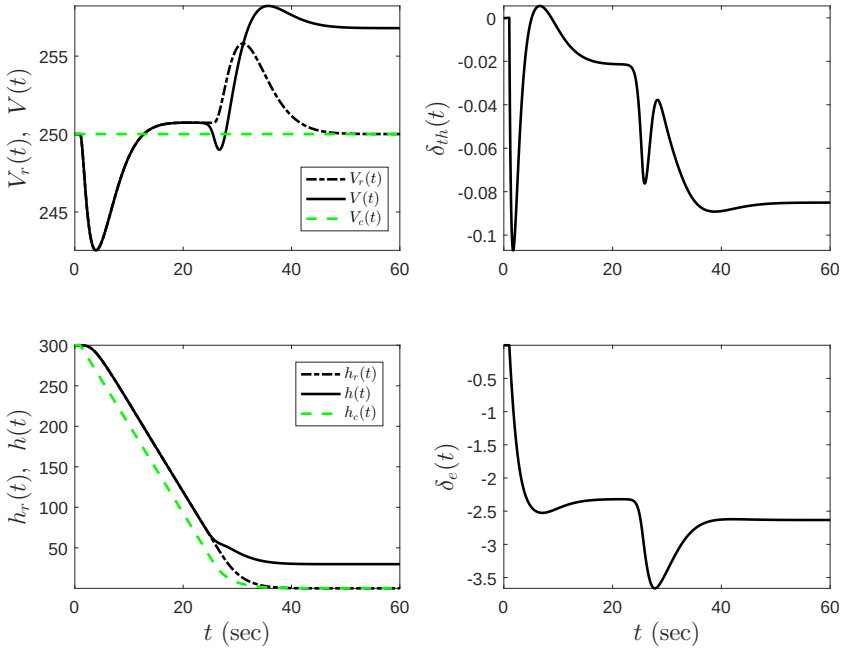

Figure 3.3: System performance with the nominal controller in transport aircraft example.

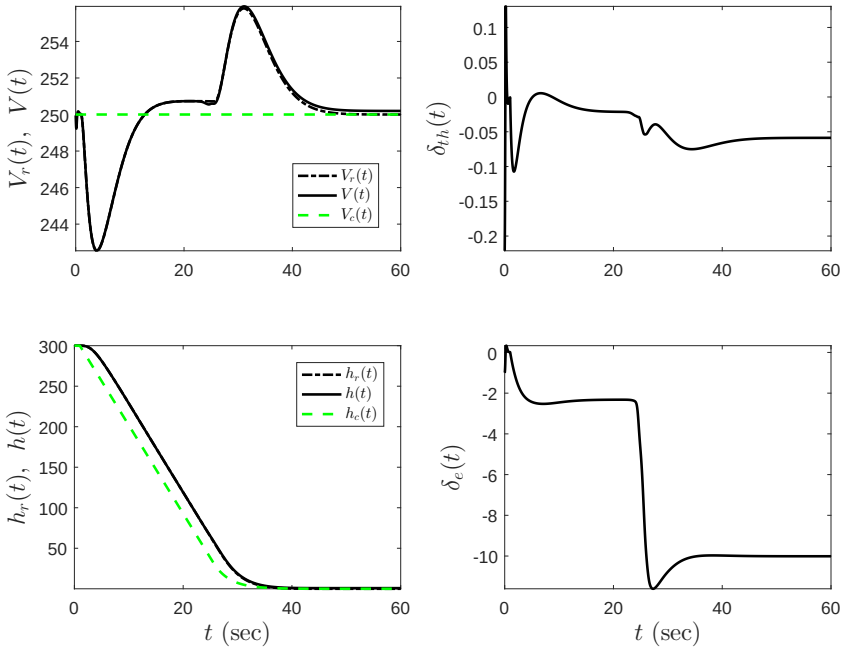

Figure 3.4: System performance with the proposed set-theoretic adaptive controller in transport aircraft example.

3.7 Conclusion

To contribute to the previous studies in neuroadaptive model reference adaptive control systems, we have reported a new architecture entitled set-theoretic model reference neuroadaptive control, which has the

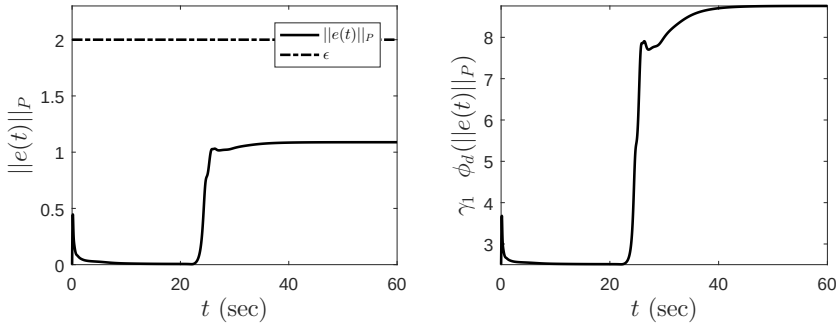

Figure 3.5: Norm of the system error trajectories with the proposed set-theoretic adaptive controller and the evolution of the effective learning rate $\gamma_1 \phi_{\mathrm{d}}(\cdot)$ in transport aircraft example.

capability to enforce strict performance guarantees on the distance between the trajectories of an uncertain dynamical system and the trajectories of a desired reference model. Specifically, our motivation behind this development stems from a major challenge in the design of neuroadaptive control laws for making the closed-loop system trajectories to evolve in a compact set where the universal function approximation properties hold. In particular, as shown in Theorem 3.5.1, by using the proposed control architecture, a control designer can adjust the deviation of the system trajectories from a given reference system; hence, as discussed in Remark 3.3.1, the system uncertainty parameterization remains valid with proper reference model selection for all time. An illustrative numerical example was also provided to complement the theoretical contribution of this paper. Future research will include extensions to the case when the entire state vector of the uncertain dynamical system is not measurable as well as experimental studies involving real-world unmanned vehicles.

CHAPTER 4: GENERALIZATIONS OF THE SET-THEORETIC MODEL REFERENCE ADAPTIVE CONTROL

This chapter presents several key generalizations of the set-theoretic model reference adaptive control architecture proposed in Chapter 2. In particular, Section 4.1 extends this control architecture for enforcing time-varying user-defined performance bounds, Section 4.2 presents a new architecture to achieve adjustable performance guarantees on a subset of system error trajectories, Section 4.3 provides performance guarantees for uncertain dynamical systems subject to actuator dynamics, and Section 4.4 generalizes the set-theoretic model reference adaptive control architecture to address disturbance rejection and system uncertainty suppression in the presence of actuator failures.

4.1 Set-Theoretic Model Reference Adaptive Control with Time-Varying Performance Bounds[1]

One of the fundamental problems in model reference adaptive control design is the ability of the controlled system to achieve not only stability but also a user-defined performance in the presence of exogenous disturbances and system uncertainties. Motivated from this standpoint, we recently proposed a set-theoretic model reference adaptive control framework, which guarantees the norm of the system error (i.e., the difference between the state of an uncertain dynamical system and the state of a given reference model) to be less than a user-defined constant performance bound. The contribution of this paper is to generalize the set-theoretic model reference adaptive control framework in order to enforce user-defined time-varying performance bounds on the system error, which gives the control designer a flexibility to control the closed-loop system performance as desired on different time intervals (e.g., transient time interval and steady-state time interval). To this end, two adaptive command following control architectures are proposed and their stability and performance properties are rigorously established using system-theoretic methods. Finally, our theoretical findings are further supported through a numerical example in order to compare these architectures and illustrate their efficacy.

[1]This section is previously published in [2]. Permission is included in Appendix H.

4.1.1 Introduction

Model reference adaptive controllers have three major components; a reference model, an update law, and a controller. The reference model captures a desired closed-loop system performance for which its output (respectively, state) is compared with the output (respectively, state) of an uncertain dynamical system. This comparison results in a system error used to drive the update law online. The controller then adapts feedback gains to suppress the system error using the information received from the update law. Although model reference adaptive controllers have the ability to guarantee closed-loop system stability in the presence of exogenous disturbances and system uncertainties, one fundamental problem is to obtain user-defined performance guarantees while utilizing these controllers in the feedback loop.

We have recently started to address this challenge by introducing a set-theoretic model reference adaptive control framework [1, 21]. Specifically, [21] and [1] respectively present this new framework for dynamical systems subject to time-invariant and time-varying system uncertainties, where the latter also captures exogenous disturbances. These results guarantee the norm of the system error (i.e., the difference between the state of an uncertain dynamical system and the state of a given reference model) to be less than a user-defined constant performance bound. We also refer to [93, 101–106] for studies extending the results of [21] and [1]. In particular, [101] focus on set-theoretic model reference adaptive control in the presence of actuator failures, [93] and [102] theoretically blend the results in [21] and [1] with neural networks to keep the trajectories of uncertain dynamical systems on a given compact set in the absence of structured system uncertainty parameterizations, and [103] and [104] consider decentralized extensions to large-scale dynamical systems. Moreover, [105] and [106] respectively consider applications of the results in [21] and [1] to a generic transport aerospace vehicle and a rigid body space vehicle on exponential coordinates.

As compared with other notable contributions in the literature enforcing similar performance bounds [18–20, 22–26, 107], the set-theoretic model reference adaptive control framework does not assume that the control signals can access every element of the state vector as in [18], does not assume that a desired trajectory along with its derivatives are all available for feedback control design as in [19], enforces user-defined performance bounds not on measurable output signals as in [20] but on measurable state signals, and does not involve a backstepping procedure for adaptive control as in [22–26, 107] (also see [1] for additional details). As noted above, in addition, the results in [1] go beyond the ones in [21] in that both the exogenous disturbances and the system uncertainties can depend on time in [1] to capture dynamic

environment conditions and changes in system dynamics. However, a common denominator of the results in [21] and [1] (including their extensions in [93, 101–106]) is that they assume the user-defined performance bound to be constant.

The contribution of this paper is to generalize the set-theoretic model reference adaptive control framework in order to enforce user-defined time-varying performance bounds on the system error, which gives the control designer a flexibility to control the closed-loop system performance as desired on different time intervals (e.g., transient time interval and steady-state time interval). To this end, two set-theoretic control architectures are proposed for adaptive command following in the presence of exogenous disturbances and system uncertainties, where the stability and performance properties of both architectures are rigorously established using system-theoretic methods. Furthermore, our theoretical findings are also supported through a numerical example in order to compare these architectures and illustrate their efficacy. Note that a preliminary conference version of this paper appeared in [108], which only considers one of the architectures proposed here. The present paper considerably goes beyond this conference version by not only providing detailed proofs for the considered architecture in [108] but also focusing on all the theoretical developments necessary for the other architecture presented here with detailed examples, added figures, and motivation.

Finally, we introduce the fairly standard notation used throughout this paper. Specifically, $\mathbb{R}^{n\times m}$ denotes the set of $n\times m$ real matrices, $\mathbb{R}_+^{n\times n}$ (respectively, $\overline{\mathbb{R}}_+^{n\times n}$) denotes the set of $n\times n$ positive-definite (respectively, nonnegative-definite) real matrices, $\mathbb{D}^{n\times n}$ denotes the set of $n\times n$ real matrices with diagonal scalar entries, $\|\cdot\|_2$ denotes the Euclidean norm, and $\|\cdot\|_{\mathrm{F}}$ denotes the Frobenius norm. In addition, we write $\|x\|_{\mathrm{A}} \triangleq \sqrt{x^{\mathrm{T}}Ax}$ for the weighted Euclidean norm of $x\in\mathbb{R}^n$ with the matrix $A\in\mathbb{R}_+^{n\times n}$, $\|A\|_2 \triangleq \sqrt{\lambda_{\max}(A^{\mathrm{T}}A)}$ for the induced 2-norm of the matrix $A\in\mathbb{R}^{n\times m}$, $\lambda_{\min}(A)$ (resp., $\lambda_{\max}(A)$) for the minimum (resp., maximum) eigenvalue of the matrix $A\in\mathbb{R}^{n\times n}$, and $\underline{x}$ (resp., $\bar{x}$) for the lower bound (resp., upper bound) of a bounded signal $x(t)\in\mathbb{R}^n$, $t\geq 0$, that is, $\underline{x}\leq\|x(t)\|_2$, $t\geq 0$ (resp., $\|x(t)\|_2\leq\bar{x}$, $t\geq 0$).

4.1.2 Problem Formulation

In this section, we introduce a benchmark adaptive command following problem formulation considered in this paper. In particular, consider the uncertain dynamical system given by

$$\dot{x}_{\mathrm{p}}(t) = A_{\mathrm{p}}x_{\mathrm{p}}(t)+B_{\mathrm{p}}\Lambda u(t)+B_{\mathrm{p}}\delta_{\mathrm{p}}(t,x_{\mathrm{p}}(t)),\quad x_{\mathrm{p}}(0)=x_{\mathrm{p}0},\quad t\geq 0. \tag{4.1}$$

In (4.1), $x_{\rm p}(t) \in \mathbb{R}^{n_{\rm p}}$, $t \geq 0$, denotes the measurable state vector, $u(t) \in \mathbb{R}^m$, $t \geq 0$, denotes the control input, $A_{\rm p} \in \mathbb{R}^{n_{\rm p} \times n_{\rm p}}$ denotes a known system matrix, and $B_{\rm p} \in \mathbb{R}^{n_{\rm p} \times m}$ denotes a known input matrix. Here, as standard, we assume that the pair $(A_{\rm p}, B_{\rm p})$ is controllable. Furthermore, $\delta_{\rm p} : \overline{\mathbb{R}}_+ \times \mathbb{R}^{n_{\rm p}} \to \mathbb{R}^m$ and $\Lambda \in \mathbb{R}_+^{m \times m} \cap \mathbb{D}^{m \times m}$ in (4.1) respectively denote a system uncertainty and an unknown control effectiveness matrix.

Considering the widely-adopted system uncertainty parameterization given by (D.1) and feedback control law given by (D.7), which has nominal $u_{\rm n}(t)$, $t \geq 0$, and adaptive $u_{\rm a}(t)$, $t \geq 0$, controller elements, one can readily rewrite (4.1) by augmenting an integrator state dynamics as

$$\dot{x}(t) \;\; = \;\; A_{\rm r} x(t) + B_{\rm r} c(t) + B\Lambda \left[u_{\rm a}(t) + W^{\rm T}(t) \sigma\big(x(t)\big) \right], \quad x(0) = x_0, \quad t \geq 0. \tag{4.2}$$

We refer to Appendix D for the standard steps in rewriting (4.2) from (4.1). In (4.2), $x(t) \triangleq [x_{\rm p}^{\rm T}(t), \; x_{\rm c}^{\rm T}(t)]^{\rm T} \in \mathbb{R}^n$, $t \geq 0$, is the augmented system state with $x_{\rm c}(t) \in \mathbb{R}^{n_{\rm c}}$, $t \geq 0$, being the integrator state and $n \triangleq n_p + n_c$, $c(t) \in \mathbb{R}^{n_{\rm c}}$, $t \geq 0$, is a given command, $W(t) \triangleq \left[\Lambda^{-1} W_{\rm p}^{\rm T}(t), \; (\Lambda^{-1} - I_{m \times m}) K \right]^{\rm T} \in \mathbb{R}^{(s+n) \times m}$, $t \geq 0$, is an unknown aggregated weight matrix, and $\sigma\big(x(t)\big) \triangleq [\sigma_{\rm p}^{\rm T}\big(x_{\rm p}(t)\big), x^{\rm T}(t)]^{\rm T} \in \mathbb{R}^{s+n}$, $t \geq 0$, is a known aggregated basis function. Motivated by the structure of the terms inside brackets in (4.2), let the adaptive control signal be given by

$$u_{\rm a}(t) = -\hat{W}^{\rm T}(t) \sigma\big(x(t)\big), \quad t \geq 0, \tag{4.3}$$

where $\hat{W}(t) \in \mathbb{R}^{(s+n) \times m}$, $t \geq 0$, is an estimate of $W(t)$, $t \geq 0$, to be defined below.

The design of an update law to construct the estimate $\hat{W}(t)$, $t \geq 0$, is crucial in any model reference adaptive control approach in order to achieve a desired level of command following performance, which is captured by the reference model given by

$$\dot{x}_{\rm r}(t) \;\; = \;\; A_{\rm r} x_{\rm r}(t) + B_{\rm r} c(t), \quad x_{\rm r}(0) = x_{\rm r0}, \quad t \geq 0, \tag{4.4}$$

with $x_{\rm r}(t) \in \mathbb{R}^n$, $t \geq 0$, being the reference state vector. While there are many update law candidates for this purpose (see, for example, [28–30], and references therein), they do not achieve practical, user-defined performance guarantees for the adaptive command following problem formulated in this section (see also Remarks 2.3 and 2.4 given in [1]). As discussed, a notable exception is entitled as set-theoretic model reference adaptive control architecture [1], where the next remark concisely overviews this result.

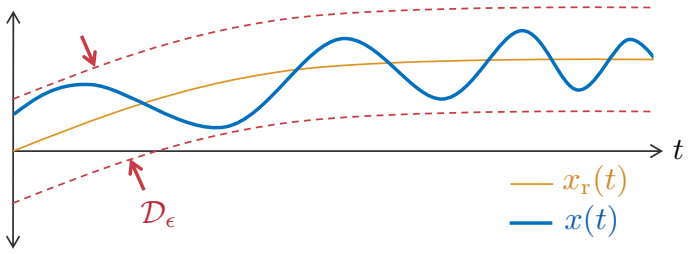

Figure 4.1: Illustration of the user-defined constant performance bound in Remark 4.1.1 for scalar reference model and uncertain dynamical system trajectories.

Remark 4.1.1 *For the highlighted problem formulation above, consider the standard set-theoretic model reference adaptive control update law [1] for (4.3) given by*

$$\dot{\hat{W}}(t) = \gamma_1 \mathrm{Proj}_{\mathrm{m}}\Big(\hat{W}(t), \phi_d(\|e(t)\|_P)\sigma\big(x(t)\big)e^{\mathrm{T}}(t)PB\Big), \quad \hat{W}(0) = \hat{W}_0, \quad t \geq 0, \tag{4.5}$$

with $\hat{W}_{\max}$ being the projection norm bound. Furthermore, $\gamma_1 \in \mathbb{R}_+$ denotes the learning rate (i.e., adaptation gain) and $e(t) \triangleq x(t) - x_{\mathrm{r}}(t)$, $t \geq 0$, denotes the system error in (4.5)*. Note that $\phi_d(\|e(t)\|_P)$ in (4.5) can be viewed as an error dependent learning rate, and hence, the term $\gamma_1\phi_d(\|e(t)\|_P)$ in (4.5) acts as the effective learning rate. Specifically, the update law given by (4.5) can be derived by considering the energy function $V(e,\tilde{W}) = \phi(\|e\|_P) + \gamma_1^{-1}\mathrm{tr}\big[(\tilde{W}\Lambda^{1/2})^{\mathrm{T}}(\tilde{W}\Lambda^{1/2})\big]$, where $\mathcal{D}_\varepsilon \triangleq \{e(t) : \|e(t)\|_P < \varepsilon\}$ and $\tilde{W}(t) \triangleq \hat{W}(t) - W(t)$, $t \geq 0$, is the weight estimation error. Note that $V(0,0) = 0$, $V\big(e,\tilde{W}\big) > 0$ for $\big(e,\tilde{W}\big) \neq (0,0)$, and $\dot{V}\big(e(t),\tilde{W}(t)\big) \leq -\frac{1}{2}\alpha V(e,\tilde{W}) + \mu$, where $\alpha \triangleq \frac{\lambda_{\min}(R)}{\lambda_{\max}(P)}$, $d \triangleq 2\gamma_1^{-1}\tilde{w}\,\dot{w}\|\Lambda\|_2$, $\mu \triangleq \frac{1}{2}\alpha\gamma_1^{-1}\tilde{w}^2\|\Lambda\|_2 + d$, and $\tilde{w} \triangleq \hat{W}_{\max} + w$ with $\|W(t)\|_{\mathrm{F}} \leq w$, $t \geq 0$, and $\|\dot{W}(t)\|_{\mathrm{F}} \leq \dot{w}$, $t \geq 0$ (we refer to the proof of Theorem 3.1 in [1] for details). By applying Lemma 1 of [23, 25], one can now conclude the boundedness of the pair $(e(t),\tilde{W}(t))$ as well as the strict performance bound on the system error given by $\|e(t)\|_P < \varepsilon$, $t \geq 0$, under the assumption $\|e(0)\|_P < \varepsilon$. Figure 4.1 illustrates this constant performance bound for scalar reference model and uncertain dynamical system trajectories.*

Remark 4.1.2 *For the standard set-theoretic model reference adaptive control framework [1] overviewed in the above remark, since ε cannot be chosen less than $\|e(0)\|_P$ by the assumption $\|e(0)\|_P < \varepsilon$, $\|e(t)\|_P$ cannot be made as small as desired unless $\|e(0)\|$ is sufficiently small. For applications when $\|e(0)\|$ is small (e.g., in the presence of almost perfect initial condition knowledge on the state of the uncertain dynamical system that yields to a sufficiently small system error initialization error), a small ε can be chosen. Yet, a*

small ε selection can lead to a large effective learning rate during the transient time interval, which may not be preferred for certain control system implementations. Motivated from the above standpoints, it is of practical interest to enforce user-defined time-varying performance bounds in set-theoretic model reference adaptive controllers (see next section) in order to give the designer a flexibility to control the closed-loop system performance as desired on different time intervals, particularly on the transient time and the steady-state time intervals.

4.1.3 Enforcing Time-Varying Performance Bounds

Based on the adaptive command following problem stated in Section 4.1.2, we now present two architectures in order to generalize the results documented in [1] that enforce user-defined constant performance bounds (see also Remarks 4.1.1 and 4.1.2). In particular, the first architecture given in Section 4.1.3.1 presents a *direct approach* in that a new control law is designed for enforcing user-defined time-varying performance bounds. The second architecture given in Section 4.1.3.2 presents an *indirect approach* in that we modify the reference model without significantly changing the control architecture of [1] to achieve the same objective of enforcing user-defined time-varying performance bounds[1].

4.1.3.1 Direct Approach

For the direct approach presented in this subsection, we first consider the generalized restricted potential function given by

$$\phi(\|z\|_{\mathrm{H}}) = \frac{\|z\|_{\mathrm{H}}^2}{\varepsilon^2(t) - \|z\|_{\mathrm{H}}^2}, \quad z \in \mathcal{D}_\varepsilon. \tag{4.6}$$

Note that (4.6) has the partial derivative $\phi_d(\|z\|_{\mathrm{H}}) = \varepsilon^2(t)/\left(\varepsilon^2(t) - \|z\|_{\mathrm{H}}^2\right)^2 > 0$, $z \in \mathcal{D}_\varepsilon$, with respect to $\|z\|_{\mathrm{H}}^2$, which satisfies $2\phi_d(\|z\|_{\mathrm{H}})\|z\|_{\mathrm{H}}^2 - \phi(\|z\|_{\mathrm{H}}) = \left(\varepsilon^2(t)\|z\|_{\mathrm{H}}^2 + \|z\|_{\mathrm{H}}^4\right)/\left(\varepsilon^2(t) - \|z\|_{\mathrm{H}}^2\right)^2 > 0$, $z \in \mathcal{D}_\varepsilon$. Thus, (4.6) satisfies all properties *i)–vi)* of generalized restricted potential functions stated in the last paragraph of Appendix F. Here, $\varepsilon(t)$ is a positive and bounded-away-from-zero user-defined parameter.

Next, let the adaptive control law be given by

$$u_{\mathrm{a}}(t) = -\hat{W}^{\mathrm{T}}(t)\sigma\big(x(t)\big) - v(t), \quad t \geq 0, \tag{4.7}$$

[1] see Appendix E for further remarks on these two approaches.

where $v(t) \in \mathbb{R}^m$, $t \geq 0$, is an additive signal, and $\hat{W}(t) \in \mathbb{R}^{(s+n)\times m}$, $t \geq 0$, is the estimate of $W(t)$, $t \geq 0$, satisfying the update law (4.5). In particular, we let the additive signal $v(t)$, $t \geq 0$, be

$$v(t) = B^{\mathrm{T}} P e(t) \hat{q}(t) \frac{|\dot{\varepsilon}(t)|}{\varepsilon(t)} \lambda_{\max}(P), \quad t \geq 0, \tag{4.8}$$

where $\hat{q}(t) \in \overline{\mathbb{R}}_+$, $t \geq 0$, is the estimate of the (partially) unknown parameter $q \triangleq \lambda_{\min}^{-1}(PB\Lambda B^{\mathrm{T}} P)$ with an unknown bound (i.e., $|q| \leq q_{\max}$) satisfying the adaptive parameter update law

$$\dot{\hat{q}}(t) = \gamma_2 \mathrm{Proj}\left(\hat{q}(t), \phi_d(\|e(t)\|_P) \|e(t)\|_2^2 \frac{|\dot{\varepsilon}(t)|}{\varepsilon(t)} \right), \quad \hat{q}(0) = \hat{q}_0 \in \overline{\mathbb{R}}_+, \quad t \geq 0, \tag{4.9}$$

with 0 and $\hat{q}_{\max}$ being the minimum and maximum projection bounds respectively and $\gamma_2 \in \mathbb{R}_+$ being the learning rate.

For the next theorem presenting the first contribution of this paper, one can write the system error dynamics, the weight estimation error dynamics, and the adaptive parameter estimation error dynamics respectively as

$$\dot{e}(t) = A_{\mathrm{r}} e(t) - B\Lambda \tilde{W}^{\mathrm{T}}(t) \sigma\big(x(t)\big) - B\Lambda v(t), \quad e(0) = e_0, \quad t \geq 0, \tag{4.10}$$

$$\dot{\tilde{W}}(t) = \gamma_1 \mathrm{Proj}_{\mathrm{m}}\big(\hat{W}(t), \phi_d(\|e(t)\|_P) \sigma\big(x(t)\big) e^{\mathrm{T}}(t) PB\big) - \dot{W}(t), \quad \tilde{W}(0) = \tilde{W}_0, \quad t \geq 0, \tag{4.11}$$

$$\dot{\tilde{q}}(t) = \gamma_2 \mathrm{Proj}\left(\hat{q}(t), \phi_d(\|e(t)\|_P) \|e(t)\|_2^2 \frac{|\dot{\varepsilon}(t)|}{\varepsilon(t)} \right), \quad \tilde{q}(0) = \tilde{q}_0, \quad t \geq 0, \tag{4.12}$$

where $\tilde{W}(t) \triangleq \hat{W}(t) - W(t)$, $t \geq 0$, is the weight estimation error and $\tilde{q}(t) \triangleq \hat{q}(t) - q$, $t \geq 0$, is the adaptive parameter estimation error. Note that we inherently assume $\varepsilon(t)$, $t \geq 0$, and $\dot{\varepsilon}(t)$, $t \geq 0$, are smooth and bounded user-defined functions.

Theorem 4.1.1 *Consider the uncertain dynamical system given by (4.1) subject to Assumption D.1, the reference model given by (4.4), and the feedback control law given by (D.7) along with (D.8), (4.5), (4.7), (4.8), and (4.9). If $\|e_0\|_P < \varepsilon(0)$, then the closed-loop dynamical system given by (4.10), (4.11), and (4.12) are bounded, where the bound on the system error satisfies the a-priori given, user-defined time-varying performance bound*

$$\|e(t)\|_P < \varepsilon(t), \quad t \geq 0. \tag{4.13}$$

Proof. To show boundedness of the closed-loop dynamical system given by (4.10), (4.11), and (4.12), consider the energy function $V : \mathcal{D}_\varepsilon \times \mathbb{R}^{(n+s)\times m} \times \mathbb{R} \to \overline{\mathbb{R}}_+$ given by

$$V(e,\tilde{W},\tilde{q}) = \phi(\|e\|_P) + \gamma_1^{-1}\mathrm{tr}\left[(\tilde{W}\Lambda^{1/2})^{\mathrm{T}}(\tilde{W}\Lambda^{1/2})\right] + \gamma_2^{-1}\tilde{q}^2\lambda_{\max}(P)\lambda_{\min}(PB\Lambda B^{\mathrm{T}}P), \tag{4.14}$$

where $\mathcal{D}_\varepsilon \triangleq \{e(t) : \|e(t)\|_P < \varepsilon(t)\}$, and $P \in \mathbb{R}_+^{n\times n}$ is a solution of the Lyapunov equation in (D.9) with $R \in \mathbb{R}_+^{n\times n}$. Note that $V(0,0,0) = 0$, $V\left(e,\tilde{W},\tilde{q}\right) > 0$ for $\left(e,\tilde{W},\tilde{q}\right) \neq (0,0,0)$, and

$$\frac{\mathrm{d}\phi(\|e(t)\|_P)}{\mathrm{d}t} = 2\phi_d(\|e(t)\|_P)e^{\mathrm{T}}(t)P\dot{e}(t) - 2\phi_d(\|e(t)\|_P)\|e(t)\|_P^2\frac{\dot{\varepsilon}(t)}{\varepsilon(t)}. \tag{4.15}$$

Specifically, the time derivative of (4.14) along the closed-loop system trajectories (4.10), (4.11), and (4.12) is given by

$$\begin{aligned}
\dot{V}\left(e(t),\tilde{W}(t),\tilde{q}(t)\right) &= \frac{\mathrm{d}\phi(\|e(t)\|_P)}{\mathrm{d}t} + 2\gamma_1^{-1}\mathrm{tr}\tilde{W}^{\mathrm{T}}(t)\dot{\tilde{W}}(t)\Lambda + 2\gamma_2^{-1}\tilde{q}(t)\dot{\tilde{q}}(t)\lambda_{\max}(P)\lambda_{\min}(PB\Lambda B^{\mathrm{T}}P)\\
&= 2\phi_d(\|e(t)\|_P)e^{\mathrm{T}}(t)P\dot{e}(t) - 2\phi_d(\|e(t)\|_P)\|e(t)\|_P^2\frac{\dot{\varepsilon}(t)}{\varepsilon(t)}\\
&\quad + 2\gamma_1^{-1}\mathrm{tr}\tilde{W}^{\mathrm{T}}(t)\left(\gamma_1\mathrm{Proj_m}\left(\hat{W}(t),\phi_d(\|e(t)\|_P)\sigma\left(x(t)\right)e^{\mathrm{T}}(t)PB\right) - \dot{W}(t)\right)\Lambda\\
&\quad + 2\gamma_2^{-1}\tilde{q}(t)\dot{\tilde{q}}(t)\lambda_{\max}(P)\lambda_{\min}(PB\Lambda B^{\mathrm{T}}P)\\
&= 2\phi_d(\|e(t)\|_P)e^{\mathrm{T}}(t)PA_{\mathrm{r}}e(t) - 2\phi_d(\|e(t)\|_P)e^{\mathrm{T}}(t)PB\Lambda\tilde{W}^{\mathrm{T}}(t)\sigma\left(x(t)\right)\\
&\quad + 2\mathrm{tr}\tilde{W}^{\mathrm{T}}(t)\mathrm{Proj_m}\left(\hat{W}(t),\phi_d(\|e(t)\|_P)\sigma\left(x(t)\right)e^{\mathrm{T}}(t)PB\right)\Lambda\\
&\quad - 2\gamma_1^{-1}\mathrm{tr}\tilde{W}^{\mathrm{T}}(t)\dot{W}(t)\Lambda - 2\phi_d(\|e(t)\|_P)e^{\mathrm{T}}(t)PB\Lambda\nu(t)\\
&\quad - 2\phi_d(\|e(t)\|_P)\|e(t)\|_P^2\frac{\dot{\varepsilon}(t)}{\varepsilon(t)} + 2\gamma_2^{-1}\tilde{q}(t)\dot{\tilde{q}}(t)\lambda_{\max}(P)\lambda_{\min}(PB\Lambda B^{\mathrm{T}}P)\\
&= 2\phi_d(\|e(t)\|_P)e^{\mathrm{T}}(t)PA_{\mathrm{r}}e(t) - 2\mathrm{tr}\left(\hat{W}^{\mathrm{T}}(t) - W^{\mathrm{T}}(t)\right)\Bigg(\phi_d(\|e(t)\|_P)\sigma\left(x(t)\right)\\
&\quad \cdot e^{\mathrm{T}}(t)PB - \mathrm{Proj_m}\left(\hat{W}(t),\phi_d(\|e(t)\|_P)\sigma\left(x(t)\right)e^{\mathrm{T}}(t)PB\right)\Bigg)\Lambda\\
&\quad - 2\gamma_1^{-1}\mathrm{tr}\tilde{W}^{\mathrm{T}}(t)\dot{W}(t)\Lambda - 2\phi_d(\|e(t)\|_P)e^{\mathrm{T}}(t)PB\Lambda\nu(t)\\
&\quad - 2\phi_d(\|e(t)\|_P)\|e(t)\|_P^2\frac{\dot{\varepsilon}(t)}{\varepsilon(t)} + 2\gamma_2^{-1}\tilde{q}(t)\dot{\tilde{q}}(t)\lambda_{\max}(P)\lambda_{\min}(PB\Lambda B^{\mathrm{T}}P).
\end{aligned} \tag{4.16}$$

Now, using the property of projection operator stated in Appendix F, one can write

$$\begin{aligned}\dot{V}\big(e(t),\tilde{W}(t),\tilde{q}(t)\big) \;\leq\; & -\phi_d(\|e(t)\|_P)e^{\mathrm{T}}(t)Re(t)+d-2\phi_d(\|e(t)\|_P)e^{\mathrm{T}}(t)PB\Lambda v(t)\\ & -2\phi_d(\|e(t)\|_P)\|e(t)\|_P^2\frac{\dot{\varepsilon}(t)}{\varepsilon(t)}+2\gamma_2^{-1}\tilde{q}(t)\dot{\tilde{q}}(t)\lambda_{\max}(P)\lambda_{\min}(PB\Lambda B^{\mathrm{T}}P). \qquad (4.17)\end{aligned}$$

In addition, using the proposed additive signal $v(t)$ in (4.8), it follows from (4.17) that

$$\begin{aligned}\dot{V}\big(e(t),\tilde{W}(t),\tilde{q}(t)\big) \;\leq\; & -\phi_d(\|e(t)\|_P)e^{\mathrm{T}}(t)Re(t)+d\\ & -2\phi_d(\|e(t)\|_P)e^{\mathrm{T}}(t)PB\Lambda B^{\mathrm{T}}Pe(t)\hat{q}(t)\frac{|\dot{\varepsilon}(t)|}{\varepsilon(t)}\lambda_{\max}(P)\\ & -2\phi_d(\|e(t)\|_P)\|e(t)\|_P^2\frac{\dot{\varepsilon}(t)}{\varepsilon(t)}+2\gamma_2^{-1}\tilde{q}(t)\dot{\tilde{q}}(t)\lambda_{\max}(P)\lambda_{\min}(PB\Lambda B^{\mathrm{T}}P)\\ \leq\; & -\phi_d(\|e(t)\|_P)e^{\mathrm{T}}(t)Re(t)+d\\ & -2\phi_d(\|e(t)\|_P)\|e(t)\|_2^2\hat{q}(t)\frac{|\dot{\varepsilon}(t)|}{\varepsilon(t)}\lambda_{\max}(P)\lambda_{\min}(PB\Lambda B^{\mathrm{T}}P)\\ & +2\phi_d(\|e(t)\|_P)\|e(t)\|_P^2\frac{|\dot{\varepsilon}(t)|}{\varepsilon(t)}+2\gamma_2^{-1}\tilde{q}(t)\dot{\tilde{q}}(t)\lambda_{\max}(P)\lambda_{\min}(PB\Lambda B^{\mathrm{T}}P)\\ \leq\; & -\phi_d(\|e(t)\|_P)e^{\mathrm{T}}(t)Re(t)+d\\ & -2\phi_d(\|e(t)\|_P)\|e(t)\|_2^2\hat{q}(t)\frac{|\dot{\varepsilon}(t)|}{\varepsilon(t)}\lambda_{\max}(P)\lambda_{\min}(PB\Lambda B^{\mathrm{T}}P)\\ & +2\phi_d(\|e(t)\|_P)e^{\mathrm{T}}(t)Pe(t)\frac{|\dot{\varepsilon}(t)|}{\varepsilon(t)}q\lambda_{\min}(PB\Lambda B^{\mathrm{T}}P)\\ & +2\gamma_2^{-1}\tilde{q}(t)\dot{\tilde{q}}(t)\lambda_{\max}(P)\lambda_{\min}(PB\Lambda B^{\mathrm{T}}P)\\ \leq\; & -\phi_d(\|e(t)\|_P)e^{\mathrm{T}}(t)Re(t)+d\\ & -2\phi_d(\|e(t)\|_P)\|e(t)\|_2^2\tilde{q}(t)\frac{|\dot{\varepsilon}(t)|}{\varepsilon(t)}\lambda_{\max}(P)\lambda_{\min}(PB\Lambda B^{\mathrm{T}}P)\\ & +2\gamma_2^{-1}\tilde{q}(t)\dot{\tilde{q}}(t)\lambda_{\max}(P)\lambda_{\min}(PB\Lambda B^{\mathrm{T}}P)\\ \leq\; & -\phi_d(\|e(t)\|_P)e^{\mathrm{T}}(t)Re(t)+d\\ & +2\big(\hat{q}(t)-q\big)\Big(\mathrm{Proj}\Big(\hat{q}(t),\phi_d(\|e(t)\|_P)\|e(t)\|_2^2\frac{|\dot{\varepsilon}(t)|}{\varepsilon(t)}\Big)\\ & -\phi_d(\|e(t)\|_P)\|e(t)\|_2^2\frac{|\dot{\varepsilon}(t)|}{\varepsilon(t)}\Big)\lambda_{\max}(P)\lambda_{\min}(PB\Lambda B^{\mathrm{T}}P). \qquad (4.18)\end{aligned}$$

Once again, using the property of projection operator stated in Appendix F, one further writes

$$\dot{V}\big(e(t),\tilde{W}(t),\tilde{q}(t)\big) \;\leq\; -\phi_d(\|e(t)\|_P)e^{\mathrm{T}}(t)Re(t)+d. \qquad (4.19)$$

Finally, it follows from (4.19) that

$$\begin{aligned}
\dot{V}\big(e(t),\tilde{W}(t),\tilde{q}(t)\big) &\leq -\alpha\phi_d(\|e(t)\|_P)e^{\mathrm{T}}(t)Pe(t)+d+\frac{1}{2}\alpha\phi(\|e(t)\|_P)-\frac{1}{2}\alpha\phi(\|e(t)\|_P)\\
&\quad+\frac{1}{2}\alpha\gamma_1^{-1}\mathrm{tr}\big[(\tilde{W}\Lambda^{1/2})^{\mathrm{T}}(\tilde{W}\Lambda^{1/2})\big]-\frac{1}{2}\alpha\gamma_1^{-1}\mathrm{tr}\big[(\tilde{W}\Lambda^{1/2})^{\mathrm{T}}(\tilde{W}\Lambda^{1/2})\big]\\
&\quad+\frac{1}{2}\alpha\gamma_2^{-1}\tilde{q}^2(t)\lambda_{\max}(P)\lambda_{\min}(PB\Lambda B^{\mathrm{T}}P)-\frac{1}{2}\alpha\gamma_2^{-1}\tilde{q}^2(t)\lambda_{\max}(P)\\
&\quad\cdot\lambda_{\min}(PB\Lambda B^{\mathrm{T}}P)\\
&\leq -\frac{1}{2}\alpha\Big(\phi(\|e(t)\|_P)+\gamma_1^{-1}\mathrm{tr}\big[(\tilde{W}\Lambda^{1/2})^{\mathrm{T}}(\tilde{W}\Lambda^{1/2})\big]+\gamma_2^{-1}\tilde{q}^2(t)\lambda_{\max}(P)\\
&\quad\cdot\lambda_{\min}(PB\Lambda B^{\mathrm{T}}P)\Big)-\alpha\Big[\phi_d(\|e(t)\|_P)e^{\mathrm{T}}(t)Pe(t)-\frac{1}{2}\phi(\|e(t)\|_P)\Big]\\
&\quad+\frac{1}{2}\alpha\gamma_1^{-1}\mathrm{tr}\big[(\tilde{W}\Lambda^{1/2})^{\mathrm{T}}(\tilde{W}\Lambda^{1/2})\big]+\frac{1}{2}\alpha\gamma_2^{-1}\tilde{q}^2(t)\lambda_{\max}(P)\lambda_{\min}(PB\Lambda B^{\mathrm{T}}P)+d\\
&\leq -\frac{1}{2}\alpha V(e,\tilde{W},\tilde{q})-\alpha\Big[\phi_d(\|e(t)\|_P)e^{\mathrm{T}}(t)Pe(t)-\frac{1}{2}\phi(\|e(t)\|_P)\Big]+\mu. \qquad (4.20)
\end{aligned}$$

Using the property (F.3), the expression (4.20) can be rewritten as

$$\dot{V}\big(e(t),\tilde{W}(t),\tilde{q}(t)\big) \leq -\frac{1}{2}\alpha V(e,\tilde{W},\tilde{q})+\mu, \qquad (4.21)$$

where $\alpha \triangleq \frac{\lambda_{\min}(R)}{\lambda_{\max}(P)}$, $d \triangleq 2\gamma_1^{-1}\tilde{w}\,\dot{w}\|\Lambda\|_2$, and $\mu \triangleq \frac{1}{2}\alpha\gamma_1^{-1}\tilde{w}^2\|\Lambda\|_2+\frac{1}{2}\alpha\gamma_2^{-1}\tilde{q}_{\max}^2+d$, with $\tilde{q}_{\max} \triangleq q_{\max}+\hat{q}_{\max}$. Now, using similar steps in Remark 3.3 of [1], it follows from (4.21) that $V(e,\tilde{W},\tilde{q})$ is upper bounded by

$$V_{\max} \triangleq \max\Big\{V_0,\frac{2\mu}{\alpha}\Big\}, \quad V_0 \triangleq V(e(0),\tilde{W}(0),\tilde{q}(0)). \qquad (4.22)$$

From (4.14), one can also write

$$\phi(\|e(t)\|_P)+\gamma_1^{-1}\mathrm{tr}\big[(\tilde{W}(t)\Lambda^{1/2})^{\mathrm{T}}(\tilde{W}(t)\Lambda^{1/2})\big]+\gamma_2^{-1}\tilde{q}^2(t)\lambda_{\max}(P)\lambda_{\min}(PB\Lambda B^{\mathrm{T}}P) \leq V_{\max},\ t\geq 0. \qquad (4.23)$$

Hence, $\phi(\|e(t)\|_P) \leq V_{\max}$, $t\geq 0$. Now, since $\|e_0\|_P < \varepsilon(0)$, it follows from (4.6) that $\|e(t)\|_P < \varepsilon(t), t\geq 0$, which gives the result. ■

Remark 4.1.3 *For visualization, block diagram of the direct approach introduced and analyzed in this subsection is given in Figure 4.2. This generalized set-theoretic model reference adaptive control architecture provides the flexibility to control the closed-loop system performance as desired on different time intervals. This flexibility results from the selection of the user-defined time-varying parameter* $\varepsilon(t)$, $t\geq 0$,

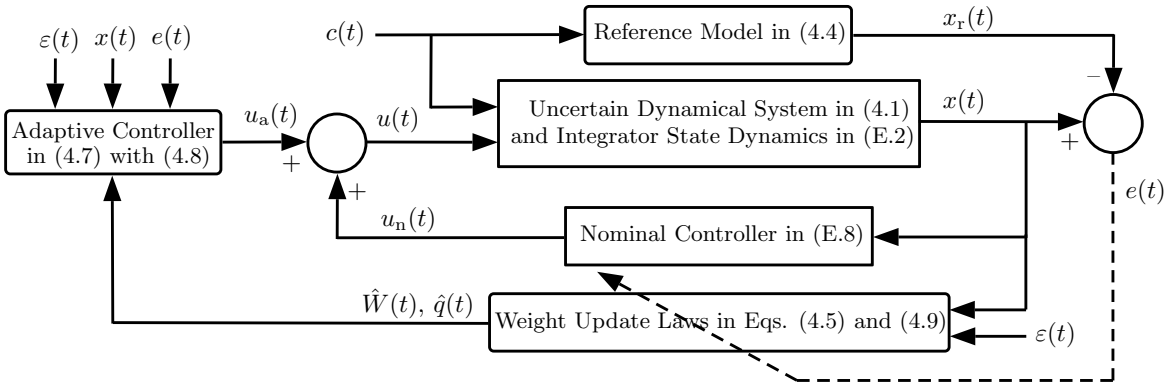

Figure 4.2: Block diagram of the set-theoretic model reference adaptive control architecture in Section 4.1.3.1.

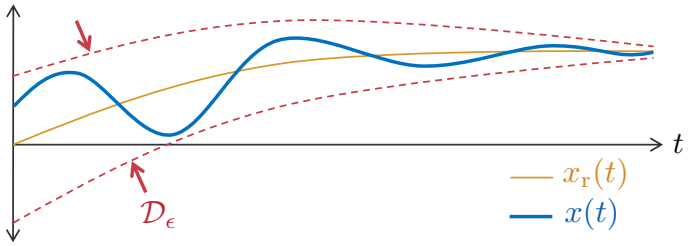

Figure 4.3: Illustration of the user-defined time-varying performance bound in Remark 4.1.3 for scalar reference model and uncertain dynamical system trajectories.

which upper bounds the system error (4.13). Comparable to Figure 4.1 depicting the constant performance bound case, Figure 4.3 illustrates this time-varying performance bound for scalar reference model and uncertain dynamical system trajectories.

4.1.3.2 Indirect Approach

In this subsection, we now present the indirect approach as an alternative to the direct approach presented above. To this end, we modify the reference model without significantly changing the control architecture of [1] to achieve the same objective of enforcing user-defined time-varying performance bounds. Mathematically speaking, we consider the modified reference model given by

$$\dot{x}_{\mathrm{r_m}}(t) = A_{\mathrm{r}}x_{\mathrm{r_m}}(t)+B_{\mathrm{r}}c(t)+\zeta(t), \quad x_{\mathrm{r_m}}(0)=x_{\mathrm{r0}}, \quad t\geq 0, \tag{4.24}$$

where $\zeta(t)\in\mathbb{R}^n$, $t\geq 0$, is an added term defined below and $x_{\mathrm{r_m}}(t)\in\mathbb{R}^n$, $t\geq 0$, is the modified reference state vector.

Now, let $e_{\rm m}(t) \triangleq x(t) - x_{\rm r_m}(t), t \geq 0$, and consider the transformation given by

$$e_\xi(t) \quad = \quad \xi(t) e_{\rm m}(t), \quad t \geq 0, \tag{4.25}$$

where $\xi(t) \in \mathbb{R}_+, t \geq 0$, is the scalar transformation parameter, which is introduced to achieve any desired performance bound as discussed below. Moreover, for the indirect approach of this subsection, we consider the generalized restricted potential function given by

$$\phi(\|z\|_{\rm H}) = \frac{\|z\|_{\rm H}^2}{\varepsilon_0 - \|z\|_{\rm H}}, \quad z \in \mathcal{D}_{\varepsilon_0}, \tag{4.26}$$

which has the partial derivative $\phi_d(\|z\|_{\rm H}) = \varepsilon_0 - \frac{1}{2}\|z\|_{\rm H}/\big(\varepsilon_0 - \|z\|_{\rm H}\big)^2 > 0$, $z \in \mathcal{D}_{\varepsilon_0}$, with respect to $\|z\|_{\rm H}^2$ satisfying $2\phi_d(\|z\|_{\rm H})\|z\|_{\rm H}^2 - \phi(\|z\|_{\rm H}) = \varepsilon_0\|z\|_{\rm H}^2/\big(\varepsilon_0 - \|z\|_{\rm H}\big)^2 > 0$, $z \in \mathcal{D}_{\varepsilon_0}$. It is clear that (4.26) satisfies all properties *i)–vi)* stated in the last paragraph of Appendix F with ε_0 being a positive and bounded-away-from-zero parameter.

Next, let the adaptive control law be given by (4.3), where $\hat{W}(t) \in \mathbb{R}^{(s+n)\times m}$, $t \geq 0$, is the estimate of $W(t)$, $t \geq 0$, satisfying the update law

$$\dot{\hat{W}}(t) = \gamma_1 {\rm Proj_m}\Big(\hat{W}(t), \xi(t)\phi_d(\|e_\xi(t)\|_P)\sigma\big(x(t)\big)e_\xi^{\rm T}(t)PB\Big), \quad \hat{W}(0) = \hat{W}_0, \quad t \geq 0, \tag{4.27}$$

with $\hat{W}_{\max}$ being the projection norm bound. In (4.27), $\gamma_1 \in \mathbb{R}_+$ is the learning rate (i.e., adaptation gain), $P \in \mathbb{R}_+^{n\times n}$ is a solution of the Lyapunov equation given by (D.9). One can readily construct the error dynamics as

$$\dot{e}_{\rm m}(t) \quad = \quad A_{\rm r} e_{\rm m}(t) - B\Lambda\tilde{W}^{\rm T}(t)\sigma\big(x(t)\big) - \zeta(t), \quad e_{\rm m}(0) = e_{\rm m0}, \quad t \geq 0, \tag{4.28}$$

where it follows from (4.25) that

$$\dot{e}_\xi(t) \quad = \quad \dot{\xi}(t)e_{\rm m}(t) + A_{\rm r}e_\xi(t) - B\xi(t)\Lambda\tilde{W}^{\rm T}(t)\sigma\big(x(t)\big) - \xi(t)\zeta(t), \quad e_\xi(0) = e_{\xi 0}, \quad t \geq 0. \tag{4.29}$$

Finally, let

$$\zeta(t) \quad \triangleq \quad \dot{\xi}(t)\xi^{-1}(t)e_{\rm m}(t), \quad t \geq 0, \tag{4.30}$$

where it now follows from (4.29) that

$$\dot{e}_{\xi}(t) \quad = \quad A_{\mathrm{r}} e_{\xi}(t) - \xi(t) B \Lambda \tilde{W}^{\mathrm{T}}(t) \sigma\big(x(t)\big), \quad e_{\xi}(0) = e_{\xi 0}, \quad t \geq 0, \tag{4.31}$$

which denotes the transformed system error dynamics. For the next theorem presenting the second contribution of this paper, one can also give the weight estimation error dynamics as

$$\dot{\tilde{W}}(t) = \gamma_1 \mathrm{Proj}_{\mathrm{m}}\big(\hat{W}(t), \xi(t) \phi_d(\|e_{\xi}(t)\|_P) \sigma\big(x(t)\big) e_{\xi}^{\mathrm{T}}(t) P B\big) - \dot{W}(t), \quad \tilde{W}(0) = \tilde{W}_0, \quad t \geq 0, \tag{4.32}$$

where $\tilde{W}(t) \triangleq \hat{W}(t) - W(t)$, $t \geq 0$. Note that we inherently assume $\xi(t)$, $t \geq 0$, and $\dot{\xi}(t)$, $t \geq 0$, are smooth and bounded user-defined functions.

Theorem 4.1.2 *Consider the uncertain dynamical system given by (4.1) subject to Assumption D.1, the reference model given by (4.4), and the feedback control law given by (D.7) along with (D.8), (4.3), and (4.27). If* $\|e_{\mathrm{m}0}\|_P < \frac{\varepsilon_0}{\xi(0)}$, *then the closed-loop dynamical system given by (4.31) and (4.32) are bounded, where the bound on the system error satisfies the a-priori given, user-defined time-varying performance bound*

$$\|e_{\mathrm{m}}(t)\|_P < \frac{\varepsilon_0}{\xi(t)}, \quad t \geq 0. \tag{4.33}$$

Proof. To show boundedness of the closed-loop dynamical system given by (4.31) and (4.32) consider the energy function $V : \mathcal{D}_{\varepsilon_0} \times \mathbb{R}^{(n+s)\times m} \to \overline{\mathbb{R}}_+$ given by

$$V(e_{\xi}, \tilde{W}) = \phi(\|e_{\xi}\|_P) + \gamma_1^{-1} \mathrm{tr}\big[(\tilde{W}\Lambda^{1/2})^{\mathrm{T}} (\tilde{W}\Lambda^{1/2})\big], \tag{4.34}$$

where $\mathcal{D}_{\varepsilon_0} \triangleq \{e_{\xi}(t) : \|e_{\xi}(t)\|_P < \varepsilon_0\}$, and $P \in \mathbb{R}_+^{n\times n}$ is a solution of the Lyapunov equation in (D.9) with $R \in \mathbb{R}_+^{n\times n}$. Note that $V(0,0) = 0$, $V\big(e_{\xi}, \tilde{W}\big) > 0$ for $\big(e_{\xi}, \tilde{W}\big) \neq (0,0)$, and it follows from similar steps in Theorem 3.1 of [1] that

$$\dot{V}\big(e_{\xi}(t), \tilde{W}(t)\big) \quad \leq \quad -\frac{1}{2}\alpha V(e_{\xi}, \tilde{W}) + \mu, \tag{4.35}$$

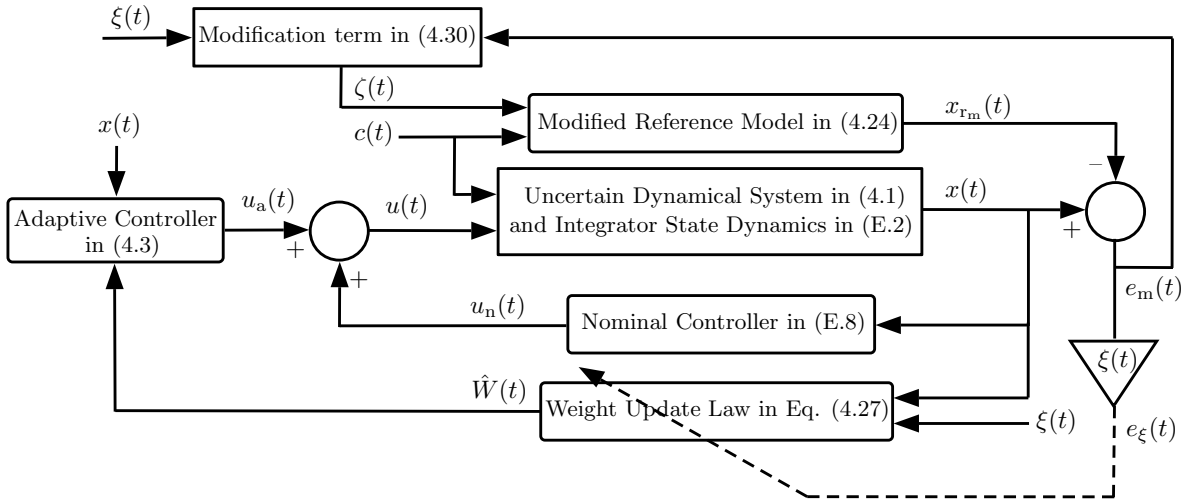

Figure 4.4: Block diagram of the set-theoretic model reference adaptive control architecture in Section 4.1.3.2.

where $\alpha \triangleq \frac{\lambda_{\min}(R)}{\lambda_{\max}(P)}$, $d \triangleq 2\gamma_1^{-1}\tilde{w}\,\dot{w}\|\Lambda\|_2$, and $\mu \triangleq \frac{1}{2}\alpha\gamma_1^{-1}\tilde{w}^2\|\Lambda\|_2 + d$. By applying Lemma 1 of [25] and [23], the boundedness of the closed-loop dynamical system (4.31) and (4.32) is immediate, where the bound on the system error satisfies the a-priori given, user-defined performance bound

$$\|e_{\xi}(t)\|_P < \varepsilon_0, \quad t \geq 0. \tag{4.36}$$

Now, by using (4.25) one can readily obtain

$$\|e_{\mathrm{m}}(t)\|_P < \frac{\varepsilon_0}{\xi(t)}, \quad t \geq 0, \tag{4.37}$$

which completes the proof. ■

Remark 4.1.4 *For visualization, block diagram of the indirect approach introduced and analyzed in this subsection is given in Figure 4.4. Specifically, as a consequence of Theorem 4.1.2 and for a given ε_0, the term $\xi(t), t \geq 0$, can be adjusted in order to control the closed-loop system performance as desired on different time intervals. Here, we note that since the modified reference model differs from the ideal, unmodified reference model in* (4.4) *by the magnitude of $\zeta(t), t \geq 0$, given by (4.30), one can readily conclude that if the time rate of change of $\xi(t), t \geq 0$, is small, then the modified reference model approximately behaves as the ideal, unmodified reference model considering that the magnitudes of $\xi^{-1}(t), t \geq 0$, and $e_{\mathrm{m}}(t), t \geq 0$, are not large.*

Remark 4.1.5 *We now make the argument given in the last sentence of Remark 4.1.4 rigorous. To this end, define* $\tilde{x}(t) \triangleq x_{\mathrm{r_m}}(t) - x_{\mathrm{r}}(t), t \geq 0$, *which captures the distance between the modified reference model state vector and the ideal, unmodified reference model state vector. Now, using* (4.4) *and* (4.24)*, one can write*

$$\dot{\tilde{x}}(t) = A_{\mathrm{r}}\tilde{x}(t) + \dot{\xi}(t)\xi^{-1}(t)e_{\mathrm{m}}(t), \quad \tilde{x}(0) = 0, \quad t \geq 0. \tag{4.38}$$

Using the fact that for an asymptotically stable matrix $A_{\mathrm{r}} \in \mathbb{R}^{n\times n}$, $\|e^{A_{\mathrm{r}}t}\| \leq \kappa e^{-\beta t}, t \geq 0$, *where* $\kappa > 0$ *and* $0 < \beta < -\alpha(A_{\mathrm{r}})$, *where* $\alpha(A_{\mathrm{r}}) \triangleq \max\{\mathrm{Re}(\lambda) : \lambda \in \mathrm{spec}(A_r)\}$ *[109], it follows that*

$$\|\tilde{x}(t)\|_2 \leq \frac{\kappa}{\beta}|\dot{\xi}(t)|\,|\xi^{-1}(t)|\,\|e_{\mathrm{m}}(t)\|_2, \quad t \geq 0. \tag{4.39}$$

Since $\xi(t)$, $t \geq 0$, *and* $\dot{\xi}(t)$, $t \geq 0$, *are considered to be smooth and bounded user-defined functions, one can write* $\xi(t) \geq \underline{\xi}, t \geq 0$, *and* $\dot{\xi}(t) \leq \overline{\dot{\xi}}, t \geq 0$*; hence, it follows from (4.37) and (4.39) that*

$$\|\tilde{x}(t)\|_2 \leq \frac{\kappa\overline{\dot{\xi}}\varepsilon_0}{\beta\underline{\xi}^2\sqrt{\lambda_{\min}(P)}}, \quad t \geq 0. \tag{4.40}$$

As expected, (4.40) now rigorously shows that if the time rate of change of $\xi(t)$ *is small, then the modified reference model approximately behaves as the ideal, unmodified reference model. Finally, one can also compute the worst-case deviation of the uncertain system trajectory from the ideal, unmodified system trajectory as*

$$\begin{aligned}\|x(t) - x_{\mathrm{r}}(t)\|_2 &= \|e_{\mathrm{m}}(t) + \tilde{x}(t)\|_2 \leq \|e_{\mathrm{m}}(t)\|_2 + \|\tilde{x}(t)\|_2 \\ &\leq \frac{\varepsilon_0}{\underline{\xi}\sqrt{\lambda_{\min}(P)}} + \frac{\kappa\overline{\dot{\xi}}\varepsilon_0}{\beta\underline{\xi}^2\sqrt{\lambda_{\min}(P)}} \\ &\leq \frac{\varepsilon_0}{\underline{\xi}\sqrt{\lambda_{\min}(P)}}\Big[1 + \frac{\kappa\overline{\dot{\xi}}}{\beta\underline{\xi}}\Big], \quad t \geq 0.\end{aligned} \tag{4.41}$$

4.1.4 Illustrative Numerical Example

We now present a numerical example to illustrate the direct and indirected generalized set-theoretic model reference adaptive control approaches presented in Theorems 4.1.1 and 4.1.2. For this purpose, consider the uncertain dynamical system representing a controlled wing rock dynamics model [32]

$$\dot{x}_{\rm p}(t) = \begin{bmatrix} 0 & 1 \\ 0 & 0 \end{bmatrix} x_{\rm p}(t) + \begin{bmatrix} 0 \\ 1 \end{bmatrix} \Big(\Lambda u(t) + \delta_{\rm p}(t, x_{\rm p}(t)) \Big), \quad x_{\rm p}(0) = 0 \quad t \geq 0, \tag{4.42}$$

where $x_{\rm p}(t) = \begin{bmatrix} x_{\rm p1}(t) & x_{\rm p2}(t) \end{bmatrix}^{\rm T}$ with $x_{\rm p1}(t)$ representing the roll angle (in rad) and $x_{\rm p2}(t)$ representing the roll rate (in rad/sec). In (4.42), $\delta_{\rm p}(t, x_{\rm p}(t))$ represents an uncertainty of the form

$$\delta_{\rm p}(t, x_{\rm p}(t)) = \alpha_1 \sin(t) + \alpha_2 x_{\rm p1} + \alpha_3 x_{\rm p2} + \alpha_4 |x_{\rm p1}| x_{\rm p2} + \alpha_5 |x_{\rm p2}| x_{\rm p2} + \alpha_6 x_{\rm p1}^3, \tag{4.43}$$

with $\alpha_1 = 0.25$, $\alpha_2 = 0.5$, $\alpha_3 = 1.0$, $\alpha_4 = -1.0$, $\alpha_5 = 1.0$, and $\alpha_6 = 1.0$, and $\Lambda = 0.75$ represents an uncertain control effectiveness matrix. For command following, we let $E_{\rm p} = \begin{bmatrix} 1, & 0 \end{bmatrix}$ in (D.2) and choose a linear nominal controller gain matrix $K = [5.49, 3.78, 2.89]$ in (D.8), which yields to the reference model given by

$$\dot{x}_{\rm r}(t) = \begin{bmatrix} 0 & 1 & 0 \\ -5.5 & -3.8 & -2.9 \\ 1 & 0 & 0 \end{bmatrix} x_{\rm r}(t) + \begin{bmatrix} 0 \\ 0 \\ -1 \end{bmatrix} c(t) \quad x_{\rm r}(0) = 0 \quad t \geq 0. \tag{4.44}$$

In addition, we choose the basis function as

$$\sigma(x) = \begin{bmatrix} 1, & x_{\rm p1}, & x_{\rm p2}, & |x_{\rm p1}| x_{\rm p2}, & |x_{\rm p2}| x_{\rm p2}, & x_{\rm p1}^3, & x^{\rm T} \end{bmatrix}^{\rm T}. \tag{4.45}$$

For the proposed set-theoretic model reference adaptive control architecture in Theorem 4.1.1, we use the generalized restricted potential function given in (4.6). We choose the smooth time-varying performance bound $\varepsilon(t), t \geq 0$. Finally, we set the projection norm bounds imposed on each element of the weight estimate and adaptive parameter estimate to $\hat{W}_{\max} = 15$ and $\hat{q}_{\max} = 10$ respectively, and use $R = I$ to calculate P from (D.9) for the resulting $A_{\rm r}$ matrix. Figures regarding the closed-loop dynamical system performance are not presented since the system response with the nominal controller is unstable. In Figure 4.5, we apply the proposed set-theoretic adaptive controller with $\gamma_1 = 1$ and $\gamma_2 = 1$, where Figure 4.6 clearly illustrates its efficacy as well as the results of Theorem 4.1.1.

For the proposed set-theoretic model reference adaptive control architecture in Theorem 4.1.2, we use the generalized restricted potential function given by (4.26) with $\varepsilon_0 = 1$ and we set the scalar

transformation parameter in (4.25) to $\varepsilon^{-1}(t)$ (to have the same time-varying performance bound we have as above in this example for Theorem 4.1.1). Furthermore, we set the projection norm bound imposed on each element of the parameter estimate to $\hat{W}_{\max} = 15$ and use $R = I$ to calculate P from (D.9) for the resulting

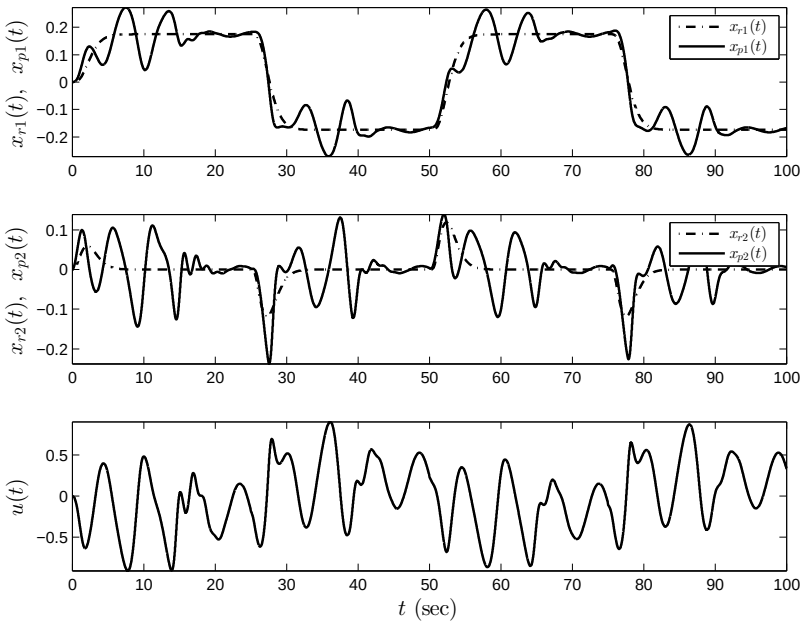

Figure 4.5: Command following performance with the generalized direct set-theoretic model reference adaptive control approach in Theorem 4.1.1.

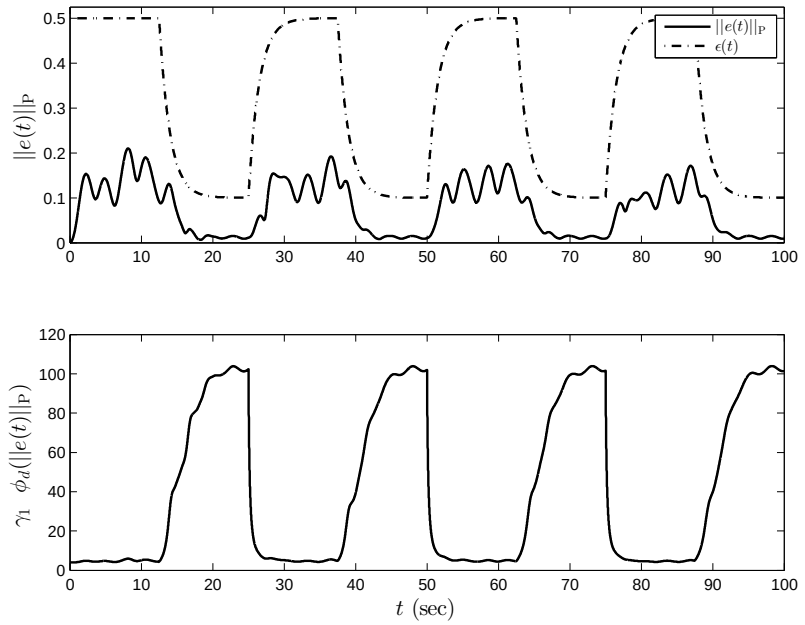

Figure 4.6: Norm of the system error trajectories with the generalized direct set-theoretic model reference adaptive control approach and the evolution of the effective learning rate $\gamma_1 \phi_{\mathrm{d}}(\cdot)$ in Theorem 4.1.1.

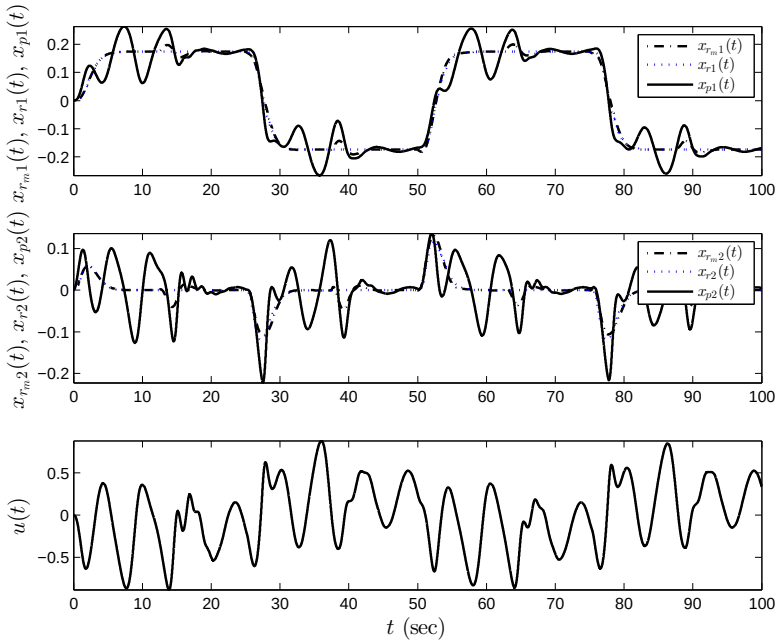

Figure 4.7: Command following performance with the generalized indirect set-theoretic model reference adaptive control approach in Theorem 4.1.2.

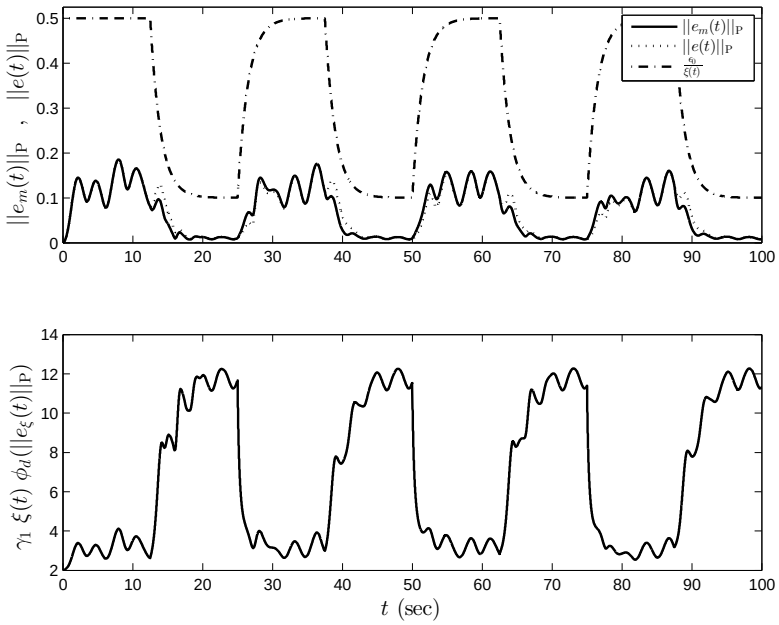

Figure 4.8: Norm of the system error trajectories with the generalized indirect set-theoretic model reference adaptive control approach and the evolution of the effective learning rate $\gamma_1 \xi(t)\phi_{\mathrm{d}}(\cdot)$ in Theorem 4.1.2.

A_{r} matrix. Figure 4.7 shows the closed-loop dynamical system performance with the proposed controller in Theorem 4.1.2 with $\gamma_1 = 1$, where Figure 4.8 clearly illustrates its efficacy and the results in Theorem 4.1.2.

4.1.5 Conclusion

In this paper, we generalized the set-theoretic model reference adaptive control framework in order to enforce user-defined time-varying performance bounds on the norm of the system error (i.e., the difference between the state of an uncertain dynamical system and the state of a given reference model). This generalization gives the designer a flexibility to control the closed-loop system performance as desired on different time intervals (e.g., transient time interval and steady-state time interval). Specifically, we presented two approaches, namely the direct approach (see Section 4.1.3.1) and the indirect approach (see Section 4.1.3.2), where the stability and performance properties of both architectures were rigorously established. It was noted that the direct approach has the capability to strictly enforce a user-defined time-varying performance bound (see Theorem 4.1.1 and Remark 4.1.3), whereas the indirect approach approximately enforces this performance bound with the approximation accuracy depending on the time rate of change of this bound (see Theorem 4.1.2, Remark 4.1.4, and Remark 4.1.5).

It was further observed from the presented illustrative numerical example (see Section 4.1.4) that both approaches work effectively as expected for the considered adaptive command following problem in the presence of exogenous disturbances and system uncertainties. While the direct approach enforces strict user-defined time-varying performance bounds as compared with the indirect approach enforcing approximate performance bounds, Figures 4.6 and 4.8 showed that the indirect approach results in significantly smaller effective learning rates as compared with the direct approach, where this can be important for certain control systems implementations. Motivated from this standpoint, future research will include high-fidelity simulation studies and experimentations on unmanned aerial vehicles to further understand this interplay between strict versus approximate time-varying performance bound enforcement and their resulting effective learning rates. Future research will also include output-feedback extensions of the proposed approaches for set-theoretic model reference adaptive control in the absence of measurable state vectors.

4.2 A Command Governor Approach to Set-Theoretic Model Reference Adaptive Control for Enforcing Partially Adjustable Performance Guarantees[2]

In feedback control, the presence of system uncertainties cause the system state trajectories to deviate from their ideal responses. In practice, a subset of these trajectories can be more critical than the rest due to physical and/or performance characteristics associated with a problem of interest. As a

[2]This section has been submitted to the *International Journal of Robust and Nonlinear Control* for possible publication.

consequence, it is desired not only to have performance guarantees on the entire system state trajectories but also to be able to adjust the resulting worst-case performance bound specifically for that critical subset. Yet, in the model reference adaptive control of uncertain dynamical systems, assigning performance bounds on a subset of system trajectories is not a trivial problem. In this paper, we address this gap by proposing a new control architecture that has the capability to enforce an a-priori given, user-defined performance bound on the selected subset of dynamical system trajectories, entitled as partially adjustable performance guarantees. The proposed control architecture is predicated on a set-theoretic treatment and utilizes a two-level constructive design framework. In particular, we first form an auxiliary state dynamics in order to construct the auxiliary system error vector between uncertain dynamical system states and this auxiliary dynamics states. This construction aids a control designer to weigh each element of the auxiliary system error vector independently, while enforcing performance bounds on the norm of this error vector. Then, a command governor mechanism is designed for driving a feasible user-selected subset of system states to a close (and user-controllable) neighborhood of the corresponding reference model states. This results in adjustable performance guarantees on a subset of system error trajectories. Two illustrative numerical examples are also provided to demonstrate the efficacy of the proposed architecture.

4.2.1 Introduction

4.2.1.1 Literature Review and Contribution

Model reference adaptive control methods are effective system-theoretical tools, which can cope with the adverse effects in the dynamics of physical systems resulting from exogenous disturbances and system uncertainties. Yet, their resulting worst-case bounds on the system error vector between the states of an uncertain dynamical system and the states of a given ideal reference model may not be practically useful for evaluating their transient and steady-state performance. This is due to (excessive) conservatism of these bounds as well as their dependence on system uncertainties. To overcome this limitation, [1, 2, 18–20, 22] present notable contributions to enforce performance guarantees on the system error vector.

Specifically, the authors of [18] present an error transformation approach to transform an uncertain dynamical system subject to performance constraints into an equivalent form without constraints. Yet, it is assumed that the control signals can access to every element of the state vector. This limitation is addressed in [19], but under the assumption that a desired trajectory and its derivatives are available. The same approach is used in [20] for enforcing constraints on measurable output signals using a switching

controller. Furthermore, restricted potential functions (barrier Lyapunov functions) are employed in [22] to address performance guarantees on the components of system error vector for the systems in Brunovsky normal form, where the system is assumed to be accurate with no uncertainties or external disturbances. We also refer to the introduction section of [1] for other approaches similar in spirit to [18–20, 22].

Unlike the control schemes in [18–20, 22], the authors of [1, 2] considered uncertain dynamical systems subject to performance constraints in the context of model reference adaptive control. In particular, the proposed approach in [1, 2], which is entitled as the set-theoretic model reference adaptive control architecture, has the capability to enforce user-defined strict performance guarantees on the entire norm of the system error vector. Yet, from a practical standpoint, a subset of system state trajectories can be more critical than the rest. As a consequence, it is often desired not only to have strict guarantees on the norm of the entire system error vector but also to be able to adjust the resulting worst-case performance bound specifically for that critical subset. This practical limitation becomes more prominent when the number of system states gets large. Therefore, although the set-theoretic model reference adaptive control architecture allows one to enforce performance guarantees, it can suffer from the fact that the performance guarantees cannot be applied in a readily adjustable way on a subset of system state trajectories (see Section 4.2.1.2 for a motivational example).

In this paper, we address the aforementioned gap by developing a new model reference adaptive control architecture that has the capability to enforce an a-priori given, user-defined performance bound on the selected subset of dynamical system trajectories, entitled as partially adjustable performance guarantees. The proposed control architecture is predicated on a set-theoretic treatment and utilizes a two-level constructive design framework. In particular:

- First, we form an auxiliary state dynamics in order to construct the auxiliary system error vector between uncertain dynamical system states and this auxiliary dynamics states. This construction aids a control designer to weigh each element of the auxiliary system error vector independently, while enforcing performance bounds on the norm of this error vector.
- Then, a command governor mechanism is designed for driving a feasible user-selected subset of system states to a close (and user-controllable) neighborhood of the corresponding reference model states.

Two illustrative numerical examples are also provided to demonstrate the efficacy of the proposed architecture.

We also note that the authors made two earlier attempts in conference papers [110, 111] on achieving partially adjustable strict performance guarantees with the set-theoretic model reference adaptive control architecture, where a convex optimization method is used in [110] (that is not only different than the two-level constructive design framework proposed in this paper but also this optimization procedure involves linear matrix inequalities that may yield to infeasible or near optimal numerical solutions system error vector dimension increases) and the technique adopted in [111] utilizes a restrictive (structural) condition (see Assumption 2 of [111]). Finally, a preliminary conference version of this paper appeared in [112]. The present paper significantly goes beyond this conference version by not only providing detailed proofs for the considered architecture in [112] but also focusing on all the theoretical developments necessary for the generalization of the results with detailed examples, added figures, and motivation.

4.2.1.2 A Motivational Example

To elucidate the motivation behind the proposed approach of this paper, consider an uncertain short-period dynamics given in Example 10.1 of [30]. In this control problem, through applying an adaptive control signal to the elevator deflection $\delta_{\rm e}(t)$, a control designer is interested in driving the short-period states, the angle of attack $\alpha(t)$ and the pitch rate $q(t)$, to a desired reference model trajectory with $\alpha_{\rm r}(t)$ and $q_{\rm r}(t)$ being its states. For this problem setup, the standard set-theoretic model reference adaptive control architecture in [1] can be used to enforce the strict performance bound on the system error vector given by

$$\begin{bmatrix} \alpha(t)-\alpha_{\rm r}(t) & q(t)-q_{\rm r}(t) \end{bmatrix} P \begin{bmatrix} \alpha(t)-\alpha_{\rm r}(t) \\ q(t)-q_{\rm r}(t) \end{bmatrix} < \varepsilon^2, \quad t \geq 0, \tag{4.46}$$

where ε is a user-defined performance bound and P is a positive definite solution for the Lyapunov equation $0 = A_{\rm r}^{\rm T}P + PA_{\rm r} + R$ for a given positive definite R with $A_{\rm r}$ being a Hurwitz system matrix of the desired reference model. Note that the structure of matrix P in (4.46) determines how the user-defined bound ε is distributed among the system error vector components — the angle of attack error and the pitch rate error signals. To further explain this point, consider a scenario where it is essential to track the angle of attack reference signal precisely, but deviation in the pitch rate can be tolerated. In this case, the standard set-theoretic model reference adaptive control architecture does not provide a constructive flexibility for a control designer to prioritize the angle of attack over the pitch rate.

This limitation clearly becomes more prominent as the number of system states gets large. To address this problem, we here present a constructive methodology to develop a new set-theoretic model reference adaptive control architecture to drive a feasible user-selected subset of system states to a close (and user-controllable) neighborhood of the corresponding reference model states, resulting in adjustable performance guarantees on a subset of system error trajectories.

4.2.1.3 Notation

A standard notation is used throughout this paper. In particular, $\mathbb{R}, \mathbb{R}^n$ and $\mathbb{R}^{n\times m}$ respectively denote the set of (real) numbers, the set of $n\times 1$ real column vectors, and the set of $n\times m$ real matrices; $\mathbb{R}_+$ (respectively, $\overline{\mathbb{R}}_+$) and $\mathbb{D}^{n\times n}$ respectively denote the set of positive (respectively, nonnegative-definite) numbers and the set of $n\times n$ matrices with diagonal scalar entries; $0_{n\times n}$ denotes the $n\times n$ zero matrix; and "$\triangleq$" denotes equality by definition. Furthermore, $(\cdot)^{\mathrm{T}}$ stands for the transpose, $(\cdot)^{-1}$ stands for the inverse, $\mathrm{tr}(\cdot)$ stands for the trace, $\|\cdot\|_2$ stands for the Euclidean norm, $\|\cdot\|_{\mathrm{F}}$ stands for the Frobenius norm, $\|\cdot\|_H$ stands for the weighted Euclidean norm (i.e., $\|x\|_A = \sqrt{x^{\mathrm{T}}Ax}$ for $x\in\mathbb{R}^n$ and $A\in\mathbb{R}_+^{n\times n}$), and $\|A\|_2 \triangleq \sqrt{\lambda_{\max}(A^{\mathrm{T}}A)}$ stands for the induced 2-norm of matrix $A\in\mathbb{R}^{n\times m}$. Finally, two key definitions, namely the definition of the projection operator and the definition of the generalized restricted potential function, is included in Appendix F for completeness.

4.2.2 Problem Formulation

In this section, we first present the adaptive command following problem formulation considered in this paper and then provide a concise overview of the set-theoretic model reference adaptive control architecture based on the results documented in [1].

4.2.2.1 Adaptive Command Following

Consider the class of uncertain dynamical systems given by

$$\dot{x}(t) \;=\; Ax(t)+B\Lambda\big(u(t)+\delta(t,x(t))\big), \quad x(0)=x_0, \quad t\geq 0. \tag{4.47}$$

In (4.47), $x(t)\in\mathbb{R}^n$, $t\geq 0$, denotes the measurable state vector, $u(t)\in\mathbb{R}^m$, $t\geq 0$, denotes the control input, $A\in\mathbb{R}^{n\times n}$ denotes a known system matrix, $B\in\mathbb{R}^{n\times m}$ denotes a known input matrix, $\Lambda\in\mathbb{R}_+^{m\times m}\cap\mathbb{D}^{m\times m}$

denotes an unknown control effectiveness matrix, and $\delta : \overline{\mathbb{R}}_+ \times \mathbb{R}^n \to \mathbb{R}^m$ denotes a time-varying system uncertainty due to exogenous disturbances and unknown model parameters. As standard, we consider here that the pair (A,B) is controllable. To capture a desired closed-loop dynamical system behavior, now consider the ideal reference model given by

$$\dot{x}_{\rm ri}(t) \quad = \quad A_{\rm r}x_{\rm ri}(t)+B_{\rm r}c_{\rm d}(t), \quad x_{\rm ri}(0)=x_{\rm ri0}, \quad t \geq 0. \tag{4.48}$$

In (4.48), $x_{\rm ri}(t) \in \mathbb{R}^n$, $t \geq 0$, denotes the ideal reference state vector, $c_{\rm d}(t) \in \mathbb{R}^{n_{\rm c}}$, $t \geq 0$, denotes a desired uniformly continuous bounded command, $A_{\rm r} \in \mathbb{R}^{n \times n}$ denotes the Hurwitz reference model matrix, and $B_{\rm r} \in \mathbb{R}^{n \times n_c}$ denotes the command input matrix. A standard assumption on system uncertainty parameterization is next introduced (see, for example, [28–30]).

Assumption 4.2.1 *Consider the parametrization for the system uncertainty $\delta : \overline{\mathbb{R}}_+ \times \mathbb{R}^n \to \mathbb{R}^m$ given by*

$$\delta(t,x(t)) \quad = \quad W_0^{\rm T}(t)\sigma_0(x(t)). \tag{4.49}$$

In (4.49)*, $W_0(t) \in \mathbb{R}^{s \times m}$, $t \geq 0$, denotes a bounded unknown weight matrix (i.e., $\|W_0(t)\|_{\rm F} \leq w_0$, $t \geq 0$) with a bounded time rate of change (i.e., $\|\dot{W}_0(t)\|_{\rm F} \leq \dot{w}_0$, $t \geq 0$) and $\sigma_0 : \mathbb{R}^n \to \mathbb{R}^s$ denotes a known basis function with the elements $\sigma_{0i}(x(t))$, $i = 1, \ldots, s$.*

Using Assumption 4.2.1, (4.47) can be rewritten as

$$\dot{x}(t) \quad = \quad Ax(t)+B\Lambda\big(u(t)+W_0^{\rm T}(t)\sigma_0(x(t))\big), \quad x(0)=x_0, \quad t \geq 0. \tag{4.50}$$

For (4.50), we now consider the feedback control algorithm given by

$$u(t) = u_{\rm n}(t)+u_{\rm a}(t), \quad t \geq 0. \tag{4.51}$$

In (4.51), $u_{\rm n}(t) \in \mathbb{R}^m$, $t \geq 0$, and $u_{\rm a}(t) \in \mathbb{R}^m$, $t \geq 0$, respectively stand for the nominal and adaptive control laws. Moreover, we consider without loss of much generality that, the nominal control law satisfies the form given by

$$u_{\rm n}(t) = -K_1x(t)+K_2c(t), \quad t \geq 0. \tag{4.52}$$

In (4.52), $K_1 \in \mathbb{R}^{m\times n}$ and $K_2 \in \mathbb{R}^{m\times n_c}$ need to be respectively selected to ensure $A_\mathrm{r} = A - BK_1$ and $B_\mathrm{r} = BK_2$. Furthermore, $c(t) \in \mathbb{R}^{n_\mathrm{c}}$ denotes the actual applied command signal (see Section 4.2.3.1). We let the desired command signal equivalent to the actual one (i.e., $c(t) \equiv c_\mathrm{d}(t), t \geq 0$) only for the results of this section.

Based on the above definitions, (4.50) can be rewritten as

$$\dot{x}(t) = A_\mathrm{r}x(t) + B_\mathrm{r}c(t) + B\Lambda\big(u_\mathrm{a}(t) + W^\mathrm{T}(t)\sigma\big(x(t),c(t)\big)\big), \quad x(0) = x_0, \quad t \geq 0. \tag{4.53}$$

In (4.53), $W(t) \triangleq \big[W_0^\mathrm{T}(t),\ (\Lambda^{-1} - I_{\mathrm{m}\times\mathrm{m}})K_1,\ -(\Lambda^{-1} - I_{\mathrm{m}\times\mathrm{m}})K_2\big]^\mathrm{T} \in \mathbb{R}^{(s+n+n_c)\times m}, t \geq 0$, denotes an unknown weight matrix and $\sigma\big(x(t),c(t)\big) \triangleq \big[\sigma_0^\mathrm{T}\big(x(t)\big),\ x^\mathrm{T}(t),\ c^\mathrm{T}(t)\big]^\mathrm{T} \in \mathbb{R}^{s+n+n_c}$, $t \geq 0$. From Assumption 4.2.1, $\|W(t)\|_\mathrm{F} \leq w, t \geq 0$, and $\|\dot{W}(t)\|_\mathrm{F} \leq \dot{w}, t \geq 0$, directly follows. From the structure of the term "$B\Lambda\big(u_\mathrm{a}(t) + W^\mathrm{T}(t)\sigma\big(x(t),c(t)\big)\big)$" in (4.53), the adaptive control law is chosen as

$$u_\mathrm{a}(t) = -\hat{W}^\mathrm{T}(t)\sigma\big(x(t),c(t)\big), \quad t \geq 0, \tag{4.54}$$

with $\hat{W}(t) \in \mathbb{R}^{(s+n+n_c)\times m}$, $t \geq 0$, being an estimate of $W(t)$, $t \geq 0$. In what follows, we present a concise overview of the main results in [1] for completeness.

4.2.2.2 Standard Set-Theoretic Model Reference Adaptive Control Overview

Following the architecture presented in [1], consider the update law for (4.54) in the form

$$\dot{\hat{W}}(t) = \gamma\mathrm{Proj}_\mathrm{m}\Big(\hat{W}(t), \phi_d(\|e_\mathrm{i}(t)\|_P)\sigma\big(x(t),c(t)\big)e_\mathrm{i}^\mathrm{T}(t)PB\Big), \quad \hat{W}(0) = \hat{W}_0, \quad t \geq 0, \tag{4.55}$$

with the projection norm bound $\hat{W}_\mathrm{max}$. In addition, $\gamma \in \mathbb{R}_+$ stands for the learning rate (i.e., adaptation gain), $P \in \mathbb{R}_+^{n\times n}$ stands for the solution to the Lyapunov equation

$$0 \quad = \quad A_\mathrm{r}^\mathrm{T}P + PA_\mathrm{r} + R, \tag{4.56}$$

with $R \in \mathbb{R}_+^{n\times n}$, and $e_\mathrm{i}(t) \triangleq x(t) - x_\mathrm{ri}(t)$, $t \geq 0$, stands for the system error. The system error dynamics and the weight estimation error dynamics can now be respectively written as

$$\dot{e}_\mathrm{i}(t) \quad = \quad A_\mathrm{r}e_\mathrm{i}(t) - B\Lambda\tilde{W}^\mathrm{T}(t)\sigma\big(x(t),c(t)\big), \quad e_\mathrm{i}(0) = e_\mathrm{i0}, \quad t \geq 0, \tag{4.57}$$

$$\dot{\hat{W}}(t) = \gamma \mathrm{Proj}_{\mathrm{m}}\Big(\hat{W}(t), \phi_d(\|e_{\mathrm{i}}(t)\|_P)\sigma\big(x(t),c(t)\big)e_{\mathrm{i}}^{\mathrm{T}}(t)PB\Big) - \dot{W}(t), \quad \tilde{W}(0) = \tilde{W}_0, \quad t \geq 0. \tag{4.58}$$

Here, $\tilde{W}(t) \triangleq \hat{W}(t) - W(t)$, $t \geq 0$, denotes the weight estimation error.

Remark 4.2.1 *The update law given by* (4.55) *for the standard set-theoretic model reference adaptive control architecture can be derived by considering the following energy function* $V(e_{\mathrm{i}}, \tilde{W}) = \phi(\|e_{\mathrm{i}}\|_P) + \gamma^{-1}\mathrm{tr}\big[(\tilde{W}\Lambda^{1/2})^{\mathrm{T}}(\tilde{W}\Lambda^{1/2})\big]$ *where* $\mathcal{D}_\varepsilon \triangleq \{e_{\mathrm{i}}(t) : \|e_{\mathrm{i}}(t)\|_P < \varepsilon\}$ *and* $P \in \mathbb{R}_+^{n\times n}$ *is the unique solution of the Lyapunov equation in (4.56). Note that* $V(0,0) = 0$, $V(e_{\mathrm{i}}, \tilde{W}) > 0$ *for* $(e_{\mathrm{i}}, \tilde{W}) \neq (0,0)$, *and* $\dot{V}\big(e_{\mathrm{i}}(t), \tilde{W}(t)\big) \leq -\frac{1}{2}\alpha V(e_{\mathrm{i}}, \tilde{W}) + \mu$, *where* $\alpha \triangleq \frac{\lambda_{\min}(R)}{\lambda_{\max}(P)}$, $d \triangleq 2\gamma^{-1}\tilde{w}\,\dot{w}\|\Lambda\|_2$, $\mu \triangleq \frac{1}{2}\alpha\gamma^{-1}\tilde{w}^2\|\Lambda\|_2 + d$, *and* $\tilde{w} = \hat{W}_{\max} + w$. *By applying Lemma 1 of [23, 25], one can now conclude the boundedness of the closed-loop dynamical system given by (4.57) and (4.58) and the strict performance bound on the system error given by*

$$\|e_{\mathrm{i}}(t)\|_P < \varepsilon, \quad t \geq 0, \tag{4.59}$$

under the condition $\|e_{\mathrm{i}}(0)\|_P < \varepsilon$.

Remark 4.2.2 *The set-theoretic model reference adaptive control architecture concisely overviewed in this section provides a strict performance bound given by (4.59) on the norm of the entire system error vector. In particular,* $e_{\mathrm{i}}^{\mathrm{T}}(t)Pe_{\mathrm{i}}(t) < \varepsilon^2$ *equivalently results from this performance bound. If the matrix P is a diagonal matrix with user-defined* $p_i \in \mathbb{R}_+$, $i = 1, \ldots, n$, *coefficients on its diagonals, then one can further write this performance bound as* $\sum_{j=1}^{n} p_j e_{ij}^2(t) = p_1 e_{\mathrm{i}1}^2(t) + \cdots + p_n e_{\mathrm{i}n}^2(t) < \varepsilon^2$; *hence, these* p_i *coefficients can be used as weights in order to adjust the performance bound as desired for enforcing strict guarantees on a subset of this system error vector, which can capture partial system errors that a control designer specifically cares. However, unfortunately, since P is obtained from (4.56), it is generally not a diagonal matrix with user-defined coefficients. This implies that, the standard set-theoretic model reference adaptive control architecture overviewed above does not readily allow for partially adjustable performance guarantees. The contribution of this paper is to address this problem (see Section 4.2.3).*

Following the discussion given in the above remark, let C be a matrix that defines a subset of the system states. To this end, define

$$y(t) \triangleq Cx(t), \quad t \geq 0, \tag{4.60}$$

$$y_{\mathrm{ri}}(t) \triangleq Cx_{\mathrm{ri}}(t), \quad t \geq 0. \tag{4.61}$$

In particular, the next section addresses the problem of driving a feasible user-selected system subset states given by (4.60) to a close (and user-controllable) neighborhood of their equivalent reference model subset states given by (4.61) for achieving adjustable strict performance guarantees on partial system errors.

4.2.3 Partially Adjustable Strict Performance Guarantees

The proposed new set-theoretic model reference adaptive control architecture of this paper involves a two-level constructive design framework, as discussed. To this end, Section 4.2.3.1 introduces an auxiliary state dynamics and develop the auxiliary system error vector between the states of an uncertain dynamical system and the states of this auxiliary dynamics, where this allows a control designer to weigh each auxiliary system error vector elements independently, while enforcing strict performance guarantees on the norm of this auxiliary system error vector. In Section 4.2.3.2, we then utilize a command governor mechanism in order to drive a feasible user-selected system subset states to a close (and user-controllable) neighborhood of their equivalent reference model subset states.

4.2.3.1 Auxiliary State Dynamics

In this subsection, based on the structure of a modified reference system, we introduce an auxiliary state dynamics. To this end, consider the modified reference dynamics given by

$$\dot{x}_{\mathrm{r}}(t) = A_{\mathrm{r}}x_{\mathrm{r}}(t)+B_{\mathrm{r}}c(t), \quad x_{\mathrm{r}}(0)=x_{\mathrm{r0}}, \quad t\geq 0. \tag{4.62}$$

In (4.62), $x_{\mathrm{r}}(t)\in\mathbb{R}^n$, $t\geq 0$, denotes the modified reference state vector and $c(t)\in\mathbb{R}^{n_{\mathrm{c}}}, t\geq 0$, denotes the actual applied command signal given by

$$c(t)\triangleq c_{\mathrm{d}}(t)+c_{\mathrm{g}}(t), \quad t\geq 0, \tag{4.63}$$

where $c_{\mathrm{g}}(t)\in\mathbb{R}^{n_{\mathrm{c}}}, t\geq 0$, is a performance modification term for the ideal command $c_{\mathrm{d}}(t), t\geq 0$ (see Section 4.2.3.2).

Now, let the auxiliary state dynamics be given by[2]

$$\dot{x}_{\mathrm{a}}(t) = A_{\mathrm{r}}x(t)+B_{\mathrm{r}}c(t)+L\big(x(t)-x_{\mathrm{a}}(t)\big), \quad x_{\mathrm{a}}(0)=x_{\mathrm{a0}}, \quad t\geq 0, \tag{4.64}$$

[2]Versions of the auxiliary state dynamics given by (4.64) and (4.65) are previously utilized by the authors of [32, 113–116] for reducing high-frequency oscillations that may occur in adaptive control systems. In this paper, however, the auxiliary state dynamics given by (4.64) and (4.65) is needed for an entirely different purpose to address the problem stated in Section 4.2.2; hence, our results are not related to those of [32, 113–116].

$$y_{\mathrm{a}}(t) \;=\; Cx_{\mathrm{a}}(t), \quad t \geq 0. \tag{4.65}$$

In (4.64) and (4.65), $x_{\mathrm{a}}(t) \in \mathbb{R}^n, t \geq 0$, denotes the auxiliary state vector, $y_{\mathrm{a}}(t) \in \mathbb{R}^{n_y}, t \geq 0$, denotes the auxiliary output signal, and $L = \mathrm{diag}[l_1, \ldots, l_n] \in \mathbb{D}^{n \times n}$ denotes a design matrix (see Remark 4.2.3). In addition, we consider the update law for (4.54) as

$$\dot{\hat{W}}(t) = \gamma \mathrm{Proj}_{\mathrm{m}}\Big(\hat{W}(t), \phi_d(\|e(t)\|_{L^{-1}})\sigma\big(x(t), c(t)\big)e^{\mathrm{T}}(t)L^{-1}B\Big), \quad \hat{W}(0) = \hat{W}_0, \quad t \geq 0. \tag{4.66}$$

In (4.66), $e(t) \triangleq x(t) - x_{\mathrm{a}}(t), t \geq 0$, denotes the auxiliary system error vector, $\phi_d(\|e(t)\|_{L^{-1}}) \in \mathbb{R}_+$ denotes an error dependent learning gain, $\gamma \in \mathbb{R}_+$ denotes a design scalar, and $\hat{W}_{\max}$ and $-\hat{W}_{\max}$ respectively denotes the maximum and minimum element-wise projection bounds. Now, the auxiliary and weight estimation error dynamics can be written as

$$\dot{e}(t) \;=\; -Le(t) - B\Lambda\tilde{W}^{\mathrm{T}}(t)\sigma\big(x(t), c(t)\big), \quad e(0) = e_0, \quad t \geq 0, \tag{4.67}$$

$$e_y(t) \;=\; Ce(t), \quad t \geq 0, \tag{4.68}$$

$$\dot{\tilde{W}}(t) \;=\; \gamma \mathrm{Proj}_{\mathrm{m}}\Big(\hat{W}(t), \phi_d(\|e(t)\|_{L^{-1}})\sigma\big(x(t), c(t)\big)e^{\mathrm{T}}(t)L^{-1}B\Big) - \dot{W}(t), \quad \tilde{W}(0) = \tilde{W}_0, \quad t \geq 0, \tag{4.69}$$

where $\tilde{W}(t) \triangleq \hat{W}(t) - W(t) \in \mathbb{R}^{(s+n+n_{\mathrm{c}}) \times m}$, $t \geq 0$, is the weight estimation error. The following theorem presents the first and intermediate result of this paper.

Theorem 4.2.1 *Consider the uncertain dynamical system given by (4.47) subject to Assumption 4.2.1, the auxiliary state dynamics given by* (4.64) *and* (4.65)*, and the feedback control law given by (4.51) along with the nominal control law* (4.52)*, the adaptive control law* (4.54)*, and the update law (4.66). If* $\|e_0\|_{L^{-1}} < \varepsilon$*, then the closed-loop dynamical system given by (4.67),* (4.68) *and (4.69) are bounded, where the bound on the system error strictly satisfies a-priori given, user-defined worst-case performance*

$$\|e(t)\|_{L^{-1}} < \varepsilon, \quad t \geq 0. \tag{4.70}$$

Proof. The boundedness of the closed-loop dynamical system in (4.67), (4.68) and (4.69) and the given strict performance bound in (4.70) follow by applying Theorem 3.1 of [1] with considering the Lyapunov function

$$V(e,\tilde{W}) = \phi(\|e\|_P) + \gamma^{-1}\mathrm{tr}\big[(\tilde{W}\Lambda^{1/2})^{\mathrm{T}}(\tilde{W}\Lambda^{1/2})\big]. \tag{4.71}$$

Since $-L$ is Hurwitz and symmetric, note that the positive-definite matrix P in (4.71) satisfies the Lyapunov equation given by

$$\begin{aligned} 0 &= -L^{\mathrm{T}}P - PL + R \\ &= -LP - PL + R, \end{aligned} \tag{4.72}$$

with $R = 2I$. This implies that $P = L^{-1} \in \mathbb{R}_+^{n\times n}$ in (4.72). ■

Remark 4.2.3 *As a direct consequence of Theorem 4.2.1, each auxiliary system error vector element can now be independently weighted while enforcing strict performance guarantees on the norm of this error vector. To this end, one needs to choose the elements of L as* $L = \mathrm{diag}[l_1,\ldots,l_n] \in \mathbb{D}^{n\times n}$ *with* l_i, $i = 1,\ldots,n$, *being design scalars. To elucidate this point, note that* (4.70) *can be written as* $\sum_{j=1}^{n} l_j^{-1}e_j^2(t) = l_1^{-1}e_1^2(t) + \cdots + l_n^{-1}e_n^2(t) < \varepsilon^2, t \geq 0$, *where* $l_1,\ldots,l_n$ *coefficients can be utilized as weights in order to adjust the performance bound as desired on the auxiliary system error vector* $e(t), t \geq 0$. *Note that this adjustable performance guarantee is an intermediate step toward our overarching aim of driving a feasible user-selected subset of system states* (4.60) *to a close (and user-controllable) neighborhood of the equivalent subset of ideal reference model system states* (4.61)*, which is addressed in the following subsection.*

4.2.3.2 Command Governor Design

To drive a feasible user-selected system subset states to a close (and user-controllable) neighborhood of their equivalent ideal reference model subset states, we design a command governor mechanism in this subsection. Mathematically speaking, let $e_{\mathrm{r}}(t) \triangleq x_{\mathrm{a}}(t) - x_{\mathrm{ri}}(t), t \geq 0$, be the error signal between the auxiliary state vector and the ideal reference state vector. Its resulting dynamics then satisfies

$$\dot{e}_{\mathrm{r}}(t) = A_{\mathrm{r}}e_{\mathrm{r}}(t) + (A_{\mathrm{r}} + L)e(t) + B_{\mathrm{r}}c_g(t), \quad e_{\mathrm{r}}(0) = x_{\mathrm{a}0} - x_{\mathrm{ri}0}, \quad t \geq 0, \tag{4.73}$$

$$e_{\mathrm{ry}}(t) = Ce_{\mathrm{r}}(t), \quad t \geq 0, \tag{4.74}$$

with $e_{\mathrm{ry}}(t) \triangleq y_{\mathrm{a}}(t) - y_{\mathrm{ri}}(t), t \geq 0$.

Similar to the procedure in, for example [117], in what follows we employ a backstepping approach to construct the command governor signal $c_g(t), t \geq 0$, to drive the norm of the output error signal $e_{\rm ry}(t), t \geq 0$, arbitrarily small as desired, and, as a result, a feasible user-selected subset of system states given in (4.60) enters a close (and user-controllable) neighborhood of the equivalent subset of ideal reference model system states given in (4.61). For this purpose, we consider (4.73) and (4.74) in the control canonical form with

$$A_{\rm r} = \begin{bmatrix} 0 & 1 & 0 & \dots & 0 \\ 0 & 0 & 1 & \dots & 0 \\ \vdots & \vdots & \vdots & \ddots & \vdots \\ 0 & 0 & 0 & \dots & 1 \\ -k_1 & -k_2 & -k_3 & \dots & -k_n \end{bmatrix}, \quad k_i \in \mathbb{R}, \tag{4.75}$$

$$B_{\rm r} = \begin{bmatrix} 0_{(\rho-1)\times m} \\ \overline{B} \end{bmatrix}, \quad \overline{B} = \begin{bmatrix} b_{\rho 1} & \dots & b_{\rho m} \\ \vdots & \ddots & \vdots \\ b_{n1} & \dots & b_{nm} \end{bmatrix} \in \mathbb{R}^{(n-\rho+1)\times m}, \quad b_i \in \mathbb{R}, \tag{4.76}$$

$$C = \begin{bmatrix} 1 & 0 & \dots & 0 \end{bmatrix}. \tag{4.77}$$

Now, let $e_{\rm f}(t) \in \mathbb{R}^n, t \geq 0$, be a low-pass filter estimate of $e(t), t \geq 0$, given by

$$\dot{e}_{\rm f}(t) = \Gamma_{\rm f}[e(t) - e_{\rm f}(t)], \quad e_{\rm f}(0) = e_{\rm f0}, \quad t \geq 0, \tag{4.78}$$

where $\Gamma_{\rm f} \in \mathbb{D}^{n\times n} \cap \mathbb{R}_+^{n\times n}$ is a filter gain matrix. Since $e_{\rm f}(t), t \geq 0$, is a low-pass filter estimate of $e(t), t \geq 0$, the matrix $\Gamma_{\rm f}$ is chosen as $\lambda_{\max}(\Gamma_{\rm f}) \leq \gamma_{\rm f,max}$ with $\gamma_{\rm f,max} > 0$ being a design parameter.

Remark 4.2.4 *From Theorem 4.2.1, $e(t), t \geq 0$, is a bounded signal and since the filter gain matrix $\Gamma_{\rm f}$ is positive-definite, it follows from* (4.78) *that $e_{\rm f}(t), t \geq 0$ and $\dot{e}_{\rm f}(t), t \geq 0$ are bounded.*

In order to obtain a recursive procedure using a backstepping control design, as standard, we first start with the second-order system given by

$$\dot{e}_{\rm r1}(t) = e_{\rm r2}(t) + l_1 e_1(t) + e_2(t), \quad e_{\rm r1}(0) = e_{\rm r10}, \quad t \geq 0, \tag{4.79}$$

$$\dot{e}_{\rm r2}(t) = -k_1 e_{\rm r1}(t) - k_2 e_{\rm r2}(t) - k_1 e_1(t) + (l_2 - k_2) e_2(t) + b_1 c_g(t), \quad e_{\rm r2}(0) = e_{\rm r2_0}, \quad t \geq 0, \tag{4.80}$$

$$e_{\rm ry}(t) = e_{\rm r1}(t), \quad t \geq 0. \tag{4.81}$$

Specifically, let $\varepsilon_1(t) \triangleq \Gamma_0 e_{\rm r1}(t) + e_{\rm r2}(t) + l_1 e_{\rm 1f}(t) + e_{\rm 2f}(t)$, $t \geq 0$, and define the command governor signal as

$$\begin{aligned} c_g(t) \;\triangleq\; & -b_1^{-1}\Big[(\Gamma_1+\Gamma_0-k_2)\varepsilon_1(t) - \big(\Gamma_0^2 - k_2\Gamma_0 + k_1\big)e_{\rm r1}(t) + (\Gamma_0-k_2)\big[l_1\big(e_1(t)-e_{\rm 1f}(t)\big)+e_2(t) \\ & -e_{\rm 2f}(t)\big] + k_2(l_1 e_1(t) + \dot{e}_{\rm 1f}(t)) + l_2 e_2(t) + \dot{e}_{\rm 2f}(t)\Big], \quad t \geq 0. \end{aligned} \tag{4.82}$$

In (4.82), $\Gamma_0 \in \mathbb{R}_+$ and $\Gamma_1 \in \mathbb{R}_+$ are design parameters. Based on the new state variable $\varepsilon_1(t), t \geq 0$, and the command governor signal (4.82), (4.79), (4.80), and (4.81) can be rewritten as

$$\dot{e}_{\rm r1}(t) = -\Gamma_0 e_{\rm r1}(t) + \varepsilon_1(t) + l_1\big(e_1(t) - e_{\rm 1f}(t)\big) + e_2(t) - e_{\rm 2f}(t), \quad e_{\rm r1}(0) = e_{\rm r10}, \quad t \geq 0, \tag{4.83}$$

$$\dot{\varepsilon}_1(t) = -\Gamma_1 \varepsilon_1(t), \quad \varepsilon_1(0) = \varepsilon_{10}, \quad t \geq 0, \tag{4.84}$$

$$e_{\rm ry}(t) = e_{\rm r1}(t), \quad t \geq 0, \tag{4.85}$$

or, equivalently, in the compact form

$$\dot{\zeta}(t) = A_1\zeta(t) + B_1\tilde{q}_1(t), \quad \zeta(0) = \zeta_0, \quad t \geq 0, \tag{4.86}$$

$$e_{\rm ry}(t) = C_1\zeta(t), \quad t \geq 0, \tag{4.87}$$

with

$$A_1 = \begin{bmatrix} -\Gamma_0 & 1 \\ 0 & -\Gamma_1 \end{bmatrix}, \quad B_1 = \begin{bmatrix} 1 \\ 0 \end{bmatrix}, \quad C_1 = \begin{bmatrix} 1 & 0 \end{bmatrix}, \tag{4.88}$$

where $\zeta(t) = [e_{\rm r1}(t),\ \varepsilon_1(t)]^{\rm T}, t \geq 0$, is the aggregated system state and $\tilde{q}_1(t) \triangleq l_1\big(e_1(t) - e_{\rm 1f}(t)\big) + e_2(t) - e_{\rm 2f}(t)$, $t \geq 0$, is a bounded signal from Remark 4.2.4.

From [79, 118], consider now the equi-induced signal

$$|\!|\!|\mathcal{G}|\!|\!|_{(\infty,2),(\infty,2)} \triangleq \sup_{\tilde{q}_1 \in \mathcal{L}_\infty} \frac{|\!|\!|e_{\rm ry}|\!|\!|_{\infty,2}}{|\!|\!|\tilde{q}_1|\!|\!|_{\infty,2}}, \tag{4.89}$$

that denotes the $\mathcal{L}_1$-system norm of (4.86) and (4.87). An upper bound to (4.89) is given by

$$|\!|\!|\mathcal{G}|\!|\!|_{(\infty,2),(\infty,2)} \leq \frac{1}{\sqrt{\alpha}}\sigma_{\max}^{1/2}(C_1 Q_\alpha C_1^{\rm T}), \tag{4.90}$$

where $\alpha > 0$ ensures that $A_1 + \frac{\alpha}{2} I$ is Hurwitz and $Q_\alpha \in \mathbb{R}^{2\times 2}$ is the (unique) nonnegative definite Lyapunov equation solution to

$$0 \quad = \quad A_1 Q_\alpha + Q_\alpha A_1^{\mathrm{T}} + \alpha Q_\alpha + B_1 B_1^{\mathrm{T}}. \tag{4.91}$$

Remark 4.2.5 *By minimizing the upper bound on the $\mathcal{L}_1$-system norm given by* (4.90)*, it follows from* (4.89) *that one can suppress the effect of $\tilde{q}_1(t)$, $t \geq 0$, which has the worst-case upper bound satisfying*

$$|\tilde{q}_1(t)| \leq (3l_1^{3/2} + 2l_2^{1/2})\varepsilon, \quad t \geq 0, \tag{4.92}$$

on the output error signal $e_{\mathrm{ry}}(t)$, $t \geq 0$. Specifically, to show how the design parameters Γ_0 and Γ_1 suppress the effect of this bounded perturbation term on the output error signal $e_{\mathrm{ry}}(t)$, $t \geq 0$, for the illustration purposes in this remark only we consider $\tilde{q}_1(t)$, $t \geq 0$, as a step input having unity amplitude. As it is shown in Figure 4.9, one can observe that by increasing $\Gamma \triangleq \Gamma_0 = \Gamma_1$ from 1 to 10, the output error signal $e_{\mathrm{ry}}(t)$, $t \geq 0$, decreases. In addition, in order to make the upper bound of the $\mathcal{L}_1$-system norm of (4.86) *and* (4.87) *arbitrarily small, one can increase the design parameter Γ as required. Note that the selection of the unit step input for $\tilde{q}_1(t)$, $t \geq 0$, in this remark is without loss of generality and in general it can be in the form of any bounded time-varying function.*

Proposition 4.2.1 *Consider the uncertain dynamical system given by (4.47) with $n = 2$, subject to Assumption 4.2.1, the auxiliary state dynamics given by* (4.64) *and* (4.65)*, and the feedback control law given by*

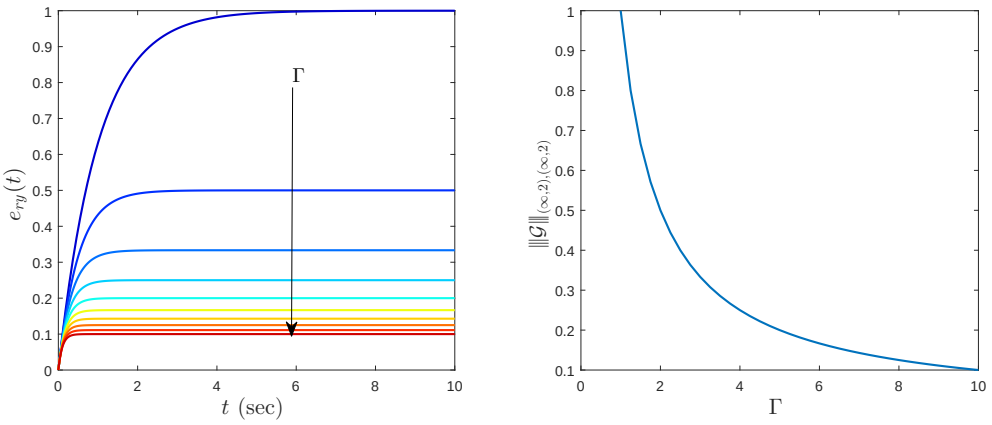

Figure 4.9: System response of (4.86) and (4.87) to step input of $\tilde{q}_1(t), t \geq 0$ (left), and the upper bound on the $\mathcal{L}_1$-system norm given in (4.90) (right).

(4.51) along with the nominal control law (4.52)*, the adaptive control law* (4.54)*, and the update law (4.66). In addition, consider the error dynamics between the auxiliary state vector and the ideal reference state vector given in* (4.79)*,* (4.80) *and* (4.81)*, and let the command governor signal be given by* (4.82)*. Then, all of the closed-loop dynamical system signals remain bounded, and the system output signal* $y(t), t \geq 0$*, converges to a close (and user-controllable) neighborhood of the ideal reference system output signal* $y_{\rm ri}(t), t \geq 0$*.*

Proof. The auxiliary system error signal $e(t), t \geq 0$, is bounded from Theorem 4.2.1. Now, based on the upper triangular structure of A_1 matrix in (4.86), the boundedness of $e_{\rm r1}(t), t \geq 0$, and $\varepsilon_1(t), t \geq 0$, is immediate [109]. Hence, from the definition of the signal $\varepsilon_1(t), t \geq 0$, one can conclude the boundedness of $e_{\rm r2}(t), t \geq 0$, where from the definition of the signal $e_{\rm r}(t)$, $t \geq 0$, the auxiliary state $x_{\rm a}(t), t \geq 0$, is also bounded. Now, from the definition of the auxiliary system error signal $e(t), t \geq 0$, the system state $x(t), t \geq 0$, is also bounded. Therefore, all of the closed-loop dynamical system signals are bounded.

For the second part of the proof, we analyze the deviation of the system output trajectory in (4.60) from the output signal of the ideal reference system in (4.61) given by

$$\begin{aligned} \big|y(t) - y_{\rm ri}(t)\big| &= \big|\big(y(t) - y_{\rm a}(t)\big) + \big(y_{\rm a}(t) - y_{\rm ri}(t)\big)\big| = \big|e_y(t) + e_{\rm ry}(t)\big| \\ &\leq \big|e_y(t)\big| + \big|e_{\rm ry}(t)\big|, \quad t \geq 0. \end{aligned} \tag{4.93}$$

Note that, based on Remark 4.2.3 one can write $l_1^{-1} e_1^2(t) \leq l_1^{-1} e_1^2(t) + l_2^{-1} e_2^2(t) < \varepsilon^2, t \geq 0$, or equivalently, $e_1^2(t) < l_1 \varepsilon^2, t \geq 0$, which can be expressed as

$$\big|e_y(t)\big| < \sqrt{l_1}\, \varepsilon, \quad t \geq 0. \tag{4.94}$$

Furthermore, it follows from Remark 4.2.5 that the effect of $\tilde{q}_1(t), t \geq 0$, (with its upper bound in (4.92)) on $\big|e_{\rm ry}(t)\big|, t \geq 0$ can be made as small as desired by choosing the design parameters Γ_1 and Γ_0. It is now clear from (4.93) that the system output signal $y(t), t \geq 0$, converges to a close (and user-controllable) neighborhood of the ideal reference system output signal $y_{\rm ri}(t), t \geq 0$, by judicious selection of the user-defined and design parameters ε, Γ_0, Γ_1 and l_1 which completes the proof. ■

Owing to the nature of the backstepping approach, the above analysis can be carried out to design the command governor signal $c_g(t), t \geq 0$, for the high-order dynamical systems to guarantee the boundedness of the auxiliary state signal $x_{\rm a}(t), t \geq 0$ and to make the output of the auxiliary dynamics arbitrarily close to

the output of the reference system by tuning the design parameters. To elucidate this point, we now consider a third-order system given by

$$\dot{e}_{\rm r1}(t) = e_{\rm r2}(t)+l_1e_1(t)+e_2(t), \quad e_{\rm r1}(0)=e_{\rm r10}, \quad t\geq 0, \tag{4.95}$$

$$\dot{e}_{\rm r2}(t) = e_{\rm r3}(t)+l_2e_2(t)+e_3(t), \quad e_{\rm r2}(0)=e_{\rm r20}, \quad t\geq 0, \tag{4.96}$$

$$\dot{e}_{\rm r3}(t) = -k_1e_{\rm r1}(t)-k_2e_{\rm r2}(t)-k_3e_{\rm r3}(t)-k_1e_1(t)-k_2e_2(t)+(l_3-k_3)e_3(t)+b_1c_g(t), \quad e_{\rm r3}(0)=e_{\rm r30}, \quad t\geq 0, \tag{4.97}$$

$$e_{\rm ry}(t) = e_{\rm r1}(t), \quad t\geq 0. \tag{4.98}$$

In particular, let

$$\varepsilon_1(t) \triangleq \Gamma_0e_{\rm r1}(t)+e_{\rm r2}(t)+l_1e_{1\rm f}(t)+e_{2\rm f}(t), \quad t\geq 0, \tag{4.99}$$

$$\varepsilon_2(t) \triangleq (\Gamma_1+\Gamma_0)\varepsilon_1(t)-\Gamma_0^2e_{\rm r1}(t)+e_{\rm r3}(t)-\Gamma_0l_1e_{1\rm f}(t)-\Gamma_0e_{2\rm f}(t)+e_{3\rm f}(t), \quad t\geq 0, \tag{4.100}$$

and define the command governor signal as

$$\begin{aligned} &c_g(t) \triangleq \\ &-b_1^{-1}\Big[\big(\Gamma_2+\Gamma_1+\Gamma_0-k_3\big)\varepsilon_2(t)-\big((\Gamma_1+\Gamma_0)(\Gamma_1-k_3)+k_2+\Gamma_0^2\big)\varepsilon_1(t)+\big(\Gamma_0^3-k_3\Gamma_0^2+k_2\Gamma_0-k_1\big)e_{\rm r1}(t) \\ &+l_1\Gamma_0\Gamma_1\big(e_1(t)-e_{1\rm f}(t)\big)+\big(\Gamma_0(\Gamma_1+l_2)+\Gamma_1l_2-k_2\big)\big(e_2(t)-e_{2\rm f}(t)\big)+\big(\Gamma_0+\Gamma_1-k_3\big)\big(e_3(t)-e_{3\rm f}(t)\big) \\ &+k_2l_1e_{1\rm f}(t)+k_3l_2e_{2\rm f}(t)-k_1e_1(t)+l_3e_3(t)+k_3l_1\dot{e}_{1\rm f}(t)+(k_3+l_2)\dot{e}_{2\rm f}(t)+\dot{e}_{3\rm f}(t)\Big], \quad t\geq 0. \end{aligned} \tag{4.101}$$

In (4.101), $\Gamma_0\in\mathbb{R}_+$,$\Gamma_1\in\mathbb{R}_+$ and $\Gamma_2\in\mathbb{R}_+$ are design parameters. Based on the new state variables $\varepsilon_1(t)$, $\varepsilon_2(t)$,$t\geq 0$, and the command governor signal (4.101), (4.95), (4.96), (4.97), and (4.98) can be rewritten as

$$\dot{e}_{\rm r1}(t) = -\Gamma_0e_{\rm r1}(t)+\varepsilon_1(t)+l_1\big(e_1(t)-e_{1\rm f}(t)\big)+e_2(t)-e_{2\rm f}(t), \quad e_{\rm r1}(0)=e_{\rm r10}, \quad t\geq 0, \tag{4.102}$$

$$\begin{aligned} \dot{\varepsilon}_1(t) = &-\Gamma_1\varepsilon_1(t)+\varepsilon_2(t)+\Gamma_0l_1\big(e_1(t)-e_{1\rm f}(t)\big)+\big(\Gamma_0+l_2\big)\big(e_2(t)-e_{2\rm f}(t)\big)+e_3(t)-e_{3\rm f}(t) \\ &+l_1\dot{e}_{1\rm f}(t)+\dot{e}_{2\rm f}(t), \quad \varepsilon_1(0)=\varepsilon_{10}, \quad t\geq 0, \end{aligned} \tag{4.103}$$

$$\dot{\varepsilon}_2(t) = -\Gamma_2\varepsilon_2(t), \quad \varepsilon_2(0)=\varepsilon_{20}, \quad t\geq 0, \tag{4.104}$$

$$e_{\rm ry}(t) = e_{\rm r1}(t), \quad t\geq 0, \tag{4.105}$$

or, equivalently, in the compact form

$$\dot{\zeta}(t) = A_2\zeta(t) + B_2\tilde{q}_2(t), \quad \zeta(0) = \zeta_0, \quad t \geq 0, \tag{4.106}$$

$$e_{\mathrm{ry}}(t) = C_2\zeta(t), \quad t \geq 0, \tag{4.107}$$

with

$$A_2 = \begin{bmatrix} -\Gamma_0 & 1 & 0 \\ 0 & -\Gamma_1 & 1 \\ 0 & 0 & -\Gamma_2 \end{bmatrix}, \quad B_2 = \begin{bmatrix} l_1 & 1 & 0 & 0 \\ l_1\Gamma_0 & \Gamma_0 + l_2 & 1 & 1 \\ 0 & 0 & 0 & 0 \end{bmatrix}, \quad C_2 = \begin{bmatrix} 1 & 0 & 0 \end{bmatrix}, \tag{4.108}$$

where $\zeta(t) = [e_{\mathrm{r1}}(t),\ \varepsilon_1(t),\ \varepsilon_2(t)]^{\mathrm{T}}, t \geq 0$ is the aggregated system state and $\tilde{q}_2(t) = \big[e_1(t) - e_{1\mathrm{f}}(t),\ \ e_2(t) - e_{2\mathrm{f}}(t),\ \ e_3(t) - e_{3\mathrm{f}}(t),\ \ l_1\Gamma_{1\mathrm{f}}[e_1(t) - e_{1\mathrm{f}}(t)] + \Gamma_{2\mathrm{f}}[e_2(t) - e_{2\mathrm{f}}(t)]\big]^{\mathrm{T}}, t \geq 0$, is a bounded signal from Remark 4.2.4. Similar to (4.89), from [79, 118], consider the equi-induced signal

$$|||\mathcal{G}|||_{(\infty,2),(\infty,2)} \triangleq \sup_{\tilde{q}_2 \in \mathcal{L}_\infty} \frac{|||e_{\mathrm{ry}}|||_{\infty,2}}{|||\tilde{q}_2|||_{\infty,2}}, \tag{4.109}$$

that denotes the $\mathcal{L}_1$-system norm of (4.106) and (4.107). An upper bound to (4.109) is given by

$$|||\mathcal{G}|||_{(\infty,2),(\infty,2)} \leq \frac{1}{\sqrt{\alpha}} \sigma_{\max}^{1/2}(C_2 Q_\alpha C_2^{\mathrm{T}}), \tag{4.110}$$

where $\alpha > 0$ ensures that $A_2 + \frac{\alpha}{2} I$ is Hurwitz and $Q_\alpha \in \mathbb{R}^{3\times 3}$ is the (unique) nonnegative definite Lyapunov equation solution to

$$0 = A_2 Q_\alpha + Q_\alpha A_2^{\mathrm{T}} + \alpha Q_\alpha + B_2 B_2^{\mathrm{T}}. \tag{4.111}$$

Remark 4.2.6 *As it is shown in Figure 4.10 and similar to the case in Remark 4.2.5, one can observe that by increasing* $\Gamma \triangleq \Gamma_0 = \Gamma_1 = \Gamma_2$ *from 1 to 10, the output error signal* $e_{\mathrm{ry}}(t)$, $t \geq 0$, *decreases. In addition, in order to make the upper bound of the* $\mathcal{L}_1$*-system norm of* (4.106) *and* (4.107) *arbitrarily small, one can increase the design parameter* Γ.

Proposition 4.2.2 *Consider the uncertain dynamical system given by (4.47) with* $n = 3$, *subject to Assumption 4.2.1, the auxiliary state dynamics given by* (4.64) *and* (4.65), *and the feedback control law given*

by (4.51) along with the nominal control law (4.52)*, the adaptive control law* (4.54)*, and the update law (4.66). In addition, consider the error dynamics between the auxiliary state vector and the ideal reference state vector given in* (4.95)*,* (4.96)*,* (4.97) *and* (4.98)*, and let the command governor signal be given by* (4.101)*. Then, all of the closed-loop dynamical system signals remain bounded, and the system output signal* $y(t), t \geq 0$*, converges to a close (and user-controllable) neighborhood of the ideal reference system output signal* $y_{\rm ri}(t), t \geq 0$*.*

Proof. The auxiliary system error signal $e(t), t \geq 0$, is bounded from Theorem 4.2.1. Now, based on the upper triangular structure of A_2 matrix in (4.106), the boundedness of $e_{\rm r1}(t), t \geq 0$, $\varepsilon_1(t), t \geq 0$, and $\varepsilon_2(t), t \geq 0$, is immediate [109]. Hence, from the definition of the signals $\varepsilon_1(t), t \geq 0$, and $\varepsilon_2(t), t \geq 0$, one can conclude the boundedness of $e_{\rm r2}(t), t \geq 0$, and $e_{\rm r3}(t), t \geq 0$, where from the definition of the signal $e_{\rm r}(t)$, $t \geq 0$, the auxiliary state $x_{\rm a}(t), t \geq 0$, is also bounded. Now, from the definition of the auxiliary system error signal $e(t), t \geq 0$, the system state $x(t), t \geq 0$, is also bounded. Therefore, all of the closed-loop dynamical system signals are bounded.

Similar to the proof of Proposition 4.2.1, for the second part of the proof we analyze the deviation of the system output trajectory in (4.60) from the output signal of the ideal reference system in (4.61) given by

$$\begin{aligned} \big|y(t) - y_{\rm ri}(t)\big| &= \big|\big(y(t) - y_{\rm a}(t)\big) + \big(y_{\rm a}(t) - y_{\rm ri}(t)\big)\big| = \big|e_y(t) + e_{\rm ry}(t)\big| \\ &\leq \big|e_y(t)\big| + \big|e_{\rm ry}(t)\big|, \quad t \geq 0. \end{aligned} \tag{4.112}$$

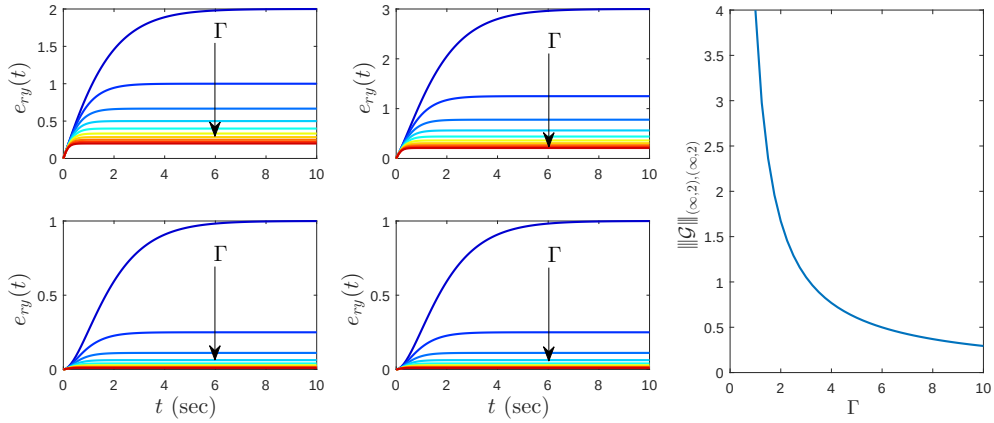

Figure 4.10: System response of (4.106) and (4.107) to step input of the first (top left), the second (top middle), the third (bottom left), and the fourth (bottom middle) components of $\tilde{q}_2(t), t \geq 0$, and the upper bound on the $\mathcal{L}_1$-system norm given in (4.110) (right).

Note that, once again based on Remark 4.2.3 one can write $l_1^{-1}e_1^2(t) \leq l_1^{-1}e_1^2(t) + l_2^{-1}e_2^2(t) + l_3^{-1}e_3^2(t) < \varepsilon^2, t \geq 0$, or equivalently, $e_1^2(t) < l_1\varepsilon^2, t \geq 0$, which can be expressed as

$$\left|e_y(t)\right| < \sqrt{l_1}\,\varepsilon, \quad t \geq 0. \tag{4.113}$$

Furthermore, it is clear based on Remark 4.2.6 that $\left|e_{\rm ry}(t)\right|, t \geq 0$, can be made as small as desired by choosing the design parameters Γ_2, Γ_1 and Γ_0. It now follows from (4.112) that the system output signal $y(t), t \geq 0$, converges to a close (and user-controllable) neighborhood of the ideal reference system output signal $y_{\rm ri}(t), t \geq 0$, by judicious selection of the user-defined and design parameters $\varepsilon, \Gamma_0, \Gamma_1, \Gamma_2$ and l_1. ■

Remark 4.2.7 *By repeating the recursive procedure in Propositions 4.2.1 and 4.2.2,* $(n-1)$*-times, one can design the command governor signal* $c_g(t), t \geq 0$, *for the general error dynamical systems given in* (4.73) *and* (4.74) *to guarantee the boundedness of the auxiliary state signal* $x_{\rm a}(t), t \geq 0$ *and to tighten the upper bound on the output error signal in* (4.74) *by tuning the design parameters* $\Gamma_0, \Gamma_1, \ldots \Gamma_{n-1}$.

4.2.4 Illustrative Numerical Examples

In this section, we present two numerical examples to demonstrate the efficacy of the proposed command governor-based adaptive control architecture.

4.2.4.1 Example 1

Consider the uncertain dynamical system given by

$$\dot{x}(t) = \begin{bmatrix} 0 & 3 \\ 3 & 1 \end{bmatrix} x(t) + \begin{bmatrix} 0 \\ 1 \end{bmatrix} \Lambda \Big(u(t) + \delta(t, x(t)) \Big), \quad x(0) = 0, \quad t \geq 0, \tag{4.114}$$

where $x(t) = \left[x_1(t),\ \ x_2(t)\right]^{\rm T}$ is the system state, $\delta(t, x(t))$ represents an uncertainty of the form given in (4.49) with

$$W_0(t) = [5\cos(0.5t),\ -15,\ 1]^{\rm T}, \quad \sigma_0(x(t)) = [x_1(t),\ x_2(t),\ 1]^{\rm T}, \quad t \geq 0, \tag{4.115}$$

and $\Lambda = 0.75$ represents an uncertain control effectiveness matrix. The linear quadratic regulator theory is used to design the nominal feedback gain matrix as $K_1 = [8.4,\ 8.5]$, where we pick $K_2 = 5.4$.

For the standard set-theoretic model reference adaptive controller in Section 4.2.2.2, we use the generalized restricted potential function given by $\phi(\|e_{\rm i}(t)\|_{\rm P}) = \|e_{\rm i}(t)\|_{\rm P}^2/\big(\varepsilon - \|e_{\rm i}(t)\|_{\rm P}\big)$, set $\varepsilon = 1$, the projection norm bound imposed on each element of the parameter estimate to $\hat{W}_{\max} = 15$, the learning rate to $\gamma = 20$, and we use $R = I$ to calculate P from (4.56) for the resulting $A_{\rm r}$ matrix. Figure 4.11 shows the closed-loop dynamical system performance with the standard set-theoretic adaptive controller in Section 4.2.2.2, where Figure 4.12 shows the norm of the system error trajectories and the evolution of the effective learning rate. One can see from these figures that the standard set-theoretic adaptive controller is not able to enforce a user-defined performance bound to a subset of the system states, unless ε is chosen to be sufficiently small. Yet, as known, this can result in high effective learning rates [1].

Next, we apply the proposed command governor-based set-theoretic adaptive control architecture, we use $L = \text{diag}([1, 10])$, $\Gamma_0 = \Gamma_1 = 10$ and set the filter gain in (4.78) to $\Gamma_f = 0.5$. It can be seen in Figure 4.13 that desired performance is obtained and the first component of the state vector converges to a close (and user-controllable) neighborhood of the reference state. The evolution of the norm of the auxiliary system error trajectories and the effective learning rate is depicted in Figure 4.14. Finally, Figure 4.15 shows the role of the command governor signal to modify the command signal for different values of $\Gamma = \Gamma_0 = \Gamma_1$, where it is clear from Figure 4.16 that a larger value of Γ, leads to a better tracking performance of output signal of the reference system. △

4.2.4.2 Example 2

For this second example, we consider a third-order uncertain dynamical system given by

$$\dot{x}(t) = \begin{bmatrix} 0 & 1 & 0 \\ 0 & 0 & 1 \\ 2 & 3 & 1 \end{bmatrix} x(t) + \begin{bmatrix} 0 \\ 0 \\ 1 \end{bmatrix} \Lambda \Big(u(t) + \delta(t, x(t)) \Big), \quad x(0) = 0, \quad t \geq 0, \tag{4.116}$$

where $x(t) = \big[x_1(t)\ \ x_2(t)\ \ x_3(t)\big]^{\rm T}$ is the system state, $\delta(t, x(t))$ represents an uncertainty of the form given in (4.49) with$W_0(t) = 10\,[\sin(0.25t),\ -0.25,\ 0.5,\ 0.5]^{\rm T}, t \geq 0$, $\sigma_0(x(t)) = [x_1(t),\ x_2(t),\ x_1(t)x_2(t),\ x_3(t)]^{\rm T}, t \geq 0$, and $\Lambda = 0.75$ represents an uncertain control effectiveness matrix. The linear quadratic regulator theory is used to design the nominal feedback gain matrix as $K_1 = [5.7,\ 9.9,\ 6.1]$, where we pick $K_2 = 3.7$.

For the standard set-theoretic model reference adaptive controller in Section 4.2.2.2, we use the generalized restricted potential function given by $\phi(\|e_{\mathrm{i}}(t)\|_{\mathrm{P}}) = \|e_{\mathrm{i}}(t)\|_{\mathrm{P}}^2/\big(\varepsilon - \|e_{\mathrm{i}}(t)\|_{\mathrm{P}}\big)$, set $\varepsilon = 1$, the

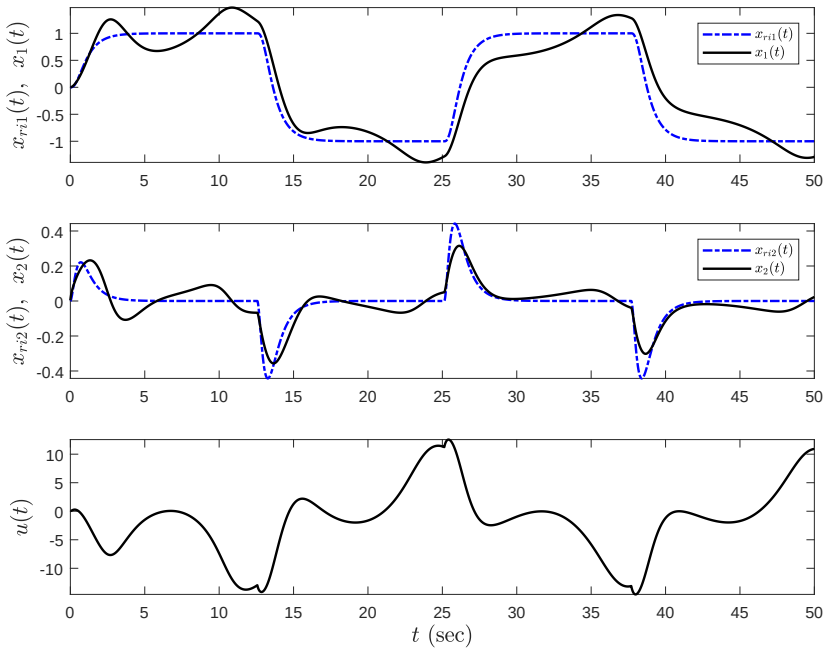

Figure 4.11: Command following performance with the standard set-theoretic model reference adaptive controller in Section 4.2.2.2.

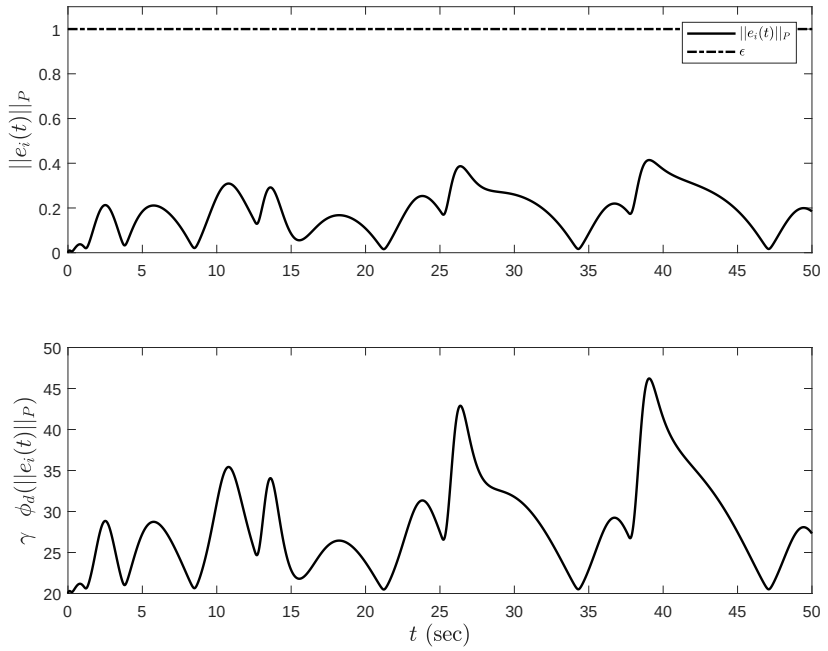

Figure 4.12: Norm of the system error trajectories and the evolution of the effective learning rate $\gamma\phi_d(\cdot)$ with the standard set-theoretic model reference adaptive controller in Section 4.2.2.2.

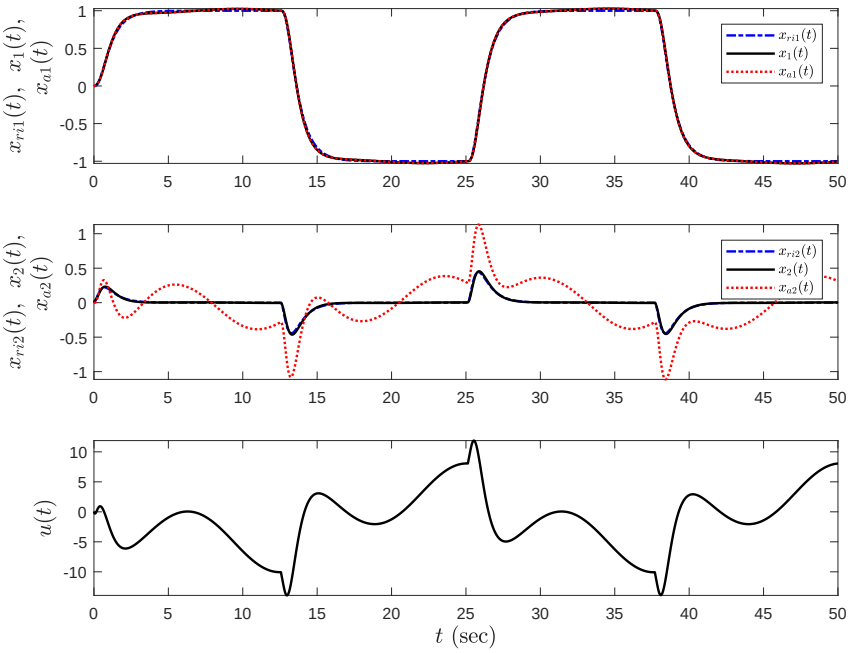

Figure 4.13: Command following performance with the proposed command governor-based set-theoretic model reference adaptive controller in Section 4.2.3.

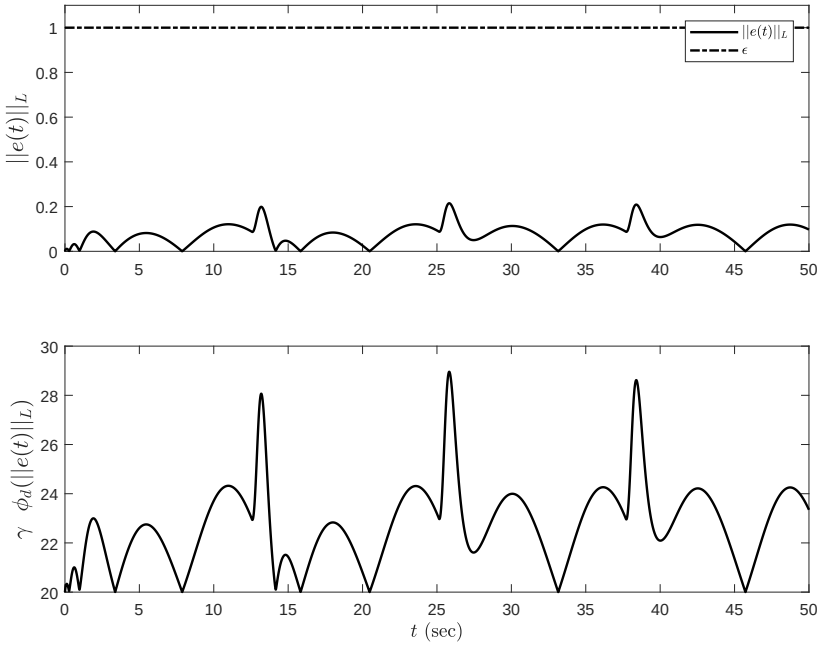

Figure 4.14: Norm of the auxiliary system error trajectories and the evolution of the effective learning rate $\gamma\phi_d(\cdot)$ with the proposed command governor-based set-theoretic model reference adaptive controller in Section 4.2.3.

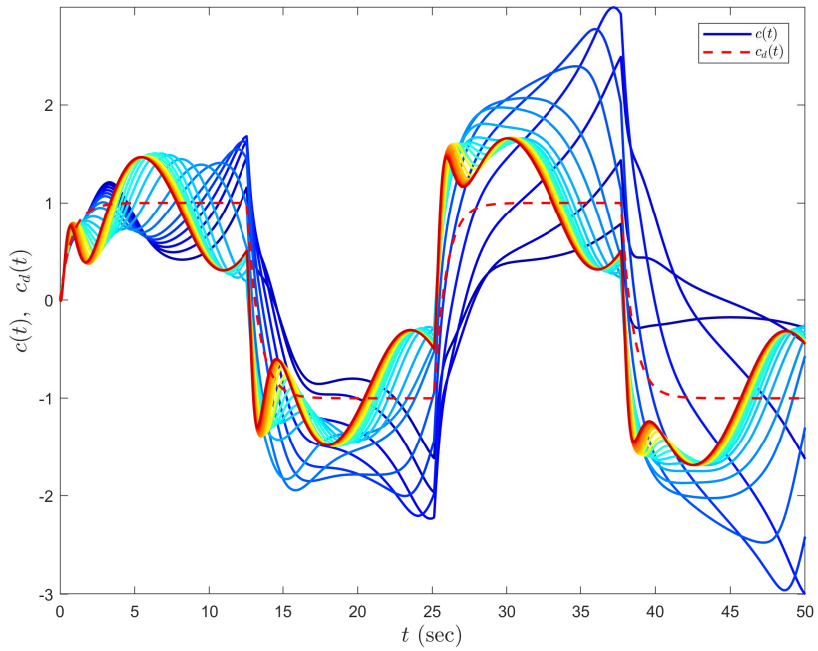

Figure 4.15: The effect of increasing the design parameter $\Gamma = \Gamma_0 = \Gamma_1$ from 0.05 to 10 (blue to red) on the modified command signal with the proposed command governor-based set-theoretic model reference adaptive controller in Section 4.2.3.

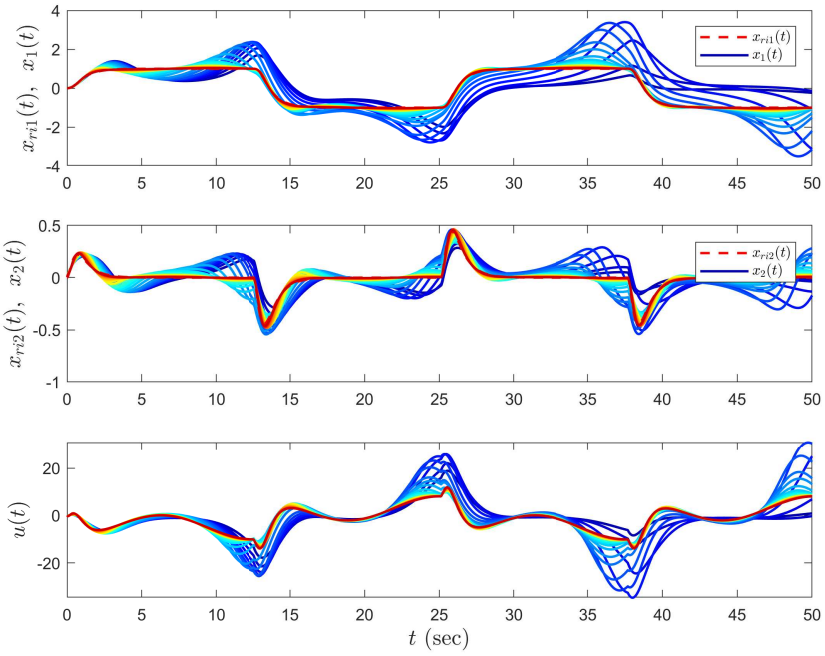

Figure 4.16: The effect of increasing the design parameter $\Gamma = \Gamma_0 = \Gamma_1$ from 0.05 to 10 (blue to red) on the system performance with the proposed command governor-based set-theoretic model reference adaptive controller in Section 4.2.3.

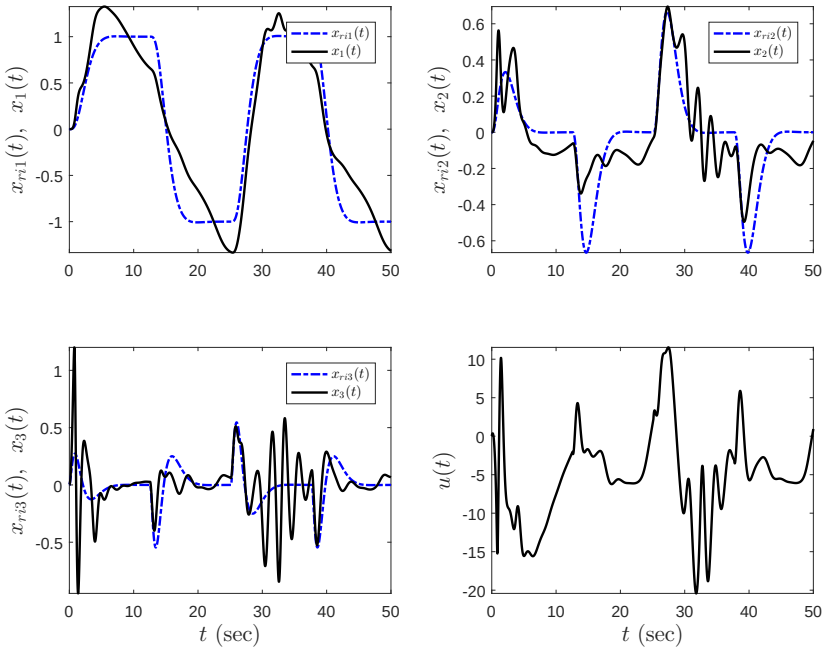

Figure 4.17: Command following performance with the standard set-theoretic model reference adaptive controller in Section 4.2.2.2.

projection norm bound imposed on each element of the parameter estimate to $\hat{W}_{\max} = 15$, the learning rate to $\gamma = 20$, and we use $R = I$ to calculate P from (4.56) for the resulting A_{r} matrix. Figure 4.17 shows the closed-loop dynamical system performance with the standard set-theoretic adaptive controller in Section 4.2.2.2 where Figure 4.18 shows the norm of the system error trajectories and the evolution of the effective learning rate. One can see from these figures that the the standard set-theoretic adaptive controller is not able to enforce a user-defined performance bound to a subset of the system states.

Next, we apply the proposed command governor-based set-theoretic adaptive control architecture, we use $L = \mathrm{diag}([1, 10, 10])$, $\Gamma_0 = \Gamma_1 = 5$ and set the filter gain in (4.78) to $\Gamma_f = 0.5$. It can be seen in Figure 4.19 that desired performance is obtained and the first component of the state vector converges to a close (and user-controllable) neighborhood of the reference state. The evolution of the norm of the auxiliary system error trajectories and the effective learning rate is depicted in Figure 4.20. Finally, Figure 4.21 shows the role of the command governor signal to modify the command signal for different values of $\Gamma = \Gamma_0 = \Gamma_1 = \Gamma_2$, where it is clear from Figure 4.22 that a larger value of Γ, leads to a better tracking performance of output signal of the reference system. $\triangle$

4.2.5 Conclusion

In this paper, we developed a new two-level set-theoretic model reference adaptive control architecture that has the ability to enforce an a-priori given, user-defined performance bound on the selected subset of dynamical system trajectories, entitled as partially adjustable performance guarantees. Specifically, we first utilized an auxiliary state dynamics that allows a control designer to weigh each auxiliary system error vector elements independently, while enforcing strict performance guarantees on the norm of this auxiliary system error vector. A command governor mechanism was then designed through a constructive backstepping procedure in order to drive a feasible user-selected subset of system states to a close (and user-controllable) neighborhood of the corresponding reference model states. This resulted in adjustable strict performance guarantees on a subset of system errors trajectories. In addition to the presented theoretical results, two illustrative numerical examples further demonstrated the efficacy of our contribution.

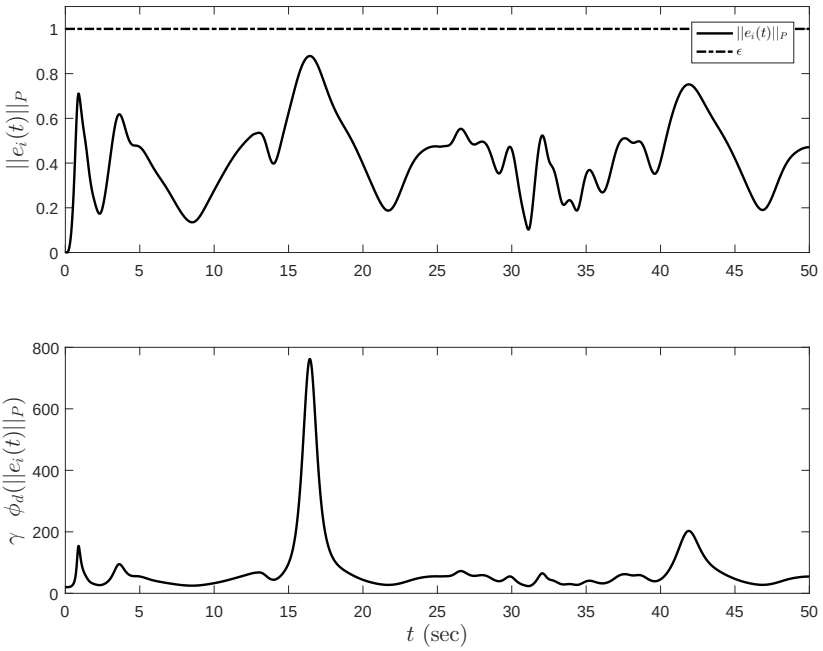

Figure 4.18: Norm of the system error trajectories and the evolution of the effective learning rate $\gamma\phi_d(\cdot)$ with the standard set-theoretic model reference adaptive controller in Section 4.2.2.2.

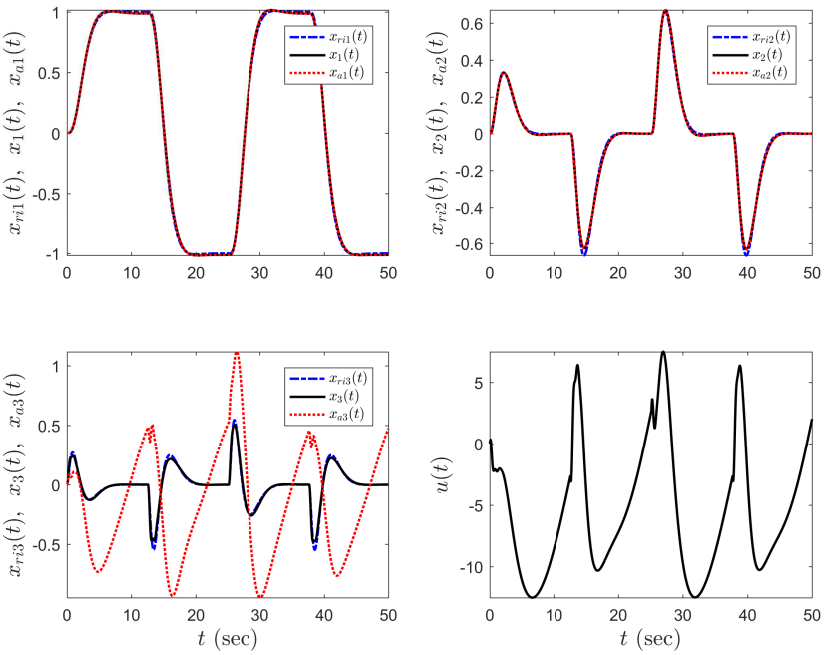

Figure 4.19: Command following performance with the proposed command governor-based set-theoretic model reference adaptive controller in Section 4.2.3.

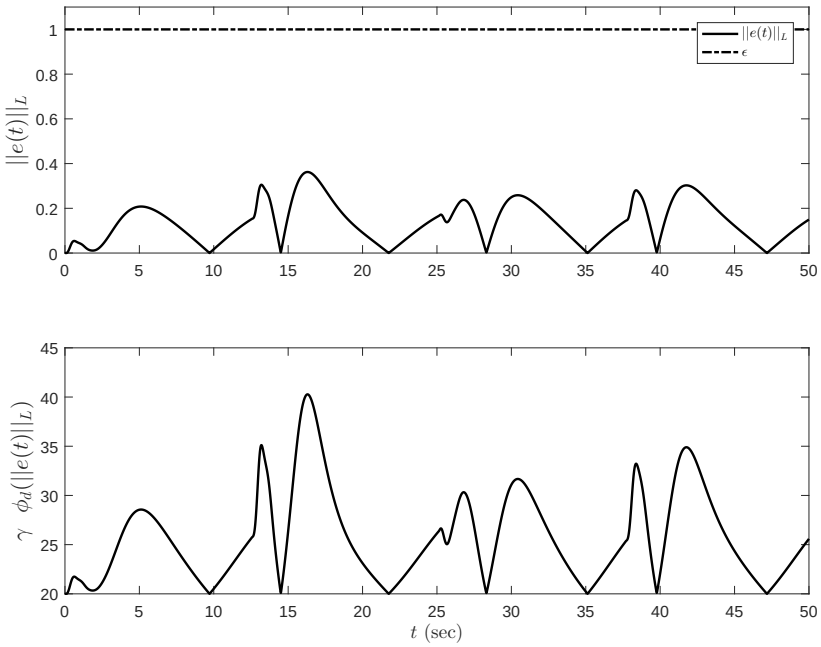

Figure 4.20: Norm of the auxiliary system error trajectories and the evolution of the effective learning rate $\gamma\phi_d(\cdot)$ with the proposed command governor-based set-theoretic model reference adaptive controller in Section 4.2.3.

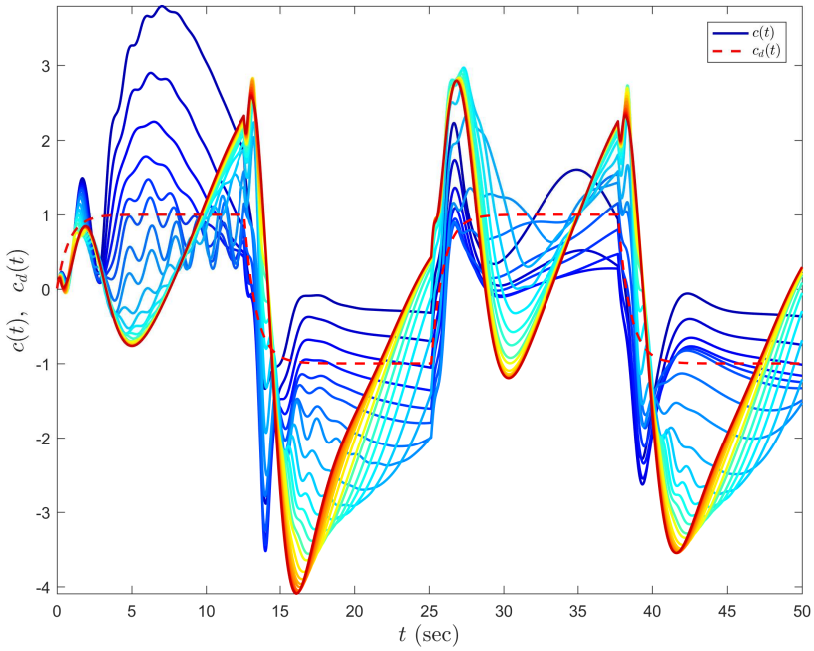

Figure 4.21: The effect of increasing the design parameter $\Gamma = \Gamma_0 = \Gamma_1 = \Gamma_2$ from 0.05 to 10 (blue to red) on the modified command signal with the proposed command governor-based set-theoretic model reference adaptive controller in Section 4.2.3.

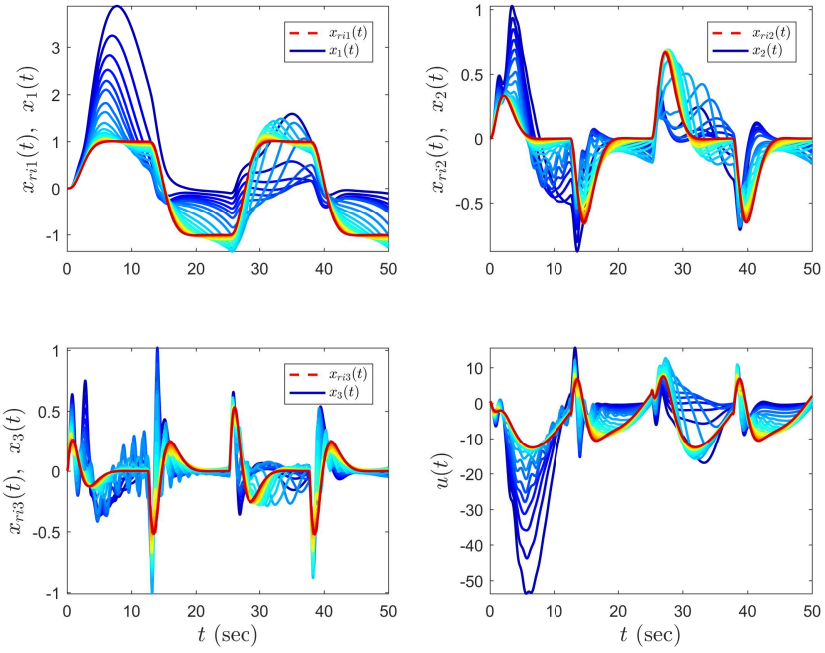

Figure 4.22: The effect of increasing the design parameter $\Gamma = \Gamma_0 = \Gamma_1 = \Gamma_2$ from 0.05 to 10 (blue to red) on the system performance with the proposed command governor-based set-theoretic model reference adaptive controller in Section 4.2.3.

4.3 On Set-Theoretic Model Reference Adaptive Control of Uncertain Dynamical Systems Subject to Actuator Dynamics[3]

In applications where the bandwidth of the actuator dynamics is not sufficiently high, the stability of model reference adaptive controllers can be degraded drastically as it is well known. To this end, one of the effective approaches for tackling the challenge of limited actuator bandwidth is the hedging method in which using a "modified" reference model, the adaptation becomes "excluded" from the actuator dynamics. With this approach, however, the performance bounds between the uncertain dynamical system trajectories and the "ideal" reference model trajectories can be conservative and depend on the bounds on the system uncertainties; therefore, no "practical" performance guarantees exist.

To address this challenge, we generalize a recently developed set-theoretic model reference adaptive control architecture, which has the capability to achieve "practical" (i.e., user-defined) performance guarantees, for uncertain dynamical systems subject to actuator dynamics. Specifically, we first show that the proposed architecture keeps the performance bounds between the uncertain dynamical system trajectories and the "modified" reference model trajectories within an a-priori, user-defined bound. We next show that the error bounds between the "ideal" reference model trajectories and the uncertain dynamical system trajectories is characterized by this user-defined bound as well as the actuator bandwidth limit, and hence, is "computable" using a given set of adaptive control design parameters. Finally, as a byproduct, our illustrative numerical example shows that the time rate of change of the actual control signal (i.e., the output of the actuator dynamics) becomes less in magnitude as compared with the the set-theoretic model reference adaptive control case without actuator dynamics.

4.3.1 Introduction

In applications where the bandwidth of the actuator dynamics is not sufficiently high, the stability of model reference adaptive controllers can be degraded drastically as it is well known. To this end, one of the effective approaches for tackling the challenge of limited actuator bandwidth is the hedging method [37] in which using a "modified" reference model (i.e., the "ideal" reference model modified by the "hedge" signal), the adaptation becomes "excluded" from the actuator dynamics (we refer to [37] as well as [38, 39] for details). While [37] introduce this method to the model reference adaptive control literature around 2000s, the authors of [40, 41] recently show not only generalizations of this method but also the sufficient condition

[3]This section is previously published in [119]. Permission is included in Appendix H.

predicated on linear matrix inequalities (LMIs) such that the modified reference model trajectories, and hence, the overall closed-loop dynamical system, become stable in the presence of actuator dynamics once this sufficient condition holds. Yet, since the contributions in [40, 41] adopt a "standard" model reference adaptive control framework, the performance bounds between the uncertain dynamical system trajectories and the "ideal" reference model trajectories can be conservative and depend on the bounds on the system uncertainties; therefore, no "practical" performance guarantees exist (e.g., see Theorem 1.4.1 of [41], where the performance bound includes unknown parameters; thus, is not readily a-priori "computable" at the pre-design stage).

To address this challenge, we generalize a recently developed set-theoretic model reference adaptive control architecture [1] (see also [21, 93, 101–104, 108]), which has the capability to achieve "practical" performance guarantees, for uncertain dynamical systems subject to actuator dynamics using tools and methods from [40, 41]. Specifically, we first show that the proposed set-theoretic model reference adaptive control architecture keeps the performance bounds between the uncertain dynamical system trajectories and the "modified" reference model trajectories within an a-priori, user-defined bound (unlike the results in [40, 41]). We next show that the error bounds between the "ideal" reference model trajectories and the uncertain dynamical system trajectories is characterized by this user-defined bound as well as the actuator bandwidth limit, and hence, is a-priori "computable" using a given set of adaptive control design parameters. Finally, as a byproduct, our illustrative numerical example shows that the time rate of change of the actual control signal (i.e., the output of the actuator dynamics) becomes less in magnitude as compared with the the set-theoretic model reference adaptive control case without actuator dynamics.

The contents of this paper are as follows. In Section 4.3.2, we overview necessary notation and definitions for the main results of this paper. In Sections 4.3.3, we present the problem formulation and an overview on the set-theoretic model reference adaptive control architecture considered in this paper. In Section 4.3.4, we present the proposed set-theoretic model reference adaptive control architecture for uncertain dynamical systems subject to actuator dynamics, where the convergence of the ("ideal" and "modified") reference models are presented in Section 4.3.5. The efficacy of our theoretical results are also demonstrated via an illustrative numerical example in Section 4.3.6. Finally, conclusions are summarized in Section 4.3.7. Once again, note that the contribution of this paper builds on the results in [1, 40, 41] and can be viewed either as the generalization of the results in [1] to uncertain dynamical systems subject to

actuator dynamics using tools and methods from [40, 41], or as the generalization of the results in [40, 41] to set-theoretic model reference adaptive control based on the theory developed in [1].

4.3.2 Notation and Definitions

The notation used throughout this paper is standard and similar to, for example, [1]. For self-containedness, note that $\mathbb{R}$ denotes the set of real numbers, $\mathbb{R}^n$ denotes the set of $n \times 1$ real column vectors, $\mathbb{R}^{n\times m}$ denotes the set of $n \times m$ real matrices, $\mathbb{R}_+$ (respectively, $\overline{\mathbb{R}}_+$) denotes the set of positive (respectively, nonnegative-definite) real numbers, $\mathbb{R}_+^{n\times n}$ (respectively, $\overline{\mathbb{R}}_+^{n\times n}$) denotes the set of $n \times n$ positive-definite (respectively, nonnegative-definite) real matrices, $\mathbb{D}^{n\times n}$ denotes the set of $n \times n$ real matrices with diagonal scalar entries, $0_{n\times n}$ denotes the $n \times n$ zero matrix, and "$\triangleq$" denotes equality by definition. We, in addition, write $(\cdot)^{\mathrm{T}}$ for the transpose operator, $(\cdot)^{-1}$ for the inverse operator, $\mathrm{tr}(\cdot)$ for the trace operator, and $\|\cdot\|_2$ for the Euclidean norm. We also write $\|x\|_{\mathrm{A}} \triangleq \sqrt{x^{\mathrm{T}}Ax}$ for the weighted Euclidean norm of $x \in \mathbb{R}^n$ with the matrix $A \in \mathbb{R}_+^{n\times n}$, $\|A\|_2 \triangleq \sqrt{\lambda_{\max}(A^{\mathrm{T}}A)}$ for the induced 2-norm of the matrix $A \in \mathbb{R}^{n\times m}$, $\lambda_{\min}(A)$ (resp., $\lambda_{\max}(A)$) for the minimum (resp., maximum) eigenvalue of the matrix $A \in \mathbb{R}^{n\times n}$, and $\underline{x}$ (resp., $\overline{x}$) for the lower bound (resp., upper bound) of a bounded signal $x(t) \in \mathbb{R}^n$, $t \geq 0$, that is, $\underline{x} \leq \|x(t)\|_2, t \geq 0$ (resp., $\|x(t)\|_2 \leq \overline{x}, t \geq 0$). We next define the projection operator. For this purpose, let $\Omega = \left\{\theta \in \mathbb{R}^n : (\theta_i^{\min} \leq \theta_i \leq \theta_i^{\max})_{i=1,2,\cdots,n}\right\}$ be a convex hypercube in $\mathbb{R}^n$, where $(\theta_i^{\min}, \theta_i^{\max})$ represent the minimum and maximum bounds for the i^{th} component of the n-dimensional parameter vector θ. Additionally, for a sufficiently small positive constant ν, a second hypercube is defined by $\Omega_\nu = \left\{\theta \in \mathbb{R}^n : (\theta_i^{\min} + \nu \leq \theta_i \leq \theta_i^{\max} - \nu)_{i=1,2,\cdots,n}\right\}$, where $\Omega_\nu \subset \Omega$. Then, the projection operator $\mathrm{Proj} : \mathbb{R}^n \times \mathbb{R}^n \to \mathbb{R}^n$ is defined componentwise by

$$\mathrm{Proj}(\theta, y) \triangleq \begin{cases} \left(\frac{\theta_i^{\max} - \theta_i}{\nu}\right) y_i, & \text{if } \theta_i > \theta_i^{\max} - \nu \\ & \text{and } y_i > 0 \\ \left(\frac{\theta_i - \theta_i^{\min}}{\nu}\right) y_i, & \text{if } \theta_i < \theta_i^{\min} + \nu \\ & \text{and } y_i < 0 \\ y_i, & \text{otherwise} \end{cases} \tag{4.117}$$

where $y \in \mathbb{R}^n$ [30]. It follows from (4.117) that $(\theta - \theta^*)^{\mathrm{T}}(\mathrm{Proj}(\theta, y) - y) \leq 0$ holds (see [30, 80] for details). This definition can be further generalized to matrices as $\mathrm{Proj}_{\mathrm{m}}(\Theta, Y) = \big(\mathrm{Proj}(\mathrm{col}_1(\Theta), \mathrm{col}_1(Y)), \ldots, \mathrm{Proj}(\mathrm{col}_m(\Theta), \mathrm{col}_m(Y))\big)$, where $\Theta \in \mathbb{R}^{n\times m}$, $Y \in \mathbb{R}^{n\times m}$ and $\mathrm{col}_i(\cdot)$ denotes ith column operator. In this

case, for a given matrix Θ^*, it follows from $(\theta-\theta^*)^{\mathrm{T}}(\mathrm{Proj}(\theta,y)-y)\leq 0$ that $\mathrm{tr}\left[(\Theta-\Theta^*)^{\mathrm{T}}(\mathrm{Proj}_{\mathrm{m}}(\Theta,Y)-Y)\right]=\sum_{i=1}^{m}\left[\mathrm{col}_i(\Theta-\Theta^*)^{\mathrm{T}}(\mathrm{Proj}(\mathrm{col}_i(\Theta),\mathrm{col}_i(Y))-\mathrm{col}_i(Y))\right]\leq 0$.

We finally define $\phi(\|z\|_{\mathrm{H}})$, $\phi:\mathbb{R}\to\mathbb{R}$, to be a "generalized restricted potential function" (generalized barrier Lyapunov function) on the set $\mathcal{D}_\varepsilon \triangleq \left\{\|z\|_{\mathrm{H}} : \|z\|_{\mathrm{H}}\in[0,\varepsilon)\right\}$ with $\varepsilon\in\mathbb{R}_+$ being a user-defined constant, if the following statements hold [1]:

i) If $\|z\|_{\mathrm{H}}=0$, then $\phi(\|z\|_{\mathrm{H}})=0$.

ii) If $\|z\|_{\mathrm{H}}\in\mathcal{D}_\varepsilon$ and $\|z\|_{\mathrm{H}}\neq 0$, then $\phi(\|z\|_{\mathrm{H}})>0$.

iii) If $\|z\|_{\mathrm{H}}\to\varepsilon$, then $\phi(\|z\|_{\mathrm{H}})\to\infty$.

iv) $\phi(\|z\|_{\mathrm{H}})$ is continuously differentiable on $\mathcal{D}_\varepsilon$.

v) If $\|z\|_{\mathrm{H}}\in\mathcal{D}_\varepsilon$, then $\phi_d(\|z\|_{\mathrm{H}})>0$, where

$$\phi_d(\|z\|_{\mathrm{H}}) \triangleq \frac{\mathrm{d}\phi(\|z\|_{\mathrm{H}})}{\mathrm{d}\|z\|_{\mathrm{H}}^2}. \tag{4.118}$$

vi) If $\|z\|_{\mathrm{H}}\in\mathcal{D}_\varepsilon$, then

$$2\phi_d(\|z\|_{\mathrm{H}})\|z\|_{\mathrm{H}}^2-\phi(\|z\|_{\mathrm{H}})>0. \tag{4.119}$$

As noted in [1], this definition generalizes the definition of the "restricted potential functions" (barrier Lyapunov functions) (e.g., see [21–26, 107]) and a candidate generalized restricted potential function satisfying the conditions given above has the form $\phi(\|z\|_{\mathrm{H}})=\|z\|_{\mathrm{H}}^2/(\varepsilon-\|z\|_{\mathrm{H}})$, $\|z\|_{\mathrm{H}}\in\mathcal{D}_\varepsilon$.

4.3.3 Set-Theoretic Model Reference Adaptive Control: A Concise Overview

We now present the problem formulation and overview the set-theoretic model reference adaptive control architecture proposed in [1]. For this purpose, consider the uncertain dynamical system given by

$$\dot{x}(t) \;=\; Ax(t)+B\big(u(t)+\delta(t,x(t))\big),\quad x(0)=x_0,\quad t\geq 0, \tag{4.120}$$

where $x(t)\in\mathbb{R}^n$, $t\geq 0$, is the available (i.e., measurable) state vector, $u(t)\in\mathbb{R}^m$, $t\geq 0$, is the control input, $A\in\mathbb{R}^{n\times n}$ is a known system matrix, $B\in\mathbb{R}^{n\times m}$ is a known input matrix, $\delta:\overline{\mathbb{R}}_+\times\mathbb{R}^n\to\mathbb{R}^m$ is a system uncertainty, and the pair (A,B) is controllable. We now introduce a linear and time-varying version of the standard "structured" system uncertainty parameterization [28–30].

Assumption 4.3.1 *The system uncertainty given by* (4.120) *is parameterized as*

$$\delta(t,x(t)) \quad = \quad W^{\mathrm{T}}(t)x(t), \quad t \geq 0, \tag{4.121}$$

where $W(t) \in \mathbb{R}^{n\times m}$, $t \geq 0$, *is a bounded unknown weight matrix (i.e.,* $\|W(t)\|_2 \leq w$, $t \geq 0$*) with a bounded time rate of change (i.e.,* $\|\dot{W}(t)\|_2 \leq \dot{w}$, $t \geq 0$*).*

Next, let desired command following characteristics be captured by the "ideal" reference model given by

$$\dot{x}_{\mathrm{r_i}}(t) \quad = \quad A_{\mathrm{r}}x_{\mathrm{r_i}}(t) + B_{\mathrm{r}}c(t), \quad x_{\mathrm{r_i}}(0) = x_{\mathrm{r_i}0}, \quad t \geq 0, \tag{4.122}$$

where $c(t) \in \mathbb{R}^{n_{\mathrm{c}}}$, $t \geq 0$, is a given bounded piecewise continuous command (i.e. $\|c(t)\|_2 \leq \bar{c}$, $t \geq 0$), and $x_{\mathrm{r_i}}(t) \in \mathbb{R}^n$, $t \geq 0$, is the reference state vector. Now, consider the feedback control law given by

$$u(t) = u_{\mathrm{n}}(t) + u_{\mathrm{a}}(t), \quad t \geq 0, \tag{4.123}$$

where $u_{\mathrm{n}}(t) \in \mathbb{R}^m$, $t \geq 0$, and $u_{\mathrm{a}}(t) \in \mathbb{R}^m$, $t \geq 0$, are the nominal and adaptive control laws, respectively. Furthermore, let the nominal control law be

$$u_{\mathrm{n}}(t) = -K_1x(t) + K_2c(t), \quad t \geq 0, \tag{4.124}$$

such that $A_{\mathrm{r}} \triangleq A - BK_1$, $K_1 \in \mathbb{R}^{m\times n}$, is Hurwitz and $B_{\mathrm{r}} \triangleq BK_2, K_2 \in \mathbb{R}^{m\times n_{\mathrm{c}}}$. Using (4.123) and (4.124) in (4.120) yields

$$\dot{x}(t) \quad = \quad A_{\mathrm{r}}x(t) + B_{\mathrm{r}}c(t) + B\left[u_{\mathrm{a}}(t) + W^{\mathrm{T}}(t)x(t)\right], \quad x(0) = x_0, \quad t \geq 0. \tag{4.125}$$

Considering (4.125), let the adaptive control law be

$$u_{\mathrm{a}}(t) = -\hat{W}^{\mathrm{T}}(t)x(t), \quad t \geq 0, \tag{4.126}$$

where $\hat{W}(t) \in \mathbb{R}^{n\times m}$, $t \geq 0$, is an estimate of $W(t)$, $t \geq 0$.

Now, following the architecture presented in [1], consider the update law for (4.126) as

$$\dot{\hat{W}}(t) = \gamma_{\mathrm{i}}\mathrm{Proj}_{\mathrm{m}}\Big(\hat{W}(t), \phi_d(\|e_{\mathrm{i}}(t)\|_P)x(t)e_{\mathrm{i}}^{\mathrm{T}}(t)PB\Big), \quad \hat{W}(0) = \hat{W}_0, \quad t \geq 0, \tag{4.127}$$

with $\hat{W}_{\max}$ being the projection norm bound and $\|\hat{W}(t)\|_2 \leq \hat{w}, t \geq 0$. In (4.127), additionally, $\gamma_{\mathrm{i}} \in R_+$ is the learning rate (i.e., adaptation gain), $P \in \mathbb{R}_+^{n\times n}$ is a solution of the Lyapunov equation given by

$$0 \quad = \quad A_{\mathrm{r}}^{\mathrm{T}}P + PA_{\mathrm{r}} + R, \tag{4.128}$$

with $R \in \mathbb{R}_+^{n\times n}$, and $e_{\mathrm{i}}(t) \triangleq x(t) - x_{\mathrm{r_i}}(t), t \geq 0$, being the system error. Note that $\phi_d(\|e_{\mathrm{i}}(t)\|_P), t \geq 0$ in (4.127) can be viewed as an error dependent learning rate.

We now state the key result presented in Theorem 3.1 of [1]. For this purpose, consider the system error dynamics and the weight estimation error dynamics respectively as

$$\dot{e}_{\mathrm{i}}(t) \quad = \quad A_{\mathrm{r}}e_{\mathrm{i}}(t) - B\tilde{W}^{\mathrm{T}}(t)x(t), \quad e_{\mathrm{i}}(0) = e_{\mathrm{i0}}, \quad t \geq 0, \tag{4.129}$$

$$\dot{\tilde{W}}(t) \quad = \quad \gamma_{\mathrm{i}}\mathrm{Proj}_{\mathrm{m}}\Big(\hat{W}(t), \phi_d(\|e_{\mathrm{i}}(t)\|_P)x(t)e_{\mathrm{i}}^{\mathrm{T}}(t)PB\Big) - \dot{W}(t), \quad \tilde{W}(0) = \tilde{W}_0, \quad t \geq 0, \tag{4.130}$$

where $\tilde{W}(t) \triangleq \hat{W}(t) - W(t)$, $t \geq 0$, is the weight estimation error. Using the energy function $V(e_{\mathrm{i}}, \tilde{W}) = \phi(\|e_{\mathrm{i}}\|_P) + \gamma_{\mathrm{i}}^{-1}\mathrm{tr}\big[\tilde{W}^{\mathrm{T}}\tilde{W}\big]$, where $\mathcal{D}_\varepsilon \triangleq \{\|e_{\mathrm{i}}(t)\|_P : \|e_{\mathrm{i}}(t)\|_P < \varepsilon\}$ with $P \in \mathbb{R}_+^{n\times n}$ being a solution of the Lyapunov equation in (4.128) for $R \in \mathbb{R}_+^{n\times n}$, we calculate $\dot{V}\big(e_{\mathrm{i}}(t), \tilde{W}(t)\big) \leq -\frac{1}{2}\alpha V(e_{\mathrm{i}}(t), \tilde{W}(t)) + \mu$ with $\alpha \triangleq \frac{\lambda_{\min}(R)}{\lambda_{\max}(P)}$, $d \triangleq 2\gamma_{\mathrm{i}}^{-1}\tilde{w}\,\dot{w}$, and $\mu \triangleq \frac{1}{2}\alpha\gamma_{\mathrm{i}}^{-1}\tilde{w}^2 + d$. To this end, we conclude the boundedness of the closed-loop dynamical system given by (4.129) and (4.130) as well as the strict performance bound on the system error given by $\|e_{\mathrm{i}}(t)\|_P < \varepsilon, t \geq 0$, where we refer to the proof of Theorem 3.1 in [1] for details.

4.3.4 Generalizations to Uncertain Dynamical Systems Subject to Actuator Dynamics

In this section, we generalize the set-theoretic adaptive control architecture overviewed in Section 4.3.3 to the uncertain dynamical systems subject to actuator dynamics. On this generalization, we consider the uncertain dynamical system given by [40]

$$\dot{x}(t) \quad = \quad Ax(t) + B\big(v(t) + \delta(t, x(t))\big), \quad x(0) = x_0, \quad t \geq 0, \tag{4.131}$$

where $v(t) \in \mathbb{R}^m$, $t \geq 0$, is the actuator output satisfying the "actuator dynamics"

$$\dot{x}_c(t) = -Mx_c(t)+u(t), \quad x_c(0)=x_{c0}, \quad t\geq 0, \tag{4.132}$$

$$v(t) = Mx_c(t), \quad v(0)=v_0, \quad t\geq 0, \tag{4.133}$$

where $x_c(t)\in\mathbb{R}^m$, $t\geq 0$, is the actuator state, $M\in\mathbb{R}_+^{m\times m}\cap\mathbb{D}^{m\times m}$ with diagonal entries $\lambda_{i,i}>0, i=1,\ldots,m$, represents the actuator bandwidth of each control channel, and $u(t)\in\mathbb{R}^m$, $t\geq 0$, is the control input signal. From a practical view, the above representation can be thought as the one given by (4.120), where each control signal is "filtered through a first-order filter" before they enter to uncertain dynamical system.

We next utilize the hedging approach [37]. To this end, we rewrite (4.131) as

$$\dot{x}(t) = Ax(t)+B\big(u(t)+W^{\mathrm{T}}(t)x(t)\big)+B\big(v(t)-u(t)\big), \quad x(0)=x_0, \quad t\geq 0. \tag{4.134}$$

Introducing (4.123), (4.124), and (4.126) in (4.134) yields

$$\dot{x}(t) = A_{\mathrm{r}}x(t)+B_{\mathrm{r}}c(t)-B\tilde{W}^{\mathrm{T}}(t)x(t)+B\big(v(t)-u(t)\big), \quad x(0)=x_0, \quad t\geq 0. \tag{4.135}$$

Applying the "hedging philosophy" here (we refer to [37] as well as [38–41] for details), the "modified" reference system is now given by

$$\dot{x}_{\mathrm{r}}(t) = A_{\mathrm{r}}x_{\mathrm{r}}(t)+B_{\mathrm{r}}c(t)+B\big(v(t)-u(t)\big), \quad x_{\mathrm{r}}(0)=x_{\mathrm{r}0}, \quad t\geq 0. \tag{4.136}$$

In (4.136), the added term to the "ideal" reference model (4.122) (i.e., "$B\big(v(t)-u(t)\big)$") is called the "hedge signal." To implement the adaptive control law given by (4.126), we consider the update law given by

$$\dot{\hat{W}}(t) = \gamma\mathrm{Proj}_{\mathrm{m}}\Big(\hat{W}(t),\phi_d(\|e(t)\|_P)x(t)e^{\mathrm{T}}(t)PB\Big), \quad \hat{W}(0)=\hat{W}_0, \quad t\geq 0. \tag{4.137}$$

While (4.137) looks similar to (4.127), it utilizes the error signal given by $e(t)\triangleq x(t)-x_{\mathrm{r}}(t)$, $t\geq 0$, which represents the difference between the uncertain dynamical system trajectories and the "modified" reference model trajectories (unlike the error signal $e_{\mathrm{i}}(t)$ used in (4.127)).

For the main result of this section, we note the following:

i) It follows from the above formulation that one can now write the system error dynamics and the weight estimation error dynamics respectively as

$$\dot{e}(t) = A_{\mathrm{r}}e(t) - B\tilde{W}^{\mathrm{T}}(t)x(t), \quad e(0) = e_0, \quad t \geq 0, \tag{4.138}$$

$$\dot{\tilde{W}}(t) = \gamma \mathrm{Proj}_{\mathrm{m}}\Big(\hat{W}(t), \phi_d(\|e(t)\|_P)x(t)e^{\mathrm{T}}(t)PB\Big) - \dot{W}(t), \quad \tilde{W}(0) = \tilde{W}_0, \quad t \geq 0. \tag{4.139}$$

ii) It follows from Lemma 3.1 of [40] or Lemma 1.3.1 of [41] that there exists a set $\kappa \triangleq \big\{\underline{\lambda} : \underline{\lambda} \leq \lambda_{i,i},\ i = 1,\ldots,m\big\} \bigcup \big\{\overline{\omega} : \hat{W}_{\max,i+(j-1)n} \leq \overline{\omega}, i = 1,\ldots,n, j = 1,\ldots,m\big\}$ such that if $(\underline{\lambda},\overline{\omega}) \in \kappa$, then

$$\mathcal{A}(\hat{W}(t),M) = \begin{bmatrix} A + B\hat{W}^{\mathrm{T}}(t) & BM \\ -K_1 - \hat{W}^{\mathrm{T}}(t) & -M \end{bmatrix}, \quad t \geq 0, \tag{4.140}$$

is quadratically stable. That is, similar to the results in [40, 41], the existence of the set κ is necessary for the feasibility of the considered adaptive control problem. To see this, let $\zeta(t) \triangleq [x_{\mathrm{r}}^{\mathrm{T}}(t), x_{\mathrm{c}}^{\mathrm{T}}(t)]^{\mathrm{T}}$, $t \geq 0$, which yields $\dot{\zeta}(t) = \mathcal{A}(\hat{W}(t),M)\zeta(t) + \omega(e(t),\hat{W}(t))$, $t \geq 0$, with

$$\omega(e(t),\hat{W}(t)) = \begin{bmatrix} B\big(\hat{W}^{\mathrm{T}}(t) + K_1\big)e(t) \\ -\big(\hat{W}^{\mathrm{T}}(t) + K_1\big)e(t) + K_2c(t) \end{bmatrix}, \quad t \geq 0. \tag{4.141}$$

Now, if the system error dynamics and the weight estimation error dynamics respectively given by (4.136) and (4.139) have bounded trajectories, then it follows that $\omega(e(t),\hat{W}(t))$, $t \geq 0$, in (4.141) is bounded. Thus, by quadratic stability of $\mathcal{A}(\hat{W}(t),M)$, $t \geq 0$, on κ, $\zeta(t)$, $t \geq 0$, is bounded. As a consequence, all closed-loop dynamical system trajectories (including $x(t)$) are bounded provided that (4.136) and (4.139) have bounded trajectories.

We are now ready to state the main result of this section.

Theorem 4.3.1 *Consider the uncertain dynamical system given by (4.131) subject to Assumption 4.3.1 and actuator dynamics (4.132) and (4.133), the modified reference model given by (4.136), the feedback control law given by (4.123) with (4.124), (4.126), and (4.137). In addition, assume $\|e_0\|_P < \varepsilon$ and $(\underline{\lambda},\overline{\omega}) \in \kappa$ hold. Then, all closed-loop system trajectories are bounded, where the bound on the system error strictly satisfies a-priori given, user-defined worst-case performance*

$$\|e(t)\|_P < \varepsilon, \quad t \geq 0. \tag{4.142}$$

Proof. The first step of the proof is similar to the discussion given in the last paragraph of Section 4.3.3. Specifically, consider the energy function given by $V(e,\tilde{W}) = \phi(\|e\|_P) + \gamma^{-1}\mathrm{tr}\big[\tilde{W}^{\mathrm{T}}\tilde{W}\big]$, where $\mathcal{D}_\varepsilon \triangleq \{\|e(t)\|_P : \|e(t)\|_P < \varepsilon\}$ with $P \in \mathbb{R}^{n\times n}_+$ being a solution of the Lyapunov equation in (4.128) for $R \in \mathbb{R}^{n\times n}_+$. Using this energy function, one can calculate $\dot{V}\big(e(t),\tilde{W}(t)\big) \leq -\frac{1}{2}\alpha V(e(t),\tilde{W}(t)) + \mu$, where $\alpha \triangleq \frac{\lambda_{\min}(R)}{\lambda_{\max}(P)}$, $d \triangleq 2\gamma_{\mathrm{i}}^{-1}\tilde{w}\,\dot{w}$, and $\mu \triangleq \frac{1}{2}\alpha\gamma_{\mathrm{i}}^{-1}\tilde{w}^2 + d$. In this calculation, we adopt similar steps as in the proof of Theorem 3.1 in [1]; thus, we refer interested readers to [1] for details. Above, we conclude the boundedness of the pair $(e(t),\tilde{W}(t))$, $t \geq 0$, for (4.138) and (4.139) as well as the result in (4.142) once $\|e_0\|_P < \varepsilon$ holds.

Note that since $\tilde{W}(t) = \hat{W}(t) - W(t)$, $t \geq 0$, and $W(t)$, $t \geq 0$, is assumed to be bounded, this conclusion implies that $\hat{W}(t)$, $t \geq 0$, is bounded. Considering $e(t) = x(t) - x_{\mathrm{r}}(t)$, $t \geq 0$, however, boundedness of $e(t)$, $t \geq 0$, does not directly imply the boundedness of $x(t)$, $t \geq 0$, here, since $x_{\mathrm{r}}(t)$, $t \geq 0$, can be unbounded in general. Thus, we now establish the boundedness of $x_{\mathrm{r}}(t)$, $t \geq 0$, using $(\underline{\lambda},\overline{\omega}) \in \kappa$. In particular, following the discussion given before Theorem 4.3.1, $(\underline{\lambda},\overline{\omega}) \in \kappa$ implies that (4.140) is quadratically stable; hence, $\zeta(t)$, $t \geq 0$, is bounded containing the pair $(x_{\mathrm{r}}(t),x_{\mathrm{c}}(t))$, $t \geq 0$ (we refer interested readers to the proofs of, for example, Theorem 3.1 in [40] or Theorem 1.3.1 in [41] for additional details). The proof is now complete since this discussion gives the boundedness of all closed-loop system trajectories. ■

From Theorem 4.3.1, if $\|e_0\|_P < \varepsilon$ and $(\underline{\lambda},\overline{\omega}) \in \kappa$ hold, then all closed-loop system trajectories are bounded and the user-defined worst-case performance bound given by (4.142) is guaranteed. Specifically, the assumption on $\|e_0\|_P < \varepsilon$ can be trivially satisfied by a judicious initialization of the "modified" reference model given by (4.136). For example, considering $x_{\mathrm{r}0} = x_0$, one has $\|e_0\|_P = \|x_0 - x_{\mathrm{r}0}\|_P = \|x_0 - x_0\|_P = 0 < \varepsilon$ that holds for any ε chosen by the control user. To satisfy the assumption on $(\underline{\lambda},\overline{\omega}) \in \kappa$, which implies the quadratic stability of $\mathcal{A}(\hat{W}(t),M)$, $t \geq 0$, given by (4.140), one can consider the following convex optimization problem from Remark 3.3 of [40] or Section 1.3 of [41]: If

$$\mathcal{A}_{i_1,\ldots,i_l} = \begin{bmatrix} A + B\overline{W}^{\mathrm{T}}_{i_1,\ldots,i_l} & BM \\ -K_1 - \overline{W}^{\mathrm{T}}_{i_1,\ldots,i_l} & -M \end{bmatrix}, \tag{4.143}$$

satisfies the matrix inequality

$$\mathcal{A}^{\mathrm{T}}_{i_1,\ldots,i_l}\mathcal{P} + \mathcal{P}\mathcal{A}_{i_1,\ldots,i_l} < 0, \quad \mathcal{P} = \mathcal{P}^{\mathrm{T}} > 0, \tag{4.144}$$

for all permutations of $\overline{W}_{i_1,\ldots,i_l} \in \mathbb{R}^{n\times m}$, then (4.140) is quadratically stable. Above, $\overline{W}_{i_1,\ldots,i_l}$ denotes

$$\overline{W}_{i_1,\ldots,i_l} = \begin{bmatrix} (-1)^{i_1}\hat{W}_{\max,1} & \cdots & (-1)^{i_{1+(m-1)n}}\hat{W}_{\max,1+(m-1)n} \\ (-1)^{i_2}\hat{W}_{\max,2} & \cdots & (-1)^{i_{2+(m-1)n}}\hat{W}_{\max,2+(m-1)n} \\ \vdots & \ddots & \vdots \\ (-1)^{i_n}\hat{W}_{\max,n} & \cdots & (-1)^{i_{mn}}\hat{W}_{\max,mn} \end{bmatrix}, \tag{4.145}$$

with $i_l \in \{1,2\}$, $l \in \{1,\ldots,2^{mn}\}$, where it essentially represents the corners of the hypercube that represents the maximum variation of $\hat{W}(t), t \geq 0$.

4.3.5 Distance Between of Uncertain Dynamical System and Ideal Reference Model Trajectories

In the previous section, we showed that using the set-theoretic adaptive control architecture, one can achieve the prescribed system performance guarantees for the error signal between the uncertain dynamical system in (4.120) and the modified reference system in (4.136). In this section, we analyze the distance between the uncertain dynamical system in (4.120) and the actual, "ideal" reference model in (4.122). For this purpose, let $e_{\mathrm{r}}(t) \triangleq x_{\mathrm{r}}(t) - x_{\mathrm{r_i}}(t), t \geq 0$, be the error between the modified and the ideal reference systems. Therefore, one can write

$$\|x(t) - x_{\mathrm{r_i}}(t)\|_{\mathcal{L}_\infty} = \|e(t) + e_{\mathrm{r}}(t)\|_{\mathcal{L}_\infty} \leq \|e(t)\|_{\mathcal{L}_\infty} + \|e_{\mathrm{r}}(t)\|_{\mathcal{L}_\infty}, \quad t \geq 0. \tag{4.146}$$

Now for the sake of the next result, let [41]

$$\mathcal{P} \triangleq \begin{bmatrix} P & PB \\ B^{\mathrm{T}}P & B^{\mathrm{T}}PB + \rho I \end{bmatrix}, \tag{4.147}$$

where $P \in \mathbb{R}_+^{n\times n}$ is a solution of the Lyapunov equation given by (4.128) with $R \in \mathbb{R}_+^{n\times n}$ and $\rho \in \mathbb{R}_+$. Note that the actuator bandwidth matrix $M_0 \in \mathbb{R}_+^{m\times m} \cap \mathbb{D}^{m\times m}$ can be related to the actual actuator bandwidth matrix $M \in \mathbb{R}_+^{m\times m} \cap \mathbb{D}^{m\times m}$ as $M \triangleq \psi M_0$, where $\psi \in \mathbb{R}_+$ and $\psi \geq 1$.

Theorem 4.3.2 *Based on the conditions given in Theorem 4.3.1, the error signal between the system state and ideal reference system state can be characterized by the user-defined parameter ε as well as ψ, which*

is related with the actuator bandwidth, and is given by

$$\begin{aligned}\|x(t)-x_{\mathrm{r_i}}(t)\|_{\mathcal{L}_\infty} \quad \leq \quad & \varepsilon\rho\sqrt{\frac{\lambda_{\max}(\mathcal{P})}{\lambda_{\min}(P)\lambda_{\min}(\mathcal{P})}}\sqrt{\frac{5\eta+(\psi-1)\beta}{\eta(\eta+(\psi-1)\beta)^2}}\Bigg(\left(\|B\|_2+1\right)\left(\hat{w}+\|K_1\|_2\right) \\ & +\frac{\sqrt{\lambda_{\min}(P)}\|K_2\|_2\bar{c}}{\varepsilon}\Bigg)+\frac{\varepsilon}{\sqrt{\lambda_{\min}(P)}}, \quad \eta\in\mathbb{R}_+, \quad t\geq 0. \end{aligned} \tag{4.148}$$

Proof. It follows from Theorem 1.4.1 of [41] that

$$\|e_{\mathrm{r}}(t)\|_{\mathcal{L}_\infty} < \rho\omega^*\sqrt{\frac{\lambda_{\max}(\mathcal{P})}{\lambda_{\min}(\mathcal{P})}}\sqrt{\frac{5\eta+(\psi-1)\beta}{\eta(\eta+(\psi-1)\beta)^2}}, \quad t\geq 0, \tag{4.149}$$

with $\beta = 2\rho\lambda_{\min}(M_0)$, $\eta\in\mathbb{R}_+$ satisfying

$$\mathcal{A}^{\mathrm{T}}(\hat{W}(t),M_0)\mathcal{P}+\mathcal{P}\mathcal{A}(\hat{W}(t),M_0)\leq -\eta I_{n+m}, \quad t\geq 0, \tag{4.150}$$

and ω^* being the upper bound on $\omega(\cdot)$ in (4.141) given by

$$\begin{aligned}\|\omega(\cdot)\|_2 \quad \leq \quad & \left\|B\left(\hat{W}^{\mathrm{T}}(t)+K_1\right)e(t)\right\|_2+\left\|-\left(\hat{W}^{\mathrm{T}}(t)+K_1\right)e(t)+K_2c(t)\right\|_2 \\ \leq \quad & \frac{\varepsilon}{\sqrt{\lambda_{\min}(P)}}\left(\left\|B\left(\hat{W}^{\mathrm{T}}(t)+K_1\right)\right\|_2+\left\|\left(\hat{W}^{\mathrm{T}}(t)+K_1\right)\right\|_2\right)+\|K_2c(t)\|_2 \\ \leq \quad & \frac{\varepsilon}{\sqrt{\lambda_{\min}(P)}}\left(\|B\|_2+1\right)\left(\hat{w}+\|K_1\|_2\right)+\|K_2\|_2\bar{c}, \quad t\geq 0. \end{aligned} \tag{4.151}$$

Furthermore, it follows from Theorem 4.3.1 that

$$\|e(t)\|_\infty \leq \|e(t)\|_2 < \frac{\varepsilon}{\sqrt{\lambda_{\min}(P)}}, \quad t\geq 0. \tag{4.152}$$

Introducing (4.149), (4.151) and (4.152) in (4.146) yields

$$\begin{aligned}\|x(t)-x_{\mathrm{r_i}}(t)\|_{\mathcal{L}_\infty} \quad \leq \quad & \frac{\varepsilon}{\sqrt{\lambda_{\min}(P)}}\Bigg(\rho\left(\left(\|B\|_2+1\right)\left(\hat{w}+\|K_1\|_2\right)+\frac{\sqrt{\lambda_{\min}(P)}\|K_2\|_2\bar{c}}{\varepsilon}\right)\sqrt{\frac{\lambda_{\max}(\mathcal{P})}{\lambda_{\min}(\mathcal{P})}} \\ & \cdot\sqrt{\frac{5\eta+(\psi-1)\beta}{\eta(\eta+(\psi-1)\beta)^2}}+1\Bigg), \quad t\geq 0, \end{aligned} \tag{4.153}$$

which simplifies to (4.148). ■

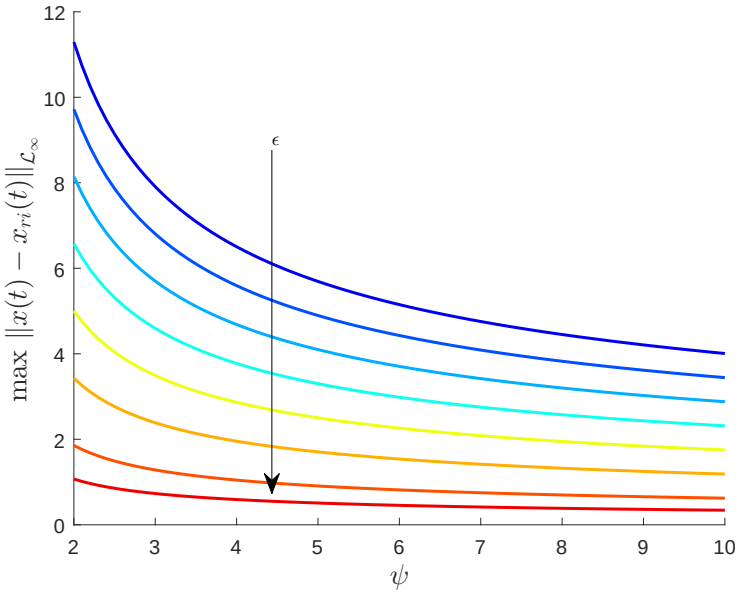

Figure 4.23: The upper bound of the error signal between the uncertain dynamical system state and the ideal reference system state given by Theorem 4.3.2.

The bound given by (4.148) captures the distance between the "ideal" reference model trajectories and the uncertain dynamical system trajectories, which is characterized by the user-defined bound ε as well as ψ related with the actuator bandwidth. From a practical standpoint, note that this bound is "computable" using a given set of adaptive control design parameters.

Remark 4.3.1 *To elucidate the effect of the controller design parameters on* (4.148)*, let* $A = 0.2$*,* $B = 1$*,* $w = 1$*,* $0.9 < \hat{w} < 1.1$*,* $K_1 = 0.4$*,* $K_2 = 1$*,* $A_r = -0.2$*,* $B_r = 1$*, which yields to* $M_0 = 2.2$*, and* $\eta = 0.1879$*. Figure 4.23 shows the effect of* $\varepsilon \in [0.05, 2]$ *and* $\psi \in [2, 10]$ *on the ultimate bounds given by* (4.148)*. Specifically, as expected, increasing* ψ *and decreasing* ε *yields smaller ultimate bound for* $\|x(t) - x_{r_i}(t)\|_{\mathcal{L}_\infty}$*,* $t \geq 0$*.*

4.3.6 Illustrative Numerical Example

Consider the uncertain dynamical system given by

$$\dot{x}(t) = \begin{bmatrix} 0 & 1 \\ 0 & 0 \end{bmatrix} x(t) + \begin{bmatrix} 0 \\ 1 \end{bmatrix} \Big(\Lambda v(t) + \delta(t, x(t)) \Big), \quad x(0) = 0, \quad t \geq 0, \tag{4.154}$$

where $x(t) = \begin{bmatrix} x_1(t) & x_2(t) \end{bmatrix}^{\mathrm{T}}$, $t \geq 0$, with $x_1(t)$, $t \geq 0$, representing the angle (in rad) and $x_2(t)$, $t \geq 0$, representing the angular rate (in rad/sec). In (4.154), $\delta(t, x(t))$, $t \geq 0$, represents an uncertainty of the form

$$\delta(t,x(t)) = w_1(t)x_1(t) + w_2x_2(t), \quad t \geq 0, \tag{4.155}$$

with $w_1(t) = \sin(0.25t) - 1$, $t \geq 0$, and $w_2 = 1$, and $\Lambda = 0.75$ represents an uncertain control effectiveness matrix. We use linear quadratic regulator design to choose $K_1 = [2.89, 3.02]$ and $K_2 = 2.89$ in (4.124), which yields to the reference model given by

$$\dot{x}_{\mathrm{r}}(t) = \begin{bmatrix} 0 & 1 \\ -2.89 & -3.02 \end{bmatrix} x_{\mathrm{r}}(t) + \begin{bmatrix} 0 \\ 2.89 \end{bmatrix} c(t) \quad x_{\mathrm{r}}(0) = 0 \quad t \geq 0. \tag{4.156}$$

First, for the case where there is no actuator dynamics, we apply the set-theoretic model reference adaptive control architecture in Section 4.3.3. The bounds on the uncertainty are set element-wise using the rectangular projection operator such that $-3 < \hat{w}_1 < 2$, and $0 < \hat{w}_2 < 2$, and we use $R = I$ to calculate P from (4.128) for the resulting A_{r} matrix. Figures 4.24(a) to 4.24(f) show the system performance with set-theoretic adaptive control architecture with $\varepsilon = 0.05$ when there is no actuator dynamics. The time derivative (generated by the `diff` function of Matlab) of the control signal $u(t), t \geq 0$, is shown in Figure 4.25.

Next, we consider a single-channel actuator dynamics given in (4.132) and (4.133) such that $M = \lambda, \lambda \in \mathbb{R}_+$. Using the bounds on $\hat{w}_1(t), t \geq 0$, and $\hat{w}_2(t), t \geq 0$, in LMI analysis, the minimum allowable actuator bandwidth is calculated as $\lambda_{\min} = 3.3$. Figures 4.26(a) to 4.26(f) show the system performance with set-theoretic adaptive control architecture with $\varepsilon = 0.05$ in presence of actuator dynamics with $\lambda = 10$ where they clearly illustrate the efficacy of the proposed architecture in this paper. The time derivative of the control signal $u(t), t \geq 0$, and the actuator output $v(t), t \geq 0$, are shown in Figure 4.28 where it is clear that compared to the previous case, the maximum rate of change in control input has decreased.

When the actuator bandwidth gets close to the calculated minimum allowable actuator bandwidth value $\lambda_{\min} = 3.3$, the system starts to exhibit some oscillations. However, the system response is still acceptable as it can be seen from Figures 4.27(a) to 4.27(f). The time derivative of the control signal $u(t), t \geq 0$, and the actuator output $v(t), t \geq 0$, are also shown in Figure 4.29.

Remark 4.3.2 *As a byproduct, our illustrative numerical example shows that the time rate of change of the (actual) control signal (i.e., the output of the actuator dynamics) becomes less in magnitude as compared with the the set-theoretic model reference adaptive control case without actuator dynamics.*

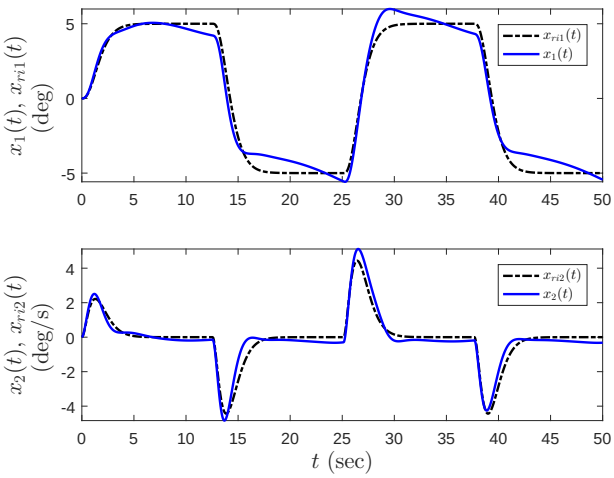

(a) Command following performance.

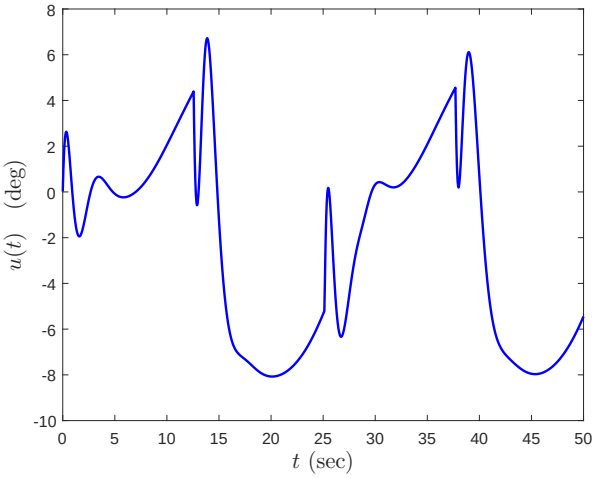

(b) Control signal.

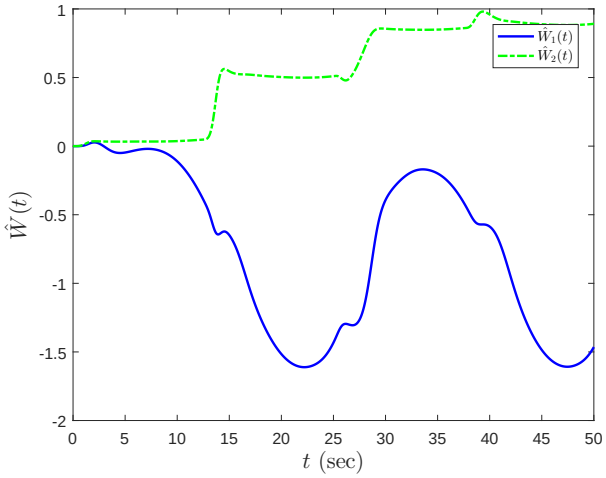

(c) Weight estimation.

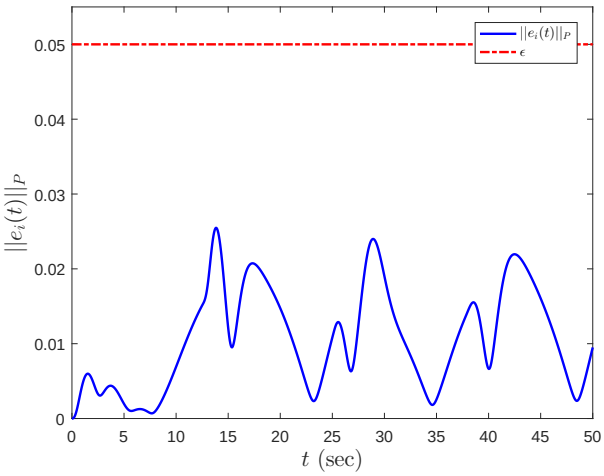

(d) Weighted error norm.

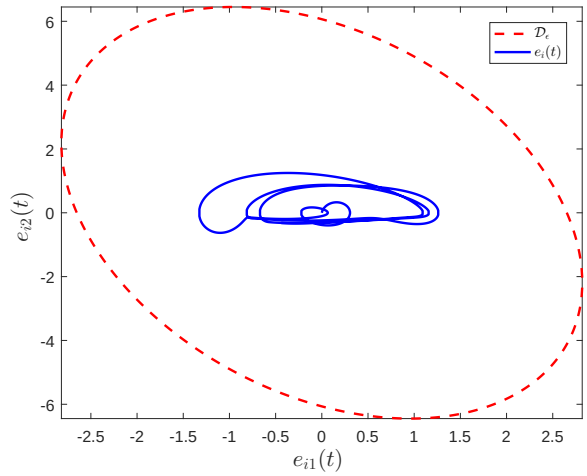

(e) 2D error plot.

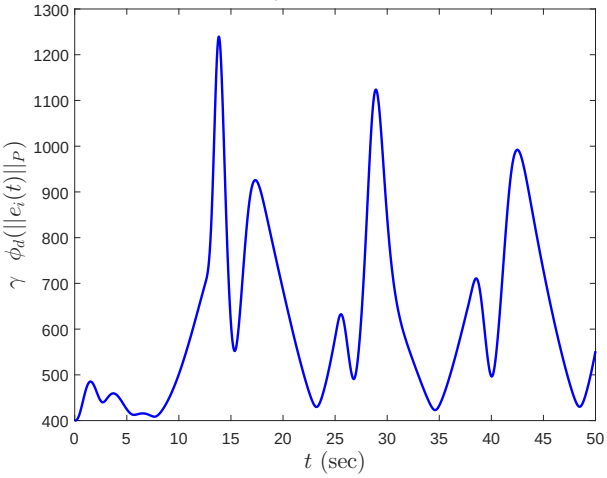

(f) Effective learning rate.

Figure 4.24: System performance with set-theoretic adaptive controller in Section 4.3.3.

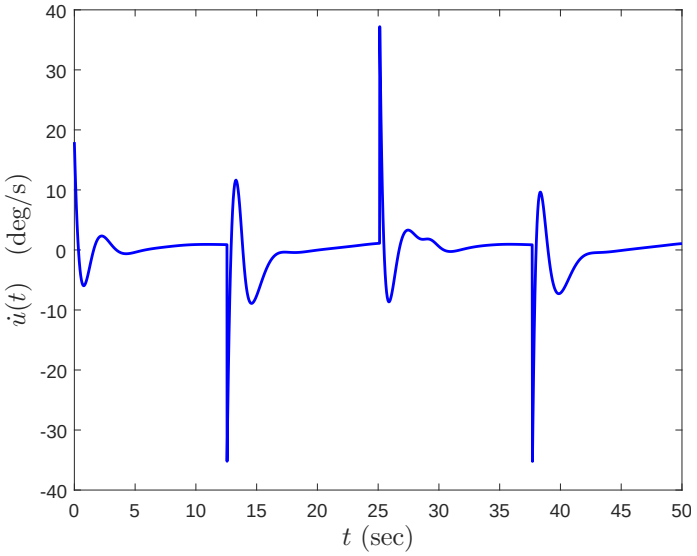

Figure 4.25: Time derivative of the control signal.

4.3.7 Conclusion

In this paper, we generalized a recently developed set-theoretic model reference adaptive control architecture, which has the capability to achieve "practical" (i.e., user-defined) performance guarantees, for uncertain dynamical systems subject to actuator dynamics. Specifically, we first showed that the proposed architecture keeps the performance bounds between the uncertain dynamical system trajectories and the "modified" reference model trajectories within an a-priori, user-defined bound. We next showed that the error bounds between the "ideal" reference model trajectories and the uncertain dynamical system trajectories is characterized by this user-defined bound as well as the actuator bandwidth limit, and hence, is "computable" using a given set of adaptive control design parameters. Our numerical example illustrated the efficacy of the proposed set-theoretic model reference adaptive controller.

4.4 Guaranteed Model Reference Adaptive Control Performance in the Presence of Actuator Failures[4]

For achieving strict closed-loop system performance guarantees in the presence of exogenous disturbances and system uncertainties, a new model reference adaptive control framework was recently proposed. Specifically, this framework was predicated on a set-theoretic adaptive controller construction using generalized restricted potential functions, where its key feature was to keep the distance between the trajectories

[4]This section is previously published in [101]. Permission is included in Appendix H.

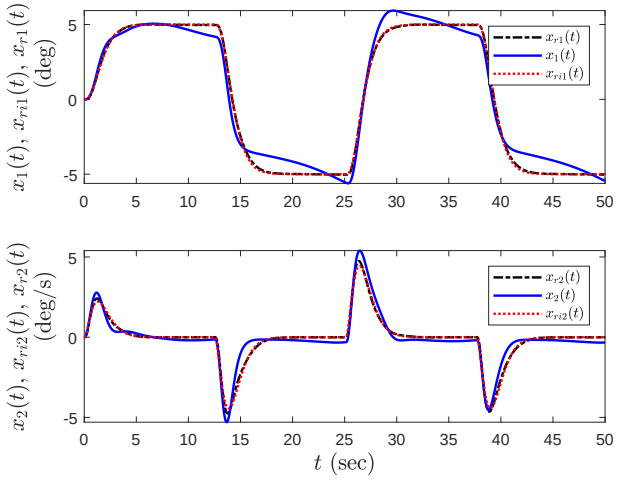

(a) Command following performance.

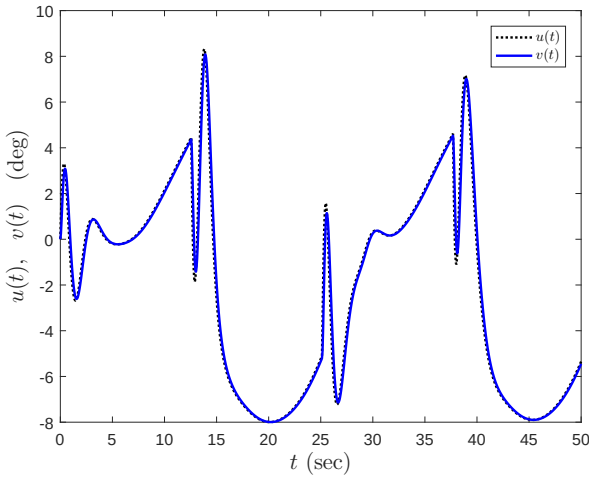

(b) Control signal.

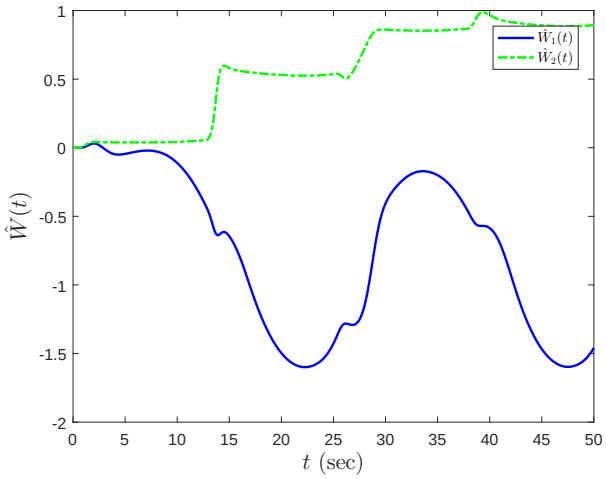

(c) Weight estimation.

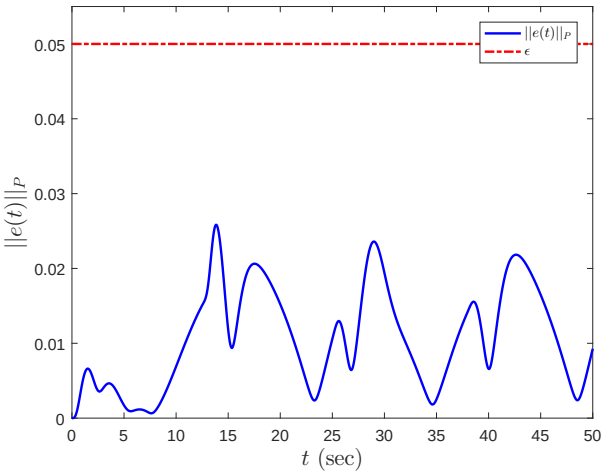

(d) Weighted error norm.

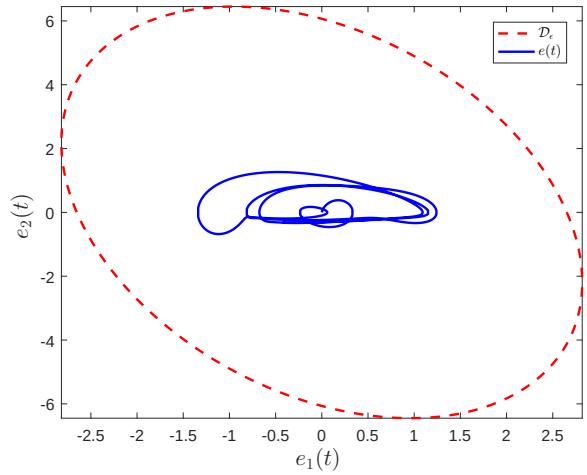

(e) 2D error plot.

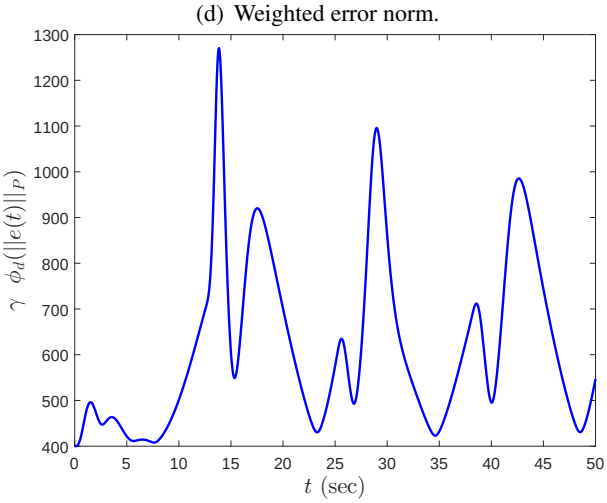

(f) Effective learning rate.

Figure 4.26: System performance with set-theoretic adaptive controller in presence of actuator dynamics with $\lambda = 10$.

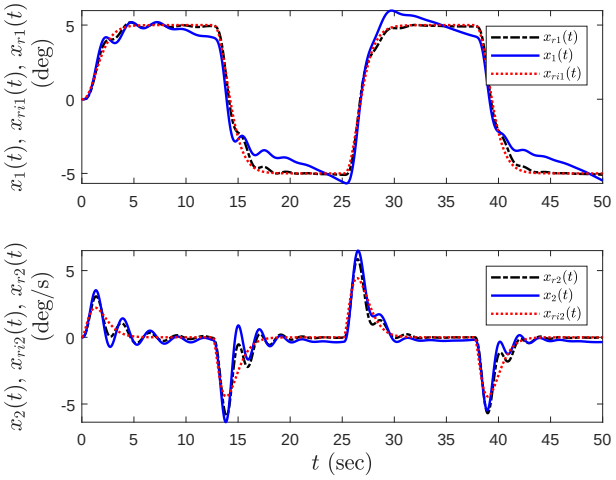

(a) Command following performance.

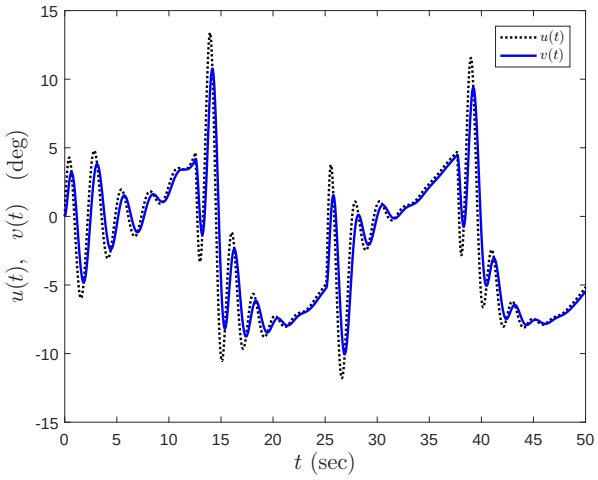

(b) Control signal.

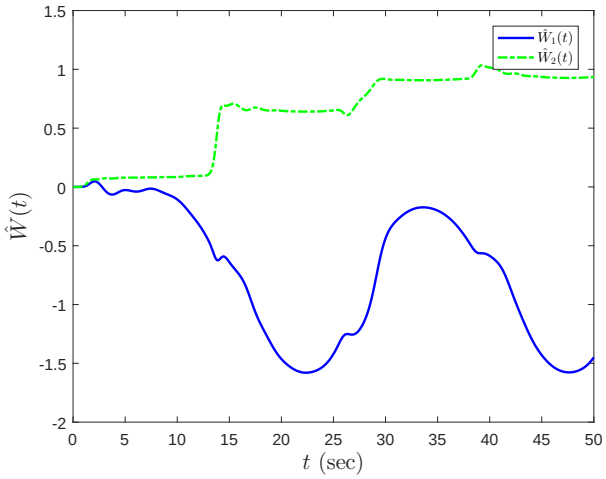

(c) Weight estimation.

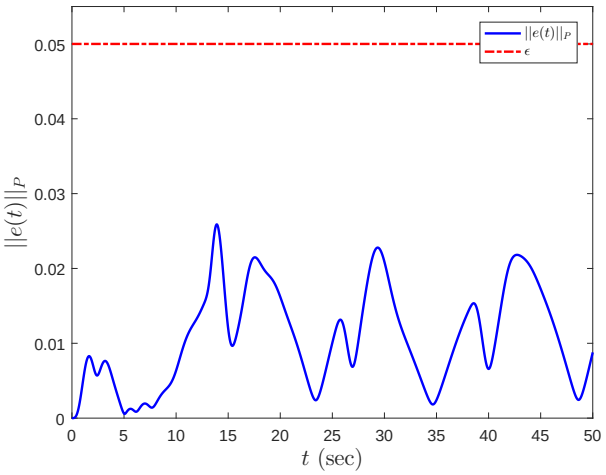

(d) Weighted error norm.

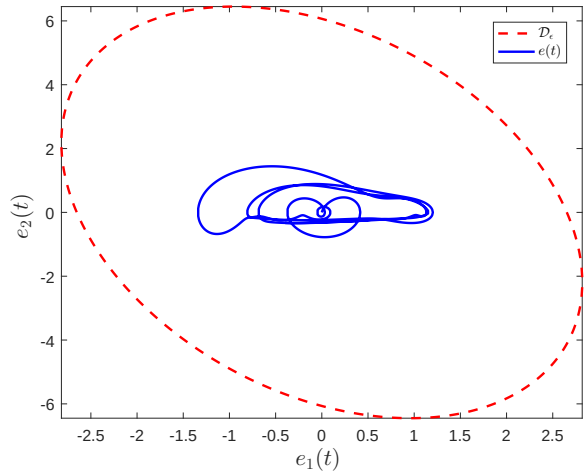

(e) 2D error plot.

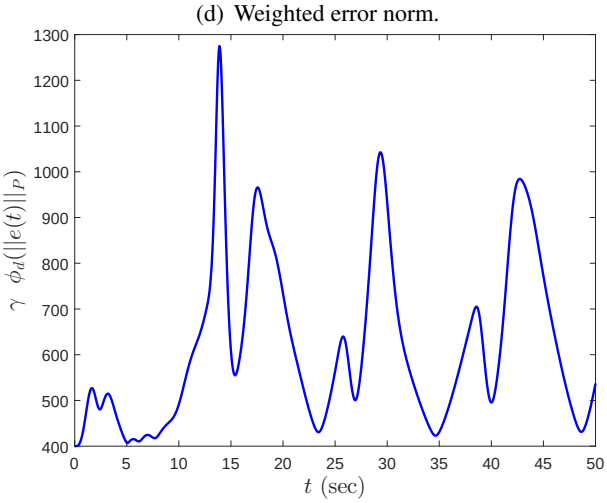

(f) Effective learning rate.

Figure 4.27: System performance with set-theoretic adaptive controller in presence of actuator dynamics with $\lambda = \lambda_{\min} = 3.3$

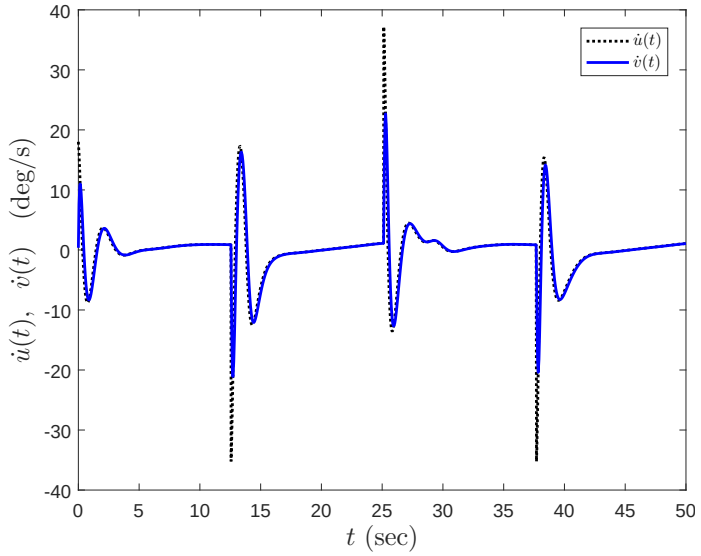

Figure 4.28: Time derivative of the actuator output signal and the control signal with $\lambda = 10$.

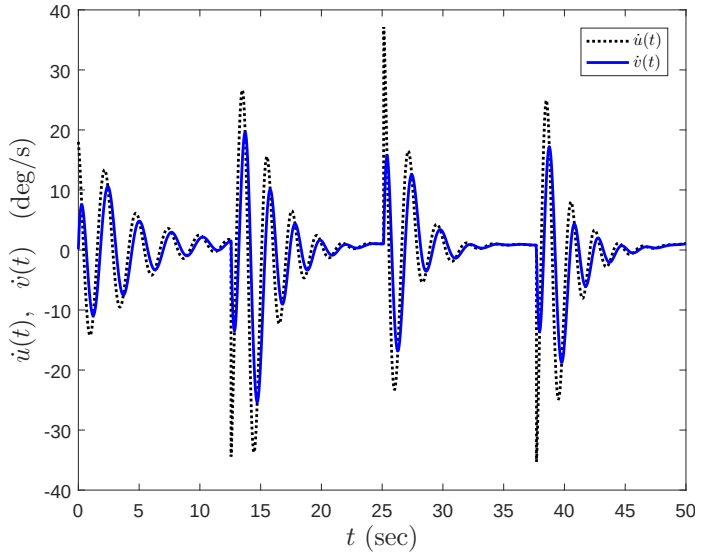

Figure 4.29: Time derivative of the actuator output signal and the control signal with $\lambda = 3.3$.

of an uncertain dynamical system and a given reference model to be less than a-priori, user-defined worst-case closed-loop system performance bound. The contribution of this paper is to generalize this framework to address disturbance rejection and system uncertainty suppression in the presence of actuator failures. A system-theoretical analysis is provided to show the strict closed-loop system performance guarantees of the proposed architecture to effectively handle actuator failures and its efficacy is demonstrated in an illustrative numerical example.

4.4.1 Introduction

One of the fundamental needs for resilient control architectures is to achieve a level of desired closed-loop system performance in the presence of adverse system conditions resulting from exogenous disturbances, imperfect system modeling, degraded modes of operation, and changes in system dynamics. Although fixed-gain robust control approaches [120–123] are helpful to cope with such adverse system conditions, they generally require the knowledge of system uncertainty bounds [124]. Characterization of these bounds is not a trivial control engineering task since it requires extensive and costly verification procedures and tests. On the other hand, adaptive control approaches [28–30, 125] have the capability to deal with adverse system conditions, require less modeling information than do fixed-gain robust control approaches, and reduce system development costs. These facts make adaptive control approaches important to achieve system resiliency.

Most adaptive control approaches adopt a model reference approach [126, 127]. Specifically, model reference adaptive control schemes have three major components; a reference model, an update law, and a controller. The reference model captures a desired closed-loop system behavior, which is compared with the behavior of an uncertain dynamical system. This comparison results in a system (tracking) error that drives the update law. The controller then adapts feedback gains to minimize this error using the information received from the update law. In practice, the behavior of an uncertain dynamical system subject to an adaptive control approach can be far different than the behavior of the reference model [31, 87, 128] especially during the transient time and in the presence of large system uncertainties.

Although there are a few approaches to address this phenomenon [79, 129, 130], their closed-loop system performance bounds not only are conservative but also depend on uncertain system parameters. Therefore, these approaches may not be practical for safety-critical resilient system applications, where strict and user-defined closed-loop system performance is required; for example, to preserve operation within safe flight envelope in aerospace applications. To this end, a new model reference adaptive control framework was recently proposed by the authors of Ref. [1] for achieving strict closed-loop system performance guarantees in the presence of exogenous disturbances and system uncertainties. Specifically, this framework was predicated on a set-theoretic adaptive controller construction using generalized restricted potential functions, where its key feature was to keep the distance between the trajectories of an uncertain dynamical

system and a given reference model to be less than a-priori, user-defined worst-case closed-loop system performance bound.

In addition to the presence of exogenous disturbances and system uncertainties, actuator failures significantly contribute to fatal accidents [42–44]. In particular, a common type of actuator failures is when one or more control surfaces suddenly become inaccessible and remain at some unknown value. If special considerations do not exist in the feedback control architecture, then the closed-loop system performance can become undesirable or even unstable. Although additional control surfaces may be provided in practice to have actuator redundancy and to preserve system controllability in the presence of one or more actuator failures, proper considerations are still needed to compensate the adverse effect of such failures in the closed-loop system performance. From an adaptive control standpoint, the authors of Refs. [45–52] (see also their references) proposed approaches to deal with actuator failures, where only the results in Ref. [52] established strict guarantees on the closed-loop system performance by utilizing a backstepping procedure and under the assumption that a desired trajectory and its derivatives are available and all bounded.

In this paper, we generalize the set-theoretic model reference adaptive control framework of Ref. [1] to address disturbance rejection and system uncertainty suppression in the presence of actuator failures, where the actuators can fail based on a common failure model in which they can be stuck at some unknown values at some unknown time, and hence, the actuator failure structure is unknown in terms of time, pattern, and value. In addition to utilizing methods from our previous work in Ref. [1], we also use methods from Ref. [49] and our contribution can be equivalently viewed as a generalization of the results in Ref. [49] to achieve strict closed-loop system performance guarantees in the presence of finite number of actuator failures. A system-theoretical analysis and an illustrative numerical example are further provided to demonstrate the efficacy of the proposed set-theoretic model reference adaptive control framework to handle actuator failures.

The notation used throughout this paper is fairly standard. Specifically, $\mathbb{R}$ denotes the set of real numbers, $\mathbb{R}^n$ denotes the set of $n \times 1$ real column vectors, $\mathbb{R}^{n\times m}$ denotes the set of $n \times m$ real matrices, $\mathbb{R}_+$ (respectively, $\overline{\mathbb{R}}_+$) denotes the set of positive (respectively, nonnegative-definite) real numbers, $\mathbb{R}_+^{n\times n}$ (respectively, $\overline{\mathbb{R}}_+^{n\times n}$) denotes the set of $n \times n$ positive-definite (respectively, nonnegative-definite) real matrices, $\mathbb{S}^{n\times n}$ denotes the set of $n \times n$ symmetric real matrices, $\mathbb{D}^{n\times n}$ denotes the set of $n \times n$ real matrices with diagonal scalar entries, $0_{n\times n}$ denotes the $n \times n$ zero matrix, and "$\triangleq$" denotes equality by definition. In addition, we write $(\cdot)^{\mathrm{T}}$ for the transpose operator, $(\cdot)^{-1}$ for the inverse operator, $\det(\cdot)$ for the determinant

operator, $\|\cdot\|_2$ for the Euclidean norm, and $\|\cdot\|_\infty$ for the infinity norm. Furthermore, we write $\lambda_{\min}(A)$ (resp., $\lambda_{\max}(A)$) for the minimum (resp., maximum) eigenvalue of the Hermitian matrix A, $\mathrm{tr}(\cdot)$ for the trace operator, $\underline{x}$ (resp., $\bar{x}$) for the lower bound (resp., upper bound) of a bounded signal $x(t) \in \mathbb{R}^n$, $t \geq 0$, that is, $\underline{x} \leq \|x(t)\|_2, t \geq 0$ (resp., $\|x(t)\|_2 \leq \bar{x}, t \geq 0$).

4.4.2 Set-Theoretic Model Reference Adaptive Control Overview

In this section, we briefly overview the standard set-theoretic model reference adaptive control architecture of Ref. [1] (in the absence of actuator failures). We begin with the following necessary definitions.

Definition 4.4.1 *Let $\psi : \mathbb{R}^n \longrightarrow \mathbb{R}$ given by $\psi(\theta) \triangleq \frac{(\varepsilon_\theta+1)\theta^{\mathrm{T}}\theta-\theta_{\max}^2}{\varepsilon_\theta\theta_{\max}^2}$, be a continuously differentiable convex function, where $\theta_{\max} \in \mathbb{R}$ is a projection norm bound imposed on $\theta \in \mathbb{R}^n$ and $\varepsilon_\theta > 0$ is a projection tolerance bound. Then, the projection operator* $\mathrm{Proj} : \mathbb{R}^n \times \mathbb{R}^n \to \mathbb{R}^n$ *is defined by*

$$\mathrm{Proj}(\theta, y) \triangleq \begin{cases} y, & \text{if } \psi(\theta) < 0, \\ y, & \text{if } \psi(\theta) \geq 0 \text{ and } \psi'(\theta)y \leq 0, \\ y - \frac{\psi'^{\mathrm{T}}(\theta)\psi'(\theta)y}{\psi'(\theta)\psi'^{\mathrm{T}}(\theta)}\psi(\theta), & \text{if } \psi(\theta) \geq 0 \text{ and } \psi'(\theta)y > 0, \end{cases} \tag{4.157}$$

where $y \in \mathbb{R}^n$ and $\psi'(\theta) \triangleq \frac{\partial\psi(\theta)}{\partial\theta}$.

It follows from Definition 4.4.1 that

$$(\theta - \theta^*)^{\mathrm{T}}\Big[\mathrm{Proj}(\theta, y) - y\Big] \leq 0, \tag{4.158}$$

holds [30, 80]. The definition of the projection operator can be generalized to matrices as

$$\mathrm{Proj}_{\mathrm{m}}(\Theta, Y) = (\mathrm{Proj}(\mathrm{col}_1(\Theta), \mathrm{col}_1(Y)), \ldots, \mathrm{Proj}(\mathrm{col}_m(\Theta), \mathrm{col}_m(Y))), \tag{4.159}$$

where $\Theta \in \mathbb{R}^{n\times m}, Y \in \mathbb{R}^{n\times m}$, and $\mathrm{col}_i(\cdot)$ denotes i th column operator. In this case, for a given matrix Θ^*, it follows from (4.158) that

$$\mathrm{tr}\left[(\Theta - \Theta^*)^{\mathrm{T}}\left[\mathrm{Proj}_{\mathrm{m}}(\Theta, Y) - Y\right]\right] = \sum_{i=1}^{m}\left[\mathrm{col}_i(\Theta - \Theta^*)^{\mathrm{T}}\Big[\mathrm{Proj}(\mathrm{col}_i(\Theta), \mathrm{col}_i(Y)) - \mathrm{col}_i(Y)\Big]\right] \leq 0. \tag{4.160}$$

Definition 4.4.2 *Let $\|z\|_H = \sqrt{z^{\mathrm{T}}Hz}$ be a weighted Euclidean norm, where $z \in \mathbb{R}^p$ is a real column vector and $H \in \mathbb{R}_+^{p\times p}$. We define $\phi(\|z\|_{\mathrm{H}})$, $\phi : \mathbb{R} \to \mathbb{R}$, to be a generalized restricted potential function (generalized barrier Lyapunov function) on the set*

$$\mathcal{D}_\varepsilon \triangleq \{\|z\|_{\mathrm{H}} : \|z\|_{\mathrm{H}} \in [0,\varepsilon)\}, \tag{4.161}$$

with $\varepsilon \in \mathbb{R}_+$ being a-priori, user-defined constant, if the following statements hold:

i) If $\|z\|_{\mathrm{H}} = 0$, then $\phi(\|z\|_{\mathrm{H}}) = 0$.

ii) If $\|z\|_{\mathrm{H}} \in \mathcal{D}_\varepsilon$ and $\|z\|_{\mathrm{H}} \neq 0$, then $\phi(\|z\|_{\mathrm{H}}) > 0$.

iii) If $\|z\|_{\mathrm{H}} \to \varepsilon$, then $\phi(\|z\|_{\mathrm{H}}) \to \infty$.

iv) $\phi(\|z\|_{\mathrm{H}})$ is continuously differentiable on $\mathcal{D}_\varepsilon$.

v) If $\|z\|_{\mathrm{H}} \in \mathcal{D}_\varepsilon$, then $\phi_d(\|z\|_{\mathrm{H}}) > 0$, where

$$\phi_d(\|z\|_{\mathrm{H}}) \triangleq \frac{\mathrm{d}\phi(\|z\|_{\mathrm{H}})}{\mathrm{d}\|z\|_{\mathrm{H}}^2}. \tag{4.162}$$

vi) If $\|z\|_{\mathrm{H}} \in \mathcal{D}_\varepsilon$, then

$$2\phi_d(\|z\|_{\mathrm{H}})\|z\|_{\mathrm{H}}^2 - \phi(\|z\|_{\mathrm{H}}) > 0. \tag{4.163}$$

Remark 4.4.1 *A candidate generalized restricted potential function satisfying the conditions given in Definition 4.4.2 has the form [1] $\phi(\|z\|_{\mathrm{H}}) = \|z\|_{\mathrm{H}}^2/\big(\varepsilon - \|z\|_{\mathrm{H}}\big)$, $\|z\|_{\mathrm{H}} \in \mathcal{D}_\varepsilon$, which has the partial derivative $\phi_d(\|z\|_{\mathrm{H}}) = \big(\varepsilon - \frac{1}{2}\|z\|_{\mathrm{H}}\big)/\big(\varepsilon - \|z\|_{\mathrm{H}}\big)^2 > 0$, $\|z\|_{\mathrm{H}} \in \mathcal{D}_\varepsilon$, with respect to $\|z\|_{\mathrm{H}}^2$, and $2\phi_d(\|z\|_{\mathrm{H}})\|z\|_{\mathrm{H}}^2 - \phi(\|z\|_{\mathrm{H}}) = \varepsilon\|z\|_{\mathrm{H}}^2/\big(\varepsilon - \|z\|_{\mathrm{H}}\big)^2 > 0$, $\|z\|_{\mathrm{H}} \in \mathcal{D}_\varepsilon$. It should be also noted that Definition 4.4.2 can be viewed as a generalized version of the restricted potential function (barrier Lyapunov function) definitions used by the authors of Refs. [21–26].*

Based on Definitions 4.4.1 and 4.4.2, we now briefly state the key results of the set-theoretic model reference adaptive control architecture of Ref. [1]. Specifically, consider the uncertain dynamical system

given by

$$\dot{x}(t) = Ax(t) + B\Lambda\big(u(t) + \delta(t, x(t))\big), \quad x(0) = x_0, \quad t \geq 0, \tag{4.164}$$

where $x(t) \in \mathbb{R}^n$, $t \geq 0$, is the measurable state vector, $u(t) \in \mathbb{R}^m$, $t \geq 0$, is the control input, $A \in \mathbb{R}^{n \times n}$ is a known system matrix, $B \in \mathbb{R}^{n \times m}$ is a known input matrix, $\delta : \overline{\mathbb{R}}_+ \times \mathbb{R}^n \to \mathbb{R}^m$ is a system uncertainty, $\Lambda \in \mathbb{R}_+^{m \times m} \cap \mathbb{D}^{m \times m}$ is an unknown control effectiveness matrix, and the pair (A, B) is controllable. The following system uncertainty parameterization is used for the main results of Ref. [1].

Assumption 4.4.1 *The system uncertainty in* (4.164) *is parameterized as*

$$\delta(t, x(t)) = W_s^{\mathrm{T}}(t)\sigma_s(x(t)), \quad x(t) \in \mathbb{R}^n \tag{4.165}$$

where $W_s(t) \in \mathbb{R}^{s \times m}$, $t \geq 0$, is a bounded unknown weight matrix (i.e., $\|W_s(t)\|_2 \leq w_s$, $t \geq 0$) with a bounded time rate of change (i.e., $\|\dot{W}_s(t)\|_2 \leq \dot{w}_s$, $t \geq 0$), and $\sigma : \mathbb{R}^n \to \mathbb{R}^s$ is a known basis function.

Now, consider the feedback control law given by

$$u(t) = u_{\mathrm{n}}(t) + u_{\mathrm{a}}(t), \quad t \geq 0, \tag{4.166}$$

where $u_{\mathrm{n}}(t) \in \mathbb{R}^m$, $t \geq 0$, and $u_{\mathrm{a}}(t) \in \mathbb{R}^m$, $t \geq 0$, are the nominal and adaptive control, respectively. Furthermore, let the nominal control law be

$$u_{\mathrm{n}}(t) = -K_1 x(t) + K_2 c(t), \quad t \geq 0, \tag{4.167}$$

where $c(t) \in \mathbb{R}^{n_c}$ is a bounded reference command, $K_1 \in \mathbb{R}^{m \times n}$ is the nominal feedback gain, and $K_2 \in \mathbb{R}^{m \times n_c}$ is the nominal feedforward gain, such that $A_{\mathrm{r}} \triangleq A - BK_1$ is Hurwitz and $B_{\mathrm{r}} \triangleq BK_2$.

Next, consider the reference model capturing a desired closed-loop system behavior given by

$$\dot{x}_{\mathrm{r}}(t) = A_{\mathrm{r}} x_{\mathrm{r}}(t) + B_{\mathrm{r}} c(t), \quad x_{\mathrm{r}}(0) = x_{\mathrm{r0}}, \quad t \geq 0, \tag{4.168}$$

where $x_r(t) \in \mathbb{R}^n$ is the reference model state vector, $A_r \in \mathbb{R}^{n \times n}$ is the desired Hurwitz system matrix, and $B_r \in \mathbb{R}^{n \times n_c}$ is the command input matrix. Using (4.164), (4.165), (4.166), (4.167) and (4.168), the system

error dynamics are given by

$$\dot{e}(t) = A_{\mathrm{r}}e(t)+B\Lambda\big(\big(\Lambda^{-1}-I_{\mathrm{m}\times\mathrm{m}}\big)\big(K_1x(t)-K_2c(t)\big)+u_{\mathrm{a}}(t)+W_s^{\mathrm{T}}(t)\sigma_s(x(t))\big), \quad e(0)=e_0, \quad t\geq 0, \tag{4.169}$$

where $e(t)\triangleq x(t)-x_{\mathrm{r}}(t)$, $t\geq 0$, is the system (tracking) error. One can rewrite (4.169) as

$$\dot{e}(t) = A_{\mathrm{r}}e(t)+B\Lambda\big(W_0^{\mathrm{T}}(t)\sigma_0(x(t))+u_{\mathrm{a}}(t)\big), \quad e(0)=e_0, \quad t\geq 0, \tag{4.170}$$

where $W_0(t)\triangleq\big[W_s^{\mathrm{T}}(t),\ (\Lambda^{-1}-I_{\mathrm{m}\times\mathrm{m}})K_1,\ -(\Lambda^{-1}-I_{\mathrm{m}\times\mathrm{m}})K_2\big]^{\mathrm{T}}\in\mathbb{R}^{(s+n+n_c)\times m}$, $t\geq 0$, is an unknown aggregated weight matrix and $\sigma_0\big(x(t),c(t)\big)\triangleq\big[\sigma^{\mathrm{T}}\big(x(t)\big),\ x^{\mathrm{T}}(t),\ c^{\mathrm{T}}(t)\big]^{\mathrm{T}}\in\mathbb{R}^{s+n+n_c}$, $t\geq 0$, is a known basis function.

Finally, let the adaptive control law be given by

$$u_{\mathrm{a}}(t)=-\hat{W}_0^{\mathrm{T}}(t)\sigma_0\big(x(t)\big), \quad t\geq 0, \tag{4.171}$$

where $\hat{W}_0(t)\in\mathbb{R}^{(s+n+n_c)\times m}$, $t\geq 0$, is the estimate of $W_0(t)$, $t\geq 0$, satisfying the set-theoretic update law

$$\dot{\hat{W}}_0(t)=\gamma\mathrm{Proj}_{\mathrm{m}}\Big(\hat{W}_0(t),\phi_d(\|e(t)\|_P)\sigma_0\big(x(t)\big)e^{\mathrm{T}}(t)PB\Big), \quad \hat{W}_0(0)=\hat{W}_{00}, \quad t\geq 0, \tag{4.172}$$

with $\hat{W}_{\max}$ being the projection norm bound, $\gamma\in R_+$ is the learning rate (i.e., adaptation gain), and $P\in\mathbb{R}_+^{n\times n}$ is a solution of the Lyapunov equation given by

$$0 = A_{\mathrm{r}}^{\mathrm{T}}P+PA_{\mathrm{r}}+R, \tag{4.173}$$

with $R\in\mathbb{R}_+^{n\times n}$, and $\phi_d(\|e(t)\|_P)$ is an error dependent learning gain.

Remark 4.4.2 *Using* (4.170)*,* (4.171)*, and* (4.172) *the system error dynamics and the weight estimation error dynamics are given by*

$$\dot{e}(t) = A_{\mathrm{r}}e(t)-B\Lambda\tilde{W}_0^{\mathrm{T}}(t)\sigma_0\big(x(t)\big), \quad e(0)=e_0, \quad t\geq 0, \tag{4.174}$$

$$\dot{\tilde{W}}_0(t) = \gamma\mathrm{Proj}_{\mathrm{m}}\big(\hat{W}_0(t),\phi_d(\|e(t)\|_P)\sigma_0\big(x(t)\big)e^{\mathrm{T}}(t)PB\big)-\dot{W}_0(t), \quad \tilde{W}_0(0)=\tilde{W}_{00}, \quad t\geq 0, \tag{4.175}$$

where $\tilde{W}_0(t) \triangleq \hat{W}_0(t) - W_0(t) \in \mathbb{R}^{(s+n+n_c)\times m}$, $t \geq 0$, *is the weight estimation error and* $e_0 \triangleq x_0 - x_{\mathrm{r}0}$. *Note that* $\|W_0(t)\|_2 \leq w_0, t \geq 0$, *and* $\|\dot{W}_0(t)\|_2 \leq \dot{w}_0, t \geq 0$, *automatically holds. Now, by considering the Lyapunov function*

$$V(e,\tilde{W}_0) = \phi(\|e\|_P) + \gamma^{-1}\mathrm{tr}\big[(\tilde{W}_0\Lambda^{1/2})^{\mathrm{T}}(\tilde{W}_0\Lambda^{1/2})\big], \tag{4.176}$$

one can calculate its derivative along the closed-loop system trajectories (4.174) and (4.175) as

$$\dot{V}\big(e(t),\tilde{W}_0(t)\big) \leq -\frac{1}{2}\alpha V(e,\tilde{W}_0) + \mu, \tag{4.177}$$

where $\alpha \triangleq \frac{\lambda_{\min}(R)}{\lambda_{\max}(P)}$ *and* $\mu \triangleq \gamma^{-1}\|\Lambda\|_2\tilde{w}_0(\frac{1}{2}\alpha\tilde{w}_0 + \dot{w}_0)$. *Following the results in Ref. [1], the boundedness of the closed-loop dynamical system given by (4.174) and (4.175) as well as the strict performance bound on the system error given by* $\|e(t)\|_P < \varepsilon$ *is immediate.*

Remark 4.4.3 *The set-theoretic model reference adaptive control architecture overviewed in this section assumes that all control surfaces are accessible at all time. However, in practice, one or more control surfaces can get stuck at some unknown values at some unknown time. In the next section, we generalize this approach to the presence of actuator failures.*

4.4.3 Adaptive Control with Strict Closed-Loop System Performance Guarantees in the Presence of Actuator Failures

In this section, we generalize the results of Section 4.4.2 to address disturbance rejection and system uncertainty suppression in the presence of finite number actuator failures. Specifically, we consider the actuator failure model in which the actuators can get stuck at some unknown values at some unknown time. This can be mathematically represented as

$$u_j(t) \quad = \quad \bar{u}_j, \quad t \geq t_j, \quad j = 1,\ldots,m, \tag{4.178}$$

where the constants, $\bar{u}_j$, and the time instants of the actuator failures, t_j, are unknown [131]. In addition, we assume if the system parameters and the actuator failure were known, then the remaining control surfaces were able to achieve the desired system performance after up to $m-1$ actuator failures. Note that this assumption is standard for addressing the actuator failures problem, which is actually an existence

assumption for a nominal solution [132]. In other words, we assume that there are $p < m$ actuator failures and they only happen at $T_i, i = 1, \ldots, p$. This implies that the actuator failure pattern is fixed on $(T_i, T_{i+1}), i = 0, 1, \ldots, p$ with $T_0 = 0$.

Next, consider the uncertain dynamical system given by

$$\dot{x}(t) = Ax(t) + B\Lambda\big(u(t) + \delta(t, x(t))\big) + B\xi_i, \quad x(0) = x_0, \quad t \geq 0, \tag{4.179}$$

where $x(t) \in \mathbb{R}^n$, $t \geq 0$, is the measurable state vector, $u(t) \in \mathbb{R}^m$, $t \geq 0$, is the control input, $A \in \mathbb{R}^{n\times n}$ is a known system matrix, $B \in \mathbb{R}^{n\times m}$ is a known input matrix, $\delta : \overline{\mathbb{R}}_+ \times \mathbb{R}^n \to \mathbb{R}^m$ is a system uncertainty, $\Lambda \in \overline{\mathbb{R}}_+^{m\times m} \cap \mathbb{D}^{m\times m}$ is an unknown control effectiveness matrix, and the pair (A, B) is controllable. In (4.179), $\xi_i \in \mathbb{R}^m$ represents an unknown vector corresponding to the constant value of the failed actuators over the interval $(T_i, T_{i+1}), i = 0, 1, \ldots, p$, (i.e., $\overline{u}_j$). We now make the following standard assumption for the actuator failures problem (see, for example, Ref. [49]).

Assumption 4.4.2 *On $(T_i, T_{i+1}), i = 0, 1, \ldots, p$, there exist matrices $K_{1i}^* \in \mathbb{R}^{m\times n}$ and $K_{2i}^* \in \mathbb{R}^{m\times n_c}$ and bias vector $\xi_i^* \in \mathbb{R}^m$ such that*

$$A + B\Lambda K_{1i}^* = A_r, \tag{4.180}$$

$$B\Lambda K_{2i}^* = B_r, \tag{4.181}$$

$$B(\Lambda\xi_i^* + \xi_i) = 0. \tag{4.182}$$

As we mentioned in the first paragraph of this section, note that Assumption 4.4.2 provides the existence of a nominal solution in case of actuator failures. Now, using (4.165), (4.168), and (4.180) to (4.182) in (4.179), one can write

$$\dot{e}(t) = A_r e(t) + B\Lambda\big(u(t) - K_{1i}^* x(t) - K_{2i}^* c(t) - \xi_i^* + W_s^{\mathrm{T}}(t)\sigma_s(x(t))\big), \quad e(0) = e_0, \quad t \geq 0, \tag{4.183}$$

or equivalently

$$\dot{e}(t) = A_r e(t) + B\Lambda\big(u(t) + W_i^{\mathrm{T}}(t)\sigma(x(t), c(t))\big), \quad e(0) = e_0, \quad t \geq 0, \tag{4.184}$$

with $W_i(t) = [-K_{1i}^*,\ -K_{2i}^*,\ -\xi_i^*,\ W_s^{\mathrm{T}}(t)]^{\mathrm{T}}$ and $\sigma(x(t), c(t)) = [x^{\mathrm{T}}(t),\ c^{\mathrm{T}}(t),\ 1,\ \sigma_s^{\mathrm{T}}(x(t))]^{\mathrm{T}}$.

Considering (4.184), let the feedback control law be given by

$$u(t) = -\hat{W}_i^{\mathrm{T}}(t)\sigma(x(t),c(t)), \quad t \geq 0, \tag{4.185}$$

where $\hat{W}_i(t) \in \mathbb{R}^{(s+n+n_c+1)\times m}$, $t \geq 0$, is the estimate of $W_i(t)$, $t \geq 0$, satisfying the update law

$$\dot{\hat{W}}_i(t) = \gamma \mathrm{Proj_m}\Big(\hat{W}_i(t), \phi_d(\|e(t)\|_P)\sigma(x(t),c(t))e^{\mathrm{T}}(t)PB\Big), \quad \hat{W}_i(0) = \hat{W}_{0i}, \quad t \geq 0, \tag{4.186}$$

with $\hat{W}_{\max}$ being the projection norm bound. In (4.186), $\gamma \in R_+$ is the learning rate, and $P \in \mathbb{R}_+^{n\times n}$ is a solution of the Lyapunov equation in (4.173). Now, one can write

$$\dot{e}(t) = A_r e(t) - B\Lambda\tilde{W}_i^{\mathrm{T}}(t)\sigma(x(t),c(t)), \quad e(0) = e_0, \quad t \geq 0, \tag{4.187}$$

$$\dot{\tilde{W}}_i(t) = \gamma \mathrm{Proj_m}\Big(\hat{W}_i(t), \phi_d(\|e(t)\|_P)\sigma(x(t),c(t))e^{\mathrm{T}}(t)PB\Big) - \dot{W}_i(t), \quad \tilde{W}_i(0) = \tilde{W}_{0i}, \quad t \geq 0, \tag{4.188}$$

where $\tilde{W}_i(t) \triangleq \hat{W}_i(t) - W_i(t) \in \mathbb{R}^{(s+n+n_c+1)\times m}$, $t \geq 0$, is the weight estimation error. Note that $\|W_i(t)\|_2 \leq w_i, t \geq 0$, and $\|\dot{W}_i(t)\|_2 \leq \dot{w}_i, t \geq 0$, automatically holds as a direct consequence of Assumptions 4.4.1 and 4.4.2. The next theorem presents the main result of this paper.

Theorem 4.4.1 *Consider the uncertain dynamical system given by (4.179) subject to Assumption 4.4.1 and a finite number of actuator failures that occur at $T_i, i = 1,\ldots,p$, based on the failure model in* (4.178) *and Assumption 4.4.2, the reference model given by (4.168), and the feedback control law given by (4.185) along with the update law (4.186). If $\|e_0\|_P < \varepsilon$, then the closed-loop dynamical system given by (4.187) and (4.188) are bounded in presence of exogenous disturbances, system uncertainties, and actuator failures, where the bound on the system error strictly satisfies a-priori given, user-defined worst-case performance bound*

$$\|e(t)\|_P < \varepsilon, \quad t \geq 0. \tag{4.189}$$

Proof. The first part of the proof follows from the results in Ref. [1]. To give readers a sketch for the first part, consider the energy function $V_i : \mathcal{D}_e \times \mathbb{R}^{(n+n_c+s+1)\times m} \to \overline{\mathbb{R}}_+$ on $(T_i, T_{i+1}), i = 0,1,\ldots,p$, given by

$$V_i(e,\tilde{W}_i\Lambda^{1/2}) = \phi(\|e\|_P) + \gamma^{-1}\mathrm{tr}(\tilde{W}_i\Lambda^{1/2})^{\mathrm{T}}(\tilde{W}_i\Lambda^{1/2}), \tag{4.190}$$

where $\mathcal{D}_e \triangleq \{e(t) : \|e(t)\|_P < \varepsilon\}$, and $P \in \mathbb{R}_+^{n\times n}$ is a solution of the Lyapunov equation in (4.173) with $R \in \mathbb{R}_+^{n\times n}$. Following the steps given in Ref. [1], the time derivative of (4.190) along the closed-loop system trajectories (4.187) and (4.188) can be computed as

$$\dot{V}_i\big(e(t),\tilde{W}_i(t)\Lambda^{1/2}\big) \;\leq\; -\frac{1}{2}\alpha V_i(e,\tilde{W}_i\Lambda^{1/2}) + \mu_i, \tag{4.191}$$

where $\mu_i \triangleq \frac{1}{2}\alpha\gamma^{-1}\tilde{w}_i^2\|\Lambda\|_2 + d_i$, $d_i \triangleq 2\gamma^{-1}\tilde{w}_i\ \dot{w}_i\|\Lambda\|_2$, and $\alpha \triangleq \frac{\lambda_{\min}(R)}{\lambda_{\max}(P)}$. Now, based on the structure of (4.191), it follows similar to Refs. [1], [23], and [25] that the closed-loop signals $e(t)$ and $\tilde{W}_i(t)\Lambda^{1/2}$ are bounded and the strict performance bound on the system error given by (4.189) over interval $(T_i, T_{i+1}), i = 1,\ldots,p$, hold.

For the second part of the proof, note that there are finite number of actuator failures and the closed-loop dynamical system given by (4.187) and (4.188) is bounded and satisfies (4.189) for every time interval $(T_i, T_{i+1}), i = 1,\ldots,p$. Thus, it follows from the continuity of the system error trajectories for all $t \geq 0$ including $t = T_i$, $i = 1,\ldots,p$, that the system error is contained inside the set $\mathcal{D}_\varepsilon$ for all $t \geq 0$ (see Figure 4.30 for a two-dimensional representation of the continuity of the system error). ■

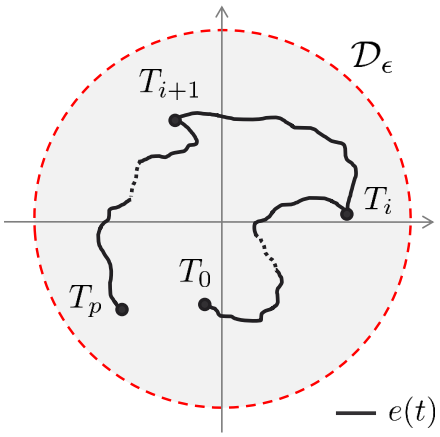

Figure 4.30: Two-dimensional representation of the continuity of the system error inside the set $\mathcal{D}_\varepsilon$.

Remark 4.4.4 *The results of this section extend the results presented in the previous work of the authors in Ref. [1] (see Section 4.4.2 for an overview) by considering that the control surfaces may not be accessible all the time due to the presence of actuator failures. As mentioned earlier, the proposed framework of this section can be equivalently viewed as a generalization of the results in Ref. [49] to achieve strict closed-loop system performance guarantees. Specifically, in Theorem 4.4.1, we show that the proposed set-theoretic*

model reference adaptive control framework has the capability to keep the closed-loop system trajectories within a-priori, user-defined compact set by compensating the adverse effect of unknown actuator failures in terms of time, pattern, and value as well as in the presence of exogenous disturbances and system uncertainties.

4.4.4 Illustrative Numerical Example

In this section, we present an illustrative numerical example to demonstrate the efficacy of the proposed set-theoretic model reference adaptive control architecture in presence of loss of control. For this purpose, consider the uncertain dynamical system given by [45]

$$\dot{x}(t) = Ax(t) + B\Lambda\Big(u(t) + W_{\mathrm{s}}^{\mathrm{T}}(t)\sigma_{\mathrm{s}}(x(t))\Big), \quad x(0) = x_0, \quad t \geq 0, \tag{4.192}$$

with

$$A = \begin{bmatrix} 0 & 1 & 0 \\ 0 & 0 & 1 \\ -1 & -2 & -2 \end{bmatrix}, \qquad B = \begin{bmatrix} 0 & 0 & 0 \\ 0 & 0 & 0 \\ 1 & 2 & 3 \end{bmatrix}. \tag{4.193}$$

In this numerical example, we choose

$$W_{\mathrm{s}}(t) = \begin{bmatrix} 0.2 + 0.1\sin(t) & 0.3 & 0.1 \\ 0.1 & 0.2 + 0.2\sin(t) & 0.1 \\ 0.2 & 0.2 & 0.2 + 0.3\sin(t) \end{bmatrix}, \tag{4.194}$$

for the unknown weight matrix, $\Lambda = 0.75I$ for the unknown control effectiveness matrix before any actuator failures, and $\sigma_{\mathrm{s}}(x(t)) = [x_1(t),\ x_1(t)x_2(t),\ x_3^2(t)]^{\mathrm{T}}$ for the basis function. In addition, we set the nominal controller matrices to

$$K_1 = \begin{bmatrix} 1 & 1 & -1 \\ 0 & -1 & 1 \\ 1 & 0 & 0 \end{bmatrix}, \quad K_2 = \begin{bmatrix} 1 \\ 0 \\ 0 \end{bmatrix}. \tag{4.195}$$

For this numerical example, we select the failure pattern parameters in (4.178) as $\bar{u}_2 = -1$ at $t_2 = 10$ sec and $\bar{u}_3 = 2$ at $t_3 = 5$ sec. In other words, this selection means that the second actuator fails at $t = 10$ sec, third actuator fails at $t = 5$ sec, and actuator 1 does not fail, which is the case in order to satisfy the existence of a nominal solution stated in Assumption 4.4.2. For the proposed set-theoretic model reference adaptive control architecture in Theorem 4.4.1, we use the generalized restricted potential function given in Remark 4.4.1 with $\varepsilon = 1$ to strictly guarantee $\|x(t) - x_{\mathrm{r}}(t)\|_P < 1$, $t \geq 0$. Finally, we set the projection norm bound imposed on the parameter estimate to 10 and use $R = 5I$ to calculate P from (4.173) for the resulting A_{r} matrix.

Figures 4.31 and 4.32 show the closed-loop dynamical system performance with the nominal controller only. One can see from Figure 4.33 that the nominal controller is incapable of keeping the system error trajectory within the compact set $\mathcal{D}_\varepsilon$. Next, we apply the proposed set-theoretic adaptive controller with $\gamma = 5$ in Figures 4.34 and 4.35, where it can be seen that a desired, user-defined closed-loop system performance is achieved. Figure 4.36 clearly shows that this controller strictly guarantees $\|x(t) - x_{\mathrm{r}}(t)\|_P < 1$.

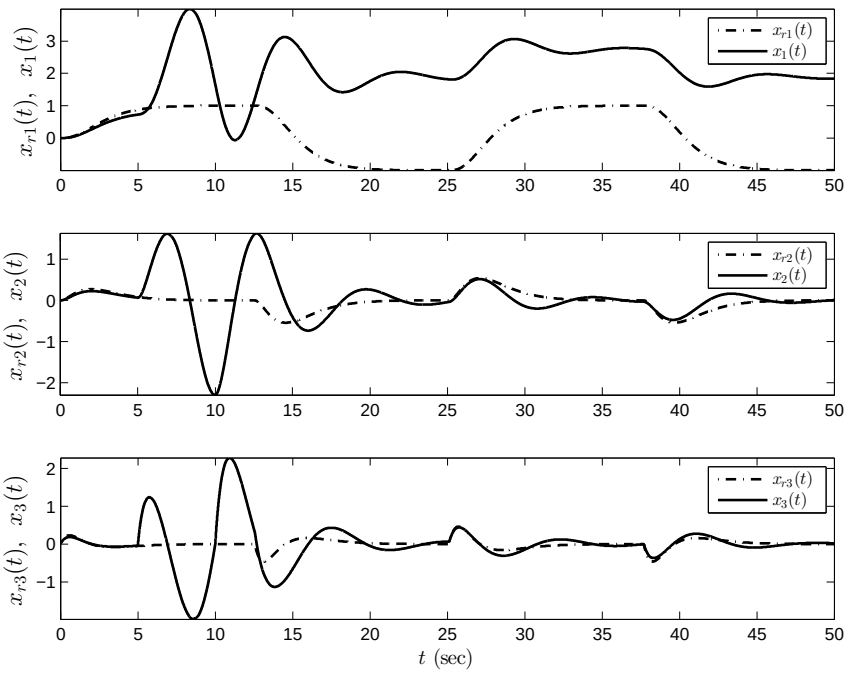

Figure 4.31: System performance with the nominal controller only.

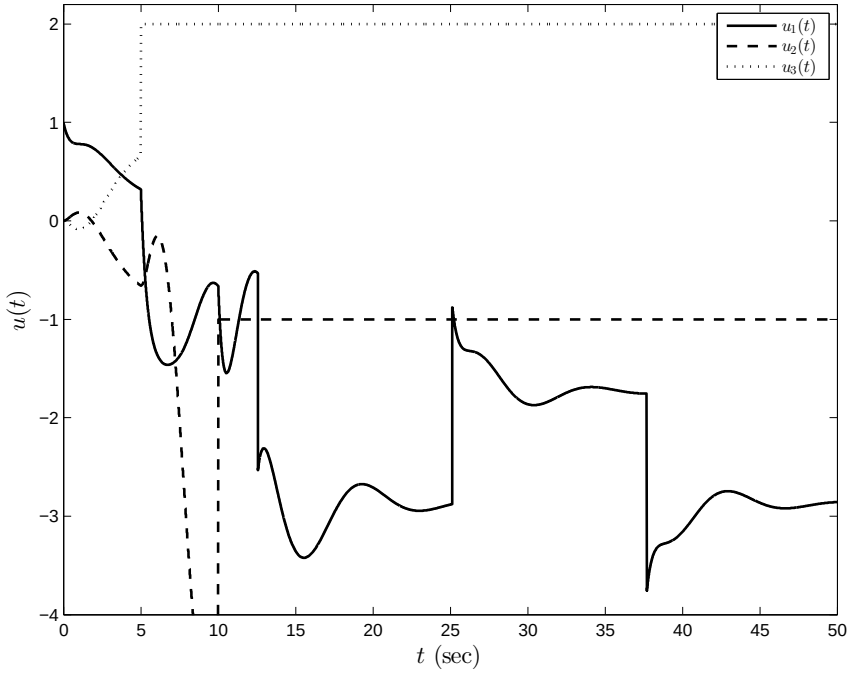

Figure 4.32: Control histories with the nominal controller only.

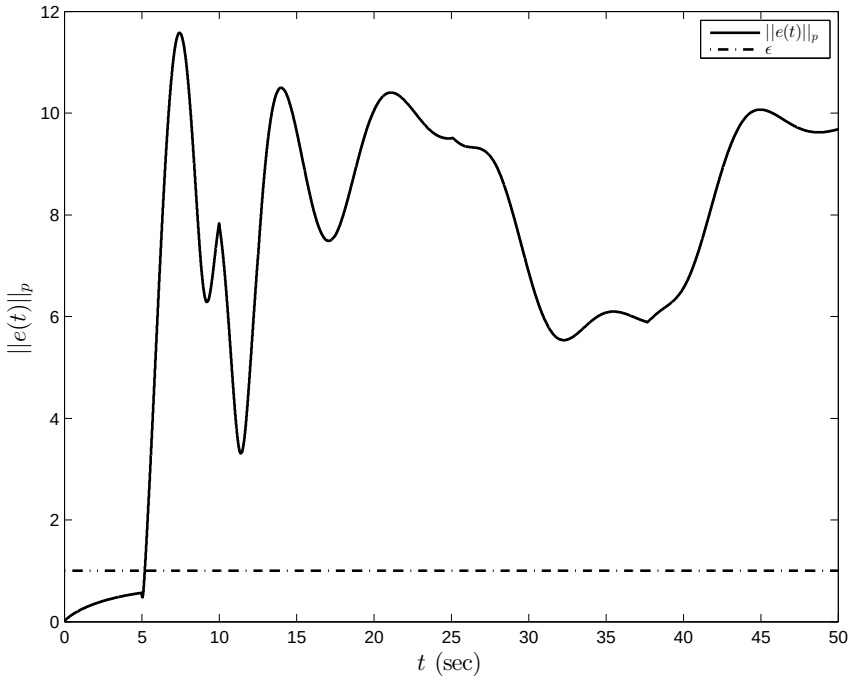

Figure 4.33: Norm of the system error trajectories and the user-defined worst-case performance bound ϵ with the nominal controller only.

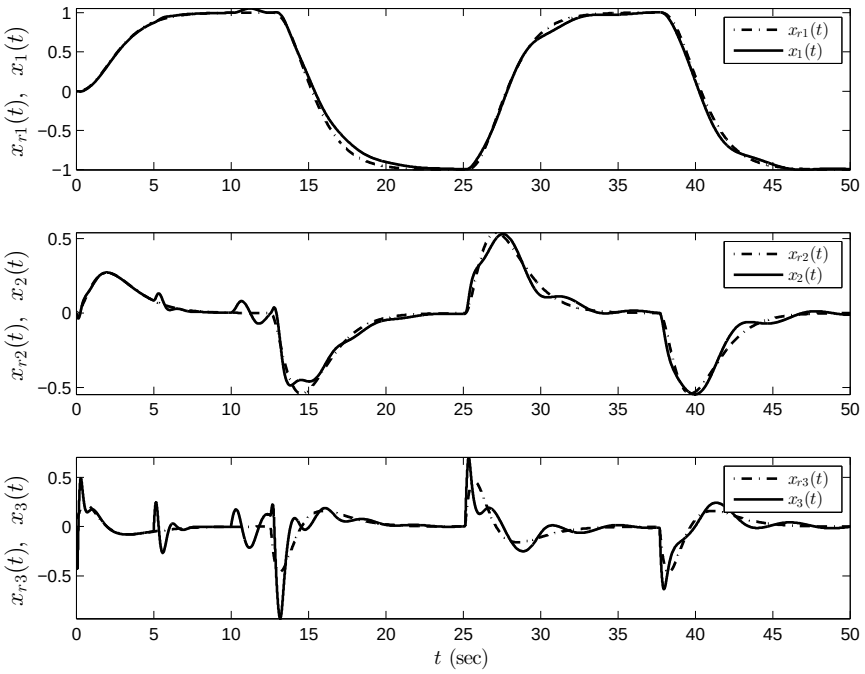

Figure 4.34: System performance with the proposed set-theoretic model reference adaptive controller in Theorem 4.4.1.

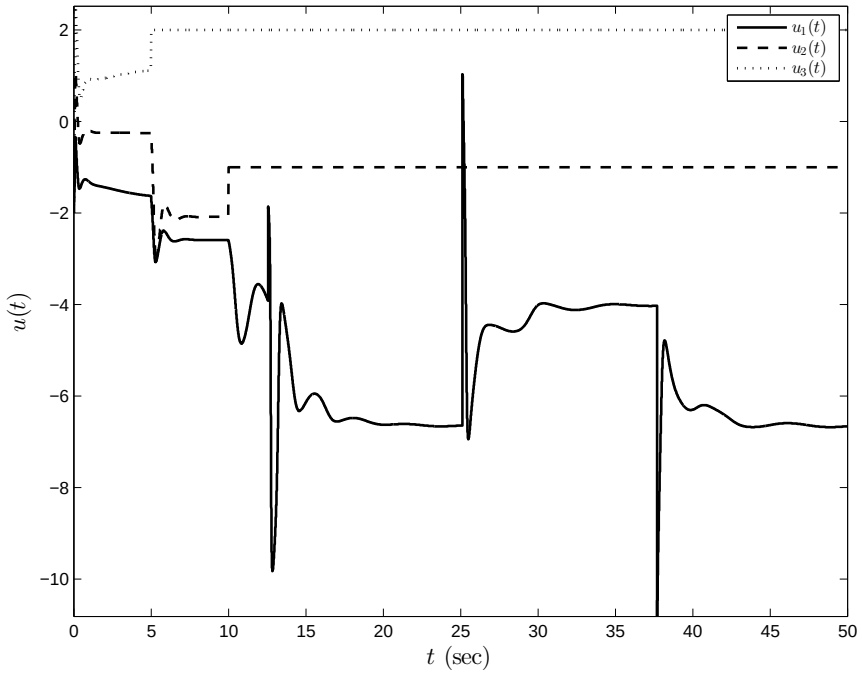

Figure 4.35: Control histories with the proposed set-theoretic model reference adaptive controller in Theorem 4.4.1.

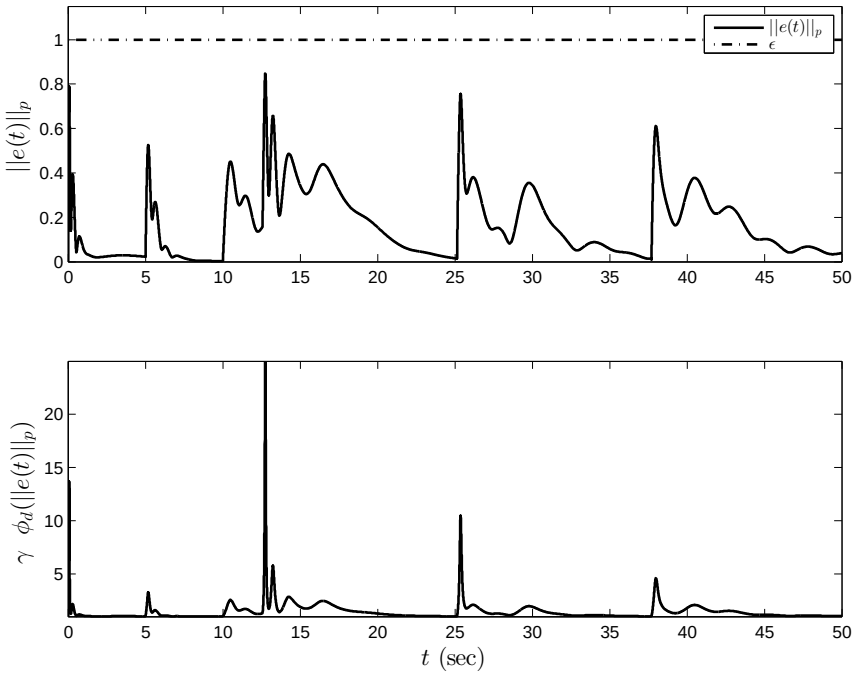

Figure 4.36: Norm of the system error trajectories, the user-defined worst-case performance bound ε, and the evolution of the effective learning rate $\gamma\phi_{\mathrm{d}}(\cdot)$ with the proposed set-theoretic model reference adaptive controller in Theorem 4.4.1.

4.4.5 Conclusion

A challenge in the design of model reference adaptive controllers is not only to achieve a level of desired system performance in the presence of exogenous disturbances and system uncertainties but also to preserve system stability and robustness against actuator failures. Motivated from this standpoint, we proposed a set-theoretic model reference adaptive control architecture in the presence of unknown actuator failures in terms of time, pattern, and value. Specifically, the key feature of the proposed approach was to keep the distance between the trajectories of an uncertain dynamical system and a given reference model to be less than a-priori, user-defined worst-case closed-loop system performance bound in the presence of finite number of actuator failures. A system-theoretical analysis and an illustrative numerical example were further provided to demonstrate the efficacy of the proposed approach.

CHAPTER 5: APPLICATIONS OF THE SET-THEORETIC MODEL REFERENCE ADAPTIVE CONTROL

This chapter presents application-oriented extensions of the set-theoretic model reference adaptive control architecture proposed in Chapters 2 and 4. Specifically, Section 5.1 presents an application of this control architecture on a generic transport model developed by NASA, where in Section 5.2 the set-theoretic model reference adaptive control with constant and time-varying performance bounds are validated on an aerospace testbed, which is configured as a dual-rotor helicopter. Section 5.3 incorporates a dead-zone effect on the set-theoretic model reference adaptive control, and finally Section 5.4 studies an application of set-theoretic model reference adaptive control for human-in-the-loop physical systems to enhance the overall system stability.

5.1 Set-Theoretic Model Reference Adaptive Control of a Generic Transport Model[1]

This paper illustrates an application of a recently developed set-theoretic model reference adaptive control architecture on a generic transport model developed by NASA. The set-theoretic model reference adaptive control allows the system error bound between the state of an uncertain dynamical system and the state of a given reference model to be less than a-priori, user-defined worst-case performance bound. Thus, it has the capability to enforce strict performance guarantees to the adaptively controlled uncertain dynamical systems. Specifically, after designing set-theoretic adaptive controllers for both longitudinal and lateral-directional dynamics here, the efficacy of this architecture is illustrated on the NASA generic transport model.

5.1.1 Introduction

Model reference adaptive control algorithms are effective system-theoretic tools to suppress the effects of adverse conditions resulting from exogenous disturbances, imperfect dynamical system modeling,

[1]This section is previously published in [105]. Permission is included in Appendix H.

degraded modes of operation, and changes in system dynamics. Yet, one of their challenges is the inability to achieve a-priori, user-defined performance guarantees. Motivated from this standpoint, a new technique entitled set-theoretic model reference adaptive control architecture is proposed in a recent set of papers by the authors [1, 21, 93, 101–104, 108, 111]. Specifically, [1, 21] respectively present this new control methodology for dynamical systems subject to time-invariant and time-varying structured uncertainties. The key feature of set-theoretic model reference adaptive control architecture is to allow the weighted Euclidean norm of the system error vector, which represents the error between the state vector of an uncertain dynamical system and the state vector of a reference model, to be less than a-priori, user-defined constant performance bound. This framework is then generalized to the unstructured system uncertainties in [93, 102] and also the extension of this architecture for guaranteeing performance in the presence of actuator failures is presented in [101]. In addition, [108] generalizes these results to the case when a-priori, user-defined performance bound is time-varying. This framework is also recently employed for decentralized control of large-scale modular systems in [103, 104]. Finally, the partial constraint problem using set-theoretic adaptive control architecture is studied in [111] and in [110] componentwise performance guarantees are developed.

Building on the results of [1], this paper illustrates an application of the set-theoretic model reference adaptive control architecture on a generic transport model developed by NASA. Specifically, after designing set-theoretic adaptive controllers for both longitudinal and lateral-directional dynamics here, the efficacy of this architecture is illustrated on the NASA generic transport model (GTM). The organization of the rest of this paper is as follows. Section 5.1.2 summarizes the architecture and properties of the set-theoretic model reference adaptive control architecture. Section 5.1.3 describes the nominal and adaptive control designs for the longitudinal and lateral-directional dynamics of the generic transport model developed by NASA, where in Section 5.1.4 the illustrative simulation results are presented. Conclusions are finally drawn in Section 5.1.5.

The notation used in this paper is fairly standard as similar to [1]. For self-containedness, $\mathbb{N}$ denotes the set of natural numbers, $\mathbb{R}$ denotes the set of real numbers, $\mathbb{R}^n$ denotes the set of $n \times 1$ real column vectors, $\mathbb{R}^{n\times m}$ denotes the set of $n \times m$ real matrices, $\mathbb{R}_+$ (respectively, $\overline{\mathbb{R}}_+$) denotes the set of positive (respectively, nonnegative-definite) real numbers, $\mathbb{R}_+^{n\times n}$ (respectively, $\overline{\mathbb{R}}_+^{n\times n}$) denotes the set of $n \times n$ positive-definite (respectively, nonnegative-definite) real matrices, $\mathbb{D}^{n\times n}$ denotes the set of $n \times n$ real matrices with diagonal scalar entries, $0_{n\times n}$ denotes the $n \times n$ zero matrix, and "$\triangleq$" denotes equality by definition. In

addition, we write $(\cdot)^{\mathrm{T}}$ for the transpose operator, $(\cdot)^{-1}$ for the inverse operator, $\det(\cdot)$ for the determinant operator, $\|\cdot\|_{\mathrm{F}}$ for the Frobenius norm, and $\|\cdot\|_2$ for the Euclidean norm. Furthermore, we write $\|x\|_{\mathrm{A}} \triangleq \sqrt{x^{\mathrm{T}}Ax}$ for the weighted Euclidean norm of $x \in \mathbb{R}^n$ with the matrix $A \in \mathbb{R}_+^{n\times n}$, $\|A\|_2 \triangleq \sqrt{\lambda_{\max}(A^{\mathrm{T}}A)}$ for the induced 2-norm of the matrix $A \in \mathbb{R}^{n\times m}$, $\lambda_{\min}(A)$ (resp., $\lambda_{\max}(A)$) for the minimum (resp., maximum) eigenvalue of the matrix $A \in \mathbb{R}^{n\times n}$, $\mathrm{tr}(\cdot)$ for the trace operator, and $\underline{x}$ (resp., $\bar{x}$) for the lower bound (resp., upper bound) of a bounded signal $x(t) \in \mathbb{R}^n$, that is, $\underline{x} \leq \|x(t)\|_2$ (resp., $\|x(t)\|_2 \leq \bar{x}$).

5.1.2 The Set-Theoretic Adaptive Control Architecture

5.1.2.1 Necessary Definitions

We first introduce the definition of the projection operator from [30].

Definition 5.1.1 *Let* $\Omega = \left\{\theta \in \mathbb{R}^n : (\theta_i^{\min} \leq \theta_i \leq \theta_i^{\max})_{i=1,2,\cdots,n}\right\}$, *be a convex hypercube in* $\mathbb{R}^n$, *where* $(\theta_i^{\min},\ \theta_i^{\max})$ *represent the minimum and maximum bounds for the* i^{th} *component of the n-dimensional parameter vector* θ. *Additionally, for a sufficiently small positive constant* ν, *define the second hypercube as* $\Omega_\nu = \left\{\theta \in \mathbb{R}^n : (\theta_i^{\min} + \nu \leq \theta_i \leq \theta_i^{\max} - \nu)_{i=1,2,\cdots,n}\right\}$, *where* $\Omega_\nu \subset \Omega$. *With* $y \in \mathbb{R}^n$, *projection operator* $\mathrm{Proj} : \mathbb{R}^n \times \mathbb{R}^n \to \mathbb{R}^n$ *is then defined componentwise by* $\mathrm{Proj}(\theta, y) \triangleq \left(\frac{\theta_i^{\max} - \theta_i}{\nu}\right) y_i$ *if* $\theta_i > \theta_i^{\max} - \nu$ *and* $y_i > 0$, $\mathrm{Proj}(\theta, y) \triangleq \left(\frac{\theta_i - \theta_i^{\min}}{\nu}\right) y_i$ *if* $\theta_i < \theta_i^{\min} + \nu$ *and* $y_i < 0$, *and* $\mathrm{Proj}(\theta, y) \triangleq y_i$ *otherwise. Based on the above formulation, note that* $\left(\theta - \theta^*\right)^{\mathrm{T}}\left(\mathrm{Proj}\left(\theta, y\right) - y\right) \leq 0$ *holds (see [30, 80] for details), where this inequality can be also readily generalized to matrices using* $\mathrm{Proj}_{\mathrm{m}}(\Theta, Y) = \big(\mathrm{Proj}(\mathrm{col}_1(\Theta), \mathrm{col}_1(Y)), \ldots,$ $\mathrm{Proj}(\mathrm{col}_m(\Theta), \mathrm{col}_m(Y))\big)$ *where* $\Theta \in \mathbb{R}^{n\times m}$, $Y \in \mathbb{R}^{n\times m}$, *and* $\mathrm{col}_i(\cdot)$ *denotes* ith *column operator.*

Throughout this paper, we assume without loss of generality that the projection norm bound imposed on each column of $\Theta \in \mathbb{R}^{n\times m}$ is $\theta_{\max}$. We next introduce the definition of the generalized restricted potential function (generalized barrier Lyapunov function) from [1, 21].

Definition 5.1.2 *Let* $\|z\|_H = \sqrt{z^{\mathrm{T}}Hz}$ *be a weighted Euclidean norm, where* $z \in \mathbb{R}^p$ *is a real column vector and* $H \in \mathbb{R}_+^{p\times p}$. *We define* $\phi(\|z\|_{\mathrm{H}})$, $\phi : \mathbb{R} \to \mathbb{R}$, *to be a generalized restricted potential function (generalized barrier Lyapunov function) on the set*

$$\mathcal{D}_\varepsilon \triangleq \{z : \|z\|_{\mathrm{H}} \in [0, \varepsilon)\}, \tag{5.1}$$

with $\varepsilon \in \mathbb{R}_+$ *being a-priori, user-defined constant, if the following statements hold [1]:*

i) *If* $\|z\|_{\mathrm{H}} = 0$, *then* $\phi(\|z\|_{\mathrm{H}}) = 0$.

ii) *If* $z \in \mathcal{D}_\varepsilon$ *and* $\|z\|_{\mathrm{H}} \neq 0$, *then* $\phi(\|z\|_{\mathrm{H}}) > 0$.

iii) *If* $\|z\|_{\mathrm{H}} \to \varepsilon$, *then* $\phi(\|z\|_{\mathrm{H}}) \to \infty$.

iv) $\phi(\|z\|_{\mathrm{H}})$ *is continuously differentiable on* $\mathcal{D}_\varepsilon$.

v) *If* $z \in \mathcal{D}_\varepsilon$, *then* $\phi_d(\|z\|_{\mathrm{H}}) > 0$, *where*

$$\phi_d(\|z\|_{\mathrm{H}}) \triangleq \frac{\mathrm{d}\phi(\|z\|_{\mathrm{H}})}{\mathrm{d}\|z\|_{\mathrm{H}}^2}. \tag{5.2}$$

vi) *If* $z \in \mathcal{D}_\varepsilon$, *then*

$$2\phi_d(\|z\|_{\mathrm{H}})\|z\|_{\mathrm{H}}^2 - \phi(\|z\|_{\mathrm{H}}) > 0. \tag{5.3}$$

Remark 5.1.1 *A candidate generalized restricted potential function satisfying the conditions given in Definition 5.1.2 has the form* $\phi(\|z\|_{\mathrm{H}}) = \|z\|_{\mathrm{H}}^2/\big(\varepsilon - \|z\|_{\mathrm{H}}\big)$, $z \in \mathcal{D}_\varepsilon$, *which has the partial derivative* $\phi_d(\|z\|_{\mathrm{H}}) = \big(\varepsilon - \frac{1}{2}\|z\|_{\mathrm{H}}\big)/\big(\varepsilon - \|z\|_{\mathrm{H}}\big)^2 > 0$, $z \in \mathcal{D}_\varepsilon$, *with respect to* $\|z\|_{\mathrm{H}}^2$, *and* $2\phi_d(\|z\|_{\mathrm{H}})\|z\|_{\mathrm{H}}^2 - \phi(\|z\|_{\mathrm{H}}) = \varepsilon\|z\|_{\mathrm{H}}^2/\big(\varepsilon - \|z\|_{\mathrm{H}}\big)^2 > 0$, $z \in \mathcal{D}_\varepsilon$ *[1].*

5.1.2.2 An Overview of the Set-Theoretic Model Reference Adaptive Control Architecture

We now overview the set-theoretic model reference adaptive control architecture introduced in [1]. To this end, consider the uncertain dynamical system given by

$$\dot{x}_{\mathrm{p}}(t) \;=\; A_{\mathrm{p}}x_{\mathrm{p}}(t) + B_{\mathrm{p}}\Lambda u(t) + B_{\mathrm{p}}\delta_{\mathrm{p}}(t, x_{\mathrm{p}}(t)), \quad x_{\mathrm{p}}(0) = x_{\mathrm{p}0}, \tag{5.4}$$

where $x_{\mathrm{p}}(t) \in \mathbb{R}^{n_{\mathrm{p}}}$ is the measurable state vector, $u(t) \in \mathbb{R}^m$ is the control input, $A_{\mathrm{p}} \in \mathbb{R}^{n_{\mathrm{p}} \times n_{\mathrm{p}}}$ is a known system matrix, $B_{\mathrm{p}} \in \mathbb{R}^{n_{\mathrm{p}} \times m}$ is a known input matrix, $\delta_{\mathrm{p}} : \overline{\mathbb{R}}_+ \times \mathbb{R}^{n_{\mathrm{p}}} \to \mathbb{R}^m$ is a system uncertainty, $\Lambda \in \mathbb{R}_+^{m \times m} \cap \mathbb{D}^{m \times m}$ is an unknown control effectiveness matrix, and the pair $(A_{\mathrm{p}}, B_{\mathrm{p}})$ is controllable. Below we introduce a standard system uncertainty parameterization [28–30].

Assumption 5.1.1 *The system uncertainty given by* (5.4) *is parameterized as*

$$\delta_{\rm p}(t,x_{\rm p}) \;=\; W_{\rm p}^{\rm T}(t)\sigma_{\rm p}(x_{\rm p}), \tag{5.5}$$

where $W_{\rm p}(t) \in \mathbb{R}^{s\times m}$ *is a bounded unknown weight matrix (i.e.,* $\|W_{\rm p}(t)\|_{\rm F} \leq w_{\rm p}$*) with a bounded time rate of change (i.e.,* $\|\dot{W}_{\rm p}(t)\|_{\rm F} \leq \dot{w}_{\rm p}$*) and* $\sigma_{\rm p} : \mathbb{R}^{n_{\rm p}} \to \mathbb{R}^s$ *is a known basis function of the form* $\sigma_{\rm p}(x_{\rm p}) = [\sigma_{\rm p1}(x_{\rm p}), \sigma_{\rm p2}(x_{\rm p}), \ldots, \sigma_{{\rm p}s}(x_{\rm p})]^{\rm T}$.

Note that by letting the first element of the basis function be a constant (i.e., $\sigma_{\rm p1}(x_{\rm p}) = b$), the parameterization given by (5.5) also captures exogenous disturbances. To address command following, let $c(t) \in \mathbb{R}^{n_{\rm c}}$ be a given bounded piecewise continuous command and $x_{\rm c}(t) \in \mathbb{R}^{n_{\rm c}}$ be the integrator state satisfying

$$\dot{x}_{\rm c}(t) = E_{\rm p}x_{\rm p}(t) - c(t), \quad x_{\rm c}(0) = x_{\rm c0}, \tag{5.6}$$

where $E_{\rm p} \in \mathbb{R}^{n_{\rm c}\times n_{\rm p}}$ allows the selection of a subset of $x_{\rm p}(t)$ to follow $c(t)$. Using (5.4) and (5.6), we write

$$\dot{x}(t) \;=\; Ax(t) + B\Lambda u(t) + BW_{\rm p}^{\rm T}(t)\sigma_{\rm p}(x_{\rm p}(t)) + B_{\rm r}c(t), \quad x(0) = x_0, \tag{5.7}$$

where $x(t) \triangleq [x_{\rm p}^{\rm T}(t),\ x_{\rm c}^{\rm T}(t)]^{\rm T} \in \mathbb{R}^n$, $n = n_{\rm p} + n_{\rm c}$, is the augmented state vector, and $x_0 \triangleq [x_{\rm p0}^{\rm T},\ x_{\rm c0}^{\rm T}]^{\rm T}$,

$$A \;\triangleq\; \begin{bmatrix} A_{\rm p} & 0_{n_{\rm p}\times n_{\rm c}} \\ E_{\rm p} & 0_{n_{\rm c}\times n_{\rm c}} \end{bmatrix} \in \mathbb{R}^{n\times n}, \tag{5.8}$$

$$B \;\triangleq\; \begin{bmatrix} B_{\rm p}^{\rm T} & 0_{n_{\rm c}\times m}^{\rm T} \end{bmatrix}^{\rm T} \in \mathbb{R}^{n\times m}, \tag{5.9}$$

$$B_{\rm r} \;\triangleq\; \begin{bmatrix} 0_{n_{\rm p}\times n_{\rm c}}^{\rm T} & -I_{n_{\rm c}\times n_{\rm c}} \end{bmatrix}^{\rm T} \in \mathbb{R}^{n\times n_{\rm c}}. \tag{5.10}$$

Next, consider the (augmenting) feedback control law given by

$$u(t) = u_{\rm n}(t) + u_{\rm a}(t), \tag{5.11}$$

where $u_{\rm n}(t) \in \mathbb{R}^m$, and $u_{\rm a}(t) \in \mathbb{R}^m$ are the nominal and adaptive control laws, respectively. Furthermore, let the nominal control law be

$$u_{\mathrm{n}}(t) = -Kx(t), \tag{5.12}$$

such that $A_{\mathrm{r}} \triangleq A - BK$, $K \in \mathbb{R}^{m\times n}$, is Hurwitz. Using (5.11) and (5.12) in (5.7) yields

$$\dot{x}(t) \;=\; A_{\mathrm{r}}x(t) + B_{\mathrm{r}}c(t) + B\Lambda\left[u_{\mathrm{a}}(t) + W^{\mathrm{T}}(t)\sigma\big(x(t)\big)\right], \quad x(0) = x_0, \tag{5.13}$$

where

$$W(t) \triangleq \left[\Lambda^{-1}W_{\mathrm{p}}^{\mathrm{T}}(t),\ (\Lambda^{-1} - I_{m\times m})K\right]^{\mathrm{T}} \in \mathbb{R}^{(s+n)\times m}, \tag{5.14}$$

is an unknown (aggregated) weight matrix and

$$\sigma\big(x(t)\big) \triangleq [\sigma_{\mathrm{p}}^{\mathrm{T}}\big(x_{\mathrm{p}}(t)\big), x^{\mathrm{T}}(t)]^{\mathrm{T}} \in \mathbb{R}^{s+n}, \tag{5.15}$$

is a known (aggregated) basis function. Considering (5.13), let the adaptive control law be

$$u_{\mathrm{a}}(t) = -\hat{W}^{\mathrm{T}}(t)\sigma\big(x(t)\big), \tag{5.16}$$

where $\hat{W}(t) \in \mathbb{R}^{(s+n)\times m}$ is an estimate of $W(t)$.

Note that the theoretical development of an update law to construct the estimate $\hat{W}(t)$ is crucial in any model reference adaptive control design for achieving desired command following characteristics captured by the reference model given by

$$\dot{x}_{\mathrm{r}}(t) \;=\; A_{\mathrm{r}}x_{\mathrm{r}}(t) + B_{\mathrm{r}}c(t), \quad x_{\mathrm{r}}(0) = x_{\mathrm{r}0}, \tag{5.17}$$

with $x_{\mathrm{r}}(t) \in \mathbb{R}^n$ being the reference state vector. Following the set-theoretic model reference adaptive control architecture developed in [1] (see also [93, 101–104, 108]), consider the update law for (5.16) given by

$$\dot{\hat{W}}(t) = \gamma\mathrm{Proj}_{\mathrm{m}}\Big(\hat{W}(t), \phi_d(\|e(t)\|_{\mathrm{P}})\sigma\big(x(t)\big)e^{\mathrm{T}}(t)PB\Big), \quad \hat{W}(0) = \hat{W}_0, \tag{5.18}$$

with $\hat{W}_{\max}$ being the projection norm bound. In (5.18), additionally, $\gamma \in \mathbb{R}_+$ is the learning rate (i.e., adaptation gain), $P \in \mathbb{R}_+^{n\times n}$ is a solution of the Lyapunov equation given by

$$0 \quad = \quad A_{\mathrm{r}}^{\mathrm{T}}P + PA_{\mathrm{r}} + R, \tag{5.19}$$

with $R \in \mathbb{R}_{+}^{n\times n}$, and $e(t) \triangleq x(t) - x_{\mathrm{r}}(t)$ is the system error.

Remark 5.1.2 *One can write the system error dynamics and the weight estimation error dynamics respectively as*

$$\dot{e}(t) \quad = \quad A_{\mathrm{r}}e(t) - B\Lambda\tilde{W}^{\mathrm{T}}(t)\sigma\big(x(t)\big), \quad e(0) = e_0, \tag{5.20}$$

$$\dot{\tilde{W}}(t) \quad = \quad \gamma \mathrm{Proj}_{\mathrm{m}}\Big(\hat{W}(t), \phi_d(\|e(t)\|_{\mathrm{P}})\sigma\big(x(t)\big)e^{\mathrm{T}}(t)PB\Big) - \dot{W}(t), \quad \tilde{W}(0) = \tilde{W}_0, \tag{5.21}$$

where $\tilde{W}(t) \triangleq \hat{W}(t) - W(t)$, is the weight estimation error. Note that $\phi_d(\|e(t)\|_{\mathrm{P}})$ in (5.18) can be viewed as an error dependent learning rate and $\|W(t)\|_{\mathrm{F}} \leq w$ and $\|\dot{W}(t)\|_{\mathrm{F}} \leq \dot{w}$ automatically holds as a direct consequence of Assumption 5.1.1. From a theoretical standpoint, the update law given by (5.18) *for the set-theoretic model reference adaptive control architecture can be derived by considering the following energy function*

$$V(e,\tilde{W}) = \phi(\|e\|_{\mathrm{P}}) + \gamma^{-1}\mathrm{tr}\big[(\tilde{W}\Lambda^{1/2})^{\mathrm{T}}(\tilde{W}\Lambda^{1/2})\big], \tag{5.22}$$

where $\mathcal{D}_\varepsilon \triangleq \{e(t) : \|e(t)\|_{\mathrm{P}} < \varepsilon\}$ and $P \in \mathbb{R}_{+}^{n\times n}$ is a solution of the Lyapunov equation in (5.19) with $R \in \mathbb{R}_{+}^{n\times n}$. Note that $V(0,0) = 0$, $V\big(e,\tilde{W}\big) > 0$ for $\big(e,\tilde{W}\big) \neq (0,0)$, and

$$\dot{V}\big(e(t),\tilde{W}(t)\big) \quad \leq \quad -\frac{1}{2}\alpha V(e,\tilde{W}) + \mu, \tag{5.23}$$

where $\alpha \triangleq \frac{\lambda_{\min}(R)}{\lambda_{\max}(P)}$, $d \triangleq 2\gamma^{-1}\tilde{w}\,\dot{w}\|\Lambda\|_2$, $\mu \triangleq \frac{1}{2}\alpha\gamma^{-1}\tilde{w}^2\|\Lambda\|_2 + d$, and $\tilde{w} = \hat{W}_{\max} + w$. By applying Lemma 1 of [23, 25], one can now conclude the boundedness of the closed-loop dynamical system given by (5.20) and (5.21) as well as the strict performance bound on the system error given by (see [1] for details)

$$\|e(t)\|_{\mathrm{P}} < \varepsilon. \tag{5.24}$$

5.1.3 Set-theoretic Model Reference Adaptive Control Architecture Design for the Generic Transport Model

We consider the NASA GTM 6-DOF rigid aircraft state space model [133] in the form of (5.4) with

$$x_{\rm p}(t) = [h(t),\ U(t),\ \alpha(t), q(t),\ \theta(t),\ \beta(t),\ p(t),\ r(t),\ \phi(t),\ \psi(t)] \in \mathbb{R}^{10}, \tag{5.25}$$

$$u(t) = [F_{\rm T}(t),\ \delta_{\rm e}(t),\ \delta_{\rm r}(t),\ \delta^{\rm L}_{\rm f_1}, \cdots,\ \delta^{\rm L}_{\rm f_{16}},\ \delta^{\rm R}_{\rm f_1}, \cdots,\ \delta^{\rm R}_{\rm f_{16}}] \in \mathbb{R}^{35}, \tag{5.26}$$

being the measurable state vector and control signal vector, respectively. In (5.4), $h(t)$ is the height (in ft), $U(t)$ is the speed (in ft/s), $\alpha(t)$ is the angle of attack (in rad), $\theta(t)$ is the pitch angle (in rad), $\beta(t)$ is the sideslip angle (in rad), $p(t), q(t)$ and $r(t)$ are the angular velocities (in rad/s), $\phi(t)$ is the roll angle (in rad), and $\psi(t)$ is the heading angle. In (5.25), $F_{\rm T}(t)$ is the thrust of the two engines (in lbs), $\delta_{\rm e}(t)$ is the elevator control input (in rad), $\delta_{\rm r}(t)$ is the rudder control input (in rad), $\delta^{\rm L}_{\rm f_1}$ and $\delta^{\rm R}_{\rm f_1}$ correspond to the furthest inboard Variable Camber Continuous Trailing Edge Flap (VCCTEF) segment on the left and the right wings, respectively (in rad). For details, we refer interested readers to [133].

In what follows in this section, we design the set-theoretic adaptive control for both longitudinal and lateral-directional dynamics under the common physical assumption that the longitudinal and lateral-directional dynamics are not strictly coupled and then we use the resulting control input signals for the coupled system given by (5.4).

5.1.3.1 Longitudinal Control Design

For the longitudinal dynamics, we consider the state vector denoted as $x_{\rm p_{lo}}(t) = [\alpha(t),\ q(t)]^{\rm T} \in \mathbb{R}^2$ and the control input is denoted as $u_{\rm lo}(t) = \delta_{\rm e}(t) \in \mathbb{R}$ with the dynamics given by

$$\dot{x}_{\rm p_{lo}}(t) \quad = \quad A_{\rm p_{lo}} x_{\rm p_{lo}}(t) + B_{\rm p_{lo}} \Lambda_{\rm lo} u_{\rm lo}(t) + B_{\rm p_{lo}} \delta_{\rm lo}(t, x_{\rm p_{lo}}(t)), \quad x_{\rm p_{lo}}(0) = x_{\rm p_{lo}0}. \tag{5.27}$$

To address command following, let $c_{\rm lo}(t) \triangleq c_\alpha(t) \in \mathbb{R}$, be a given bounded piecewise continuous command for the angle of attack and $x_{\rm c_\alpha}(t) \in \mathbb{R}$, be the integrator state satisfying $\dot{x}_{\rm c_\alpha}(t) = E_{\rm p_{lo}} x_{\rm p_{lo}}(t) - c_\alpha(t), x_{\rm c_\alpha}(0) = x_{\rm c_\alpha 0}$, where $E_{\rm p_{lo}} = [1,\ 0]$. Now using Assumption 5.1.1, (5.27) can be written as $\dot{x}_{\rm lo}(t) = A_{\rm lo} x_{\rm lo}(t) + B_{\rm lo}\Lambda_{\rm lo} u(t) + B_{\rm lo} W^{\rm T}_{\rm p_{lo}}(t) \sigma_{\rm p_{lo}}(x_{\rm p_{lo}}(t)) + B_{\rm r_{lo}} c_\alpha(t), x_{\rm lo}(0) = x_{\rm lo0}$ where $x_{\rm lo}(t) \triangleq [x^{\rm T}_{\rm p_{lo}}(t),\ x^{\rm T}_{\rm c_\alpha}(t)]^{\rm T} \in \mathbb{R}^3$, is the

augmented state vector, and $x_{\mathrm{lo}0} \triangleq [x_{\mathrm{p_{lo}}0}^{\mathrm{T}}, x_{\mathrm{c}_\alpha 0}^{\mathrm{T}}]^{\mathrm{T}}$,

$$A_{\mathrm{lo}} \triangleq \begin{bmatrix} A_{\mathrm{p_{lo}}} & 0_{2\times 1} \\ E_{\mathrm{p_{lo}}} & 0 \end{bmatrix} \in \mathbb{R}^{3\times 3}, \tag{5.28}$$

$$B_{\mathrm{lo}} \triangleq \begin{bmatrix} B_{\mathrm{p_{lo}}}^{\mathrm{T}} & 0 \end{bmatrix}^{\mathrm{T}} \in \mathbb{R}^3, \tag{5.29}$$

$$B_{\mathrm{r_{lo}}} \triangleq \begin{bmatrix} 0 & 0 & -1 \end{bmatrix}^{\mathrm{T}} \in \mathbb{R}^3. \tag{5.30}$$

Now, by taking similar steps as introduced in Section 5.1.2, one can get

$$\dot{x}_{\mathrm{lo}}(t) = A_{\mathrm{r_{lo}}} x_{\mathrm{lo}}(t) + B_{\mathrm{r_{lo}}} c_{\mathrm{lo}}(t) + B_{\mathrm{lo}} \Lambda_{\mathrm{lo}} \left[u_{\mathrm{a_{lo}}}(t) + W_{\mathrm{lo}}^{\mathrm{T}}(t) \sigma_{\mathrm{lo}}\big(x_{\mathrm{lo}}(t)\big) \right], \quad x_{\mathrm{lo}}(0) = x_{\mathrm{lo}0}, \tag{5.31}$$

where $A_{\mathrm{r_{lo}}} \triangleq A_{\mathrm{lo}} - B_{\mathrm{lo}} K_{\mathrm{lo}}$, $K_{\mathrm{lo}} \in \mathbb{R}^{1\times 3}$, $W_{\mathrm{lo}}(t) \triangleq \left[\Lambda_{\mathrm{lo}}^{-1} W_{\mathrm{p_{lo}}}^{\mathrm{T}}(t),\ (\Lambda_{\mathrm{lo}}^{-1} - 1) K_{\mathrm{lo}} \right]^{\mathrm{T}} \in \mathbb{R}^5$ is an unknown weight matrix and $\sigma_{\mathrm{lo}}\big(x_{\mathrm{lo}}(t)\big) \triangleq [\sigma_{\mathrm{p_{lo}}}^{\mathrm{T}}\big(x_{\mathrm{p_{lo}}}(t)\big), x_{\mathrm{lo}}^{\mathrm{T}}(t)]^{\mathrm{T}} \in \mathbb{R}^5$ is a known basis function.

Therefore, we consider the feedback control law for the longitudinal dynamics given by

$$u_{\mathrm{lo}}(t) = u_{\mathrm{n_{lo}}}(t) + u_{\mathrm{a_{lo}}}(t), \tag{5.32}$$

with

$$u_{\mathrm{n_{lo}}}(t) = -K_{\mathrm{lo}} x_{\mathrm{lo}}(t), \tag{5.33}$$

$$u_{\mathrm{a_{lo}}}(t) = -\hat{W}_{\mathrm{lo}}^{\mathrm{T}}(t) \sigma_{\mathrm{lo}}\big(x_{\mathrm{lo}}(t)\big), \tag{5.34}$$

where $\hat{W}_{\mathrm{lo}}(t) \in \mathbb{R}^5$ is the estimate of $W_{\mathrm{lo}}(t)$ satisfying the update law

$$\dot{\hat{W}}_{\mathrm{lo}}(t) = \gamma_{\mathrm{lo}} \mathrm{Proj_m}\Big(\hat{W}_{\mathrm{lo}}(t), \phi_d(\|e_{\mathrm{lo}}(t)\|_{\mathrm{P_{lo}}}) \sigma_{\mathrm{lo}}\big(x_{\mathrm{lo}}(t)\big) e_{\mathrm{lo}}^{\mathrm{T}}(t) P_{\mathrm{lo}} B_{\mathrm{lo}} \Big), \quad \hat{W}_{\mathrm{lo}}(0) = \hat{W}_{\mathrm{lo}0}, \tag{5.35}$$

with $\hat{W}_{\mathrm{max_{lo}}}$ being the projection norm bound. In (5.35), $\gamma_{\mathrm{lo}} \in \mathbb{R}_+$ is the learning rate, $P_{\mathrm{lo}} \in \mathbb{R}_+^{3\times 3}$ is a solution of the Lyapunov equation given by

$$0 = A_{\mathrm{r_{lo}}}^{\mathrm{T}} P_{\mathrm{lo}} + P_{\mathrm{lo}} A_{\mathrm{r_{lo}}} + R_{\mathrm{lo}}, \tag{5.36}$$

with $R_{\rm lo} \in \mathbb{R}^{3\times 3}_{+}$, and $e_{\rm lo}(t) \triangleq x_{\rm lo}(t) - x_{\rm r_{lo}}(t)$ is the system error in longitudinal dynamics with $x_{\rm r_{lo}}(t)$ being the reference state vector, which satisfies the reference model for the longitudinal dynamics given by

$$\dot{x}_{\rm r_{lo}}(t) = A_{\rm r_{lo}} x_{\rm r_{lo}}(t) + B_{\rm r_{lo}} c_{\rm lo}(t), \quad x_{\rm r_{lo}}(0) = x_{\rm r_{lo}0}. \tag{5.37}$$

Finally, one can write the system error dynamics and weight estimation error dynamics respectively as

$$\dot{e}_{\rm lo}(t) = A_{\rm r_{lo}} e_{\rm lo}(t) - B_{\rm lo}\Lambda_{\rm lo}\tilde{W}^{\rm T}_{\rm lo}(t)\sigma_{\rm lo}\big(x_{\rm lo}(t)\big), \quad e_{\rm lo}(0) = e_{\rm lo0}, \tag{5.38}$$

$$\dot{\tilde{W}}_{\rm lo}(t) = \gamma_{\rm lo}{\rm Proj_m}\Big(\hat{W}_{\rm lo}(t), \phi_d(\|e_{\rm lo}(t)\|_{\rm P_{lo}})\sigma_{\rm lo}\big(x_{\rm lo}(t)\big)e^{\rm T}_{\rm lo}(t)P_{\rm lo}B_{\rm lo}\Big) - \dot{W}_{\rm lo}(t), \quad \tilde{W}_{\rm lo}(0) = \tilde{W}_{\rm lo0}, \tag{5.39}$$

where $\tilde{W}_{\rm lo}(t) \triangleq \hat{W}_{\rm lo}(t) - W_{\rm lo}(t)$, is the weight estimation error. Based on the result overviewed in Section 5.1.2, one can easily conclude the boundedness of the closed-loop dynamical system given by (5.38) and (5.39) as well as the strict performance bound on the system error in longitudinal dynamics given by

$$\|e_{\rm lo}(t)\|_{P_{\rm lo}} < \varepsilon_{\rm lo}. \tag{5.40}$$

5.1.3.2 Lateral-Directional Control Design

The control design for the lateral-directional dynamics follows similarly. In particular, we consider the state vector denoted as $x_{\rm p_{la}}(t) = [\beta(t),\ p(t),\ r(t),\ \phi(t)]^{\rm T} \in \mathbb{R}^4$ and the control input denoted as $u_{\rm la}(t) = [\delta_{\rm r}(t),\ \delta^{\rm L}_{\rm f_1}(t), \cdots,\ \delta^{\rm L}_{\rm f_{16}}(t),\ \delta^{\rm R}_{\rm f_1}(t), \cdots,\ \delta^{\rm R}_{\rm f_{16}}(t)] \in \mathbb{R}^{33}$ with the dynamics given by

$$\dot{x}_{\rm p_{la}}(t) = A_{\rm p_{la}} x_{\rm p_{la}}(t) + B_{\rm p_{la}}\Lambda_{\rm la}u_{\rm la}(t) + B_{\rm p_{la}}\delta_{\rm la}(t, x_{\rm p_{la}}(t)), \quad x_{\rm p_{la}}(0) = x_{\rm p_{la}0}. \tag{5.41}$$

To address command following, let $c_\beta(t) \in \mathbb{R}$ and $c_\phi(t) \in \mathbb{R}$ be a given bounded piecewise continuous command for the sideslip angle (in rad) and roll angle (in rad), respectively. In addition, let $c_{\rm la}(t) \triangleq [c_\beta(t),\ c_\phi(t)]^{\rm T} \in \mathbb{R}^2$ be the augmented command signal for the lateral-directional dynamics and $x_{\rm c_{la}}(t) \in \mathbb{R}^2$, be the integrator state satisfying

$$\dot{x}_{\rm c_{la}}(t) = E_{\rm p_{la}} x_{\rm p_{la}}(t) - c_{\rm la}(t), \quad x_{\rm c_{la}}(0) = x_{\rm c_{la}0}, \quad E_{\rm p_{la}} = \begin{bmatrix} 1 & 0 & 0 & 0 \\ 0 & 0 & 0 & 1 \end{bmatrix}. \tag{5.42}$$

Now using Assumption 5.1.1, (5.41) can be augmented with (5.42) as

$$\dot{x}_{\mathrm{la}}(t) = A_{\mathrm{la}}x_{\mathrm{la}}(t) + B_{\mathrm{la}}\Lambda_{\mathrm{la}}u(t) + B_{\mathrm{la}}W_{\mathrm{p_{la}}}^{\mathrm{T}}(t)\sigma_{\mathrm{p_{la}}}(x_{\mathrm{p_{la}}}(t)) + B_{\mathrm{r_{la}}}c_{\mathrm{la}}(t), \quad x_{\mathrm{la}}(0) = x_{\mathrm{la0}}, \tag{5.43}$$

where $x_{\mathrm{la}}(t) \triangleq [x_{\mathrm{p_{la}}}^{\mathrm{T}}(t),\ x_{\mathrm{c_{la}}}^{\mathrm{T}}(t)]^{\mathrm{T}} \in \mathbb{R}^6$, is the augmented state vector, and $x_{\mathrm{la0}} \triangleq [x_{\mathrm{p_{la}}0}^{\mathrm{T}}, x_{\mathrm{c_{la}}0}^{\mathrm{T}}]^{\mathrm{T}}$,

$$A_{\mathrm{la}} \triangleq \begin{bmatrix} A_{\mathrm{p_{la}}} & 0_{4\times 2} \\ E_{\mathrm{p_{la}}} & 0_{2\times 2} \end{bmatrix} \in \mathbb{R}^{6\times 6}, \tag{5.44}$$

$$B_{\mathrm{la}} \triangleq \begin{bmatrix} B_{\mathrm{p_{la}}}^{\mathrm{T}} & 0_{2\times 33}^{\mathrm{T}} \end{bmatrix}^{\mathrm{T}} \in \mathbb{R}^{6\times 33}, \tag{5.45}$$

$$B_{\mathrm{r_{la}}} \triangleq \begin{bmatrix} 0_{2\times 4} & -I_{2\times 2} \end{bmatrix}^{\mathrm{T}} \in \mathbb{R}^{6\times 2}. \tag{5.46}$$

Now, by taking similar steps as introduced in Section 5.1.2, one can get

$$\dot{x}_{\mathrm{la}}(t) = A_{\mathrm{r_{la}}}x_{\mathrm{la}}(t) + B_{\mathrm{r_{la}}}c_{\mathrm{la}}(t) + B_{\mathrm{la}}\Lambda_{\mathrm{la}}\left[u_{\mathrm{a_{la}}}(t) + W_{\mathrm{la}}^{\mathrm{T}}(t)\sigma_{\mathrm{la}}\left(x_{\mathrm{la}}(t)\right)\right], \quad x_{\mathrm{la}}(0) = x_{\mathrm{la0}}, \tag{5.47}$$

where $A_{\mathrm{r_{la}}} \triangleq A_{\mathrm{la}} - B_{\mathrm{la}}K_{\mathrm{la}}$, $K_{\mathrm{la}} \in \mathbb{R}^{33\times 6}$, $W_{\mathrm{la}}(t) \triangleq \left[\Lambda_{\mathrm{la}}^{-1}W_{\mathrm{p_{la}}}^{\mathrm{T}}(t),\ (\Lambda_{\mathrm{la}}^{-1} - 1)K_{\mathrm{la}}\right]^{\mathrm{T}} \in \mathbb{R}^{10\times 33}$ is an unknown weight matrix and $\sigma_{\mathrm{la}}\left(x_{\mathrm{la}}(t)\right) \triangleq [\sigma_{\mathrm{p_{la}}}^{\mathrm{T}}\left(x_{\mathrm{p_{la}}}(t)\right), x_{\mathrm{la}}^{\mathrm{T}}(t)]^{\mathrm{T}} \in \mathbb{R}^{10}$ is a known basis function.

Therefore, we consider the feedback control law for the lateral-directional dynamics given by

$$u_{\mathrm{la}}(t) = u_{\mathrm{n_{la}}}(t) + u_{\mathrm{a_{la}}}(t), \tag{5.48}$$

with

$$u_{\mathrm{n_{la}}}(t) = -K_{\mathrm{la}}x_{\mathrm{la}}(t), \tag{5.49}$$

$$u_{\mathrm{a_{la}}}(t) = -\hat{W}_{\mathrm{la}}^{\mathrm{T}}(t)\sigma_{\mathrm{la}}\left(x_{\mathrm{la}}(t)\right), \tag{5.50}$$

where $\hat{W}_{\mathrm{la}}(t) \in \mathbb{R}^{10\times 33}$ is the estimate of $W_{\mathrm{la}}(t)$ satisfying the update law

$$\dot{\hat{W}}_{\mathrm{la}}(t) = \gamma_{\mathrm{la}}\mathrm{Proj_m}\left(\hat{W}_{\mathrm{la}}(t), \phi_d(\|e_{\mathrm{la}}(t)\|_{\mathrm{P_{la}}})\sigma_{\mathrm{la}}\left(x_{\mathrm{la}}(t)\right)e_{\mathrm{la}}^{\mathrm{T}}(t)P_{\mathrm{la}}B_{\mathrm{la}}\right), \quad \hat{W}_{\mathrm{la}}(0) = \hat{W}_{\mathrm{la0}}, \tag{5.51}$$

with $\hat{W}_{\mathrm{max_{la}}}$ being the projection norm bound. In (5.51), $\gamma_{\mathrm{la}} \in \mathbb{R}_+$ is the learning rate, $P_{\mathrm{la}} \in \mathbb{R}_+^{6\times 6}$ is a solution of the Lyapunov equation given by

$$0 = A_{\mathrm{r_{la}}}^{\mathrm{T}}P_{\mathrm{la}} + P_{\mathrm{la}}A_{\mathrm{r_{la}}} + R_{\mathrm{la}}, \tag{5.52}$$

with $R_{\mathrm{la}} \in \mathbb{R}_{+}^{6\times 6}$, and $e_{\mathrm{la}}(t) \triangleq x_{\mathrm{la}}(t) - x_{\mathrm{r_{la}}}(t)$ is the system error in the lateral-directional dynamics with $x_{\mathrm{r_{la}}}(t)$ being the reference state vector, which satisfies the reference model for the lateral-directional dynamics given by

$$\dot{x}_{\mathrm{r_{la}}}(t) = A_{\mathrm{r_{la}}} x_{\mathrm{r_{la}}}(t) + B_{\mathrm{r_{la}}} c_{\mathrm{la}}(t), \quad x_{\mathrm{r_{la}}}(0) = x_{\mathrm{r_{la}}0}. \tag{5.53}$$

Finally, one can write the system error dynamics and weight estimation error dynamics respectively as

$$\dot{e}_{\mathrm{la}}(t) = A_{\mathrm{r_{la}}} e_{\mathrm{la}}(t) - B_{\mathrm{la}} \Lambda_{\mathrm{la}} \tilde{W}_{\mathrm{la}}^{\mathrm{T}}(t) \sigma_{\mathrm{la}}\big(x_{\mathrm{la}}(t)\big), \quad e_{\mathrm{la}}(0) = e_{\mathrm{la}0}, \tag{5.54}$$

$$\dot{\tilde{W}}_{\mathrm{la}}(t) = \gamma_{\mathrm{la}} \mathrm{Proj_m}\Big(\hat{W}_{\mathrm{la}}(t), \phi_d(\|e_{\mathrm{la}}(t)\|_{\mathrm{P_{la}}}) \sigma_{\mathrm{la}}\big(x_{\mathrm{la}}(t)\big) e_{\mathrm{la}}^{\mathrm{T}}(t) P_{\mathrm{la}} B_{\mathrm{la}}\Big) - \dot{W}_{\mathrm{la}}(t), \quad \tilde{W}_{\mathrm{la}}(0) = \tilde{W}_{\mathrm{la}0}, \tag{5.55}$$

where $\tilde{W}_{\mathrm{la}}(t) \triangleq \hat{W}_{\mathrm{la}}(t) - W_{\mathrm{la}}(t)$, is the weight estimation error. Once again, based on the result overviewed in Section 5.1.2, one can easily conclude the boundedness of the closed-loop dynamical system given by (5.54) and (5.55) as well as the strict performance bound on the system error in the lateral-directional dynamics given by

$$\|e_{\mathrm{la}}(t)\|_{P_{\mathrm{la}}} < \varepsilon_{\mathrm{la}}. \tag{5.56}$$

5.1.4 Evaluation of Set-Theoretic Model Reference Adaptive Control Architecture on the Generic Transport Model

In this section, we evaluate the NASA GTM performance using the set-theoretic adaptive control architecture that we developed in Section 5.1.3. Specifically, the control signal in (5.32) and (5.48) that are designed for the longitudinal and the lateral-directional dynamics, respectively, are applied to the coupled dynamical system of the NASA GTM. The feedback mechanism of the architecture used in this paper is illustrated in Figure 5.1.

For the configuration with 80% fuel ratio, an altitude of 3600 feet, and a Mach number of 0.797, a linearized model under nominal conditions is obtained, where for a detailed description and the system matrices we refer to [133]. Moreover, linear quadratic regulator (LQR) theory is used to design the nominal controller gain matrices in the longitudinal dynamics with the weighting matrices as $Q_{\mathrm{lo}} = \mathrm{diag}([15, 10, 50])$ to penalize $x_{\mathrm{lo}}(t)$ and $R_{\mathrm{lo}} = 10$ to penalize $u_{\mathrm{lo}}(t)$, resulting in $K_{\mathrm{lo}} = [-1.6958, -1.3820, -2.2361]$. Similarly,

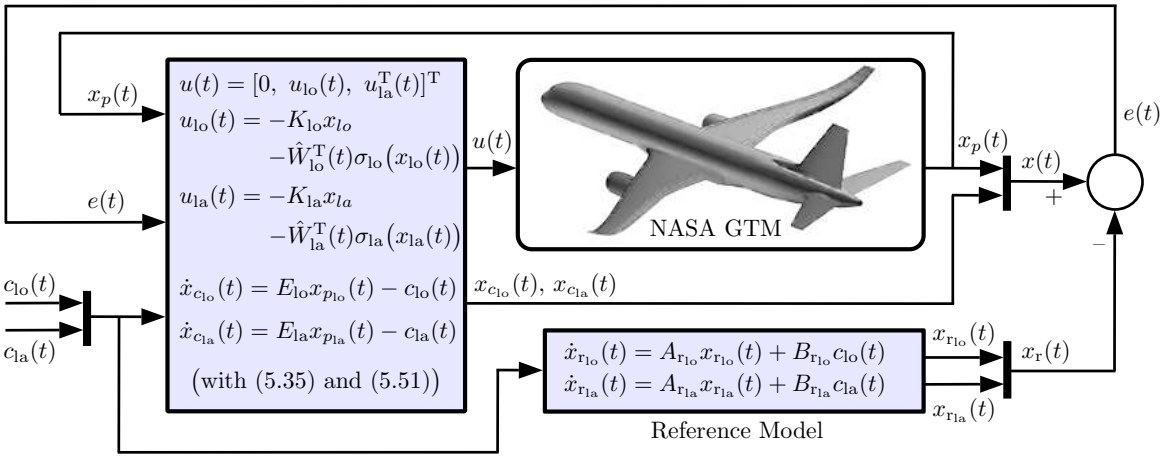

Figure 5.1: Set-theoretic model reference adaptive control architecture.

for the lateral-directional dynamics we choose the weighting matrices as $Q_{\mathrm{la}} = \mathrm{diag}([15,5,5,10,50,50])$ to penalize $x_{\mathrm{la}}(t)$ and $R_{\mathrm{la}} = 10I_{33\times 33}$ to penalize $u_{\mathrm{la}}(t)$, resulting in the corresponding gain matrix $K_{\mathrm{la}} \in \mathbb{R}^{33\times 6}$ that is not presented due to its high dimension. Figures 5.2 and 5.3 show the system response with the nominal controller in absence of system uncertainties.

In what follows we illustrate the performance of the set-theoretic adaptive control architecture for several adverse condition scenarios. For the set-theoretic adaptive control design in all of the scenarios, we set the projection norm bound imposed on each element of the parameter estimate to $\hat{W}_{\mathrm{lo}_{\max}} = 10$ and $\hat{W}_{\mathrm{la}_{\max}} = 20$ and we select $\gamma_{\mathrm{lo}} = 200$ and $\gamma_{\mathrm{la}} = 100$. We use the generalized restricted potential function given in Remark 5.1.1 with two choices for the performance bound ε for each scenario as $\varepsilon_{\mathrm{lo}} = \varepsilon_{\mathrm{la}} = 0.15$ and $\varepsilon_{\mathrm{lo}} = \varepsilon_{\mathrm{la}} = 0.3$ in order to strictly guarantee $\|x_{\mathrm{lo}}(t) - x_{\mathrm{r_{lo}}}(t)\|_{P_{\mathrm{lo}}} = \|x_{\mathrm{la}}(t) - x_{\mathrm{r_{la}}}(t)\|_{P_{\mathrm{la}}} < 0.15$ and $\|x_{\mathrm{lo}}(t) - x_{\mathrm{r_{lo}}}(t)\|_{P_{\mathrm{lo}}} = \|x_{\mathrm{la}}(t) - x_{\mathrm{r_{la}}}(t)\|_{P_{\mathrm{la}}} < 0.3$, respectively.

5.1.4.1 Uncertainties in C_{m_α} and C_{l_p}

We first consider the case when the variation of pitching moment coefficient with angle of attack C_{m_α} and the variation of rolling moment coefficient with roll rate C_{l_p} are both reduced by 360% and we set $\Lambda_{\mathrm{lo}} = \Lambda_{\mathrm{la}} = I$. Figures 5.4 and 5.5 show the system response with the nominal controller in presence of these system uncertainties. Figures 5.6 to 5.8 show the system response with the set-theoretic adaptive control architecture with $\varepsilon_{\mathrm{lo}} = \varepsilon_{\mathrm{la}} = 0.3$ and one can see that the proposed controller is able to recover the system and enforce the required user-defined performance bounds on the system error trajectories. In order

to get a closer tracking of the reference dynamics trajectories, we decrease the performance bounds on both longitudinal and lateral-directional channels to $\varepsilon_{\text{lo}} = \varepsilon_{\text{la}} = 0.15$ as it can be seen from Figures 5.9 to 5.11.

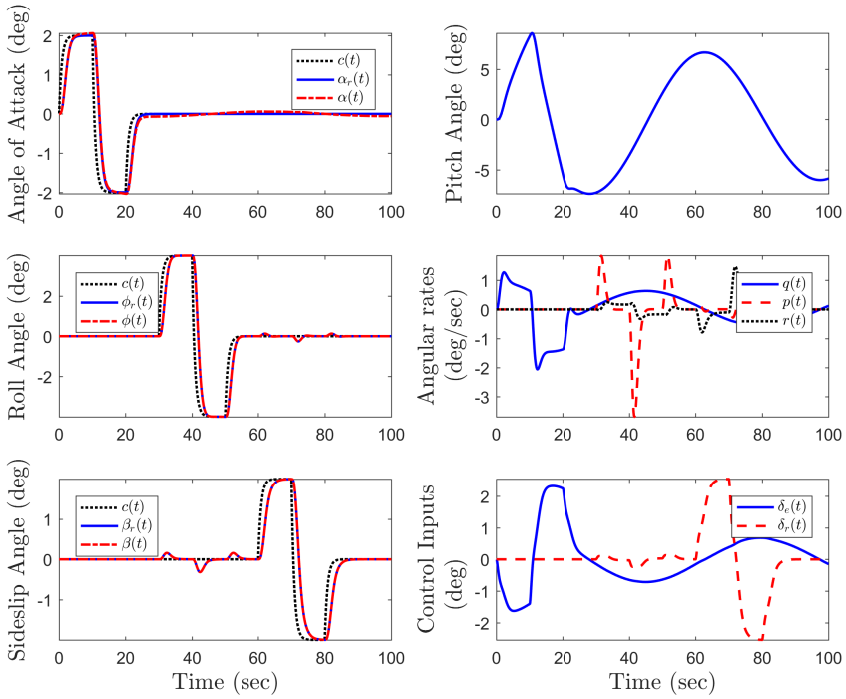

Figure 5.2: System response with the nominal controller.

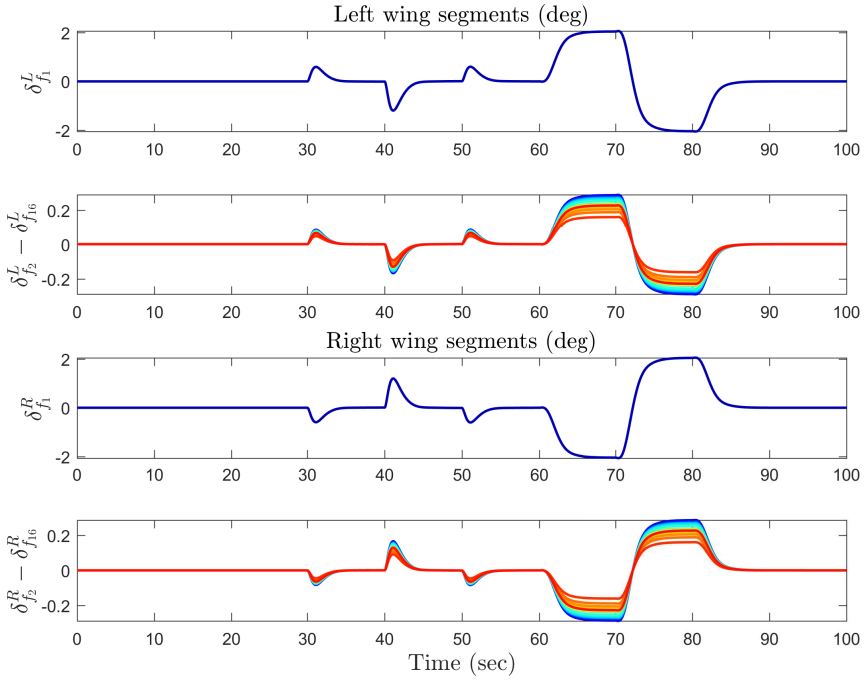

Figure 5.3: Control signals of the VCCTEF segments on the left and the right wings with the nominal controller.

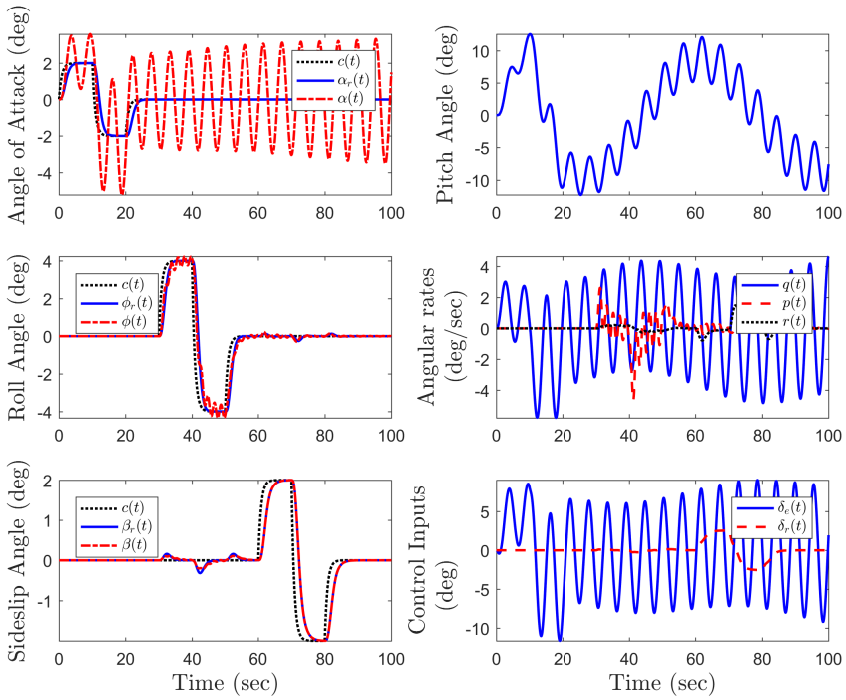

Figure 5.4: System response with the nominal controller under scenario 5.1.4.1.

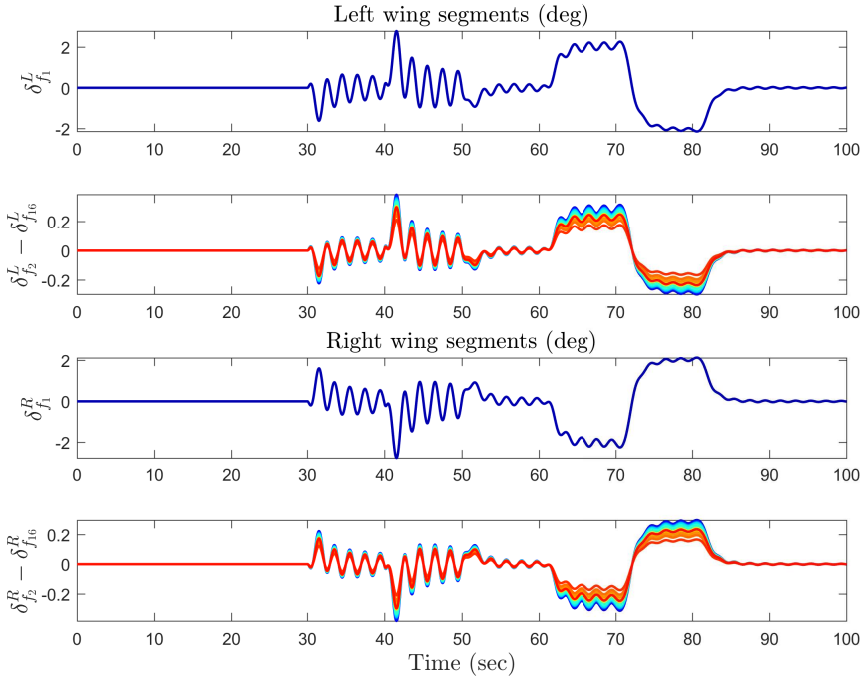

Figure 5.5: Control signals of the VCCTEF segments on the left and the right wings with the nominal controller under scenario 5.1.4.1.

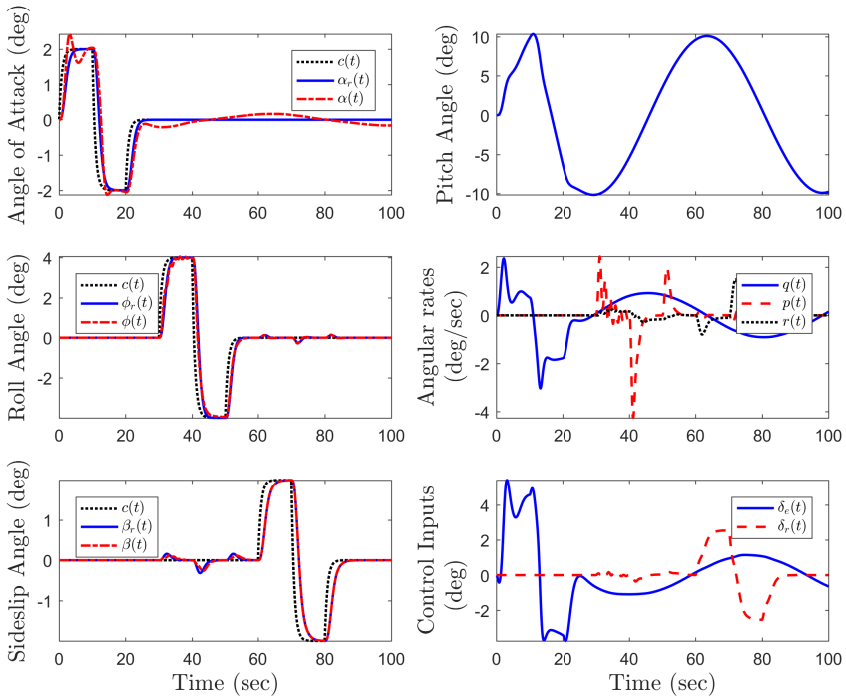

Figure 5.6: Set-theoretic controller response with $\varepsilon_{\text{lo}} = \varepsilon_{\text{la}} = 0.3$ under scenario 5.1.4.1.

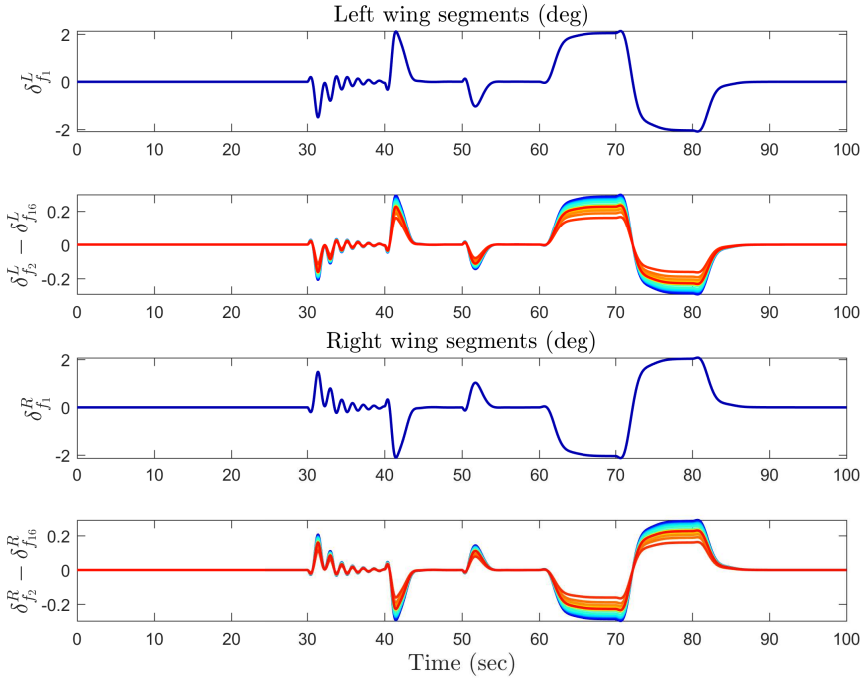

Figure 5.7: Control signals of the VCCTEF segments on the left and the right wings for the case where $\varepsilon_{\text{lo}} = \varepsilon_{\text{la}} = 0.3$ under scenario 5.1.4.1.

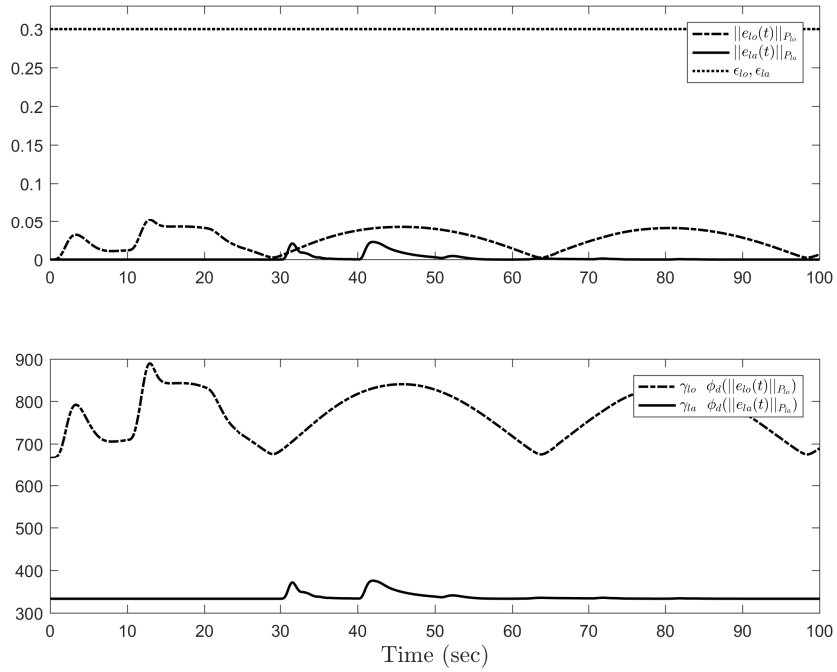

Figure 5.8: The error norm (top) and the effective error dependent adaptation rate (bottom) for the case where $\varepsilon_{\text{lo}} = \varepsilon_{\text{la}} = 0.3$ under scenario 5.1.4.1.

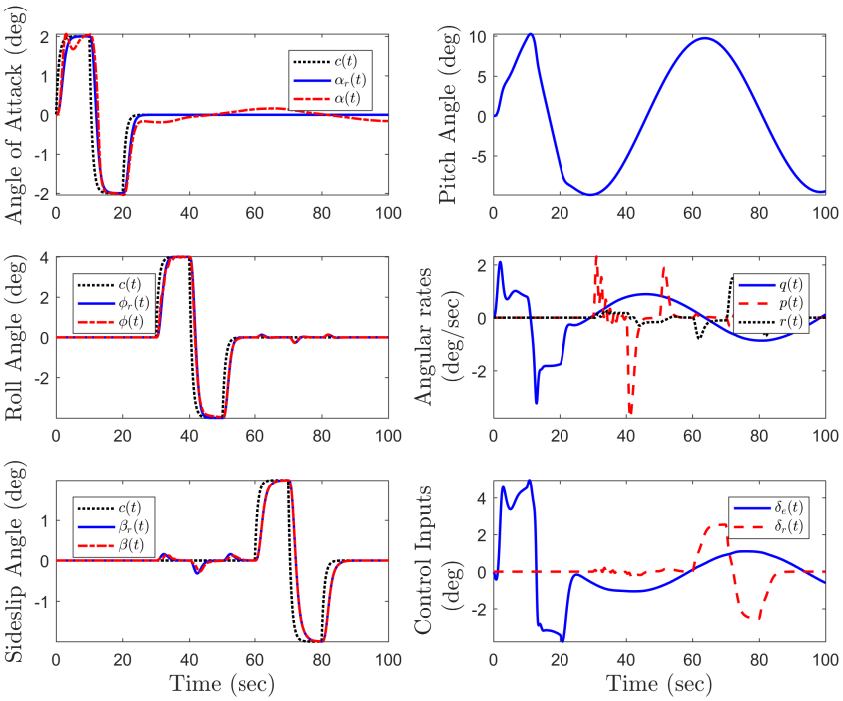

Figure 5.9: Set-theoretic controller response with $\varepsilon_{\text{lo}} = \varepsilon_{\text{la}} = 0.15$ under scenario 5.1.4.1.

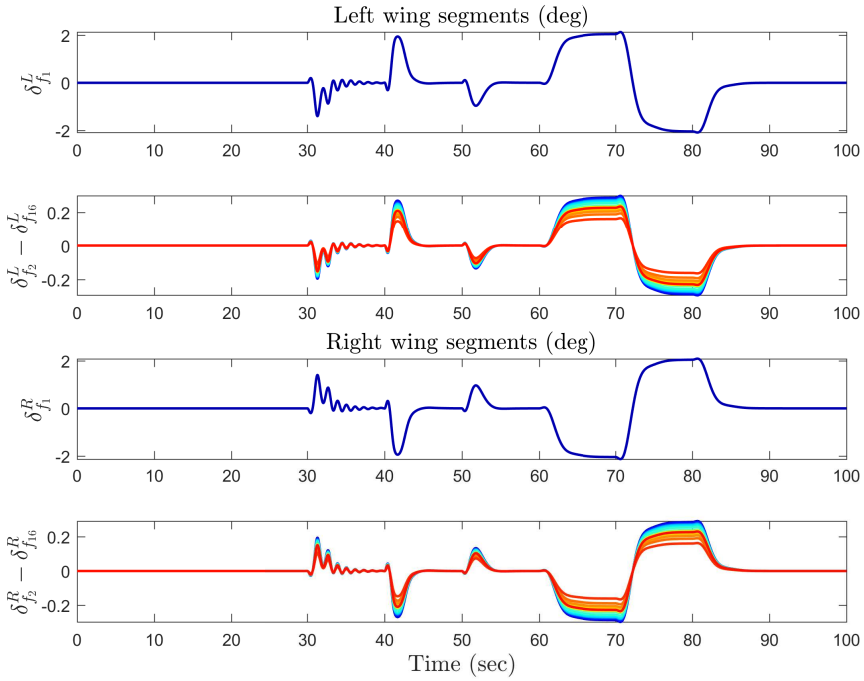

Figure 5.10: Control signals of the VCCTEF segments on the left and the right wings for the case where $\varepsilon_{\text{lo}} = \varepsilon_{\text{la}} = 0.15$ under scenario 5.1.4.1.

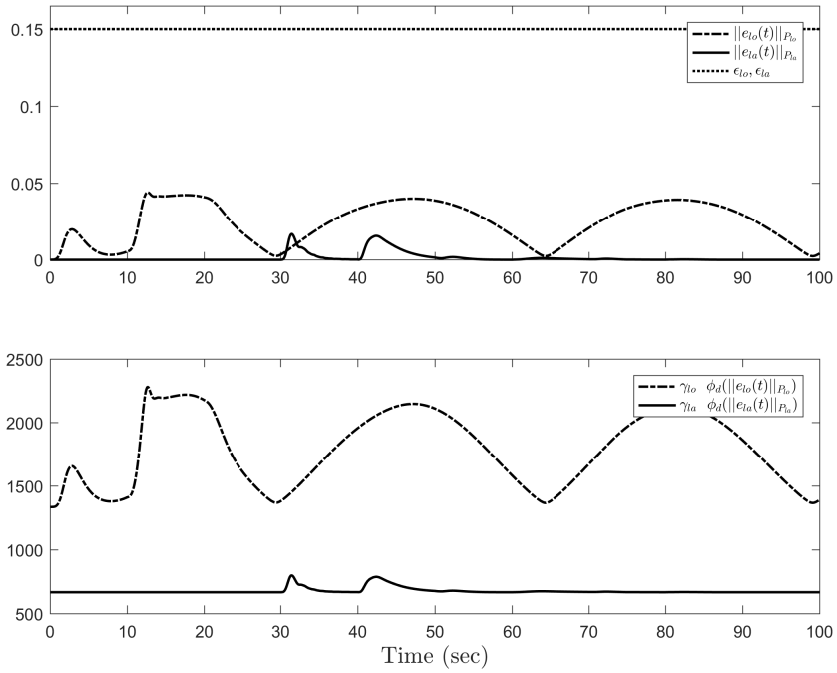

Figure 5.11: The error norm (top) and the effective error dependent adaptation rate (bottom) for the case where $\varepsilon_{\text{lo}} = \varepsilon_{\text{la}} = 0.15$ under scenario 5.1.4.1.

5.1.4.2 Uncertainties in C_{n_β} and C_{l_β}

As the second scenario, we consider the case when the variation of yawing moment coefficient with sideslip angle C_{n_β} and the variation of rolling moment coefficient with sideslip angle C_{l_β} are both reduced by 300%, and we set $\Lambda_{\text{lo}} = \Lambda_{\text{la}} = I$. Figures 5.12 and 5.13 show the system response with the nominal controller in presence of these system uncertainties. Figures 5.14 to 5.16 show the system response with the set-theoretic adaptive control architecture with $\varepsilon_{\text{lo}} = \varepsilon_{\text{la}} = 0.3$ and one can see that the proposed controller is able to recover the system and strictly enforce the user-defined performance bounds on the system error trajectories. Once again, to achieve a better tracking performance, we decrease the performance bounds on both longitudinal and lateral-directional channels to $\varepsilon_{\text{lo}} = \varepsilon_{\text{la}} = 0.15$ as it can be seen from Figures 5.17 to 5.19.

5.1.4.3 Uncertainties in C_{m_α}, C_{l_β}, C_{n_β} and C_{l_p}

Finally, we consider the case when the variation of pitching moment coefficient with angle of attack C_{m_α} and the variation of rolling moment coefficient with sideslip angle C_{l_β} are both reduced by 150%, and also the variation of yawing moment coefficient with sideslip angle C_{n_β} and the variation of rolling moment coefficient with roll rate C_{l_p} are reduced by 100%. We further consider that the control effectiveness matrices

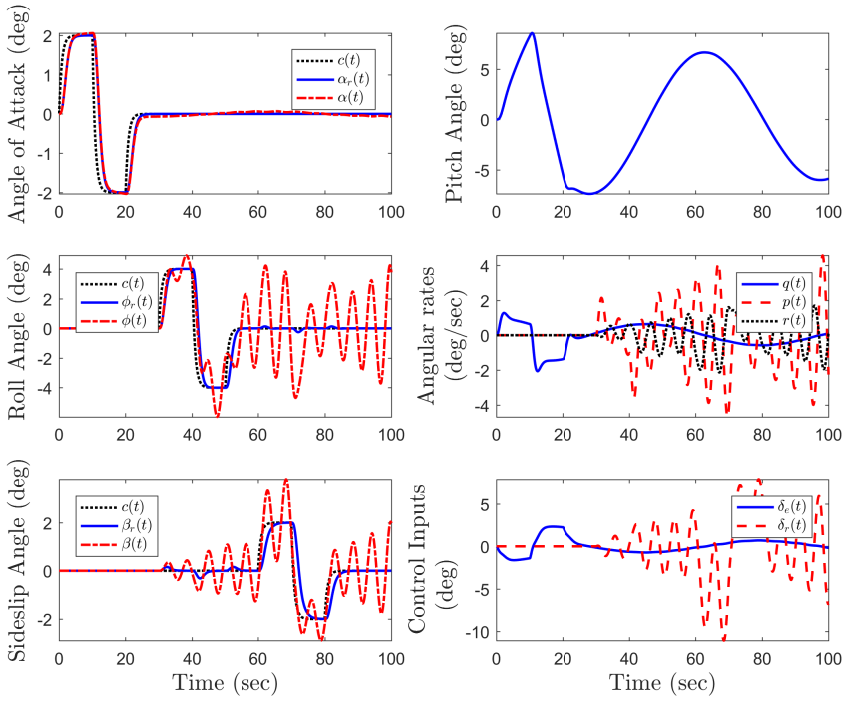

Figure 5.12: System response with the nominal controller under scenario 5.1.4.2.

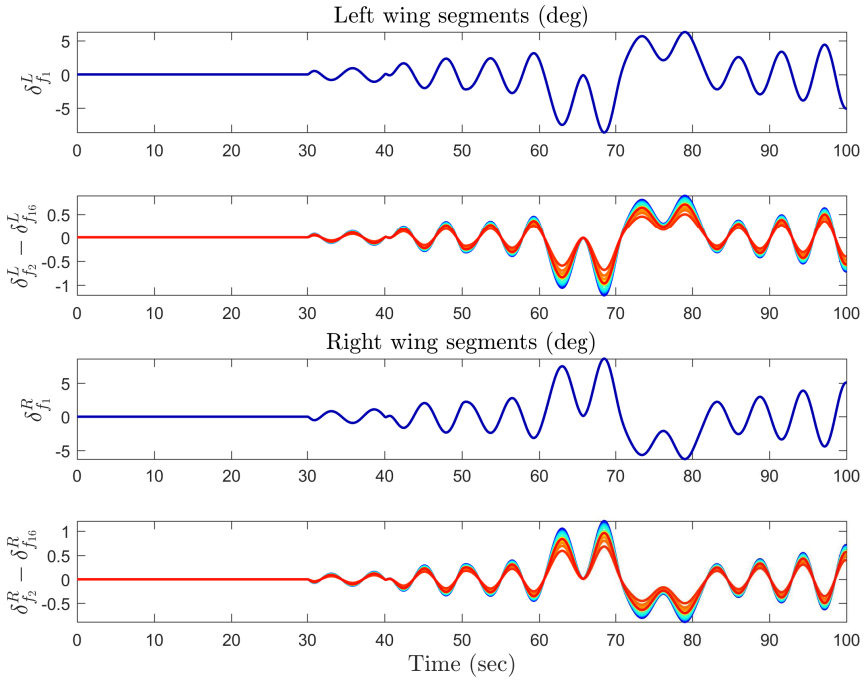

Figure 5.13: Control signals of the VCCTEF segments on the left and the right wings with the nominal controller under scenario 5.1.4.2.

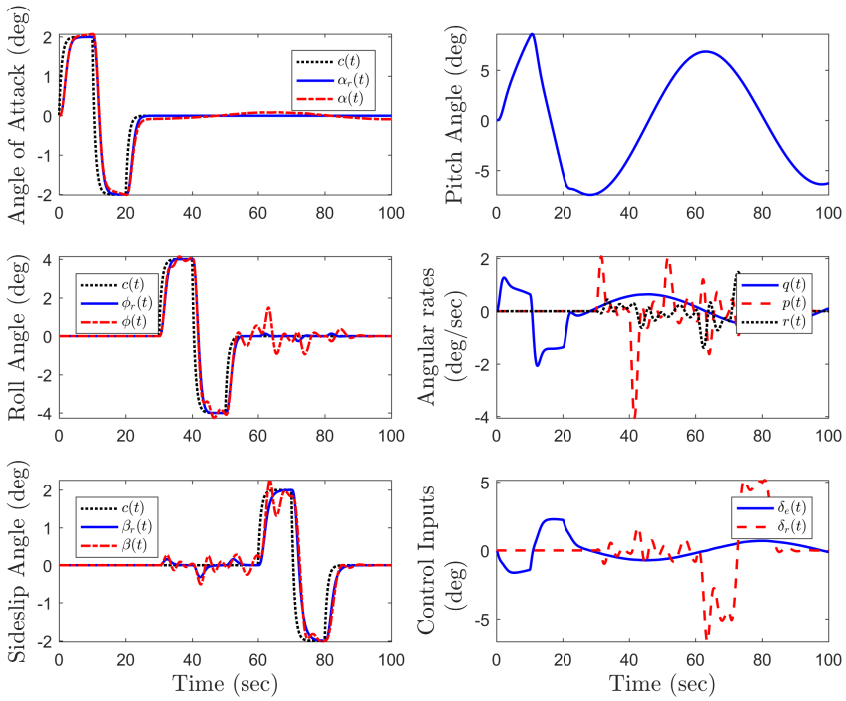

Figure 5.14: Set-theoretic controller response with $\varepsilon_{\text{lo}} = \varepsilon_{\text{la}} = 0.3$ under scenario 5.1.4.2.

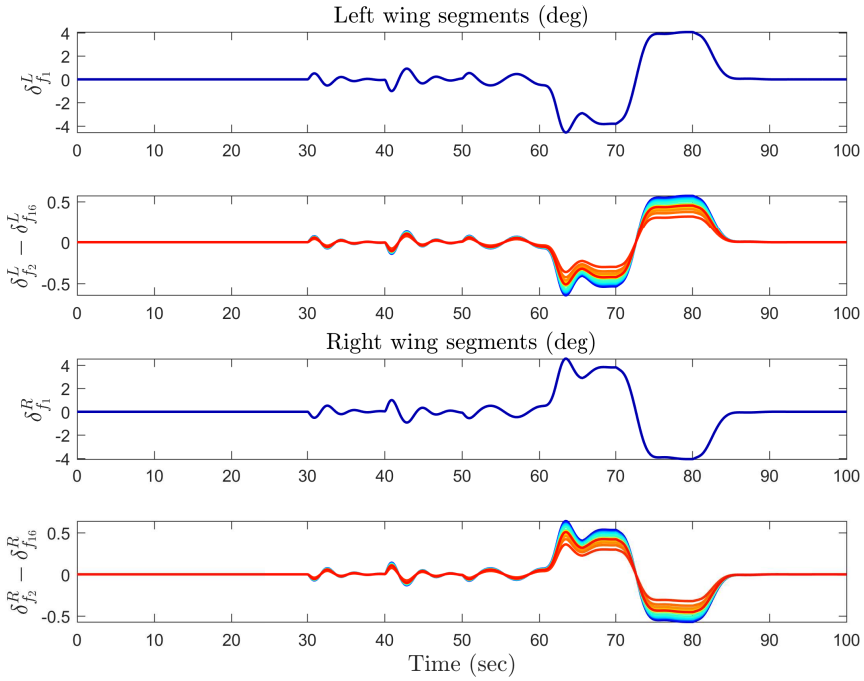

Figure 5.15: Control signals of the VCCTEF segments on the left and the right wings for the case where $\varepsilon_{\text{lo}} = \varepsilon_{\text{la}} = 0.3$ under scenario 5.1.4.2.

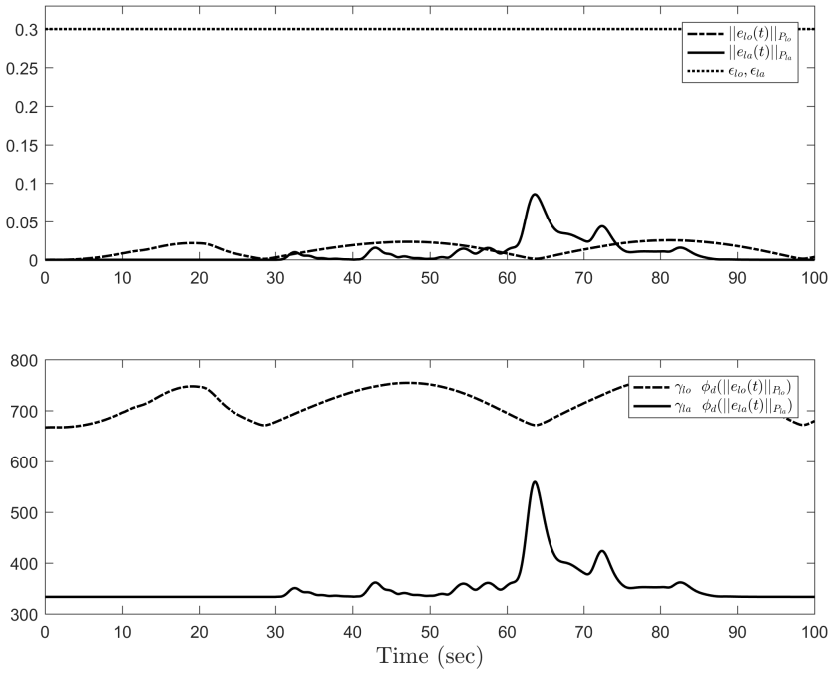

Figure 5.16: The error norm (top) and the effective error dependent adaptation rate (bottom) for the case where $\varepsilon_{\text{lo}} = \varepsilon_{\text{la}} = 0.3$ under scenario 5.1.4.2.

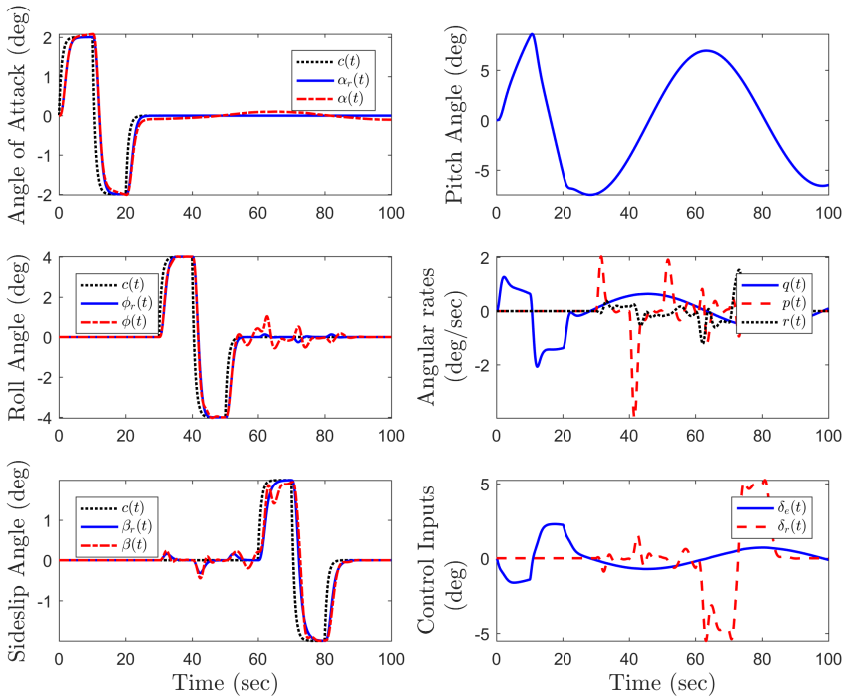

Figure 5.17: Set-theoretic controller response with $\varepsilon_{\text{lo}} = \varepsilon_{\text{la}} = 0.15$ under scenario 5.1.4.2.

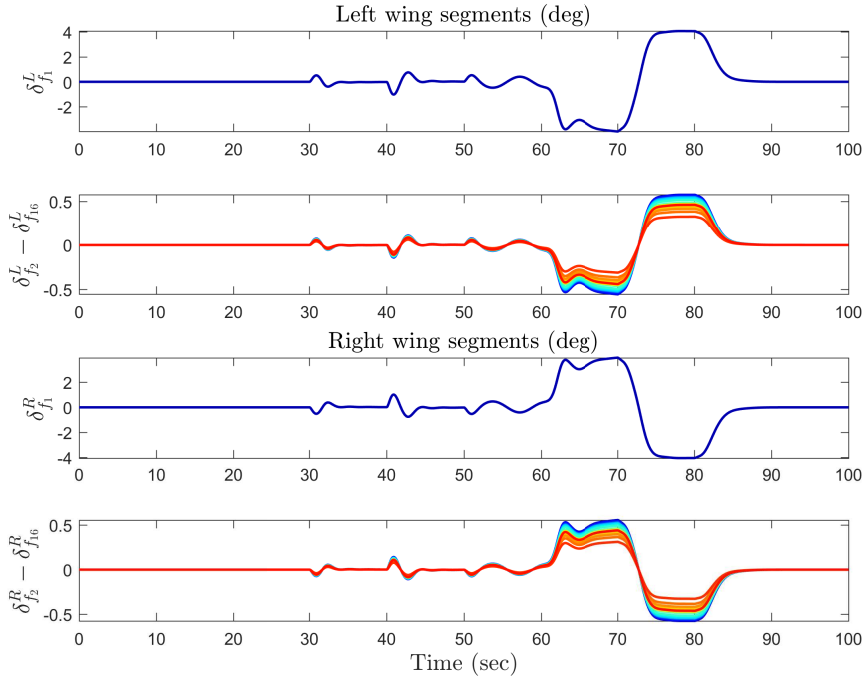

Figure 5.18: Control signals of the VCCTEF segments on the left and the right wings for the case where $\varepsilon_{\text{lo}} = \varepsilon_{\text{la}} = 0.15$ under scenario 5.1.4.2.

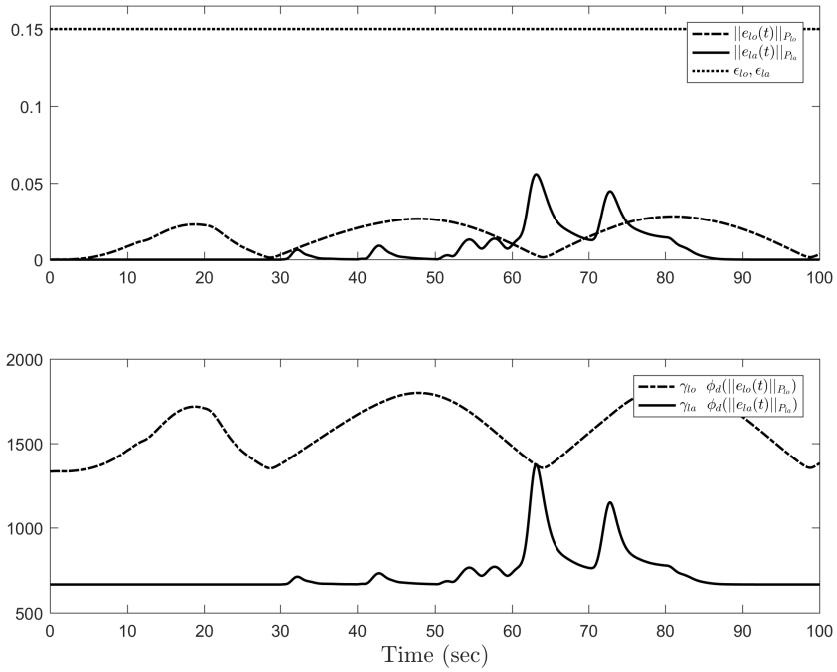

Figure 5.19: The error norm (top) and the effective error dependent adaptation rate (bottom) for the case where $\varepsilon_{\text{lo}} = \varepsilon_{\text{la}} = 0.15$ under scenario 5.1.4.2.

on both longitudinal and lateral-directional channels are given by $\Lambda_{\text{lo}} = 0.25$, $\Lambda_{\text{la}} = 0.25 I_{33\times 33}$. Figures 5.20 and 5.21 show the system response with the nominal controller in presence of these system uncertainties. Figures 5.22 to 5.24 show the system response with the set-theoretic adaptive control architecture with $\varepsilon_{\text{lo}} = \varepsilon_{\text{la}} = 0.3$ where it can be seen that the proposed controller is able to recover the system and strictly enforce the required user-defined performance bounds on the system error trajectories. In order to achieve a closer tracking of the reference dynamics trajectories, once again we decrease the performance bounds on both longitudinal and lateral-directional channels to $\varepsilon_{\text{lo}} = \varepsilon_{\text{la}} = 0.15$ as it can be seen from Figures 5.25 to 5.27.

5.1.5 Conclusion

A set-theoretic model reference adaptive control architecture was applied to the longitudinal and lateral-directional dynamics of the NASA generic transport model. The simulation results showed that this control framework was capable of enforcing user-defined performance guarantees on this model without knowledge on the upper and lower bounds on the system uncertainties.

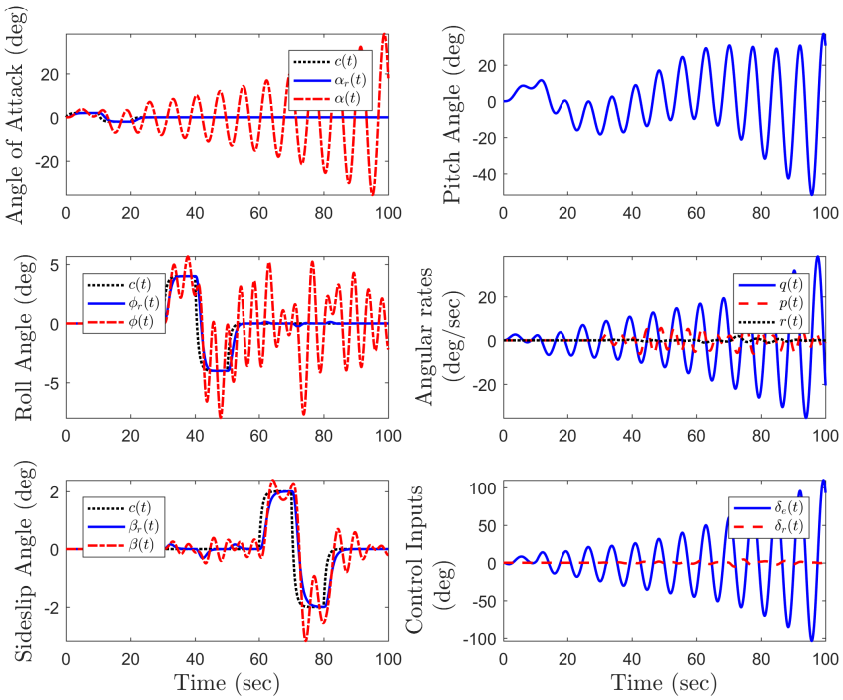

Figure 5.20: System response with the nominal controller under scenario 5.1.4.3.

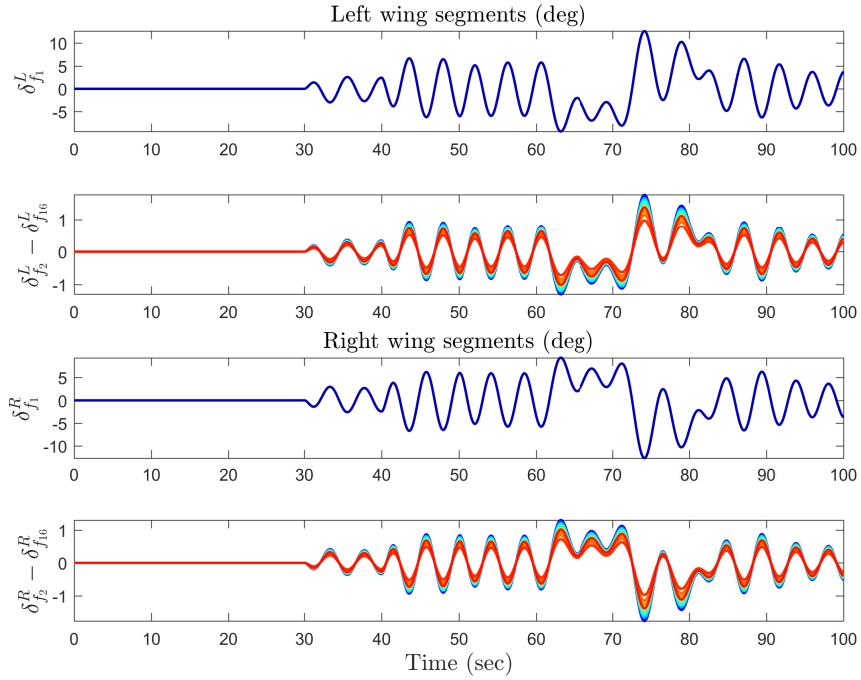

Figure 5.21: Control signals of the VCCTEF segments on the left and the right wings with the nominal controller under scenario 5.1.4.3.

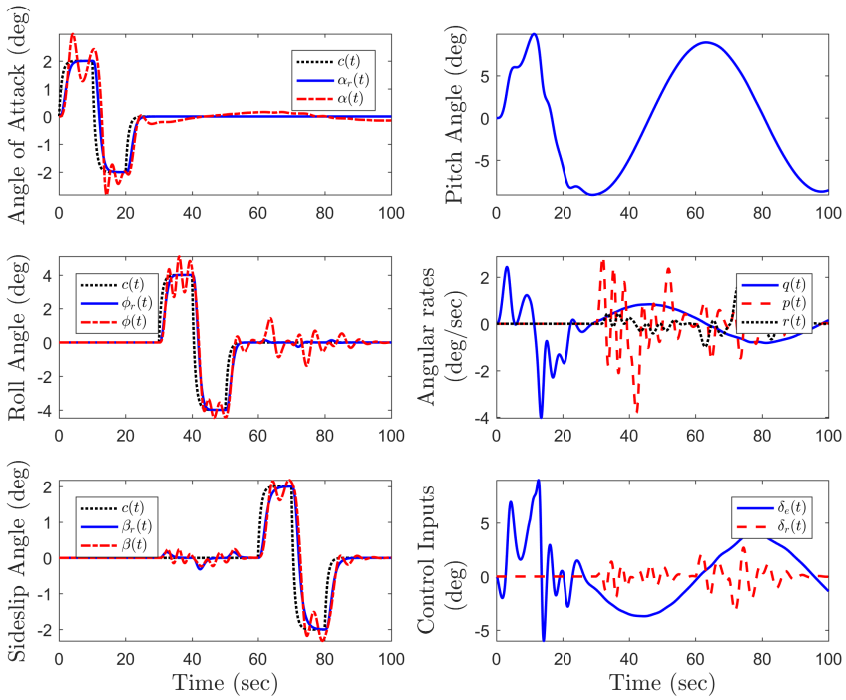

Figure 5.22: Set-theoretic controller response with $\varepsilon_{\text{lo}} = \varepsilon_{\text{la}} = 0.3$. under scenario 5.1.4.3.

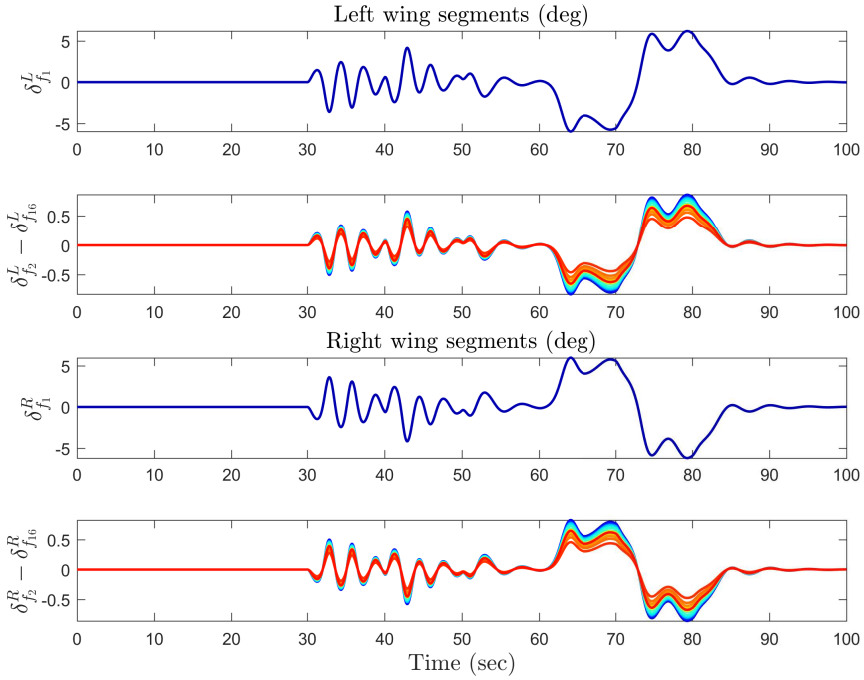

Figure 5.23: Control signals of the VCCTEF segments on the left and the right wings for the case where $\varepsilon_{\text{lo}} = \varepsilon_{\text{la}} = 0.3$ under scenario 5.1.4.3.

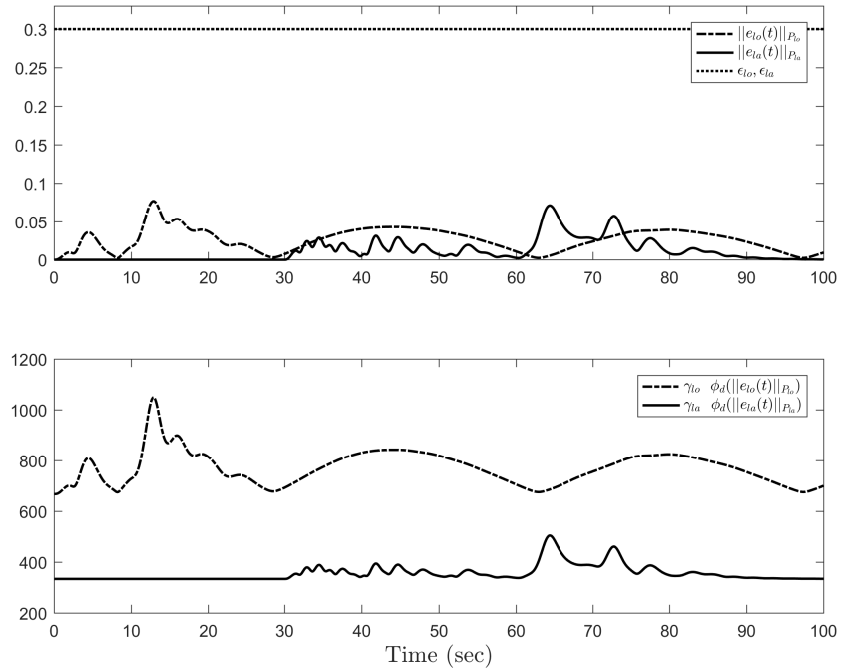

Figure 5.24: The error norm (top) and the effective error dependent adaptation rate (bottom) for the case where $\varepsilon_{\text{lo}} = \varepsilon_{\text{la}} = 0.3$ under scenario 5.1.4.3.

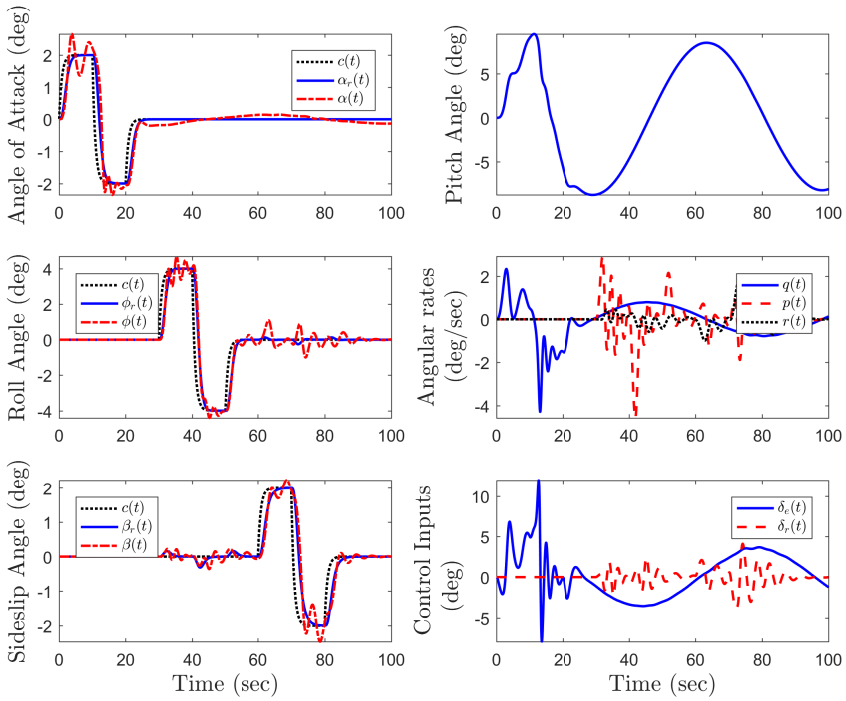

Figure 5.25: Set-theoretic controller response with $\varepsilon_{\text{lo}} = \varepsilon_{\text{la}} = 0.15$ under scenario 5.1.4.3.

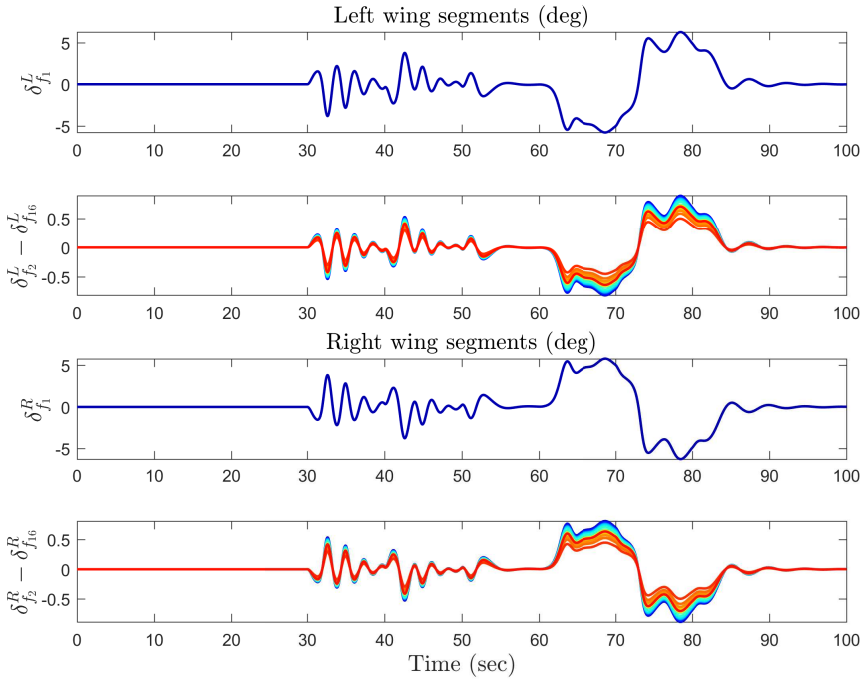

Figure 5.26: Control signals of the VCCTEF segments on the left and the right wings for the case where $\varepsilon_{\text{lo}} = \varepsilon_{\text{la}} = 0.15$ under scenario 5.1.4.3.

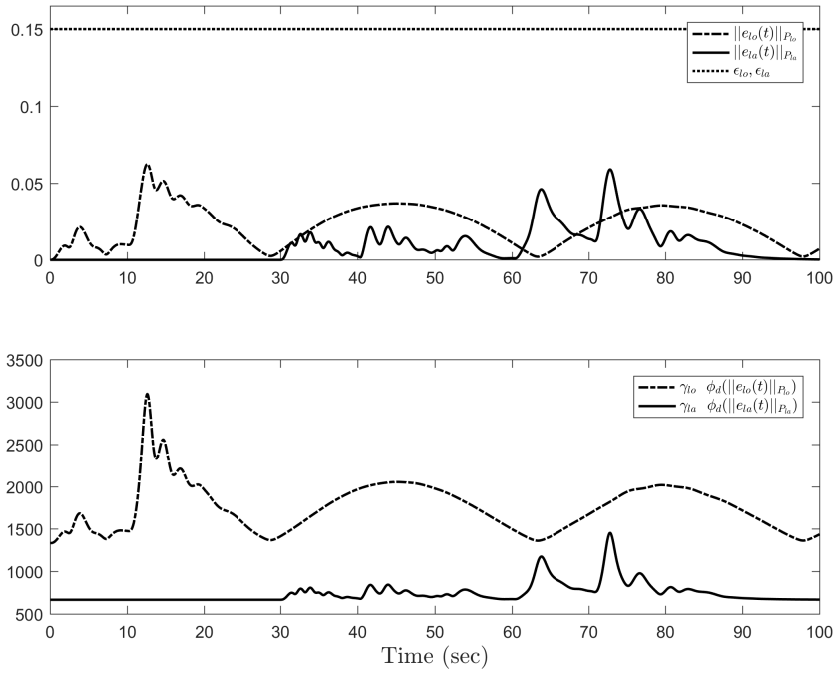

Figure 5.27: The error norm (top) and the effective error dependent adaptation rate (bottom) for the case where $\varepsilon_{\text{lo}} = \varepsilon_{\text{la}} = 0.15$ under scenario 5.1.4.3.

5.2 Experimental Results with the Set-Theoretic Model Reference Adaptive Control Architecture on an Aerospace Testbed[2]

In this paper, we present experimental results of a recently developed set-theoretic model reference adaptive control architecture on an aerospace testbed, which is configured as a conventional dual-rotor helicopter. The key feature of this architecture allows the system error bound between the state of an uncertain dynamical system and the state of a reference model, which captures a desired closed-loop system performance, to be less than a-priori, user-defined worst-case performance bound. This means that this proposed architecture is suitable for enforcing strict performance guarantees during the transient and steady-state response of the adaptation process. Specifically, we first experimentally demonstrate the practical capabilities of this adaptive control algorithm with constant performance bounds on the considered testbed. We then consider the time-varying performance bounds, where we highlight how a control designer is empowered by the set-theoretic model reference adaptive control architecture to control the closed-loop system performance as desired on different time intervals (e.g. transient time interval and steady-state time interval) and also how to handle a possible system initialization error that can happen in practice.

5.2.1 Introduction

Although model reference adaptive control architectures are capable of guaranteeing closed-loop system stability in the presence of exogenous disturbances and system uncertainties, one of the major drawbacks to adopting these control frameworks is the inability to obtain user-defined performance guarantees. For addressing this limitation, we recently proposed set-theoretic model reference adaptive control architecture in a set of papers [1, 2, 93, 101–106, 108, 119]. The key feature of set-theoretic model reference adaptive control architecture allows the system error bound between the state of an uncertain dynamical system and the state of a reference model, which captures a desired closed-loop system performance, to be less than a-priori, user-defined worst-case performance bound. This means that this architecture is suitable for enforcing strict performance guarantees during the transient and steady-state response of the adaptation process. Specifically, [1] presents this control framework for achieving time-invariant performance bounds, where in [2, 108] this framework is further extended to guarantee time-varying user-defined performance bounds. The generalization of the set-theoretic model reference adaptive control architecture to the unstructured system uncertainties is studied in [93, 102] and also the extension of this architecture

[2]This section has been submitted to the *AIAA Guidance, Navigation, and Control Conference*.

for guaranteeing performance in the presence of actuator failures and actuator dynamics are respectively presented in [101, 119]. This framework is also recently employed for decentralized control of large-scale modular systems in [103, 104]. In [105, 106] an application of the set-theoretic model reference adaptive control architecture are respectively presented on the NASA generic transport model and a rigid body vehicle on exponential coordinates.

Primarily building on the results of [1, 2, 108], this paper presents experimental results of a recently developed set-theoretic model reference adaptive control architecture on an aerospace testbed, configured as a conventional dual-rotor helicopter. Specifically, we first experimentally demonstrate the practical capabilities of this adaptive control algorithm with constant performance bounds in [1] compared with the standard model reference adaptive controller. From a practical standpoint, we then show how the extension of the set-theoretic model reference adaptive control architecture to time-varying performance bounds in [2, 108] gives the control designer a flexibility to control the closed-loop system performance as desired on different time intervals (e.g. transient time interval and steady-state time interval). In addition, we demonstrate the efficacy of this control framework for handling the initialization error that can happen in practical settings.

The organization of the rest of this paper is as follows. Section 5.2.2 provides the problem formulation. Section 5.2.3 overviews the set-theoretic model reference adaptive control architecture with constant and time-varying performance bounds. Section 5.2.4 illustrates the efficacy of the set-theoretic model reference adaptive control architecture applied to the AERO platform. Finally, the conclusions are drawn in Section 5.2.5. The notation used in this paper is fairly standard as similar to [1, 2, 108]. To be self-contained, $\mathbb{N}$ denotes the set of natural numbers, $\mathbb{R}$ denotes the set of real numbers, $\mathbb{R}^n$ denotes the set of $n \times 1$ real column vectors, $\mathbb{R}^{n\times m}$ denotes the set of $n \times m$ real matrices, $\mathbb{R}_+$ (respectively, $\overline{\mathbb{R}}_+$) denotes the set of positive (respectively, nonnegative-definite) real numbers, $\mathbb{R}_+^{n\times n}$ (respectively, $\overline{\mathbb{R}}_+^{n\times n}$) denotes the set of $n \times n$ positive-definite (respectively, nonnegative-definite) real matrices, $\mathbb{D}^{n\times n}$ denotes the set of $n \times n$ real matrices with diagonal scalar entries, $0_{n\times n}$ denotes the $n \times n$ zero matrix, and "$\triangleq$" denotes equality by definition. In addition, we write $(\cdot)^{\mathrm{T}}$ for the transpose operator, $(\cdot)^{-1}$ for the inverse operator, $\|\cdot\|_{\mathrm{F}}$ for the Frobenius norm, and $\|\cdot\|_2$ for the Euclidean norm. Furthermore, we write $\|A\|_2 \triangleq \sqrt{\lambda_{\max}(A^{\mathrm{T}}A)}$ for the induced 2-norm of the matrix $A \in \mathbb{R}^{n\times m}$, $\lambda_{\min}(A)$ (resp., $\lambda_{\max}(A)$) for the minimum (resp., maximum) eigenvalue of the matrix $A \in \mathbb{R}^{n\times n}$, and $\mathrm{tr}(\cdot)$ for the trace operator.

5.2.2 Problem Formulation

Consider the uncertain dynamical system given by

$$\dot{x}_{\rm p}(t) \;=\; A_{\rm p}x_{\rm p}(t)+B_{\rm p}\Lambda u(t)+B_{\rm p}\delta_{\rm p}(t,x_{\rm p}(t)),\quad x_{\rm p}(0)=x_{\rm p0}. \tag{5.57}$$

In the above expression, $x_{\rm p}(t)\in\mathbb{R}^{n_{\rm p}}$ denotes the measurable state vector, $u(t)\in\mathbb{R}^{m}$ denotes the control input, $A_{\rm p}\in\mathbb{R}^{n_{\rm p}\times n_{\rm p}}$ denotes a known system matrix, $B_{\rm p}\in\mathbb{R}^{n_{\rm p}\times m}$ denotes a known input matrix, $\delta_{\rm p}:\overline{\mathbb{R}}_{+}\times\mathbb{R}^{n_{\rm p}}\to\mathbb{R}^{m}$ denotes a system uncertainty, and $\Lambda\in\mathbb{R}_{+}^{m\times m}\cap\mathbb{D}^{m\times m}$ denotes an unknown control effectiveness matrix. As standard, it is assumed that the pair $(A_{\rm p},B_{\rm p})$ is controllable. Note that the considered uncertain dynamical system dynamics given in (5.57) fits appropriately to the experimental aerospace testbed (see Section 5.2.4 for details). Here, we also consider that the system uncertainty given by (5.57) is parameterized as

$$\delta_{\rm p}(t,x_{\rm p}) \;=\; W_{\rm p}^{\rm T}(t)\sigma_{\rm p}(x_{\rm p}), \tag{5.58}$$

where $W_{\rm p}(t)\in\mathbb{R}^{s\times m}$ is a bounded unknown weight matrix (i.e., $\|W_{\rm p}(t)\|_{\rm F}\leq w_{\rm p}$) with a bounded time rate of change (i.e., $\|\dot{W}_{\rm p}(t)\|_{\rm F}\leq \dot{w}_{\rm p}$) and $\sigma_{\rm p}:\mathbb{R}^{n_{\rm p}}\to\mathbb{R}^{s}$ is a known basis function of the form $\sigma_{\rm p}(x_{\rm p})=[\sigma_{\rm p1}(x_{\rm p}),\sigma_{\rm p2}(x_{\rm p}),\ \ldots\ ,\sigma_{{\rm p}s}(x_{\rm p})]^{\rm T}$ that includes locally Lipschitz elements.

To address command following, it is of practice to consider an integral state $x_{\rm c}(t)\in\mathbb{R}^{n_{\rm c}}$ satisfying

$$\dot{x}_{\rm c}(t)=E_{\rm p}x_{\rm p}(t)-c(t),\quad x_{\rm c}(0)=x_{\rm c0}. \tag{5.59}$$

Here, $c(t)\in\mathbb{R}^{n_{\rm c}}$ is a piecewise continuous command and $E_{\rm p}\in\mathbb{R}^{n_{\rm c}\times n_{\rm p}}$ is a matrix introduced to select a subset of $x_{\rm p}(t)$ to follow $c(t)$. Considering this integral state, one can now defined the augmented state vector as $x(t)\triangleq[x_{\rm p}^{\rm T}(t),\ x_{\rm c}^{\rm T}(t)]^{\rm T}\in\mathbb{R}^{n}$, $n=n_{\rm p}+n_{\rm c}$, and write

$$\dot{x}(t) \;=\; Ax(t)+B\Lambda u(t)+BW_{\rm p}^{\rm T}(t)\sigma_{\rm p}(x_{\rm p}(t))+B_{\rm r}c(t),\quad x(0)=x_{0}, \tag{5.60}$$

using (5.57) and (5.59), where

$$A \;\triangleq\; \begin{bmatrix} A_{\rm p} & 0_{n_{\rm p}\times n_{\rm c}} \\ E_{\rm p} & 0_{n_{\rm c}\times n_{\rm c}} \end{bmatrix}\in\mathbb{R}^{n\times n}, \tag{5.61}$$

$$B \triangleq \begin{bmatrix} B_{\mathrm{p}}^{\mathrm{T}} & 0_{n_{\mathrm{c}}\times m}^{\mathrm{T}} \end{bmatrix}^{\mathrm{T}} \in \mathbb{R}^{n\times m}, \tag{5.62}$$

$$B_{\mathrm{r}} \triangleq \begin{bmatrix} 0_{n_{\mathrm{p}}\times n_{\mathrm{c}}}^{\mathrm{T}} & -I_{n_{\mathrm{c}}\times n_{\mathrm{c}}} \end{bmatrix}^{\mathrm{T}} \in \mathbb{R}^{n\times n_{\mathrm{c}}}. \tag{5.63}$$

Next, consider the feedback control law given by

$$u(t) = u_{\mathrm{n}}(t) + u_{\mathrm{a}}(t). \tag{5.64}$$

In (5.64), $u_{\mathrm{n}}(t) \in \mathbb{R}^m$ represents the nominal control law of the form given by

$$u_{\mathrm{n}}(t) = -Kx(t), \tag{5.65}$$

such that $A_{\mathrm{r}} \triangleq A - BK$, $K \in \mathbb{R}^{m\times n}$, is Hurwitz and $u_{\mathrm{a}}(t) \in \mathbb{R}^m$ represents the adaptive control law to be introduced in Section 5.2.3. It is now straightforward to write

$$\dot{x}(t) = A_{\mathrm{r}}x(t) + B_{\mathrm{r}}c(t) + B\Lambda\left[u_{\mathrm{a}}(t) + W^{\mathrm{T}}(t)\sigma\big(x(t)\big)\right], \quad x(0) = x_0, \tag{5.66}$$

using (5.64) and (5.65) in (5.60), where $W(t) \triangleq \left[\Lambda^{-1}W_{\mathrm{p}}^{\mathrm{T}}(t),\ (\Lambda^{-1} - I_{m\times m})K\right]^{\mathrm{T}} \in \mathbb{R}^{(s+n)\times m}$ is an unknown weight matrix and $\sigma\big(x(t)\big) \triangleq [\sigma_{\mathrm{p}}^{\mathrm{T}}\big(x_{\mathrm{p}}(t)\big), x^{\mathrm{T}}(t)]^{\mathrm{T}} \in \mathbb{R}^{s+n}$ is a known basis function.

5.2.3 Set-Theoretic Model Reference Adaptive Control Architecture [1, 2]

As it is well-known, the selection of the adaptive control law and its corresponding update law plays a crucial role in any model reference adaptive control design for achieving desired command following characteristics captured by the reference model given by

$$\dot{x}_{\mathrm{r}}(t) = A_{\mathrm{r}}x_{\mathrm{r}}(t) + B_{\mathrm{r}}c(t), \quad x_{\mathrm{r}}(0) = x_{\mathrm{r}0}, \tag{5.67}$$

with $x_{\mathrm{r}}(t) \in \mathbb{R}^n$ being the reference state vector. In this section, we concisely overview the set-theoretic model reference adaptive control architecture proposed in [1] and [2, 108] for respectively enforcing constant and time-varying user-defined performance bound guarantees on the norm of system error vector.

5.2.3.1 Constant Performance Bound Guarantees

We begin with the set-theoretic model reference adaptive control architecture developed in [1] for enforcing constant performance bound guarantees. To this end, we let the adaptive control law be given by

$$u_{\mathrm{a}}(t) = -\hat{W}^{\mathrm{T}}(t)\sigma\big(x(t)\big), \tag{5.68}$$

where $\hat{W}(t) \in \mathbb{R}^{(s+n)\times m}$ is an estimate of $W(t)$. We now use the well-known projection operator. Based on its definition (e.g., see [30, 80]), $\big(\theta - \theta^*\big)^{\mathrm{T}}\big(\mathrm{Proj}\,(\theta, y) - y\big) \leq 0$ holds for any vector y, where the vector θ is the estimation of the unknown vector θ^*. This definition can be further generalized to matrices as $\mathrm{Proj}_{\mathrm{m}}(\Theta, Y) = \big(\mathrm{Proj}(\mathrm{col}_1(\Theta), \mathrm{col}_1(Y)), \ldots, \mathrm{Proj}(\mathrm{col}_m(\Theta), \mathrm{col}_m(Y))\big)$, where $\Theta \in \mathbb{R}^{n\times m}$, $Y \in \mathbb{R}^{n\times m}$, and $\mathrm{col}_i(\cdot)$ denotes ith column operator resulting in $\mathrm{tr}\left[(\Theta - \Theta^*)^{\mathrm{T}}(\mathrm{Proj}_{\mathrm{m}}(\Theta, Y) - Y)\right] \leq 0$. Now, consider the update law for (5.68) given by

$$\dot{\hat{W}}(t) = \gamma \mathrm{Proj}_{\mathrm{m}}\Big(\hat{W}(t), \phi_d(\|e(t)\|_{\mathrm{P}})\sigma\big(x(t)\big)e^{\mathrm{T}}(t)PB\Big), \quad \hat{W}(0) = \hat{W}_0, \tag{5.69}$$

with $\hat{W}_{\max}$ being the projection norm bound. In (5.69), $\gamma \in \mathbb{R}_+$ is the learning rate (i.e., adaptation gain), $P \in \mathbb{R}_+^{n\times n}$ is a solution of the Lyapunov equation given by

$$0 \quad = \quad A_{\mathrm{r}}^{\mathrm{T}}P + PA_{\mathrm{r}} + R, \tag{5.70}$$

with $R \in \mathbb{R}_+^{n\times n}$, and $e(t) \triangleq x(t) - x_{\mathrm{r}}(t)$ is the system error. In (5.69), in addition, $\phi(\|e(t)\|_{\mathrm{P}})$ is the generalized restricted potential function defined on the set $\mathcal{D}_\varepsilon \triangleq \{e(t) : \|e(t)\|_{\mathrm{P}} \in [0, \varepsilon)\}$ with $\|e(t)\|_P = \sqrt{e^{\mathrm{T}}(t)Pe(t)}$ being the weighted system error and $\varepsilon \in \mathbb{R}_+$ being a-priori, user-defined constant, satisfying

i) If $\|e(t)\|_{\mathrm{P}} = 0$, then $\phi(\|e(t)\|_{\mathrm{P}}) = 0$.

ii) If $e(t) \in \mathcal{D}_\varepsilon$ and $\|e(t)\|_{\mathrm{P}} \neq 0$, then $\phi(\|e(t)\|_{\mathrm{P}}) > 0$.

iii) If $\|e(t)\|_{\mathrm{P}} \to \varepsilon$, then $\phi(\|e(t)\|_{\mathrm{P}}) \to \infty$.

iv) $\phi(\|e(t)\|_{\mathrm{P}})$ is continuously differentiable on $\mathcal{D}_\varepsilon$.

v) If $e(t) \in \mathcal{D}_\varepsilon$, then $\phi_d(\|e(t)\|_{\mathrm{P}}) > 0$, where $\phi_d(\|e(t)\|_{\mathrm{P}}) \triangleq \frac{\mathrm{d}\phi(\|e(t)\|_{\mathrm{P}})}{\mathrm{d}\|e(t)\|_{\mathrm{P}}^2}$.

vi) If $e(t) \in \mathcal{D}_\varepsilon$, then $2\phi_d(\|e(t)\|_{\mathrm{P}})\|e(t)\|_{\mathrm{P}}^2 - \phi(\|e(t)\|_{\mathrm{P}}) > 0$.

Remark 5.2.1 *From a theoretical standpoint, the update law given by* (5.69) *for the set-theoretic model reference adaptive control architecture can be derived by considering the following energy function [1]*

$$V(e,\tilde{W}) = \phi(\|e\|_{\mathrm{P}}) + \gamma^{-1}\mathrm{tr}\big[(\tilde{W}\Lambda^{1/2})^{\mathrm{T}}(\tilde{W}\Lambda^{1/2})\big]. \tag{5.71}$$

where $\tilde{W}(t) \triangleq \hat{W}(t) - W(t)$. *As shown in [1], the time derivative of this energy function is upper bounded by*

$$\dot{V}\big(e(t),\tilde{W}(t)\big) \quad \leq \quad -\frac{1}{2}\alpha V(e,\tilde{W}) + \mu, \tag{5.72}$$

where $\alpha \triangleq \frac{\lambda_{\min}(R)}{\lambda_{\max}(P)}$, $d \triangleq 2\gamma^{-1}\tilde{w}\,\dot{w}\|\Lambda\|_2$, $\mu \triangleq \frac{1}{2}\alpha\gamma^{-1}\tilde{w}^2\|\Lambda\|_2 + d$, $\tilde{w} = \hat{W}_{\max} + w$, $\|W(t)\|_{\mathrm{F}} \leq w$, *and* $\|\dot{W}(t)\|_{\mathrm{F}} \leq \dot{w}$. *In particular,* (5.72) *is sufficient to conclude that* $V(e,\tilde{W})$ *is upper bounded. Hence, one can now conclude with* $\|e_0\|_P < \varepsilon$ *that the pair* $(e(t),\tilde{W}(t))$ *is bounded and the system error satisfies the strict bound given by* $\|e(t)\|_{\mathrm{P}} < \varepsilon, t \geq 0$. *Once again, we refer to Theorem 3.1 of [1] for details.*

5.2.3.2 Time-Varying Performance Bound Guarantees

We now overview the results in [2] for enforcing time-varying performance bound guarantees. For this purpose, we consider the modified reference model given by

$$\dot{x}_{\mathrm{r_m}}(t) \quad = \quad A_{\mathrm{r}}x_{\mathrm{r_m}}(t) + B_{\mathrm{r}}c(t) + \zeta(t), \quad x_{\mathrm{r_m}}(0) = x_{\mathrm{r0}}, \tag{5.73}$$

where $x_{\mathrm{r_m}}(t) \in \mathbb{R}^n$ is the modified reference state vector and $\zeta(t) \in \mathbb{R}^n$ is an added term to be defined below.

Letting $e_{\mathrm{m}}(t) \triangleq x(t) - x_{\mathrm{r_m}}(t)$, we consider the error transformation given by

$$e_{\xi}(t) \quad = \quad \xi(t)e_{\mathrm{m}}(t), \tag{5.74}$$

where $\xi(t) \in \mathbb{R}_+$ is a user-defined scalar transformation function that is used later to enforce a time-varying performance bound on the system error vector. We also let

$$\zeta(t) \quad \triangleq \quad \dot{\xi}(t)\xi^{-1}(t)e_{\mathrm{m}}(t). \tag{5.75}$$

Furthermore, we utilize the generalized restricted potential function introduced in Section 5.2.3.1 and con-

sider the update law for (5.68) given by

$$\dot{\hat{W}}(t) = \gamma \mathrm{Proj}_{\mathrm{m}}\Big(\hat{W}(t), \xi(t)\phi_d(\|e_\xi(t)\|_P)\sigma\big(x(t)\big)e_\xi^{\mathrm{T}}(t)PB\Big), \quad \hat{W}(0) = \hat{W}_0, \tag{5.76}$$

with $\hat{W}_{\max}$ being the projection bound and $\gamma \in \mathbb{R}_+$ being the learning rate.

Remark 5.2.2 *From a theoretical standpoint, the update law given by* (5.76) *for the set-theoretic model reference adaptive control architecture can be derived by considering the following energy function [2]*

$$V(e_\xi, \tilde{W}) = \phi(\|e_\xi\|_P) + \gamma^{-1}\mathrm{tr}\big[(\tilde{W}\Lambda^{1/2})^{\mathrm{T}}(\tilde{W}\Lambda^{1/2})\big], \tag{5.77}$$

where $\tilde{W}(t) \triangleq \hat{W}(t) - W(t)$. *The time derivative on this energy function satisfies the upper bound given by*

$$\dot{V}\big(e_\xi(t), \tilde{W}(t)\big) \quad \leq \quad -\frac{1}{2}\alpha V(e_\xi, \tilde{W}) + \mu, \tag{5.78}$$

holds, where $\alpha \triangleq \frac{\lambda_{\min}(R)}{\lambda_{\max}(P)}$, $d \triangleq 2\gamma^{-1}\tilde{w}\,\dot{w}\|\Lambda\|_2$, $\mu \triangleq \frac{1}{2}\alpha\gamma^{-1}\tilde{w}^2\|\Lambda\|_2 + d$, $\tilde{w} = \hat{W}_{\max} + w$, $\|W(t)\|_{\mathrm{F}} \leq w$, *and* $\|\dot{W}(t)\|_{\mathrm{F}} \leq \dot{w}$. *In particular,* (5.78) *is sufficient to conclude boundedness of* $V(e_\xi, \tilde{W})$. *Hence, one can now conclude with* $\|e_{\mathrm{m}0}\|_P < \varepsilon/\xi(0)$ *that the closed-loop system state* $(e_\xi(t), \tilde{W}(t))$ *is bounded and the system error satisfies the strict performance bound given by* $\|e_{\mathrm{m}}(t)\|_P < \varepsilon/\xi(t), \quad t \geq 0$. *Once again, we refer to Theorem 3.2 of [2] for details.*

To enforce strict time-varying performance guarantees, one can also use Theorem 3.1 of [2] instead of Theorem 3.2 of [2]. We note here that the former theorem if used requires an extra condition that is $\lambda_{\min}(PB\Lambda B^{\mathrm{T}}P) \neq 0$. However, if $\lambda_{\min}(PB\Lambda B^{\mathrm{T}}P) = 0$ and $\lambda_{\min}(R) - 2\overline{\varepsilon}\lambda_{\max}(P) > 0$ both hold at the same time with $\overline{\varepsilon} \triangleq \max_{t \in \overline{\mathbb{R}}_+} \frac{\dot{\varepsilon}(t)}{\varepsilon(t)}$, then it readily follows from Theorem 3.1 of [2] that it can be utilized without this extra condition.

5.2.4 Experimental Study with an Aerospace Testbed

In this section, we experimentally demonstrate the practical capabilities of the set-theoretic model reference adaptive control architecture with constant and time-varying performance bounds on the Quanser AERO platform in dual-rotor helicopter configuration [3]. For this purpose, we follow the presented control algorithms in Section 5.2.3 as illustrated in Figure 5.28.

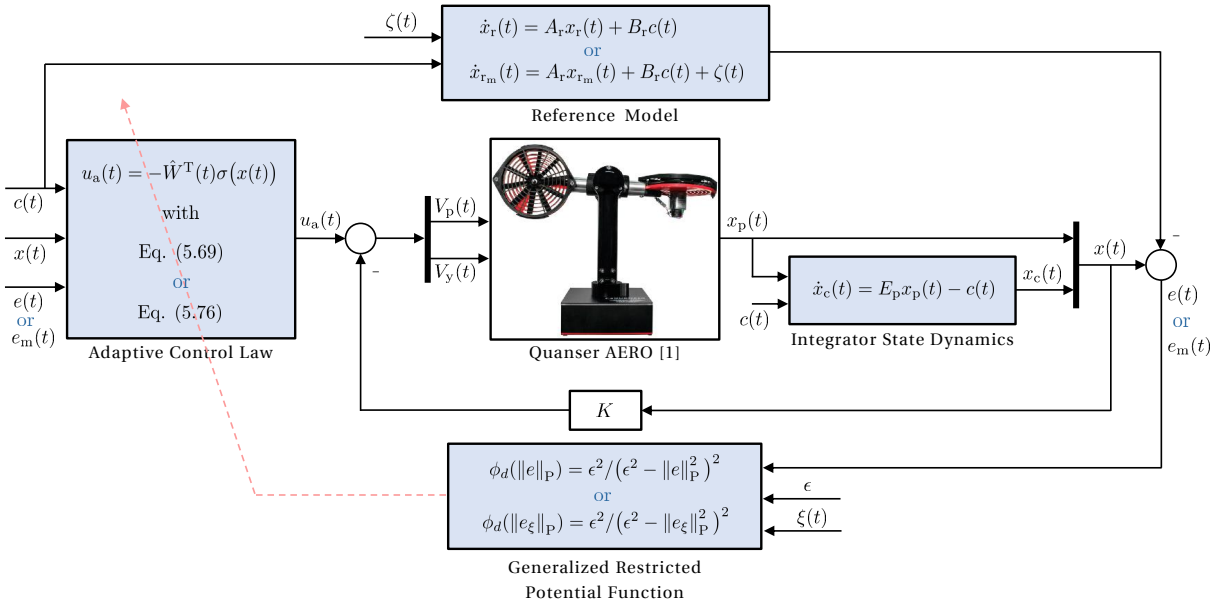

Figure 5.28: Set-theoretic model reference adaptive control architecture.

5.2.4.1 Physical Setup

For the control design, we consider the linearized model of the considered aerospace testbed given by

$$J_{\mathrm{p}}\ddot{\theta}(t) + D_{\mathrm{p}}\dot{\theta}(t) + K_{\mathrm{sp}}\theta(t) = \tau_{\mathrm{p}}(t), \quad \theta(0) = \theta_0, \tag{5.79}$$

$$J_{\mathrm{y}}\ddot{\psi}(t) + D_{\mathrm{y}}\dot{\psi}(t) = \tau_{\mathrm{y}}(t), \quad \psi(0) = \psi_0, \tag{5.80}$$

where $\theta(t)$ is the pitch angle (in radians), $\psi(t)$ is the yaw angle (in radians), J_{p} (respectively, J_{y}) is the total moment of inertia about the pitch (respectively, yaw) axis, D_{p} (respectively, D_{y}) is the damping about the pitch (respectively, yaw) axis, and K_{sp} is the stiffness about the pitch axis. The control torques acting on the pitch and yaw axes are given by

$$\tau_{\mathrm{p}}(t) = K_{\mathrm{pp}}V_{\mathrm{p}}(t) + K_{\mathrm{py}}V_{\mathrm{y}}(t), \tag{5.81}$$

$$\tau_{\mathrm{y}}(t) = K_{\mathrm{yp}}V_{\mathrm{p}}(t) + K_{\mathrm{yy}}V_{\mathrm{y}}(t). \tag{5.82}$$

where $V_{\mathrm{p}}(t)$ and $V_{\mathrm{y}}(t)$ are respectively the motor voltages applied to the pitch and yaw rotors, K_{pp} (respectively, K_{yy}) is the torque thrust gain from the pitch (respectively, yaw) rotor, and K_{py} (respectively, K_{yp}) is the cross-torque thrust gain acting on the pitch (respectively, yaw) from the yaw (respectively, pitch) rotor.

Table 5.1: The Quanser AERO platform parameters.

J_p $[\mathrm{kg\,m^2}]$	0.0219	D_y $[\mathrm{kg\,m^2s^{-1}}]$	0.0220	K_pp $[\mathrm{kg\,m^2s^{-2}V^{-1}}]$	0.0011
J_y $[\mathrm{kg\,m^2}]$	0.0220	K_sp $[\mathrm{kg\,m^2s^{-2}}]$	0.0375	K_yy $[\mathrm{kg\,m^2s^{-2}V^{-1}}]$	0.0022
D_p $[\mathrm{kg\,m^2s^{-1}}]$	0.0071	K_yp $[\mathrm{kg\,m^2s^{-2}V^{-1}}]$	-0.0027	K_py $[\mathrm{kg\,m^2s^{-2}V^{-1}}]$	0.0021

Using (5.79) to (5.82), one can equivalently write the system dynamics in the form

$$\dot{x}_\mathrm{p}(t) \quad = \quad A_\mathrm{p}x_\mathrm{p}(t)+B_\mathrm{p}u(t), \quad x_\mathrm{p}(0)=x_\mathrm{p0}, \tag{5.83}$$

with

$$A_\mathrm{p}=\begin{bmatrix} 0 & 0 & 1 & 0 \\ 0 & 0 & 0 & 1 \\ -K_\mathrm{sp}/J_\mathrm{p} & 0 & -D_\mathrm{p}/J_\mathrm{p} & 0 \\ 0 & 0 & 0 & -D_\mathrm{y}/J_\mathrm{y} \end{bmatrix}, \quad B_\mathrm{p}=\begin{bmatrix} 0 & 0 \\ 0 & 0 \\ K_\mathrm{pp}/J_\mathrm{p} & K_\mathrm{py}/J_\mathrm{p} \\ K_\mathrm{yp}/J_\mathrm{y} & K_\mathrm{yy}/J_\mathrm{y} \end{bmatrix}, \tag{5.84}$$

where $x_\mathrm{p}(t)=[\theta(t),\psi(t),\dot{\theta}(t),\dot{\psi}(t)]^\mathrm{T}\in\mathbb{R}^4$ denotes the measurable state vector and $u(t)=[V_\mathrm{p}(t),V_\mathrm{y}(t)]^\mathrm{T}\in\mathbb{R}^2$ denotes the control input. The system parameters are obtained from the Quanser AERO user manual [3] as shown in Table 5.1. Note that (5.83) is derived based on the ideal system conditions. However, in practical application scenarios where system uncertainties are present, one can alternatively consider the uncertain system dynamics in the form given by

$$\dot{x}_\mathrm{p}(t) \quad = \quad A_\mathrm{p}x_\mathrm{p}(t)+B_\mathrm{p}\Lambda(u(t)+W_\mathrm{p}^\mathrm{T}(t)\sigma_\mathrm{p}(x_\mathrm{p}(t))), \quad x_\mathrm{p}(0)=x_\mathrm{p0}, \tag{5.85}$$

where Λ denotes an uncertain control effectiveness matrix, $W_\mathrm{p}(t)$ denotes a bounded unknown weight matrix, and $\sigma_\mathrm{p}(x_\mathrm{p}(t))$ denotes a known basis function.

Linear quadratic regulator theory is used to design the nominal controller gain matrix with the weighting matrices as $Q=\mathrm{diag}([2,2,0,0,50,50])$ to penalize $x(t)$ and $R=0.001I_{2\times2}$ to penalize $u(t)$ resulting in

$$K=\begin{bmatrix} 82.85 & -124.21 & 29.70 & -32.29 & 125.18 & -185.28 \\ 117.26 & 78.55 & 38.95 & 19.04 & 185.28 & 125.18 \end{bmatrix}, \tag{5.86}$$

for (5.65). In this experiment, a 30 degree yaw maneuver is considered as the control objective; hence, from a practical point of view, we pass the desired command through a low-pass filter to generate a smooth yaw command. In addition, note that the pitch and yaw motor voltages saturate at 24 V and we consider $W_{\rm p}(t) = 0$ and the uncertain control effectiveness matrix to be assumed as $\Lambda = 0.1I_{2\times 2}$ (i.e., 90% reduction in control channel efforts) resulting in $W = 9I_{2\times 2}$.

5.2.4.2 Experimental Results with Constant Performance Bound Guarantees

In this subsection, we illustrate the efficacy of the set-theoretic model reference adaptive controller for enforcing constant strict performance guarantees. For this purpose, we start with the implementation of the nominal and standard adaptive control laws to the AERO platform.

Figure 5.29 shows the performance of the nominal controller for command following. Introducing the uncertain control effectiveness matrix, it is evident from Figure 5.30 that the nominal controller yields to instability. As it is well-known [30], the standard adaptive control architecture can be implemented by setting $\phi_d(\|e(t)\|_{\rm P}) = 1$ in (5.69) for all time. Furthermore, we use rectangular projection operator and set the upper and lower projection bounds imposed on each element of the parameter estimate as $\hat{W}_{\rm upper} = 16I_{2\times 2}$ and $\hat{W}_{\rm lower} = 2I_{2\times 2}$. Moreover, we use $R = 1.5I_{6\times 6}$ to calculate P from (5.70) for the resulting $A_{\rm r}$ matrix. Figure 5.31 presents the command following performance of the adaptive controller with $\gamma = 5$, where the evolution of norm of the system error and the weight estimation are shown in Figure 5.32. Assuming that we need a close tracking of the reference system such that the norm of the system error (i.e., $\|e(t)\|_{\rm P}$) be less than 0.4, this adaptive controller is not able to achieve this requirement. In order to improve the performance, a control designer can increase the adaptation rate as well-known. Figure 5.33 presents the command following performance of the adaptive controller with $\gamma = 30$, where the evolution of norm of the system error and the weight estimation are shown in Figure 5.34. Although, the performance is improved in this setting, the control objective (i.e., $\|e(t)\|_{\rm P} < 0.4$) is not yet achieved. By further increasing the adaptation rate to $\gamma = 70$, one can eventually obtain satisfactory results as it can be seen from Figures 5.35 and 5.36. Note that, even though the desired performance is obtained using $\gamma = 70$, this performance is not guaranteed and is subject to change if the system uncertainties vary. In addition, one needs to perform ad-hoc process to come up with this adaptation rate, which should be avoided in real-world safety-critical scenarios.

Next, in order to demonstrate the efficacy of the set-theoretic model reference adaptive controller for enforcing constant strict performance guarantees by utilization of the error-dependent learning rate

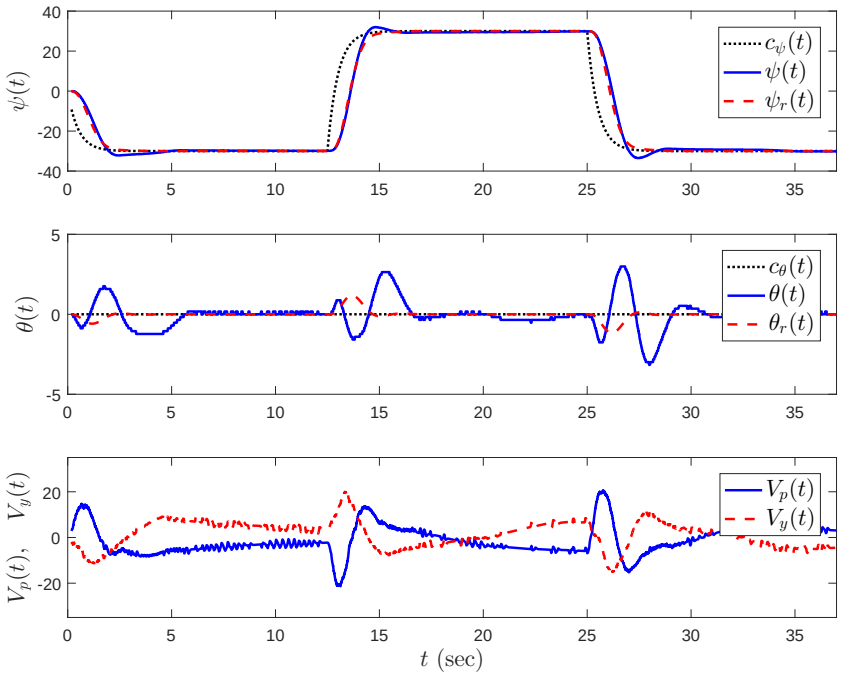

Figure 5.29: Command following performance with the nominal controller in the absence of the system uncertainty.

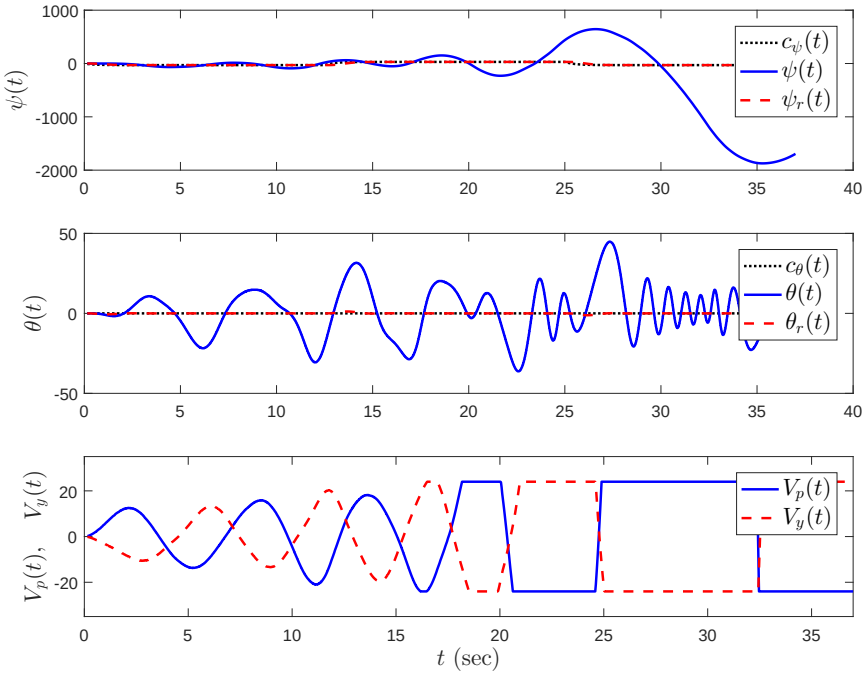

Figure 5.30: Command following performance with the nominal controller in the presence of the system uncertainty.

$\phi_d(\|e(t)\|_{\mathrm{P}})$, we use the generalized restricted potential function of the form $\phi(\|e(t)\|_{\mathrm{P}}) = \|e(t)\|_{\mathrm{P}}^2/(\varepsilon^2 - \|e(t)\|_{\mathrm{P}}^2)$, $e(t) \in \mathcal{D}_\varepsilon$ [2, 108], with $\varepsilon = 0.4$, and we set the constant learning rate to $\gamma = 5$. Figure 5.37 shows the closed-loop dynamical system performance with the set-theoretic adaptive controller in Section 5.2.3.1,

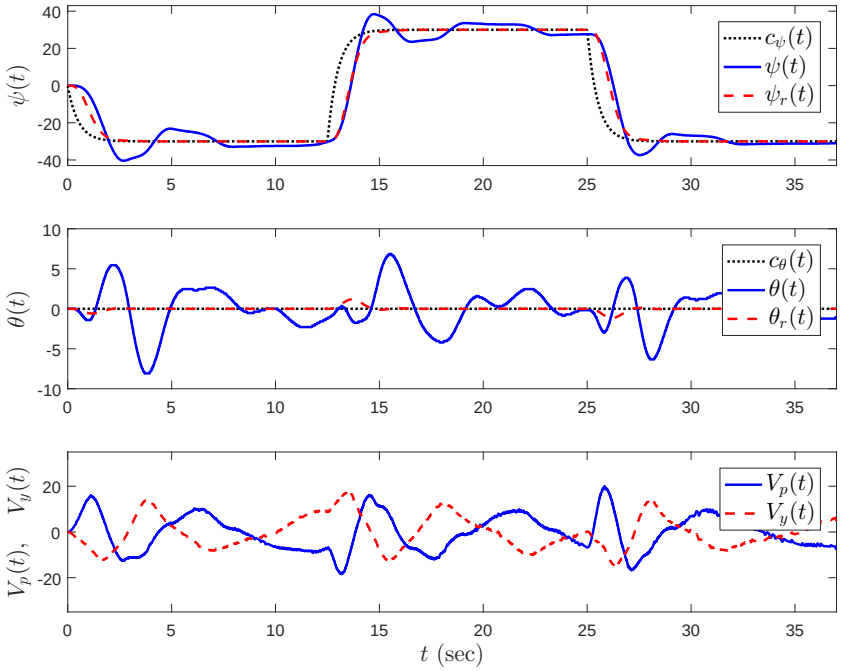

Figure 5.31: Command following performance with the adaptive controller using $\gamma = 5$.

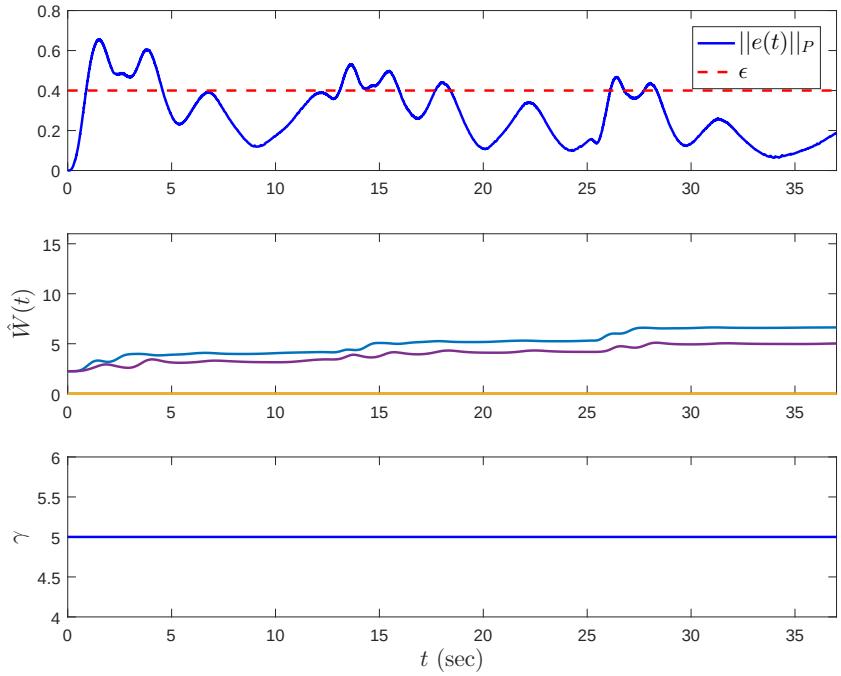

Figure 5.32: Norm of the system error trajectories and the evolution of the weight estimation $\hat{W}(t)$ with the adaptive controller using $\gamma = 5$.

where Figure 5.38 shows the norm of the system error trajectories, the evolution of the weight estimate $\hat{W}(t)$, and the evolution of the effective learning rate. One can see from these figures that the expected performance is achieved and the norm of the system error is guaranteed to be less than $\varepsilon = 0.4$. Note that,

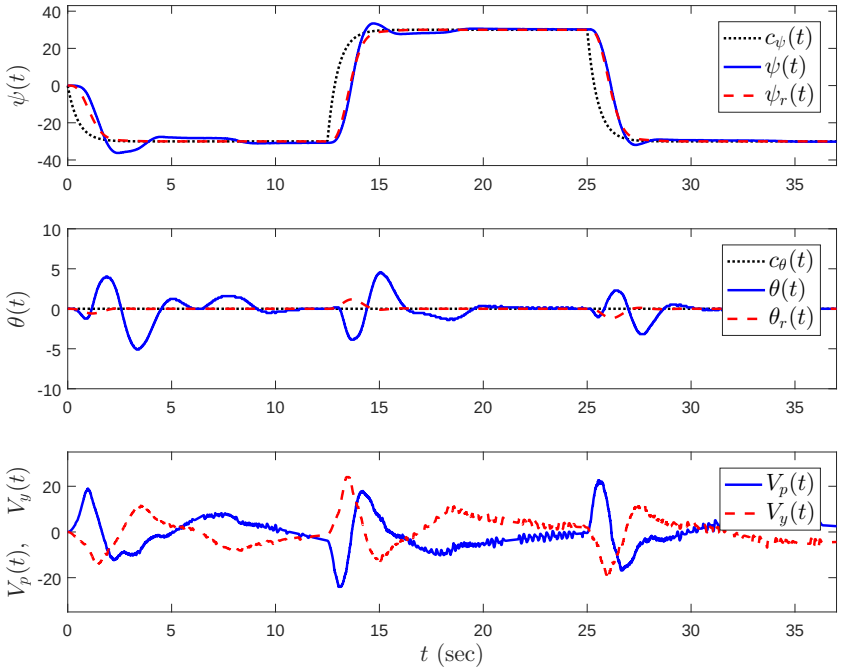

Figure 5.33: Command following performance with the adaptive controller using $\gamma = 30$.

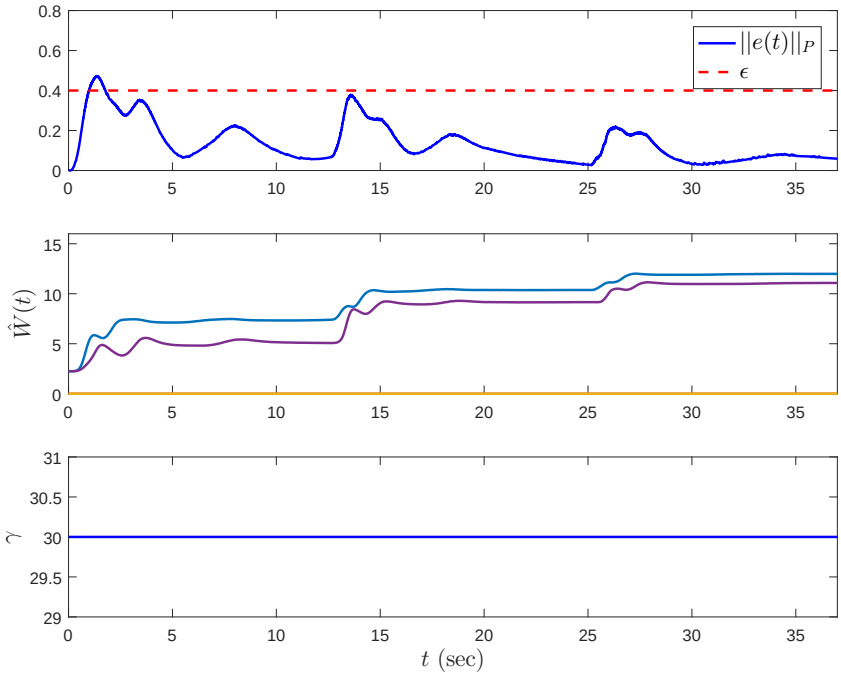

Figure 5.34: Norm of the system error trajectories and the evolution of the weight estimation $\hat{W}(t)$ with the adaptive controller using $\gamma = 30$.

any other values for learning rate γ can be used alternatively in this control architecture without violating the desired user-defined performance guarantee (e.g., see [1]). In addition, unlike the standard adaptive controller with $\gamma = 70$, this performance is obtained independent of the bound on the system uncertainties

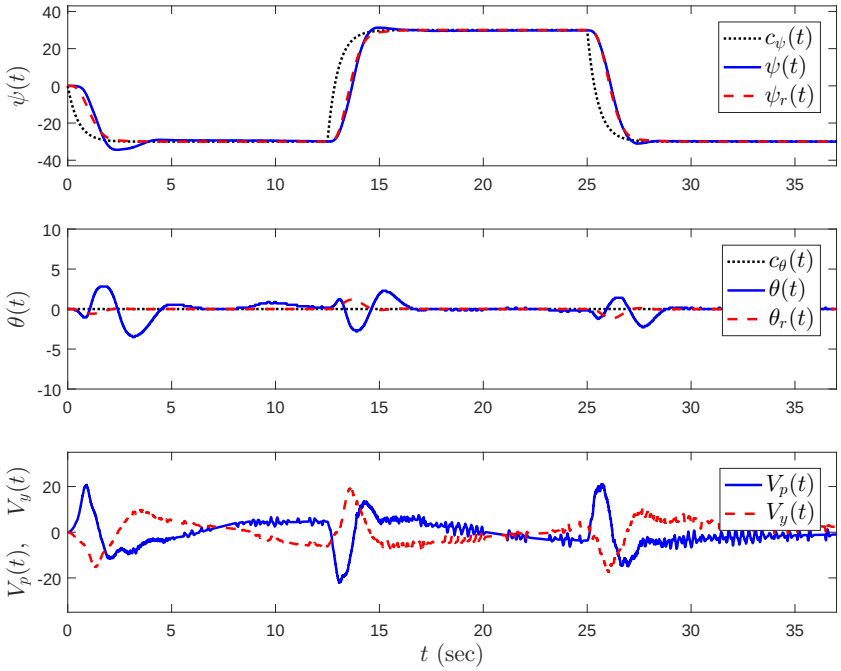

Figure 5.35: Command following performance with the adaptive controller using $\gamma = 70$.

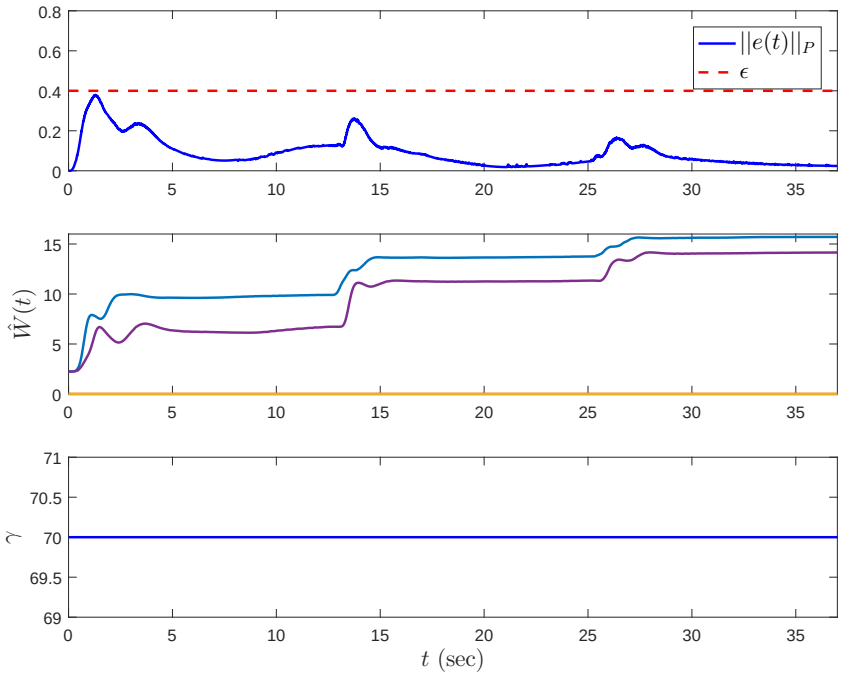

Figure 5.36: Norm of the system error trajectories and the evolution of the weight estimation $\hat{W}(t)$ with the adaptive controller using $\gamma = 70$.

and, more importantly, it does not require an ad-hoc tuning process – in fact, it tunes "$\gamma\phi_d(\|e(t)\|_P)$" in response to the system error to ensure the desired user-defined performance, automatically. This subsection

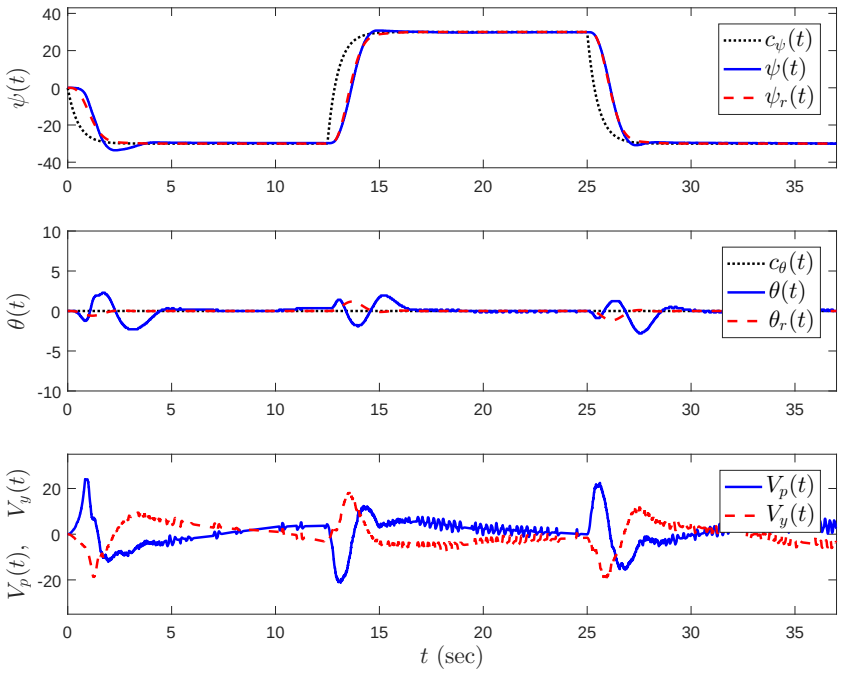

Figure 5.37: Command following performance with the set-theoretic model reference adaptive controller in Section 5.2.3.1.

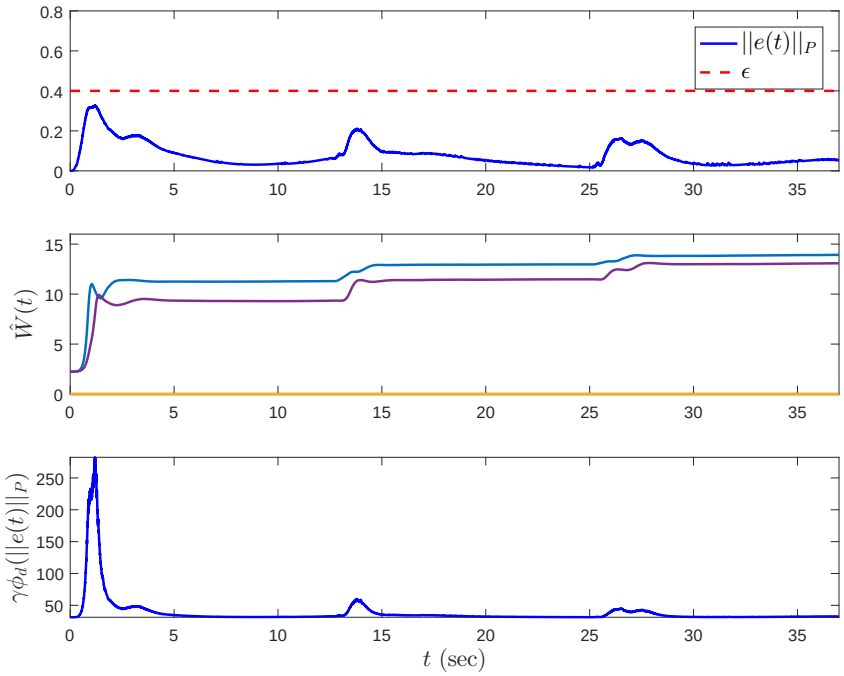

Figure 5.38: Norm of the system error trajectories, the evolution of the weight estimation $\hat{W}(t)$, and the effective learning rate $\gamma\phi_d(\cdot)$ with the set-theoretic model reference adaptive controller in Section 5.2.3.1.

highlighted how the set-theoretic model reference adaptive control architecture empowers a control designer for enforcing desirable system performance requirements, without concerning about the selection of the adaptation rate and requiring the knowledge of the upper bound on the system uncertainty.

5.2.4.3 Experimental Results with Time-Varying Performance Bound Guarantees

In this subsection, we now demonstrate the efficacy of the set-theoretic model reference adaptive controller for enforcing time-varying strict performance guarantees. In particular, we utilize the generalized restricted potential function of the form $\phi(\|e_\xi(t)\|_{\mathrm{P}}) = \|e_\xi(t)\|_{\mathrm{P}}^2/(\varepsilon^2 - \|e_\xi(t)\|_{\mathrm{P}}^2)$, $e_\xi(t) \in \mathcal{D}_\varepsilon$ [2, 108], with $\varepsilon = 1$, and we set the constant learning rate to $\gamma = 5$. Furthermore, we choose the user-defined function $\xi(t)$ such that its inverse ($\xi^{-1}(t)$) changes smoothly from 0.4 to 0.2 such that it allows more deviation at the transient time interval ($\xi_{\max}^{-1} = 0.4$) and then it enforces more restricted bound for the steady-state time interval ($\xi_{\min}^{-1} = 0.2$) in order to obtain a closer tracking performance by guaranteeing $\|x(t) - x_{\mathrm{r_m}}(t)\|_P < \xi^{-1}(t)$.

Figure 5.39 shows the closed-loop dynamical system performance with the set-theoretic adaptive controller with time-varying performance bound, where Figure 5.40 shows the norm of the system error trajectories, the evolution of the weight estimate $\hat{W}(t)$, and the evolution of the effective learning rate. One can see from these figures that the set-theoretic control architecture in Section 5.2.3.2 enables the designer to control the closed-loop system performance as desired on different time intervals (e.g. transient time interval and steady-state time interval). Once again, we note that, any other values for learning rate γ can be used alternatively in this control architecture without violating the desired user-defined performance guarantee.

As mentioned in Remark 5.2.1, to implement the set-theoretic control architecture in Section 5.2.3.1, the initial error has to satisfy $\|e_0\|_P < \varepsilon$. From a practical standpoint, and due to the possible initialization error, this requirement may be restrictive. In what follows, we demonstrate the efficacy of the set-theoretic model reference adaptive controller in Section 5.2.3.2 for addressing this limitation by enforcing time-varying strict performance guarantees. To this end, we consider 10 degrees initialization error in the yaw angle. We now utilize the error-dependent learning rate $\phi_d(\|e_\xi(t)\|_{\mathrm{P}})$ and we set the constant learning rate to $\gamma = 5$. Furthermore, we choose the user-defined function $\xi(t)$ such that the resulting bound on the system error behaves exponentially. This allows more deviation at the initial stage ($\xi^{-1}(0) = 2$), and then gradually enforces more restriction ($\xi_{\min}^{-1} = 0.4$) in order to obtain a closer tracking performance by guaranteeing $\|x(t) - x_{\mathrm{r_m}}(t)\|_P < \xi^{-1}(t)$. Figure 5.41 shows the command following performance of the set-theoretic

model reference adaptive controller in Section 5.2.3.2, where satisfactory result is obtained for tracking the desired command. Once again, the key feature of the proposed control algorithm in practical applications

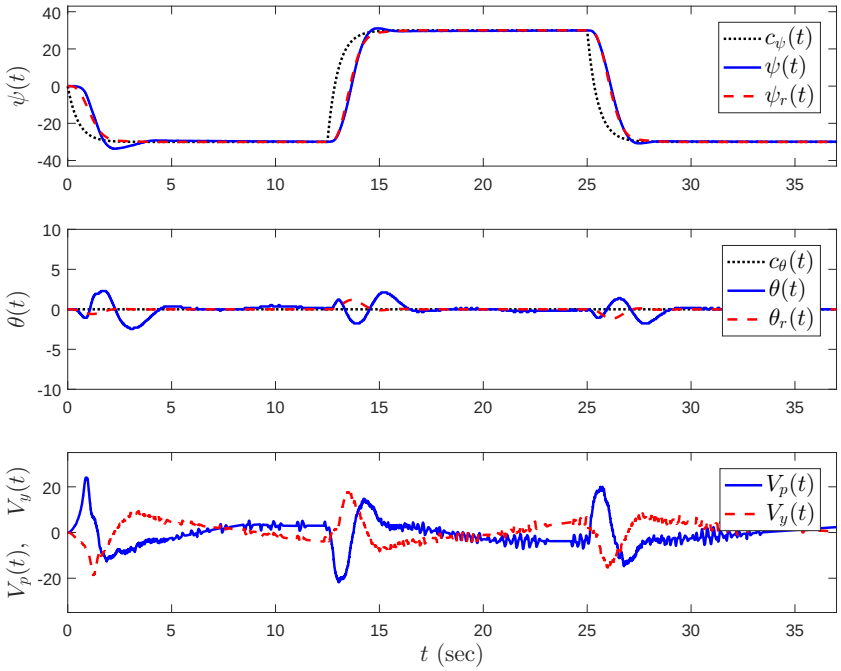

Figure 5.39: Command following performance with the set-theoretic model reference adaptive controller in Section 5.2.3.2.

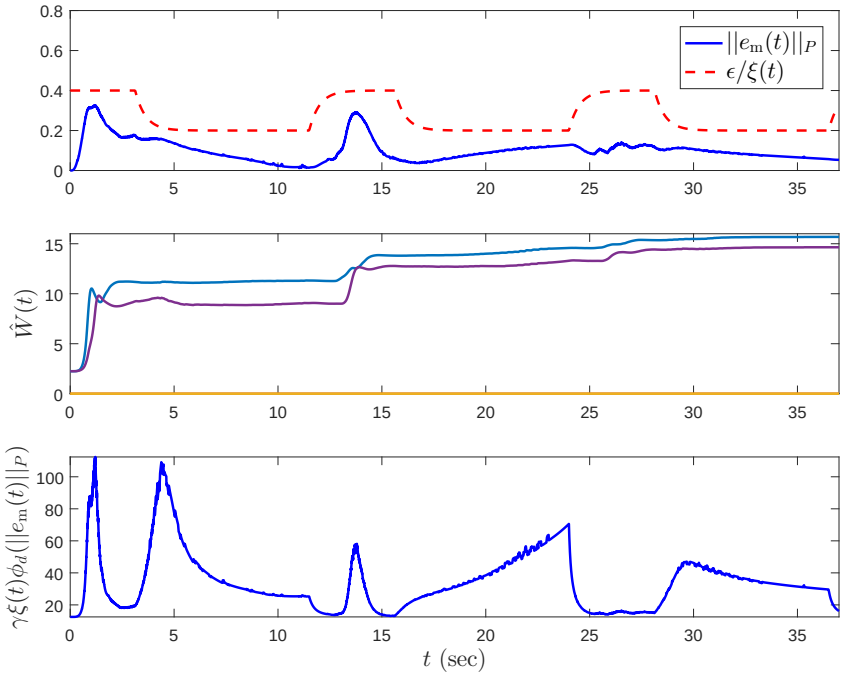

Figure 5.40: Norm of the system error trajectories, the evolution of the weight estimation $\hat{W}(t)$, and the effective learning rate $\gamma\xi(t)\phi_d(\cdot)$ with the set-theoretic model reference adaptive controller in Section 5.2.3.2.

is evident from Figure 5.42. Specifically, one can see from this figure that due to the initialization error, the system error norm is large initially, therefore a time-varying performance bound is needed such that it

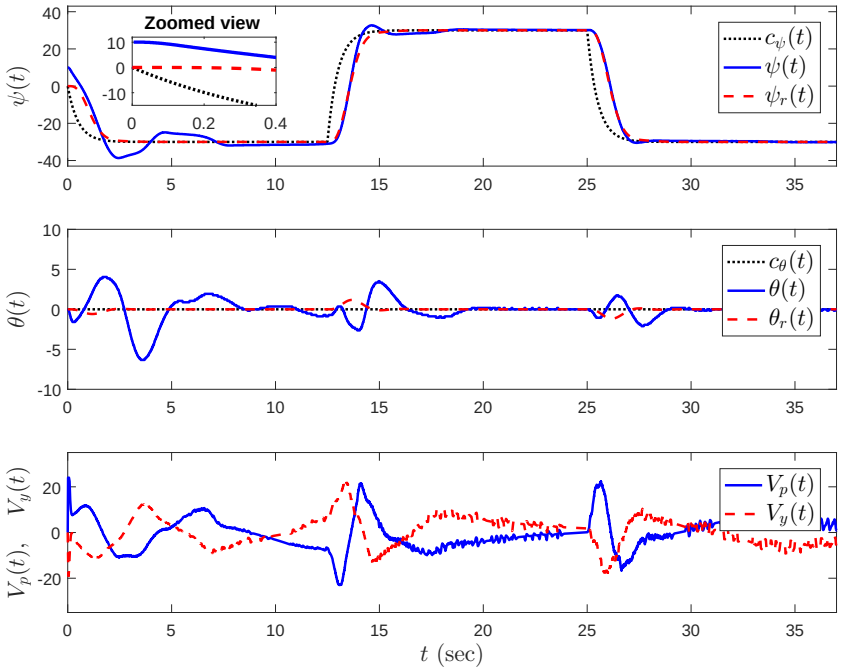

Figure 5.41: Command following performance with the set-theoretic model reference adaptive controller in Section 5.2.3.2.

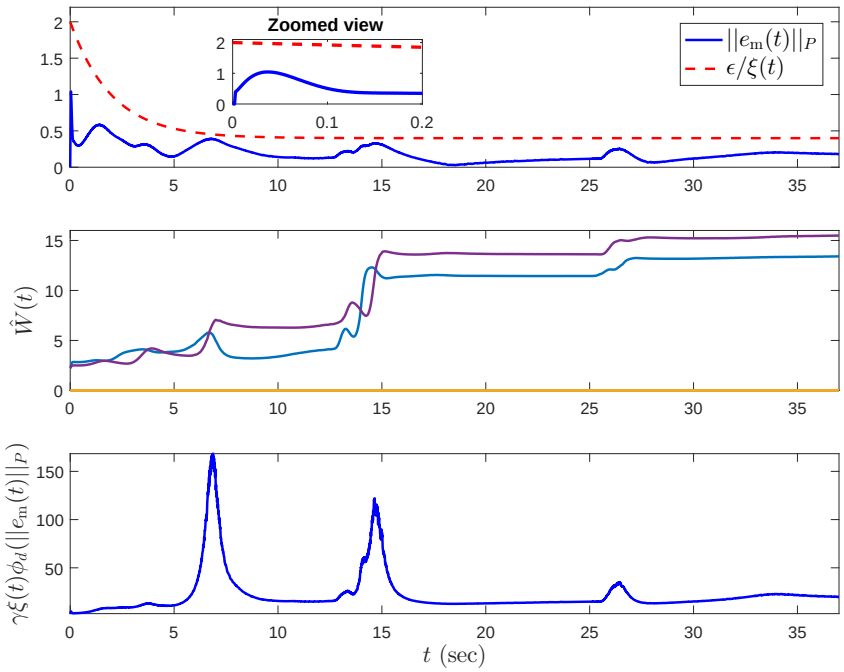

Figure 5.42: Norm of the system error trajectories, the evolution of the weight estimation $\hat{W}(t)$, and the effective learning rate $\gamma\xi(t)\phi_d(\cdot)$ with the set-theoretic model reference adaptive controller in Section 5.2.3.2.

decreases from a large initial value to a small final value in order to handle the initial large system error norm and eventually obtain the desired tracking performance.

5.2.5 Conclusion

In this paper, set-theoretic model reference adaptive control architectures with constant and time-varying performance bounds were tested on an aerospace testbed, configured as a conventional dual-rotor helicopter. The experimental results demonstrated that this control framework was capable of enforcing user-defined performance guarantees without requiring strict knowledge of the upper and lower bounds on the system uncertainties. Furthermore, the set-theoretic model reference adaptive control architecture with time-varying performance bounds enhanced the overall system performance by not only controlling the closed-loop system performance as desired on different time intervals (e.g. transient time interval and steady-state time interval), but also by handling the initialization error.

5.3 A Set-Theoretic Model Reference Adaptive Control Architecture with Dead-Zone Effect[3]

In contrast to standard model reference adaptive control architectures with fixed learning rates, set-theoretic model reference adaptive control architectures predicated on *system error-dependent learning rates* have the capability to enforce *user-defined* worst-case performance bounds on the closed-loop uncertain dynamical system trajectories. When learning is *not* needed (e.g., in the presence of small system errors that often contain high-frequency residual signal contents), however, it is *not* theoretically straightforward to *stop* the adaptation process with set-theoretic architectures using the *common* dead-zone function — a practice that is widely-adopted in applications of standard model reference adaptive control architectures. Motivated from this standpoint, the *contribution* of this paper is a set-theoretic model reference adaptive control architecture with *dead-zone effect*. Specifically, the key feature of our framework utilizes a *new and continuous generalized restricted potential function*, where it not only *stops* the adaptation process inside the *dead-zone* but also *allows* the norm of the system error to be less than a user-defined performance bound. The stability of the proposed technique is rigorously analyzed through several steps by showing the boundedness of an energy function in all possible variations in the system error trajectories, which goes *well beyond* the analyses of standard adaptive control schemes with the common dead-zone function. For cases when this performance bound is *time-varying*, in addition, we show that this dead-zone also *scales* its

[3]This section has been submitted to the *IFAC Journal Control Engineering Practice*.

size automatically to give the designer a flexibility to control the closed-loop system performance as desired on different time intervals. Finally, we also *experimentally validate* the efficacy of the proposed technique through an aerospace testbed.

5.3.1 Introduction

5.3.1.1 Literature Review and Contribution

In any model reference adaptive control algorithm, the *system error* between an uncertain dynamical system and a reference model, which captures a *desired closed-loop dynamical system response*, is *critical*. In particular, this error drives the update law and then the update law adjusts the feedback control gains online in order to suppress this system error, and therefore, to make the uncertain dynamical system *behave close* to the desired closed-loop dynamical system response. The update laws of standard model reference adaptive control architectures utilize *fixed learning rates* and their resulting upper bounds on the norm of the system error can be calculated based on Lyapunov arguments (see, for example, [16, 17, 28–30]). Yet, as it is well-known (see, for example, [1]), these calculated upper bounds are usually *conservative*. As a consequence, they may *not* give tight practical insights to a control designer for correctly assessing a *worst-case performance* in the implementation process of these standard algorithms.

In contrast to standard model reference adaptive control algorithms, *set-theoretic* model reference adaptive control architectures (see, for example, [1]), which are predicated on *system error-dependent learning rates*, have a capability to directly enforce *user-defined* worst-case performance bounds on the system errors, and therefore, on the closed-loop uncertain dynamical system trajectories (see also [1, Section 1] on how this architecture compares with other relevant literature works). When learning is *not* needed (e.g., in the presence of small system errors), however, it is *not* theoretically straightforward to *stop* the adaptation process with set-theoretic architectures using the *common* dead-zone function due to their generalized restricted potential function-based constructions. In particular, the use of the common dead-zone functions is a *widely-adopted practice* (see, for example, [30, 134, 135]) in applications of standard model reference adaptive control algorithms. This is motivated from the observation that small system errors generally contain, for example, *high-frequency residual content* of exogenous disturbances and/or measurement noise. Specifically, a model reference adaptive control algorithm with dead-zone is originally proposed by the authors of [134] to *stop* the adaptation process when the system error is less than a prescribed value. The authors of [135] also propose a *smooth* dead-zone version to the literature (see also [30, Section 11.2] for

details). Yet, these contributions also utilize standard *fixed learning rates* and, once again, it is a challenge to correctly assess a *worst-case performance* in a non-conservative way in the implementation process of these algorithms.

The *contribution* of this paper is a set-theoretic model reference adaptive control architecture with a *dead-zone effect*. The key feature of our framework utilizes a *new and continuous generalized restricted potential function*. Instead of directly using the common dead-zone function, in particular, this potential function is theoretically constructed in order not only to *stop* the adaptation process inside the *dead-zone* but also to *allow* the norm of the system error to be less than a user-defined performance bound for achieving strict closed-loop dynamical system response guarantees. Specifically, Section 5.3.3.1 first presents the proposed approach with a user-defined *constant* performance bound on the system error, where dead-zone effect is also treated as a *constant* region. We next address in Section 5.3.3.2 the case when this performance bound is desired to be *time-varying* and show that this dead-zone also *scales* its size automatically to give the designer a flexibility to control the closed-loop system performance as desired on *different time intervals*. We refer to Section 5.3.1.2 for a motivational example.

We note here that the provided new stability analysis of the proposed architecture goes *well beyond* the analyses of standard model reference adaptive control schemes with the common dead-zone function. In particular, the stability of the proposed technique is rigorously analyzed through several steps by showing the boundedness of an energy function in all possible variations in the system error trajectories, and hence, it does not trivially follow from, for example, [1]. Finally, we also show the efficacy of the proposed architecture through two illustrative numerical examples and, more importantly, through an *aerospace testbed experimentation* in Section 5.3.4.

5.3.1.2 A Motivational Example

To elucidate the motivation behind the proposed model reference adaptive control architecture, consider a simple-yet-representative scenario. Specifically, let $x(t)$ be the scalar state of an uncertain dynamical system and let $x_{\rm r}(t)$ be the scalar state of a reference model. If we only focus on the problem where the system error $e(t) = x(t) - x_{\rm r}(t)$ needs to stay on the fixed set $\mathcal{S}$ capturing a constant worst-case performance as depicted in Figure 5.43(a), then the original set-theoretic model reference adaptive control architecture [1] can be utilized to address this problem. In addition to enforcing a worst-case performance to the adaptation process through constraining the system error to stay in the set $\mathcal{S}$, a control designer may

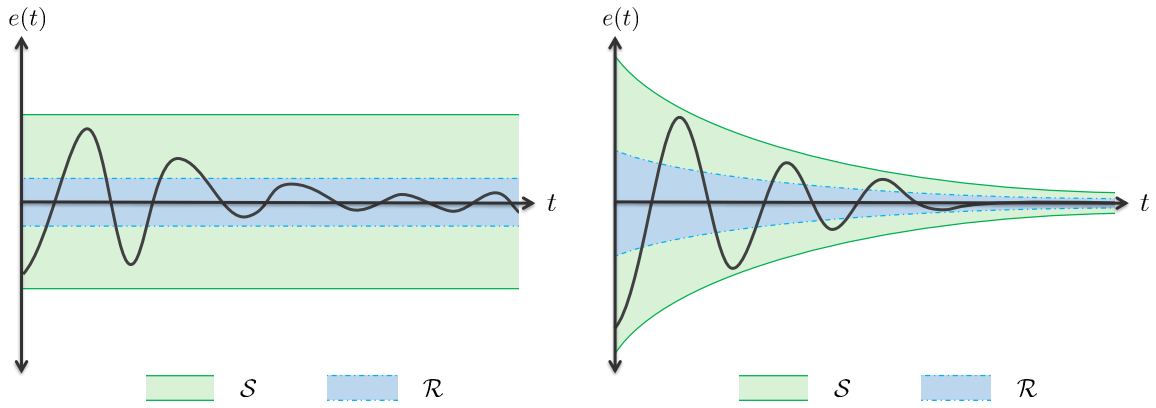

(a) Constant performance bound.

(b) Time-varying performance bound.

Figure 5.43: Graphical representations for the motivational example in Section 5.3.1.2.

also want to stop the adaptation when this system error belongs to a smaller set $\mathcal{R} \subset \mathcal{S}$ (dead-zone) as also shown in this figure. As discussed above, this expectation is common in practice since small system errors often contain high-frequency residual signal contents that the update laws should *not* take into account. This problem is addressed in Section 5.3.3.1 through a new and continuous generalized restricted potential function in the set-theoretic model reference adaptive control law.

Next, consider the case when a control designer wants to enforce a time-varying worst-case performance to the adaptation process in order to shape the closed-loop system performance as desired on different time intervals; that is, $e(t)$ needs to obey to the time-varying set $\mathcal{S}$ as shown in Figure 5.43(b). For example, while deviation from an ideal reference model trajectory can be tolerated within the transient time interval (i.e., a larger user-defined performance bound), it is usually required to have a close command following performance after this transition period (i.e., a tighter user-defined performance bound). This example also motivates the smaller set $\mathcal{R}$ (dead-zone) to be time-varying. Specifically, the dead-zone is expected to become smaller after the aforementioned transition period in order to incorporate more information from the system error signal in to the update law. This problem is addressed in Section 5.3.3.2 through expanding the results in Section 5.3.3.1, which allows the dead-zone to automatically scale its size based on the time-varying changes on the assigned worst-case performance.

5.3.2 Mathematical Preliminaries

Before presenting the theoretical contributions of this paper in Sections 5.3.3.1 and 5.3.3.2 followed by an experimental validation in Section 5.3.4, we first cover the notation used in this paper (Section 5.3.2.1),

the considered problem formulation (Section 5.3.2.2), and a concise overview of the original set-theoretic model reference adaptive control approach (Section 5.3.2.3).

5.3.2.1 Notation

In this paper, $\mathbb{R}$ denotes the set of real numbers, $\mathbb{R}^n$ denotes the set of $n \times 1$ real column vectors, $\mathbb{R}^{n\times m}$ denotes the set of $n \times m$ real matrices, $\mathbb{R}_+$ (respectively, $\overline{\mathbb{R}}_+$) denotes the set of positive (respectively, nonnegative) real numbers, $\mathbb{R}_+^{n\times n}$ (respectively, $\overline{\mathbb{R}}_+^{n\times n}$) denotes the set of positive-definite (respectively, nonnegative-definite) $n \times n$ real matrices, $\mathbb{D}^{n\times n}$ denotes the set of $n \times n$ real matrices with diagonal scalar entries, $0_{n\times n}$ denotes the $n \times n$ zero matrix, and "$\triangleq$" denotes equality by definition. In addition, we write $(\cdot)^{\mathrm{T}}$ for the transpose, $(\cdot)^{-1}$ for the inverse, $\mathrm{tr}(\cdot)$ for the trace, $\|\cdot\|_2$ for the Euclidean norm, $\|\cdot\|_{\mathrm{F}}$ for the Frobenius norm, $\|x\|_A \triangleq \sqrt{x^{\mathrm{T}}Ax}$ for the weighted Euclidean norm with $x \in \mathbb{R}^n$ and $A \in \mathbb{R}_+^{n\times n}$, and $\|A\|_2 \triangleq \sqrt{\lambda_{\max}(A^{\mathrm{T}}A)}$ for the induced two-norm with $A \in \mathbb{R}^{n\times m}$.

5.3.2.2 Problem Formulation

This paper focuses on a class of uncertain dynamical systems given by

$$\dot{x}(t) \;=\; Ax(t) + B\Lambda\big(u(t) + \delta(t,x(t))\big), \quad x(0) = x_0, \quad t \geq 0. \tag{5.87}$$

In (5.87), $x(t) \in \mathbb{R}^n$, $t \geq 0$, denotes the measurable state vector, $u(t) \in \mathbb{R}^m$, $t \geq 0$, denotes the control input, $A \in \mathbb{R}^{n\times n}$ denotes a known system matrix, $B \in \mathbb{R}^{n\times m}$ denotes a known input matrix, $\delta : \overline{\mathbb{R}}_+ \times \mathbb{R}^n \to \mathbb{R}^m$ denotes a system uncertainty, and $\Lambda \in \mathbb{R}_+^{m\times m} \cap \mathbb{D}^{m\times m}$ denotes an unknown control effectiveness matrix. Here, the pair (A,B) is considered to be controllable. We now introduce a standard assumption [28–30] on the system uncertainty parameterization.

Assumption 5.3.1 *The system uncertainty* (5.87) *is parameterized as*

$$\delta(t,x(t)) \;=\; W_0^{\mathrm{T}}(t)\sigma_0(x(t)), \quad x(t) \in \mathbb{R}^n, \tag{5.88}$$

where $W_0(t) \in \mathbb{R}^{s\times m}$, $t \geq 0$, is a bounded unknown weight matrix (i.e., $\|W_0(t)\|_{\mathrm{F}} \leq w_0$, $t \geq 0$) with a bounded time rate of change (i.e., $\|\dot{W}_0(t)\|_{\mathrm{F}} \leq \dot{w}_0$, $t \geq 0$) and $\sigma_0 : \mathbb{R}^n \to \mathbb{R}^s$ is a known basis function of the form $\sigma_0(x(t)) = [\sigma_{01}(x(t)), \sigma_{02}(x(t)), \ldots, \sigma_{0s}(x(t))]^{\mathrm{T}}$ that includes locally Lipschitz elements.

We consider that a desired closed-loop dynamical system performance is captured by the reference model dynamics given by

$$\dot{x}_{\mathrm{r}}(t) \quad = \quad A_{\mathrm{r}}x_{\mathrm{r}}(t)+B_{\mathrm{r}}c(t), \quad x_{\mathrm{r}}(0)=x_{\mathrm{r0}}, \quad t\geq 0. \tag{5.89}$$

In (5.89), $x_{\mathrm{r}}(t)\in\mathbb{R}^n$, $t\geq 0$, denotes the reference state vector, $c(t)\in\mathbb{R}^{n_c}$ denotes the uniformly continuous bounded command, $A_{\mathrm{r}}\in\mathbb{R}^{n\times n}$ denotes the Hurwitz reference model matrix, and $B_{\mathrm{r}}\in\mathbb{R}^{n\times n_c}$ denotes the command input matrix. Using Assumption 5.3.1 in (5.87), one can write

$$\dot{x}(t) \quad = \quad Ax(t)+B\Lambda\big(u(t)+W_0^{\mathrm{T}}(t)\sigma_0(x(t))\big), \quad x(0)=x_0, \quad t\geq 0. \tag{5.90}$$

In what follows, without loss of any generality, we consider a nominal control law with feedback and feedforward terms (see Section 5.3.4 for a different type of nominal control law selection using an integrator state). Specifically, let the feedback control law be given by

$$u(t)=\underbrace{-K_1x(t)+K_2c(t)}_{u_{\mathrm{n}}(t)}\ \underbrace{-\hat{W}^{\mathrm{T}}(t)\sigma\big(x(t),c(t)\big)}_{u_{\mathrm{a}}(t)}, \quad t\geq 0, \tag{5.91}$$

where $u_{\mathrm{n}}(t)\in\mathbb{R}^m$, $t\geq 0$, and $u_{\mathrm{a}}(t)\in\mathbb{R}^m$, $t\geq 0$, are the nominal and adaptive control laws, respectively. Here, the feedback $K_1\in\mathbb{R}^{m\times n}$ and the feedforward $K_2\in\mathbb{R}^{m\times n_c}$ gains in (5.91) are selected such that $A_{\mathrm{r}}=A-BK_1$ and $B_{\mathrm{r}}=BK_2$ hold. Using (5.91) in (5.90) now results in

$$\dot{x}(t) \quad = \quad A_{\mathrm{r}}x(t)+B_{\mathrm{r}}c(t)-B\Lambda\tilde{W}^{\mathrm{T}}(t)\sigma\big(x(t),c(t)\big), \quad x(0)=x_0, \quad t\geq 0, \tag{5.92}$$

where $\sigma\big(x(t),c(t)\big)\triangleq\big[\sigma_0^{\mathrm{T}}\big(x(t)\big),\ x^{\mathrm{T}}(t),\ c^{\mathrm{T}}(t)\big]^{\mathrm{T}}\in\mathbb{R}^{s+n+n_c}$, $t\geq 0$, and $\tilde{W}(t)\triangleq\hat{W}(t)-W(t)\in\mathbb{R}^{(s+n+n_c)\times m}$ is the weight estimation error with $W(t)\triangleq\big[W_0^{\mathrm{T}}(t),\ (\Lambda^{-1}-I_{\mathrm{m}\times\mathrm{m}})K_1,\ -(\Lambda^{-1}-I_{\mathrm{m}\times\mathrm{m}})K_2\big]^{\mathrm{T}}\in\mathbb{R}^{(s+n+n_c)\times m}$, $t\geq 0$, being an unknown weight matrix and $\hat{W}(t)\in\mathbb{R}^{(s+n+n_c)\times m}$, $t\geq 0$, being an estimate of $W(t)$, $t\geq 0$. Considering Assumption 5.3.1, note that $\|W(t)\|_{\mathrm{F}}\leq w, t\geq 0$, and $\|\dot{W}(t)\|_{\mathrm{F}}\leq\dot{w}, t\geq 0$, automatically hold.

5.3.2.3 Set-Theoretic Model Reference Adaptive Control Overview

Based on the problem formulation introduced above, we now overview the standard set-theoretic model reference adaptive control architecture [1]. We begin with the following definitions.

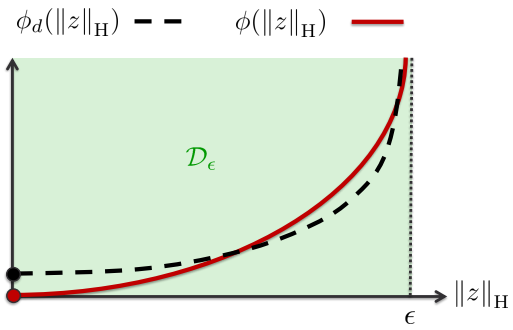

Figure 5.44: Graphical representation of $\phi(\|z\|_{\mathrm{H}})$ and $\phi_d(\|z\|_{\mathrm{H}})$ in Remark 5.3.1.

Definition 5.3.1 *For $z \in \mathbb{R}^p$ and $H \in \mathbb{R}_+^{p\times p}$, $\phi(\|z\|_{\mathrm{H}})$, $\phi : \mathbb{R} \to \mathbb{R}$, is called a generalized restricted potential function (generalized barrier Lyapunov function) on the set*

$$\mathcal{D}_\varepsilon \triangleq \{z : \|z\|_{\mathrm{H}} \in [0, \varepsilon)\}, \tag{5.93}$$

with $\varepsilon \in \mathbb{R}_+$ being a-priori, user-defined constant, when the following statements hold [1]: i) If $\|z\|_{\mathrm{H}} = 0$, then $\phi(\|z\|_{\mathrm{H}}) = 0$. ii) If $z \in \mathcal{D}_\varepsilon$ and $\|z\|_{\mathrm{H}} \neq 0$, then $\phi(\|z\|_{\mathrm{H}}) > 0$. iii) If $\|z\|_{\mathrm{H}} \to \varepsilon$, then $\phi(\|z\|_{\mathrm{H}}) \to \infty$. iv) $\phi(\|z\|_{\mathrm{H}})$ is continuously differentiable on $\mathcal{D}_\varepsilon$. v) If $z \in \mathcal{D}_\varepsilon$, then $\phi_d(\|z\|_{\mathrm{H}}) > 0$, where $\phi_d(\|z\|_{\mathrm{H}}) \triangleq \mathrm{d}\phi(\|z\|_{\mathrm{H}})/\mathrm{d}\|z\|_{\mathrm{H}}^2$. vi) If $z \in \mathcal{D}_\varepsilon$, then $2\phi_d(\|z\|_{\mathrm{H}})\|z\|_{\mathrm{H}}^2 - \phi(\|z\|_{\mathrm{H}}) > 0$.

Remark 5.3.1 *As discussed in [2], a candidate generalized restricted potential function satisfying all the conditions given in Definition 5.3.1 has the form $\phi(\|z\|_{\mathrm{H}}) = \|z\|_{\mathrm{H}}^2/\left(\varepsilon^2 - \|z\|_{\mathrm{H}}^2\right)$, $z \in \mathcal{D}_\varepsilon$. Figure 5.44 shows a graphical representation of this generalized restricted potential function.*

Definition 5.3.2 *Let $\Omega = \left\{\theta \in \mathbb{R}^n : (\theta_i^{\min} \leq \theta_i \leq \theta_i^{\max})_{i=1,2,\cdots,n}\right\}$ be a convex hypercube in $\mathbb{R}^n$, where $(\theta_i^{\min}, \theta_i^{\max})$ represent the minimum and maximum bounds for the i^{th} component of the n-dimensional parameter vector θ. Moreover, for a sufficiently small positive constant ν, define a second hypercube as $\Omega_\nu = \left\{\theta \in \mathbb{R}^n : (\theta_i^{\min} + \nu \leq \theta_i \leq \theta_i^{\max} - \nu)_{i=1,2,\cdots,n}\right\}$, where $\Omega_\nu \subset \Omega$. The projection operator $\mathrm{Proj} : \mathbb{R}^n \times \mathbb{R}^n \to \mathbb{R}^n$ is then defined componentwise by $\mathrm{Proj}(\theta, y) \triangleq \left(\frac{\theta_i^{\max} - \theta_i}{\nu}\right) y_i$ if $\theta_i > \theta_i^{\max} - \nu$ and $y_i > 0$, $\mathrm{Proj}(\theta, y) \triangleq \left(\frac{\theta_i - \theta_i^{\min}}{\nu}\right) y_i$ if $\theta_i < \theta_i^{\min} + \nu$ and $y_i < 0$, and $\mathrm{Proj}(\theta, y) \triangleq y_i$ otherwise. Based on the above definition, note that $\left(\theta - \theta^*\right)^{\mathrm{T}}\left(\mathrm{Proj}\left(\theta, y\right) - y\right) \leq 0$, holds [30, 80]. This definition can be further generalized to matrices as $\mathrm{Proj}_{\mathrm{m}}(\Theta, Y) = \left(\mathrm{Proj}(\mathrm{col}_1(\Theta), \mathrm{col}_1(Y)), \ldots, \mathrm{Proj}(\mathrm{col}_m(\Theta), \mathrm{col}_m(Y))\right)$, where $\Theta \in \mathbb{R}^{n\times m}$, $Y \in$*

$\mathbb{R}^{n\times m}$ *and* $\mathrm{col}_i(\cdot)$ *denotes* ith *column operator. In this case, for a given matrix* Θ^**, it follows that* $\mathrm{tr}\left[(\Theta-\Theta^*)^{\mathrm{T}}(\mathrm{Proj}_{\mathrm{m}}(\Theta,Y)-Y)\right]=\sum_{i=1}^{m}\left[\mathrm{col}_i(\Theta-\Theta^*)^{\mathrm{T}}(\mathrm{Proj}(\mathrm{col}_i(\Theta),\mathrm{col}_i(Y))-\mathrm{col}_i(Y))\right]\leq 0$.

Following the theory presented in [1], consider next the update law for (5.91) given by

$$\dot{\hat{W}}(t)=\gamma\mathrm{Proj}_{\mathrm{m}}\Big(\hat{W}(t),\phi_d(\|e(t)\|_P)\sigma\big(x(t),c(t)\big)e^{\mathrm{T}}(t)PB\Big),\quad \hat{W}(0)=\hat{W}_0,\quad t\geq 0, \tag{5.94}$$

with $\hat{W}_{\max}$ being the projection norm bound. In (5.94), $\gamma\in\mathbb{R}_+$ denotes the adaptation gain, $e(t)\triangleq x(t)-x_{\mathrm{r}}(t)$, $t\geq 0$, denotes the system error, and $P\in\mathbb{R}_+^{n\times n}$ denotes a solution of the Lyapunov equation given by

$$0 \;=\; A_{\mathrm{r}}^{\mathrm{T}}P+PA_{\mathrm{r}}+R, \tag{5.95}$$

with $R\in\mathbb{R}_+^{n\times n}$. Since A_{r} is Hurwitz, it follows from converse Lyapunov theory [109, 136] that there exists a unique positive-definite P satisfying (5.95) for a given positive-definite R. The system error dynamics and the weight estimation error dynamics can now be written as

$$\dot{e}(t) \;=\; A_{\mathrm{r}}e(t)-B\Lambda\tilde{W}^{\mathrm{T}}(t)\sigma\big(x(t),c(t)\big),\quad e(0)=e_0,\quad t\geq 0, \tag{5.96}$$

$$\dot{\tilde{W}}(t) \;=\; \gamma\mathrm{Proj}_{\mathrm{m}}\Big(\hat{W}(t),\phi_d(\|e(t)\|_P)\sigma\big(x(t),c(t)\big)e^{\mathrm{T}}(t)PB\Big)-\dot{W}(t),\quad \tilde{W}(0)=\tilde{W}_0,\quad t\geq 0. \tag{5.97}$$

Remark 5.3.2 *The update law* (5.94) *for the set-theoretic model reference adaptive control approach can be derived using the energy function of the form* $V(e,\tilde{W})=\phi(\|e\|_P)+\gamma^{-1}\mathrm{tr}\big[(\tilde{W}\Lambda^{1/2})^{\mathrm{T}}(\tilde{W}\Lambda^{1/2})\big]$ *with* $\|e(0)\|_P<\varepsilon$*, where* $\mathcal{D}_\varepsilon\triangleq\{e(t):\|e(t)\|_P<\varepsilon\}$*. From this energy function, one can calculate* $\dot{V}\big(e(t),\tilde{W}(t)\big)\leq -\frac{1}{2}\alpha V(e,\tilde{W})+\mu$ *[1], where* $\alpha\triangleq\frac{\lambda_{\min}(R)}{\lambda_{\max}(P)}$*,* $d\triangleq 2\gamma^{-1}\tilde{w}\,\dot{w}\|\Lambda\|_2$*,* $\mu\triangleq\frac{1}{2}\alpha\gamma^{-1}\tilde{w}^2\|\Lambda\|_2+d$*, and* $\tilde{w}=\hat{W}_{\max}+w$*. One can now conclude the boundedness of* $V(e,\tilde{W})$ *and the closed-loop dynamical system given by (5.96) and (5.97) as well as the strict performance bound on the system error given by* $\|e(t)\|_P<\varepsilon$*,* $t\geq 0$*.*

Note that the original set-theoretic model reference adaptive control architecture overviewed in this section provides a strict performance guarantee by utilizing the error-dependent adaptation rate $\phi_d(\|e(t)\|_P)$, $t\geq 0$. Since small system errors often contain high-frequency residual signal contents as discussed in Section 5.3.1, it is practically desired to *stop* the adaptation process in the presence of such small errors. This problem is addressed in the next section with a new set-theoretic model reference adaptive control synthesis and analysis.

5.3.3 Set-Theoretic Model Reference Adaptive Control with Dead-Zone Effect

In this section, we first utilize a new and continuous *generalized restricted potential function* with a constant user-defined bound in the adaptation process such that this potential function not only *stops* the adaptation process inside the dead-zone when the system error is small but also it allows the norm of the system error to be less than a-priori, user-defined worst-case performance bound (Section 5.3.3.1). Next, we address the case when this performance bound is desired to be time-varying and show that this dead-zone *scales* its size automatically to give the designer a flexibility to control the closed-loop system performance as desired on different time intervals (Section 5.3.3.2).

5.3.3.1 Constant User-Defined Performance Guarantees

We begin with the following new definition, which embeds a *user-defined dead-zone effect* into the generalized restricted potential function in Definition 5.3.1.

Definition 5.3.3 *For $z \in \mathbb{R}^p$ and $H \in \mathbb{R}_+^{p\times p}$, $\psi(\|z\|_{\mathrm{H}})$, $\psi : \mathbb{R}^p \to \mathbb{R}$, is called a shifted generalized restricted potential function on the set $\mathcal{D}_\varepsilon \triangleq \mathcal{D}_{\varepsilon_1} \cup \mathcal{D}_{\varepsilon_2}$, where $\mathcal{D}_{\varepsilon_1} \triangleq \{z : \|z\|_{\mathrm{H}} \in [0, \varepsilon_1)\}$ and $\mathcal{D}_{\varepsilon_2} \triangleq \{z : \|z\|_{\mathrm{H}} \in [\varepsilon_1, \varepsilon_2)\}$, $0 \leq \varepsilon_1 < \varepsilon_2$ with $\varepsilon_1, \varepsilon_2 \in \mathbb{R}_+$ being a-priori, user-defined constants, if the following statements hold: i) If $\|z\|_{\mathrm{H}} \leq \varepsilon_1$, then $\psi(\|z\|_{\mathrm{H}}) = 0$. ii) If $z \in \mathcal{D}_{\varepsilon_2}$ and $\|z\|_{\mathrm{H}} \neq 0$, then $\psi(\|z\|_{\mathrm{H}}) > 0$. iii) If $\|z\|_{\mathrm{H}} \to \varepsilon_2$, then $\psi(\|z\|_{\mathrm{H}}) \to \infty$. iv) $\psi(\|z\|_{\mathrm{H}})$ is continuously differentiable on $\mathcal{D}_{\varepsilon_2}$. v) If $z \in \mathcal{D}_{\varepsilon_2}$, then $\psi_d(\|z\|_{\mathrm{H}}) > 0$, where $\psi_d(\|z\|_{\mathrm{H}}) \triangleq \mathrm{d}\psi(\|z\|_{\mathrm{H}})/\mathrm{d}\|z\|_{\mathrm{H}}^2$. vi) If $z \in \mathcal{D}_{\varepsilon_2}$, then $2\psi_d(\|z\|_{\mathrm{H}})\|z\|_{\mathrm{H}}^2 - \psi(\|z\|_{\mathrm{H}}) > 0$.*

Remark 5.3.3 *A candidate shifted generalized restricted potential function satisfying the conditions given in Definition 5.3.3 has the form*

$$\psi(\|z\|_{\mathrm{H}}) \triangleq \begin{cases} \dfrac{\left(\|z\|_{\mathrm{H}} - \varepsilon_1\right)^2}{\varepsilon_2^2 - \|z\|_{\mathrm{H}}^2}, & \text{if } z \in \mathcal{D}_{\varepsilon_2} \\ 0, & \text{if } z \in \mathcal{D}_{\varepsilon_1} \end{cases} \tag{5.98}$$

where $\mathcal{D}_{\varepsilon_1} \triangleq \{z : \|z\|_{\mathrm{H}} \in [0, \varepsilon_1)\}$ and $\mathcal{D}_{\varepsilon_2} \triangleq \{z : \|z\|_{\mathrm{H}} \in [\varepsilon_1, \varepsilon_2)\}$ with the partial derivative

$$\psi_d(\|z\|_{\mathrm{H}}) \triangleq \begin{cases} \dfrac{(\|z\|_{\mathrm{H}} - \varepsilon_1)(\varepsilon_2^2 - \varepsilon_1\|z\|_{\mathrm{H}})}{\|z\|_{\mathrm{H}}\left(\varepsilon_2^2 - \|z\|_{\mathrm{H}}^2\right)^2}, & \text{if } z \in \mathcal{D}_{\varepsilon_2} \\ 0, & \text{if } z \in \mathcal{D}_{\varepsilon_1} \end{cases} \tag{5.99}$$

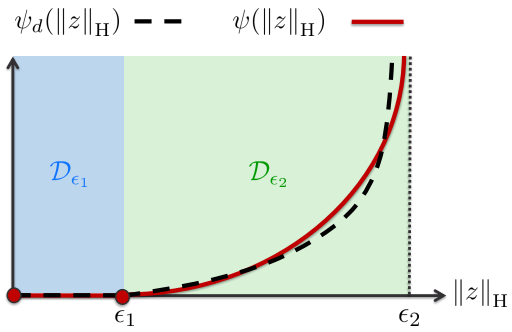

Figure 5.45: Graphical representation of $\psi(\|z\|_{\mathrm{H}})$ and $\psi_d(\|z\|_{\mathrm{H}})$ in Remark 5.3.3. Here, $\mathcal{D}_{\varepsilon_1}$ denotes the dead-zone.

with respect to $\|z\|_{\mathrm{H}}^2$. *Based on this new potential function, one can readily verify that* $2\psi_d(\|z\|_{\mathrm{H}})\|z\|_{\mathrm{H}}^2 - \psi(\|z\|_{\mathrm{H}}) > 0$ *for* $z \in \mathcal{D}_{\varepsilon_2}$. *A graphical representation of* $\psi(\|z\|_{\mathrm{H}})$ *is shown in Figure 5.45, where the region* $\mathcal{D}_{\varepsilon_1}$ *represents a dead-zone. Note that setting* $\varepsilon_1 = 0$ *reduces this shifted generalized restricted potential function* $\psi(\|z\|_{\mathrm{H}})$ *to* $\phi(\|z\|_{\mathrm{H}})$ *in Remark 5.3.1.*

Consider next the proposed update law for (5.91) given by

$$\dot{\hat{W}}(t) = \gamma \mathrm{Proj}_{\mathrm{m}}\Big(\hat{W}(t), \psi_d(\|e(t)\|_P)\sigma\big(x(t),c(t)\big)e^{\mathrm{T}}(t)PB\Big), \quad \hat{W}(0) = \hat{W}_0, \quad t \geq 0, \tag{5.100}$$

with $\hat{W}_{\max}$ being the projection bound. In (5.100), $\gamma \in \mathbb{R}_+$ denotes the adaptation gain and $P \in \mathbb{R}_+^{n\times n}$ denotes a solution of the Lyapunov equation given in (5.95) with $R \in \mathbb{R}_+^{n\times n}$. One can now write the system error dynamics and the weight estimation error dynamics respectively as

$$\dot{e}(t) = A_{\mathrm{r}}e(t) - B\Lambda\tilde{W}^{\mathrm{T}}(t)\sigma\big(x(t),c(t)\big), \quad e(0) = e_0, \quad t \geq 0, \tag{5.101}$$

$$\dot{\tilde{W}}(t) = \gamma \mathrm{Proj}_{\mathrm{m}}\Big(\hat{W}(t), \psi_d(\|e(t)\|_P)\sigma\big(x(t),c(t)\big)e^{\mathrm{T}}(t)PB\Big) - \dot{W}(t), \quad \tilde{W}(0) = \tilde{W}_0, \quad t \geq 0. \tag{5.102}$$

The following theorem presents the main result of this section.

Theorem 5.3.1 *Consider the uncertain dynamical system given by (5.87) subject to Assumption 5.3.1, the reference model given by (5.89), and the feedback control law given by (5.91) with (5.100). If* $\|e_0\|_P < \varepsilon_2$, *then the closed-loop dynamical system given by (5.101) and (5.102) are bounded, where the bound on the system error satisfies a-priori given, user-defined worst-case performance given by*

$$\|e(t)\|_P < \varepsilon_2, \quad t \geq 0. \tag{5.103}$$

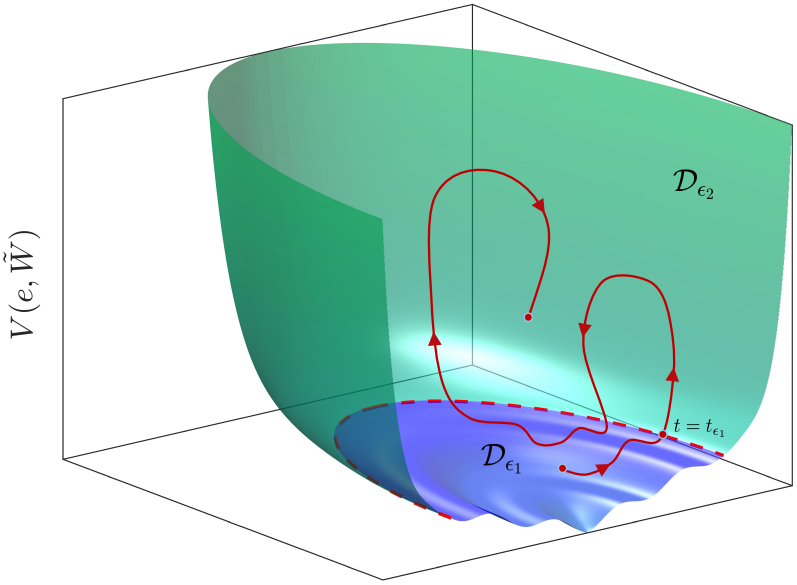

Figure 5.46: Graphical representation of the energy function in (5.104) and the transitions between the sets $\mathcal{D}_{\varepsilon_1}$ and $\mathcal{D}_{\varepsilon_2}$. Here, $\mathcal{D}_{\varepsilon_1}$ denotes the dead-zone.

Proof. To show boundedness of the closed-loop dynamical system given by (5.101) and (5.102), consider the energy function $V : \mathcal{D}_{\varepsilon} \times \mathbb{R}^{(s+n+n_c)\times m} \to \overline{\mathbb{R}}_+$ given by

$$V(e,\tilde{W}) = \psi(\|e\|_P) + \gamma^{-1}\mathrm{tr}\big[(\tilde{W}\Lambda^{1/2})^{\mathrm{T}}(\tilde{W}\Lambda^{1/2})\big], \tag{5.104}$$

where $\mathcal{D}_{\varepsilon} \triangleq \mathcal{D}_{\varepsilon_1} \cup \mathcal{D}_{\varepsilon_2}$ with $\mathcal{D}_{\varepsilon_1} \triangleq \{e(t) : \|e(t)\|_P \in [0,\varepsilon_1)\}$ and $\mathcal{D}_{\varepsilon_2} \triangleq \{e(t) : \|e(t)\|_P \in [\varepsilon_1,\varepsilon_2)\}$ (a graphical representation of this energy function is shown in Figure 5.46). To analyze the closed-loop system trajectories (5.101) and (5.102), we now consider two *cases*.

In Case 1, we first focus on the case where the initial error $\|e_0\|_P$ starts at the set $\mathcal{D}_{\varepsilon_1}$, i.e. $\|e_0\|_P < \varepsilon_1$. We assume *without loss of any generality* that the weight estimation is initialized at zero, i.e., $\hat{W}_0 = 0$. From (5.98), we know that $\psi(\|e(t)\|_P) = 0, t \geq 0$, for $e(t) \in \mathcal{D}_{\varepsilon_1}, t \geq 0$; hence, the energy function $V(e,\tilde{W})$ in the set $\mathcal{D}_{\varepsilon_1}$ can be written as

$$V(\cdot) = \gamma^{-1}\mathrm{tr}\big[(W\Lambda^{1/2})^{\mathrm{T}}(W\Lambda^{1/2})\big]. \tag{5.105}$$

We now consider two *subcases*:

i) Starting from $\|e_0\|_P \in \mathcal{D}_{\varepsilon_1}$, as long as the system error trajectory stays within the set $\mathcal{D}_{\varepsilon_1}$, the energy function $V(\cdot)$ remains bounded by

$$V(e,\tilde{W}) \leq V_1, \tag{5.106}$$

where $V_1 \triangleq \gamma^{-1}w^2\|\Lambda\|_2$. Note that in this subcase, while there can be some variations in the energy function resulting from the time-varying unknown weight matrix $W(t), t \geq 0$, the key point is that $V(e,\tilde{W})$ remains bounded, as it is also depicted in Figure 5.46.

ii) Next, assume that the error trajectory leaves from the set $\mathcal{D}_{\varepsilon_1}$ to the set $\mathcal{D}_{\varepsilon_2}$ at some $t = t_{\varepsilon_1}$. Then right before leaving the set $\mathcal{D}_{\varepsilon_1}$ at $t = t_{\varepsilon_1^-}$, we have

$$V(\cdot) = V_{\varepsilon_1^-} \triangleq \gamma^{-1}\mathrm{tr}\big[(W(t_{\varepsilon_1^-})\Lambda^{1/2})^{\mathrm{T}}(W(t_{\varepsilon_1^-})\Lambda^{1/2})\big]. \tag{5.107}$$

In addition, from continuity of $\psi(\|z\|_{\mathrm{H}})$ in (5.98), we have $\psi(\varepsilon_1^-) = \psi(\varepsilon_1^+) = \psi(\varepsilon_1) = 0$. Now, one can write the expression for the energy function $V(\cdot)$ at $t = t_{\varepsilon_1^+}$ as

$$V(\cdot) = V_{\varepsilon_1^+} \triangleq \gamma^{-1}\mathrm{tr}\big[(W(t_{\varepsilon_1^+})\Lambda^{1/2})^{\mathrm{T}}(W(t_{\varepsilon_1^+})\Lambda^{1/2})\big]. \tag{5.108}$$

From (5.107), (5.108), and the continuity of the system uncertainty, $W(t), t \geq 0$, we conclude that the energy function $V(\cdot)$ is continuous in the whole set $\mathcal{D}_{\varepsilon}$.

Now that the error trajectory is in the set $\mathcal{D}_{\varepsilon_2}$, we have

$$V(e,\tilde{W}) = \psi(\|e\|_P) + \gamma^{-1}\mathrm{tr}\big[(\tilde{W}\Lambda^{1/2})^{\mathrm{T}}(\tilde{W}\Lambda^{1/2})\big]. \tag{5.109}$$

Note that

$$\frac{\mathrm{d}\psi(\|e(t)\|_P)}{\mathrm{d}t} = \frac{\mathrm{d}\psi(\|e(t)\|_P)}{\mathrm{d}\|e(t)\|_P^2}\,\frac{\mathrm{d}\|e(t)\|_P^2}{\mathrm{d}t} = 2\psi_d(\|e(t)\|_P)e^{\mathrm{T}}(t)P\dot{e}(t), \quad t \geq t_{\varepsilon_1}. \tag{5.110}$$

Following the proof of Theorem 3.1 in [1], the time derivative of (5.109) along the closed-loop system trajectories (5.101) and (5.102) is given by

$$
\begin{aligned}
\dot{V}\big(e(t),\tilde{W}(t)\big) &= \frac{\mathrm{d}\psi(\|e(t)\|_P)}{\mathrm{d}t} + 2\gamma^{-1}\mathrm{tr}\tilde{W}^{\mathrm{T}}(t)\dot{\tilde{W}}(t)\Lambda \\
&= 2\psi_d(\|e(t)\|_P)e^{\mathrm{T}}(t)P\dot{e}(t) \\
&\quad +2\gamma^{-1}\mathrm{tr}\tilde{W}^{\mathrm{T}}(t)\Big(\gamma\mathrm{Proj}_{\mathrm{m}}\Big(\hat{W}(t),\psi_d(\|e(t)\|_P)\sigma\big(x(t)\big)e^{\mathrm{T}}(t)PB\Big) - \dot{W}(t)\Big)\Lambda \\
&\leq -\frac{1}{2}\alpha V\big(e(t),\tilde{W}(t)\big) - \alpha\Big[\psi_d(\|e(t)\|_P)e^{\mathrm{T}}(t)Pe(t) - \frac{1}{2}\psi(\|e(t)\|_P)\Big] + \mu, \quad t \geq t_{\varepsilon_1},
\end{aligned}
\tag{5.111}
$$

and it follows from Definition 5.3.3 that

$$
\dot{V}\big(e(t),\tilde{W}(t)\big) \leq -\frac{1}{2}\alpha V\big(e(t),\tilde{W}(t)\big) + \mu, \quad t \geq t_{\varepsilon_1}, \tag{5.112}
$$

where $\alpha \triangleq \frac{\lambda_{\min}(R)}{\lambda_{\max}(P)}$, $d \triangleq 2\gamma^{-1}\tilde{w}\,\dot{w}\|\Lambda\|_2$, and $\mu \triangleq \frac{1}{2}\alpha\gamma^{-1}\tilde{w}^2\|\Lambda\|_2 + d$. It now follows from (5.112) that $V(e,\tilde{W})$ is upper bounded by $V_2 \triangleq \max\big\{V_{\varepsilon_1}, \frac{2\mu}{\alpha}\big\}$, where $V_{\varepsilon_1} \triangleq V(e(t_{\varepsilon_1}),\tilde{W}(t_{\varepsilon_1}))$.

Thus, in both subcases *i)* and *ii)*, the energy function $V(e,\tilde{W})$ is upper bounded by $V_{\max} \triangleq \max\big\{V_1, V_2\big\}$ and using (5.109) one can write $\psi(\|e(t)\|_P) + \gamma^{-1}\mathrm{tr}(\tilde{W}(t)\Lambda^{1/2})^{\mathrm{T}}(\tilde{W}(t)\Lambda^{1/2}) \leq V_{\max}$, $t \geq 0$; hence, $\psi(\|e(t)\|_P) \leq V_{\max}$, $t \geq 0$, which proves that the $\|e(t)\|_P, t \geq 0$, *never leaves* the set $\mathcal{D}_\varepsilon$, or equivalently, (5.103) holds.

In Case 2, next consider that the initial error $\|e_0\|_P$ starts at the set $\mathcal{D}_{\varepsilon_2}$, i.e., $\varepsilon_1 \leq \|e_0\|_P < \varepsilon_2$. Similar to the discussion in subcase *ii)* of Case 1, one can obtain the time derivative of $V(e,\tilde{W})$ in (5.104) to conclude the boundedness of the energy function and the shifted generalized restricted potential function $\psi(\|e(t)\|_P), t \geq 0$, resulting in $\|e(t)\|_P < \varepsilon_2, t \geq 0$. Thus, the proof is now complete. ■

To demonstrate the performance of the proposed adaptive control algorithm in Theorem 5.3.1, we now present an illustrative numerical example. Consider the second-order uncertain dynamical system given by

$$
\dot{x}(t) = \begin{bmatrix} 0 & 1 \\ 0 & 0 \end{bmatrix} x(t) + \begin{bmatrix} 0 \\ 1 \end{bmatrix} \Big(\Lambda u(t) + \delta_0(t,x(t))\Big), \quad x(0) = 0, \quad t \geq 0, \tag{5.113}
$$

where $x(t) = \big[x_1(t) \;\; x_2(t)\big]^{\mathrm{T}}$. In (5.113), $\delta_0(t,x(t))$ represents an uncertainty of the form

$$
\delta_0(t,x(t)) = \alpha_1 \sin(t) + \alpha_2 x_1 + \alpha_3 x_2^2, \tag{5.114}
$$

with $\alpha_1 = 0.5$, $\alpha_2 = 1$, $\alpha_3 = 0.25$, and $\Lambda = 0.75$ represents an uncertain control effectiveness matrix. The linear quadratic regulator theory is used to design the nominal feedback gain matrices as $K_1 = [2.2,\ 2.5]$ and $K_2 = 2.2$ in (5.91). We now apply the proposed set-theoretic model reference adaptive control with dead-zone effect in Theorem 5.3.1, where we use the shifted generalized restricted potential function given in Remark 5.3.3 with $\varepsilon_2 = 0.25$ to strictly guarantee $\|x(t) - x_{\mathrm{r}}(t)\|_P < 0.25$, $t \geq 0$. In addition, we set the projection norm bound imposed on each element of the parameter estimate to $\hat{W}_{\max} = 2$, the learning rate to $\gamma = 1$, and we use $R = 5I$ to calculate P from (5.95) for the resulting A_{r} matrix. Figures 5.47 and 5.48 show the effects of utilizing different user-defined parameter $\varepsilon_1 \in [0, 0.1]$ on the proposed set-theoretic model reference adaptive control with dead-zone effect in Theorem 5.3.1. One can see from these figures that the adaptation process *stops* for small system errors and the average effective adaptation rate is decreased. ▲

5.3.3.2 Time-Varying User-Defined Performance Guarantees

We now generalize the results in Section 5.3.3.1 to the case of time-varying user-defined performance bounds using [2, Section 3.2]. This generalization also allows the dead-zone to automatically scale its size on different time intervals in the light of the changes on the user-defined performance bound. To begin with, let $\zeta(t) \in \mathbb{R}^n, t \geq 0$, be a signal (see below) that modifies the reference model given by (5.89) to allow the enforcement of user-defined time-varying performance bounds. Specifically, consider the modified reference model given by

$$\dot{x}_{\mathrm{r_m}}(t) = A_{\mathrm{r}} x_{\mathrm{r_m}}(t) + B_{\mathrm{r}} c(t) + \zeta(t), \quad x_{\mathrm{r_m}}(0) = x_{\mathrm{r0}}, \quad t \geq 0, \tag{5.115}$$

where $x_{\mathrm{r_m}}(t) \in \mathbb{R}^n, t \geq 0$, is the modified reference state vector. Next, consider the modified system error $e_{\mathrm{m}}(t) \triangleq x(t) - x_{\mathrm{r_m}}(t), t \geq 0$, and the error transformation $e_\xi(t) = \xi(t) e_{\mathrm{m}}(t), t \geq 0$, where $\xi(t) \in \mathbb{R}_+, t \geq 0$, is a user-defined scalar for adjusting the worst-case performance bound (see Theorem 5.3.2) such that both $\xi(t)$ and its time-derivative are smooth and bounded.

Using the shifted generalized restricted potential function candidate given in Remark 5.3.3, we now propose the update law for (5.91) given by

$$\dot{\hat{W}}(t) = \gamma \mathrm{Proj_m}\Big(\hat{W}(t), \psi_d(\|e_\xi(t)\|_P)\sigma\big(x(t), c(t)\big)\xi(t)e_\xi^{\mathrm{T}}(t)PB\Big), \quad \hat{W}(0) = \hat{W}_0, \quad t \geq 0, \tag{5.116}$$

with $\hat{W}_{\max}$ being the projection bound. Using (5.92) and (5.115), one can write the modified system error dynamics as

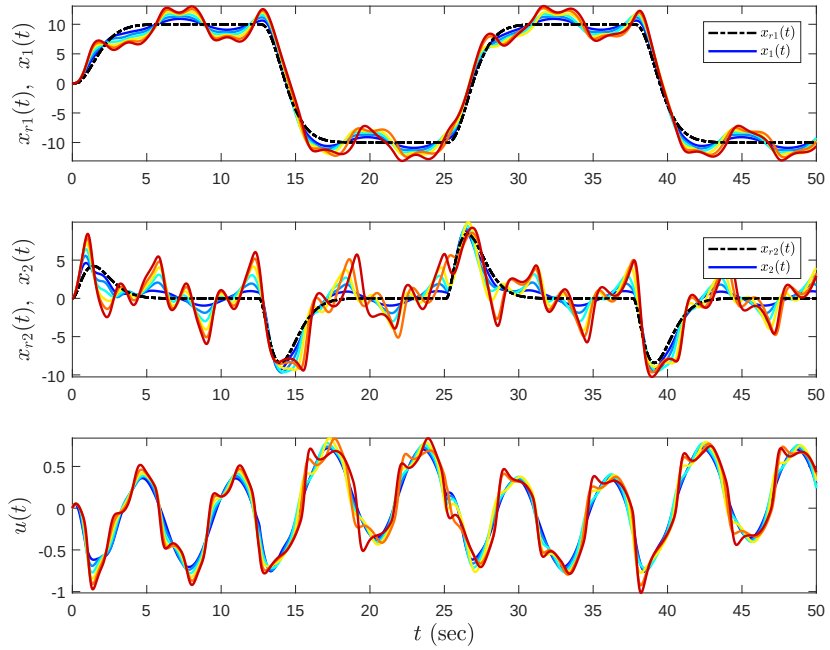

Figure 5.47: Closed-loop system performance with the set-theoretic model reference adaptive control architecture in Theorem 5.3.1 when $\varepsilon_1 \in [0, 0.1]$ (blue to red) and $\varepsilon_2 = 0.25$.

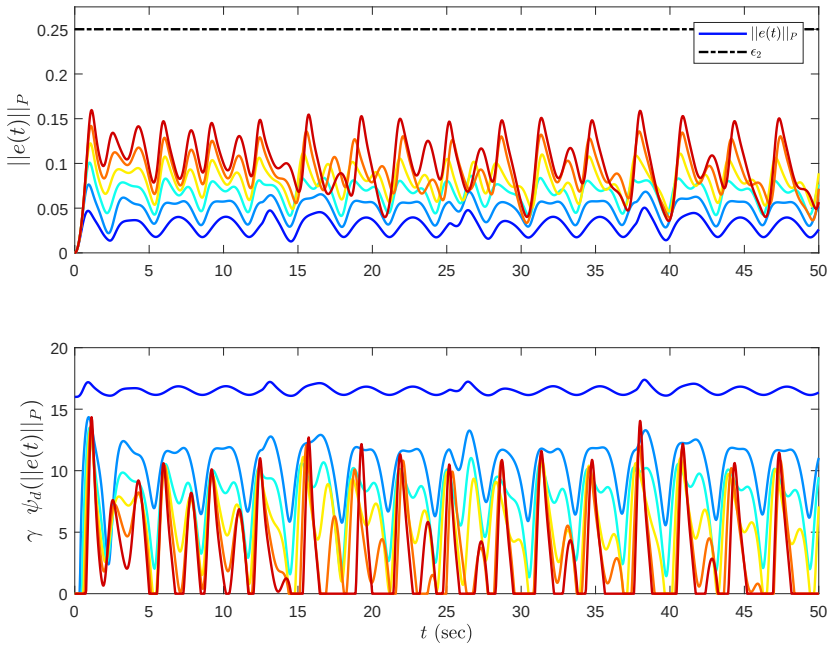

Figure 5.48: History of the system error trajectories and the effective learning rates with the set-theoretic model reference adaptive control architecture in Theorem 5.3.1 when $\varepsilon_1 \in [0, 0.1]$ (blue to red) and $\varepsilon_2 = 0.25$.

$$\dot{e}_{\rm m}(t) \;=\; A_{\rm r}e_{\rm m}(t) - B\Lambda\tilde{W}^{\rm T}(t)\sigma\big(x(t),c(t)\big) - \zeta(t), \quad e_{\rm m}(0) = e_{\rm m0}, \quad t \geq 0, \tag{5.117}$$

where it follows from the considered error transformation given by $e_\xi(t) = \xi(t)e_{\rm m}(t), t \geq 0$, that

$$\dot{e}_\xi(t) = \dot{\xi}(t)e_{\rm m}(t) + A_{\rm r}e_\xi(t) - B\Lambda\tilde{W}^{\rm T}(t)\sigma\big(x(t),c(t)\big)\xi(t) - \xi(t)\zeta(t), \quad e_\xi(0) = e_{\xi 0}, \quad t \geq 0. \tag{5.118}$$

Next, let $\zeta(t) \triangleq \dot{\xi}(t)\xi^{-1}(t)e_{\rm m}(t), t \geq 0$, which puts (5.118) into the form given by

$$\dot{e}_\xi(t) \;=\; A_{\rm r}e_\xi(t) - \xi(t)B\Lambda\tilde{W}^{\rm T}(t)\sigma\big(x(t),c(t)\big), \quad e_\xi(0) = e_{\xi 0}, \quad t \geq 0. \tag{5.119}$$

Finally the weight estimation error dynamics can be also written as

$$\dot{\tilde{W}}(t) = \gamma{\rm Proj}_{\rm m}\big(\hat{W}(t), \psi_d(\|e_\xi(t)\|_P)\sigma\big(x(t),c(t)\big)\xi(t)e_\xi^{\rm T}(t)PB\big) - \dot{W}(t), \quad \tilde{W}(0) = \tilde{W}_0, \quad t \geq 0. \tag{5.120}$$

The following theorem presents the main result of this section.

Theorem 5.3.2 *Consider the uncertain dynamical system given by (5.87) subject to Assumption 5.3.1, the modified reference model given by (5.115), and the feedback control law given by (5.91) with (5.116). If* $\|e_{\rm m0}\|_P < \frac{\varepsilon_2}{\xi(0)}$, *then the closed-loop dynamical system given by (5.119) and (5.120) are bounded, where the bound on the system error satisfies a-priori given, user-defined worst-case performance given by*

$$\|e_{\rm m}(t)\|_P < \frac{\varepsilon_2}{\xi(t)}, \quad t \geq 0. \tag{5.121}$$

Proof. The error dynamics given by (5.119) and (5.120) is similar to the error dynamics given by (5.96) and (5.97). Since the condition given by $\|e_{\rm m0}\|_P < \frac{\varepsilon_2}{\xi(0)}$ can be equivalently written as $\|e_{\xi 0}\|_P < \varepsilon_2$, then based on the energy function $V : \mathcal{D}_\varepsilon \times \mathbb{R}^{(s+n+n_c)\times m} \to \overline{\mathbb{R}}_+$ given by

$$V(e_\xi, \tilde{W}) = \psi(\|e_\xi\|_P) + \gamma^{-1}{\rm tr}\big[(\tilde{W}\Lambda^{1/2})^{\rm T}(\tilde{W}\Lambda^{1/2})\big], \tag{5.122}$$

where $\mathcal{D}_\varepsilon \triangleq \mathcal{D}_{\varepsilon_1} \cup \mathcal{D}_{\varepsilon_2}$ with $\mathcal{D}_{\varepsilon_1} \triangleq \{e_\xi(t) : \|e_\xi(t)\|_P \in [0, \varepsilon_1)\}$ and $\mathcal{D}_{\varepsilon_2} \triangleq \{e_\xi(t) : \|e_\xi(t)\|_P \in [\varepsilon_1, \varepsilon_2)\}$, it identically follows from the proof of Theorem 5.3.1 that $\|e_\xi(t)\|_P < \varepsilon_2$. Clearly, this yields to (5.121) using the error transformation $e_\xi(t) = \xi(t)e_{\rm m}(t)$. Hence, the proof is now complete. ■

Remark 5.3.4 *Based on the results shown in Theorem 5.3.2, the user-defined function* $\xi(t), t \geq 0$, *can be chosen such that the adaptation process stops when* $\|e_{\mathrm{m}}(t)\|_P < \frac{\varepsilon_1}{\xi(t)}$, *while enforcing the worst-case time-varying performance bound* $\|e_{\mathrm{m}}(t)\|_P < \frac{\varepsilon_2}{\xi(t)}$. *Furthermore, we also note that if the time rate of change of* $\xi(t), t \geq 0$, *is small, then the modified reference model approximately behaves as the ideal, unmodified reference model. We refer to Remarks 3.2 and 3.3 of [2] for more details on how the modified reference model in* (5.115) *can behave close to the ideal, unmodified reference model in* (5.89) *with proper selection of* $\xi(t), t \geq 0$.

Remark 5.3.5 *The proposed adaptive control architecture of this section for enforcing time-varying performance guarantees with dead-zone effect can also be viewed as an extension of [2, Theorem 3.2] that does not consider dead-zone. In addition, one can also utilize the approach in [2, Theorem 3.1] for enforcing the time-varying bound* $\varepsilon(t), t \geq 0$, *with the required additional assumption that* $\lambda_{\min}(PB\Lambda B^{\mathrm{T}}P)$ *is nonzero. Yet, for the case where* $\lambda_{\min}(PB\Lambda B^{\mathrm{T}}P)$ *is zero, one can readily show that if* $\lambda_{\min}(R) - 2\overline{\varepsilon}\lambda_{\max}(P) > 0$ *holds with* $\overline{\varepsilon} \triangleq \max_{t \in \overline{\mathbb{R}}_+} \frac{\dot{\varepsilon}(t)}{\varepsilon(t)}$, *then the result of [2, Theorem 3.1] still holds and the user-defined time-varying system performance bound* $\varepsilon(t)$ *can be enforced on the system error trajectories (i.e.,* $\|e(t)\|_{\mathrm{P}} < \varepsilon(t)$*).*

Consider the same numerical example in Section 5.3.3.1 with the same nominal feedback gain matrices. We now apply the proposed set-theoretic model reference adaptive control with dead-zone effect in Theorem 5.3.2, where we use the candidate shifted generalized restricted potential function given in Remark 5.3.3 with $\varepsilon_2 = 1$. We also select the user-defined function $\xi(t), t \geq 0$, such that its inverse $(\xi^{-1}(t), t \geq 0)$ changes smoothly from 0.25 to 0.15. This selection allows more deviation at the beginning of the applied command signal $(\xi^{-1}_{\max} = 0.25)$ and then it enforces a tighter bound $(\xi^{-1}_{\min} = 0.15)$ in order to obtain a closer tracking performance by guaranteeing $\|x(t) - x_{\mathrm{r_m}}(t)\|_P < \xi^{-1}(t)$, $t \geq 0$. In addition, we set the projection norm bound imposed on each element of the parameter estimate to $\hat{W}_{\max} = 2$, the learning rate to $\gamma = 1$, and we use $R = 5I$ to calculate P from (5.95) for the resulting A_{r} matrix. Figures 5.49 and 5.50 show the effects of utilizing different user-defined parameter $\varepsilon_1 \in [0, 0.4]$ on the proposed set-theoretic model reference adaptive control with dead-zone effect in Theorem 5.3.2. One can see from these figures that the adaptation process *stops* for small system errors and, once again, the average effective adaptation rate is decreased. ▲

Remark 5.3.6 *The proposed set-theoretic model reference adaptive control architectures with dead-zone effect presented in Sections 5.3.3.1 and 5.3.3.2 utilize user-defined performance bounds* ε_1 *and* ε_2 *such that the adaptation process stops when the system error is small. Furthermore, the continuous nature of the*

proposed shifted generalized restricted potential function avoids, for example, chattering during transitions to/from the dead-zone. We should also note that while the system error trajectory can go between the sets

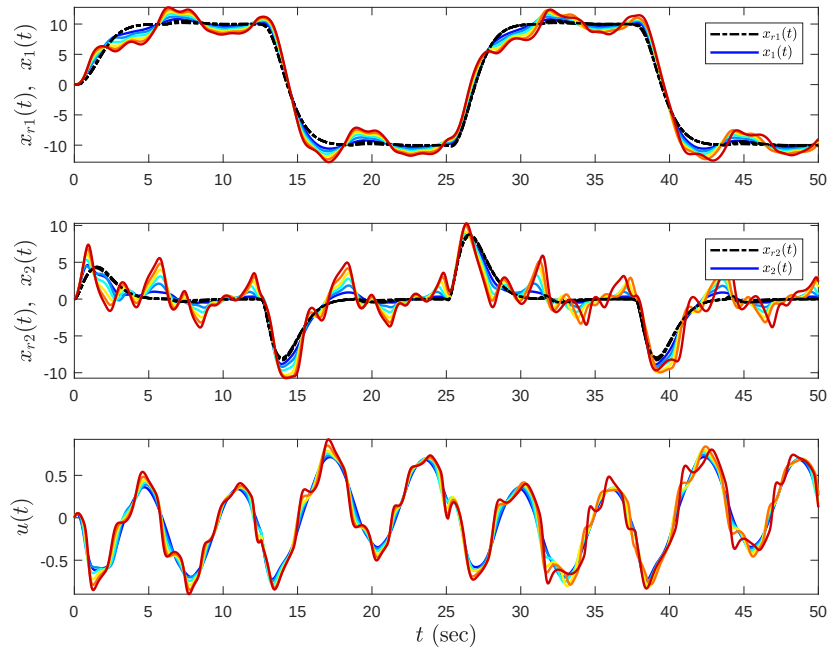

Figure 5.49: Closed-loop system performance with the set-theoretic model reference adaptive control architecture in Theorem 5.3.2 when $\varepsilon_1 \in [0, 0.4]$ (blue to red) and $\varepsilon_2 = 1$.

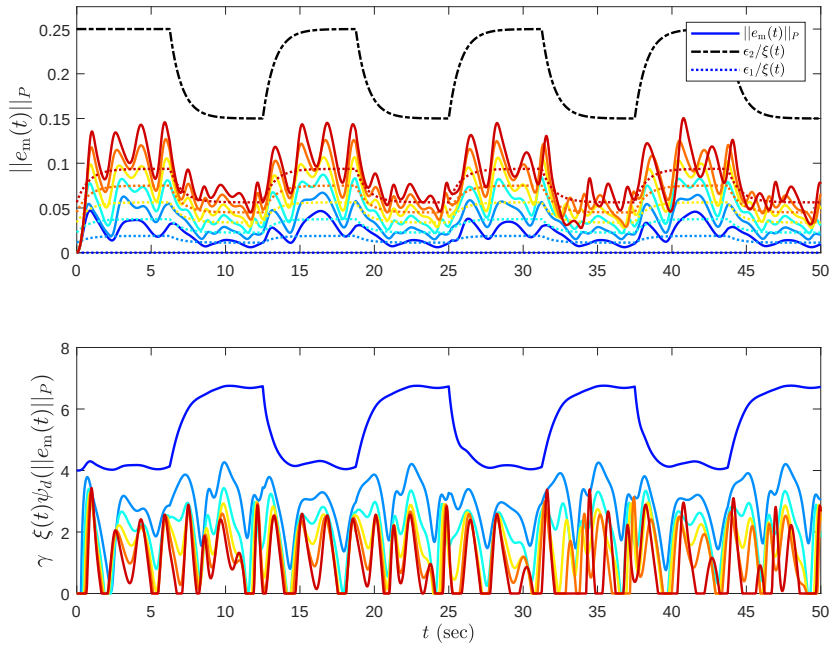

Figure 5.50: History of the system error trajectories and the effective learning rates with the set-theoretic model reference adaptive control architecture in Theorem 5.3.2 when $\varepsilon_1 \in [0, 0.4]$ (blue to red) and $\varepsilon_2 = 1$.

$\mathcal{D}_{\varepsilon_1}$ and $\mathcal{D}_{\varepsilon_2}$ multiple times, the above arguments hold for all these transitions and the energy functions given by (5.104) *and* (5.122) *are guaranteed to be bounded for all time. A graphical representation of these transitions is also depicted in Figure 5.46.*

5.3.4 Experimental Verification

We now present an experimental study on the Quanser AERO platform in dual-rotor helicopter configuration[1] [3] (see Figure 5.51). To begin with the control design, consider the (linearized) model of the this testbed given by

$$J_{\mathrm{p}}\ddot{\theta}(t)+D_{\mathrm{p}}\dot{\theta}(t)+K_{\mathrm{sp}}\theta(t) = \tau_{\mathrm{p}}(t), \quad \theta(0)=\theta_0, \quad t\geq 0, \tag{5.123}$$

$$J_{\mathrm{y}}\ddot{\psi}(t)+D_{\mathrm{y}}\dot{\psi}(t) = \tau_{\mathrm{y}}(t), \quad \psi(0)=\psi_0, \quad t\geq 0. \tag{5.124}$$

In (5.123) and (5.124), $\theta(t), t\geq 0$, is the pitch angle (in radians), $\psi(t), t\geq 0$, is the yaw angle (in radians), J_{p} (respectively, J_{y}) is the total moment of inertia about the pitch (respectively, yaw) axis, D_{p} (respectively, D_{y}) is the damping about the pitch (respectively, yaw) axis, and K_{sp} is the stiffness about the pitch axis. The control torques acting on the pitch and yaw axes satisfy

$$\tau_{\mathrm{p}}(t) = K_{\mathrm{pp}}V_{\mathrm{p}}(t)+K_{\mathrm{py}}V_{\mathrm{y}}(t), \quad t\geq 0, \tag{5.125}$$

$$\tau_{\mathrm{y}}(t) = K_{\mathrm{yp}}V_{\mathrm{p}}(t)+K_{\mathrm{yy}}V_{\mathrm{y}}(t), \quad t\geq 0. \tag{5.126}$$

Figure 5.51: Quanser AERO platform [3].

[1] We have previously evaluated the set-theoretic model reference adaptive control architecture on this aerospace platform in [137] without the dead-zone effect.

In (5.125) and (5.126), $V_{\rm p}(t), t \geq 0$, and $V_{\rm y}(t), t \geq 0$, are the motor voltages applied to the pitch and yaw rotors, respectively, $K_{\rm pp}$ (respectively, $K_{\rm yy}$) is the torque thrust gain from the pitch (respectively, yaw) rotor, and $K_{\rm py}$ (respectively, $K_{\rm yp}$) is the cross-torque thrust gain acting on the pitch (respectively, yaw) from the yaw (respectively, pitch) rotor.

Using (5.123), (5.124), (5.125) and (5.126), one can write the system dynamics in the state space form given by

$$\dot{x}_{\rm p}(t) \;=\; A_{\rm p}x_{\rm p}(t) + B_{\rm p}\Lambda u(t), \quad x_{\rm p}(0) = x_{\rm p0}, \quad t \geq 0, \tag{5.127}$$

with the corresponding matrices

$$A_{\rm p} = \begin{bmatrix} 0 & 0 & 1 & 0 \\ 0 & 0 & 0 & 1 \\ -K_{\rm sp}/J_{\rm p} & 0 & -D_{\rm p}/J_{\rm p} & 0 \\ 0 & 0 & 0 & -D_{\rm y}/J_{\rm y} \end{bmatrix}, \quad B_{\rm p} = \begin{bmatrix} 0 & 0 \\ 0 & 0 \\ K_{\rm pp}/J_{\rm p} & K_{\rm py}/J_{\rm p} \\ K_{\rm yp}/J_{\rm y} & K_{\rm yy}/J_{\rm y} \end{bmatrix}, \tag{5.128}$$

where $x_{\rm p}(t) = [\theta(t), \psi(t), \dot{\theta}(t), \dot{\psi}(t)]^{\rm T} \in \mathbb{R}^4$, $t \geq 0$, denotes the measurable state vector, Λ denotes an introduced uncertain control effectiveness matrix, and $u(t) = [V_{\rm p}(t), V_{\rm y}(t)]^{\rm T} \in \mathbb{R}^2$, $t \geq 0$, denotes the control input. The system parameters are obtained from the Quanser AERO user manual as $J_{\rm p} = 0.0219$ $(\mathrm{kg\,m^2})$, $J_{\rm y} = 0.0220$ $(\mathrm{kg\,m^2})$, $D_{\rm p} = 0.0071$ $(\mathrm{kg\,m^2 s^{-1}})$, $D_{\rm y} = 0.0220$ $(\mathrm{kg\,m^2 s^{-1}})$, $K_{\rm pp} = 0.0011$ $(\mathrm{kg\,m^2 s^{-2} V^{-1}})$, $K_{\rm sp} = 0.0375$ $(\mathrm{kg\,m^2 s^{-2}})$, $K_{\rm yy} = 0.0022$ $(\mathrm{kg\,m^2 s^{-2} V^{-1}})$, $K_{\rm yp} = -0.0027$ $(\mathrm{kg\,m^2 s^{-2} V^{-1}})$, and $K_{\rm py} = 0.0021$ $(\mathrm{kg\,m^2 s^{-2} V^{-1}})$.

To address command following for the pitch and yaw angles, let $c(t) = [c_\theta(t), c_\psi(t)]^{\rm T} \in \mathbb{R}^2$, $t \geq 0$, be given bounded piecewise continuous commands and $x_{\rm c}(t) \in \mathbb{R}^2$, $t \geq 0$, be the integrator state that satisfies the dynamics given by

$$\dot{x}_{\rm c}(t) = E_{\rm p}x_{\rm p}(t) - c(t), \quad x_{\rm c}(0) = x_{\rm c0}, \quad t \geq 0, \quad \text{with} \quad E_{\rm p} = \begin{bmatrix} 1 & 0 & 0 & 0 \\ 0 & 1 & 0 & 0 \end{bmatrix}. \tag{5.129}$$

Next, (5.127) can be augmented with (5.129) as

$$\dot{x}(t) \;=\; Ax(t) + B\Lambda u(t) + B_{\rm r}c(t), \quad x(0) = x_0, \quad t \geq 0, \tag{5.130}$$

where $x(t) \triangleq [x_{\mathrm{p}}^{\mathrm{T}}(t),\ x_{\mathrm{c}}^{\mathrm{T}}(t)]^{\mathrm{T}} \in \mathbb{R}^6$, $t \geq 0$, is the augmented state vector, $x_0 \triangleq [x_{\mathrm{p}0}^{\mathrm{T}}, x_{\mathrm{c}0}^{\mathrm{T}}]^{\mathrm{T}}$, and

$$A \triangleq \begin{bmatrix} A_{\mathrm{p}} & 0_{4\times 2} \\ E_{\mathrm{p}} & 0_{2\times 2} \end{bmatrix} \in \mathbb{R}^{6\times 6}, \tag{5.131}$$

$$B \triangleq \begin{bmatrix} B_{\mathrm{p}}^{\mathrm{T}} & 0_{2\times 2}^{\mathrm{T}} \end{bmatrix}^{\mathrm{T}} \in \mathbb{R}^{6\times 2}, \tag{5.132}$$

$$B_{\mathrm{r}} \triangleq \begin{bmatrix} 0_{4\times 2}^{\mathrm{T}} & -I_{2\times 2} \end{bmatrix}^{\mathrm{T}} \in \mathbb{R}^{6\times 2}. \tag{5.133}$$

We now consider the feedback control law given by

$$u(t) = u_{\mathrm{n}}(t) + u_{\mathrm{a}}(t), \quad t \geq 0, \tag{5.134}$$

where $u_{\mathrm{n}}(t) \in \mathbb{R}^2$, $t \geq 0$, and $u_{\mathrm{a}}(t) \in \mathbb{R}^2$, $t \geq 0$, are the nominal and adaptive control laws, respectively. Moreover, linear quadratic regulator theory is used to design the nominal controller gain matrix with the weighting matrices as $Q = \mathrm{diag}([2,2,0,0,50,50])$ to penalize $x(t)$ and $R = 0.001I_{2\times 2}$ to penalize $u(t)$, resulting in

$$u_{\mathrm{n}}(t) = -Kx(t), \quad t \geq 0, \tag{5.135}$$

with

$$K = \begin{bmatrix} 82.85 & -124.21 & 29.70 & -32.29 & 125.18 & -185.28 \\ 117.26 & 78.55 & 38.95 & 19.04 & 185.28 & 125.18 \end{bmatrix}, \tag{5.136}$$

such that $A_{\mathrm{r}} \triangleq A - BK$ is Hurwitz, $K \in \mathbb{R}^{2\times 6}$. Using (5.134) and (5.135) in (5.130) yields

$$\dot{x}(t) = A_{\mathrm{r}}x(t) + B_{\mathrm{r}}c(t) + B\Lambda\left[u_{\mathrm{a}}(t) + W^{\mathrm{T}}\sigma\big(x(t)\big)\right], \quad x(0) = x_0, \quad t \geq 0, \tag{5.137}$$

where $W \triangleq (\Lambda^{-1} - I_{2\times 2}) \in \mathbb{R}^{2\times 2}$ is an unknown weight matrix and $\sigma\big(x(t)\big) \triangleq Kx(t) \in \mathbb{R}^2$, $t \geq 0$, is a known basis function. In this experimental study, a 30 degree yaw maneuver is considered as the control objective[2], the pitch and yaw motor voltages saturate at 24 V, and the uncertain control effectiveness matrix is set to $\Lambda = 0.1I_{2\times 2}$ (that yields $W = 9I_{2\times 2}$).

[2]From a practical point of view, we pass the desired command through a low-pass filter to generate a smooth yaw command.

Figure 5.52 shows the performance of the nominal controller for command following in the absence of the system uncertainty (i.e., $\Lambda = I_{2\times 2}$ that yields $W = 0_{2\times 2}$). Introducing the uncertain control effectiveness matrix, it is evident from Figure 5.53 that the nominal controller alone yields to an unstable closed-loop dynamical system performance. For all the adaptive controllers discussed below, we use a rectangular projection operator and set the upper and lower projection bounds imposed on each element of the parameter estimate respectively to $\hat{W}_{\text{upper}} = 16I_{2\times 2}$ and $\hat{W}_{\text{lower}} = 2I_{2\times 2}$. Moreover, we use $R = 1.5I_{6\times 6}$ to calculate P from (5.95) for the resulting A_{r} matrix.

5.3.4.1 Evaluation of Standard Model Reference Adaptive Control Method

We begin with evaluating the performance of a standard model reference adaptive control method (i.e., $\phi_d(\|e(t)\|_P) \equiv 1$ in (5.94)); see, for example, [16, 17, 28–30]. Figure 5.54 present the command following performance of the adaptive controller with $\gamma = 1$, where the evolution of norm of the system error and the weight estimation are shown in Figures 5.55. Considering that one designs to achieve a close tracking of the reference system such that the norm of the system error be less than 0.5, this adaptive controller is not able to achieve this requirement with $\gamma = 1$. In order to obtain a better performance, a control designer can increase the adaptation gain. Figures 5.56 and 5.57 show the command following performance

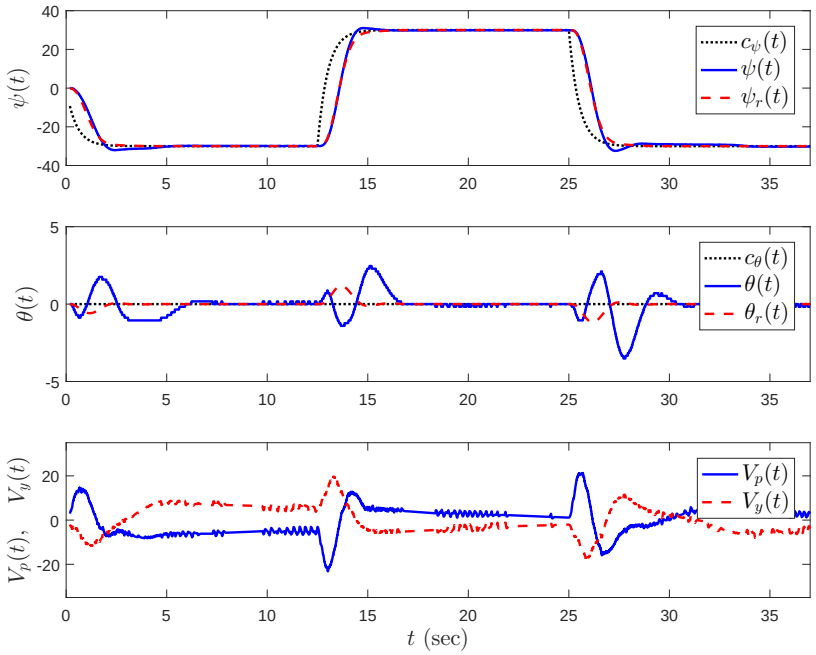

Figure 5.52: Command following performance with the nominal controller in the absence of the system uncertainty.

of the adaptive controller with $\gamma = 5$, where the desired requirement is still not met. By increasing the adaptation rate further to $\gamma = 40$ one can obtain the desired tracking performance as it can be seen from

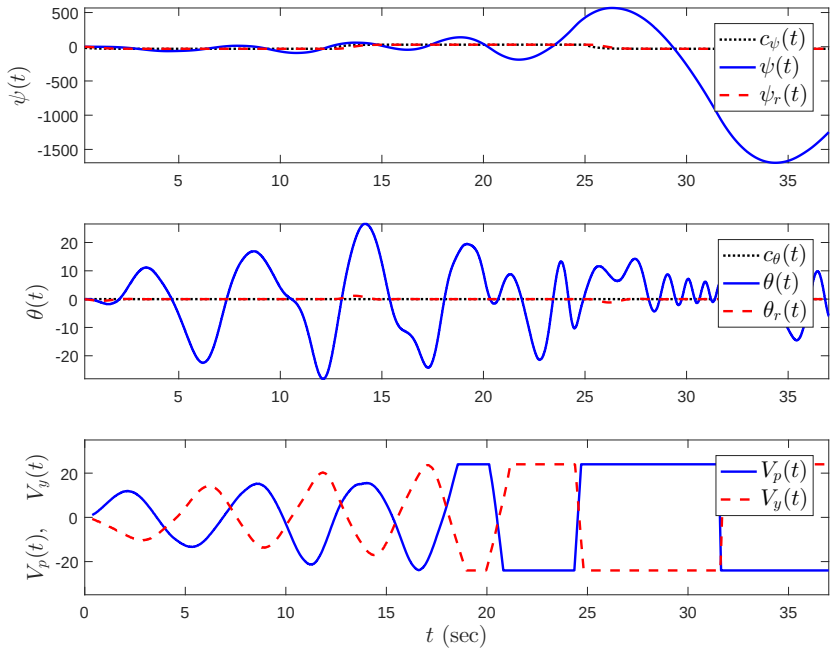

Figure 5.53: Command following performance with the nominal controller in the presence of the system uncertainty.

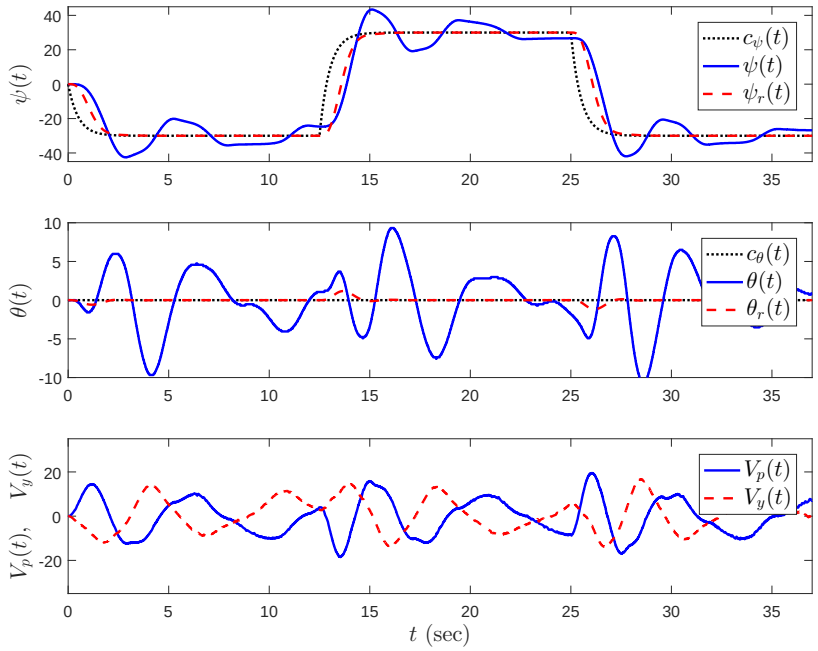

Figure 5.54: Command following performance with the standard model reference adaptive controller (i.e., $\phi_d(\|e(t)\|_P) \equiv 1$ in (5.94)) using $\gamma = 1$.

Figures 5.58 and 5.59. Note that, even though satisfactory results are obtained through an *ad-hoc* tuning process that results in $\gamma = 40$, this performance is *not* guaranteed for different system uncertainties.

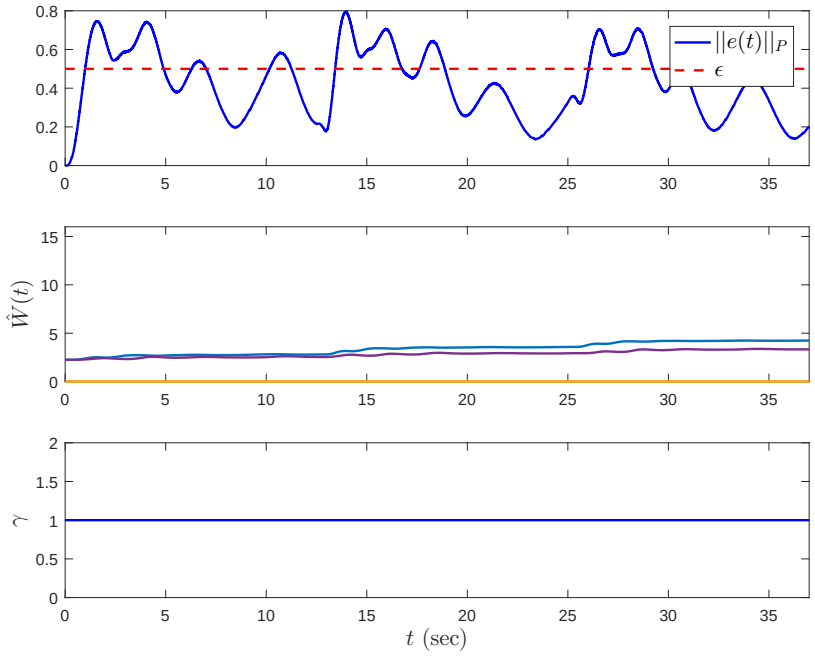

Figure 5.55: Norm of the system error trajectories, the evolution of the weight estimation $\hat{W}(t), t \geq 0$, and the effective learning rate γ with the standard model reference adaptive controller (i.e., $\phi_d(\|e(t)\|_P) \equiv 1$ in (5.94)) using $\gamma = 1$.

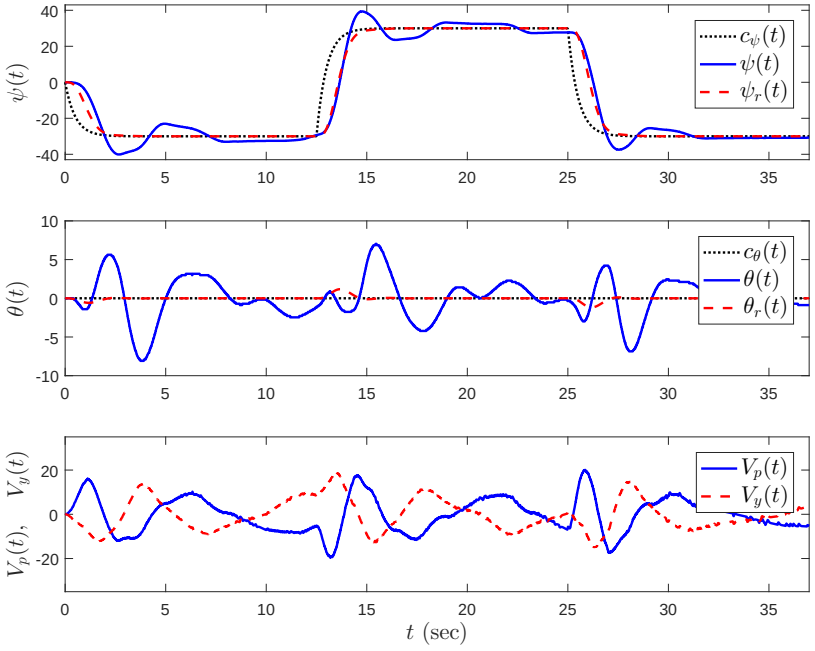

Figure 5.56: Command following performance with the standard model reference adaptive controller (i.e., $\phi_d(\|e(t)\|_P) \equiv 1$ in (5.94)) using $\gamma = 5$.

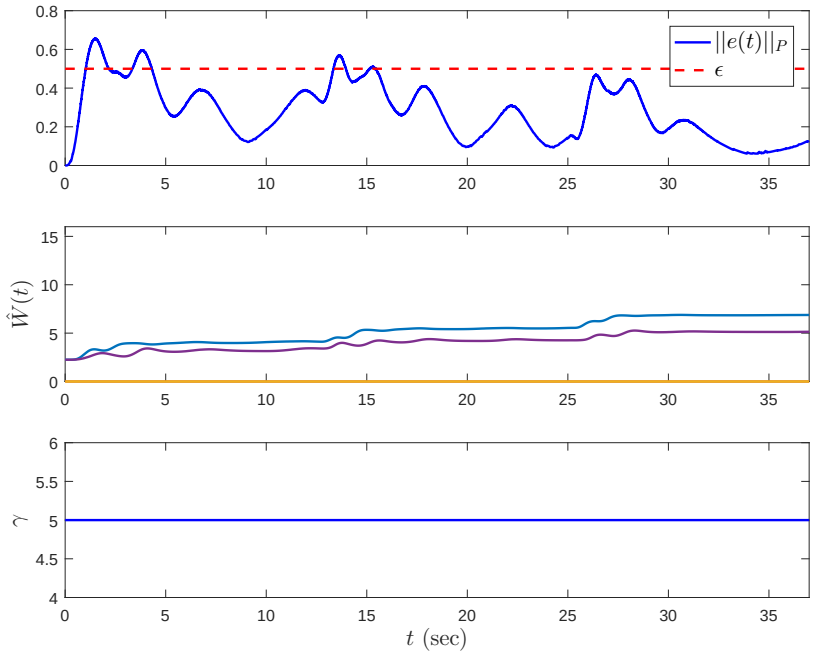

Figure 5.57: Norm of the system error trajectories, the evolution of the weight estimation $\hat{W}(t), t \geq 0$, and the effective learning rate γ with the standard model reference adaptive controller (i.e., $\phi_d(\|e(t)\|_P) \equiv 1$ in (5.94)) using $\gamma = 5$.

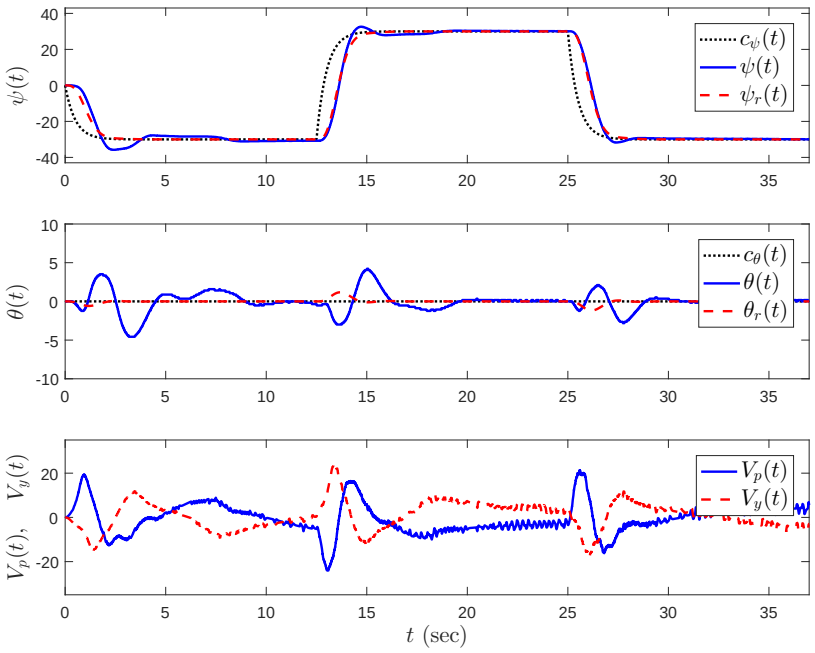

Figure 5.58: Command following performance with the standard model reference adaptive controller (i.e., $\phi_d(\|e(t)\|_P) \equiv 1$ in (5.94)) using $\gamma = 40$.

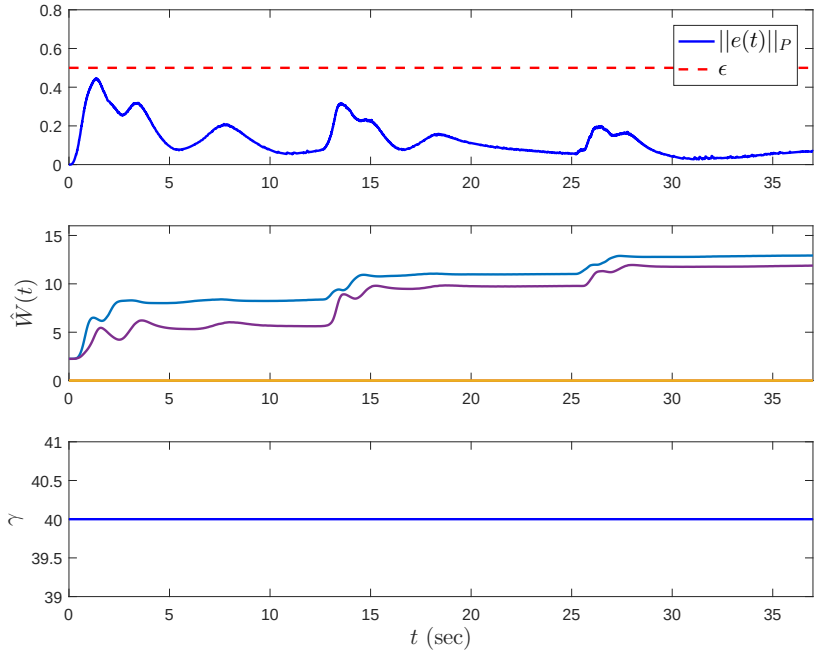

Figure 5.59: Norm of the system error trajectories, the evolution of the weight estimation $\hat{W}(t), t \geq 0$, and the effective learning rate γ with the standard model reference adaptive controller (i.e., $\phi_d(\|e(t)\|_P) \equiv 1$ in (5.94)) using $\gamma = 40$.

5.3.4.2 Evaluation of Standard and Proposed Set-Theoretic Model Reference Adaptive Control Methods with Constant Performance Bounds

We first demonstrate the standard set-theoretic model reference adaptive controller for enforcing strict performance guarantees by utilization of the system error-dependent learning rate $\phi_d(||e(t)||_P)$. Specifically, we use the generalized restricted potential function given in Section 5.3.2.3 with $\varepsilon = 0.5$ and we set the constant learning rate to $\gamma = 5$. Figure 5.60 shows the closed-loop dynamical system performance with the standard set-theoretic model reference adaptive controller concisely overviewed in Section 5.3.2.3, where Figure 5.61 shows the norm of the system error trajectories, the evolution of the weight estimate $\hat{W}(t), t \geq 0$, and the evolution of the effective learning rate. As expected from these figures, the adaptation is always *active* with the standard set-theoretic method.

We next apply the proposed set-theoretic model reference adaptive control with dead-zone effect in Theorem 5.3.1, where we use the new shifted generalized restricted potential function given in Remark 5.3.3 with $\varepsilon_1 = 0.15$ and $\varepsilon_2 = 0.5$ to guarantee $\|x(t) - x_{\mathrm{r}}(t)\|_P < 0.5, t \geq 0$. It can be seen in Figure 5.62 that desired performance is obtained and the evolution of the norm of the system error trajectories, the evolution of the weight estimate $\hat{W}(t), t \geq 0$, and the effective learning rate are depicted in Figure 5.63. The key

feature of the proposed control algorithm in practical applications is evident from Figure 5.63. Specifically, the proposed set-theoretic model reference adaptive control with dead-zone effect stops the adaptation in the set $\mathcal{D}_{\varepsilon_1}$.

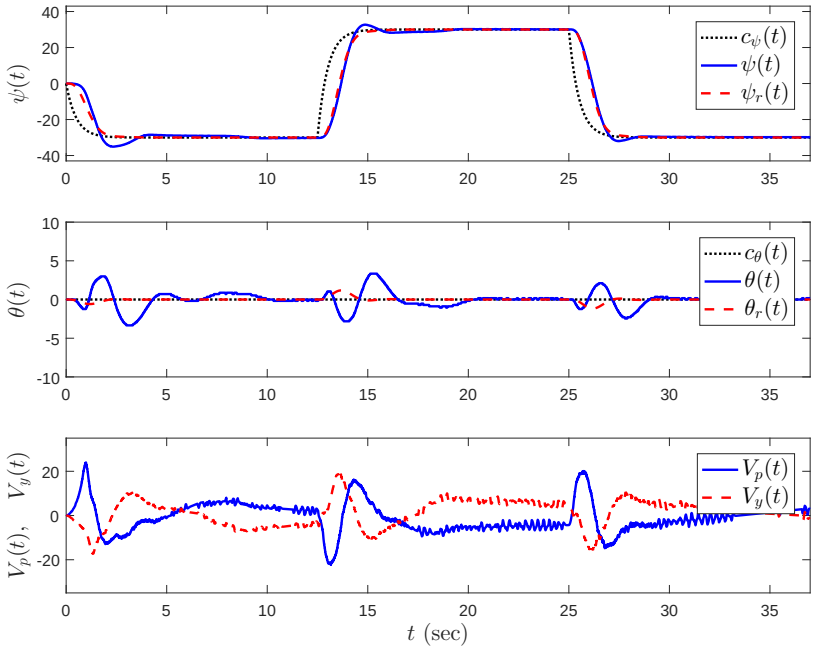

Figure 5.60: Command following performance with the standard set-theoretic model reference adaptive controller [1].

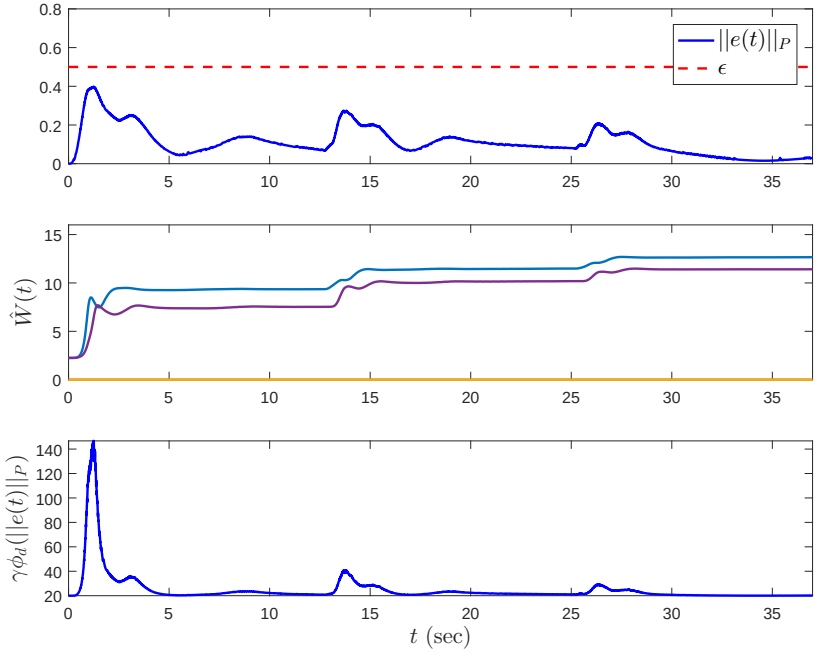

Figure 5.61: Norm of the system error trajectories, the evolution of the weight estimation $\hat{W}(t), t \geq 0$, and the effective learning rate $\gamma\phi_d(\cdot)$ with the standard set-theoretic model reference adaptive controller [1].

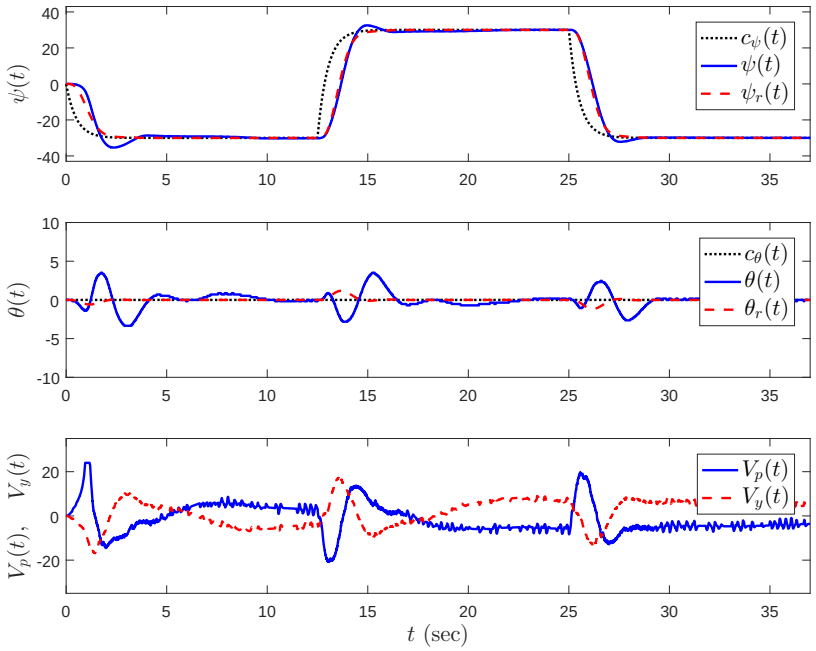

Figure 5.62: Command following performance with the proposed controller in Theorem 5.3.1.

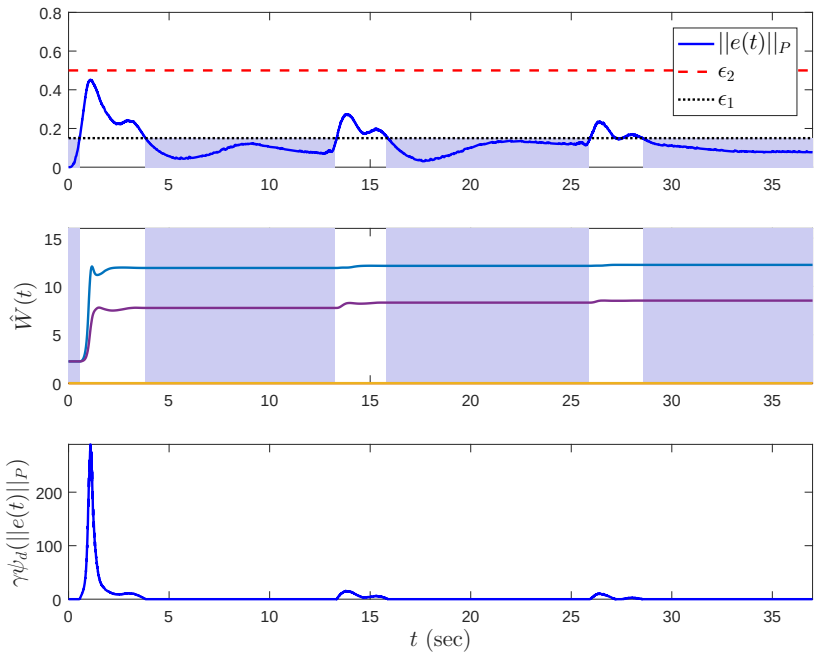

Figure 5.63: Norm of the system error trajectories, the evolution of the weight estimation $\hat{W}(t), t \geq 0$, and the effective learning rate $\gamma\psi_d(\cdot)$ with the proposed controller in Theorem 5.3.1.

5.3.4.3 Evaluation of Standard and Proposed Set-Theoretic Model Reference Adaptive Control Methods with Time-Varying Performance Bounds

We first demonstrate the performance of the standard set-theoretic model reference adaptive controller with time-varying performance bound in [2, Theorem 3.2], we use the shifted generalized restricted potential function given in Remark 5.3.3 with $\varepsilon_1 = 0$ and we set the constant learning rate to $\gamma = 5$. Furthermore, we set $\varepsilon_2 = 1$ and choose the user-defined function $\xi(t), t \geq 0$, such that its inverse $(\xi^{-1}(t), t \geq 0)$ changes smoothly from 0.5 to 0.25 to allow larger deviation at the beginning of the applied command signal $(\xi^{-1}_{\max} = 0.5)$ and then it enforces a tighter bound $(\xi^{-1}_{\min} = 0.25)$ to obtain a closer tracking performance thorough $\|x(t) - x_{\mathrm{r_m}}(t)\|_P < \xi^{-1}(t), t \geq 0$. Figure 5.64 shows the closed-loop dynamical system performance with the standard set-theoretic adaptive controller with time-varying performance bound, where Figure 5.65 shows the norm of the system error trajectories, the evolution of the weight estimate $\hat{W}(t), t \geq 0$, and the evolution of the effective learning rate. Once again, the adaptation is always *active* as it can be seen from these figures.

We finally apply the proposed set-theoretic model reference adaptive control with dead-zone effect in Theorem 5.3.2, where we use the new shifted generalized restricted potential function given in Remark 5.3.3 with $\varepsilon_2 = 1$ and $\varepsilon_1 = 0.3$ such that there is always 30% dead-zone effect in the adaptation process. We

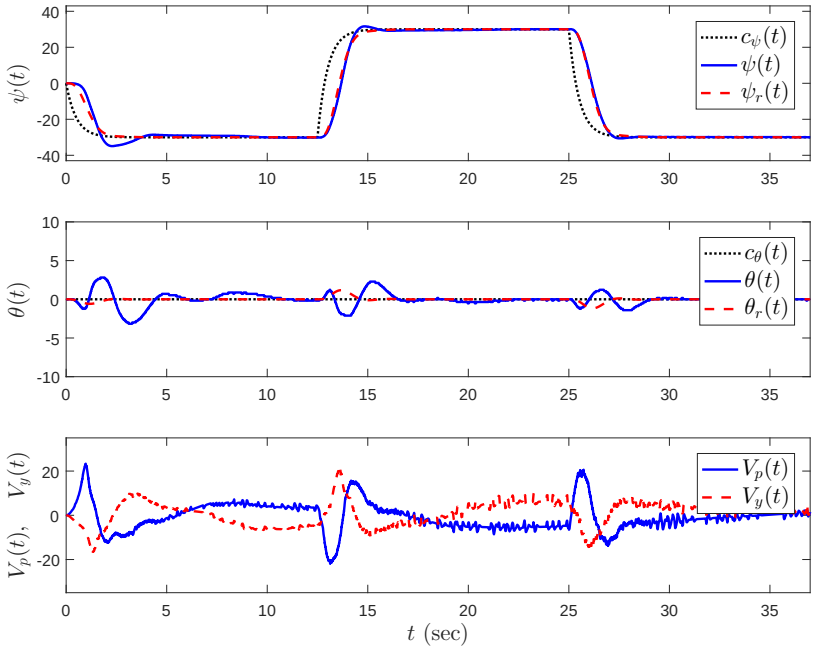

Figure 5.64: Command following performance with the standard set-theoretic model reference adaptive controller with time-varying bound [2].

also select the user-defined function $\xi(t), t \geq 0$, such that its inverse $(\xi^{-1}(t), t \geq 0)$ changes smoothly from 0.5 to 0.25 as explained above to enforce the performance guarantee through $\|x(t) - x_{\mathrm{r_m}}(t)\|_P < \xi^{-1}(t)$, $t \geq 0$. It can be seen in Figure 5.66 that desired performance is obtained and the evolution of the norm

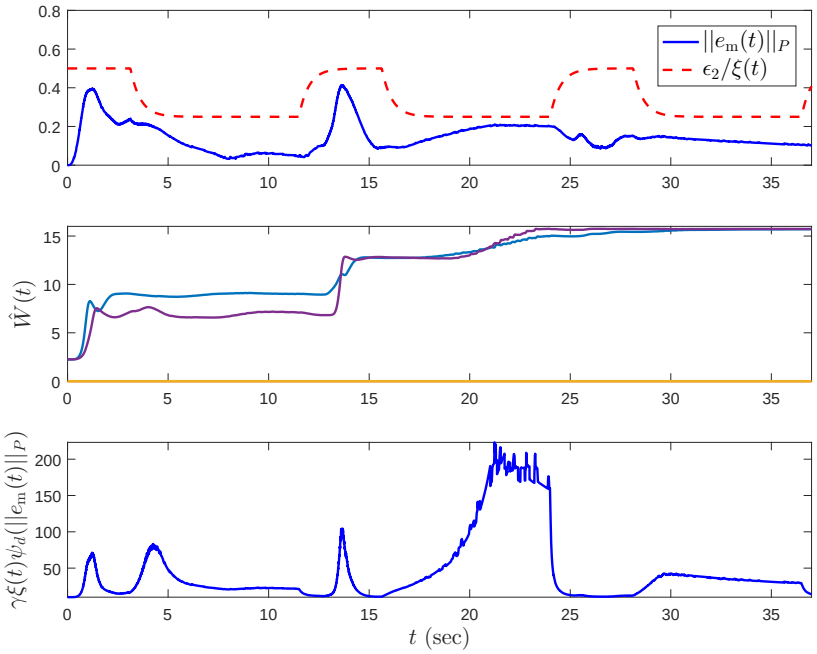

Figure 5.65: Norm of the system error trajectories, the evolution of the weight estimation $\hat{W}(t), t \geq 0$, and the effective learning rate $\gamma\xi(t)\psi_d(\cdot)$ with the standard set-theoretic model reference adaptive controller with time-varying bound [2].

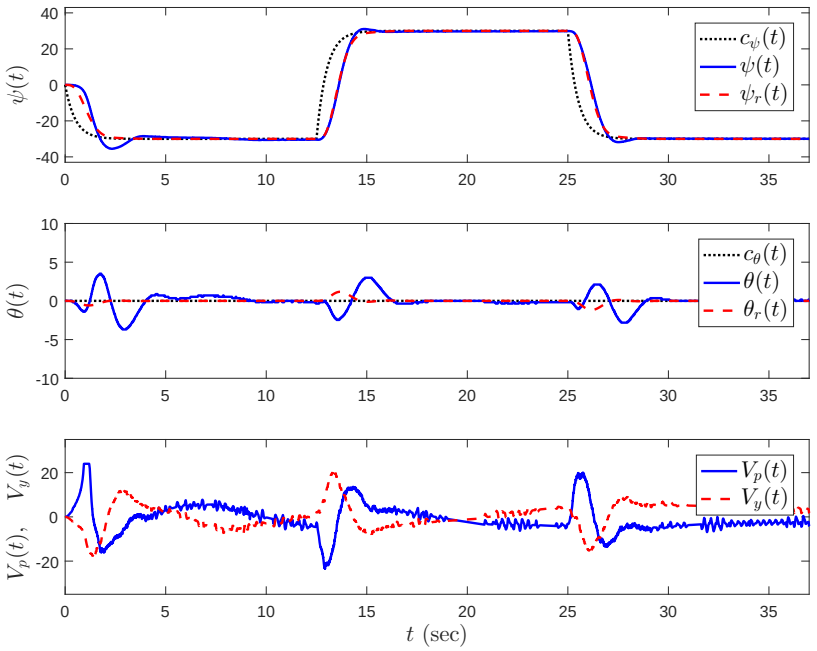

Figure 5.66: Command following performance with the proposed controller in Theorem 5.3.2.

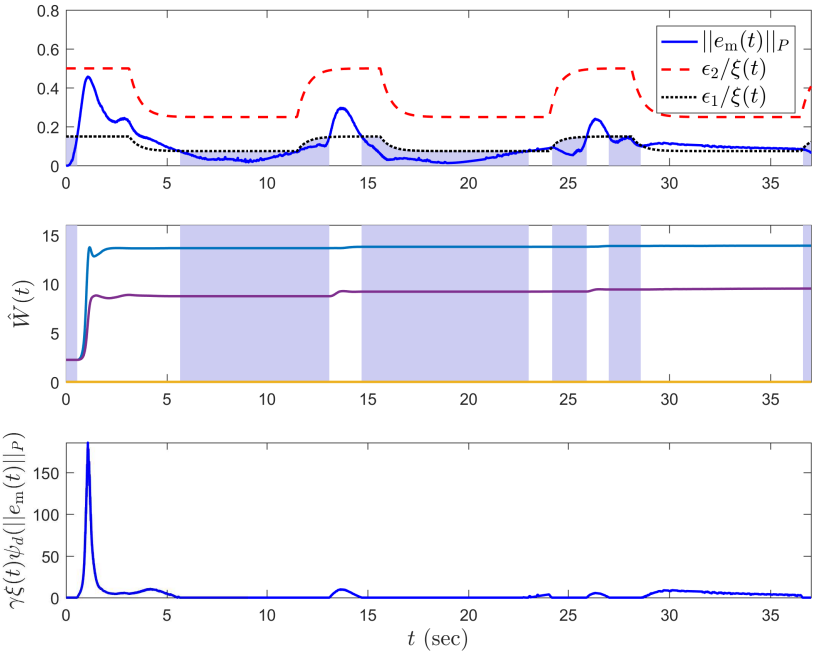

Figure 5.67: Norm of the system error trajectories, the evolution of the weight estimation $\hat{W}(t), t \geq 0$, and the effective learning rate $\gamma\xi(t)\psi_d(\cdot)$ with the proposed controller in Theorem 5.3.2.

of the system error trajectories, the evolution of the weight estimate $\hat{W}(t), t \geq 0$, and the effective learning rate are depicted in Figure 5.67. Once again, the key feature of the proposed control algorithm in practical applications is evident from Figure 5.67, where the proposed set-theoretic model reference adaptive control with dead-zone effect stops the adaptation in the set $\mathcal{D}_{\varepsilon_1}$.

5.3.5 Conclusion

In the presence of small system errors, which often contain high-frequency residual content of exogenous disturbances and/or measurement noise, it is a widely-adopted practice to *stop* the adaptation process in applications of model reference adaptive control algorithms. Specifically, standard model reference adaptive control architectures with fixed learning rates generally use the *common* dead-zone function to *stop* their adaptation in a straightforward fashion; however, they *cannot* enforce user-defined worst-case performance bounds on the closed-loop uncertain dynamical system trajectories, which is necessary for safety-critical applications. While set-theoretic adaptive control architectures have the capability to enforce such bounds, stopping their adaptation process without still violating these worst-case bounds is *not* a theoretically trivial task. To this end, we presented a set-theoretic model reference adaptive control

architecture with *dead-zone effect*. Based on a *continuous shifted generalized restricted potential function*, in particular, we analytically showed that the proposed architecture not only *stops* the learning process inside the *dead-zone* but also allows the norm of the system error to be less than a user-defined constant or time-varying performance bound. In addition to the provided new theoretical findings, we efficacy of the proposed technique was also demonstrated through illustrative numerical examples and, importantly, through an aerospace testbed experimentation.

5.4 Human-in-the-Loop Systems with Inner and Outer Feedback Control Loops: Adaptation, Stability Conditions, and Performance Constraints[4]

In this paper, we focus on human-in-the-loop physical systems with inner and outer feedback control loops. Specifically, our problem formulation considers that inner loop control laws use a model reference adaptive control approach to suppress the effect of system uncertainties such that the overall physical system operates close to its ideal behavior as desired in the presence of adverse conditions due to failures and/or modeling inaccuracies. Moreover, we consider that the outer loop control laws exist owing to employing either sequential loop closure and/or high-level guidance methods. As it is true in practice, in addition, humans are considered to inject commands directly to the outer loop dynamics in response to the changes in the physical system, where the outer loop commands affect inner loop dynamics in response to the commands received from the humans as well as in response to the changes in the physical system.

The presence of humans can result in system instability, even when the resulting physical system augmented with inner and outer feedback control loops yield to stable trajectories in the absence of humans. This paper addresses this problem by proving a sufficient stability condition for the overall physical system with human dynamics modeled as a linear time-invariant system with human reaction time-delay, where this condition does not depend on system uncertainties similar to our recent theoretical results. Furthermore, inner loop system errors during the transient phase of adaptively suppressing system uncertainties can severely affect the human-outer loop interactions. We also address this issue by utilizing a recently proposed set-theoretic model reference adaptive control approach at the inner loop for enforcing a user-defined performance constraint on the norm of the system error trajectories, where we show how the selection of this constraint affects the overall physical system. Finally, the efficacy of our results is demonstrated through an illustrative numerical example for an adaptive flight control application with a Neal-Smith pilot model.

[4]This section has been submitted to the *AIAA Guidance, Navigation, and Control Conference*.

5.4.1 Introduction

This paper focuses on human-in-the-loop physical systems with inner and outer feedback control loops. Building on our recent results documented in [138], our problem formulation considers that inner loop control laws use a model reference adaptive control approach to suppress the effect of system uncertainties such that the overall physical system operates close to its ideal behavior in the presence of adverse conditions due to failures and/or modeling inaccuracies (we refer to [138] and references therein for relevant literature). Specifically, the model reference adaptive control approach of this paper has the capability to enforce performance constraints on the transient system performance (see below), unlike the results in [138]. Moreover, it theoretically augments a general nominal dynamic compensator structure; that is, the nominal control law utilized in [138] becomes a special case of the nominal dynamic compensator considered in this paper. Here, we also explicitly consider outer loop control laws within our problem formulation. From an application standpoint, these outer loop control laws can exist owing to employing either sequential loop closure and/or high-level guidance methods. While the results in [138] can consider entire system dynamics to enforce objectives achieved by such methods, it is well-known that sequential loop closure approaches can ease the control design task through several low-order control laws (see, for example, [139, 140] and references therein) and/or one would like to simply add a guidance algorithm to an existing inner loop feedback control architecture.

As it is true in practice, humans are considered to inject commands directly to the outer loop dynamics in response to the changes in the physical system within our problem formulation, where the outer loop commands affect inner loop dynamics in response to the commands received from the humans as well as in response to the changes in the physical system. In particular, the presence of humans can result in system instability especially due to human reaction time-delays (see, for example, [138, 141–145] and references therein), even when the resulting physical system augmented with inner and outer feedback control loops yield to stable trajectories in the absence of humans. In this paper, we address this problem by proving a sufficient stability condition for the overall physical system with human dynamics modeled as a linear time-invariant system with human reaction time-delay, where this condition does not depend on system uncertainties similar to the results in [138]. Furthermore, inner loop system errors during the transient phase of adaptively suppressing system uncertainties can severely affect the human-outer loop

interactions. This paper also addresses this issue by utilizing a recent model reference adaptive control approach discussed next.

Specifically, with conventional model reference adaptive control algorithms like the one adopted in [138], only a conservative bound on the system errors can be theoretically developed that depends on the bound on the system uncertainties. Thus, without a complete knowledge of the upper bound on the system uncertainties, the adaptively controlled overall system may exhibit unsatisfactory performance (i.e., large system error signal) resulting in poor human-physical system interaction, unless a high adaptation gain is used for all time that may not be practically desirable. To overcome this limitation of conventional model reference adaptive control laws, the authors recently proposed the set-theoretic model reference adaptive control architecture in [1] for achieving time-invariant user-defined performance bounds, where in [2, 108] this framework was further extended to guarantee time-varying user-defined performance bounds. The generalizations of the set-theoretic model reference adaptive control architecture to the unstructured system uncertainties, actuator failures, actuator dynamics were then studied in [1, 93, 101, 102]. Within the scope of this paper, we use this new architecture in [1] for enforcing a user-defined performance constraint on the norm of the system error trajectories, where we explicitly show how the selection of this constraint affects the overall physical system. Finally, the efficacy of the overall human-in-the-loop physical system architecture of this paper with inner and outer feedback control loops is demonstrated through an illustrative numerical example for an adaptive flight control application with a Neal-Smith pilot model.

The organization of this paper is as follows. Section 5.4.2 provides the mathematical preliminaries. Section 5.4.3 presents the problem formulation, where Section 5.4.4 shows the stability and performance guarantees analysis for the overall human-in-the-loop physical system architecture. Section 5.4.5 presents the aforementioned illustrative numerical example, where the conclusions are finally drawn in Section 5.4.6.

5.4.2 Mathematical Preliminaries

5.4.2.1 Notation

The notation used throughout this paper is consistent with our prior work [138]. Specifically, $\mathbb{R}$ denotes the set of real numbers, $\mathbb{C}$ denotes the set of complex numbers, $\mathbb{R}^n$ denotes the set of $n \times 1$ real column vectors, $\mathbb{R}^{n\times m}$ denotes the set of $n \times m$ real matrices, $\mathbb{R}_+$ denotes the set of positive real numbers, $\mathbb{R}_+^{n\times n}$ denotes the set of $n \times n$ positive definite matrices, $\mathbb{D}^{n\times n}$ denotes the set of $n \times n$ real matrices with diagonal scalar entries, $0_{n\times n}$ denotes the $n \times n$ zero matrix, and "$\triangleq$" denotes equality by definition. In

addition, we write $(\cdot)^{\mathrm{T}}$ for the transpose, $(\cdot)^{-1}$ for the inverse, $\mathrm{tr}(\cdot)$ for the trace, $\|\cdot\|_2$ for the Euclidean norm, $\|\cdot\|_{\mathrm{F}}$ for the Frobenius norm, and $\|A\|_2 \triangleq \sqrt{\lambda_{\max}(A^{\mathrm{T}}A)}$ for the induced 2-norm of the matrix $A \in \mathbb{R}^{n\times m}$.

5.4.2.2 Necessary Definitions

The following definitions are used in the main results of this paper.

Definition 5.4.1 ([30, 80]) *Let* $\Omega = \left\{\theta \in \mathbb{R}^n : (\theta_i^{\min} \leq \theta_i \leq \theta_i^{\max})_{i=1,2,\cdots,n}\right\}$ *be a convex hypercube in* $\mathbb{R}^n$, *where* $(\theta_i^{\min}, \theta_i^{\max})$ *represent the minimum and maximum bounds for the* i^{th} *component of the n-dimensional parameter vector* θ. *In addition, for a sufficiently small positive constant* ν, *a second hypercube is defined by* $\Omega_\nu = \left\{\theta \in \mathbb{R}^n : (\theta_i^{\min} + \nu \leq \theta_i \leq \theta_i^{\max} - \nu)_{i=1,2,\cdots,n}\right\}$, *where* $\Omega_\nu \subset \Omega$. *The projection operator* $\mathrm{Proj} : \mathbb{R}^n \times \mathbb{R}^n \to \mathbb{R}^n$ *is then defined componentwise by* $\mathrm{Proj}(\theta, y) \triangleq \left(\frac{\theta_i^{\max} - \theta_i}{\nu}\right) y_i$, *if* $\theta_i > \theta_i^{\max} - \nu$ *and* $y_i > 0$, $\mathrm{Proj}(\theta, y) \triangleq \left(\frac{\theta_i - \theta_i^{\min}}{\nu}\right) y_i$, *if* $\theta_i < \theta_i^{\min} + \nu$ *and* $y_i < 0$, *and* $\mathrm{Proj}(\theta, y) \triangleq y_i$, *otherwise, where* $y \in \mathbb{R}^n$ *[30]. Based on this definition and* $\theta^* \in \Omega_\nu$, *note that*

$$(\theta - \theta^*)^{\mathrm{T}} (\mathrm{Proj}\,(\theta, y) - y) \leq 0, \tag{5.138}$$

holds for $\theta \in \Omega$ *and* $y \in \mathbb{R}^n$*[30, 80]. This definition can be further generalized to matrices as* $\mathrm{Proj}_{\mathrm{m}}(\Theta, Y) = \big(\mathrm{Proj}(\mathrm{col}_1(\Theta), \mathrm{col}_1(Y)), \ldots, \mathrm{Proj}(\mathrm{col}_m(\Theta), \mathrm{col}_m(Y))\big)$, *where* $\Theta \in \mathbb{R}^{n\times m}$, $Y \in \mathbb{R}^{n\times m}$ *and* $\mathrm{col}_i(\cdot)$ *denotes* ith *column operator. In this case, for a given matrix* Θ^* *it follows from* (5.138) *that* $\mathrm{tr}\left[(\Theta - \Theta^*)^{\mathrm{T}}(\mathrm{Proj}_{\mathrm{m}}(\Theta, Y) - Y)\right] = \sum_{i=1}^{m}\left[\mathrm{col}_i(\Theta - \Theta^*)^{\mathrm{T}}(\mathrm{Proj}(\mathrm{col}_i(\Theta), \mathrm{col}_i(Y)) - \mathrm{col}_i(Y))\right] \leq 0$.

Definition 5.4.2 ([1]) *Let* $\|z\|_H = \sqrt{z^{\mathrm{T}}Hz}$ *be a weighted Euclidean norm, where* $z \in \mathbb{R}^p$ *is a real column vector and* $H \in \mathbb{R}_+^{p\times p}$. *We define* $\phi(\|z\|_{\mathrm{H}})$, $\phi : \mathbb{R} \to \mathbb{R}$, *to be a generalized restricted potential function (generalized barrier Lyapunov function) on the set*

$$\mathcal{D}_\varepsilon \triangleq \{z : \|z\|_{\mathrm{H}} \in [0, \varepsilon)\}, \tag{5.139}$$

with $\varepsilon \in \mathbb{R}_+$ *being a-priori, user-defined constant, if the following statements hold [1]: i) If* $\|z\|_{\mathrm{H}} = 0$, *then* $\phi(\|z\|_{\mathrm{H}}) = 0$. *ii) If* $z \in \mathcal{D}_\varepsilon$ *and* $\|z\|_{\mathrm{H}} \neq 0$, *then* $\phi(\|z\|_{\mathrm{H}}) > 0$. *iii) If* $\|z\|_{\mathrm{H}} \to \varepsilon$, *then* $\phi(\|z\|_{\mathrm{H}}) \to \infty$. *iv)* $\phi(\|z\|_{\mathrm{H}})$ *is continuously differentiable on* $\mathcal{D}_\varepsilon$. *v) If* $z \in \mathcal{D}_\varepsilon$, *then* $\phi_d(\|z\|_{\mathrm{H}}) > 0$, *where* $\phi_d(\|z\|_{\mathrm{H}}) \triangleq \mathrm{d}\phi(\|z\|_{\mathrm{H}})/\mathrm{d}\|z\|_{\mathrm{H}}^2$. *vi) If* $z \in \mathcal{D}_\varepsilon$, *then* $2\phi_d(\|z\|_{\mathrm{H}})\|z\|_{\mathrm{H}}^2 - \phi(\|z\|_{\mathrm{H}}) > 0$.

5.4.3 Problem Formulation

In this paper, we consider a human-machine system in which the machine behavior $y(t)$ is observed by the human. Based on this observation, the human then generates a decision and commands the actuator for tracking purposes. To improve the overall tracking performance with the human, instead of direct interaction of the human with the machine, we consider outer and inner control loops with which human commands are properly delegated to the machine to stabilize the error dynamics. To start the control design, consider the block diagram representation of the human-in-the-loop physical systems with inner and outer feedback control loops as given in Figure 5.68. Note that in this setting, the human input (i.e., the reference command) is what the human aims to achieve in a given task and the uncertain dynamical system is the physical system on which this task is being performed. The outer loop architecture then uses the initial command constructed by the human loop and generates the command signal that is fed into the inner loop. The inner loop architecture includes the uncertain dynamical system as well as the model reference adaptive controller components (i.e., the reference model, the parameter adjustment mechanism, and the controller).

In what follows, we provide detailed discussion for each of these three loops. Specifically, we consider the uncertain dynamics representing a physical system given by

$$\dot{x}^*(t) = \begin{bmatrix} A_{\mathrm{p}} & 0_{n_{\mathrm{p}}\times n_{\phi_{\mathrm{p}}}} \\ G_{\mathrm{p}} & F_{\mathrm{p}} \end{bmatrix} x^*(t) + \begin{bmatrix} B_{\mathrm{p}} \\ 0^{\mathrm{T}}_{n_{\mathrm{c}}\times m} \end{bmatrix} \Big(\Lambda u(t) + \delta_{\mathrm{p}}(x_{\mathrm{p}}(t)) \Big), \tag{5.140}$$

where $A_{\mathrm{p}} \in \mathbb{R}^{n_{\mathrm{p}}\times n_{\mathrm{p}}}$, $B_{\mathrm{p}} \in \mathbb{R}^{n_{\mathrm{p}}\times m}$, $F_{\mathrm{p}} \in \mathbb{R}^{n_{\phi_{\mathrm{p}}}\times n_{\phi_{\mathrm{p}}}}$, and $G_{\mathrm{p}} \in \mathbb{R}^{n_{\phi_{\mathrm{p}}}\times n_{\mathrm{p}}}$ are the system matrices, $u(t) \in \mathbb{R}^m$ is the control input, $\delta_{\mathrm{p}} : \mathbb{R}^{n_{\mathrm{p}}} \to \mathbb{R}^m$ is a system uncertainty, $\Lambda \in \mathbb{R}^{m\times m}_{+} \cap \mathbb{D}^{m\times m}$ is an unknown control effectiveness matrix, and we assume that the overall system is controllable. Letting $x^*(t) = [x^{\mathrm{T}}_{\mathrm{p}}(t), \phi^{\mathrm{T}}_{\mathrm{p}}(t)]^{\mathrm{T}} \in \mathbb{R}^{n_{\mathrm{p}}+n_{\phi_{\mathrm{p}}}}$, where $x_{\mathrm{p}}(t) \in \mathbb{R}^{n_{\mathrm{p}}}$ is the primary measurable state vector and $\phi_{\mathrm{p}} \in \mathbb{R}^{n_{\phi_{\mathrm{p}}}}$ is the secondary measurable state vector, one can equivalently write (5.140) as

$$\dot{x}_{\mathrm{p}}(t) = A_{\mathrm{p}}x_{\mathrm{p}}(t) + B_{\mathrm{p}}\Lambda u(t) + B_{\mathrm{p}}\delta_{\mathrm{p}}(x_{\mathrm{p}}(t)), \quad x_{\mathrm{p}}(0) = x_{\mathrm{p}0}, \tag{5.141}$$

$$\dot{\phi}_{\mathrm{p}}(t) = F_{\mathrm{p}}\phi_{\mathrm{p}}(t) + G_{\mathrm{p}}x_{\mathrm{p}}(t), \quad \phi_{\mathrm{p}}(0) = \phi_{\mathrm{p}0}. \tag{5.142}$$

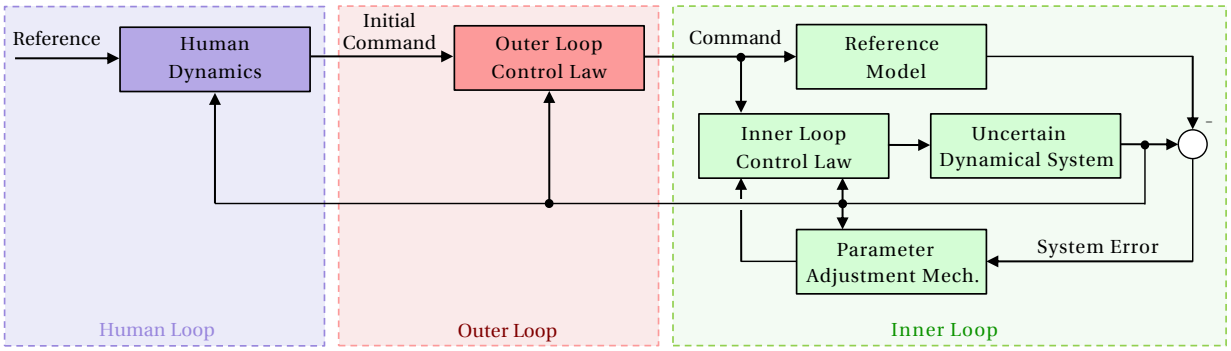

Figure 5.68: Block diagram of the human-in-the-loop model reference adaptive control architecture.

Specifically, we design the controller at the inner loop based on the structure given by (5.141). We then utilize (5.142) to design an outer loop dynamic compensator for generating the command signal that is fed to the inner loop.

5.4.3.1 Inner Loop Architecture

At the inner loop architecture, we consider the uncertain dynamical system given in (5.141) and assume that the system uncertainty $\delta_{\rm p}(x_{\rm p}(t))$ is parameterized as

$$\delta_{\rm p}(x_{\rm p}(t)) \;=\; W_{\rm p}^{\rm T}(t)\sigma_{\rm p}(x_{\rm p}(t)), \tag{5.143}$$

where $W_{\rm p}(t) \in \mathbb{R}^{s\times m}$ is a bounded unknown weight matrix (i.e., $\|W_0(t)\|_{\rm F} \leq w_0$) with a bounded time rate of change (i.e., $\|\dot{W}_0(t)\|_{\rm F} \leq \dot{w}_0$) and $\sigma_{\rm p} : \mathbb{R}^{n_{\rm p}} \to \mathbb{R}^s$ is a known basis function of the form $\sigma_{\rm p}(x_{\rm p}(t)) = [\sigma_{\rm p1}(x_{\rm p}(t)), \sigma_{\rm p2}(x_{\rm p}(t)), \ldots, \sigma_{\rm ps}(x_{\rm p}(t))]^{\rm T}$.

To address command following at the inner loop architecture, let $x_{\rm c}(t) \in \mathbb{R}^{n_{\rm c}}$, be the dynamic compensator state satisfying

$$\dot{x}_{\rm c}(t) \;=\; A_{\rm c}x_{\rm c}(t) + B_{\rm c}e_{\rm p}(t), \quad x_{\rm c}(0) = x_{\rm c0}, \tag{5.144}$$

$$z_{\rm c}(t) \;=\; C_{\rm c}x_{\rm c}(t) + D_{\rm c}e_{\rm p}(t), \tag{5.145}$$

where $A_{\rm c} \in \mathbb{R}^{n_{\rm c}\times n_{\rm p}}$, $B_{\rm c} \in \mathbb{R}^{n_{\rm c}\times n_{\rm y}}$, $C_{\rm c} \in \mathbb{R}^{n_{\rm z}\times n_{\rm c}}$, $D_{\rm c} \in \mathbb{R}^{n_{\rm z}\times n_{\rm y}}$, $z(t) \in \mathbb{R}^z$ is the output of the dynamic compensator, $e_{\rm p}(t) \triangleq y(t) - c(t)$, and $y(t) \triangleq C_{\rm p}x_{\rm p}(t)$ with $C_{\rm p} \in \mathbb{R}^{n_{\rm y}\times n_{\rm p}}$. We now consider the inner loop control law given by

$$u(t) = u_{\rm n}(t) + u_{\rm a}(t), \tag{5.146}$$

where $u_{\rm n}(t) \in \mathbb{R}^m$ and $u_{\rm a}(t) \in \mathbb{R}^m$ are the nominal and adaptive control laws, respectively. Furthermore, let the nominal control law be

$$u_{\rm n}(t) = -K_{\rm p}x_{\rm p}(t) - K_{\rm c}z_{\rm c}(t), \tag{5.147}$$

with $K_{\rm p} \in \mathbb{R}^{m\times n_{\rm p}}$ and $K_{\rm c} \in \mathbb{R}^{m\times n_z}$. Now, (5.141) can be augmented with (5.144) as

$$\dot{x}(t) \;\; = \;\; A_{\rm r}x(t) + B_{\rm r}c(t) + B\Lambda\big(u_{\rm a}(t) + W^{\rm T}(t)\sigma\big(x(t),c(t)\big)\big), \quad x(0) = x_0, \tag{5.148}$$

where $x(t) \triangleq [x_{\rm p}^{\rm T}(t),\ x_{\rm c}^{\rm T}(t)]^{\rm T} \in \mathbb{R}^n$, $n = n_{\rm p} + n_{\rm c}$, is the augmented state vector, $W(t) \triangleq \big[W_{\rm p}^{\rm T}(t),\ (\Lambda^{-1} - I_{m\times m})(K_{\rm p} + K_{\rm c}D_{\rm c}C_{\rm p}),\ (\Lambda^{-1} - I_{m\times m})K_{\rm c}C_{\rm c},\ -(\Lambda^{-1} - I_{m\times m})K_{\rm c}D_{\rm c}\big]^{\rm T} \in \mathbb{R}^{(s+n+n_y)\times m}$ is an unknown (aggregated) weight matrix, $\sigma\big(x(t),c(t)\big) \triangleq [\sigma_{\rm p}^{\rm T}\big(x_{\rm p}(t)\big), x_{\rm p}^{\rm T}(t), x_{\rm c}^{\rm T}(t), c(t)]^{\rm T} \in \mathbb{R}^{s+n+n_y}$ is a known (aggregated) basis function, $x_0 \triangleq [x_{\rm p0}^{\rm T}, x_{\rm c0}^{\rm T}]^{\rm T}$,

$$A_{\rm r} \;\; \triangleq \;\; \begin{bmatrix} A_{\rm p} - B_{\rm p}K_{\rm p} - B_{\rm p}K_{\rm c}D_{\rm c}C_{\rm p} & -B_{\rm p}K_{\rm c}C_{\rm c} \\ B_{\rm c}C_{\rm p} & A_{\rm c} \end{bmatrix} \in \mathbb{R}^{n\times n}, \tag{5.149}$$

$$B_{\rm r} \;\; \triangleq \;\; \begin{bmatrix} B_{\rm p}K_{\rm c}D_{\rm c} \\ -B_{\rm c} \end{bmatrix} \in \mathbb{R}^{n\times n_y} \tag{5.150}$$

$$B \;\; \triangleq \;\; \begin{bmatrix} B_{\rm p}^{\rm T} & 0_{n_{\rm c}\times m}^{\rm T} \end{bmatrix}^{\rm T} \in \mathbb{R}^{n\times m}. \tag{5.151}$$

Considering (5.148), let the adaptive control law be in the form given by

$$u_{\rm a}(t) = -\hat{W}^{\rm T}(t)\sigma\big(x(t),c(t)\big), \tag{5.152}$$

where $\hat{W}(t) \in \mathbb{R}^{(s+n+n_y)\times m}$ is the estimate of $W(t)$. Following the set-theoretic model reference adaptive control architecture presented in [1] (see also [1, 2, 93, 101, 102, 108]), let the update law for (5.152) be given by

$$\dot{\hat{W}}(t) = \gamma{\rm Proj}_{\rm m}\Big(\hat{W}(t), \phi_d(\|e(t)\|_P)\sigma\big(x(t)\big)e^{\rm T}(t)PB\Big), \quad \hat{W}(0) = \hat{W}_0 \tag{5.153}$$

with $\hat{W}_{\max}$ being the projection norm bound. In (5.153), $\gamma \in \mathbb{R}_+$ is the learning rate (i.e., adaptation gain), $P \in \mathbb{R}_+^{n\times n}$ is a solution of the Lyapunov equation given by

$$0 \quad = \quad A_{\mathrm{r}}^{\mathrm{T}}P + PA_{\mathrm{r}} + R, \tag{5.154}$$

with $R \in \mathbb{R}_+^{n\times n}$, and $e(t) \triangleq x(t) - x_{\mathrm{r}}(t)$, is the system error with $x_{\mathrm{r}}(t) \in \mathbb{R}^n$ being the reference state vector of a reference model dynamics at the inner loop that captures a desired inner loop dynamical system performance given by

$$\dot{x}_{\mathrm{r}}(t) \quad = \quad A_{\mathrm{r}}x_{\mathrm{r}}(t) + B_{\mathrm{r}}c(t), \quad x_{\mathrm{r}}(0) = x_{\mathrm{r}0}. \tag{5.155}$$

Using (5.152), (5.153), and (5.155), the inner loop system error dynamics is given by

$$\dot{e}(t) \quad = \quad A_{\mathrm{r}}e(t) - B\Lambda\tilde{W}^{\mathrm{T}}(t)\sigma\big(x(t),c(t)\big), \quad e(0) = e_0, \tag{5.156}$$

$$\dot{\tilde{W}}(t) \quad = \quad \gamma\mathrm{Proj}_{\mathrm{m}}\Big(\hat{W}(t), \phi_d(\|e(t)\|_P)\sigma\big(x(t),c(t)\big)e^{\mathrm{T}}(t)PB\Big) - \dot{W}(t), \quad \tilde{W}(0) = \tilde{W}_0, \tag{5.157}$$

where $\tilde{W}(t) \triangleq \hat{W}(t) - W(t) \in \mathbb{R}^{(s+n+n_y)\times m}$ is the weight estimation error and $e_0 \triangleq x_0 - x_{\mathrm{r}0}$. Once again, we note that the unknown weight matrix $W(t)$ and its derivative have unknown upper bounds (i.e., $\|W(t)\|_{\mathrm{F}} \leq w$ and $\|\dot{W}(t)\|_{\mathrm{F}} \leq \dot{w}$ with unknown w and $\dot{w}$).

Comment 5.4.1 *The update law given by* (5.153) *for the set-theoretic model reference adaptive control architecture can be derived by considering the following energy function*

$$V(e,\tilde{W}) = \phi(\|e\|_P) + \gamma^{-1}\mathrm{tr}\big[(\tilde{W}\Lambda^{1/2})^{\mathrm{T}}(\tilde{W}\Lambda^{1/2})\big]. \tag{5.158}$$

As shown in [1], the time derivative of this energy function is upper bounded by

$$\dot{V}\big(e(t),\tilde{W}(t)\big) \quad \leq \quad -\frac{1}{2}\alpha_1 V(e,\tilde{W}) + \alpha_2, \tag{5.159}$$

where $\alpha_1 \triangleq \frac{\lambda_{\min}(R)}{\lambda_{\max}(P)}$, $d \triangleq 2\gamma^{-1}\tilde{w}\,\dot{w}\|\Lambda\|_2$, $\alpha_2 \triangleq \frac{1}{2}\alpha_1\gamma^{-1}\tilde{w}^2\|\Lambda\|_2 + d$, *and* $\tilde{w} = \hat{W}_{\max} + w$. *In particular,* (5.159) *is sufficient to conclude that* $V(e,\tilde{W})$ *is upper bounded. Hence, one can now conclude with* $\|e_0\|_P < \varepsilon$ *that*

the pair $(e(t),\tilde{W}(t))$ *is bounded and the system error satisfies the strict bound given by*

$$\|e(t)\|_P < \varepsilon, \quad t \geq 0. \tag{5.160}$$

5.4.3.2 Outer Loop Architecture

We now construct the outer loop control law for (5.142). Specifically, consider the dymanic compensator given by

$$\dot{\phi}_{\rm c}(t) = F_{\rm c}\phi_{\rm c}(t) + G_{\rm c}\eta_{\rm p}(t), \quad \phi_{\rm p}(0) = \phi_{\rm p0}, \tag{5.161}$$

$$c(t) = H_{\rm c}\phi_{\rm c}(t) - J_{\rm c}\eta_{\rm p}(t), \tag{5.162}$$

$$\eta_{\rm p}(t) = M_{\rm p}\phi_{\rm p}(t) - c_0(t), \tag{5.163}$$

where $F_{\rm c} \in \mathbb{R}^{n_y \times n_y}$, $G_{\rm c} \in \mathbb{R}^{n_y \times n_{c0}}$, $\eta_{\rm p}(t) \in \mathbb{R}^{n_{c0}}$, $M_{\rm p} \in \mathbb{R}^{n_{c0} \times n_{\phi_{\rm p}}}$, $H_{\rm c} \in \mathbb{R}^{n_y \times n_y}$, $J_{\rm c} \in \mathbb{R}^{n_y \times n_{c0}}$, $\phi_{\rm c}(t) \in \mathbb{R}^{n_y}$ is the outer loop state vector, $c_0(t) \in \mathbb{R}^{n_{c0}}$ is the initial command signal produced by the human, which is the input to the outer loop architecture, and $c(t) \in \mathbb{R}^{n_y}$ is the generated command at the outer loop as shown in Figure 5.68. As discussed earlier, these outer loop dynamics can exist owing to employing either sequential loop closure and/or high-level guidance methods.

Now by letting $\phi(t) = [x_{\rm r}^{\rm T}(t),\ \phi_{\rm p}^{\rm T}(t),\ \phi_{\rm c}^{\rm T}(t)]^{\rm T} \in \mathbb{R}^{n_\phi}$, $n_\phi = n + n_{\phi_{\rm p}} + n_y$, one can write (5.142), (5.155), and (5.161) in a compact form as

$$\dot{\phi}(t) = F_{\rm r}\phi(t) + G_{\rm r}c_0(t) + Ge(t), \quad \phi(0) = \phi_0, \tag{5.164}$$

where

$$F_{\rm r} \triangleq \begin{bmatrix} A_{\rm r} & -B_{\rm r}J_{\rm c}M_{\rm p} & B_{\rm r}H_{\rm c} \\ G_{\rm p}N & F_{\rm p} & 0 \\ 0 & G_{\rm c}M_{\rm p} & F_{\rm c} \end{bmatrix} \in \mathbb{R}^{(n+n_{\phi_{\rm p}}+n_y)\times(n+n_{\phi_{\rm p}}+n_y)}, \tag{5.165}$$

$$G_{\rm r} \triangleq \begin{bmatrix} B_{\rm r}J_{\rm c} \\ 0 \\ -G_{\rm c} \end{bmatrix} \in \mathbb{R}^{(n+n_{\phi_{\rm p}}+n_y)\times n_{c0}}, \quad G \triangleq \begin{bmatrix} 0 \\ G_{\rm p}N \\ 0 \end{bmatrix} \in \mathbb{R}^{(n+n_{\phi_{\rm p}}+n_y)\times n}, \tag{5.166}$$

with $N = [I_{n_p \times n_p}, 0_{n_p \times n_c}]$. Note that F_r should be made a Hurwitz matrix by design to capture stability when $c_0(t)$ is bounded a-priori in the absence of uncertainties; this is discussed in the next comment.

Comment 5.4.2 *If $c_0(t)$ is bounded, then it follows from F_r being Hurwitz and $e(t)$ being bounded (see Comment 5.4.1) that the solution $\phi(t)$ to* (5.164) *is bounded. Yet, since humans make decisions in response to the system states received from the dynamical system as shown in the human loop part of Figure 5.68, $c_0(t)$ cannot be assumed to be a-priori bounded signal. We refer to the next subsection and Section 5.4.4 for more details concerning this point.*

5.4.3.3 Human Loop Architecture

For the human loop, we consider a general class of linear human models with constant time-delay [138]

$$\dot{\xi}(t) = A_h \xi(t) + B_h \theta(t-\tau), \quad \xi(0) = \xi_0 \tag{5.167}$$

$$c_0(t) = C_h \xi(t) + D_h \theta(t-\tau), \tag{5.168}$$

where $\xi(t) \in \mathbb{R}^{n_\xi}$ is the internal human state vector, $\tau \in \mathbb{R}_+$ is the human reaction time-delay, $A_h \in \mathbb{R}^{n_\xi \times n_\xi}$, $B_h \in \mathbb{R}^{n_\xi \times n_r}$, $C_h \in \mathbb{R}^{n_{c0} \times n_\xi}$, and $D_h \in \mathbb{R}^{n_{c0} \times n_r}$. Here, the input to the human dynamics is given by

$$\theta(t) = r(t) - E_h \phi_p(t), \tag{5.169}$$

where $\theta(t) \in \mathbb{R}^{n_r}$, and $r(t) \in \mathbb{R}^{n_r}$ is the bounded reference signal. In (5.169), $E_h \in \mathbb{R}^{n_r \times n}$ selects the appropriate states to be compared with $r(t)$. Note that the dynamics given by (5.167), (5.168) and (5.169) captures a wide range of linear time-invariant human models with time-delay including Neal-Smith model and its extensions [146–150] and is also utilized as-is by the authors of [138] in their analysis.

5.4.4 Stability and Performance Guarantee Analysis

Based on the structure of the inner, outer, and human loops presented in the previous section, we now analyze the closed-loop system performance and show how the system error at the inner loop affects the human loop. We then demonstrate the effectiveness of the set-theoretic model reference adaptive control architecture at the inner loop for guaranteeing a user-defined performance constraint on the norm

of system error trajectory without any knowledge of the upper bound on the system uncertainties, which results in an acceptable human performance in accomplishing a given task. For this purpose, letting $x_0(t) \triangleq [\phi^{\mathrm{T}}(t),\ \xi^{\mathrm{T}}(t)]^{\mathrm{T}} \in \mathbb{R}^{n_0}$, $n_0 \triangleq n_\phi + n_\xi$, one can write the dynamics in (5.164) and (5.167) as

$$\dot{x}_0(t) \quad = \quad A_0 x_0(t) + A_1 x_0(t-\tau) + B_0 r(t-\tau) + B_1 e(t), \quad x_0(t) = \psi_0(t) \quad \text{for} \quad t \in [-\tau,\ 0], \tag{5.170}$$

where $\psi_0(t) \in \mathbb{R}^{n_0}$ is the initial condition and

$$A_0 \quad \triangleq \quad \begin{bmatrix} F_{\mathrm{r}} & G_{\mathrm{r}} C_{\mathrm{h}} \\ 0 & A_{\mathrm{h}} \end{bmatrix} \in \mathbb{R}^{n_0 \times n_0}, \quad A_1 \triangleq \begin{bmatrix} -G_{\mathrm{r}} D_{\mathrm{h}} E_{\mathrm{h}} N_0 & 0 \\ -B_{\mathrm{h}} E_{\mathrm{h}} N_0 & 0 \end{bmatrix} \in \mathbb{R}^{n_0 \times n_0}, \tag{5.171}$$

$$B_0 \quad \triangleq \quad \begin{bmatrix} G_{\mathrm{r}} D_{\mathrm{h}} \\ B_{\mathrm{h}} \end{bmatrix} \in \mathbb{R}^{n_0 \times n_{\mathrm{r}}} \quad , \quad B_1 \triangleq \begin{bmatrix} G \\ 0 \end{bmatrix} \in \mathbb{R}^{n_0 \times n}, \tag{5.172}$$

with $N_0 = [0_{n_{\phi_{\mathrm{p}}} \times n},\ I_{n_{\phi_{\mathrm{p}}} \times n_{\phi_{\mathrm{p}}}},\ 0_{n_{\phi_{\mathrm{p}}} \times n_y}]$. Now, we consider the overall nominal system performance as the case where there is no uncertainty in the system at the inner loop. In other words, the overall performance of the human interacting with the physical system in absence of any uncertainties is viewed as the ideal behavior represented by

$$\dot{\hat{x}}_0(t) \quad = \quad A_0 \hat{x}_0(t) + A_1 \hat{x}_0(t-\tau) + B_0 r(t-\tau), \quad \hat{x}_0(t) = \hat{\psi}_0(t) \quad \text{for} \quad t \in [-\tau,\ 0]. \tag{5.173}$$

Now letting $\tilde{x}(t) \triangleq x_0(t) - \hat{x}(t)$ and using (5.170) and (5.173), the error dynamics can be written as

$$\dot{\tilde{x}}_0(t) \quad = \quad A_0 \tilde{x}_0(t) + A_1 \tilde{x}_0(t-\tau) + B_1 e(t), \quad \tilde{x}_0(t) = \psi(t) \quad \text{for} \quad t \in [-\tau,\ 0], \tag{5.174}$$

where $\psi(t) \triangleq \psi_0(t) - \hat{\psi}_0(t)$.

Comment 5.4.3 *Setting $e(t) = 0$ in* (5.174)*, the nominal system is obtained as*

$$\dot{\tilde{x}}_0(t) \quad = \quad A_0 \tilde{x}_0(t) + A_1 \tilde{x}_0(t-\tau). \tag{5.175}$$

Notice here that the delay term appears only in the state but not in the derivative of the state. This class of dynamics are known as retarded *type [151–153], which exhibits certain continuity properties in their spectrum useful for assessing their stability characteristics. To elaborate on this, let us write the*

characteristic function of the system as

$$f(s, e^{-s\tau}) \triangleq \det[sI - A_0 - A_1 e^{-s\tau}], \tag{5.176}$$

where I is the identity matrix, s is the Laplace variable, and the delay term τ appears in exponentials in the Laplace sense. The zeros of (5.176)*, which are called the* characteristic roots*, determine the stability of the nominal system as follows. The nominal system is asymptotically stable for a given delay $\tau \geq 0$ and system matrices A_0, A_1, if and only if the characteristic roots all lie on the left-half complex plane $s \in \mathbb{C}$ [151].*

Stability of (5.175) *can be assessed with respect to τ by observing certain features of the system characteristic roots. The real part of these roots is continuous with respect to τ and hence as τ is varied, the only way the system can switch from stable to unstable behavior, or vice versa, is that a root touches the imaginary axis at $s = \mp j\omega^*$ for some critical delays $\tau = \tau^*$ [154]. In general, as the critical delay is slightly increased, a pair of complex conjugate roots cross over the imaginary axis. Depending on the direction of crossing, the system will have two more, or two less, unstable roots.*

Considering all the delays causing crossings over the imaginary axis, starting with $\tau = 0$, one can decompose the delay axis into countably many intervals, where the upper/lower boundaries of each interval is determined by τ^*, and neighboring intervals have two or more less unstable roots depending on the direction of crossing of the respective root $s = \mp j\omega^*$. Ultimately, the intervals for which the number of unstable roots is zero are labeled as stable, otherwise unstable. The principle behind this approach is known as the τ-decomposition property [155, 156].

For stability assessment, it is crucial to detect all τ for which system characteristic roots touch the imaginary axis $s = \mp j\omega$. Notice however that this is not a trivial task mainly because the exponential terms in (5.176) *make the system infinite dimensional. That is, there exist infinitely many roots of the system, and accurate and exhaustive detection of those touching the imaginary axis is a challenge. This very likely explains more than six decades of research on this particular problem, see a review in [157]. Without getting into details, here we mention that we will utilize the approach in [158] to compute the imaginary crossings and their corresponding delay values. To compute the rightmost (dominant) roots of the system, we will utilize the TRACE-DDE toolbox [159].*

Comment 5.4.4 (Section 5.6.2, [160]) *Consider a system with single time-delay given by*

$$\dot{z}(t) \;=\; A_0 z(t) + A_1 z(t-\tau), \quad z(t) = \psi(t) \;\; \textit{for} \;\; t \in [-\tau,\, 0], \tag{5.177}$$

where $z(t) \in \mathbb{R}^n$ is the system state, $A_0 \in \mathbb{R}^{n\times n}$ and $A_1 \in \mathbb{R}^{n\times n}$ are constant matrices, and τ is a positive time-delay. Then, its solution satisfies

$$z(t,\psi) \;=\; \Psi(t)\psi(0) + \int_{-\tau}^{0} \Psi(t-\tau-\theta) A_1 \psi(\theta)\mathrm{d}\theta, \quad t \geq 0, \tag{5.178}$$

where $\Psi(t) \in \mathbb{R}^{n\times n}$ is the fundamental solution satisfying

$$\dot{\Psi}(t) \;=\; A_0\Psi(t) + A_1\Psi(t-\tau), \quad t \geq 0, \tag{5.179}$$

and the initial condition $\Psi(0) = I$ and $\Psi(t) = 0$ for $t < 0$. Furthermore, assuming that the system given by (5.177) *is asymptotically stable, then there exist an $\alpha > 0$ such that*

$$\|\Psi(t)\|_2 \leq K e^{-\alpha t}, \quad t \geq 0, \tag{5.180}$$

for some $K > 1$.

Let us now apply Comment 5.4.4 to bound the error dynamics in (5.174). For this, one first needs to guarantee that the nominal system ($e(t) = 0$) must be asymptotically stable. This can be assessed from Comment 5.4.3. Under asymptotic stability assumption, notice that the fundamental solution $\Psi(t)$ of the nominal system respects (5.180). Therefore, the solution of the error dynamics in (5.174)

$$\tilde{x}(t,\psi) \;=\; \Psi(t)\psi(0) + \int_{-\tau}^{0} \Psi(t-\tau-\theta) A_1 \psi(\theta)\mathrm{d}\theta + \int_{0}^{t} \Psi(t-r) B_1 e(r)\mathrm{d}r, \quad t \geq 0, \tag{5.181}$$

can be bounded by

$$\begin{aligned}
\|\tilde{x}(t,\psi)\|_2 \;&\leq\; K e^{-\alpha t}\|\psi(0)\|_2 + K\int_{-\tau}^{0} e^{-\alpha(t-\tau-\theta)}\|A_1\psi(\theta)\|_2\mathrm{d}\theta + K\int_{0}^{t} e^{-\alpha(t-r)}\|B_1 e(r)\|_2\mathrm{d}r, \\
&\leq\; K e^{-\alpha t}\|\psi(0)\|_2 + K\|A_1\|_2\big(\sup_{-\tau\leq\theta\leq 0}\psi(\theta)\big)\int_{-\tau}^{0} e^{-\alpha(t-\tau-\theta)}\mathrm{d}\theta \\
&\quad + K\|B_1\|_2\big(\sup_{0\leq r\leq t} e(r)\big)\int_{0}^{t} e^{-\alpha(t-r)}\mathrm{d}r.
\end{aligned} \tag{5.182}$$

Solving the integrals in (5.182) now results in

$$\|\tilde{x}(t,\psi)\|_2 \leq Ke^{-\alpha t}\|\psi(0)\|_2 + \frac{K}{\alpha}\left[\|A_1\|_2 e^{-\alpha t}\left(e^{\alpha\tau}-1\right)\sup_{-\tau\leq\theta\leq 0}\psi(\theta) + \|B_1\|_2\left(1-e^{-\alpha t}\right)\sup_{0\leq r\leq t}e(r)\right]. \tag{5.183}$$

We now evaluate (5.183) in a worst-case setting. That is, one can write

$$\|\tilde{x}(t,\psi)\|_2 \leq K\|\psi(0)\|_2 + \frac{K}{\alpha}\left[\|A_1\|_2\left(e^{\alpha\tau}-1\right)\sup_{-\tau\leq\theta\leq 0}\psi(\theta) + \|B_1\|_2\sup_{0\leq r\leq t}e(r)\right], \tag{5.184}$$

from (5.183). Finally, it also follows from (5.160) that

$$\|e(t)\|_2 < \frac{\varepsilon}{\sqrt{\lambda_{\min}(P)}}. \tag{5.185}$$

Thus, (5.184) can be further simplified as

$$\|\tilde{x}(t,\psi)\|_2 \leq K\|\psi(0)\|_2 + \frac{K}{\alpha}\left[\|A_1\|_2\overline{\psi}\left(e^{\alpha\tau}-1\right) + \|B_1\|_2\frac{\varepsilon}{\sqrt{\lambda_{\min}(P)}}\right], \tag{5.186}$$

where $\overline{\psi} \triangleq \sup_{-\tau\leq\theta\leq 0}\psi(\theta)$.

Comment 5.4.5 *Without loss of generality, we assume that the the initial condition of the system in* (5.170) *is equal to that of the ideal behavior of the system in* (5.173) *(i.e.* $\psi_0(t) = \hat{\psi}_0(t)$ *for* $t \in [-\tau,\ 0]$*) or, equivalently,* $\psi(t) \equiv 0$ *for* $t \in [-\tau,\ 0]$ *and* $\overline{\psi} = 0$*. Therefore, one can rewrite* (5.186) *as*

$$\|\tilde{x}(t,\psi)\|_2 \leq \varepsilon\mu, \qquad \mu \triangleq \frac{K\|B_1\|_2}{\alpha\sqrt{\lambda_{\min}(P)}}. \tag{5.187}$$

The upper bound on the error signal $\tilde{x}(t,\psi)$ *obtained in* (5.187) *implies that the user-defined performance parameter* ε *can be utilized to control the deviation of the system from the ideal behavior in* (5.173)*.*

5.4.5 Illustrative Numerical Example

In this section, we demonstrate the efficacy of the presented architecture for an adaptive flight control application with a Neal-Smith pilot model. For this purpose, consider the linearized longitudinal flight dynamics of a generic hypersonic vehicle [140, 161] given by

$$\dot{x}_{\mathrm{g}} = A_{\mathrm{g}} x_{\mathrm{g}} + B_{\mathrm{g}} u_{\mathrm{g}}, \tag{5.188}$$

where $x_{\mathrm{g}} = [v(t),\ \alpha(t),\ q(t),\ \theta(t)]^{\mathrm{T}} \in \mathbb{R}^4$, with $v(t)$ being the velocity in feet per second, $\alpha(t)$ being the angle of attack in radians, $q(t)$ being the pitch rate in radians per second, and $\theta(t)$ being the pitch angle in radians. In addition, $u_{\mathrm{g}} = [u_{\mathrm{th}}(t),\ u_{\mathrm{e}}(t)]^{\mathrm{T}}$, where $u_{\mathrm{th}}(t)$ denotes the throttle equivalence ratio, and $u_{\mathrm{e}}(t)$ denotes the elevator deflection angle in degrees. The system matrices in (5.188) for steady level flight condition of Mach 6 and an altitude of 80,000 feet are given by

$$A_{\mathrm{g}} = \begin{bmatrix} -0.0037 & -0.7169 & 0 & -31.818 \\ 0 & -0.2398 & 1 & 0 \\ 0 & 4.5689 & -0.1189 & 0 \\ 0 & 0 & 1 & 0 \end{bmatrix}, \quad B_{\mathrm{g}} = \begin{bmatrix} 27.262 & 0.06525 \\ 0 & -0.0001 \\ 0 & -0.18561 \\ 0 & 0 \end{bmatrix}. \tag{5.189}$$

One can simplify this dynamics [140] and obtain the decoupled velocity dynamics given by

$$\dot{v}(t) = a_v v(t) + b_v u_{\mathrm{th}}, \tag{5.190}$$

with $a_v = -0.0037$ and $b_v = 27.262$, and the decoupled longitudinal dynamics given by

$$\dot{x}^*(t) = \begin{bmatrix} A_{\mathrm{p}} & 0_{2\times 2} \\ G_{\mathrm{p}} & F_{\mathrm{p}} \end{bmatrix} x^*(t) + \begin{bmatrix} B_{\mathrm{p}} \\ 0_{2\times 1} \end{bmatrix} \Big(\Lambda u_{\mathrm{e}}(t) + \delta_{\mathrm{p}}(x_{\mathrm{p}}(t)) \Big), \tag{5.191}$$

where $x^*(t) = [x_{\mathrm{p}}^{\mathrm{T}}(t), \phi_{\mathrm{p}}^{\mathrm{T}}(t)]^{\mathrm{T}} \in \mathbb{R}^3$ with $x_{\mathrm{p}}(t) = [\alpha(t),\ q(t)]^{\mathrm{T}} \in \mathbb{R}^2$, $\phi_{\mathrm{p}}(t) = \theta(t) \in \mathbb{R}$, and

$$A_{\mathrm{p}} = \begin{bmatrix} -0.2398 & 1 \\ 4.5689 & -0.1189 \end{bmatrix}, \quad B_{\mathrm{p}} = \begin{bmatrix} -0.0001 \\ -0.18561 \end{bmatrix}, G_{\mathrm{p}} = \begin{bmatrix} 0 & 1 \end{bmatrix}, \quad F_{\mathrm{p}} = 0. \tag{5.192}$$

In (5.191), $\delta_{\mathrm{p}}(x_{\mathrm{p}}(t))$ represents an uncertainty of the form given in (5.143) with

$$W_{\mathrm{p}}(t) = [20\sin(0.05t),\ -5,\ 20]^{\mathrm{T}}, \quad \sigma_{\mathrm{p}}(x_{\mathrm{p}}(t)) = [\alpha(t),\ q(t),\ \alpha(t)q(t)]^{\mathrm{T}}, \tag{5.193}$$

and $\Lambda = 0.25$ represents the uncertain control effectiveness.

Based on the model simplifications mentioned above, the control loop for the velocity dynamics can be designed independent from the longitudinal dynamics. For this purpose, we consider the velocity dynamics in (5.190) and we let $x_{\rm vc}(t) \in \mathbb{R}$ to be a velocity integrator state satisfying

$$\dot{x}_{\rm cv}(t) \quad = \quad v(t) - c_v(t), \quad x_{\rm vc}(0) = 0, \tag{5.194}$$

such that the velocity can track the desired command $c_v(t)$. Considering this integral state, one can now defined the augmented state vector as $x_v(t) \triangleq [v(t),\ x_{\rm cv}(t)]^{\rm T}$, and write

$$\dot{x}_v(t) \quad = \quad \begin{bmatrix} a_v & 0 \\ 1 & 0 \end{bmatrix} x_v(t) + \begin{bmatrix} b_v \\ 0 \end{bmatrix} u_{\rm th}(t) + \begin{bmatrix} 0 \\ -1 \end{bmatrix} c_v(t), \quad x_v(0) = 0. \tag{5.195}$$

Linear quadratic regulator theory is used to design the nominal controller gain matrix for the velocity dynamics with the weighting matrices as $Q_v = {\rm diag}([10,\ 1])$ to penalize $x_v(t)$ and $R_v = 10$ to penalize $u_{\rm th}(t)$ resulting in $u_{\rm th}(t) = -K_v x_v(t)$ with

$$K_v = \begin{bmatrix} 1.0114 & 0.3162 \end{bmatrix}. \tag{5.196}$$

In what follows, we design the controller for $u_{\rm e}(t)$ and provide the necessary details. Specifically, the control objective considered in this simulation is for the generic hypersonic vehicle to track the pitch angle $\theta_{\rm cmd}(t)$ as commanded by the human. Therefore, the human is generating a pitch angle command (i.e., $c_0(t) = \theta_{\rm cmd}(t)$), where the outer loop utilizes this command to generate the pitch rate command (i.e., $c(t) = q_{\rm cmd}(t)$). Then, using this pitch rate command, the inner loop generates the elevator command signal so that the system can track the desired pitch angle.

5.4.5.1 Inner Loop Control Design

For command following at the inner loop using the pitch rate command $q_{\rm cmd}(t)$ generated by the outer loop, we consider the dynamic compensator in (5.144) and (5.145) with $A_{\rm c} = 0$, $B_{\rm c} = 1$, $C_{\rm c} = 1$, $D_{\rm c} = 0$, and $C_{\rm p} = [0 \quad 1]$. We next use linear quadratic regulator theory to design the nominal controller gain matrix with the weighting matrices as $Q_{\rm i} = {\rm diag}([5,\ 5,\ 10])$ to penalize $x(t)$ and $R_{\rm i} = 0.01$ to penalize $u_{\rm e}(t)$ resulting in $K_{\rm p} = [-36.3125,\ -34.4585]$, and $K_{\rm c} = -31.6228$ in (5.147). For the set-theoretic model

reference adaptive control architecture at the inner loop, we use the generalized restricted potential function given by $\phi(\|e(t)\|_P) = \|e(t)\|_P^2/\big(\varepsilon - \|e(t)\|_P\big)$, $e(t) \in \mathcal{D}_\varepsilon$, having the partial derivative $\phi_d(\|e(t)\|_P) = \big(\varepsilon - \frac{1}{2}\|e(t)\|_P\big)/\big(\varepsilon - \|e(t)\|_P\big)^2$, $e(t) \in \mathcal{D}_\varepsilon$, that satisfies all of the conditions given in Definition 5.4.2 [1]. Furthermore, we choose $\gamma = 1$, set the projection norm bound imposed on each element of the parameter estimate to $\hat{W}_{\max} = 80$, use $R = I$ to calculate P from (5.154) for the resulting A_{r} matrix, and set $\varepsilon = 0.1$ such that the set-theoretic model reference adaptive control guarantees $||e(t)||_P < 0.1$.

5.4.5.2 Outer Loop Control Design

The outer loop utilizes the pitch command $\theta_{\mathrm{cmd}}(t)$ from the human loop to generate the pitch rate command $q_{\mathrm{cmd}}(t)$ that is fed to the inner loop. For this purpose, we consider the feedback controller from $\theta_{\mathrm{cmd}}(t)$ to $q_{\mathrm{cmd}}(t)$ given by [140]

$$G_{\theta q} = k_{\theta q}\frac{s + z_{\theta q}}{s + p_{\theta q}}. \tag{5.197}$$

For this numerical example, we set $k_{\theta q} = 5$, $z_{\theta q} = 1$, and $p_{\theta q} = 4$.

5.4.5.3 Human Loop Transfer Function

To generate the pith command $\theta_{\mathrm{cmd}}(t)$ at the human loop, we assume that the considered generic hypersonic vehicle is operated by a pilot whose Neal-Smith model is given by [146]

$$G_{h\theta} = k_p\frac{T_p s + 1}{T_z s + 1}e^{-\tau s}, \tag{5.198}$$

where k_p is the positive scalar pilot gain, T_p and T_z are positive scalar time constants, and τ is the pilot reaction time-delay. For the sake of this numerical example we set $k_p = 0.5$, $T_p = 1$, $T_z = 5$ and $\tau = 0.5$.

5.4.5.4 Simulation Results

We first construct the matrices A_0 and A_1 in Comment 5.4.3 to assess asymptotic stability with respect to delay τ. To start with, it is easy to show that the delay-free system ($\tau = 0$) is asymptotically stable since $A_0 + A_1$ is a Hurwitz matrix. Next, we investigate following from [158] whether or not a characteristic root $s = \mp j\omega$ can touch the imaginary axis for some delay $\tau > 0$. Suppressing the details, we find out that

there exists no $\tau > 0$ that can cause a root on the imaginary axis. This implies that system stability will never be lost. That is, we have delay-independent stability. Consequently, the theoretical results for obtaining the upper bound on the error signal $\tilde{x}(t, \psi)$ in Section 5.4.4 can be validated in simulations for any delay.

Figures 5.69 and 5.70 show the pitch command following performance with the nominal controller in the absence of any system uncertainties, where it is clear from Figures 5.71 and 5.72 that once the uncertainties are introduced to the system, the nominal controller is not able to achieve the desired performance and the system becomes unstable. Next, we show the command following performance with the standard adaptive control architecture at the inner loop. As mentioned earlier, without the knowledge of the upper bound on the system uncertainties, an appropriate adaptation gain cannot be set a priori. Therefore, as one can see from Figures 5.73 to 5.75, while the standard model reference adaptive control architecture can stabilize the system, the desired level of system performance (i.e., $||e(t)||_P < 0.1$) cannot be guaranteed. Specifically, since a low adaptation gain $\gamma = 1$ is utilized, the standard model reference adaptive controller exhibits poor transient performance as the angle of attack reaches to over 20 degrees, pitch angle reaches to over 30 degrees, and the pitch rate reaches to over 40 degrees per second during the transient time. Furthermore, Figures 5.76 to 5.78 illustrate the effect of having different human reaction time-delays on the command following performance using this architecture. Once again, we note that, although increasing the adaptation gain can improve the transient performance in this setting, one can not set a suitable adaptation gain at the pre-design stage without a complete knowledge of the upper bound on the system uncertainties. Alternatively, if a very large adaptation gain is used for all time, the adaptive control system can excite the high-frequency content of the system.

Next, we utilize the set-theoretic model reference adaptive control at the inner loop to enforce the desired system performance $||e(t)||_P < 0.1$. Figures 5.79 to 5.81 present the command following performance with this controller. It can be seen from these figures that the transient performance is greatly improved compared to Figures 5.73 to 5.75. In particular, the set-theoretic model reference architecture at the inner loop is now enabling the overall control system to achieve the desired level of system performance (i.e., $||e(t)||_P < 0.1$) through increasing the effective adaptation gain based on the norm of system error. Finally, Figures 5.82 to 5.84 present the effect of having different human reaction time-delays on the command following performance using the set-theoretic model reference adaptive control at the inner loop. It is evident from these figures that the proposed control architecture can guarantee a desired level of system performance even in the presence of large human reaction time-delays.

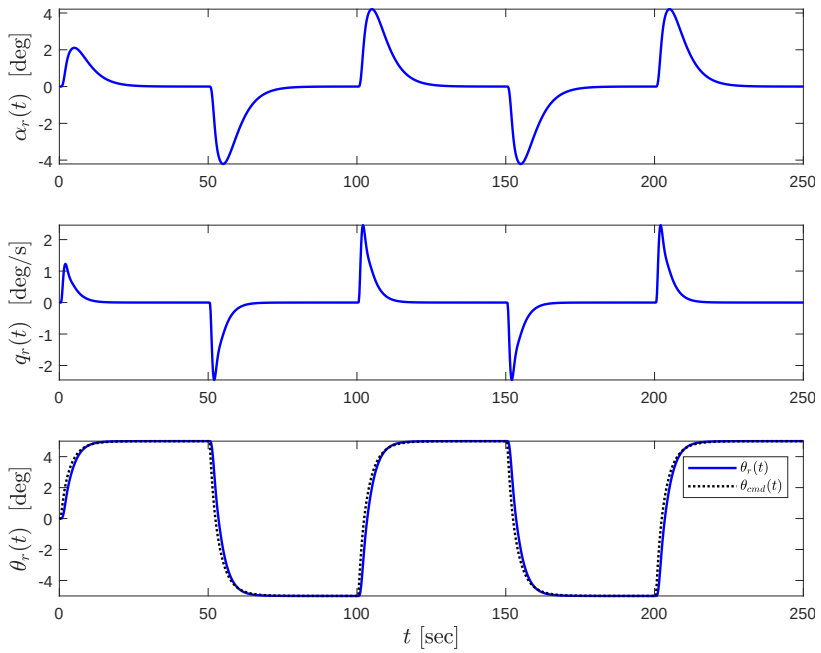

Figure 5.69: Command following performance with the nominal controller in the absence of the system uncertainty.

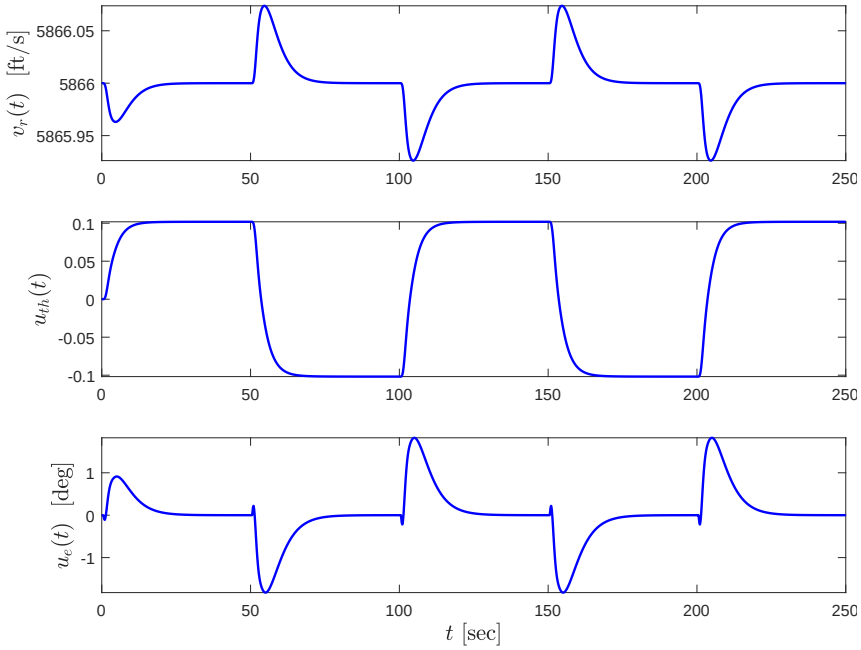

Figure 5.70: Velocity, altitude, and the control signals with the nominal controller in the absence of the system uncertainty.

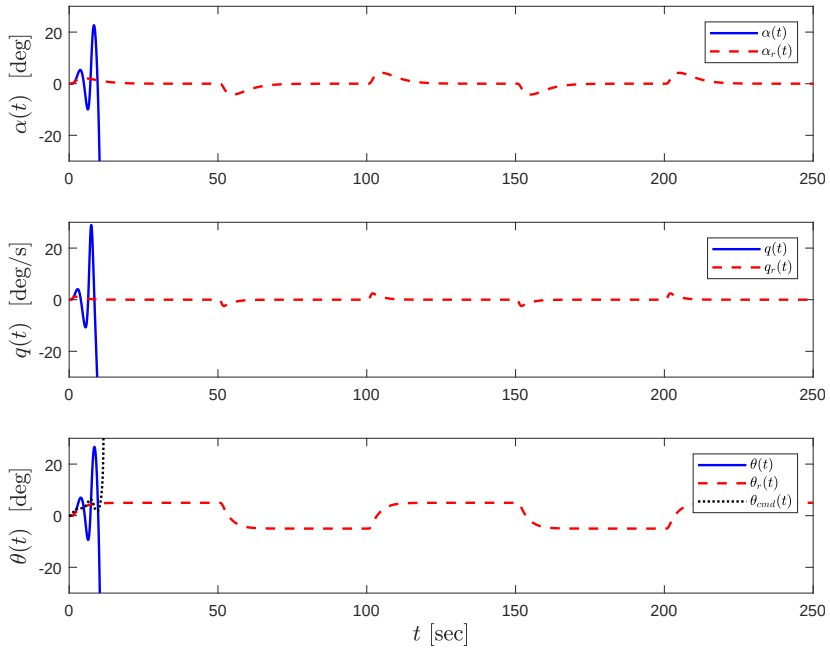

Figure 5.71: Command following performance with the nominal controller in the presence of the system uncertainty.

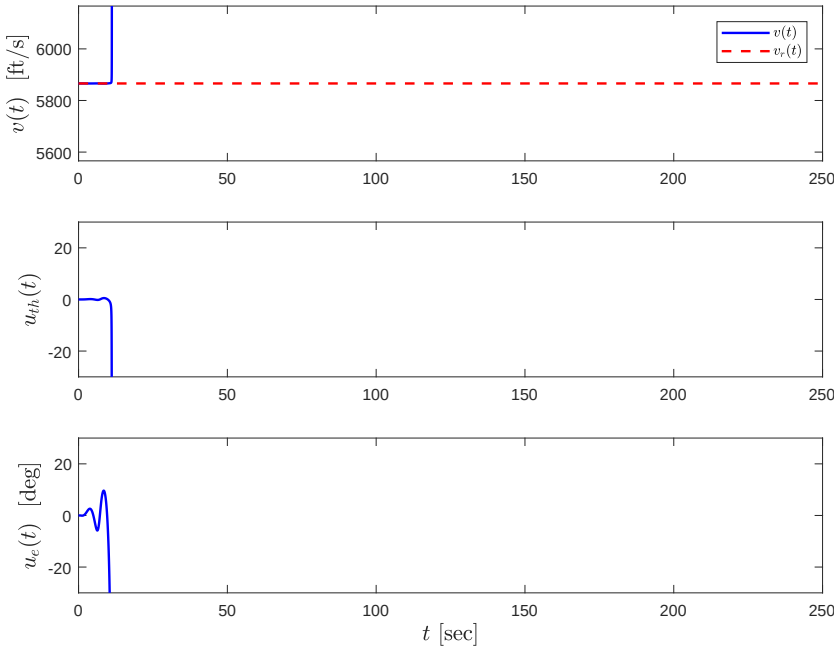

Figure 5.72: Velocity, altitude, and the control signals with the nominal controller in the presence of the system uncertainty.

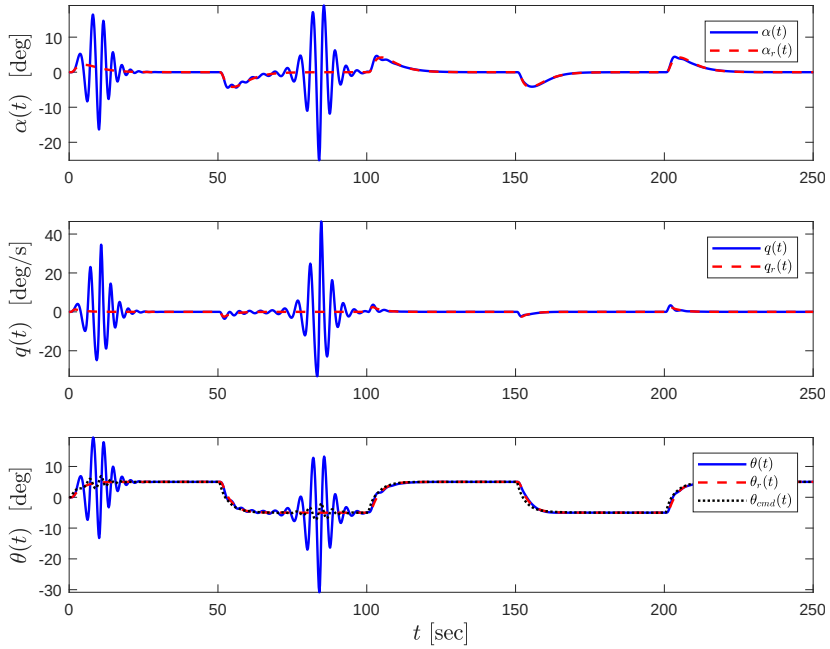

Figure 5.73: Command following performance with the standard model reference adaptive controller at the inner loop.

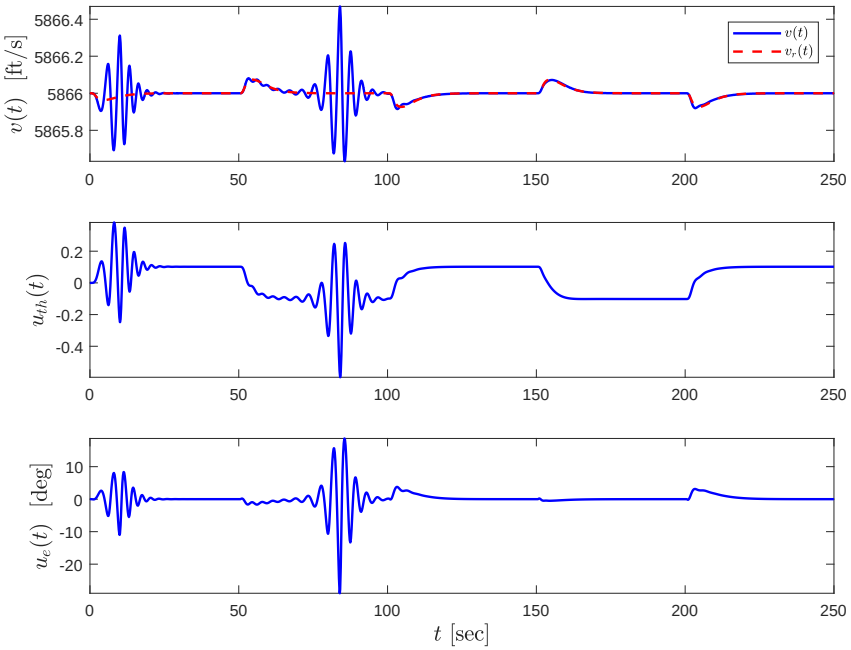

Figure 5.74: Velocity, altitude, and the control signals with the standard model reference adaptive controller at the inner loop.

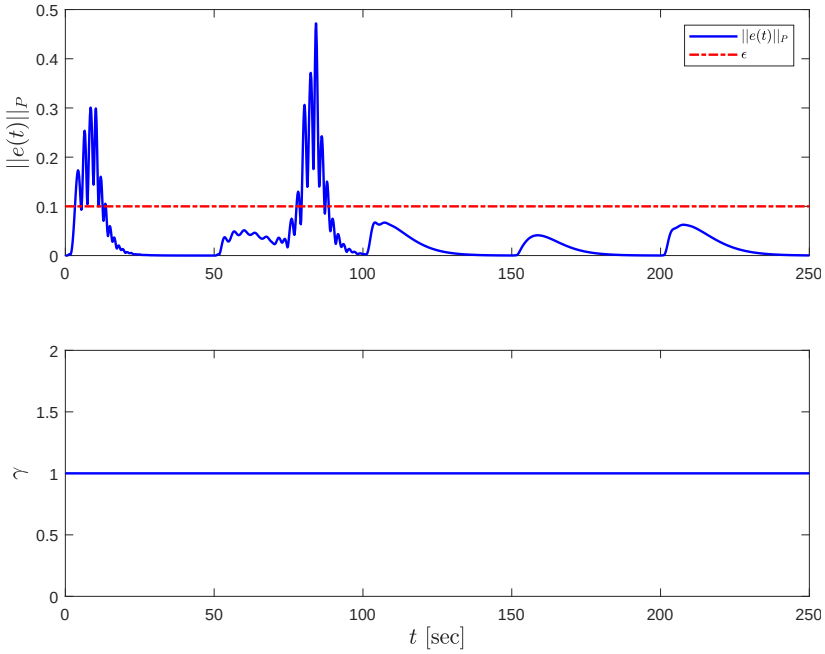

Figure 5.75: Norm of the system error trajectories with the standard model reference adaptive controller at the inner loop.

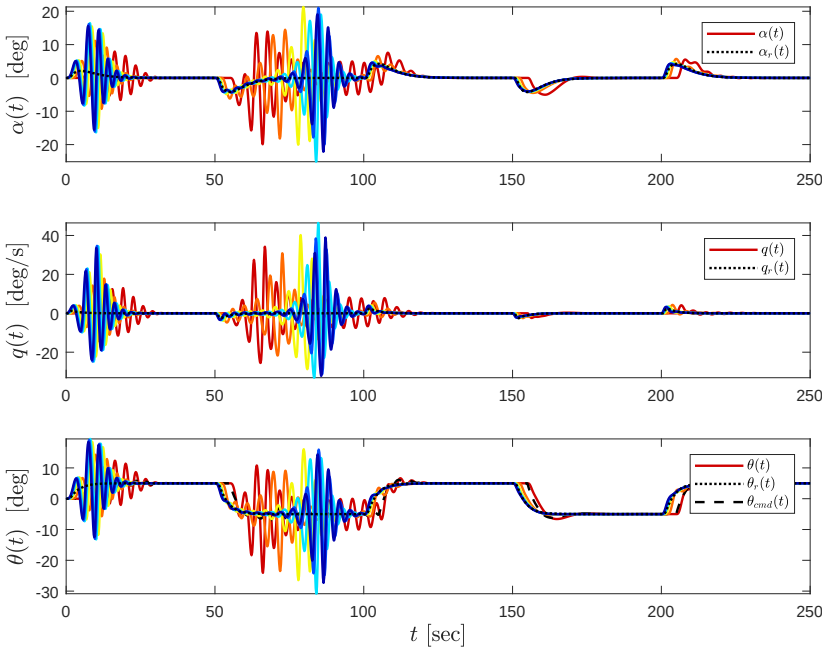

Figure 5.76: The effect of increase in the human reaction time-delay τ from 0 to 5 (blue to red) on the command following performance with the standard model reference adaptive controller at the inner loop.

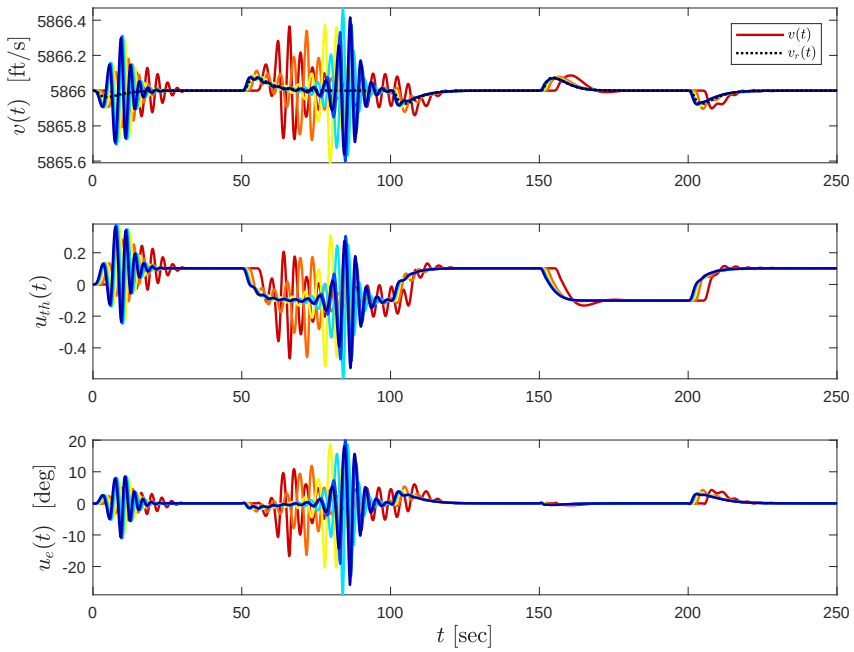

Figure 5.77: The effect of increase in the human reaction time-delay τ from 0 to 5 (blue to red) on velocity, altitude, and the control signals with the standard model reference adaptive controller at the inner loop.

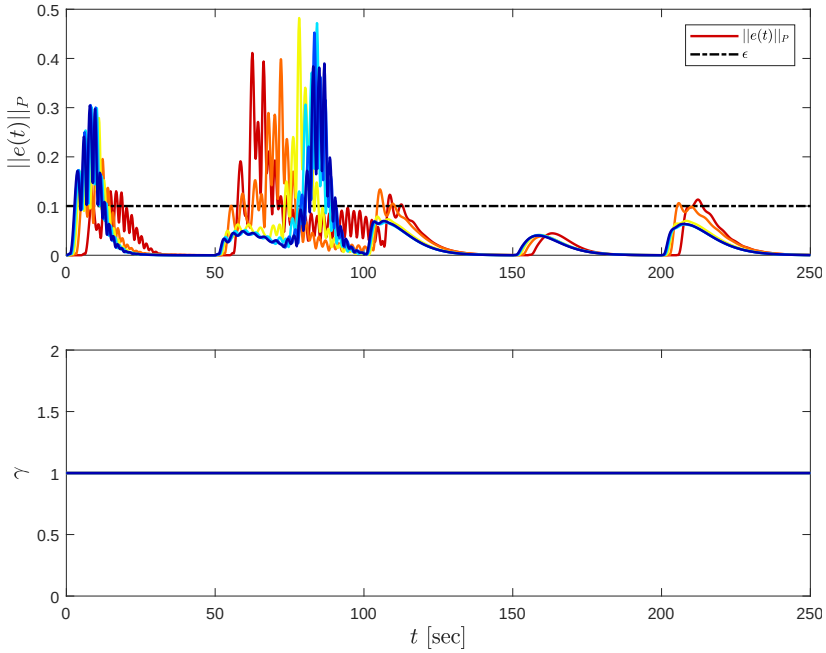

Figure 5.78: The effect of increase in the human reaction time-delay τ from 0 to 5 (blue to red) on the norm of the system error trajectories with the standard model reference adaptive controller at the inner loop.

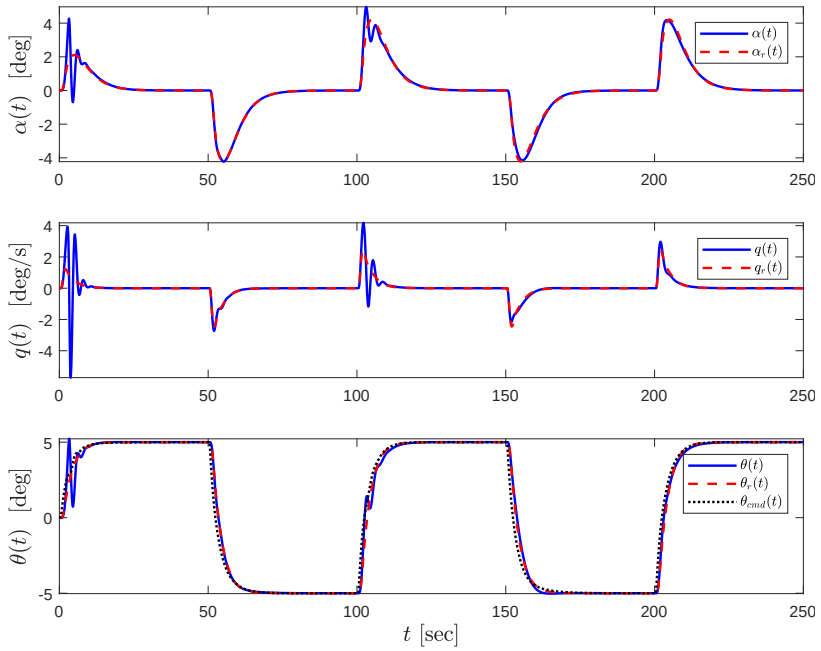

Figure 5.79: Command following performance with the proposed set-theoretic model reference adaptive controller at the inner loop.

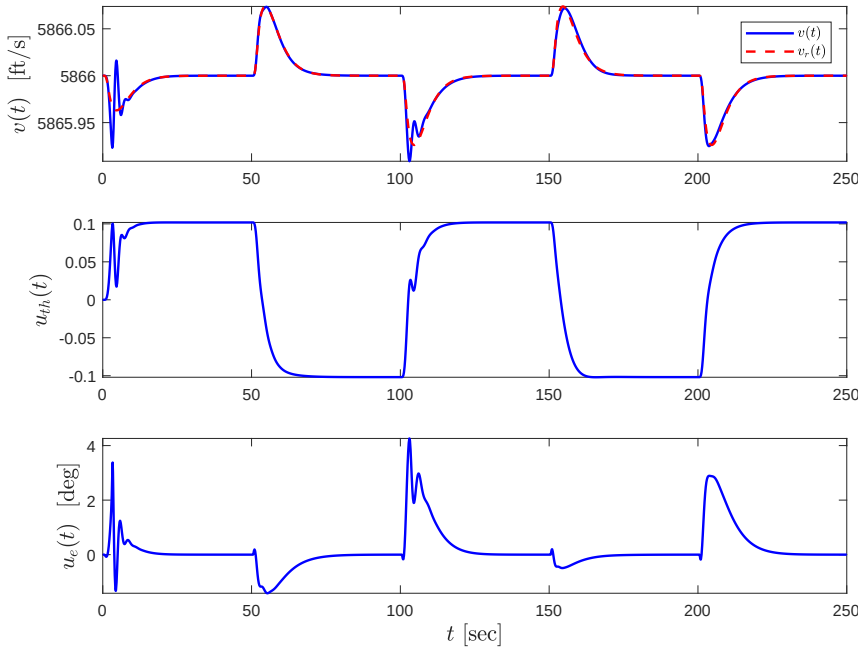

Figure 5.80: Velocity, altitude, and the control signals with the proposed set-theoretic model reference adaptive controller at the inner loop.

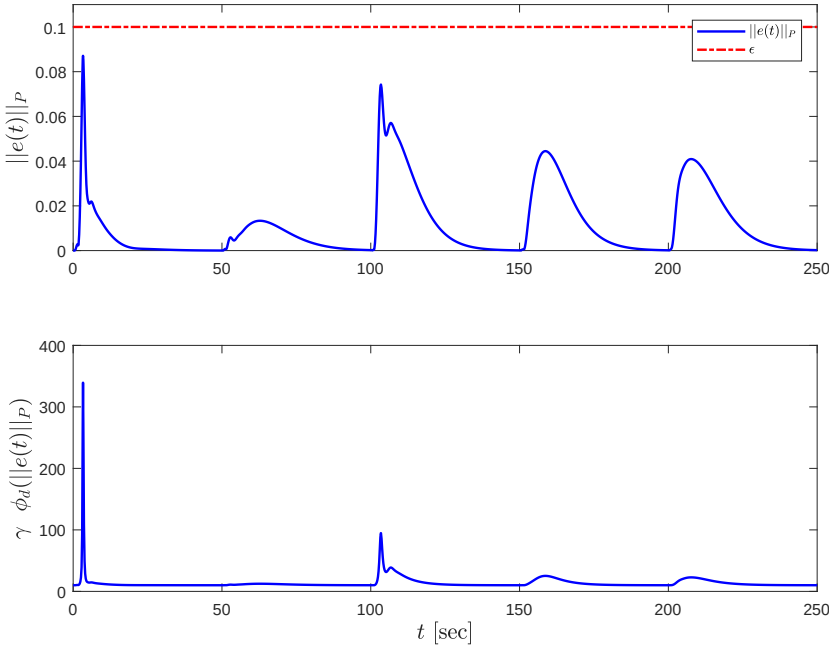

Figure 5.81: Norm of the system error trajectories and the evolution of the effective learning rate $\gamma\phi_d(\cdot)$ with the proposed set-theoretic model reference adaptive controller at the inner loop.

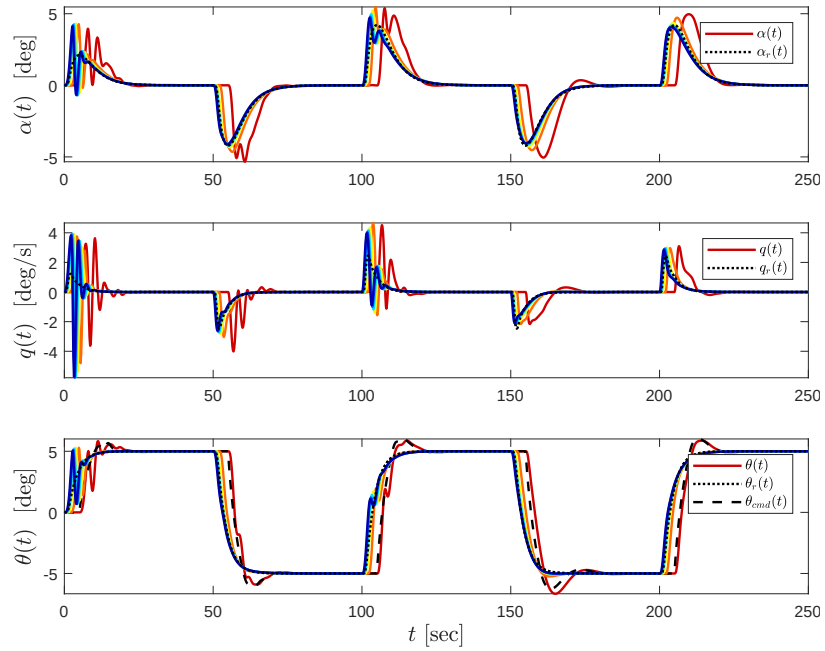

Figure 5.82: The effect of increase in the human reaction time-delay τ from 0 to 5 (blue to red) on the command following performance with the proposed set-theoretic model reference adaptive controller at the inner loop.

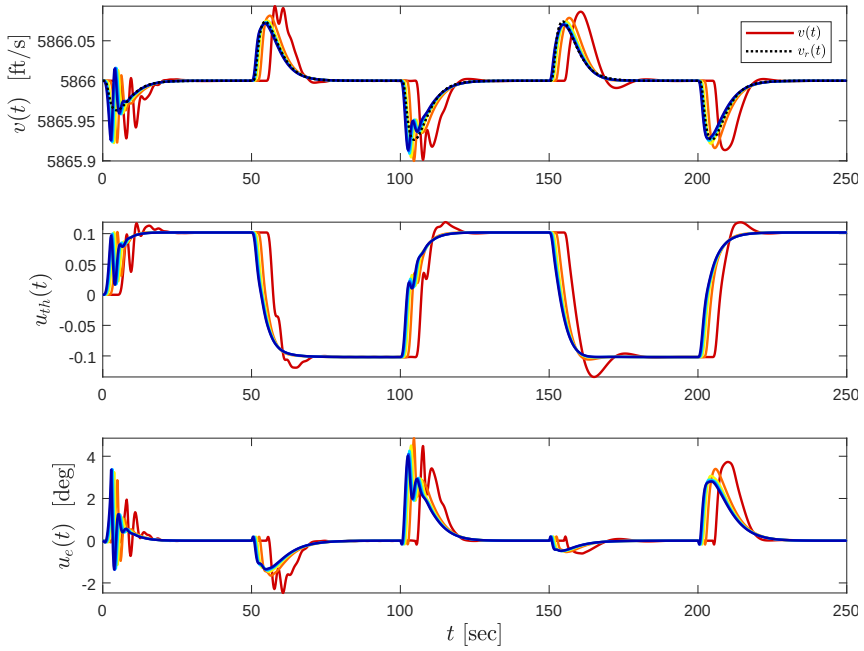

Figure 5.83: The effect of increase in the human reaction time-delay τ from 0 to 5 (blue to red) on velocity, altitude, and the control signals with the proposed set-theoretic model reference adaptive controller at the inner loop.

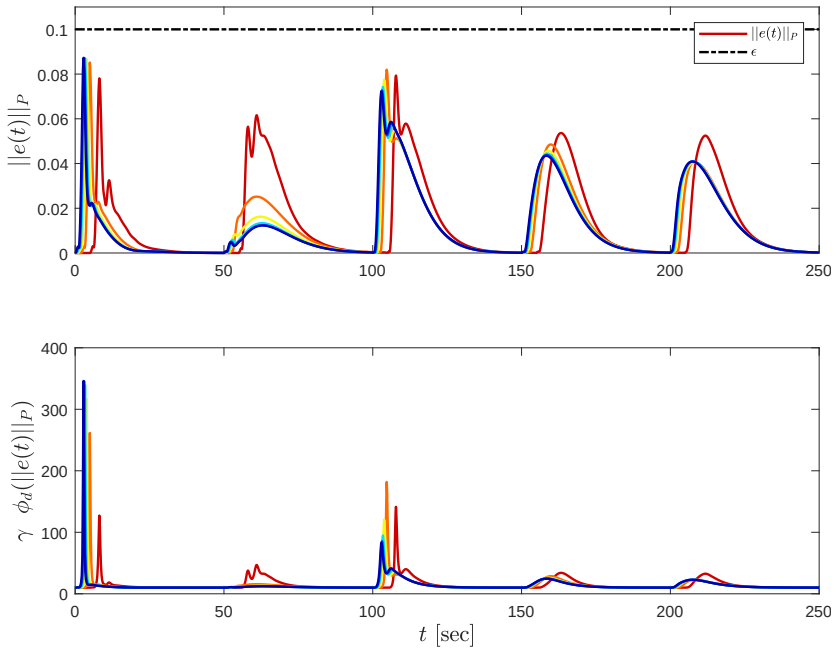

Figure 5.84: The effect of increase in the human reaction time-delay τ from 0 to 5 (blue to red) on the norm of the system error trajectories and the evolution of the effective learning rate $\gamma\phi_d(\cdot)$ with the proposed set-theoretic model reference adaptive controller at the inner loop.

5.4.6 Conclusion

We studied human-in-the-loop physical systems with uncertainties due to failures and/or modeling inaccuracies, a set-theoretic model reference adaptive control law at the inner loop that augments a general nominal dynamic compensator structure, and a dynamic outer loop compensator to capture either sequential loop closure methods and/or high-level guidance algorithms. Specifically, to complement and extend our recent studies, we first provided a sufficient stability condition for the overall physical system; that is, asymptotic stability of the system given by (5.177) with A_0 and A_1 in (5.171). We then showed how to constrain the system error trajectories in order to minimally affect the performance of the overall human-in-the-loop physical system; that is, the upper bound given by (5.187) with ε denoting a user-defined constraint. Finally, we demonstrated the efficacy of our theoretical results through an illustrative numerical example.

5.4.7 Acknowledgments

Our appreciations to Prof. Keqin Gu (Department of Mechanical and Industrial Engineering, Southern Illinois University Edwardsville) for his time to provide feedback on our developments related to Comment 5.4.4.

CHAPTER 6: FINITE-TIME DISTRIBUTED CONTROL ARCHITECTURE WITH TIME TRANSFORMATION

This chapter presents a novel distributed control architecture with a-priori given, user-defined finite-time convergence guarantees using a time transformation technique. In particular, Section 6.1 presents this architecture for networked multiagent systems having first-order dynamics, where Section 6.2 extent this result to second-order multiagent systems.

6.1 Robustness of Finite-Time Distributed Control Algorithm with Time Transformation[1]

The focus of this paper is distributed control of multiagent systems in a-priori given, user-defined finite-time interval using a recently developed time transformation approach, where our contribution is twofold. First, a generalized time transformation function is proposed that converts the user-defined finite-time interval to a stretched infinite-time interval, where one can design a distributed control algorithm on this stretched interval and then transform it back to the original finite-time interval for achieving a given multiagent system objective. Second, for a specific time transformation function, we analytically establish the robustness properties of the resulting finite-time distributed control algorithms against vanishing and non-vanishing system uncertainties. In contrast to existing finite-time approaches, it is shown that the proposed algorithms can preserve a-priori given, user-defined finite-time convergence regardless of the initial conditions of the multiagent system and without requiring a knowledge of the upper bounds of the considered class of system uncertainties. An illustrative numerical example is further included to demonstrate the presented results.

6.1.1 Introduction

Distributed control algorithms for multiagent systems can be broadly classified as the algorithms that guarantee asymptotic convergence (see, for example, [162–167] and references therein) and the algorithms that guarantee finite-time convergence (see, for example, [53–58, 168–170] and references therein).

[1] This section has been submitted to the *American Control Conference*.

Depending on the application of interest, one class of these algorithms can be preferred versus the other. Building on our recent results [72, 73, 171], this paper studies finite-time distributed control algorithms motivated by the time-critical multiagent systems applications.

Specifically, utilizing and generalizing the non-Lipschitz control methods proposed in, for example, [10, 11], the algorithms presented by the authors of [53–58, 168–170] can achieve finite-time convergence. However, this convergence depends on the initial conditions of agents. The authors of [12, 13, 61–65] partially address this problem by proposing algorithms with fixed-time convergence properties. While these algorithms provide an upper bound on the convergence time independent of the initial conditions, the calculated bounds do not necessarily hold globally for all initial conditions and/or they can be (overly) conservative [12]. This implies that it may not be possible to assign a-priori, user-defined finite-time with these algorithms. Furthermore, the finite-time convergence can depend on the bound of system uncertainties in fixed-time algorithms. Notable contributions that can achieve a-priori, user-defined finite-time convergence (also referred to as predefined-time) are documented by the authors of [14, 15, 69, 70]. In particular, the authors of [14] and [15] propose a sliding mode approach; however, their algorithm applies only to single systems and it does require a knowledge of the upper bounds of the considered class of system uncertainties in order to achieve system robustness. The method proposed in [69] similarly applies to single systems and the authors do not account for any system uncertainties. In addition, the algorithm proposed in [70] is predicated on an optimal control framework; however, it is also in the context of single systems.

A novel idea, namely the time transformation method, is proposed in our recent results documented in [72, 73, 171] for achieving a-priori, user-defined smooth finite-time convergence, where these results consider distributed control algorithms for multiagent systems. The key feature of this method is to perform analysis of a given finite-time distributed control algorithm in a stretched infinite-time interval, where one can readily utilize tools from, for example, standard Lyapunov stability theory, to conclude stability and convergence guarantees on the original user-defined finite-time interval. While the authors of [67, 68, 71, 172] use similar distributed control algorithms to the ones presented in [72, 73, 171] (note that the studies in [67, 68, 172] can be considered as a multiagent systems generalization of the idea documented in [66]), the results documented in [72] are not limited to time-invariant graph topologies and the results documented in [73, 171] are not limited to multiagent systems with static equilibrium points[1]. More importantly, due to a

[1]The authors of [173] and [174] provide extensions of [67, 68, 172]; however, the boundedness of their proposed control signals are not discussed.

lack of complete systematic design and analysis framework, the results in [67, 68, 172] may not readily be extendable and system-theoretic robustness tradeoffs of these algorithms are completely unknown.

The focus of this paper is distributed control of multiagent systems in a-priori given, user-defined finite-time interval using the recently developed time transformation approach [72, 73, 171] discussed above. Specifically, our contribution is twofold. First, a generalized time transformation function is proposed that converts the user-defined finite-time interval to a stretched infinite-time interval, where one can design a distributed control algorithm on this stretched interval and then transform it back to the original finite-time interval for achieving a given multiagent system objective. Second, for a specific time transformation function, we analytically establish the complete robustness properties of the resulting finite-time distributed control algorithms against vanishing (i.e., state-dependent) and non-vanishing (i.e., state-independent) system uncertainties in our systematic time transformation framework[2]. In contrast to existing finite-time approaches, it is shown that the proposed algorithms can preserve a-priori given, user-defined finite-time convergence regardless of the initial conditions of the multiagent system and without requiring a knowledge of the upper bounds of the considered class of system uncertainties. An illustrative numerical example is further included to demonstrate the presented results. For the notation used throughout this paper and related mathematical preliminaries we refer to Appendix G.

6.1.2 Problem Formulation

In this section, we introduce the leader-follower problem also considered in [73]. While we consider this benchmark problem, this is without loss of generality in the sense that the presented distributed control architecture can be extended to other multiagent control problems. In particular, consider a multiagent system that consists of N agents exchanging information based on a connected and undirected graph $\mathfrak{G}$. Furthermore, assume that a subset of the agents have access to the position of a time-varying leader given by

$$p(t) \quad = \quad \int_0^t v(\tau)\mathrm{d}\tau + p(0), \quad p(t) \in \mathbb{R}^n, \quad n \in \{1,2,3\}, \tag{6.1}$$

[2]While the analysis performed in [73, 171] can also be utilized for non-vanishing system uncertainties, these prior works do not make any attempts in showing robustness against state-dependent vanishing system uncertainties. Note that such vanishing system uncertainties can destabilize dynamical systems unlike the non-vanishing ones; hence, they are more critical to the overall system stability and convergence.

where $v(t) \in \mathbb{R}^n, n \in \{1,2,3\}$, denotes the bounded and piecewise continuous velocity (with unknown bound) of the leader. For the sake of simplicity and without loss of generality, we let $n = 1$ in what follows[3].

Next, we consider that dynamics of the agents are in the form given by

$$\dot{x}_i(t) \quad = \quad u_i(t) + \omega_i x_i(t) + \rho_i(t), \quad x_i(0) = x_{i0}, \quad i \in \{1,2,\ldots,N\}, \tag{6.2}$$

where $x_i(t) \in \mathbb{R}, i \in \{1,2,\ldots,N\}$ and $u_i(t) \in \mathbb{R}, i \in \{1,2,\ldots,N\}$ are the position and the control signal of each agent, respectively. In (6.2), $\omega_i \in \mathbb{R}, i \in \{1,2,\ldots,N\}$, and $\rho_i(t) \in \mathbb{R}, i \in \{1,2,\ldots,N\}$, represent vanishing and non-vanishing uncertainties in each agent's dynamics. Here, while we assume that the unknown term ω_i is bounded and the unknown term $\rho_i(t)$ is bounded and piecewise continuous for the well-posedness of the considered problem, we do not require the knowledge of their upper bound. In the next section, we propose a generalized time transformation function for finite-time distributed control with a-priori given, user-defined finite-time convergence; that is,

$$\lim_{t \to T} \big(x_i(t) - p(t)\big) = 0, \quad i \in \{1,2,\ldots,N\}, \tag{6.3}$$

where $T \in \mathbb{R}_+$ is this user-defined finite time.

6.1.3 Finite-Time Distributed Control with a Generalized Time Transformation

This section presents the first contribution of this paper. In particular, we propose a generalized time transformation function that converts the user-defined finite-time interval to a stretched infinite-time interval, where one can design a distributed control algorithm on this stretched interval. Specifically, let $t = \theta(s)$ denote this generalized time transformation function. Here, $\theta(s)$ is strictly increasing and continuously differentiable with respect to s, which transforms the infinite time interval $s \in [0,\infty)$ to the finite time interval $t \in [0,T)$ with $T \in \mathbb{R}_+$ being the user-defined finite time[4]. To this end, we propose the distributed control algorithm given by

$$u_i(t) \quad = \quad -\alpha\big(\theta'(\theta^{-1}(t))\big)^{-1}\left(\sum_{i\sim j}\big(x_i(t) - x_j(t)\big) + k_i\big(x_i(t) - p(t)\big)\right), \quad i \in \{1,2,\ldots,N\}, \tag{6.4}$$

[3]The presented results can be applied as they are to the cases when $n > 1$ (see Section 6.1.5).

[4]It is considered that $s = \theta^{-1}(t)$ exists for the results of this paper, where this is clearly possible by properly selecting the generalized time transformation function in the control design process.

defined on $t \in [0,T)$ with $\alpha \in \mathbb{R}_+$. Note that in (6.4), $k_i = 1$ for the subset of the agents having access to the position of a time-varying leader in (6.1) and $k_i = 0$ for other agents.

Let $\tilde{x}_i(t) \triangleq x_i(t) - p(t), i \in \{1,2,\ldots,N\}$, be the error between the position of each agent and that of the leader. Based on the proposed distributed control signal given by (6.4), the resulting error dynamics becomes

$$\dot{\tilde{x}}_i(t) = -\alpha\big(\theta'(\theta^{-1}(t))\big)^{-1}\Bigg(\sum_{i\sim j}\big(\tilde{x}_i(t)-\tilde{x}_j(t)\big)+k_i\tilde{x}_i(t)\Bigg)+\omega_i\big(\tilde{x}_i(t)+p(t)\big)+\rho_i(t)-v(t), \quad \tilde{x}_i(0)=\tilde{x}_{i0}, \quad i\in\{1,2,\ldots,N\}. \tag{6.5}$$

Defining now the augmented error state as $\tilde{x}(t) \triangleq [\tilde{x}_1(t),\tilde{x}_2(t),\ldots,\tilde{x}_N(t)]^{\mathrm{T}} \in \mathbb{R}^N$, the error dynamics in (6.5) can be written in the compact form given by

$$\dot{\tilde{x}}(t) = -\alpha\big(\theta'(\theta^{-1}(t))\big)^{-1}\mathcal{F}(\mathfrak{G})\tilde{x}(t)+\Omega\big(\tilde{x}(t)+\mathbf{1}_N p(t)\big)+\rho(t)-\mathbf{1}_N v(t), \tag{6.6}$$

$$= \big(-\alpha\big(\theta'(\theta^{-1}(t))\big)^{-1}\mathcal{F}(\mathfrak{G})+\Omega\big)\tilde{x}(t)+h(t), \quad \tilde{x}(0)=\tilde{x}_0, \tag{6.7}$$

where $h(t) \triangleq \Omega\mathbf{1}_N p(t)+\rho(t)-\mathbf{1}_N v(t)$, $\Omega \triangleq \mathrm{diag}(\omega_1,\omega_2,\ldots,\omega_N) \in \mathbb{R}^{N\times N}$ and $\rho(t) \triangleq [\rho_1(t),\rho_2(t),\ldots,\rho_N(t)]^{\mathrm{T}} \in \mathbb{R}^N$.

Considering the time transformation function $t = \theta(s)$, let $\xi(t) \in \mathbb{R}^N, t \in [0,T)$, be a solution to the dynamical system given by (6.7) such that $\tilde{x}_s(s) = \xi(t)$, $s \in [0,\infty)$. It now follows from Remark G.1 (see the appendix) that

$$\tilde{x}_s'(s) = \big(-\alpha\mathcal{F}(\mathfrak{G})+\Omega\theta'(s)\big)\tilde{x}_s(s)+\theta'(s)h_s(s), \quad \tilde{x}_s(\theta^{-1}(0))=\tilde{x}_0, \tag{6.8}$$

where $h_s(s) = h(\theta(s))$ based on Remark G.2. Note that $h_s(s)$ consists of bounded terms; hence, it is a bounded function. Using $\theta'(s) = \mathrm{d}\theta(s)/\mathrm{d}s = \mathrm{d}t/\mathrm{d}s$ in (6.8) yields

$$\tilde{x}_s'(s) = \Bigg(-\alpha\mathcal{F}(\mathfrak{G})+\Omega\frac{\mathrm{d}t}{\mathrm{d}s}\Bigg)\tilde{x}_s(s)+\frac{\mathrm{d}t}{\mathrm{d}s}h_s(s), \quad \tilde{x}_s(0)=\tilde{x}_0. \tag{6.9}$$

As noted in Remark G.1, the solution of (6.7) and (6.9) are equivalent with different argument domains; that is, $\tilde{x}_s(s) = \tilde{x}(t)$. We now write the introduced control signal (6.4) in the compact form given by

$$u(t) = -\alpha\frac{\mathrm{d}s}{\mathrm{d}t}\mathcal{F}(\mathfrak{G})\tilde{x}(t), \tag{6.10}$$

which has the following time derivative with respect to t

$$\begin{aligned}\dot{u}(t) &= -\alpha\frac{\mathrm{d}^2 s}{\mathrm{d}t^2}\mathcal{F}(\mathfrak{G})\tilde{x}(t) - \alpha\frac{\mathrm{d}s}{\mathrm{d}t}\mathcal{F}(\mathfrak{G})\dot{\tilde{x}}(t),\\ &= \frac{\mathrm{d}^2 s}{\mathrm{d}t^2}\frac{\mathrm{d}t}{\mathrm{d}s}u(t) - \alpha\frac{\mathrm{d}s}{\mathrm{d}t}\mathcal{F}(\mathfrak{G})\big(u(t)+\Omega\big(\tilde{x}(t)+\mathbf{1}_N p(t)\big)+\rho(t)-\mathbf{1}_N v(t)\big),\\ &= \frac{\mathrm{d}^2 s}{\mathrm{d}t^2}\frac{\mathrm{d}t}{\mathrm{d}s}u(t) - \alpha\frac{\mathrm{d}s}{\mathrm{d}t}\mathcal{F}(\mathfrak{G})\big(u(t)+\Omega\tilde{x}(t)+h(t)\big), \quad u(0)=u_0. \end{aligned} \tag{6.11}$$

Similar to how we obtain (6.9) from (6.7), one can rewrite (6.11) in the infinite time interval $s\in[0,\infty)$ as

$$u_s'(s) \;=\; -\alpha\mathcal{F}(\mathfrak{G})\Omega\tilde{x}_s(s) - \left(\alpha\mathcal{F}(\mathfrak{G}) - \frac{\mathrm{d}^2 s}{\mathrm{d}t^2}\Big(\frac{\mathrm{d}t}{\mathrm{d}s}\Big)^2 I_N\right)u_s(s) - \alpha\mathcal{F}(\mathfrak{G})h_s(s), \quad u_s(0)=u_0. \tag{6.12}$$

One can now augment the state error dynamics in (6.9) and control signal dynamics in (6.12) as

$$\begin{aligned}\begin{bmatrix}\tilde{x}_s'(s)\\ u_s'(s)\end{bmatrix} \;=\; &\begin{bmatrix}-\alpha\mathcal{F}(\mathfrak{G})+\Omega\frac{\mathrm{d}t}{\mathrm{d}s} & 0\\ -\alpha\mathcal{F}(\mathfrak{G})\Omega & -\alpha\mathcal{F}(\mathfrak{G})+\frac{\mathrm{d}^2 s}{\mathrm{d}t^2}\big(\frac{\mathrm{d}t}{\mathrm{d}s}\big)^2 I_N\end{bmatrix}\begin{bmatrix}\tilde{x}_s(s)\\ u_s(s)\end{bmatrix} + \begin{bmatrix}\frac{\mathrm{d}t}{\mathrm{d}s}I_N\\ -\alpha\mathcal{F}(\mathfrak{G})\end{bmatrix}h_s(s),\\ &\begin{bmatrix}\tilde{x}_s(0)\\ u_s(0)\end{bmatrix} = \begin{bmatrix}\tilde{x}_0\\ u_0\end{bmatrix}. \end{aligned} \tag{6.13}$$

Remark 6.1.1 *The time transformation function $t=\theta(s)$ should be chosen by the control user such that (i) the state error dynamics and control signal dynamics given by* (6.13) *are stable, which results in bounded error state $\tilde{x}_s(s)$ and control signal $u_s(s)$, and (ii) the asymptotic stability for the error state $\tilde{x}_s(s)$ is achieved (i.e., $\lim_{s\to\infty}\tilde{x}_s(s)=0$). By Remark G.1, the above discussion implies that the error state $\tilde{x}(t)$ and control signal $u(t)$ are bounded in the original time interval $t\in[0,T)$ and $\lim_{t\to T}\big(x_i(t)-p(t)\big)=0$. The latter result implies that the agents converge to the position of the time-varying leader at the user-defined finite time T.*

As discussed in Remark 6.1.1, the selection of the time transformation function $t=\theta(s)$ plays a crucial role on the stability of the closed-loop system dynamics given in (6.13). Adopted from the previous work of the authors in [72, 73], a candidate time transformation function satisfying the conditions in Remark 6.1.1, along with rigorous and detailed analysis on stability of the closed-loop system dynamics, is presented in the next section.

6.1.4 Robustness to Vanishing and Non-Vanishing System Uncertainties

This section presents the second contribution of this paper. Specifically, using the time transformation function candidate proposed in [72, 73], we now analytically analyze the robustness properties of the overall multiagent system with the time transformation-based finite-time distributed control algorithm in (6.4) in presence of vanishing and non-vanishing system uncertainties (i.e., $\omega_i \in \mathbb{R}, i \in \{1,2,\ldots,N\}$, and $\rho_i(t) \in \mathbb{R}, i \in \{1,2,\ldots,N\}$, in (6.2)). To this end, consider the time transformation candidate function given by

$$t \quad = \quad \theta(s) \triangleq T(1-e^{-s}), \tag{6.14}$$

where $T \in \mathbb{R}_+$ is the a-priori given, user-defined finite time. Note that this time transformation function has the derivative with respect to $s \in [0,\infty)$ given by

$$\frac{\mathrm{d}t}{\mathrm{d}s} = \theta'(s) = Te^{-s} = T - t. \tag{6.15}$$

Introducing (6.15) in (6.4) results in the control signal given by

$$u_i(t) \quad = \quad -\frac{\alpha}{T-t}\Bigg(\sum_{i\sim j}\big(x_i(t)-x_j(t)\big)+k_i\big(x_i(t)-p(t)\big)\Bigg), \quad i \in \{1,2,\ldots,N\}, \tag{6.16}$$

or in the compact form

$$u(t) \quad = \quad -\frac{\alpha}{T-t}\mathcal{F}(\mathfrak{G})\tilde{x}(t). \tag{6.17}$$

Furthermore, using (6.15) in the error dynamics given by (6.5) yields

$$\dot{\tilde{x}}(t) \quad = \quad \Big(-\frac{\alpha}{T-t}\mathcal{F}(\mathfrak{G})+\Omega\Big)\tilde{x}(t)+h(t), \quad \tilde{x}(0)=\tilde{x}_0. \tag{6.18}$$

Similar to the steps shown in the previous section, one can now write (6.18) in the infinite-time interval $s \in [0,\infty)$ as

$$\tilde{x}_s'(s) = \Big(-\alpha\mathcal{F}(\mathfrak{G})+\Omega Te^{-s}\Big)\tilde{x}_s(s)+Te^{-s}h_s(s), \quad \tilde{x}_s(0)=\tilde{x}_0. \tag{6.19}$$

The augmented form of the state error and the control signal dynamics can also be obtained similar to (6.13) as

$$\begin{bmatrix} \tilde{x}_s'(s) \\ u_s'(s) \end{bmatrix} = \begin{bmatrix} -\alpha\mathcal{F}(\mathfrak{G}) + \Omega T e^{-s} & 0 \\ -\alpha\mathcal{F}(\mathfrak{G})\Omega & -\mathcal{S} \end{bmatrix} \begin{bmatrix} \tilde{x}_s(s) \\ u_s(s) \end{bmatrix} + \begin{bmatrix} Te^{-s} I_N \\ -\alpha\mathcal{F}(\mathfrak{G}) \end{bmatrix} h_s(s), \quad \begin{bmatrix} \tilde{x}_s(0) \\ u_s(0) \end{bmatrix} = \begin{bmatrix} \tilde{x}_0 \\ u_0 \end{bmatrix}, \quad (6.20)$$

where

$$\mathcal{S} \triangleq \alpha\mathcal{F}(\mathfrak{G}) - I_N \in \mathbb{R}^{N\times N}. \quad (6.21)$$

Remark 6.1.2 *Letting* $\mathcal{A}(t) \triangleq -\frac{\alpha}{T-t}\mathcal{F}(\mathfrak{G}) + \Omega$*, the error dynamics given in* (6.18) *can be rewritten in the form*

$$\dot{\tilde{x}}(t) = \mathcal{A}(t)\tilde{x}(t) + h(t), \quad \tilde{x}(0) = \tilde{x}_0. \quad (6.22)$$

Now, since $\mathcal{A}(t)$ *and* $h(t)$ *are integrable functions of* t *over the finite-time interval* $t \in [0, T-\delta]$ *for every small positive constant* δ*, it follows from [175, p. 97] that the error dynamics given in* (6.18) *has a unique solution on the finite-time interval* $[0,T)$*. Alternatively, by analyzing the transferred error dynamics in the infinite-time interval given in* (6.19)*, one can conclude the existence and uniqueness of the solution* $\tilde{x}_s(s)$ *over the infinite-time interval* $s \in [0,\infty)$*. Hence, there exist a unique solution for the error dynamics given in* (6.18) *over the finite-time interval* $[0,T)$*.*

Theorem 6.1.1 *Consider the multiagent system that consists of* N *agents on a connected, undirected graph* $\mathfrak{G}$*, where the uncertain dynamics of agent* $i \in \{1,\ldots,N\}$ *is given by* (6.2)*. In addition, assume that there exists at least one agent sensing the position of the time-varying leader given by* (6.1)*, which has bounded but unknown velocity. Considering the local control algorithm* $u_i(t)$*,* $i = 1,\ldots,N$*, for each agent given by* (6.16)*, let the design parameter* α *be chosen to make* $\mathcal{S} = \alpha\mathcal{F}(\mathfrak{G}) - I_N$ *positive definite*[5]*. Then, the closed-loop system signals including the control signals remain bounded and all agents converge to the position of the leader in the a-priori given, user-defined finite time* T *(i.e.,* $\lim_{t\to T}\tilde{x}(t) = 0$*) for all initial conditions of agents and for all finite pairs* $(\omega_i, \rho_i(t)), i \in \{1,\ldots,N\}$*.*

[5]While the design parameter α needs to be chosen to make $\mathcal{S}$ in (6.21) positive definite, the proposed control signal in (6.16) is still implemented in a distributed fashion.

Proof. To show boundedness of the closed-loop system signals and convergence of all agents to the position of the leader at the user-defined finite time T, we consider the closed-loop system dynamics after applying the time transformation function as given in (6.20). We first consider the system error dynamics in the infinite time interval $s \in [0,\infty)$ and let $\mathcal{V}(\tilde{x}_s(s)) \in \overline{\mathbb{R}}_+$ be an energy function given by

$$\mathcal{V}(\tilde{x}_s(s)) \quad = \quad \tilde{x}_s^{\mathrm{T}}(s)\tilde{x}_s(s) = \|\tilde{x}_s(s)\|_2^2. \tag{6.23}$$

The derivative of (6.23) with respect to the stretched time $s \in [0,\infty)$ along the trajectories of (6.19) is given by

$$\begin{aligned}
\mathcal{V}'(\tilde{x}_s(s)) &= 2\tilde{x}_s^{\mathrm{T}}(s)\tilde{x}_s'(s),\\
&= 2\tilde{x}_s^{\mathrm{T}}(s)\Big(\big(-\alpha\mathcal{F}(\mathfrak{G})+\Omega Te^{-s}\big)\tilde{x}_s(s)+Te^{-s}h_s(s)\Big),\\
&= -2\alpha\tilde{x}_s^{\mathrm{T}}(s)\mathcal{F}(\mathfrak{G})\tilde{x}_s(s)+2Te^{-s}\tilde{x}_s^{\mathrm{T}}(s)\Omega\tilde{x}_s(s)+2Te^{-s}\tilde{x}_s^{\mathrm{T}}(s)h_s(s),\\
&\leq -2\alpha\lambda_{\min}(\mathcal{F}(\mathfrak{G}))\|\tilde{x}_s(s)\|_2^2+2Te^{-s}\omega_{\max}\|\tilde{x}_s(s)\|_2^2+2Te^{-s}\|\tilde{x}_s(s)\|_2\|h_s(s)\|_2,
\end{aligned} \tag{6.24}$$

where $\omega_{\max} \triangleq \max\{\omega_1,\ldots,\omega_N\}$. Using $2\|\tilde{x}_s(s)\|_2\|h_s(s)\|_2 \leq \|\tilde{x}_s(s)\|_2^2+\|h_s(s)\|_2^2$ on the last term and replacing $\|\tilde{x}_s(s)\|_2^2$ with $\mathcal{V}(\tilde{x}_s(s))$ in (6.24) results in

$$\begin{aligned}
\mathcal{V}'(\tilde{x}_s(s)) &\leq \mathcal{V}(\tilde{x}_s(s))\big(-2\alpha\lambda_{\min}(\mathcal{F}(\mathfrak{G}))+2Te^{-s}\omega_{\max}\big)+Te^{-s}\big(\mathcal{V}(\tilde{x}_s(s))+\|h_s(s)\|_2^2\big),\\
&\leq \mathcal{V}(\tilde{x}_s(s))\big(-2\alpha\lambda_{\min}(\mathcal{F}(\mathfrak{G}))+Te^{-s}(2\omega_{\max}+1)\big)+Te^{-s}\|h_s(s)\|_2^2.
\end{aligned} \tag{6.25}$$

For the sake of simplicity of the rest of the analysis, we define $a_0 \triangleq 2\alpha\lambda_{\min}(\mathcal{F}(\mathfrak{G})) \in \mathbb{R}_+$ by Lemma G.1, $b_0 \triangleq \max\{0, T(2\omega_{\max}+1)\} \in \mathbb{R}_+$ and $c_0 \in \mathbb{R}_+$ to be the upper bound on $T\|h_s(s)\|_2^2$, i.e., $T\|h_s(s)\|_2^2 \leq c_0$. This simplifies (6.25) to

$$\mathcal{V}'(\tilde{x}_s(s))+(a_0-b_0e^{-s})\mathcal{V}(\tilde{x}_s(s)) \quad \leq \quad e^{-s}c_0. \tag{6.26}$$

Defining the integrating factor $\mu(s) \triangleq \exp(a_0s+b_0e^{-s}) \in \mathbb{R}_+$ and multiplying both sides of (6.26) with this factor, one would get

$$\mu(s)\mathcal{V}'(\tilde{x}_s(s))+\mu(s)(a_0-b_0e^{-s})\mathcal{V}(\tilde{x}_s(s)) \quad \leq \quad \mu(s)e^{-s}c_0, \tag{6.27}$$

or equivalently,

$$\frac{\mathrm{d}}{\mathrm{d}s}\big(\mu(s)\mathcal{V}(\tilde{x}_s(s))\big) \quad \leq \quad \mu(s)e^{-s}c_0. \tag{6.28}$$

Next, we integrate both sides of (6.28) over the s domain that yields

$$\mu(s)\mathcal{V}(\tilde{x}_s(s)) \leq c_0 \int_0^s e^{-\tau}\exp(a_0\tau + b_0 e^{-\tau})\mathrm{d}\tau + \mathcal{V}_0, \tag{6.29}$$

where $\mathcal{V}_0 \triangleq \mu(0)\mathcal{V}(\tilde{x}(0)) = e^{b_0}\|\tilde{x}(0)\|_2^2$. We now set $\nu(\tau) \triangleq e^{-\tau} \in \mathbb{R}_+$ with the derivative $\mathrm{d}\nu(\tau) = -e^{-\tau}\mathrm{d}\tau$ to get

$$\begin{aligned}
\mu(s)\mathcal{V}(\tilde{x}_s(s)) &\leq -c_0 \int_1^{e^{-s}} \exp(-a_0\ln(\nu(\tau)) + b_0\nu(\tau))\mathrm{d}\nu(\tau) + \mathcal{V}_0, \\
&\leq c_0 \int_{e^{-s}}^1 \big(\nu(\tau)\big)^{-a_0} e^{b_0\nu(\tau))}\mathrm{d}\nu(\tau) + \mathcal{V}_0, \\
&\leq d_0 \int_{e^{-s}}^1 \big(\nu(\tau)\big)^{-a_0}\mathrm{d}\nu(\tau) + \mathcal{V}_0,
\end{aligned} \tag{6.30}$$

where $d_0 \triangleq c_0 e^{b_0} \in \mathbb{R}_+$ is the upper bound on $c_0 e^{b_0\nu(\tau)}$. Note that since $\tau \in [0,s)$ with $s \in [0,\infty)$, we have $\nu(\tau) \in (0,1]$ showing the existence of d_0.

We now solve the integral in (6.30) for two possible a_0 cases. In particular, if $a_0 = 1$, we have

$$\begin{aligned}
\mu(s)\mathcal{V}(\tilde{x}_s(s)) &\leq d_0 \int_{e^{-s}}^1 \big(\nu(\tau)\big)^{-1}\mathrm{d}\nu(\tau) + \mathcal{V}_0, \\
&\leq d_0 \ln \nu(\tau)\Big|_{e^{-s}}^1 + \mathcal{V}_0, \\
&\leq d_0 s + \mathcal{V}_0.
\end{aligned} \tag{6.31}$$

Introducing the integral factor $\mu(s) = \exp(s + b_0 e^{-s})$ in (6.31), the bound on the energy function is now given by

$$\mathcal{V}(\tilde{x}_s(s)) \quad \leq \quad \frac{d_0 s}{e^{s+b_0 e^{-s}}} + \mathcal{V}_0 e^{-s-b_0 e^{-s}}. \tag{6.32}$$

We are interested in the limit of this bound when $s \to \infty$ given by

$$\begin{aligned}
\lim_{s\to\infty} \mathcal{V}(\tilde{x}_s(s)) &\leq \lim_{s\to\infty} \frac{d_0 s}{e^{s+b_0 e^{-s}}} + \lim_{s\to\infty} \mathcal{V}_0 e^{-s-b_0 e^{-s}}, \\
&= \lim_{s\to\infty} \frac{d_0}{(1-b_0 e^{-s})e^{s+b_0 e^{-s}}} \;=\; 0,
\end{aligned} \tag{6.33}$$

where we applied the L'Hospital's Rule to the first limit term. Next, since $\mathcal{V}(\tilde{x}_s(s))$ is a positive definite function we can conclude

$$\lim_{s\to\infty} \mathcal{V}(\tilde{x}_s(s)) = 0. \tag{6.34}$$

For the case when $a_0 \neq 1$, one can write

$$\begin{aligned} \mu(s)\mathcal{V}(\tilde{x}_s(s)) &\leq d_0 \int_{e^{-s}}^{1} \big(\nu(\tau)\big)^{-a_0} \mathrm{d}\nu(\tau) + \mathcal{V}_0, \\ &\leq d_0 \frac{\big(\nu(\tau)\big)^{(1-a_0)}}{1-a_0}\Big|_{e^{-s}}^{1} + \mathcal{V}_0, \\ &\leq \frac{d_0}{1-a_0}\big(1 - e^{(a_0-1)s}\big) + \mathcal{V}_0. \end{aligned} \tag{6.35}$$

Introducing the integral factor $\mu(s)$ in (6.35), the bound on the energy function is now given by

$$\mathcal{V}(\tilde{x}_s(s)) \leq \frac{d_0}{1-a_0}\big(e^{-a_0 s - b_0 e^{-s}} - e^{-s - b_0 e^{-s}}\big) + \mathcal{V}_0 e^{-a_0 s - b_0 e^{-s}}. \tag{6.36}$$

Once again, we take the limit on the bound on the energy function in (6.36) when $s \to \infty$ as

$$\lim_{s\to\infty} \mathcal{V}(\tilde{x}_s(s)) \leq \lim_{s\to\infty} \frac{d_0}{1-a_0}\big(e^{-a_0 s - b_0 e^{-s}} - e^{-s - b_0 e^{-s}}\big) + \lim_{s\to\infty} \mathcal{V}_0 e^{-a_0 s - b_0 e^{-s}} = 0. \tag{6.37}$$

Therefore in all cases we have $\lim_{s\to\infty} \mathcal{V}(\tilde{x}_s(s)) = 0$ resulting in

$$\lim_{s\to\infty} \tilde{x}_s(s) = 0. \tag{6.38}$$

Since $\tilde{x}_s(s) = \tilde{x}(t)$ by Remark G.1 and $t \to T$ as $s \to \infty$, one can obtain

$$\lim_{t\to T} \tilde{x}(t) = 0. \tag{6.39}$$

Furthermore, it follows from (6.32) and (6.36) that the energy function $\mathcal{V}(\tilde{x}_s(s))$, and consequently the state error vector $\tilde{x}_s(s)$, remain bounded for all $s \in [0,\infty)$. Equivalently, the state error vector $\tilde{x}(t)$, remains bounded in the finite time interval for all $t \in [0,T)$.

Finally, to show the boundedness of the control signal $u_s(s)$, consider the second equation in (6.20) given by

$$u_s'(s) = -\mathcal{S}u_s(s) - \alpha\mathcal{F}(\mathfrak{G})\Omega\tilde{x}_s(s) - \alpha\mathcal{F}(\mathfrak{G})h_s(s), \quad u(0) = u_0. \tag{6.40}$$

As noted earlier, from the boundedness of the position and velocity of the leader as well as the boundedness of the system uncertainties, it follows that $h_s(s)$ is a bounded function. Now, since the last two terms in (6.40) are bounded, and $-\mathcal{S}$ is Hurwitz by the assumption of the theorem, then $u_s(s)$ is bounded. Equivalently, $u(t)$ remains bounded in the finite interval $t \in [0, T)$ which concludes the proof. ■

Remark 6.1.3 *The notable feature of the proposed distributed control algorithm in this section for handling system uncertainties while achieving an a-priori given, user-defined finite-time multiagent system performance arises mainly from the utilization of the time transformation function in* (6.14). *Specifically, the aforementioned time transformation method converts the problem under study from its finite interval $t \in [0, T)$ to the infinite-time interval $s \in [0, \infty)$. This then enables a control user to exploit any standard (i.e., over infinite horizon) system-theoretic tools for synthesis and analysis purposes. The finite-time stability and convergence guarantees are then immediate by transforming the time to the original interval.*

6.1.5 Illustrative Numerical Example

In this section, we present an illustrative numerical example to demonstrate the efficacy of the presented results of this paper. To this end, consider a multiagent systems that consists of $N = 8$ agents exchanging information based on an undirected, connected circle graph $\mathfrak{G}$ as shown in Figure 6.1, where the first two agents have access to the position of the time-varying leader given by $p(t) = 2.5 + 5\sin(0.5t) + 0.5\sin(5t)$ (i.e., $k_i = 1$ for $i \in \{1, 2\}$, and $k_i = 0$ for $i \in \{3, 4, \ldots, 8\}$ in (6.16)). Furthermore, the vanishing and non-vanishing system uncertainties are selected for this numerical example respectively as $w_i = -0.3, i \in \{1, \ldots, 8\}$, and $\rho_i(t) = \sin(2t), i \in \{1, \ldots, 8\}$. Finally, we note that the initial positions of the agents are selected randomly using the `randn` function in MATLAB.

For the proposed distributed control algorithm, we use the time transformation function given in (6.14) with $T = 4$ in order to enforce the finite-time convergence value equal to 4 seconds and we set $\alpha = 10$ that results in a positive definite matrix $\mathcal{S}$ in (6.21). Figure 6.2 shows the performance of the proposed distributed control algorithm in presence of vanishing and non-vanishing system uncertainties. As expected from Theorem 6.1.1, the position of each agent converges to that of the leader at the chosen user-defined finite time with bounded agent states and control signals. Moreover, for further illustrating the robustness

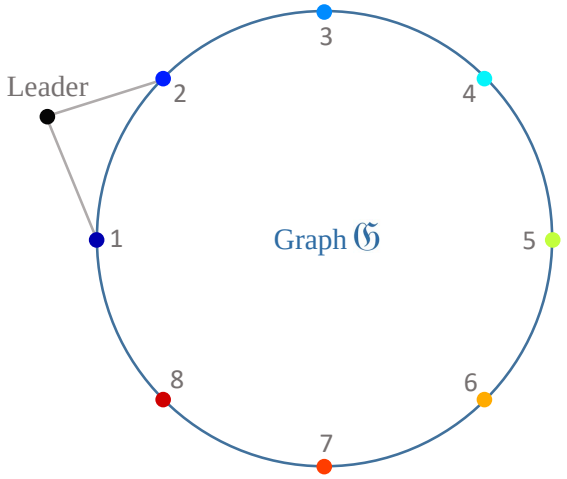

Figure 6.1: An example multiagent system on an undirected, connected circle graph $\mathfrak{G}$.

of the proposed distributed control algorithm to different vanishing and non-vanishing system uncertainties, consider four additional uncertainty scenarios as

$$A: \begin{cases} w_i = 0 \\ \rho_i(t) = 0 \end{cases}, \quad B: \begin{cases} w_i = -0.1 \\ \rho_i(t) = 2\sin(4t) \end{cases}, \tag{6.41}$$

$$C: \begin{cases} w_i = -0.5 \\ \rho_i(t) = -4\sin(0.5t) \end{cases}, \quad D: \begin{cases} w_i = 0.5 \\ \rho_i(t) = -6\sin(2t) \end{cases}. \tag{6.42}$$

The initial condition of the agents are selected randomly in the interval $[14,16]$ for scenario A, $[8,10]$ for scenario B, $[-1,1]$ for scenario C, and $[-6,-4]$ for scenario D. Figure 6.4 shows that in all cases the proposed algorithm can preserve the user-defined finite-time convergence, regardless of the initial conditions of the agents and without requiring the knowledge of the upper bounds of the system uncertainties.

As discussed in Section 6.1.2, the proposed algorithm can also be utilized for a-priori given, user-defined finite-time convergence in higher dimensions (i.e., n>1). For demonstrating this fact in a two dimensional case (i.e., $n = 2$), we next consider the same multiagent system having the same vanishing and non-vanishing system uncertainties for both dimensions, where the first two agents have access to the position of the time-varying leader given by $p(t) = [4\sin(1.5t),\ 4\cos(1.5t)]^{\mathrm{T}}$. Figure 6.5 shows the performance of the proposed distributed control algorithm applied to both dimensions simultaneously. Once again, the position of each agent converges to that of the leader at the user-defined finite time.

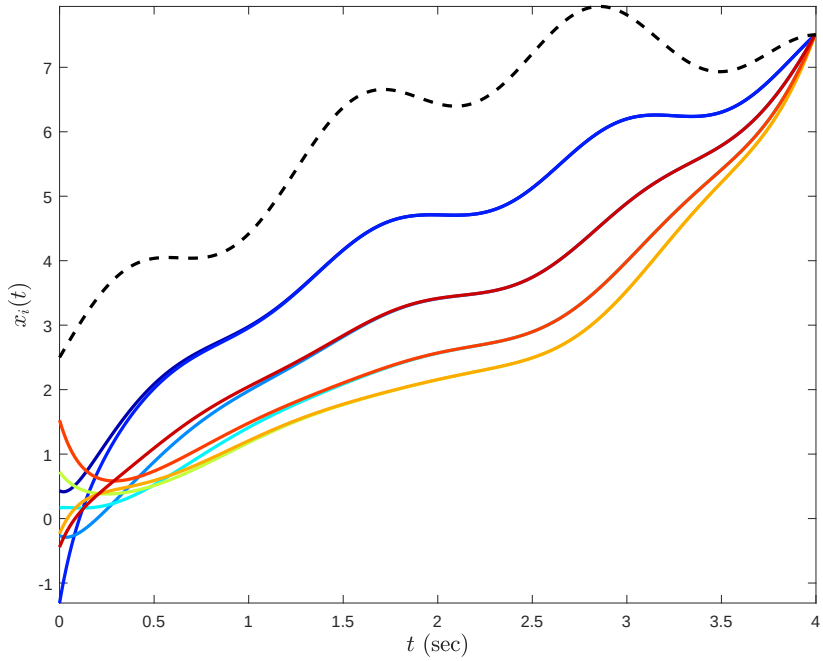

Figure 6.2: Leader-follower performance with the proposed finite-time control algorithm ($T = 4$ and $\alpha = 10$) in the presence of vanishing and non-vanishing uncertainties (dashed line shows the position of the leader and solid lines show the position of agents).

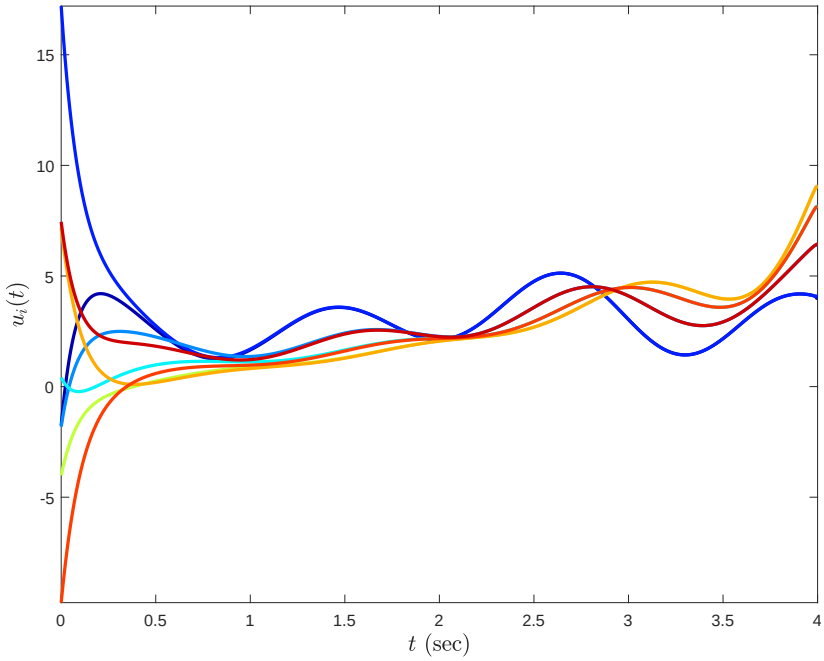

Figure 6.3: Control signal of each agent with the proposed finite-time control algorithm ($T = 4$ and $\alpha = 10$) in the presence of vanishing and non-vanishing uncertainties (dashed line shows the position of the leader and solid lines show the position of agents).

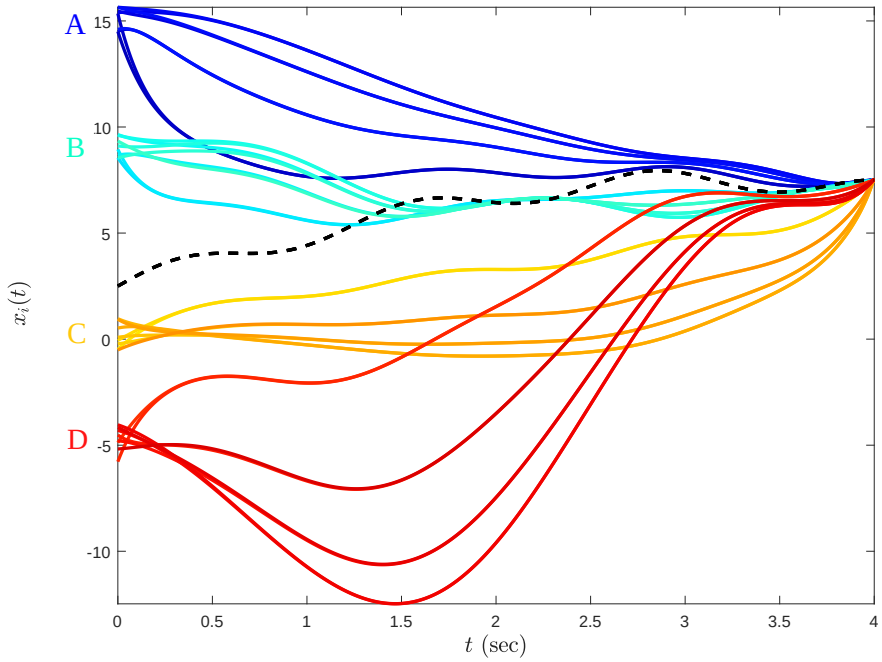

Figure 6.4: Leader-follower performance with the proposed finite-time control algorithm ($T = 4$ and $\alpha = 10$) in the presence of different system uncertainty scenarios (dashed line shows the position of the leader and solid lines show the position of agents).

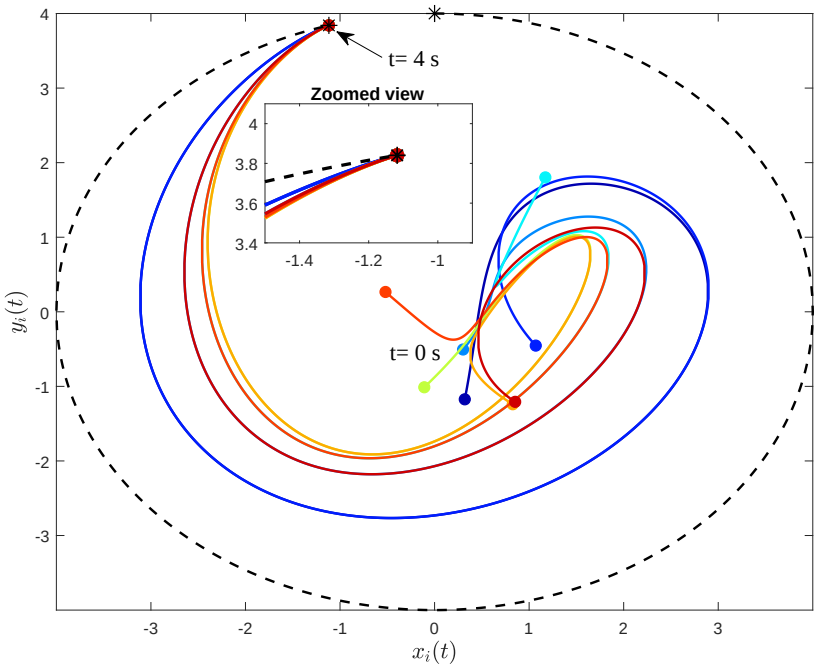

Figure 6.5: Two dimensional leader-follower performance with the proposed finite-time control algorithm ($T = 4$ and $\alpha = 10$) in the presence of vanishing and non-vanishing uncertainties (dashed line shows the position of the leader and solid lines show the position of agents).

6.1.6 Conclusion

To contribute to the previous studies in multiagent systems, we proposed a distributed control algorithm for achieving a-priori given, user-defined finite-time convergence using the time transformation approach. Specifically, we first introduced a generalized time transformation function that converts the user-defined finite-time interval $t \in [0, T)$ to a stretched infinite-time interval $s \in [0, \infty)$, where one can construct a distributed control algorithm for achieving a given multiagent system objective. Based on the structure of a time transformation function candidate, we then established the robustness properties of the resulting finite-time distributed control algorithms against vanishing and non-vanishing system uncertainties. Furthermore, we showed that, in contrast to the existing finite-time approaches, the proposed distributed control algorithm can preserve a-priori given, user-defined finite-time convergence regardless of the initial conditions of the multiagent system and without requiring a knowledge of the upper bounds of the considered class of system uncertainties. Finally, the efficacy of the presented results was demonstrated through an illustrative numerical example.

6.2 Further Results on Finite-Time Distributed Control of Multiagent Systems with Time Transformation[2]

In previous work, a (smooth) finite-time distributed control algorithm with time transformation was introduced for first-order multiagent systems, which guarantees convergence of the single state of agents to a time-varying leader at a-priori given, user-defined time T from any arbitrary initial conditions with bounded local control signals. In this paper, we present an extension of this previous work to second-order multiagent systems. Specifically, utilizing a user-defined finite-time interval of interest $t \in [0, T)$, we time transform this class of multiagent systems subject to the considered (smooth) distributed control algorithm to an infinite-time interval $s \in [0, \infty)$ with s being the stretched time. Based on a property of this time transformation, this results in finite-time convergence as the regular time t approaches to T from any arbitrary initial conditions with bounded local control and internal signals. Finally, two numerical examples illustrate the efficacy of the proposed algorithm.

[2]This section is previously published in [171]. Permission is included in Appendix H.

6.2.1 Introduction

Finite-time distributed control algorithms have paramount importance to time-critical applications of multiagent systems such as simultaneous strike and multiagent automation. Yet, a drawback of standard finite-time algorithms is that their convergence time depends on the initial conditions of agents; hence, a user cannot assign a desired convergence time with these algorithms. Motivated from this standpoint, [12, 13, 61–65] study control algorithms with fixed-time convergence ability. While these algorithms can upper bound the convergence time independently from the initial conditions, the calculated bounds do not necessarily hold globally and/or can be conservative, or some of these results considering system uncertainties can require a knowledge of uncertainty upper bounds for stability. To address this problem, [14, 15, 66–71] study control algorithms that can guarantee convergence at a user-defined finite-time. However, these algorithms are proposed in the context of either sole systems or first-order multiagent systems, or some of these results considering system uncertainties can require, once again, a knowledge of uncertainty upper bounds for stability. We refer to [4, 72, 73] for more details.

Recently, we introduce (smooth) finite-time distributed control algorithm with time transformation for first-order multiagent systems subject to time-varying graph topologies [72], time-invariant graph topologies with dynamic equilibrium points [73], and time-invariant graph topologies with dynamic equilibrium points and system uncertainties [4]. In particular, closely related prior studies to the results of this paper are documented in [4, 73], which guarantee convergence of the single state of agents to a time-varying leader at a-priori given, user-defined time T from any arbitrary initial conditions with bounded local control signals. The former study achieves the convergence without requiring an upper bound on the velocity of this time-varying leader and the latter study achieves the convergence with structured but otherwise completely unknown uncertainties (i.e., without resorting to a knowledge of uncertainty upper bounds). In contrast to the references cited in the first paragraph, [4, 72, 73] utilize a novel time transformation method along with results from infinite horizon stability theory in their respective finite-time convergence analyses (see [4, 72, 73] for details).

Building on our previous studies highlighted above, this paper presents further results for second-order multiagent systems. Specifically, utilizing a user-defined finite-time interval of interest $t \in [0, T)$, we time transform this class of multiagent systems subject to the considered (smooth) distributed control algorithm to an infinite-time interval $s \in [0, \infty)$ with s being the stretched time. Based on a property of this

time transformation, this results in finite-time convergence as the regular time t approaches to T from any arbitrary initial conditions with bounded local control and internal signals. Finally, two numerical examples illustrate the efficacy of the proposed algorithm. We note here that [15, 172–174] consider studies with user-defined finite-time convergence guarantees for systems beyond first-order dynamics. However, the results in [15] can be sensitive to system initial conditions and these results are outside the context of multiagent systems. Moreover, while the results in [172–174] consider second-order multiagent systems and utilize a time-varying control gain, they neither discuss boundedness of their local control signals nor consider system uncertainties.

The notation used in this paper is fairly standard. Specifically, $\mathbb{R}$ denotes the set of real numbers, $\mathbb{R}^n$ denotes the set of $n \times 1$ real column vectors, $\mathbb{R}^{n\times m}$ denotes the set of $n \times m$ real matrices, $\mathbb{R}_+$ denotes the set of positive real numbers, $\mathbb{R}_+^{n\times n}$ (resp., $\overline{\mathbb{R}}_+^{n\times n}$) denotes the set of $n \times n$ positive-definite (resp., nonnegative-definite) real matrices, $\mathbb{Z}_+$ (resp., $\overline{\mathbb{Z}}_+$) denotes the set of positive (resp., nonnegative) integers, 0_n denotes the $n \times 1$ zero vector, $\mathbf{1}_n$ denotes the $n \times 1$ ones vector, $0_{n\times m}$ denotes the $n \times m$ zero matrix, and "$\triangleq$" denotes equality by definition. In addition, we write $(\cdot)^{\mathrm{T}}$ for the transpose function, $(\cdot)^{-1}$ for the inverse function, $\det(\cdot)$ for the determinant function, and $\|\cdot\|_2$ for the Euclidean norm. Furthermore, we write $\lambda_i(A)$ for the ith eigenvalue of the square matrix A (with eigenvalues ordered from minimum to maximum value), and $[A]_{ij}$ for the (i, j)th entry of the matrix A.

6.2.2 Problem Formulation

In this section, we first present the problem formulation of this paper. Specifically, we focus on the leader-follower problem in a multiagent system with N agents exchanging information based on a connected, undirected graph $\mathfrak{G}$ (see below for graph-theoretic notions). Note that considering this benchmark problem is without loss of much generality and the proposed distributed control algorithm can be extended to other multiagent control problems. Mathematically speaking, we consider that the agents have second-order dynamics given by

$$\dot{x}_i(t) = v_i(t), \quad x_i(0) = x_{i0}, \tag{6.43}$$

$$\dot{v}_i(t) = u_i(t), \quad v_i(0) = v_{i0}, \tag{6.44}$$

where $x_i(t) \in \mathbb{R}$ and $v_i(t) \in \mathbb{R}$ respectively denote the position and velocity of agent i, $i \in \{1,2,\ldots,N\}$, and $u_i(t) \in \mathbb{R}$, is the corresponding control signal.

Next, we consider a leader with second-order dynamics

$$\dot{x}_0(t) = v_0(t), \quad x_0(0) = x_{00}, \tag{6.45}$$

$$\dot{v}_0(t) = a_0(t), \quad v_0(0) = v_{00}, \tag{6.46}$$

where $x_0(t) \in \mathbb{R}$ and $v_0(t) \in \mathbb{R}$ respectively denote the position and velocity of the leader. In addition, $a_0(t) \in \mathbb{R}$ in (6.46) stands for a time-varying, bounded, and piecewise continuous acceleration signal of the leader (with unknown bound) under the assumption that this signal results in bounded position and velocity of the leader. Our objective here is to design a distributed control algorithm for achieving finite-time convergence with a-priori given, user-defined finite time $T \in \mathbb{R}_+$; that is,

$$\lim_{t \to T} \big(x_i(t) - x_0(t)\big) = 0, \quad i \in \{1,2,\ldots,N\}. \tag{6.47}$$

We now overview some basic notions from graph theory (see, e.g., [176, 177] for details). In particular, graphs are broadly adopted in the multiagent systems literature for encoding interactions between networked systems. An undirected graph $\mathfrak{G}$ is defined by a set $\mathcal{V}_{\mathfrak{G}} = \{1,\ldots,N\}$ of *nodes* and a set $\mathcal{E}_{\mathfrak{G}} \subset \mathcal{V}_{\mathfrak{G}} \times \mathcal{V}_{\mathfrak{G}}$ of *edges*. If $(i,j) \in \mathcal{E}_{\mathfrak{G}}$, then nodes i and j are neighbors and the neighboring relation is indicated by $i \sim j$. The *degree* of a node is given by the number of its neighbors. Letting d_i denote the degree of node i, then the *degree matrix* of a graph $\mathfrak{G}$, denoted by $\mathcal{D}(\mathfrak{G}) \in \mathbb{R}^{N \times N}$, is given by $\mathcal{D}(\mathfrak{G}) \triangleq \operatorname{diag}[d]$, where $d = [d_1,\ldots,d_N]^{\mathrm{T}}$. A *path* $i_0 i_1 \cdots i_L$ of a graph $\mathfrak{G}$ is a finite sequence of nodes such that $i_{k-1} \sim i_k$, $k = 1,\ldots,L$, and if every pair of distinct nodes has a path, then the graph $\mathfrak{G}$ is connected. We write $\mathcal{A}(\mathfrak{G}) \in \mathbb{R}^{N \times N}$ for the *adjacency matrix* of a graph $\mathfrak{G}$ defined by $[\mathcal{A}(\mathfrak{G})]_{ij} \triangleq 1$, if $(i,j) \in \mathcal{E}_{\mathfrak{G}}$, and $[\mathcal{A}(\mathfrak{G})]_{ij} \triangleq 0$, otherwise, and $\mathcal{B}(\mathfrak{G}) \in \mathbb{R}^{N \times M}$ for the (node-edge) *incidence matrix* of a graph $\mathfrak{G}$ defined by $[\mathcal{B}(\mathfrak{G})]_{ij} \triangleq 1$, if node i is the head of edge j, $[\mathcal{B}(\mathfrak{G})]_{ij} \triangleq -1$, if node i is the tail of edge j, and $[\mathcal{B}(\mathfrak{G})]_{ij} \triangleq 0$, otherwise, where M is the number of edges, i is an index for the node set, and j is an index for the edge set. The *graph Laplacian matrix*, denoted by $\mathcal{L}(\mathfrak{G}) \in \overline{\mathbb{R}}_+^{N \times N}$, is defined by $\mathcal{L}(\mathfrak{G}) \triangleq \mathcal{D}(\mathfrak{G}) - \mathcal{A}(\mathfrak{G})$ or, equivalently, $\mathcal{L}(\mathfrak{G}) = \mathcal{B}(\mathfrak{G})\mathcal{B}(\mathfrak{G})^{\mathrm{T}}$, and the spectrum of the graph Laplacian of a connected, undirected graph $\mathfrak{G}$ can be ordered as $0 = \lambda_1(\mathcal{L}(\mathfrak{G})) < \lambda_2(\mathcal{L}(\mathfrak{G})) \leq \cdots \leq \lambda_N(\mathcal{L}(\mathfrak{G}))$, with 1_N being the eigenvector corresponding to

the zero eigenvalue $\lambda_1(\mathcal{L}(\mathfrak{G}))$, and $\mathcal{L}(\mathfrak{G})1_N = 0_N$ and $e^{\mathcal{L}(\mathfrak{G})}1_N = 1_N$. Throughout this paper, we model a given multiagent system by a connected, undirected graph $\mathfrak{G}$ (nodes and edges respectively represent agents and inter-agent communication links).

In addition to the above notions from graph theory, the following lemma and remarks are used in this paper.

Lemma 6.2.1 (Lemma 3.3, [178]) *Let $K = diag(k)$, $k = [k_1, k_2, \ldots, k_N]^{\mathrm{T}}$, $k_i \in \overline{\mathbb{Z}}_+$, $i = 1, \ldots, N$, and assume that at least one element of k is nonzero. Then, $\mathcal{F}(\mathfrak{G}) \triangleq \mathcal{L}(\mathfrak{G}) + K \in \mathbb{R}_+^{N\times N}$ and $\det(\mathcal{F}(\mathfrak{G})) \neq 0$ for the Laplacian of a connected, undirected graph.*

Remark 6.2.1 *From Lemma 6.2.1, $-\mathcal{F}(\mathfrak{G})$ is clearly a symmetric and Hurwitz matrix. As a consequence, $-\mathcal{F}(\mathfrak{G})$ satisfies the Lyapunov equation $R = \mathcal{F}(\mathfrak{G})P + P\mathcal{F}(\mathfrak{G})$ for a given $R \in \mathbb{R}_+^{N\times N}$.*

Remark 6.2.2 *We use a notion from Section 1.1.1.4 of [179]. Specifically, let $\xi(t)$ denote a solution to the dynamical system*

$$\dot{x}(t) = f(t, x(t)), \quad x(0) = x_0. \tag{6.48}$$

In addition, let $t = \theta(s)$ denote a time transformation, where $\theta(s)$ is a strictly increasing and continuously differentiable function, and define $\chi(s) = \xi(t)$. Then,

$$\chi'(s) = \theta'(s) f(\theta(s), \chi(s)), \quad \chi(\theta^{-1}(0)) = x_0, \tag{6.49}$$

where $\chi'(s) \triangleq d\chi(s)/ds$, and $\theta'(s) \triangleq d\theta(s)/ds$.

6.2.3 Finite-Time Distributed Control of Second-Order Multiagent Systems with Time Transformation

In this section, we propose a time transformation-based finite-time distributed control algorithm for addressing the leader-follower problem stated in Section 6.2.2. To this end, we consider the time transformation function [72, 73] given by

$$t \quad = \quad \theta(s) \triangleq T(1 - e^{-s}), \tag{6.50}$$

where $T \in \mathbb{R}_+$ is the a-priori given, user-defined finite time (see Figure 6.6). Note that this function converts the infinite-time interval $s \in [0,\infty)$ to the finite-time interval of interest $t \in [0,T)$ (vice versa), and it has the derivative with respect to $s \in [0,\infty)$

$$\frac{\mathrm{d}t}{\mathrm{d}s} = \theta'(s) = Te^{-s} = T - t. \tag{6.51}$$

For addressing (6.47), we next introduce the distributed control signal of the form given by

$$\begin{aligned} u_i(t) &= -\alpha \frac{k_\varepsilon + 1}{(T-t)^2}\Big(\sum_{i\sim j}\big(x_i(t)-x_j(t)\big) + k_i\big(x_i(t)-x_0(t)\big)\Big) \\ &\quad -\frac{\alpha}{T-t}\Big(\sum_{i\sim j}\big(v_i(t)-v_j(t)\big) + k_i\big(v_i(t)-v_0(t)\big)\Big) - \frac{k_\varepsilon}{T-t}v_i(t), \quad i \in \{1,2,\ldots,N\}, \end{aligned} \tag{6.52}$$

where $k_\varepsilon \in \mathbb{R}_+$ and $\alpha \in \mathbb{R}_+$ are design parameters. Note that in (6.52), $k_i = 1$ for the subset of the agents having access to the states of the a time-varying leader in (6.45) and (6.46), and $k_i = 0$ for other agents. Now, let $\tilde{x}_i(t) \triangleq x_i(t) - x_0(t)$, $i \in \{1,2,\ldots,N\}$, and $\tilde{v}_i(t) \triangleq v_i(t) - v_0(t)$, $i \in \{1,2,\ldots,N\}$, be the position and the velocity error states, respectively. Furthermore, define an auxiliary state of the form

$$\begin{aligned} \varepsilon_i(t) &\triangleq v_i(t) + \frac{\alpha}{T-t}\big(\sum_{i\sim j}\big(x_i(t)-x_j(t)\big) + k_i(x_i(t)-x_0(t))\big) \\ &= v_i(t) + \frac{\alpha}{T-t}\big(\sum_{i\sim j}\big(\tilde{x}_i(t)-\tilde{x}_j(t)\big) + k_i\tilde{x}_i(t)\big), \quad i \in \{1,2,\ldots,N\}. \end{aligned} \tag{6.53}$$

One can now use (6.53) to write the position error dynamics as

$$\begin{aligned} \dot{\tilde{x}}_i(t) &= v_i(t) - v_0(t), \\ &= -\frac{\alpha}{T-t}\big(\sum_{i\sim j}\big(\tilde{x}_i(t)-\tilde{x}_j(t)\big) + k_i\tilde{x}_i(t)\big) + \varepsilon_i(t) - v_0(t), \quad \tilde{x}_i(0) = \tilde{x}_{i0}. \end{aligned} \tag{6.54}$$

The derivative of the auxiliary state in (6.53) satisfies

$$\dot{\varepsilon}_i(t) = -\frac{k_\varepsilon}{T-t}\varepsilon_i(t), \quad \varepsilon_i(0) = \varepsilon_{i0}, \tag{6.55}$$

where (6.52) is used.

We now define the augmented position error state, velocity error state, and the auxiliary state respectively as $\tilde{x}(t) \triangleq [\tilde{x}_1(t),\tilde{x}_2(t),\ldots,\tilde{x}_N(t)]^{\mathrm{T}} \in \mathbb{R}^N$, $\tilde{v}(t) \triangleq [\tilde{v}_1(t),\tilde{v}_2(t),\ldots,\tilde{v}_N(t)]^{\mathrm{T}} \in \mathbb{R}^N$, and $\varepsilon(t) \triangleq [\varepsilon_1(t),\varepsilon_2(t),\ldots,\varepsilon_N(t)]^{\mathrm{T}} \in \mathbb{R}^N$. One can then write the system dynamics in (6.54) and (6.55) in the compact form

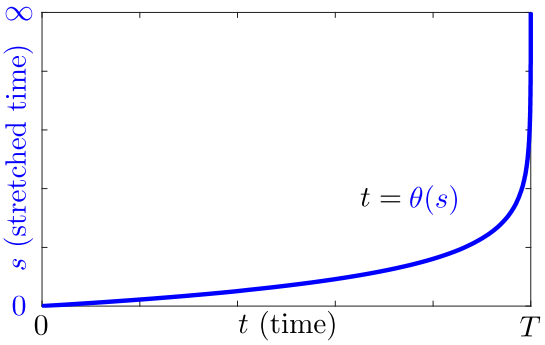

Figure 6.6: The time transformation function in (6.50).

$$\dot{\tilde{x}}(t) = -\frac{\alpha}{T-t}\mathcal{F}(\mathfrak{G})\tilde{x}(t) + \varepsilon(t) - \mathbf{1}_N v_0(t), \quad \tilde{x}(0) = \tilde{x}_0, \tag{6.56}$$

$$\dot{\varepsilon}(t) = -\frac{k_\varepsilon}{T-t}\varepsilon(t), \quad \varepsilon(0) = \varepsilon_0. \tag{6.57}$$

Remark 6.2.3 *Considering the time transformation $t = \theta(s)$ and any signal $\eta(t)$, we write $\eta_s(s)$ to denote the transformed signal in the interval s for notational simplicity in what follows; that is, $\eta_s(s) \triangleq \eta(\theta(s))$.*

Based on the time transformation function in (6.50), let $\xi(t) \in \mathbb{R}^N$, $t \in [0, T)$, be a solution to the dynamical system in (6.56) and define $\tilde{x}_s(s) = \xi(t)$, $s \in [0, \infty)$. It follows from Remark 6.2.2 that

$$\tilde{x}_s'(s) = -\alpha\mathcal{F}(\mathfrak{G})\tilde{x}_s(s) + \theta'(s)\varepsilon_s(s) - \theta'(s)\mathbf{1}_N v_{0_s}(s), \quad \tilde{x}_s(0) = \tilde{x}_0, \tag{6.58}$$

where the subscript s is used; see Remark 6.2.3. As noted in Remark 6.2.2, the solution of (6.56) and (6.58) are equivalent with different argument domains. Introducing (6.51) in (6.58) yields

$$\tilde{x}_s'(s) = -\alpha\mathcal{F}(\mathfrak{G})\tilde{x}_s(s) + Te^{-s}\big(\varepsilon_s(s) - \mathbf{1}_N v_{0_s}(s)\big), \quad \tilde{x}_s(0) = \tilde{x}_0, \tag{6.59}$$

Similarly, one can use the time transformation function in (6.50) to convert (6.57) into the infinite-time interval given by

$$\varepsilon_s'(s) = -k_\varepsilon\varepsilon_s(s), \quad \varepsilon_s(0) = \varepsilon_0. \tag{6.60}$$

As a consequence, the solution of the auxiliary state in the infinite-time horizon can be written as

$$\varepsilon_s(s) = \varepsilon_0 e^{-k_\varepsilon s}. \tag{6.61}$$

Using (6.61) in (6.59) yields

$$\tilde{x}_s'(s) = -\alpha\mathcal{F}(\mathfrak{G})\tilde{x}_s(s) + e^{-s}\beta(s), \quad \tilde{x}_s(0) = \tilde{x}_0, \tag{6.62}$$

where $\beta(s) \triangleq T(\varepsilon_0 e^{-k_\varepsilon s} - \mathbf{1}_N v_{0_s}(s))$ is a bounded function (i.e., $\|\beta(s)\|_2 \leq \overline{\beta}$). For the following result, we also define

$$\mathcal{R} \triangleq \alpha\mathcal{F}(\mathfrak{G}) - 2I_N \in \mathbb{R}^{N\times N}. \tag{6.63}$$

Theorem 6.2.1 *Consider the multiagent system that consists of N agents on a connected, undirected graph* $\mathfrak{G}$*, where the agents have the second-order dynamics given by* (6.43) *and* (6.44)*. Furthermore, assume that there exists at least one agent exchanging information with the leader with bounded position and velocity given by* (6.45) *and* (6.46)*, where this leader is subject to a bounded but otherwise unknown acceleration signal. Based on the distributed control algorithm* $u_i(t)$*,* $i = 1,\ldots,N$*, for each agent given by* (6.52)*, let the design parameter* α *be chosen to make* $\mathcal{R}$ *in* (6.63) *positive definite and* $k_\varepsilon > 1$*. Then, the closed-loop system signals including the control and internal signals remain bounded and all agents' positions converge to the position of the leader in the a-priori given, user-defined finite time T (i.e.,* $\lim_{t\to T}\tilde{x}(t) = 0$*) for all initial conditions of agents.*

Next, we discuss robustness of the proposed distributed control algorithm against non-vanishing, time-dependent system uncertainties (i.e., external disturbances). To this end, consider the second-order agent dynamics given by

$$\dot{x}_i(t) = v_i(t), \quad x_i(0) = x_{i0}, \tag{6.64}$$

$$\dot{v}_i(t) = u_i(t) + \rho_i(t), \quad v_i(0) = v_{i0}, \tag{6.65}$$

where $\rho_i(t) \in \mathbb{R}$ represents external disturbances in the dynamics of each agent. For well-posedness of the considered problem, we here assume that $\rho_i(t)$ and $\dot{\rho}_i(t)$ are bounded but we do not require a knowledge of their upper bounds.

One can write the derivative of the auxiliary state in (6.53) as

$$\dot{\varepsilon}_i(t) = -\frac{k_\varepsilon}{T-t}\varepsilon_i(t) + \rho_i(t), \quad \varepsilon_i(0) = \varepsilon_{i0}, \tag{6.66}$$

where (6.52) is used. Here, (6.66) can also be compactly written as

$$\dot{\varepsilon}(t) \quad = \quad -\frac{k_\varepsilon}{T-t}\varepsilon(t)+\rho(t), \quad \varepsilon(0)=\varepsilon_0, \tag{6.67}$$

with $\rho(t) \triangleq [\rho_1(t),\rho_2(t),\ldots,\rho_N(t)]^{\mathrm{T}} \in \mathbb{R}^N$. Using the time transformation function (6.50), one can convert (6.67) to the infinite-time interval as

$$\varepsilon_s'(s) \quad = \quad -k_\varepsilon\varepsilon_s(s)+Te^{-s}\rho_s(s), \quad \varepsilon_s(0)=\varepsilon_0. \tag{6.68}$$

We can now augment the system dynamics in (6.59) and (6.68) as

$$\begin{bmatrix}\tilde{x}_s'(s)\\ \varepsilon_s'(s)\end{bmatrix} = \begin{bmatrix}-\alpha\mathcal{F} & Te^{-s}I_N\\ 0_{N\times N} & -k_\varepsilon I_N\end{bmatrix}\begin{bmatrix}\tilde{x}_s(s)\\ \varepsilon_s(s)\end{bmatrix}+Te^{-s}\begin{bmatrix}-\mathbf{1}_N v_{0_s}(s)\\ \rho_s(s)\end{bmatrix}, \quad \begin{bmatrix}\tilde{x}_s(0)\\ \varepsilon_s(0)\end{bmatrix}=\begin{bmatrix}\tilde{x}_0\\ \varepsilon_0\end{bmatrix}. \tag{6.69}$$

Theorem 6.2.2 *Consider the multiagent system that consists of N agents on a connected, undirected graph* $\mathcal{G}$*, where the agents have the second-order dynamics as given by* (6.64) *and* (6.65) *having non-vanishing external disturbances. Furthermore, assume that there exists at least one agent exchanging information with the leader with bounded position and velocity given by* (6.45) *and* (6.46)*, where this leader is subject to a bounded but otherwise unknown acceleration signal. Based on the distributed control algorithm* $u_i(t)$*,* $i=1,\ldots,N$*, for each agent given by* (6.52)*, let the design parameter* α *be chosen to make* $\mathcal{R}$ *in* (6.63) *positive definite and* $k_\varepsilon > 1$*. Then, the closed-loop system signals including the control signals remain bounded and all agents' positions converge to the position of the leader in the a-priori given, user-defined finite time T (i.e.,* $\lim_{t\to T}\tilde{x}(t)=0$*) for all initial conditions of agents and for all finite* $\rho_i(t), i\in\{1,\ldots,N\}$*.*

The proof of the above results will be reported elsewhere.

6.2.4 Illustrative Numerical Examples

In this section, we present two numerical examples to demonstrate the utility and efficacy of the proposed distributed control algorithm for achieving user-defined finite-time convergence guarantees.

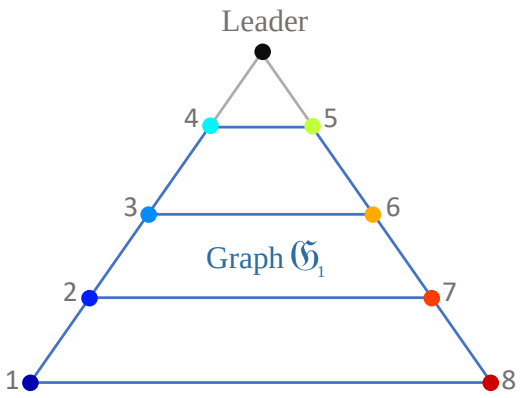

Figure 6.7: An example multiagent system on an undirected, connected line graph $\mathfrak{G}_1$.

6.2.5 Example 1

Consider a multiagent systems that consists of $N = 8$ agents exchanging information based on an undirected, connected line graph $\mathfrak{G}_1$ as shown in Figure 6.7, where agents 4 and 5 have access to the position and velocity of the leader given by $\dot{x}_0(t) = v_0(t), \dot{v}_0(t) = -2x_0(t)$ (i.e., $k_i = 1$ for $i \in \{4,5\}$ and $k_i = 0$ for the rest of the agents in (6.52)). We note that the initial positions and velocities of the agents are respectively selected randomly in the intervals [0,2] and [-2,0].

For the proposed distributed control algorithm, we use the time transformation function given in (6.50) with $T = 5$ in order to enforce the finite-time convergence value equal to 5 seconds and we set $k_\varepsilon = 10$ and $\alpha = 20$ that results in a positive definite matrix $\mathcal{R}$ in (6.63). Figures 6.8 and 6.9 show the performance of the proposed distributed control algorithm in the absence of external disturbances. As expected from Theorem 6.2.1, the position of each agent converges to that of the leader at the chosen user-defined finite time with bounded agent states and control signals.

In order to demonstrate the robustness of the proposed algorithm to external disturbances, we now consider that the non-vanishing external disturbances satisfy $\rho_i(t) = 0.5\sin(2t), i \in \{1,\ldots,8\}$. Figures 6.10 and 6.11 show the performance of the proposed distributed control algorithm in the presence of external disturbances. As expected from Theorem 6.2.2, the position of each agent once again converges to that of the leader at the chosen user-defined finite time with bounded agent states and control signals.

Finally, for illustrating the robustness of the proposed distributed control algorithm to different initial conditions and different non-vanishing external disturbances, consider four additional external disturbance scenarios as

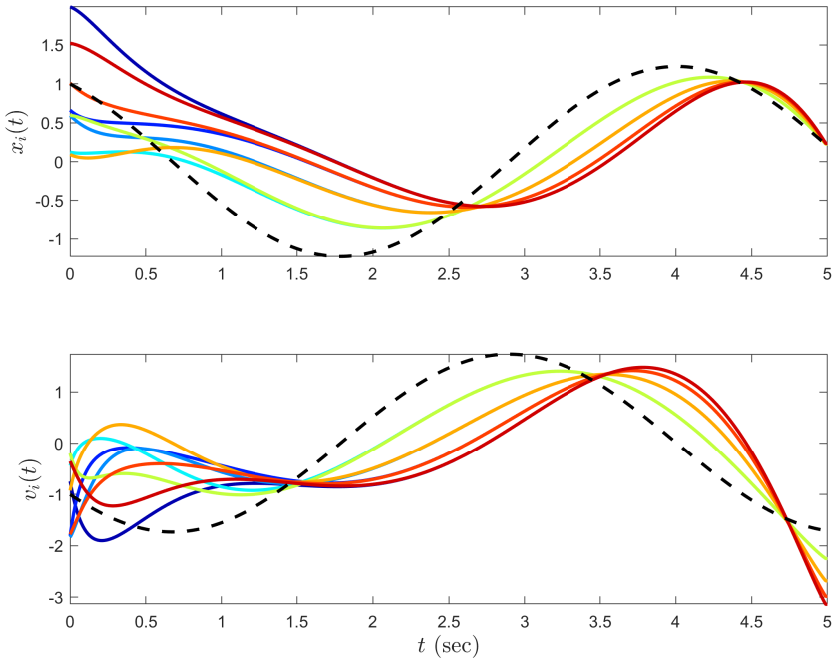

Figure 6.8: Leader-follower performance with the proposed finite-time control algorithm ($T = 5$, $k_\varepsilon = 10$ and $\alpha = 20$) in the absence of external disturbances in Example 1 (dashed line shows the position and velocity of the leader and solid lines show those of the agents).

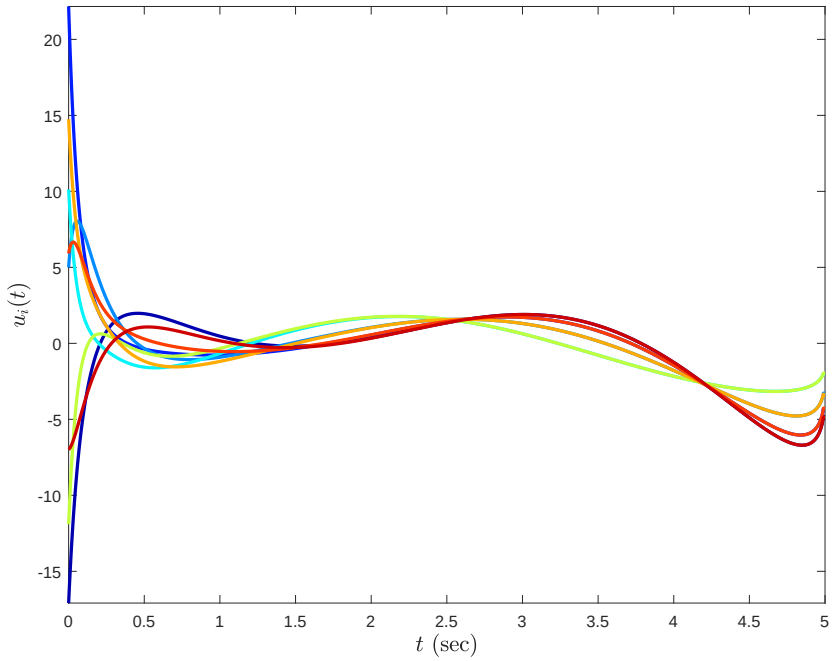

Figure 6.9: Control signal of each agent with the proposed finite-time control algorithm in Example 1 ($T = 5$, $k_\varepsilon = 10$ and $\alpha = 20$) in the absence of external disturbances.

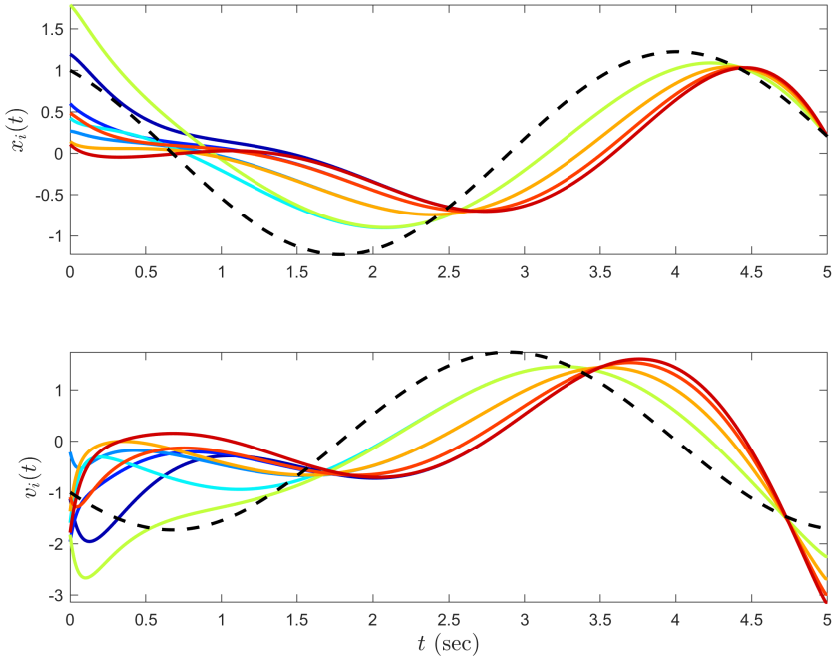

Figure 6.10: Leader-follower performance with the proposed finite-time control algorithm ($T = 5$, $k_\varepsilon = 10$ and $\alpha = 20$) in the presence of non-vanishing uncertainties in Example 1 (dashed line shows the position and velocity of the leader and solid lines show those of the agents).

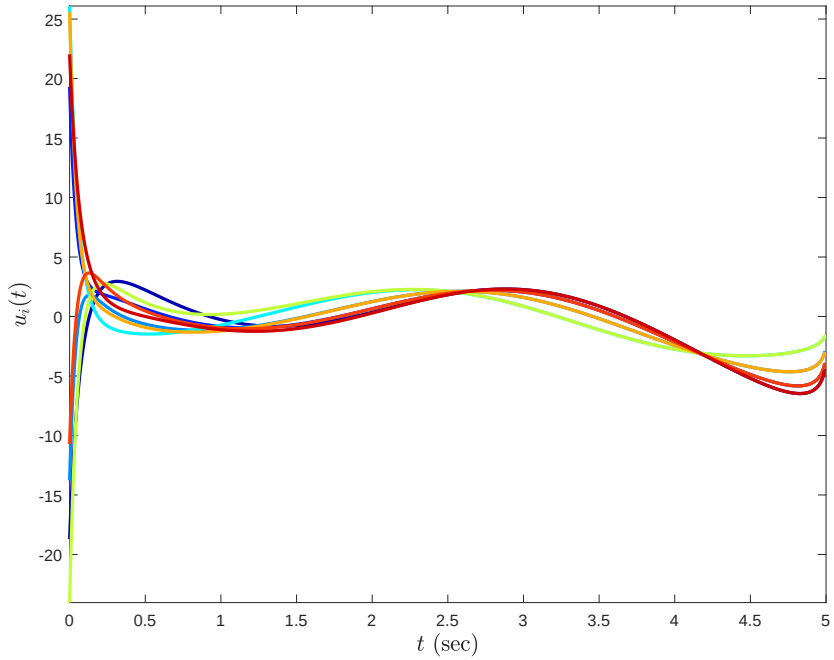

Figure 6.11: Control signal of each agent with the proposed finite-time control algorithm in Example 1 ($T = 5$, $k_\varepsilon = 10$ and $\alpha = 20$) in the presence of non-vanishing uncertainties.

$$\text{A:}\quad \rho_i(t) = 0, \qquad \text{B:}\quad \rho_i(t) = 2\sin(4t), \tag{6.70}$$

$$\text{C:}\quad \rho_i(t) = 3\sin(0.5t), \qquad \text{D:}\quad \rho_i(t) = -5\sin(2t). \tag{6.71}$$

Furthermore, the initial position and velocity of the agents are selected randomly respectively in the intervals $[6,8]$ and $[-8,-6]$ for scenario A, $[2,4]$ and $[-4,-2]$ for scenario B, $[-4,-2]$ and $[2,4]$ for scenario C, and $[-8,-6]$ and $[6,8]$ for scenario D. Figures 6.13 and 6.14 show that in all of these scenarios the proposed algorithm can preserve the user-defined finite-time convergence, regardless of the initial conditions of the agents and without requiring the knowledge of the upper bounds of the external disturbances.

6.2.6 Example 2

In this example, we analyze the proposed control algorithm on a different graph topology by considering a multiagent systems that consists of $N = 8$ agents exchanging information based on an undirected, connected line graph $\mathfrak{G}_2$ as shown in Figure 6.12, where agents 4 and 5 have access to the position and velocity of the leader given by $\dot{x}_0(t) = v_0(t), \dot{v}_0(t) = -2x_0(t)$ (i.e., $k_i = 1$ for $i \in \{4,5\}$, and $k_i = 0$ for the rest of the agents in (6.52)). Similar to the Example 1, the initial positions and velocities of the agents are respectively selected randomly in the intervals [0,2] and [-2,0].

For the proposed distributed control algorithm, we use the time transformation function given in (6.50) with $T = 5$ in order to enforce the finite-time convergence value equal to 5 seconds and we similarly set $k_\varepsilon = 10$ and $\alpha = 20$ that results in a positive definite matrix $\mathcal{R}$ in (6.63). Figures 6.15 and 6.16 show

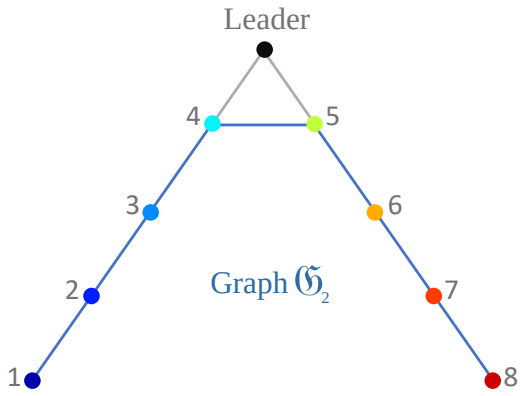

Figure 6.12: An example multiagent system on an undirected, connected line graph $\mathfrak{G}_2$.

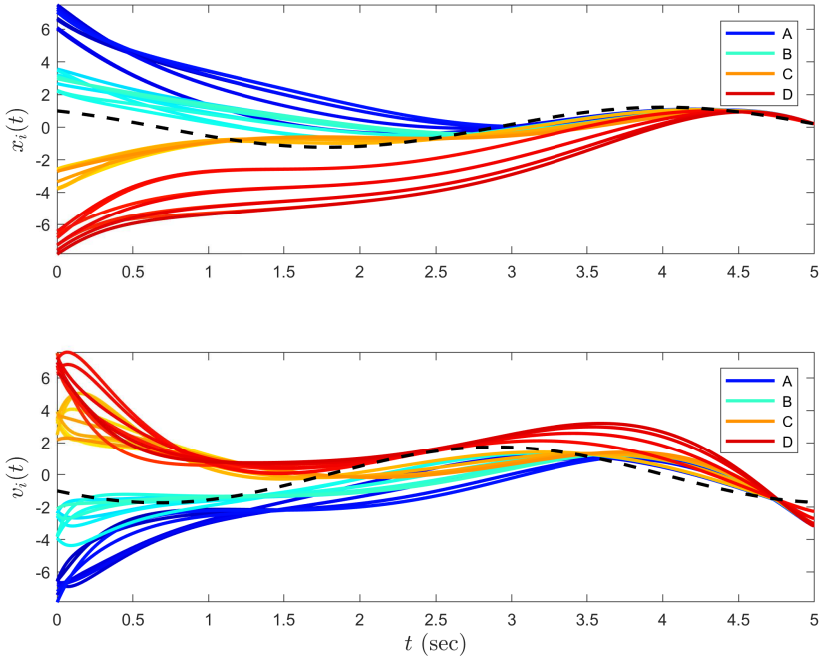

Figure 6.13: Leader-follower performance with the proposed finite-time control algorithm ($T = 5$, $k_\varepsilon = 10$ and $\alpha = 20$) in the presence of different external disturbance scenarios in Example 1 (dashed line shows the position and velocity of the leader and solid lines show those of the agents).

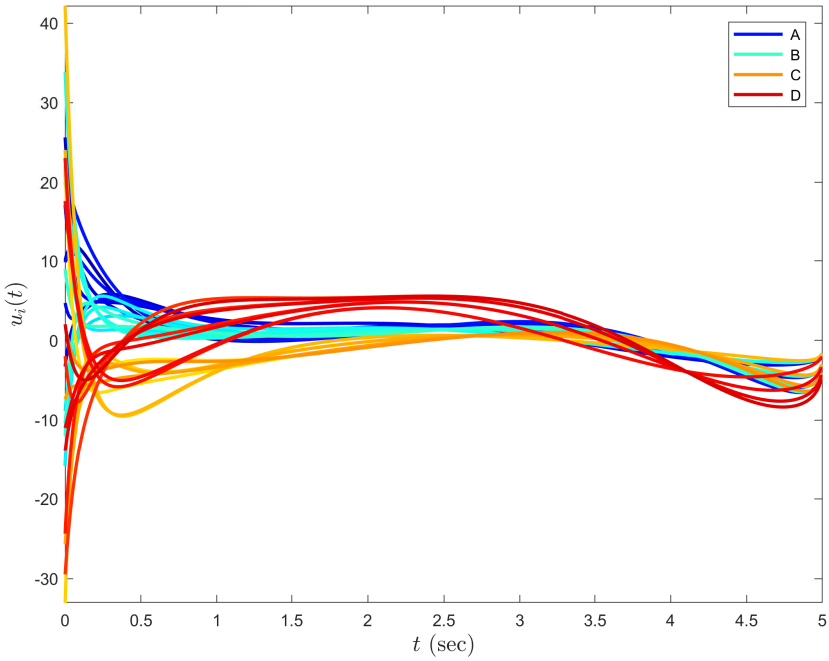

Figure 6.14: Control signal of each agent with the proposed finite-time control algorithm in Example 1 ($T = 5$, $k_\varepsilon = 10$ and $\alpha = 20$) in the presence of different external disturbance scenarios.

the performance of the proposed distributed control algorithm in the absence of external disturbances. Once again, as expected from Theorem 6.2.1, the position of each agent converges to that of the leader at the chosen user-defined finite time with bounded agent states and control signals.

Similar to the Example 1, in order to demonstrate the robustness of the proposed algorithm to external disturbances, we now consider that the non-vanishing external disturbances satisfy $\rho_i(t) = 0.5\sin(2t), i \in \{1,\ldots,8\}$. Figures 6.17 and 6.18 show the performance of the proposed distributed control algorithm in the presence of external disturbances. As expected from Theorem 6.2.2, the position of each agent once again converges to that of the leader at the chosen user-defined finite time with bounded agent states and control signals.

Finally, for illustrating the robustness of the proposed distributed control algorithm to different initial conditions and different non-vanishing external disturbances, we consider four additional external disturbance scenarios as given in (6.70) and (6.71) in Example 1. Figures 6.19 and 6.20 show that in all of these scenarios the proposed algorithm can preserve the user-defined finite-time convergence, regardless of

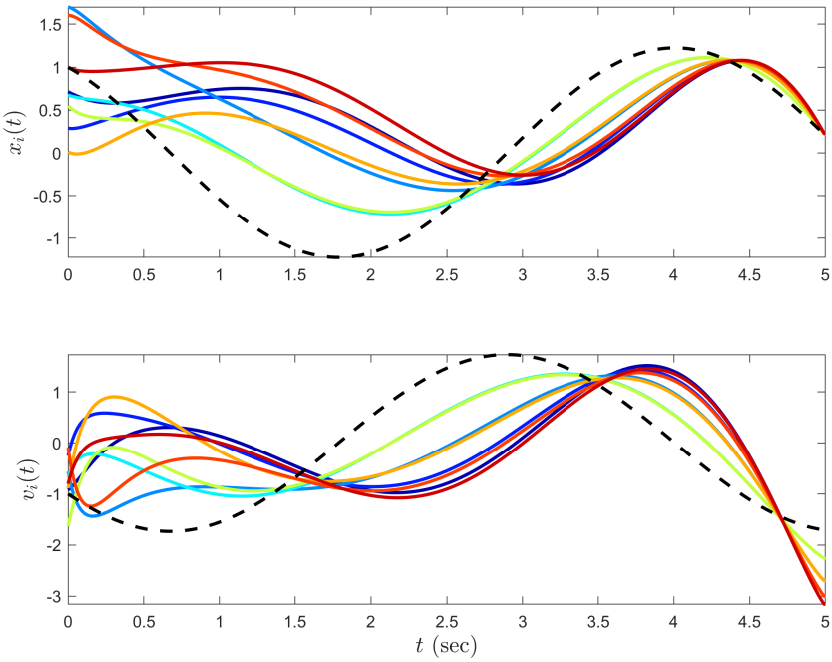

Figure 6.15: Leader-follower performance with the proposed finite-time control algorithm ($T = 5$, $k_\varepsilon = 10$ and $\alpha = 20$) in the absence of external disturbances in Example 2 (dashed line shows the position and velocity of the leader and solid lines show those of the agents).

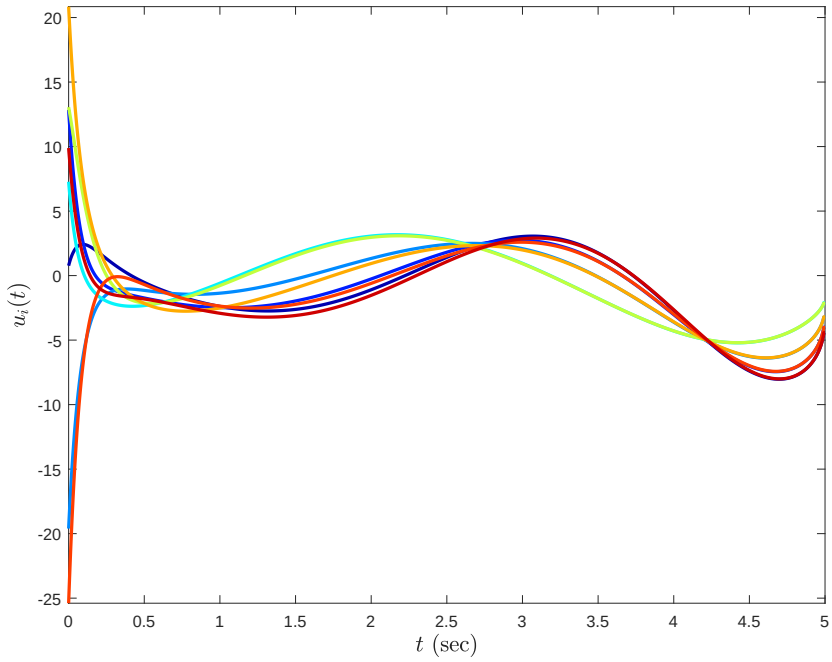

Figure 6.16: Control signal of each agent with the proposed finite-time control algorithm in Example 2 ($T = 5$, $k_\varepsilon = 10$ and $\alpha = 20$) in the absence of external disturbances.

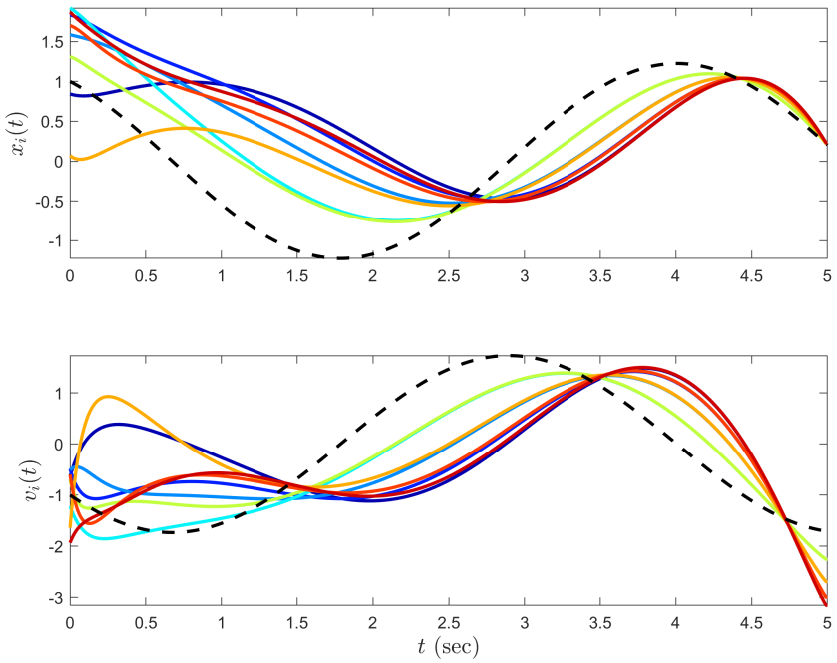

Figure 6.17: Leader-follower performance with the proposed finite-time control algorithm ($T = 5$, $k_\varepsilon = 10$ and $\alpha = 20$) in the presence of non-vanishing uncertainties in Example 2 (dashed line shows the position and velocity of the leader and solid lines show those of the agents).

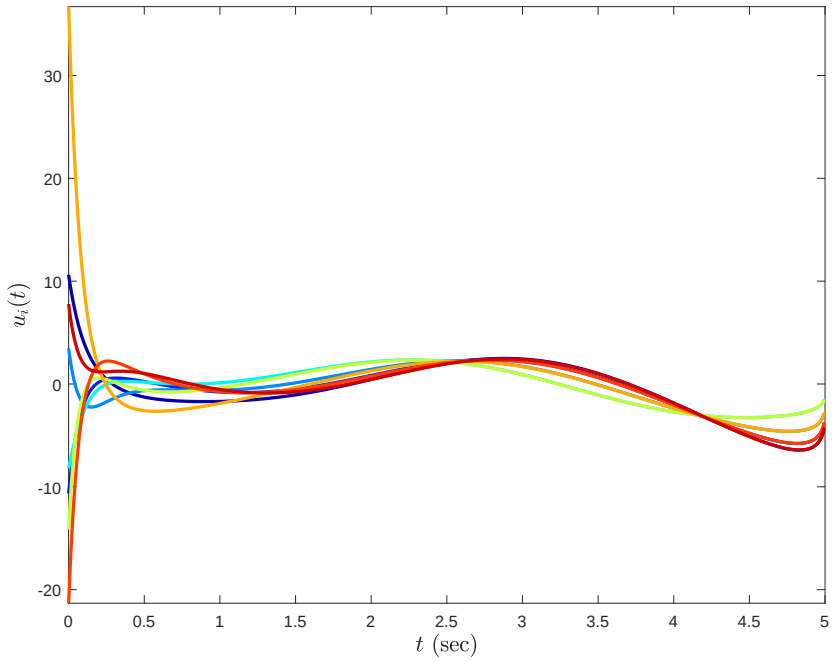

Figure 6.18: Control signal of each agent with the proposed finite-time control algorithm in Example 2 ($T = 5$, $k_\varepsilon = 10$ and $\alpha = 20$) in the presence of non-vanishing uncertainties.

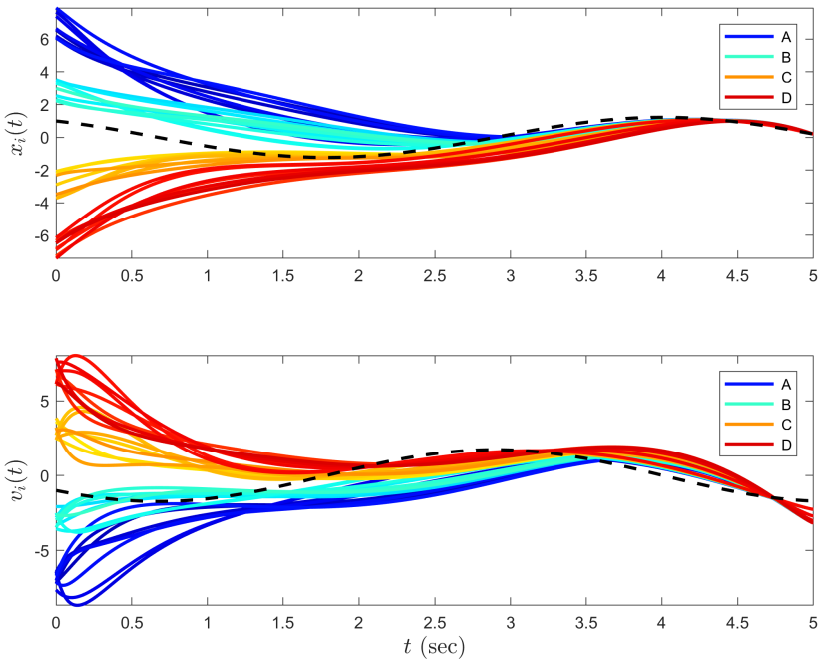

Figure 6.19: Leader-follower performance with the proposed finite-time control algorithm ($T = 5$, $k_\varepsilon = 10$ and $\alpha = 20$) in the presence of different external disturbance scenarios in Example 2 (dashed line shows the position and velocity of the leader and solid lines show those of the agents).

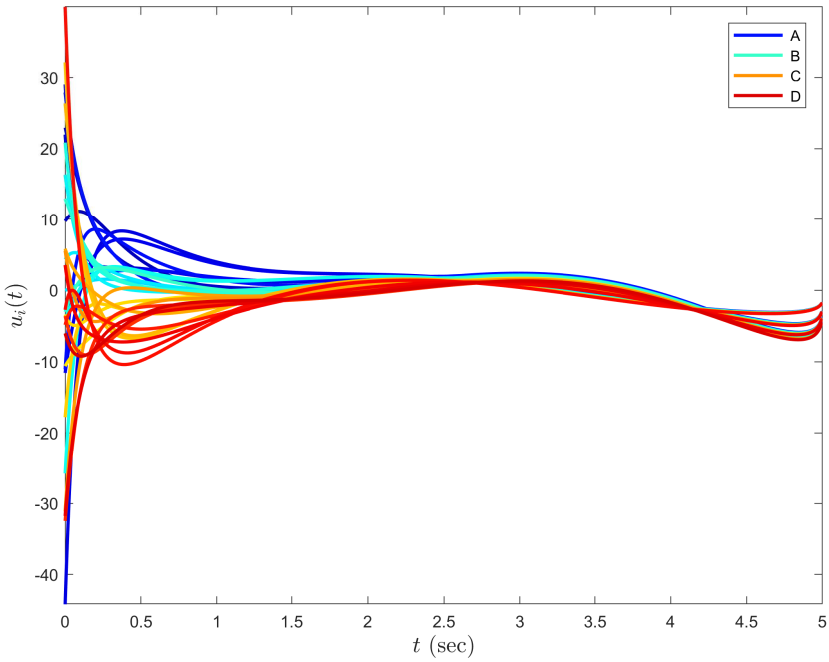

Figure 6.20: Control signal of each agent with the proposed finite-time control algorithm in Example 2 ($T = 5$, $k_\varepsilon = 10$ and $\alpha = 20$) in the presence of different external disturbance scenarios.

the initial conditions of the agents and without requiring the knowledge of the upper bounds of the external disturbances.

6.2.7 Conclusion

Further results on finite-time distributed control of multiagent systems with time transformation were reported. In particular, second-order multiagent systems with a (smooth) finite-time distributed control algorithm were considered and it was discussed through time transformation-based methods that the position state of agents converge to the position of a time-varying leader at a-priori-given, user-defined time from any arbitrary initial conditions with bounded local control and internal signals. Two illustrative numerical examples were also presented in order to demonstrate the efficacy of our results. Building on the contribution of this paper, future research can include generalizations to directed graph topologies as well as agents having higher state dynamics.

CHAPTER 7: MITIGATING THE EFFECTS OF SENSOR UNCERTAINTIES IN NETWORKED MULTIAGENT SYSTEMS[1]

Networked multiagent systems consist of interacting agents that locally exchange information, energy, or matter. Since these systems do not in general have a centralized architecture to monitor the activity of each agent, resilient distributed control system design for networked multiagent systems is essential in providing high system performance, reliability, and operation in the presence of system uncertainties. An important class of such system uncertainties that can significantly deteriorate the achievable closed-loop system performance is sensor uncertainties, which can arise due to low sensor quality, sensor failure, sensor bias, or detrimental environmental conditions. This paper presents a novel distributed adaptive control architecture for networked multiagent systems with undirected communication graph topologies to mitigate the effect of sensor uncertainties. Specifically, we consider agents having identical high-order, linear dynamics with agent interactions corrupted by unknown exogenous disturbances. We show that the proposed adaptive control architecture guarantees asymptotic stability of the closed-loop dynamical system when the exogenous disturbances are time-invariant and uniform ultimate boundedness when the exogenous disturbances are time-varying. Two numerical examples are provided to illustrate the efficacy of the proposed distributed adaptive control architecture.

7.1 Introduction

Networked multiagent systems (e.g., communication networks, power systems, and process control systems) consist of interacting agents that locally exchange information, energy, or matter [162, 176, 181, 182]. These systems require a resilient distributed control system design architecture for providing high system performance, reliability, and operation in the presence of system uncertainties [183–187]. An important class of such system uncertainties that can significantly deteriorate achievable closed-loop dynamical system performance is sensor uncertainties, which can arise due to low sensor quality, sensor failure, sensor bias, or

[1]This chapter is previously published in [180]. Permission is included in Appendix H.

detrimental environmental conditions [74–77]. If relatively cheap sensor suites are used for low-cost, small-scale unmanned vehicle applications, then this can result in inaccurate sensor measurements. Alternatively, sensor measurements can be corrupted by malicious attacks if these dynamical systems are controlled through large-scale, multilayered communication networks as in the case of cyber-physical systems.

Early approaches that deal with sensor uncertainties focus on classical fault detection, isolation, and recovery schemes (see, for example, [188, 189]). In these approaches sensor measurements are compared with an analytical model of the dynamical system by forming a residual signal and analyzing this signal to determine if a fault has occurred. However, in practice it is difficult to identify a single residual signal per failure mode, and as the number of failure modes increase this becomes prohibitive. In addition, a common underlying assumption of the classical fault detection, isolation, and recovery schemes is that all dynamical system signals remain bounded during the fault detection process, which may not always be a valid assumption.

More recently, the authors of [190] consider the fundamental limitations of attack detection and identification methods for linear systems. However, their approach is not only computationally expensive but also it is not linked to the controller design. In [191], adversarial attacks on actuator and sensors are modeled as exogenous disturbances. However, the presented control methodology cannot address situations where more than half of the sensors are compromised and the set of attacked nodes change over time. Finally, the authors in [192] analyze a case where the interaction between networked agents are corrupted by exogenous disturbances. However, their approach is limited to agents having scalar dynamics and is not linked to the controller design in order to mitigate the effect of such sensor uncertainties.

In this paper, we present a novel distributed adaptive control architecture for networked multiagent systems with undirected communication graph topologies to mitigate the effect of sensor uncertainties. Specifically, we consider multiagent systems having identical high-order, linear dynamics with agent interactions corrupted by unknown exogenous disturbances. We show that the proposed adaptive control architecture guarantees asymptotic stability of the closed-loop dynamical system when the exogenous disturbances are time-invariant and uniform ultimate boundedness when the exogenous disturbances are time-varying. A preliminary conference version of this paper appeared in [193]. The present paper considerably expands on [193] by providing detailed proofs of all the results along with additional examples and motivation.

The contents of the paper are as follows. In Section 7.1, we present mathematical preliminaries and give the problem formulation. In Section 7.2.2, we develop a distributed adaptive control architecture for

the case of time-invariant sensor uncertainties, whereas Section 7.2.2 extends this architecture to the case of time-varying sensor uncertainties. Two illustrative examples are provided in Section 7.5 and conclusions are drawn in Section 7.6.

7.2 Mathematical Preliminaries and Problem Formulation

7.2.1 Mathematical Preliminaries

The notation used in this paper is fairly standard. Specifically, $\mathbb{R}$ denotes the set of real numbers, $\mathbb{R}^n$ denotes the set of $n \times 1$ real column vectors, $\mathbb{R}^{n\times m}$ denotes the set of $n \times m$ real matrices, $\mathbb{R}_+$ denotes the set of positive real numbers, $\mathbb{P}^n$ (resp., $\mathbb{N}^n$) denotes the set of $n \times n$ positive definite (resp., nonnegative definite) real matrices, 0_n denotes the $n \times 1$ zero vector, $\mathbf{1}_n$ denotes the $n \times 1$ ones vector, $0_{n\times m}$ denotes the $n \times m$ zero matrix, and "$\triangleq$" denotes equality by definition. In addition, we write $(\cdot)^{\mathrm{T}}$ for the transpose operator, $(\cdot)^{-1}$ for the inverse operator, $\det(\cdot)$ for the determinant operator, $(\cdot)'$ for the Frechet derivative, $\|\cdot\|_2$ for the Euclidean norm, and $\otimes$ for the Kronecker product. Furthermore, we write $\lambda_{\min}(A)$ (resp., $\lambda_{\max}(A)$) for the minimum (resp., maximum) eigenvalue of the square matrix A, $\lambda_i(A)$ for the ith eigenvalue of the square matrix A (with eigenvalues ordered from minimum to maximum value), $\mathrm{spec}(A)$ for the spectrum of the square matrix A including multiplicity, $[A]_{ij}$ for the (i,j)th entry of the matrix A, and $\underline{x}$ (resp., $\bar{x}$) for the lower bound (resp., upper bound) of a bounded signal $x(t) \in \mathbb{R}^n$, $t \geq 0$, that is, $\underline{x} \leq \|x(t)\|_2$, $t \geq 0$ (resp., $\|x(t)\|_2 \leq \bar{x}$, $t \geq 0$).

Next, we recall some basic notions from graph theory, where we refer the reader to [176, 177] for further details. Specifically, graphs are broadly adopted in the multiagent systems literature to encode interactions between networked systems. An undirected graph $\mathfrak{G}$ is defined by a set $\mathcal{V}_{\mathfrak{G}} = \{1,\ldots,N\}$ of *nodes* and a set $\mathcal{E}_{\mathfrak{G}} \subset \mathcal{V}_{\mathfrak{G}} \times \mathcal{V}_{\mathfrak{G}}$ of *edges*. If $(i,j) \in \mathcal{E}_{\mathfrak{G}}$, then nodes i and j are neighbors and the neighboring relation is indicated by $i \sim j$. The *degree* of a node is given by the number of its neighbors. Letting d_i denote the degree of node i, then the *degree matrix* of a graph $\mathfrak{G}$, denoted by $\mathcal{D}(\mathfrak{G}) \in \mathbb{R}^{N\times N}$, is given by $\mathcal{D}(\mathfrak{G}) \triangleq \mathrm{diag}\,[d]$, where $d = [d_1,\ldots,d_N]^{\mathrm{T}}$. A *path* $i_0 i_1 \cdots i_L$ of a graph $\mathfrak{G}$ is a finite sequence of nodes such that $i_{k-1} \sim i_k$, $k = 1,\ldots,L$, and if every pair of distinct nodes has a path, then the graph $\mathfrak{G}$ is connected. We write $\mathcal{A}(\mathfrak{G}) \in \mathbb{R}^{N\times N}$ for the *adjacency matrix* of a graph $\mathfrak{G}$ defined by

$$[\mathcal{A}(\mathfrak{G})]_{ij} \triangleq \begin{cases} 1, & \text{if } (i,j) \in \mathcal{E}_{\mathfrak{G}}, \\ 0, & \text{otherwise}, \end{cases} \tag{7.1}$$

and $\mathcal{B}(\mathfrak{G}) \in \mathbb{R}^{N\times M}$ for the (node-edge) *incidence matrix* of a graph $\mathfrak{G}$ defined by

$$[\mathcal{B}(\mathfrak{G})]_{ij} \triangleq \begin{cases} 1, & \text{if node } i \text{ is the head of edge } j, \\ -1, & \text{if node } i \text{ is the tail of edge } j, \\ 0, & \text{otherwise,} \end{cases} \tag{7.2}$$

where M is the number of edges, i is an index for the node set, and j is an index for the edge set.

The *graph Laplacian matrix*, denoted by $\mathcal{L}(\mathfrak{G}) \in \mathbb{N}^N$, is defined by $\mathcal{L}(\mathfrak{G}) \triangleq \mathcal{D}(\mathfrak{G}) - \mathcal{A}(\mathfrak{G})$ or, equivalently, $\mathcal{L}(\mathfrak{G}) = \mathcal{B}(\mathfrak{G})\mathcal{B}(\mathfrak{G})^{\mathrm{T}}$, and the spectrum of the graph Laplacian of a connected, undirected graph $\mathfrak{G}$ can be ordered as $0 = \lambda_1(\mathcal{L}(\mathfrak{G})) < \lambda_2(\mathcal{L}(\mathfrak{G})) \leq \cdots \leq \lambda_N(\mathcal{L}(\mathfrak{G}))$, with 1_N being the eigenvector corresponding to the zero eigenvalue $\lambda_1(\mathcal{L}(\mathfrak{G}))$, and $\mathcal{L}(\mathfrak{G})1_N = 0_N$ and $e^{\mathcal{L}(\mathfrak{G})}1_N = 1_N$. Finally, we partition the incidence matrix $\mathcal{B}(\mathfrak{G}) = \left[\mathcal{B}_{\mathrm{L}}(\mathfrak{G})^{\mathrm{T}}, \mathcal{B}_{\mathrm{F}}(\mathfrak{G})^{\mathrm{T}}\right]^{\mathrm{T}}$, where $\mathcal{B}_{\mathrm{L}}(\mathfrak{G}) \in \mathbb{R}^{N_{\mathrm{L}}\times M}$, $\mathcal{B}_{\mathrm{F}}(\mathfrak{G}) \in \mathbb{R}^{N_{\mathrm{F}}\times M}$, $N_{\mathrm{L}} + N_{\mathrm{F}} = N$, and N_{L} and N_{F}, respectively denote the cardinalities of the leader and follower groups [176]. Furthermore, without loss of generality, we assume that the leader agents are indexed first and the follower agents are indexed last in the graph $\mathfrak{G}$ so that $\mathcal{L}(\mathfrak{G}) = \mathcal{B}(\mathfrak{G})\mathcal{B}(\mathfrak{G})^{\mathrm{T}}$ is given by

$$\mathcal{L}(\mathfrak{G}) = \begin{bmatrix} L(\mathfrak{G}) & G(\mathfrak{G})^{\mathrm{T}} \\ G(\mathfrak{G}) & F(\mathfrak{G}) \end{bmatrix}, \tag{7.3}$$

where $L(\mathfrak{G}) \triangleq \mathcal{B}_{\mathrm{L}}(\mathfrak{G})\mathcal{B}_{\mathrm{L}}(\mathfrak{G})^{\mathrm{T}}$, $G(\mathfrak{G}) \triangleq \mathcal{B}_{\mathrm{F}}(\mathfrak{G})\mathcal{B}_{\mathrm{L}}(\mathfrak{G})^{\mathrm{T}}$, and $F(\mathfrak{G}) \triangleq \mathcal{B}_{\mathrm{F}}(\mathfrak{G})\mathcal{B}_{\mathrm{F}}(\mathfrak{G})^{\mathrm{T}}$. Note that $F(\mathfrak{G}) \in \mathbb{P}^{N_{\mathrm{F}}}$ for a connected, undirected graph $\mathfrak{G}$ and satisfies $F(\mathfrak{G})\mathbf{1}_{N_{\mathrm{F}}} = -G(\mathfrak{G})\mathbf{1}_{N_{\mathrm{L}}}$. This implies that each row sum of $-F(\mathfrak{G})^{-1}G(\mathfrak{G})$ is equal to 1.

7.2.2 Problem Formulation

Consider a networked multiagent system consisting of N agents with the dynamics of agent i, $i \in \{1,\ldots,N\}$, given by

$$\dot{x}_i(t) \quad = \quad Ax_i(t) + Bu_i(t), \quad x_i(0) = x_{i0}, \quad t \geq 0, \tag{7.4}$$

where $x_i(t) \in \mathbb{R}^n$, $t \geq 0$, is the state vector of agent i, $u_i(t) \in \mathbb{R}^m$, $t \geq 0$, is the control input of agent i, and $A \in \mathbb{R}^{n\times n}$ and $B \in \mathbb{R}^{n\times m}$ are system matrices. We assume that the pair (A,B) is controllable and the control

input $u_i(\cdot)$, $i = 1,\ldots,N$, is restricted to the class of admissible controls consisting of measurable functions such that $u_i(t) \in \mathbb{R}^m$, $t \geq 0$. In addition, we assume that the agents can measure their own state and can locally exchange information via a connected, undirected graph $\mathfrak{G}$ with nodes and edges representing agents and interagent information exchange links, respectively, resulting in a static network topology; that is, the time evolution of the agents do not result in edges appearing or disappearing in the network.

Here, we consider a networked multiagent system, where the agents lie on an agent layer and their local controllers lie on a control layer as depicted in Figure 7.1. Furthermore, we assume that the graph for the controller structure is the same as the graph for the agents' communication. Specifically, agent $i \in \{1,\ldots,N\}$ sends its state measurement to its corresponding local controller at a given control layer and this controller sends its control input to agent i lying on the agent layer. In addition, we assume that the compromised state measurement

$$\tilde{x}_i(t) = x_i(t) + \delta_i(t), \quad i = 1,\ldots,N, \tag{7.5}$$

is available to the local controller and the neighboring agents of agent $i \in \{1,\ldots,N\}$, where $\tilde{x}_i(t) \in \mathbb{R}^n$, $t \geq 0$, and $\delta_i(t) \in \mathbb{R}^n$, $t \geq 0$, captures sensor uncertainties. In particular, if $\delta_i(\cdot)$ is nonzero, then the state vector $x_i(t)$, $t \geq 0$, of agent $i \in \{1,\ldots,N\}$ is corrupted with a faulty or malicious signal $\delta_i(\cdot)$. Alternatively, if $\delta_i(\cdot)$ is zero, then $\tilde{x}_i(t) = x_i(t)$, $t \geq 0$, and the uncompromised state measurement is available to the local controller of agent $i \in \{1,\ldots,N\}$.

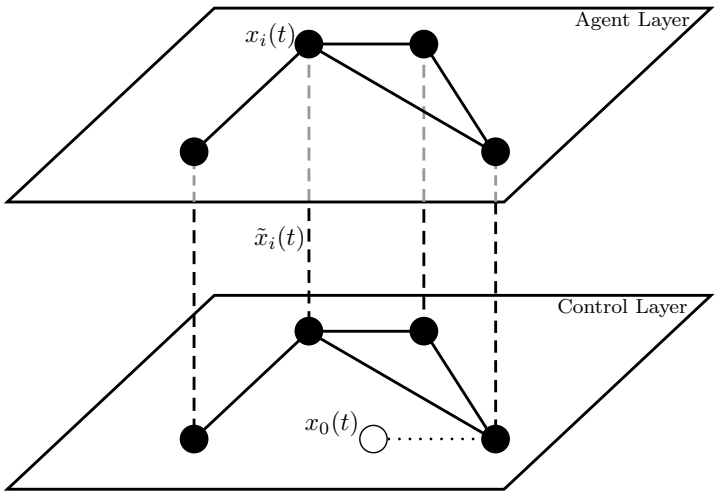

Figure 7.1: A networked multiagent system with agents lying on an agent layer and their local controllers lying on a control layer.

Given the two-layer networked multiagent system hierarchy, we are interested in the problem of asymptotically (or approximately) driving the state vector of each agent $x_i(t)$, $i = 1,\ldots,N$, $t \geq 0$, to the state vector of a (virtual) leader $x_0(t) \in \mathbb{R}^n$, $t \geq 0$, that lies on the control layer with dynamics

$$\dot{x}_0(t) = A_0 x_0(t), \quad x_0(0) = x_{00}, \quad t \geq 0, \tag{7.6}$$

where $A_0 \in \mathbb{R}^{n\times n}$ is Lyapunov stable and is given by $A_0 \triangleq A - BK_0$ with $K_0 \in \mathbb{R}^{m\times n}$.

For the case where the uncompromised state measurement is available to the local controller of agent $i \in \{1,\ldots,N\}$, that is, $\delta_i(t) \equiv 0$, then the controller

$$u_i(t) = -K_0 x_i(t) - cK\left[l_i\big(x_i(t) - x_0(t)\big) + \sum_{i\sim j}\big(x_i(t) - x_j(t)\big)\right], \tag{7.7}$$

guarantees that $\lim_{t\to\infty} x_i(t) = x_0(t)$ for all $i = 1,\ldots,N$, where $l_i = 1$ for a set of $N_{\rm L}$ agents that have access to the state of the leader $x_0(t)$, $t \geq 0$, and $l_i = 0$ for the remaining $N_{\rm F}$ agents with $N = N_{\rm L} + N_{\rm F}$, and where $K \in \mathbb{R}^{m\times n}$ and $c \in \mathbb{R}_+$ denote an appropriate feedback gain matrix and coupling strength, respectively, such that $A_\xi \triangleq A_0 - \eta_i cBK$ is Hurwitz for all $\eta_i \in \mathrm{spec}(F(\mathfrak{G}))$. To see this, let $\xi_i(t) \triangleq x_i(t) - x_0(t)$ and note that using (7.4), (7.6), and (7.7),

$$\dot{\xi}_i(t) = A_0\xi_i(t) - cBK\left[l_i\xi_i(t) + \sum_{i\sim j}\big(\xi_i(t) - \xi_j(t)\big)\right], \quad \xi_i(0) = \xi_{i0}, \quad t \geq 0, \tag{7.8}$$

with $\xi_{i0} \triangleq x_{i0} - x_0$. In addition, defining the augmented state $\xi(t) \triangleq [\xi_1^{\rm T}(t),\ldots,\xi_N^{\rm T}(t)]^{\rm T}$, (7.8) can be written in compact form as

$$\dot{\xi}(t) = \big[I_N \otimes A_0 - cF(\mathfrak{G}) \otimes BK\big]\xi(t), \quad \xi(0) = \xi_0, \quad t \geq 0. \tag{7.9}$$

Now, using the results in [187, 194, 195], it can be shown that $I_N \otimes A_0 - cF(\mathfrak{G}) \otimes BK$ is Hurwitz when A_ξ is Hurwitz for all $\eta_i \in \mathrm{spec}(F(\mathfrak{G}))$. Hence, $\lim_{t\to\infty}\xi(t) = 0$, that is, $\lim_{t\to\infty} x_i(t) = x_0(t)$ for all $i = 1,\ldots,N$.

For $\delta(\cdot) \neq 0$, our objective is to design a local controller for each agent $i \in \{1,\ldots,N\}$ of the form

$$u_i(t) = -K_0\tilde{x}_i(t) - cK\left[l_i\big(\tilde{x}_i(t) - x_0(t)\big) + \sum_{i\sim j}\big(\tilde{x}_i(t) - \tilde{x}_j(t)\big)\right] + v_i(t), \tag{7.10}$$

where $v_i(t) \in \mathbb{R}^m$, $t \geq 0$, is a local corrective signal that suppresses or counteracts the effect of $\delta_i(t)$, $t \geq 0$, to asymptotically (or approximately) recover the ideal system performance (i.e., $\lim_{t\to\infty} x_i(t) = x_0(t)$ for all $i = 1,\ldots,N$) that is achieved when the state vector is available for feedback. Thus, assuming that A_ξ is Hurwitz for all $\eta_i \in \mathrm{spec}(F(\mathfrak{G}))$ implies that there exists an ideal system performance that can be recovered by designing the local corrective signals $v_i(t) \in \mathbb{R}^m$, $t \geq 0$, for each agent $i \in \{1,\ldots,N\}$. Although we consider this specific problem in this paper, the proposed approach dealing with sensor uncertainties can be used in many other problems that exist in the networked multiagent systems literature [176, 182].

7.3 Adaptive Leader Following with Time-Invariant Sensor Uncertainties

In this section, we design the local corrective signal $v_i(t)$, $i = 1,\ldots,N$, $t \geq 0$, in (7.10) to achieve asymptotic adaptive leader following in the presence of time-invariant sensor uncertainties, that is, $\delta_i(t) \equiv \delta_i$, $i = 1,\ldots,N$, $t \geq 0$. For this problem, we propose the corrective signal

$$v_i(t) = K_0\hat{\delta}_i(t) + cK\left[l_i\hat{\delta}_i(t) + \sum_{i\sim j}\big(\hat{\delta}_i(t) - \hat{\delta}_j(t)\big)\right], \tag{7.11}$$

where

$$\dot{\hat{\delta}}_i(t) = -\gamma A^{\mathrm{T}}P\big(\tilde{x}_i(t) - \hat{x}_i(t) - \hat{\delta}_i(t)\big), \quad \hat{\delta}_i(0) = \hat{\delta}_{i0}, \quad t \geq 0, \tag{7.12}$$

$$\dot{\hat{x}}_i(t) = A_0\hat{x}_i(t) - cBK\left[l_i\big(\hat{x}_i(t) - x_0(t)\big) + \sum_{i\sim j}\big(\hat{x}_i(t) - \hat{x}_j(t)\big)\right] + \big(\gamma A^{\mathrm{T}}P + \mu I_n\big)\big(\tilde{x}_i(t) - \hat{x}_i(t) - \hat{\delta}_i(t)\big), \quad \hat{x}_i(0) = \hat{x}_{i0}, \quad t \geq 0, \tag{7.13}$$

$\hat{\delta}_i(t) \in \mathbb{R}^n$, $t \geq 0$, is the estimate of the sensor uncertainty $\delta_i(t)$, $t \geq 0$, $\hat{x}_i(t) \in \mathbb{R}^n$, $t \geq 0$, is the state estimate of the uncompromised state vector $x_i(t)$, $t \geq 0$, $\gamma \in \mathbb{R}_+$ and $\mu \in \mathbb{R}_+$ are design gains, and $P \in \mathbb{P}^n$ is a solution to the linear matrix inequality (LMI) given by

$$I_N \otimes (A_0^{\mathrm{T}}P + PA_0 - 2\mu P) - cF(\mathfrak{G}) \otimes (K^{\mathrm{T}}B^{\mathrm{T}}P + PBK) < 0. \tag{7.14}$$

For the statement of next result, we note from (7.4) and (7.10) that

$$\dot{x}_i(t) = Ax_i(t) - BK_0x_i(t) - cBK\left[l_i\big(x_i(t) - x_0(t)\big) + \sum_{i\sim j}\big(x_i(t) - x_j(t)\big)\right] - cBK\sum_{i\sim j}\big(\delta_i - \delta_j\big) - B\big(cl_iK + K_0\big)\delta_i + Bv_i(t), \quad x_i(0) = x_{i0}, \quad t \geq 0. \tag{7.15}$$

Now, define $x(t) \triangleq [x_1^{\mathrm{T}}(t),\ldots,x_N^{\mathrm{T}}(t)]^{\mathrm{T}}$, $\delta \triangleq [\delta_1^{\mathrm{T}},\ldots,\delta_N^{\mathrm{T}}]^{\mathrm{T}}$, and $v(t) \triangleq [v_1(t),\ldots,v_N(t)]^{\mathrm{T}}$, and note that (7.15) can be written in a compact form as

$$\begin{aligned}\dot{x}(t) &= [I_N \otimes A_0 - cF(\mathfrak{G}) \otimes BK]x(t) + (cG(\mathfrak{G}) \otimes BK)x_0(t) - \big(cF(\mathfrak{G}) \otimes BK + I_N \otimes BK_0\big)\delta \\ &\quad + (I_N \otimes B)v(t), \quad x(0) = x_0, \quad t \geq 0. \end{aligned} \tag{7.16}$$

Using (7.5) and (7.16), the dynamics for $\tilde{x}(t)$, $t \geq 0$, with $\tilde{x}(t) \triangleq [\tilde{x}_1^{\mathrm{T}}(t),\ldots,\tilde{x}_N^{\mathrm{T}}(t)]^{\mathrm{T}}$, can also be written in compact form as

$$\begin{aligned}\dot{\tilde{x}}(t) &= [I_N \otimes A_0 - cF(\mathfrak{G}) \otimes BK]\tilde{x}(t) + (cG(\mathfrak{G}) \otimes BK)x_0(t) - (I_N \otimes A)\delta \\ &\quad + (I_N \otimes B)v(t), \quad \tilde{x}(0) = \tilde{x}_0, \quad t \geq 0. \end{aligned} \tag{7.17}$$

Next, letting $\hat{x}(t) \triangleq [\hat{x}_1^{\mathrm{T}}(t),\ldots,\hat{x}_N^{\mathrm{T}}(t)]^{\mathrm{T}}$, a compact form for the dynamics of $\hat{x}(t)$, $t \geq 0$, is given by

$$\begin{aligned}\dot{\hat{x}}(t) &= [I_N \otimes A_0 - cF(\mathfrak{G}) \otimes BK]\hat{x}(t) + (cG(\mathfrak{G}) \otimes BK)x_0(t) - \big(cF(\mathfrak{G}) \otimes BK + I_N \otimes BK_0\big)\hat{\delta}(t) \\ &\quad + (I_N \otimes B)v(t) + \phi(t), \quad \hat{x}(0) = \hat{x}_0, \quad t \geq 0, \end{aligned} \tag{7.18}$$

where $\phi(t) \triangleq [\phi_1^{\mathrm{T}}(t),\ldots,\phi_N^{\mathrm{T}}(t)]^{\mathrm{T}}$ with $\phi_i(t) \triangleq -\dot{\hat{\delta}}_i(t) + \mu e_i(t)$. Finally, define $e_i(t) \triangleq \tilde{x}_i(t) - \hat{x}_i(t) - \hat{\delta}_i(t)$ and $\tilde{\delta}_i(t) \triangleq \delta_i - \hat{\delta}_i(t)$, and note that

$$\dot{e}(t) = (A_r - \mu I_{nN})e(t) - (I_N \otimes A)\tilde{\delta}(t), \quad e(0) = e_0, \quad t \geq 0, \tag{7.19}$$

$$\dot{\tilde{\delta}}(t) = (I_N \otimes \gamma A^{\mathrm{T}}P)e(t), \quad \tilde{\delta}(0) = \tilde{\delta}_0, \quad t \geq 0, \tag{7.20}$$

where $A_r \triangleq I_N \otimes A_0 - cF(\mathfrak{G}) \otimes BK$, $e(t) \triangleq [e_1^{\mathrm{T}}(t),\ldots,e_N^{\mathrm{T}}(t)]^{\mathrm{T}}$, and $\tilde{\delta}(t) \triangleq [\tilde{\delta}_1^{\mathrm{T}}(t),\ldots,\tilde{\delta}_N^{\mathrm{T}}(t)]^{\mathrm{T}}$.

Theorem 7.3.1 *Consider the networked multiagent system consisting of N agents on a connected, undirected graph $\mathfrak{G}$, where the dynamics of agent $i \in \{1,\ldots,N\}$ is given by (7.4). In addition, assume that the local controller $u_i(t)$, $i = 1,\ldots,N$, $t \geq 0$, for each agent is given by (7.10) with the corrective signal $v_i(t)$, $i = 1,\ldots,N$, $t \geq 0$, given by (7.11). Moreover, assume that $\delta_i(t) \equiv \delta_i$, $t \geq 0$, and $\det(A) \neq 0$. Then, the zero solution $\big(e(t),\tilde{\delta}(t)\big) \equiv \big(0,0\big)$ of the closed-loop system given by (7.19) and (7.20) is Lyapunov stable and $\lim_{t\to\infty} e(t) = 0$ and $\lim_{t\to\infty} \tilde{\delta}(t) = 0$ for all $\big(e_0,\tilde{\delta}_0\big) \in \mathbb{R}^{nN} \times \mathbb{R}^{nN}$.*

Proof. To show Lyapunov stability of the zero solution $\big(e(t),\tilde{\delta}(t)\big)\equiv\big(0,0\big)$ of the closed-loop system given by (7.19) and (7.20), consider the Lyapunov function candidate given by

$$V\big(e,\tilde{\delta}\big)=\sum_{i=1}^{N}(e_i^{\mathrm{T}}Pe_i+\gamma^{-1}\tilde{\delta}_i^{\mathrm{T}}\tilde{\delta}_i)=e^{\mathrm{T}}(I_N\otimes P)e+\gamma^{-1}\tilde{\delta}^{\mathrm{T}}\tilde{\delta}, \tag{7.21}$$

where P is a solution to the LMI given by (7.14). Note that $V(0,0)=0$, $V\big(e,\tilde{\delta}\big)>0$ for all $\big(e,\tilde{\delta}\big)\neq(0,0)$, and $V\big(e,\tilde{\delta}\big)$ is radially unbounded. The time derivative of (7.21) along the trajectories of (7.19) and (7.20) is given by

$$\dot{V}\big(e(t),\tilde{\delta}(t)\big)=e^{\mathrm{T}}(t)\Big(I_N\otimes(A_0^{\mathrm{T}}P+PA_0-2P\mu)-cF(\mathfrak{G})\otimes(K^{\mathrm{T}}B^{\mathrm{T}}P+PBK)\Big)e(t)\leq 0,\quad t\geq 0. \tag{7.22}$$

Hence, the zero solution $\big(e(t),\tilde{\delta}(t)\big)\equiv\big(0,0\big)$ of the closed-loop system given by (7.19) and (7.20) is Lyapunov stable for all $\big(e_0,\tilde{\delta}_0\big)\in\mathbb{R}^{nN}\times\mathbb{R}^{nN}$.

To show $\lim_{t\to\infty}e(t)=0$, note that $\ddot{V}\big(e(t),\tilde{\delta}(t)\big)=2e^{\mathrm{T}}(t)\big[I_N\otimes(A_0^{\mathrm{T}}P+PA_0-2P\mu)-cF(\mathfrak{G})\otimes(K^{\mathrm{T}}B^{\mathrm{T}}P+PBK)\big]\dot{e}(t)$. Now, it follows from the Lyapunov stability of the zero solution $\big(e(t),\tilde{\delta}(t)\big)\equiv(0,0)$ of (19) and (20), and the boundedness of $\dot{e}(t),t\geq 0$, that $\ddot{V}\big(e(t),\tilde{\delta}(t)\big)$ is bounded for all $t\geq 0$. Thus, $\dot{V}\big(e(t),\tilde{\delta}(t)\big)$, $t\geq 0$, is uniformly continuous in t. Now, it follows from Barbalat's lemma [109] that $\lim_{t\to\infty}\dot{V}\big(e(t),\tilde{\delta}(t)\big)=0$, and hence, $\lim_{t\to\infty}e(t)=0$. Finally, to show $\lim_{t\to\infty}\tilde{\delta}(t)=0$, define $\mathcal{R}\triangleq\{(e,\tilde{\delta}):\dot{V}(e,\tilde{\delta})=0\}$ and let $\mathcal{M}$ be the largest invariant set contained in $\mathcal{R}$. In this case, it follows from (7.19) that $(I_N\otimes A)\tilde{\delta}=0$, and hence, $\tilde{\delta}=0$ since $\det(A)\neq 0$. Thus, $\big(e(t),\tilde{\delta}(t)\big)\to\mathcal{M}=\{(0,0)\}$ as $t\to\infty$. ■

Remark 7.3.1 *It follows from (7.4), (7.10), and (7.11) that*

$$\begin{aligned}\dot{x}_i(t) &= A_0x_i(t)-cBK\left[l_i\big(x_i(t)-x_0(t)\big)+\sum_{i\sim j}\big(x_i(t)-x_j(t)\big)\right]-BK_0\tilde{\delta}_i(t)\\ &\quad -cBK\left[l_i\tilde{\delta}_i(t)+\sum_{i\sim j}\big(\tilde{\delta}_i(t)-\tilde{\delta}_j(t)\big)\right],\quad x_i(0)=x_{i0},\quad t\geq 0,\end{aligned} \tag{7.23}$$

which, using the boundedness of $\tilde{\delta}_i(t)$, $i=1,\ldots,N$, $t\geq 0$, and the assumption that A_ξ is Hurwitz for all $\eta_i\in\operatorname{spec}(F(\mathfrak{G}))$, implies that $x_i(t)$ is bounded for all $t\geq 0$ and $i\in\{1,\ldots,N\}$. Hence, using (7.5), $\tilde{x}_i(t)$ is bounded for all $t\geq 0$ and $i\in\{1,\ldots,N\}$. Furthermore, since $e_i(t)$, $t\geq 0$, $\tilde{x}_i(t)$, $t\geq 0$, and $\hat{\delta}_i(t)$, $t\geq 0$, are bounded for all $i\in\{1,\ldots,N\}$, it follows that $\hat{x}_i(t)$ is bounded for all $t\geq 0$ and $i\in\{1,\ldots,N\}$.

Remark 7.3.2 *Since, by Theorem 7.3.1,* $\lim_{t\to\infty}\tilde{\delta}(t)=0$ *it follows from (7.23) that each agent subject to the dynamics given by (7.4) asymptotically recovers the ideal system performance (i.e.,* $\lim_{t\to\infty}x_i(t)=x_0(t)$ *for all* $i=1,\ldots,N$*), which is a direct consequence of the discussion given in Section 7.2.2 and the assumption that* A_ξ *is Hurwitz for all* $\eta_i\in\operatorname{spec}(F(\mathfrak{G}))$*,* $i=1,\ldots,N$*. In addition,* $\lim_{t\to\infty}e(t)=0$ *and* $\lim_{t\to\infty}\tilde{\delta}(t)=0$ *imply that* $\lim_{t\to\infty}\big(x(t)-\hat{x}(t)\big)=0$*, which shows that the state estimate* $\hat{x}(t)$*,* $t\geq 0$*, converges to the uncompromised state measurement* $x(t)$*,* $t\geq 0$*.*

Remark 7.3.3 *It is important to note that the local controller* $u_i(t)$ *and corrective signal* $v_i(t)$*,* $i=1,\ldots,N$*,* $t\geq 0$*, are independent of the system initial conditions. The same remark holds for Theorem 7.4.1 below.*

Let $Q\in\mathbb{P}^m$, set $K=Q^{-1}B^{\mathrm{T}}P$, and assume that A_ξ is Hurwitz for all $\eta_i\in\operatorname{spec}(F(\mathfrak{G}))$, $i=1,\ldots,N$ for the given selection of K. Substituting $K=Q^{-1}B^{\mathrm{T}}P$ in (7.14) yields

$$I_N\otimes(A_0^{\mathrm{T}}P+PA_0-2\mu P)-2cF(\mathfrak{G})\otimes(PBQ^{-1}B^{\mathrm{T}}P)<0. \tag{7.24}$$

Let T be such that $TF(\mathfrak{G})T^{-1}=J$, where J is the Jordan form of $F(\mathfrak{G})$. Multiplying (7.24) by $T\otimes I_N$ from the left and by $T^{-1}\otimes I_N$ from the right yields

$$(T\otimes I_N)(I_N\otimes(A_0^{\mathrm{T}}P+PA_0-2\mu P))(T^{-1}\otimes I_N)-2(T\otimes I_N)(cF(\mathfrak{G})\otimes(PBQ^{-1}B^{\mathrm{T}}P))(T^{-1}\otimes I_N)<0, \tag{7.25}$$

which can be equivalently written as

$$I_N\otimes(A_0^{\mathrm{T}}P+PA_0-2\mu P)-2cJ\otimes(PBQ^{-1}B^{\mathrm{T}}P)<0. \tag{7.26}$$

Note that since $F(\mathfrak{G})$ is symmetric, $F(\mathfrak{G})$ is real diagonalizable. Hence, the diagonal form of J allows one to rewrite (7.26) as

$$A_0^{\mathrm{T}}P+PA_0-2\mu P-2c\eta_iPBQ^{-1}B^{\mathrm{T}}P<0, \tag{7.27}$$

where $\eta_i\in\operatorname{spec}(F(\mathfrak{G}))$, $i=1,\ldots,N$. Now, letting the coupling strength be such that $c\geq\frac{1}{\min\{\eta_i\}}$, $i=1,\ldots,N$, it follows from (7.27), using the results in [196], that

$$A_0^{\mathrm{T}}P+PA_0-2\mu P-2c\eta_iPBQ^{-1}B^{\mathrm{T}}P\leq A_0^{\mathrm{T}}P+PA_0-2\mu P-2PBQ^{-1}B^{\mathrm{T}}P, \tag{7.28}$$

since $-c\eta_i \leq -1, i = 1, \ldots, N$, and hence, one can equivalently solve the LMI

$$(A_0 - \mu I_n)^{\mathrm{T}} P + P(A_0 - \mu I_n) - 2PBQ^{-1}B^{\mathrm{T}}P < 0 \tag{7.29}$$

to obtain $P \in \mathbb{P}^n$ rather than the LMI given by (7.14).

Remark 7.3.4 *By setting $S \triangleq P^{-1}$ [197], the LMI given by (7.29) can be further simplified to*

$$(A_0 - \mu I_n)S + S(A_0 - \mu I_n)^{\mathrm{T}} - 2BQ^{-1}B^{\mathrm{T}} < 0. \tag{7.30}$$

Thus, one can alternatively solve (7.30) for $S \in \mathbb{P}^n$ and then set $P = S^{-1}$ to obtain $P \in \mathbb{P}^n$ for (7.12) and (7.13). Note that since one can solve (7.30) *instead of* (7.14)*, the computational complexity does not increase as the number of agents gets large.*

Finally, note that in this paper we consider the case where each agent is subject to sensor uncertainties. If, however, only a fraction of the agents are subject to sensor uncertainties, then the proposed corrective signal in (7.11) can be applied to only those agents subject to sensor uncertainty and not to all the agents.

7.4 Adaptive Leader Following with Time-Varying Sensor Uncertainties

In this section, we generalize the results of the previous section by designing the local corrective signal $v_i(t)$, $i = 1, \ldots, N$, $t \geq 0$, in (7.10) to achieve approximate adaptive leader following in the presence of time-varying sensor uncertainties $\delta_i(t)$, $i = 1, \ldots, N$, $t \geq 0$. We assume that the time-varying sensor uncertainties are bounded and have bounded time rates of change; that is, $\|\delta_i(t)\|_2 \leq \overline{\delta}, t \geq 0$, and $\|\dot{\delta}_i(t)\|_2 \leq \overline{\dot{\delta}}, t \geq 0$, for all $i = 1, \ldots, N$.

For the statement of our next result, it is necessary to introduce the projection operator [80]. Specifically, let $\phi : \mathbb{R}^n \longrightarrow \mathbb{R}$ be a continuously differentiable convex function given by $\phi(\theta) \triangleq \frac{(\varepsilon_\theta + 1)\theta^{\mathrm{T}}\theta - \theta_{\max}^2}{\varepsilon_\theta \theta_{\max}^2}$, where $\theta_{\max} \in \mathbb{R}$ is a *projection norm bound* imposed on $\theta \in \mathbb{R}^n$ and $\varepsilon_\theta > 0$ is a *projection tolerance bound*. Then, the *projection operator* $\mathrm{Proj} : \mathbb{R}^n \times \mathbb{R}^n \to \mathbb{R}^n$ is defined by

$$\mathrm{Proj}(\theta, y) \triangleq \begin{cases} y, & \text{if } \phi(\theta) < 0, \\ y, & \text{if } \phi(\theta) \geq 0 \text{ and } \phi'(\theta)y \leq 0, \\ y - \frac{\phi'^{\mathrm{T}}(\theta)\phi'(\theta)y}{\phi'(\theta)\phi'^{\mathrm{T}}(\theta)}\phi(\theta), & \text{if } \phi(\theta) \geq 0 \text{ and } \phi'(\theta)y > 0, \end{cases} \tag{7.31}$$

where $y \in \mathbb{R}^n$ and $\phi'(\theta) \triangleq \frac{\partial \phi(\theta)}{\partial \theta}$. Note that it follows from the definition of the projection operator that $(\theta^* - \theta)^{\mathrm{T}} \Big[\mathrm{Proj}(\theta, y) - y \Big] \geq 0$.

Next, for the controller given by (7.10), we use the local corrective signal

$$v_i(t) = K_0 \hat{\delta}_i(t) + cK \left[l_i \hat{\delta}_i(t) + \sum_{i \sim j} \big(\hat{\delta}_i(t) - \hat{\delta}_j(t) \big) \right], \tag{7.32}$$

where

$$\dot{\hat{\delta}}_i(t) = \gamma \mathrm{Proj} \Big(\hat{\delta}_i(t), -A^{\mathrm{T}} P \big(\tilde{x}_i(t) - \hat{x}_i(t) - \hat{\delta}_i(t) \big) \Big), \quad \hat{\delta}_i(0) = \hat{\delta}_{i0}, \quad t \geq 0, \tag{7.33}$$

$$\begin{aligned} \dot{\hat{x}}_i(t) &= A_0 \hat{x}_i(t) - cBK \left[l_i \big(\hat{x}_i(t) - x_0(t) \big) + \sum_{i \sim j} \big(\hat{x}_i(t) - \hat{x}_j(t) \big) \right] + \mu I_n \big(\tilde{x}_i(t) - \hat{x}_i(t) - \hat{\delta}_i(t) \big) \\ &\quad - \gamma \mathrm{Proj} \Big(\hat{\delta}_i(t), -A^{\mathrm{T}} P \big(\tilde{x}_i(t) - \hat{x}_i(t) - \hat{\delta}_i(t) \big) \Big), \quad \hat{x}_i(0) = \hat{x}_{i0}, \quad t \geq 0, \end{aligned} \tag{7.34}$$

and $P \in \mathbb{P}^n$ is the solution to the LMI given by

$$I_N \otimes (A_0^{\mathrm{T}} P + P A_0 - 2\mu P) - cF(\mathfrak{G}) \otimes (K^{\mathrm{T}} B^{\mathrm{T}} P + PBK) < 0. \tag{7.35}$$

(See Remark 7.3.4 for solving the LMI given by (7.35).)

For the statement of the next theorem, define

$$-R \triangleq I_N \otimes (A_0^{\mathrm{T}} P + P A_0 - 2\mu P) - cF(\mathfrak{G}) \otimes (K^{\mathrm{T}} B^{\mathrm{T}} P + PBK) < 0, \tag{7.36}$$

where $R \in \mathbb{P}^{Nn}$, and note that, using similar steps as given in the previous section, the dynamics for $e(t) = \tilde{x}(t) - \hat{x}(t) - \hat{\delta}(t)$ and $\tilde{\delta}(t) = \delta(t) - \hat{\delta}(t)$ are given by

$$\dot{e}(t) = (A_r - \mu I_{nN}) e(t) - (I_N \otimes A) \tilde{\delta}(t) + \dot{\delta}(t), \quad e(0) = e_0, \quad t \geq 0, \tag{7.37}$$

$$\dot{\tilde{\delta}}(t) = \dot{\delta}(t) - \gamma \hat{\delta}_{\mathrm{P}}(t), \quad \hat{\delta}_{\mathrm{P}}(t) \triangleq \big[\hat{\delta}_{\mathrm{P}1}^{\mathrm{T}}(t), \ldots, \hat{\delta}_{\mathrm{P}N}^{\mathrm{T}}(t) \big]^{\mathrm{T}}, \quad \tilde{\delta}(0) = \tilde{\delta}_0, \quad t \geq 0, \tag{7.38}$$

where $\hat{\delta}_{\mathrm{P}i}(t) \triangleq \mathrm{Proj} \Big(\hat{\delta}_i(t), -A^{\mathrm{T}} P e_i(t) \Big)$, $i = 1, \ldots, N$, $t \geq 0$.

Theorem 7.4.1 *Consider the networked multiagent system consisting of N agents on a connected, undirected graph $\mathfrak{G}$, where the dynamics of agent $i \in \{1, \ldots, N\}$ is given by (7.4). In addition, assume that the*

local controller $u_i(t)$, $i=1,\ldots,N$, $t\geq 0$, *for each agent is given by (7.10) with the corrective signal* $v_i(t)$, $i=1,\ldots,N$, $t\geq 0$, *given by (7.32). Moreover, assume that the sensor uncertainties are time-varying and* $\det(A)\neq 0$. *Then, the closed-loop system dynamics given by (7.37) and (7.38) are uniformly bounded for all* $\left(e_0,\tilde{\delta}_0\right)\in\mathbb{R}^{nN}\times\mathbb{R}^{nN}$ *with the ultimate bounds*

$$\|e(t)\|_2 \leq \left[\frac{\lambda_{\max}(P)}{\lambda_{\min}(P)}\eta_1^2+\frac{1}{\gamma\lambda_{\min}(P)}\eta_2^2\right]^{\frac{1}{2}}, \quad t\geq T, \tag{7.39}$$

$$\|\tilde{\delta}(t)\|_2 \leq \left[\gamma\lambda_{\max}(P)\eta_1^2+\eta_2^2\right]^{\frac{1}{2}}, \quad t\geq T, \tag{7.40}$$

where $\eta_1\triangleq\frac{1}{\sqrt{d_1}}\left[\frac{d_2}{2\sqrt{d_1}}+\left(\frac{d_2^2}{4d_1}+d_3\right)^{\frac{1}{2}}\right]$, $\eta_2\triangleq\hat{\delta}_{\max}+\overline{\delta}$, $d_1\triangleq\lambda_{\min}(R)$, $d_2\triangleq 2N\lambda_{\max}(P)\overline{\dot{\delta}}$, *and* $d_3\triangleq 2N\gamma^{-1}\bar{\dot{\delta}}\cdot(\hat{\delta}_{\max}+\bar{\delta})$.

Proof. To show uniform boundedness of the system dynamics given by (7.37) and (7.38), consider the Lyapunov-like function given by (7.21), where P satisfies (7.35). Note that $V(0,0)=0$, $V\left(e,\tilde{\delta}\right)>0$ for all $\left(e,\tilde{\delta}\right)\neq(0,0)$, and $V\left(e,\tilde{\delta}\right)$ is radially unbounded. The time derivative of (7.21) along the closed-loop system trajectories of (7.37) and (7.38) is given by

$$\begin{aligned}
\dot{V}\left(e(t),\tilde{\delta}(t)\right) &= \sum_{i=1}^{N}\Bigg[2e_i^{\mathrm{T}}(t)PA_0e_i(t)-2e_i^{\mathrm{T}}(t)PBK\sum_{i\sim j}\left(e_i(t)-e_j(t)\right)-2e_i^{\mathrm{T}}(t)PA\tilde{\delta}_i(t)\\
&\quad +2e_i^{\mathrm{T}}(t)P\dot{\delta}_i(t)-2e_i^{\mathrm{T}}(t)PBKl_ie_i(t)-2e_i^{\mathrm{T}}(t)P\mu e_i(t)\\
&\quad +2\gamma^{-1}\tilde{\delta}_i^{\mathrm{T}}(t)\left(\dot{\delta}_i(t)-\gamma\mathrm{Proj}\left(\hat{\delta}_i(t),-A^{\mathrm{T}}Pe_i(t)\right)\right)\Bigg]\\
&= -e^{\mathrm{T}}(t)Re(t)+\sum_{i=1}^{N}\Bigg[-2e_i^{\mathrm{T}}(t)PA\tilde{\delta}_i(t)+2e_i^{\mathrm{T}}(t)P\dot{\delta}_i(t)+2\gamma^{-1}\tilde{\delta}_i^{\mathrm{T}}(t)\dot{\delta}_i(t)\\
&\quad -2\tilde{\delta}_i^{\mathrm{T}}(t)\mathrm{Proj}(\hat{\delta}_i(t),-A^{\mathrm{T}}Pe_i(t))\Bigg],\\
&= -e^{\mathrm{T}}(t)Re(t)+\sum_{i=1}^{N}\Bigg[2\left(\hat{\delta}_i(t)-\delta_i(t)\right)^{\mathrm{T}}\left(\mathrm{Proj}(\hat{\delta}_i(t),-A^{\mathrm{T}}Pe_i(t))-\left(-A^{\mathrm{T}}Pe_i(t)\right)\right)\\
&\quad +2e_i^{\mathrm{T}}(t)P\dot{\delta}_i(t)+2\gamma^{-1}\tilde{\delta}_i^{\mathrm{T}}(t)\dot{\delta}_i(t)\Bigg],\\
&\leq -e^{\mathrm{T}}(t)Re(t)+\sum_{i=1}^{N}\left[2e_i^{\mathrm{T}}(t)P\dot{\delta}_i(t)+2\gamma^{-1}\tilde{\delta}_i^{\mathrm{T}}(t)\dot{\delta}_i(t)\right],\\
&\leq -d_1\|e(t)\|_2^2+d_2\|e(t)\|_2+d_3,\\
&= -\left[\sqrt{d_1}\|e(t)\|_2-\frac{d_2}{2\sqrt{d_1}}\right]^2+\frac{d_2^2}{4d_1}+d_3, \quad t\geq 0,
\end{aligned} \tag{7.41}$$

and hence, $\dot{V}\left(e(t),\tilde{\delta}(t)\right)<0$ outside the compact set $\Omega \triangleq \left\{\left(e,\tilde{\delta}\right)\colon \|e\|_2 \leq \eta_1 \text{ and } \|\tilde{\delta}\|_2 \leq \eta_2\right\}$. This proves the uniform boundedness of the solution $\left(e(t),\tilde{\delta}(t)\right)$ of the system dynamics given by (7.37) and (7.38) for all $\left(e_0,\tilde{\delta}_0\right)\in \mathbb{R}^{nN}\times\mathbb{R}^{nN}$ [136].

To show the ultimate bounds for $e(t), t \geq T$, and $\tilde{\delta}(t), t \geq T$, given by (7.39) and (7.40), respectively, note that $\lambda_{\min}(P)\|e(t)\|_2^2+\gamma^{-1}\|\tilde{\delta}(t)\|_2^2 \leq \lambda_{\max}(P)\eta_1^2+\gamma^{-1}\eta_2^2, t \geq T$, or, equivalently, $\lambda_{\min}(P)\|e(t)\|_2^2 \leq \lambda_{\max}(P)\eta_1^2+\gamma^{-1}\eta_2^2, t \geq T$, and $\gamma^{-1}\|\tilde{\delta}(t)\|_2^2 \leq \lambda_{\max}(P)\eta_1^2+\gamma^{-1}\eta_2^2, t \geq T$, which proves (7.39) and (7.40). ■

Remark 7.4.1 *A similar remark to Remark 7.3.1 holds for Theorem 7.4.1. Namely, all signals used to construct the local controller $u_i(t)$, $i=1,\ldots,N$, $t\geq 0$, for each agent given by (7.10) with the local corrective signal $v_i(t)$, $i=1,\ldots,N$, $t\geq 0$, given by (7.32), (7.33), and (7.34) are bounded.*

Note that the projection operator is used in order to guarantee a bounded estimate of the unknown parameter, since otherwise one cannot conclude uniform ultimate boundedness from (7.41). The ultimate bounds given by (7.39) and (7.40) characterize the controller design parameters that need to be chosen in order to achieve small excursions of $\|e(t)\|_2$ and $\|\tilde{\delta}(t)\|_2$ for $t \geq T$. This is particularly important to obtain accurate estimates for $\hat{x}_i(t)$, $i=1,\ldots,N$, $t\geq T$, and $\hat{\delta}_i(t)$, $i=1,\ldots,N$, $t\geq T$, as well as suppress the effect of $\tilde{\delta}_i(t)$, $i=1,\ldots,N$, $t\geq T$. To elucidate the effect of the controller design parameters on (7.39) and (7.40),

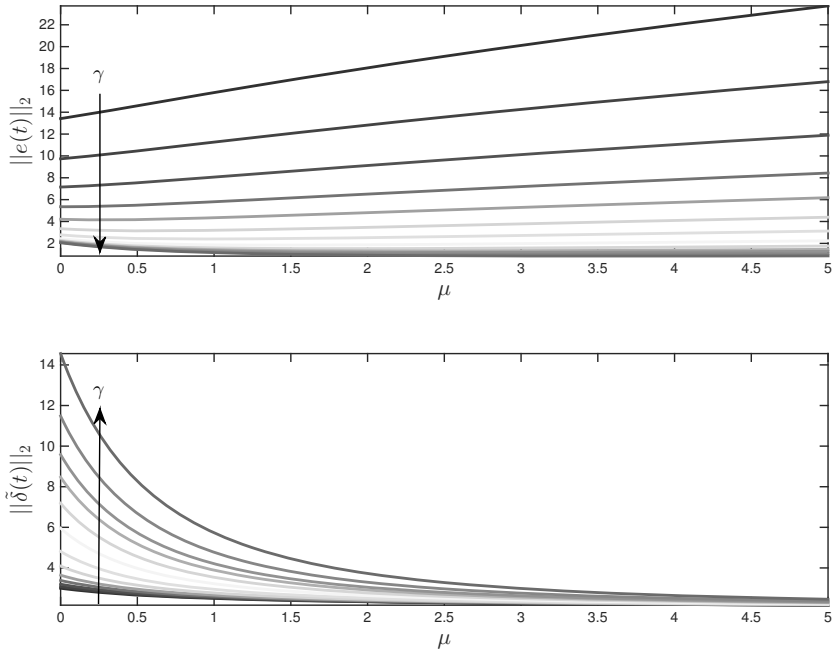

Figure 7.2: Effect of μ and γ on the ultimate bounds given by (7.39) and (7.40) (arrow directions denote the increase of γ from 0.1 to 100).

let $A=1$, $B=1$, $K=1$, $A_0=0$, $K_0=1$, $N=1$, $c=1$, $\hat{\delta}_{\max}=1$, $\underline{\delta}=1$, and $\overline{\delta}=2$. In this case, it follows from (7.36) that $P=0.5(1+\mu)^{-1}R$, where we set $R=1$. Figure 7.2 shows the effect of $\mu\in[0,5]$ and $\gamma\in[0.1,100]$ on the ultimate bounds given by (7.39) and (7.40). Specifically, as expected, increasing both μ and γ yields smaller ultimate bounds for $\|e(t)\|_2$ and $\|\tilde{\delta}(t)\|_2$ for $t\geq T$.

7.5 Illustrative Numerical Examples

In this section, we present two numerical examples to demonstrate the utility and efficacy of the proposed distributed control architectures for networked multiagent systems to mitigate the effect of time-invariant and time-varying sensor uncertainties.

7.5.1 Example 1: Time-Invariant Sensor Uncertainties Case

To illustrate the key ideas presented in Section 7.2.2, consider a group of $N=4$ agents subject to a connected, undirected graph $\mathfrak{G}$ given in Figure 7.1, where the dynamics of agent i satisfy

$$\begin{bmatrix}\dot{x}_i^1(t)\\ \dot{x}_i^2(t)\\ \dot{x}_i^3(t)\end{bmatrix}=\begin{bmatrix}0&1&0\\0&0&1\\-4&-4&-1\end{bmatrix}\begin{bmatrix}x_i^1(t)\\ x_i^2(t)\\ x_i^3(t)\end{bmatrix}+\begin{bmatrix}0\\0\\1\end{bmatrix}u(t),\quad i=1,\ldots,4,\quad t\geq 0, \tag{7.42}$$

with initial conditions $x_1(0)=[0,0,0]^{\mathrm{T}}$, $x_2(0)=[1,2,-1]^{\mathrm{T}}$, $x_3(0)=[3,1,0]^{\mathrm{T}}$, and $x_4(0)=[2,2,2]^{\mathrm{T}}$. Note that $\det(A)\neq 0$, where A is the system matrix of (7.42). For this example, we are interested in the problem of asymptotically driving the state vector of each agent $x_i(t)$, $i=1,\ldots,4$, $t\geq 0$, to the state vector of a leader $x_0(t)$, $t\geq 0$, having dynamics given by v

$$\begin{bmatrix}\dot{x}_0^1(t)\\ \dot{x}_0^2(t)\\ \dot{x}_0^3(t)\end{bmatrix}=\begin{bmatrix}0&1&0\\0&0&1\\-4&-4&-1\end{bmatrix}\begin{bmatrix}x_0^1(t)\\ x_0^2(t)\\ x_0^3(t)\end{bmatrix},\quad x_0(0)=\begin{bmatrix}1\\1\\3\end{bmatrix},\quad t\geq 0. \tag{7.43}$$

For this problem, $A_0=A-BK_0$ holds with $K_0=[0,0,0]$ as a direct consequence of (7.42) and (7.43).

To design the proposed local controllers, let $K=Q^{-1}B^{\mathrm{T}}P$ and set $Q=0.1I_3$, $\mu=0.2$, and $c=6\geq\frac{1}{\min\{\eta_i\}}$, $i=1,\ldots,4$, so that the LMI given by (7.30) for $P=S^{-1}$ (see Remark 7.3.4) is satisfied with

$$P = \begin{bmatrix} 0.0850 & 0.0316 & 0.0224 \\ 0.0316 & 0.0467 & 0.0090 \\ 0.0224 & 0.0090 & 0.0187 \end{bmatrix}, \tag{7.44}$$

and hence, $K = \begin{bmatrix} 0.22, & 0.09, & 0.19 \end{bmatrix}$. Note that with this selection for K, A_ξ is Hurwitz for all $\eta_i \in \text{spec}(F(\mathfrak{G}))$, $i = 1, \ldots, 4$. The nominal system performance for the case when the uncompromised state measurement is available to the local controller of agent i, $i \in \{1, \ldots, 4\}$, (i.e., $\delta_i(\cdot) = 0$), is shown in Figure 7.3 using (7.7).

Next, consider a time-invariant sensor uncertainty given by (7.5) with

$$\delta_1 = \begin{bmatrix} 5 \\ -7 \\ -3 \end{bmatrix}, \quad \delta_2 = \begin{bmatrix} 4 \\ -5 \\ 4 \end{bmatrix}, \quad \delta_3 = \begin{bmatrix} 6 \\ 3 \\ -5 \end{bmatrix}, \quad \delta_4 = \begin{bmatrix} -4 \\ 1 \\ 2 \end{bmatrix}. \tag{7.45}$$

The system performance for the case when the compromised state measurement is available to the local controller of agent $i \in \{1, \ldots, 4\}$ (i.e., $\delta_i(\cdot) \neq 0$), is shown in Figure 7.4 using (7.7) (i.e., $v_i(t) \equiv 0$, $i = 1, \ldots, 4$). Now, to illustrate the results of Theorem 7.3.1, we use the proposed local controller $u_i(t)$, $i = 1, \ldots, 4$, $t \geq 0$, for each agent given by (7.10) and the local corrective signal $v_i(t)$, $i = 1, \ldots, 4$, $t \geq 0$, given

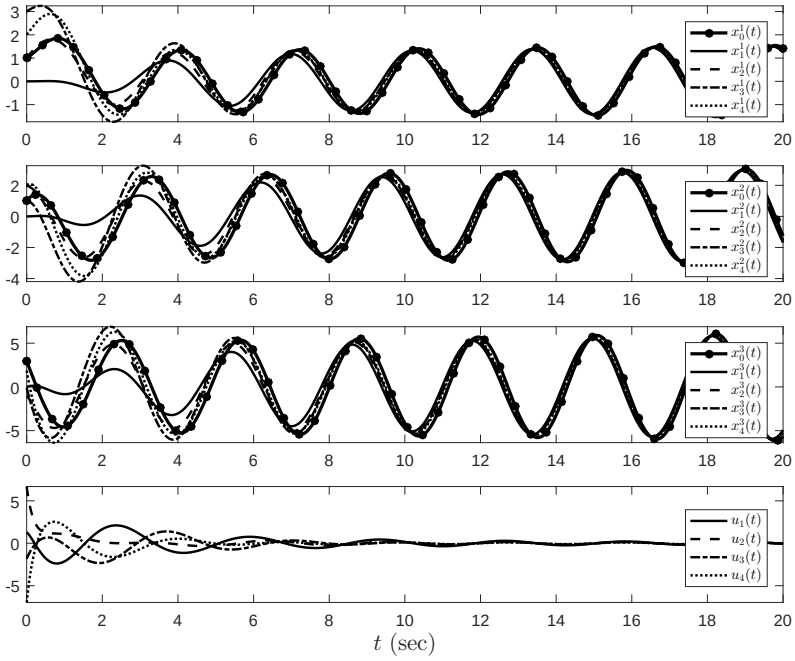

Figure 7.3: Nominal system performance for a group of agents in Example 1 with the local controller given by (7.7) (i.e., $v_i(t) \equiv 0$, $i = 1, \ldots, 4$) when the uncompromised state measurement is available for feedback.

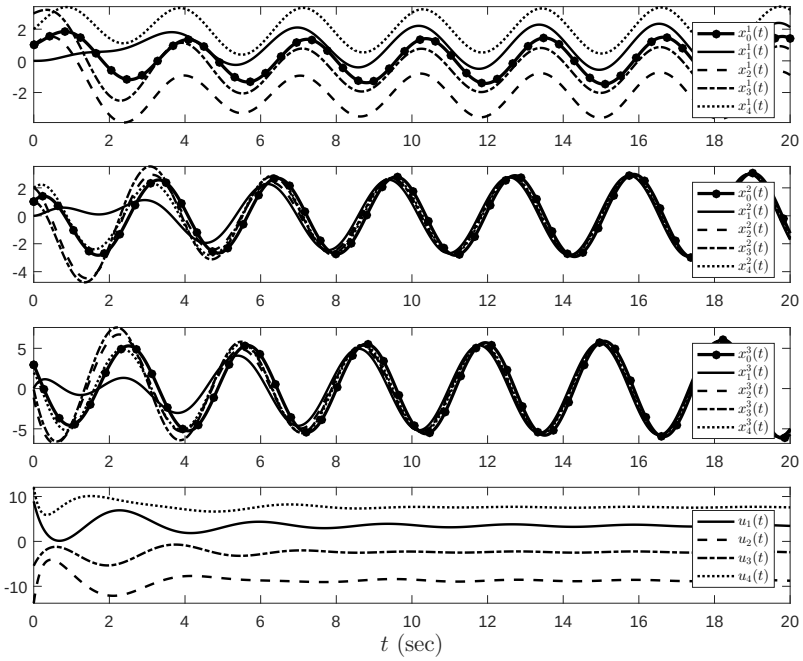

Figure 7.4: System performance for a group of agents in Example 1 with the local controller given by (7.7) (i.e., $v_i(t) \equiv 0$, $i = 1,\ldots,4$) when the compromised state measurement is available for feedback.

by (7.11) with $\gamma = 100$. For this case, the system performance in the presence of time-invariant sensor uncertainties is shown in Figure 7.5. As expected, the proposed distributed control architecture of Theorem 7.3.1 allows the state vector of each agent $x_i(t)$, $i = 1,\ldots,4$, $t \geq 0$, to asymptotically track the state vector of the leader $x_0(t)$, $t \geq 0$. Finally, the time evolution of the error signals given by $e(t), t \geq 0$, and $\tilde{\delta}(t), t \geq 0$, are shown respectively in Figures 7.6 and 7.7 for the closed-loop system with the proposed distributed control architecture. The values of the design gains γ and μ are chosen to obtain acceptable system performance without excessive control oscillations.

7.5.2 Example 2: Time-Varying Sensor Uncertainties Case

To illustrate the key ideas presented in Section 7.2.2, consider the same group of agents as in Example 1 given in Figure 7.1, where the dynamics of agent i satisfy

$$\begin{bmatrix} \dot{x}_i^1(t) \\ \dot{x}_i^2(t) \end{bmatrix} = \begin{bmatrix} 0 & 1.5 \\ -2 & 0 \end{bmatrix} \begin{bmatrix} x_i^1(t) \\ x_i^2(t) \end{bmatrix} + \begin{bmatrix} 0 \\ 1 \end{bmatrix} u(t), \quad i = 1,\ldots,4, \quad t \geq 0, \tag{7.46}$$

with initial conditions $x_1(0) = [0,0]^{\mathrm{T}}$, $x_2(0) = [1,2]^{\mathrm{T}}$, $x_3(0) = [3,1]^{\mathrm{T}}$, and $x_4(0) = [2,2]^{\mathrm{T}}$. Note that $\det(A) \neq 0$, where A is the system matrix of (7.46). For this example, we are interested in the problem of approxi-

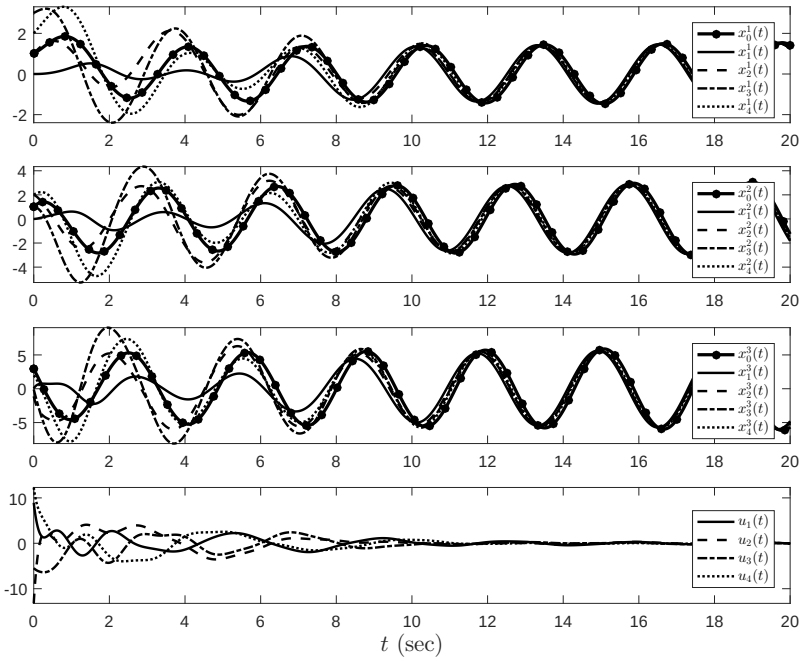

Figure 7.5: System performance for a group of agents in Example 1 with the proposed local controller given by (7.10) and the local corrective signal given by (7.11) when the compromised state measurement is available for feedback.

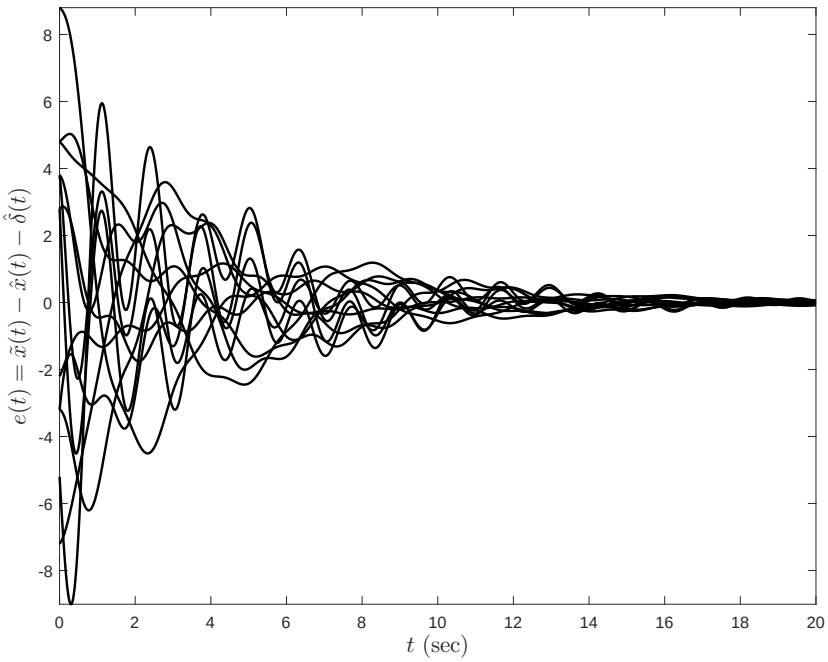

Figure 7.6: Time evolution of $e(t), t \geq 0$, in Example 1 with the proposed local controller given by (7.10) and the local corrective signal given by (7.11) when the compromised state measurement is available for feedback.

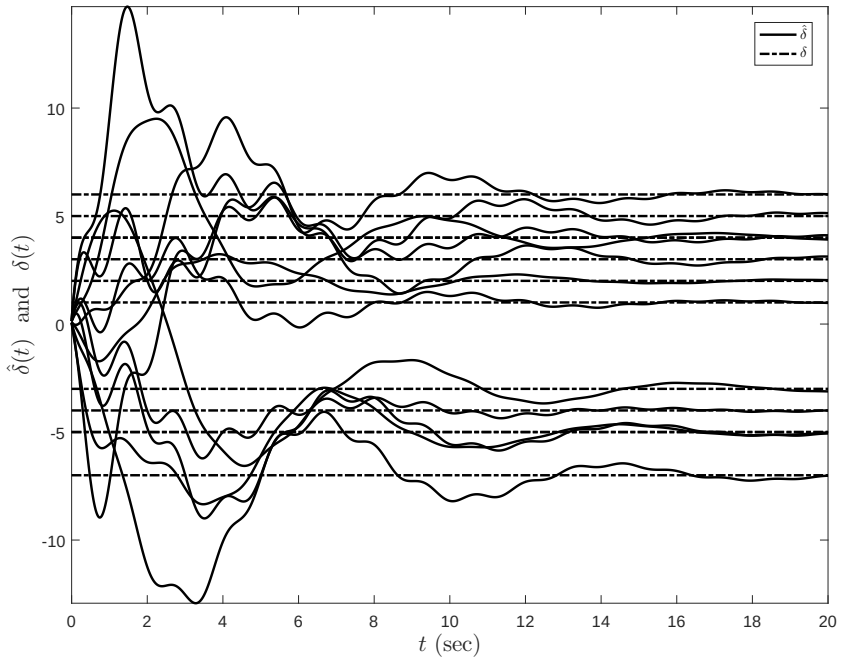

Figure 7.7: Time evolution of $\tilde{\delta}(t), t \geq 0$, in Example 1 with the proposed local controller given by (7.10) and the local corrective signal given by (7.11) when the compromised state measurement is available for feedback.

mately driving the state vector of each agent $x_i(t)$, $i = 1,\ldots,4$, $t \geq 0$, to the state vector of a leader $x_0(t)$, $t \geq 0$, having dynamics given by

$$\begin{bmatrix} \dot{x}_0^1(t) \\ \dot{x}_0^2(t) \end{bmatrix} = \begin{bmatrix} 0 & 1.5 \\ -2 & 0 \end{bmatrix} \begin{bmatrix} x_0^1(t) \\ x_0^2(t) \end{bmatrix}, \quad x_0(0) = \begin{bmatrix} 1 \\ 1 \end{bmatrix}, \quad t \geq 0. \tag{7.47}$$

For this problem, $A_0 = A - BK_0$ holds with $K_0 = [0,0]$ as a direct consequence of (7.46) and (7.47).

To design the proposed local controllers, let $K = Q^{-1}B^{\mathrm{T}}P$ and set $Q = 0.1I_2$, $\mu = 1$, and $c = 6 \geq \frac{1}{\min\{\eta_i\}}, i = 1,\ldots,4$, so that the LMI given by (7.30) for $P = S^{-1}$ (see Remark 7.3.4) is satisfied with

$$P = \begin{bmatrix} 0.0398 & 0.0037 \\ 0.0037 & 0.0360 \end{bmatrix}, \tag{7.48}$$

and hence, $K = \begin{bmatrix} 0.04, & 0.36 \end{bmatrix}$. Note that with this selection for K, A_ξ is Hurwitz for all $\eta_i \in \mathrm{spec}(F(\mathfrak{G}))$, $i = 1,\ldots,4$. The nominal system performance for the case when the uncompromised state measurement is available to the local controller of agent i, $i \in \{1,\ldots,4\}$, (i.e., $\delta_i(\cdot) = 0$), is shown in Figures 7.8 and 7.9 using (7.7).

Next, consider the time-varying sensor uncertainty given by (7.5) with

$$\delta_1(t) = 2 + \sin(0.6t) \begin{bmatrix} 0.1 \\ 0.2 \end{bmatrix}, \quad \delta_2(t) = -1 + \sin(0.85t) \begin{bmatrix} 0.2 \\ 0.4 \end{bmatrix}, \tag{7.49}$$

$$\delta_3(t) = -4 + \sin(0.25t) \begin{bmatrix} 0.3 \\ 0.6 \end{bmatrix}, \quad \delta_4(t) = 1 + \sin(0.25t) \begin{bmatrix} 0.4 \\ 0.8 \end{bmatrix}. \tag{7.50}$$

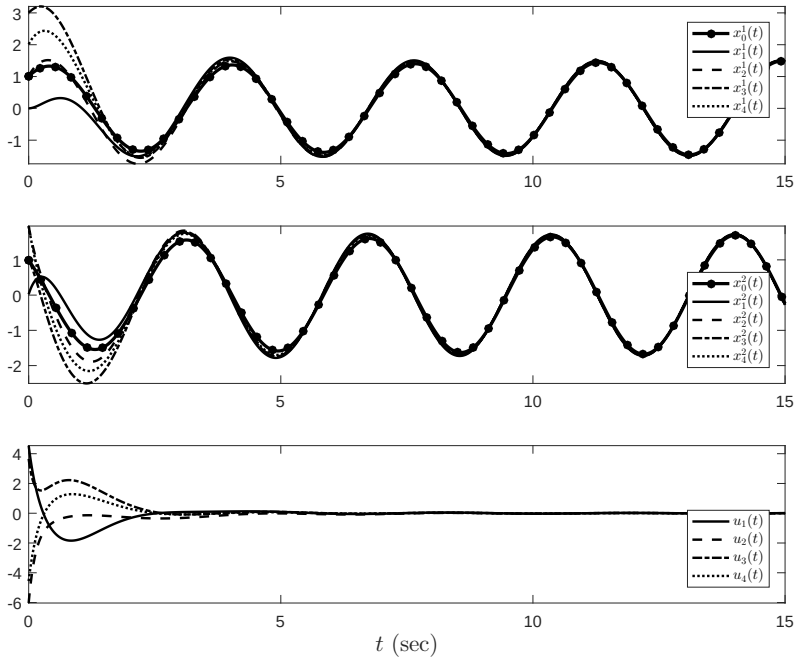

Figure 7.8: Nominal system performance for a group of agents in Example 2 with the local controller given by (7.7) (i.e., $v_i(t) \equiv 0$, $i = 1, \ldots, 4$) when the uncompromised state measurement is available for feedback.

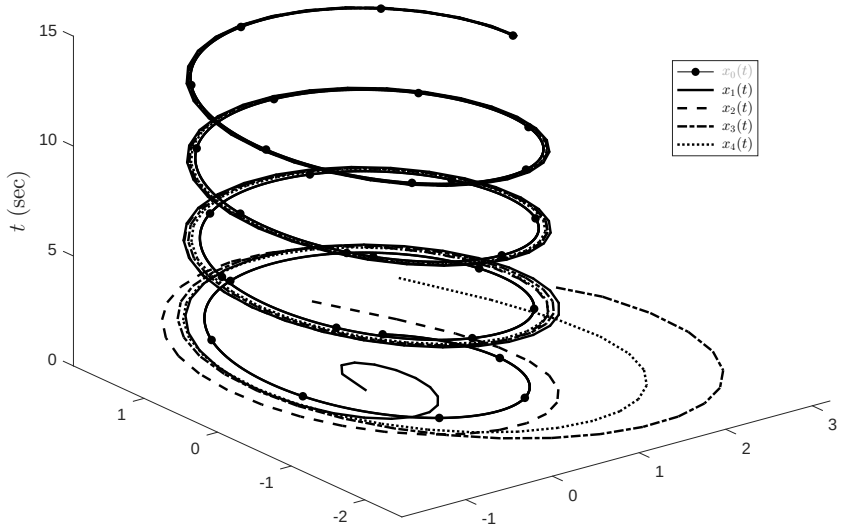

Figure 7.9: System trajectories of each agent in Figure 7.8.

The system performance for the case when the compromised state measurement is available to the local controller of agent $i \in \{1,\ldots,4\}$ (i.e., $\delta_i(t) \neq 0$), is shown in Figures 7.10 and 7.11 using (7.7) (i.e., $v_i(t) \equiv 0$, $i = 1,\ldots,4$). Now, to illustrate the results of Theorem 7.4.1, we use the proposed local controller $u_i(t)$, $i = 1,\ldots,4$, $t \geq 0$, for each agent given by (7.10) and the local corrective signal $v_i(t)$, $i = 1,\ldots,4$, $t \geq 0$, given by (7.32) with $\gamma = 100$, and $\hat{\delta}_{\max} = 100$. For this case, the system performance in the presence of time-varying sensor uncertainties is shown in Figures 7.12 and 7.13. As expected, the proposed distributed control architecture of Theorem 7.4.1 allows the state vector of each agent $x_i(t)$, $i = 1,\ldots,4$, $t \geq 0$, to approximately track the state vector of the leader $x_0(t)$, $t \geq 0$. Finally, the time evolution of the error signals given by (7.37) and (7.38) are, respectively, shown in Figures 7.14 and 7.15. As for the previous example, the values of the design gains γ and μ are chosen to obtain acceptable system performance with minimal control oscillations. In particular, after choosing $\gamma = 100$ to achieve an acceptable small ultimate bound on $\|e(t)\|_2$, we chose $\mu = 1$ to achieve an acceptable small ultimate bound on $\|\tilde{\delta}(t)\|_2$.

7.6 Conclusion

Sensor uncertainties in networked multiagent systems, which may result from low sensor quality, sensor failure, sensor bias, or detrimental environmental conditions, can significantly deteriorate achievable

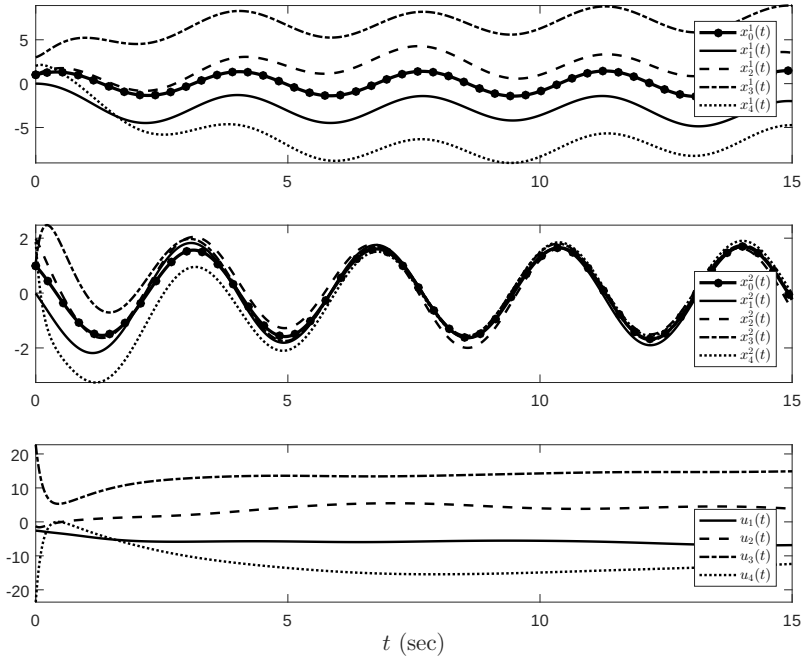

Figure 7.10: System performance for a group of agents in Example 2 with the local controller given by (7.7) (i.e., $v_i(t) \equiv 0$, $i = 1,\ldots,4$) when the compromised state measurement is available for feedback.

closed-loop system performance. In this paper, we presented two distributed adaptive control architectures to mitigate the effect of time-invariant and time-varying sensor uncertainties in networked multiagent systems with agents having high-order, linear dynamics. Specifically, we modeled agent uncertainty between

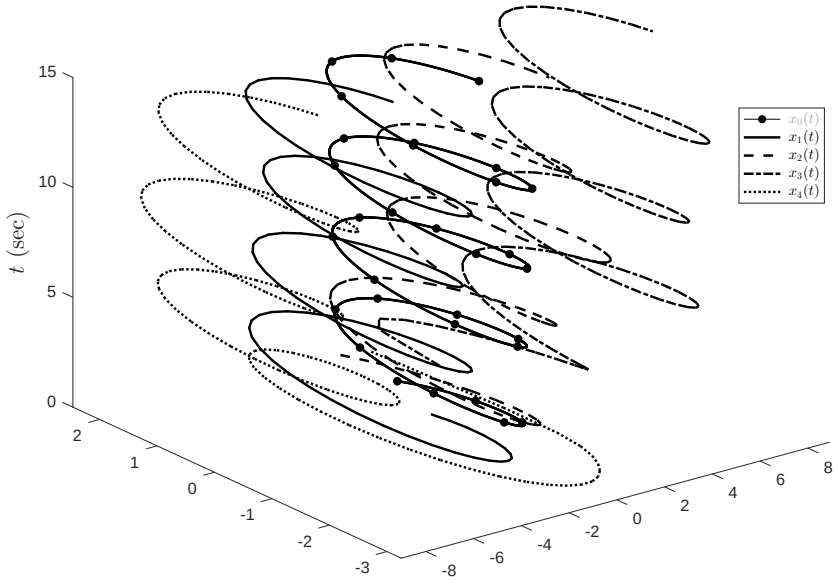

Figure 7.11: System trajectories of each agent in Figure 7.10.

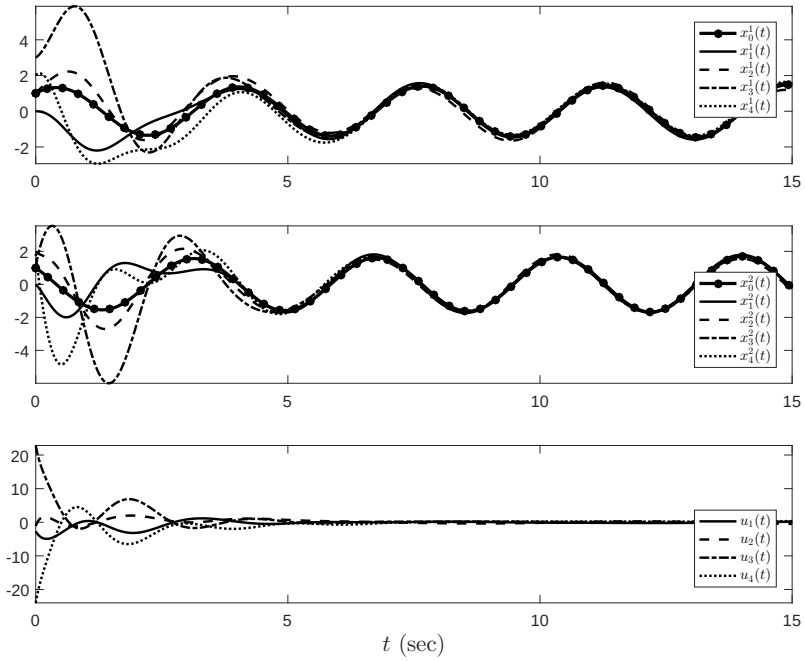

Figure 7.12: System performance for a group of agents in Example 2 with the proposed local controller given by (7.10) and the local corrective signal given by (7.32) when the compromised state measurement is available for feedback.

networked agents using unknown exogenous disturbances and showed that the proposed adaptive control architectures guarantee asymptotic stability of the closed-loop dynamical system when the exogenous disturbances are time-invariant and uniform ultimate boundedness when the exogenous disturbances are time-

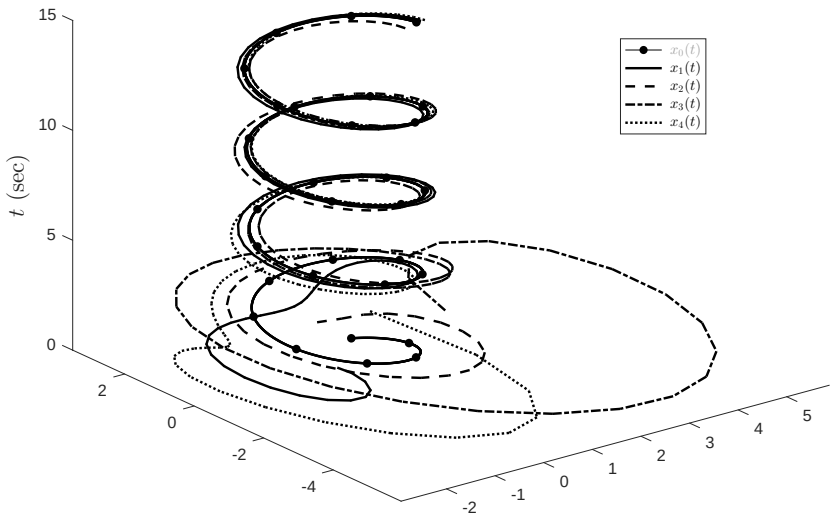

Figure 7.13: System trajectories of each agent in Figure 7.11.

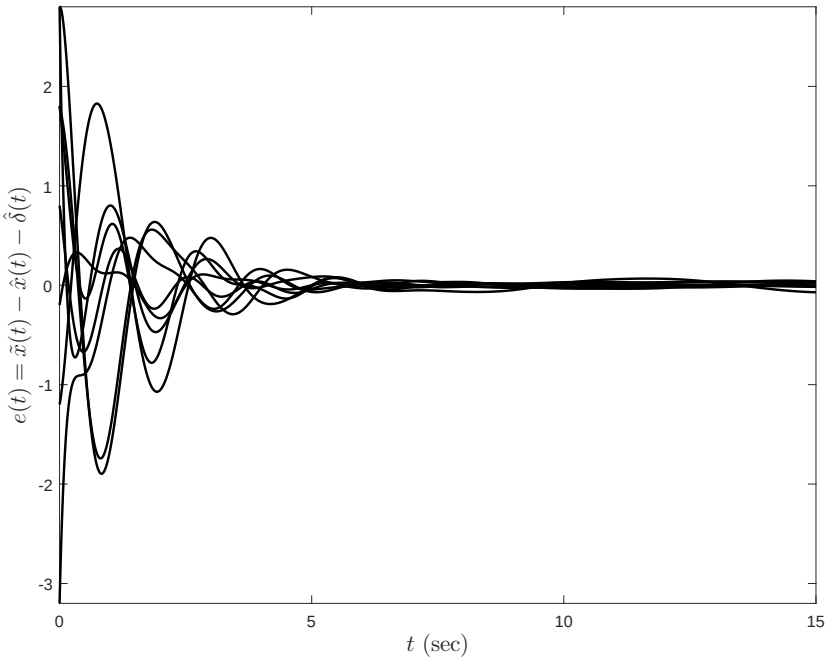

Figure 7.14: Time evolution of (7.37) in Example 2 with the proposed local controller given by (7.10) and the local corrective signal given by (7.32) when the compromised state measurement is available for feedback.

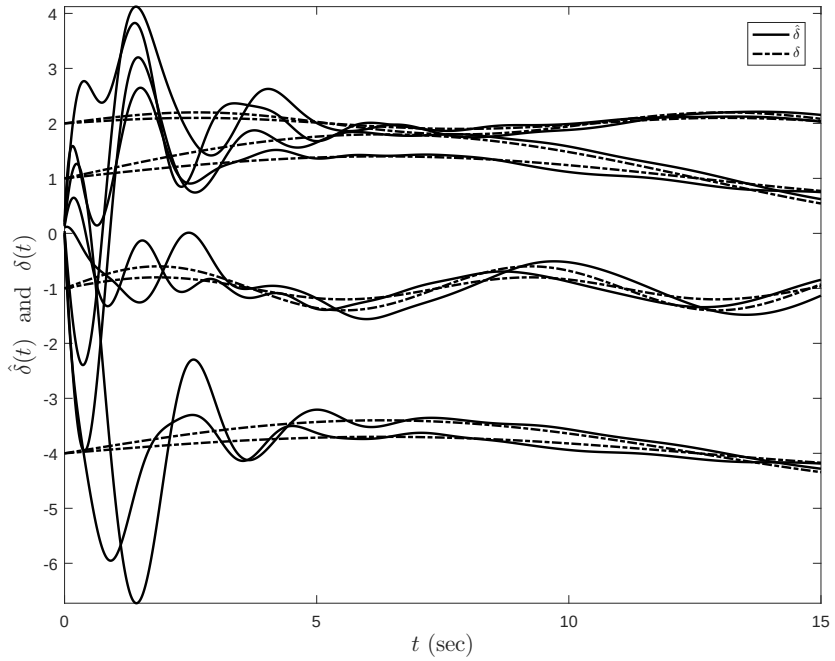

Figure 7.15: Time evolution of (7.38) in Example 2 with the proposed local controller given by (7.10) and the local corrective signal given by (7.32) when the compromised state measurement is available for feedback.

varying. Future extensions will focus on output feedback distributed adaptive control strategies that can suppress the effect of simultaneous sensor and actuator uncertainties. Generalizations to agents having nonlinear and uncertain dynamics, as well as time-varying communication graph topologies will also be developed.

CHAPTER 8: CONTROL OF UNCERTAIN MULTIAGENT SYSTEMS WITH SPATIOTEMPORAL CONSTRAINTS[1]

This paper focuses on control of uncertain multiagent systems with spatial and temporal constraints. Specifically, we propose a new distributed control algorithm to simultaneously guarantee *i)* a user-defined performance by limiting the distance between the state trajectories of agents and their reference state trajectories to be less than given bounds (spatial constraints) and *ii)* a finite-time convergence to the position of a time-varying leader at a user-defined time (temporal constraint). The key feature of the proposed distributed control architecture is to address these spatiotemporal constraints regardless of the initial conditions of agents and without requiring a strict knowledge of the upper bounds of the considered class of system uncertainties. In particular, based on a distributed adaptive control law, which utilizes an error-dependent learning rate derived from a (generalized) restricted potential function, the proposed algorithm is capable of enforcing user-defined performance bounds on the distance between the state trajectories of agents and their distributed reference models. In addition, a user-defined finite-time convergence is achieved using a time transformation approach that links a prescribed time interval and a stretched infinite-time interval, where we perform the stability analysis on the latter interval. The efficacy of the proposed control architecture is also demonstrated through a numerical example.

8.1 Introduction

Multiagent systems consist of a group of networked agents that exchange local information within each other in order to address given global objectives. In many practical applications, these systems are subject to spatial and temporal constraints. However, it is not a trivial task to satisfy these constraints especially when agents operate under system uncertainties.

[1]This chapter has been submitted to the *American Control Conference*.

8.1.1 Spatial Constraints

Spatial constraints often arise from the structural and operational limitations in critical control systems applications. Specifically, severely or unpredictably deviating from an ideal agent response, which is characterized to obey certain spatial limits on the states of agents, is not desired and needs to be avoided in practice. Therefore, a feedback control algorithm must have the ability to keep the trajectories of each agent close enough to the trajectories of a reference model, which denotes ideal responses for agents forming the multiagent system.

To this end, model reference adaptive control architectures can be effective system-theoretical methods in dealing with system uncertainties. However, their derived worst-case performance bounds based on Lyapunov or Lyapunov-like functions are usually (overly) conservative and not user-defined due to their dependence on system uncertainties [1]. Hence, these bounds are not always practical in establishing precise performance bounds on the system errors denoting the distance between uncertain system dynamics and given reference models. The authors of, for example, [1, 2, 18–20, 181] (also see references therein as well as introduction section of [1] for additional details) develop adaptive control algorithms that provide remedies to this problem for achieving performance guarantees defined by user-defined bounds. Yet, these results do not consider any temporal constraints in the control system development.

8.1.2 Temporal Constraints

Temporal constraints are generally related with time-critical applications (e.g., engagement of a vehicle with another one), where it is necessary to perform and complete a given task over a desired time interval. As it is well-known, however, the convergence time achieved through classical finite-time control architectures depends on the initial conditions of considered physical systems [10, 11, 53–60]. To address this drawback in time-critical applications, control algorithms with fixed-time convergence properties are proposed (see, for example, [12, 13, 61–65]) and control algorithms with predefined-time convergence properties are developed (see, for example, [14, 15]).

Yet, in these notable approaches, either the calculated upper bound on the convergence time do not necessarily hold globally for all initial conditions and they can be conservative [12] or they can require a strict knowledge of the upper bounds of the considered class of system uncertainties in their design (also see introduction sections of [4, 171] for additional details). Recently, the authors of [4, 72, 73, 171]

develop distributed control algorithms based on the time transformation approach in order to guarantee the completion of a given control task at T seconds, where T denotes a user-defined finite time convergence parameter that does not depend on the initial conditions of agents or knowledge of the upper bounds of system uncertainties. However, these results do not take spatial constraints into account; hence, system uncertainties can significantly deviate agents from their ideal responses during transient time (see Section 8.5 of this paper for an example illustrating this transient performance problem).

8.1.3 Contribution

In this paper, we focus on control of uncertain multiagent systems with spatiotemporal constraints. Specifically, we propose a new distributed control algorithm to simultaneously guarantee *i)* a user-defined performance by limiting a distance between the state trajectories of agents and their reference state trajectories to be less than given bounds (spatial constraints) and *ii)* a finite-time convergence to the position of a time-varying leader at a user-defined time (temporal constraint). The key feature of the proposed distributed control architecture is to address these spatiotemporal constraints regardless of the initial conditions of agents and without requiring a strict knowledge of the upper bounds of the considered class of system uncertainties.

In particular, with a distributed adaptive control law, which utilizes a set-theoretic error-dependent learning rate derived from a (generalized) restricted potential function based on the results documented in [1, 2, 181], the proposed algorithm is capable of enforcing user-defined performance bounds on the distance between the state trajectories of agents and their distributed reference models. In addition, a user-defined finite-time convergence is achieved using the time transformation approach [4, 72, 73, 171] that links a prescribed time interval $t \in [0,T)$ and a stretched infinite-time interval $s \in [0,\infty)$, where we perform the stability analysis on the latter interval. The efficacy of the proposed control architecture is also demonstrated through a numerical example.

8.2 Mathematical Preliminaries

We begin with the notation used in this paper. Specifically, $\mathbb{R}$, $\mathbb{R}^n$, and $\mathbb{R}^{n\times m}$ respectively denote the set of real numbers, the set of $n\times 1$ real column vectors, and the set of $n\times m$ real matrices; $\mathbb{R}_+$ and $\mathbb{R}_+^{n\times n}$ (resp., $\overline{\mathbb{R}}_+^{n\times n}$) denote the set of positive real numbers and the set of $n\times n$ positive-definite (resp., nonnegative-definite) real matrices; $\mathbb{Z}_+$ (resp., $\overline{\mathbb{Z}}_+$) denotes the set of positive (resp., nonnegative) integers; 0_n and $\mathbf{1}_n$

respectively denote the $n \times 1$ zero vector and the $n \times 1$ ones vector; and "$\triangleq$" denotes equality by definition. In addition, we use $(\cdot)^{\mathrm{T}}$ to denote the transpose operator, $(\cdot)^{-1}$ to denote the inverse operator, $\det(\cdot)$ to denote the determinant operator, $\|\cdot\|_2$ to denote the Euclidean norm, and $\|\cdot\|_H$ to denote the weighted Euclidean norm (i.e., $\|x\|_A = \sqrt{x^{\mathrm{T}}Ax}$ for $x \in \mathbb{R}^n$ and $A \in \mathbb{R}^{n\times n}_+$). We also write $\lambda_{\min}(A)$ (resp., $\lambda_{\max}(A)$) for the minimum (resp., maximum) eigenvalue of the square matrix A, $\lambda_i(A)$ for the ith eigenvalue of the square matrix A, and $[A]_{ij}$ for the (i,j)th entry of the matrix A.

Next, we overview several basic notions from graph theory (see [176, 177] for further reading). In particular, an undirected graph $\mathfrak{G}$ is defined by a set $\mathcal{V}_{\mathfrak{G}} = \{1,\ldots,N\}$ of *nodes* and a set $\mathcal{E}_{\mathfrak{G}} \subset \mathcal{V}_{\mathfrak{G}} \times \mathcal{V}_{\mathfrak{G}}$ of *edges*. When $(i,j) \in \mathcal{E}_{\mathfrak{G}}$, we say that nodes i and j are neighbors and $i \sim j$ indicates the neighboring relation. The *degree* of a node is given by the number of its neighbors; that is, if we let d_i to stand for the degree of node i, then the *degree matrix* of a graph $\mathfrak{G}$, $\mathcal{D}(\mathfrak{G}) \in \mathbb{R}^{N\times N}$, is given by $\mathcal{D}(\mathfrak{G}) \triangleq \operatorname{diag}[d]$ where $d = [d_1,\ldots,d_N]^{\mathrm{T}}$. A *path* $i_0 i_1 \cdots i_L$ of a graph $\mathfrak{G}$ is a finite sequence of nodes such that $i_{k-1} \sim i_k$, $k = 1,\ldots,L$. Specifically, when every pair of distinct nodes has a path, then we say that the graph $\mathfrak{G}$ is connected. We write $\mathcal{A}(\mathfrak{G}) \in \mathbb{R}^{N\times N}$ for the *adjacency matrix* of a graph $\mathfrak{G}$, which is defined by $[\mathcal{A}(\mathfrak{G})]_{ij} \triangleq 1$ when $(i,j) \in \mathcal{E}_{\mathfrak{G}}$ and $[\mathcal{A}(\mathfrak{G})]_{ij} \triangleq 0$ otherwise. We also write $\mathcal{B}(\mathfrak{G}) \in \mathbb{R}^{N\times M}$ for the (node-edge) *incidence matrix* of a graph $\mathfrak{G}$, which is defined by $[\mathcal{B}(\mathfrak{G})]_{ij} \triangleq 1$ when node i is the head of edge j, $[\mathcal{B}(\mathfrak{G})]_{ij} \triangleq -1$ when node i is the tail of edge j, and $[\mathcal{B}(\mathfrak{G})]_{ij} \triangleq 0$ otherwise. Above, M is the number of edges, i is an index for the node set, and j is an index for the edge set. Finally, the *graph Laplacian matrix*, $\mathcal{L}(\mathfrak{G}) \in \overline{\mathbb{R}}^{N\times N}_+$, is defined by $\mathcal{L}(\mathfrak{G}) \triangleq \mathcal{D}(\mathfrak{G}) - \mathcal{A}(\mathfrak{G})$ or, equivalently, $\mathcal{L}(\mathfrak{G}) = \mathcal{B}(\mathfrak{G})\mathcal{B}(\mathfrak{G})^{\mathrm{T}}$. In what follows, a given multiagent system is modeled as a connected, undirected graph $\mathfrak{G}$ with nodes and edges respectively representing agents and interagent communication links.

The following results and definitions are needed for the theoretical content of this paper.

Remark 8.2.1 *As in [4, 72, 73], we use a key notion from Section 1.1.1.4 of [179]. Let $\xi(t)$ denote the solution to the dynamical system given by*

$$\dot{x}(t) = f(t,x(t)), \quad x(0) = x_0. \tag{8.1}$$

where $f : \overline{\mathbb{R}}_+ \times \mathbb{R}^n \to \mathbb{R}^n$. Furthermore, let $t = \theta(s)$ denote a time transformation with $\theta(s)$ being a strictly increasing and continuously differentiable function. In addition, define $\psi(s) = \xi(t)$. Then, we have

$$\psi'(s) = \theta'(s) f(\theta(s), \psi(s)), \quad \psi(\theta^{-1}(0)) = x_0, \tag{8.2}$$

with $\psi'(s) \triangleq d\psi(s)/ds$ *and* $\theta'(s) \triangleq d\theta(s)/ds$.

Remark 8.2.2 *Let* $\eta(t)$ *be a given signal. Following the time transformation concept discussed in Remark 8.2.1, we write* $\eta_s(s)$ *to denote the corresponding transformed signal in the sense that* $\eta_s(s) \triangleq \eta(\theta(s))$.

Lemma 8.2.1 ([Lemma 3.3, 178]) *Let* $K = diag(k)$, $k = [k_1, k_2, \ldots, k_N]^{\mathrm{T}}$, $k_i \in \overline{\mathbb{Z}}_+$, $i = 1, \ldots, N$. *In addition, consider that at least one entry of* k *is nonzero. Then,* $\mathcal{F}(\mathfrak{G}) \triangleq \mathcal{L}(\mathfrak{G}) + K \in \mathbb{R}_+^{N \times N}$ *for a connected, undirected graph* $\mathfrak{G}$.

Lemma 8.2.2 *Consider a dynamical system given by*

$$\psi'(s) = A_r \psi(s) + \eta(s), \quad \psi(0) = \psi_0, \tag{8.3}$$

with $A_r \in \mathbb{R}^{n \times n}$ *being a Hurwitz system matrix and* $\psi(s) \in \mathbb{R}^n$ *being the system state. For any bounded input* $\eta(s)$, $\psi(s)$ *is then bounded. If, in addition* $\lim_{s \to \infty} \eta(s) = 0$, *then* $\lim_{s \to \infty} \psi(s) = 0$.

Proof. The result follows from Chapter 4.9 and Exercise 4.58 in [136]. ■

Definition 8.2.1 *Let a convex hypercube in* $\mathbb{R}^n$ *be defined as* $\Omega = \left\{\theta \in \mathbb{R}^n : (\theta_i^{\min} \leq \theta_i \leq \theta_i^{\max})_{i=1,2,\cdots,n}\right\}$, *where* $(\theta_i^{\min}, \theta_i^{\max})$ *denote the minimum and maximum bounds for the* i^{th} *component of the n-dimensional parameter vector* θ. *Furthermore, for a sufficiently small positive constant* ν, *let the second hypercube be* $\Omega_\nu = \left\{\theta \in \mathbb{R}^n : (\theta_i^{\min} + \nu \leq \theta_i \leq \theta_i^{\max} - \nu)_{i=1,2,\cdots,n}\right\}$, *where* $\Omega_\nu \subset \Omega$. *With* $y \in \mathbb{R}^n$, *the projection operator* $\text{Proj} : \mathbb{R}^n \times \mathbb{R}^n \to \mathbb{R}^n$ *is then defined (componentwise) as* $\text{Proj}(\theta, y) \triangleq \left([\theta_i^{\max} - \theta_i]/\nu\right) y_i$ *when* $\theta_i > \theta_i^{\max} - \nu$ *and* $y_i > 0$, $\text{Proj}(\theta, y) \triangleq \left([\theta_i - \theta_i^{\min}]/\nu\right) y_i$ *when* $\theta_i < \theta_i^{\min} + \nu$ *and* $y_i < 0$, *and* $\text{Proj}(\theta, y) \triangleq y_i$ *otherwise. It then follows that* $\left(\theta - \theta^*\right)^{\mathrm{T}} \left(\text{Proj}\left(\theta, y\right) - y\right) \leq 0$ *[30, 80].*

Definition 8.2.2 *For* $z \in \mathbb{R}^p$ *and* $H \in \mathbb{R}_+^{p \times p}$, *we define* $\phi(\|z\|_{\mathrm{H}})$, $\phi : \mathbb{R} \to \mathbb{R}$, *to be a generalized restricted potential function (generalized barrier Lyapunov function) on the set given by*

$$\mathcal{D}_\varepsilon \triangleq \{z : \|z\|_{\mathrm{H}} \in [0, \varepsilon)\}, \tag{8.4}$$

where $\varepsilon \in \mathbb{R}_+$ *is a user-defined constant, when the following statements hold [1]:*

i) *If* $\|z\|_{\mathrm{H}} = 0$, *then* $\phi(\|z\|_{\mathrm{H}}) = 0$.

ii) *If* $z \in \mathcal{D}_\varepsilon$ *and* $\|z\|_{\mathrm{H}} \neq 0$, *then* $\phi(\|z\|_{\mathrm{H}}) > 0$.

iii) *If* $\|z\|_{\mathrm{H}} \to \varepsilon$, *then* $\phi(\|z\|_{\mathrm{H}}) \to \infty$.

iv) $\phi(\|z\|_{\mathrm{H}})$ *is continuously differentiable on* $\mathcal{D}_\varepsilon$.

v) *If* $z \in \mathcal{D}_\varepsilon$, *then* $\phi_d(\|z\|_{\mathrm{H}}) > 0$, *where* $\phi_d(\|z\|_{\mathrm{H}}) \triangleq \frac{\mathrm{d}\phi(\|z\|_{\mathrm{H}})}{\mathrm{d}\|z\|_{\mathrm{H}}^2}$.

vi) *If* $z \in \mathcal{D}_\varepsilon$, *then* $2\phi_d(\|z\|_{\mathrm{H}})\|z\|_{\mathrm{H}}^2 - \phi(\|z\|_{\mathrm{H}}) > 0$.

8.3 Problem Formulation

In this paper, we focus on a leader-follower problem in a multiagent system, where this system has N agents that exchange information over a connected, undirected graph $\mathfrak{G}$. Specifically, we consider that a subset of these agents has access to the position of a time-varying leader given by

$$p(t) \quad = \quad \int_0^t v(\tau)\mathrm{d}\tau + p(0), \quad p(t) \in \mathbb{R}, \tag{8.5}$$

where $v(t) \in \mathbb{R}$ is the bounded (with unknown bound) and piecewise continuous velocity of the leader. In addition, we consider that the dynamics of each agent satisfies

$$\dot{x}_i(t) = u_i(t) + \omega_i x_i(t), \quad x_i(0) = x_{i0}, \quad i \in \{1,2,\ldots,N\}, \tag{8.6}$$

where $x_i(t) \in \mathbb{R},\ i \in \{1,2,\ldots,N\}$ and $u_i(t) \in \mathbb{R},\ i \in \{1,2,\ldots,N\}$ are respectively the position and the control signal of an agent and $\omega_i \in \mathbb{R},\ i \in \{1,2,\ldots,N\}$ represents an agentwise system uncertainty. In a compact form, (8.6) can be equivalently written as

$$\dot{x}(t) \quad = \quad u(t) + \Omega x(t), \quad x(0) = x_0, \tag{8.7}$$

where $x(t) \triangleq [x_1(t),\ldots,x_N(t)]^{\mathrm{T}} \in \mathbb{R}^N$ represents the aggregated state vector and $\Omega \triangleq \mathrm{diag}([\omega_1,\ldots,\omega_N]) \in \mathbb{R}^{N\times N}$.

In order to theoretically discuss the performance guarantees on the above multiagent system in the presence of system uncertainties, we introduce the reference model capturing an ideal leader-follower

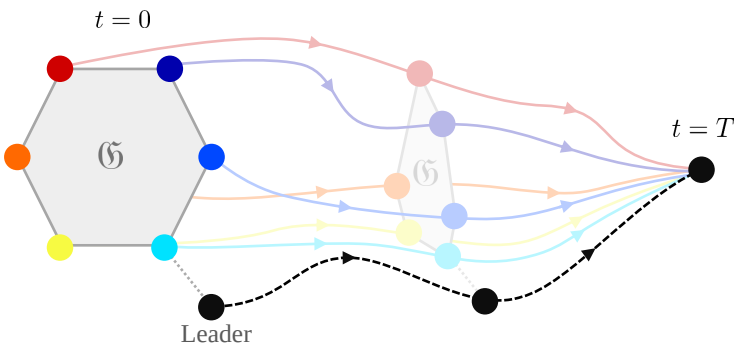

Figure 8.1: Illustration of the considered leader-follower problem over a prescribed time interval $t \in [0,T)$, where uncertain agents exchange information over a connected, undirected graph $\mathfrak{G}$.

behavior given by

$$\dot{r}_i(t) \;=\; -\alpha\lambda(t)\Big(\sum_{i\sim j}\big(r_i(t)-r_j(t)\big)+k_i\big(r_i(t)-p(t)\big)\Big), \quad r_i(0)=r_{i0}, \quad i\in\{1,2,\ldots,N\}, \tag{8.8}$$

with $r_i(t)\in\mathbb{R}$, $i\in\{1,2,\ldots,N\}$ being the ideal reference model state. From [4] with $\lambda(t)=1/(T-t)$, which is also utilized here, it now follows that the reference model given by (8.8) generates a bounded trajectory that converges to the time-varying leader given by (8.5) at the user-defined finite time T; that is,

$$\lim_{t\to T}\big(r_i(t)-p(t)\big)=0, \quad i\in\{1,2,\ldots,N\}. \tag{8.9}$$

In (8.8), each state of the reference model needs to communicate with its neighbor on the graph $\mathfrak{G}$. In order to remove this dependence and motivated by the results in [198], we introduce the reference model given by

$$\dot{x}_{ri}(t) \;=\; -\alpha\lambda(t)\Big(\sum_{i\sim j}\big(x_{ri}(t)-x_j(t)\big)+k_i\big(x_{ri}(t)-p(t)\big)\Big), \quad x_{ri}(0)=x_{ri0}, \quad i\in\{1,2,\ldots,N\}, \tag{8.10}$$

where $x_{ri}(t)\in\mathbb{R}$, $i\in\{1,2,\ldots,N\}$ denotes the reference model state. We refer to Remark 8.4.2 for a discussion on how the proposed distributed control algorithm considered in this paper can drive the reference model arbitrarily close the ideal one. Furthermore, as a byproduct, the reference model given in (8.10) also avoids a possible centralized control design (see Section 8.4).

The objective of this paper is to present a distributed control algorithm to drive the position of each agent to that of the leader in a user-defined finite time $T\in\mathbb{R}_+$ (see Figure 8.1), while guaranteeing user-defined performance bounds ε_i, $i\in\{1,2,\ldots,N\}$, on the system error trajectories (i.e., the error between the

agent's position $x_i(t)$ and an ideal system trajectory $x_{ri}(t)$); that is,

$$\lim_{t\to T}\big(x_i(t)-p(t)\big)=0,\quad i\in\{1,2,\ldots,N\}, \tag{8.11}$$

$$|x_i(t)-x_{ri}(t)|<\varepsilon_i,\quad i\in\{1,2,\ldots,N\}. \tag{8.12}$$

8.4 Proposed Control Architecture

This section presents the proposed distributed control algorithm for simultaneously achieving user-defined performance guarantees as well as user-defined finite-time convergence to the position of the time-varying leader. Mathematically speaking, consider the distributed control algorithm given by

$$u_i(t) \;=\; -\alpha\lambda(t)\Bigg(\sum_{i\sim j}\big(x_i(t)-x_j(t)\big)+k_i\big(x_i(t)-p(t)\big)\Bigg)-\hat{\omega}_i(t)x_i(t),\quad i\in\{1,2,\ldots,N\}, \tag{8.13}$$

where $\hat{\omega}_i(t)$ is an estimation of the system uncertainty ω_i, $i\in\{1,2,\ldots,N\}$. In (8.13), $k_i=1$ for the subset of the agents having access to the position of a time-varying leader in (8.5) and $k_i=0$ for other agents. Furthermore, the update law for $\hat{\omega}_i(t)$, $i\in\{1,2,\ldots,N\}$ in (8.13) is given by

$$\dot{\hat{\omega}}_i(t)=\gamma_i\mathrm{Proj}\big(\hat{\omega}_i(t),\phi_{d_i}(|e_i(t)|)x_i(t)e_i(t)\big),\quad \hat{\omega}_i(0)=\hat{\omega}_{i0},\quad i\in\{1,2,\ldots,N\}, \tag{8.14}$$

where $e_i(t)\triangleq x_i(t)-x_{ri}(t)$, $i\in\{1,2,\ldots,N\}$, is the error between the position of an agent and its corresponding reference model state from (8.10) and $\hat{\omega}_{\max}$ is the projection bound. Note that the proposed control algorithm given by (8.13) along with (8.14) can be executed distributively when a user-defined finite time T is selected for $\lambda(t)$ and when α is fixed according to Theorem 8.4.1 below. Here, (8.13) can be expressed in the compact form as

$$u(t) \;=\; -\alpha\lambda(t)\mathcal{F}(\mathfrak{G})\tilde{x}(t)-\hat{\Omega}(t)x(t). \tag{8.15}$$

where $\tilde{x}(t)\triangleq x(t)-\mathbf{1}_N p(t)\in\mathbb{R}^N$ denotes the aggregated error vector between the position of each agent and that of the leader with the dynamics

$$\begin{aligned}\dot{\tilde{x}}(t) &= \dot{x}(t)-\mathbf{1}_N v(t),\\ &= u(t)+\Omega x(t)-\mathbf{1}_N v(t),\quad \tilde{x}(0)=\tilde{x}_0,\end{aligned} \tag{8.16}$$

and $\hat{\Omega}(t)\triangleq\mathrm{diag}([\hat{\omega}_1,\ldots,\hat{\omega}_N])\in\mathbb{R}^{N\times N}$.

We now rewrite the reference model given by (8.10) as

$$\begin{aligned}\dot{x}_{\mathrm{r}i}(t) &= -\alpha\lambda(t)\Bigg(\sum_{i\sim j}\big(x_{\mathrm{r}i}(t)-x_{\mathrm{r}j}(t)+x_{\mathrm{r}j}(t)-x_j(t)\big)+k_i\big(x_{\mathrm{r}i}(t)-p(t)\big)\Bigg),\\ &= -\alpha\lambda(t)\Bigg(\sum_{i\sim j}\big(x_{\mathrm{r}i}(t)-x_{\mathrm{r}j}(t)\big)+k_i\big(x_{\mathrm{r}i}(t)-p(t)\big)\Bigg)+\alpha\lambda(t)\sum_{i\sim j}e_j(t),\ x_{\mathrm{r}i}(0)=x_{\mathrm{r}i0},\ i\in\{1,2,\ldots,N\},\end{aligned} \tag{8.17}$$

and define $\tilde{x}_{\mathrm{r}i}(t)\triangleq x_{\mathrm{r}i}(t)-p(t),\ i\in\{1,2,\ldots,N\}$, to capture the error between the reference trajectory and the position of the time-varying leader. To this end, the error dynamics for $\tilde{x}_{\mathrm{r}i}(t)$ can now be written as

$$\dot{\tilde{x}}_{\mathrm{r}i}(t) \;=\; -\alpha\lambda(t)\Bigg(\sum_{i\sim j}\big(\tilde{x}_{\mathrm{r}i}(t)-\tilde{x}_{\mathrm{r}j}(t)\big)+k_i\tilde{x}_{\mathrm{r}i}(t)\Bigg)-v(t)+\alpha\lambda(t)\sum_{i\sim j}e_j(t),\ \ x_{\mathrm{r}i}(0)=x_{\mathrm{r}i0},\ \ i\in\{1,2,\ldots,N\}, \tag{8.18}$$

In the compact form, (8.18) can be equivalently written as

$$\dot{\tilde{x}}_{\mathrm{r}}(t) \;=\; -\alpha\lambda(t)\mathcal{F}(\mathfrak{G})\tilde{x}_{\mathrm{r}}(t)+\alpha\lambda(t)\mathcal{A}(\mathfrak{G})e(t)-v(t)\mathbf{1}_N,\quad x_{\mathrm{r}}(0)=x_{\mathrm{r}0}, \tag{8.19}$$

where $\tilde{x}_{\mathrm{r}}(t)\triangleq[\tilde{x}_{\mathrm{r}1}(t),\ldots,\tilde{x}_{\mathrm{r}N}(t)]^{\mathrm{T}}\in\mathbb{R}^N$ and $e(t)\triangleq[e_1(t),\ldots,e_N(t)]^{\mathrm{T}}\in\mathbb{R}^N$ denote the aggregated error vectors. Consider now the time transformation function given by

$$t \;=\; \theta(s)\triangleq T(1-e^{-s}). \tag{8.20}$$

This time transformation links a prescribed finite-time interval of interest $t\in[0,T)$ to the stretched infinite-time interval $s\in[0,\infty)$ and vice versa. Based on this time transformation function, let $\xi(t)\in\mathbb{R}^N, t\in[0,T)$, be a solution to the dynamical system given by (8.19) and define $\tilde{x}_{\mathrm{r}s}(s)=\tilde{x}_{\mathrm{r}}(t), s\in[0,\infty)$. It follows from Remark 8.2.1 that

$$\tilde{x}'_{\mathrm{r}s}(s) \;=\; -\alpha\mathcal{F}(\mathfrak{G})\tilde{x}_{\mathrm{r}s}(s)+M_s(s)\quad x_{\mathrm{r}s}(0)=x_{\mathrm{r}s0}, \tag{8.21}$$

where $M_s(s)\triangleq\alpha\mathcal{A}(\mathfrak{G})e_s(s)-Te^{-s}v_s(s)\mathbf{1}_N\in\mathbb{R}^N$.

Using (8.6), (8.10), and (8.13), we next write the error dynamics for $e_i(t)$ as

$$\begin{aligned}\dot{e}_i(t) &= \dot{x}_i(t) - \dot{x}_{ri}(t),\\ &= -\alpha\lambda(t)\Big(\sum_{i\sim j}\big(x_i(t)-x_{ri}(t)\big)+k_i e_i(t)\Big) - \tilde{\omega}_i(t)x_i(t),\\ &= -\alpha\lambda(t)\big(d_i+k_i\big)e_i(t) - \tilde{\omega}_i(t)x_i(t), \quad e_i(0)=e_{i0}, \quad i\in\{1,2,\ldots,N\},\end{aligned} \tag{8.22}$$

where $\tilde{\omega}_i(t) \triangleq \hat{\omega}_i(t) - \omega_i,\ i\in\{1,2,\ldots,N\}$ and $e_{i0} \triangleq x_{i0} - x_{ri0},\ i\in\{1,2,\ldots,N\}$. Similar to how (8.21) is derived from (8.19) using the time transformation function given by (8.20) according to Remark 8.2.1, one can also rewrite (8.22) as

$$e'_{is}(s) = -\alpha\big(d_i+k_i\big)e_{is}(s) - Te^{-s}\tilde{\omega}_{is}(s)x_{is}(s), \quad e_{is}(0)=e_{i0}, \quad i\in\{1,2,\ldots,N\}, \tag{8.23}$$

where the subscript s is used; see Remark 8.2.2. Using (8.14), the weight estimation error dynamics can be also expressed in the infinite-time interval as

$$\tilde{\omega}'_{is}(s) = \gamma_i Te^{-s}\mathrm{Proj}\big(\hat{\omega}_{is}(s), \phi_{di}(|e_i(s)|)x_{is}(s)e_{is}(s)\big), \quad \tilde{\omega}_{is}(0)=\hat{\omega}_{i0}-\omega_i, \quad i\in\{1,2,\ldots,N\}. \tag{8.24}$$

The following theorem presents the main contribution of this paper that addresses our objective stated in the last paragraph of Section 8.3.

Theorem 8.4.1 *Consider the multiagent system consisting of N agents on a connected, undirected graph $\mathfrak{G}$, where the uncertain dynamics of an agent $i\in\{1,\ldots,N\}$ is given by* (8.6)*. Consider, in addition, that there exists at least one agent sensing the position of the time-varying leader given by* (8.5)*, which has bounded (but unknown) velocity. For the distributed control algorithm $u_i(t)$ given by* (8.13) *along with its update law given by* (8.14)*, let the design parameter α be chosen such that $\mathcal{S} \triangleq \alpha\mathcal{F}(\mathfrak{G}) - I_N$ is positive-definite. If $|e_i(0)| < \varepsilon_i,\ i\in\{1,2,\ldots,N\}$, then the closed-loop system signals (including all the distributed control signals) remain bounded and all agents converge to the position of the leader at the user-defined finite time T (i.e., $\lim_{t\to T}\tilde{x}_i(t)=0,\ i\in\{1,2,\ldots,N\}$) for all initial conditions of agents, while guaranteeing user-defined performance bounds $|e_i(t)| < \varepsilon_i,\ i\in\{1,2,\ldots,N\}$.*

Proof. Considering the error dynamics in (8.23) and (8.24), let $\mathcal{V}_i : \mathcal{D}_\varepsilon \times \mathbb{R} \to \overline{\mathbb{R}}_+$ be an energy function given by

$$\mathcal{V}_i(e_{is},\tilde{\omega}_{is}) = \phi_i(|e_{is}|) + \gamma_i^{-1}\tilde{\omega}_{is}^2, \quad i \in \{1,2,\ldots,N\}, \tag{8.25}$$

where $\mathcal{D}_\varepsilon \triangleq \{|e_{is}(s)| : |e_{is}(s)| < \varepsilon_i\},\ i \in \{1,2,\ldots,N\}$. The derivative of (8.25) with respect to s along the closed-loop system trajectories of (8.23) and (8.24) is given by

$$\begin{aligned}\mathcal{V}_i'\big(e_{is}(s),\tilde{\omega}_{is}(s)\big) &= \frac{\mathrm{d}\phi(|e_{is}(s)|)}{\mathrm{d}s} + 2\gamma_i^{-1}\tilde{\omega}_{is}(s)\tilde{\omega}_{is}'(s)\\ &= 2\phi_{d_i}(|e_{is}(s)|)e_{is}(s)e_{is}'(s) + 2\tilde{\omega}_{is}(s)\Big(Te^{-s}\mathrm{Proj}\big(\hat{\omega}_{is}(s),\phi_{d_i}(|e_{is}(s)|)x_{is}(s)e_{is}(s)\big)\Big). \end{aligned}\tag{8.26}$$

Using (8.23) in (8.26) now yields

$$\begin{aligned}\mathcal{V}_i'\big(e_{is}(s),\tilde{\omega}_{is}(s)\big) &= -2\alpha\phi_{d_i}(|e_{is}(s)|)(d_i+k_i)e_{is}^2(s) - 2Te^{-s}\big(\hat{\omega}_{is}(s)-\omega_i\big)\Big(\phi_{d_i}(|e_{is}(s)|)x_{is}(s)e_{is}(s)\\ &\quad -\mathrm{Proj}\Big(\hat{\omega}_{is}(s),\phi_{d_i}(|e_{is}(s)|)x_{is}(s)e_{is}(s)\Big)\Big). \end{aligned}\tag{8.27}$$

Now, using the property of projection operator from Definition 8.2.1, one can write

$$\begin{aligned}\mathcal{V}_i'\big(e_{is}(s),\tilde{\omega}_{is}(s)\big) &\le -\beta_i\phi_{d_i}(|e_{is}(s)|)e_{is}^2(s),\\ &\le -\beta_i\phi_{d_i}(|e_{is}(s)|)e_{is}^2(s)\\ &\quad +\big[\frac{1}{2}\beta_i\phi(|e_{is}(s)|) - \frac{1}{2}\beta_i\phi(|e_{is}(s)|)\big] + \big[\frac{1}{2}\beta_i\gamma_i^{-1}\tilde{\omega}_{is}^2(s) - \frac{1}{2}\beta_i\gamma_i^{-1}\tilde{\omega}_{is}^2(s)\big],\\ &\le -\frac{1}{2}\beta_i\mathcal{V}_i\big(e_{is}(s),\tilde{\omega}_{is}(s)\big)+\mu, \end{aligned}\tag{8.28}$$

with $\beta_i \triangleq 2\alpha(d_i+k_i) \in \mathbb{R}_+$, $\mu \triangleq \frac{1}{2}\beta_i\gamma_i^{-1}(\hat{\omega}_{\max}^2+\omega_{\max}^2)$, and $\omega_{\max} \triangleq \max\{\omega_1,\ldots,\omega_N\}$, where we also utilized the last property of Definition 8.2.2 for the generalized restricted potential function. It now follows from (8.28) that $\mathcal{V}_i\big(e_{is}(s),\tilde{\omega}_{is}(s)\big)$ is upper bounded by $\mathcal{V}_{i,\max} \triangleq \max\Big\{\mathcal{V}_{i0}, \frac{2\mu}{\beta_i}\Big\}$, where $\mathcal{V}_{i0} \triangleq \mathcal{V}_i(e_{is}(0),\tilde{\omega}_{is}(0))$. From (8.25), the boundedness of the energy function results in $\phi_i(|e_{is}(s)|) + \gamma_i^{-1}\tilde{\omega}_{is}^2(s) \le \mathcal{V}_{i,\max}$, and hence, $\phi(|e_{is}(s)|) \le \mathcal{V}_{i,\max}$ that proves $|e_{is}(s)| < \varepsilon_i,\ s \in [0,\infty)$. From Remark 8.2.1, one can now conclude that $|e_i(t)|$ stays in the set $\mathcal{D}_\varepsilon$ within the finite-time interval of interest for all agents; that is, $|e_i(t)| < \varepsilon_i, t \in [0,T),\ i \in \{1,2,\ldots,N\}$.

Since $e_s(s)$ is bounded based on the above arguments, $M_s(s)$ in (8.21) also remains bounded. Considering (8.21), it now follows from Lemma 8.2.2 that $\tilde{x}_{\mathrm{rs}}(s)$ is bounded. This implies the boundedness of the reference system trajectories $x_{\mathrm{rs}}(s)$ (or equivalently, $x_{\mathrm{r}}(t)$) and consequently the position of the agents

$x_s(s)$ (and $x(t)$). Hence, from $\mathcal{V}_i'\big(e_{is}(s),\tilde{\omega}_{is}(s)\big)\leq -\beta_i\phi_{d_i}(|e_{is}(s)|)e_{is}^2(s)$ given as the first inequality in (8.28), it follows from and the steps in the proof of Theorem 5.3 of [21] (based on [199, 200]) that $\lim_{s\to\infty} e_s(s)=0$. Since $e_s(s)=e(t)$ by definition (see Remark 8.2.1) and $t\to T$ as $s\to\infty$, one obtains

$$\lim_{t\to T} e(t)=0. \tag{8.29}$$

Turning back to (8.21), now that $\lim_{s\to\infty} e_s(s)=0$, one can conclude $\lim_{s\to\infty} M_s(s)=0$. Once again, using Lemma 8.2.2, it follows that $\lim_{s\to\infty}\tilde{x}_{\mathrm{rs}}(s)=0$, that is,

$$\lim_{t\to T}\tilde{x}_{\mathrm{r}}(t)=0. \tag{8.30}$$

Using the sum law for the well-defined limits in (8.29) and (8.30) now results in $\lim_{t\to T}\big(x(t)-\mathbf{1}_N p(t)\big)=0$ (see Section 1.6 of [201]).

Finally, we show that the control signal $u(t), t\in[0,T)$, remains bounded. For this purpose, letting $z(t)\triangleq -\alpha\lambda(t)\mathcal{F}(\mathfrak{G})\tilde{x}(t)$, we rewrite (8.15) as

$$u(t) \;=\; z(t)-\hat{\Omega}(t)x(t). \tag{8.31}$$

Since $\hat{\Omega}(t)$ and $x(t)$ are both bounded from the above part of the proof, we need to ensure that $z(t)$ remains bounded to conclude the boundedness of $u(t)$. Motivated from this standpoint, we take the time derivative of $z(t)$ as

$$\dot{z}(t)=-\alpha\lambda(t)\mathcal{F}(\mathfrak{G})\dot{\tilde{x}}(t)-\alpha\lambda^2(t)\mathcal{F}(\mathfrak{G})\tilde{x}(t),\quad z(0)=z_0. \tag{8.32}$$

Substituting (8.16) in (8.32) then yields

$$\begin{aligned}\dot{z}(t)&=-\alpha\lambda(t)\mathcal{F}(\mathfrak{G})\big(u(t)+\Omega x(t)-\mathbf{1}_N v(t)\big)+z(t)\lambda(t)\\&=-\alpha\lambda(t)\mathcal{F}(\mathfrak{G})\big(z(t)-\tilde{\Omega}(t)x(t)-\mathbf{1}_N v(t)\big)+z(t)\lambda(t),\\&=-\mathcal{S}\lambda(t)z(t)+\alpha\lambda(t)\mathcal{F}(\mathfrak{G})\big(\tilde{\Omega}(t)x(t)+\mathbf{1}_N v(t)\big),\quad z(0)=z_0,\end{aligned} \tag{8.33}$$

where $\mathcal{S}=\alpha\mathcal{F}(\mathfrak{G})-I_N$. Similar to how (8.21) is derived from (8.19) using the time transformation function given by (8.20) according to Remark 8.2.1, one can also rewrite (8.33) as

$$z_s'(s) = -\mathcal{S}z_s(s) + \alpha\mathcal{F}(\mathfrak{G})N_s(s), \quad z_s(0) = z_0, \tag{8.34}$$

where $N_s(s) \triangleq \tilde{\Omega}_s(s)x_s(s) + \mathbf{1}_N v_s(s) \in \mathbb{R}^N$. From the boundedness of the velocity of the leader as well as the boundedness of $\tilde{\Omega}_s(s)x_s(s)$, it follows that $N_s(s)$ is a bounded function. Therefore, from $-\mathcal{S}$ being Hurwitz by the assumption given in the theorem, it follows from Lemma 8.2.2 that $z_s(s)$ is bounded. Hence, $z(t)$ and therefore $u(t)$ remain bounded for all $t \in [0,T)$. ■

Remark 8.4.1 *The proposed distributed control algorithm given by* (8.13) *along with* (8.14) *simultaneously addresses the spatial and temporal constraints problem discussed in Section 8.3 for multiagent systems regardless of the initial conditions of agents and without requiring a strict knowledge of the upper bounds of the considered class of system uncertainties. Specifically, by using a time transformation function in* (8.20)*, this framework provides user-defined finite-time convergence properties for a given multiagent system with uncertain agents in the sense that is* $\lim_{t\to T}\big(x_i(t) - p(t)\big) = 0,\ i \in \{1,2,\ldots,N\}$. *The generalized restricted potential functions utilized in the update law* (8.14) *also enforces each agent to stay close to the reference trajectories during this user-defined interval, that is,* $|x_i(t) - x_{ri}(t)| < \varepsilon_i,\ i \in \{1,2,\ldots,N\}$.

Remark 8.4.2 *As mentioned earlier, the reference model given by* (8.10) *is utilized to avoid a possible centralized control design. Comparing* (8.10) *or, equivalently,* (8.17) *with* (8.8)*, one can directly see that when the error signal of the neighboring agents* $e_j(t)$ *are small, then* (8.10) *evolves close to the ideal reference model given by* (8.8)*. Now, it results from Theorem 8.4.1 that each error signal is bounded by a user-defined parameter, i.e.,* $|e_i(t)| < \varepsilon_i$*; hence, the reference model given by* (8.10) *can be made arbitrarily close by design to the ideal reference model given by* (8.8) *(i.e., by judicious selection of the user-defined bounds* $\varepsilon_i,\ i \in \{1,2,\ldots,N\}$ *and* $x_{ri}(0) = r_i(0),\ i \in \{1,2,\ldots,N\}$ *without loss of any generality).*

Remark 8.4.3 *For applications in which the system uncertainties are small, the result in [4] can be used alternatively for achieving a user-defined finite-time convergence. However, as discussed in Section 8.1, the proposed distributed control algorithm in this paper considerably goes beyond those results in that here the system performance during the transient time is also enforced by user-defined parameters* $\varepsilon_i,\ i \in \{1,2,\ldots,N\}$. *Hence, the proposed algorithm can provide additional level of performance freedom for the critical control systems.*

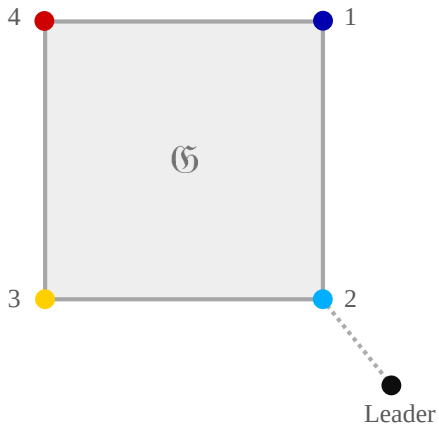

Figure 8.2: A multiagent system consisting of four agents on an undirected, connected circle graph $\mathfrak{G}$.

8.5 Illustrative Numerical Example

This section presents an illustrative numerical example to demonstrate the efficacy of the proposed distributed control algorithm. Specifically, we consider a multiagent system consisting of four agents on an undirected, connected circle graph $\mathfrak{G}$ as depicted in Figure 8.2. The agent 2 has access to the position of a time-varying leader given by $p(t) = -1.5 - 0.5\sin(0.15t) + 0.5\cos(0.3t)$. We let the system uncertainties in (8.6) be $\omega_1 = -1, \omega_2 = -1, \omega_3 = 1, \omega_4 = 1$, and set the initial positions of the agents randomly over the interval $[-0.5, 0.5]$.

Considering a desired finite-time convergence of $T = 10$ seconds, one can implement the results given in [4] (i.e., (8.13) without the term "$\hat{\omega}_i(t)x_i(t)$") with $\alpha = 6$ for addressing this temporal constraint problem. However, as mentioned in Section 8.1, this framework is not able to enforce a (transient) performance guarantee on the system error vector. Figures 8.3 and 8.4 show the finite-time convergence of the agents using the control algorithm in [4]. The dashed line shows the position of the leader, solid lines show the position of agents, and dotted lines show the ideal reference trajectories. We note that, although the agents converge to the position of the leader in $T = 10$ seconds, they are deviating from their ideal reference trajectories during the transient time. In particular, Figure 8.5 presents the evolution of $e_i(t)$ that is the distance between the agent's position and their corresponding reference position. It is clear from this figure that if a performance constraint of $\varepsilon_i = \varepsilon = 0.15,\ i \in \{1, 2, \ldots, N\}$, is required such that the agents stay close to the position of their reference model, the presented method in [4] is not able to meet such requirement.

We now implement the proposed distributed control algorithm in this paper (i.e., (8.13) along with (8.14)). We use the time transformation function given in (8.20) with $T = 10$ in order to enforce the finite-

time convergence of 10 seconds and, once again, set $\alpha = 6$ that results in a positive-definite matrix $\mathcal{S}$. In addition, we set the projection bound imposed on each element of the parameter estimate to $\hat{W}_{\max} = 2$ and the adaptation rate to $\gamma_i = 1,\ i \in \{1,2,\ldots,N\}$. We also select the generalized restricted potential function

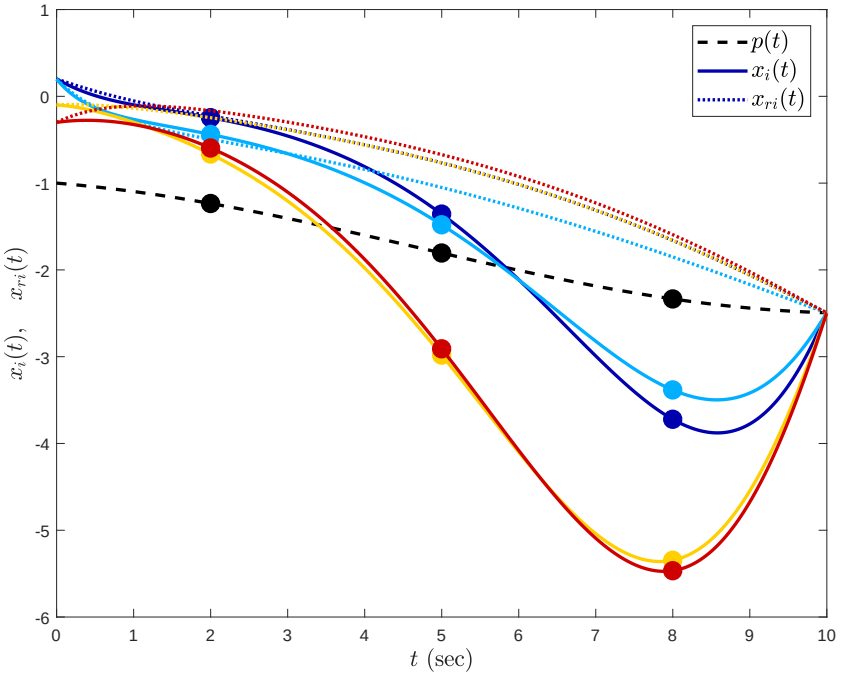

Figure 8.3: Leader-follower performance with the finite-time control algorithm in [4] ($T = 10$ and $\alpha = 6$).

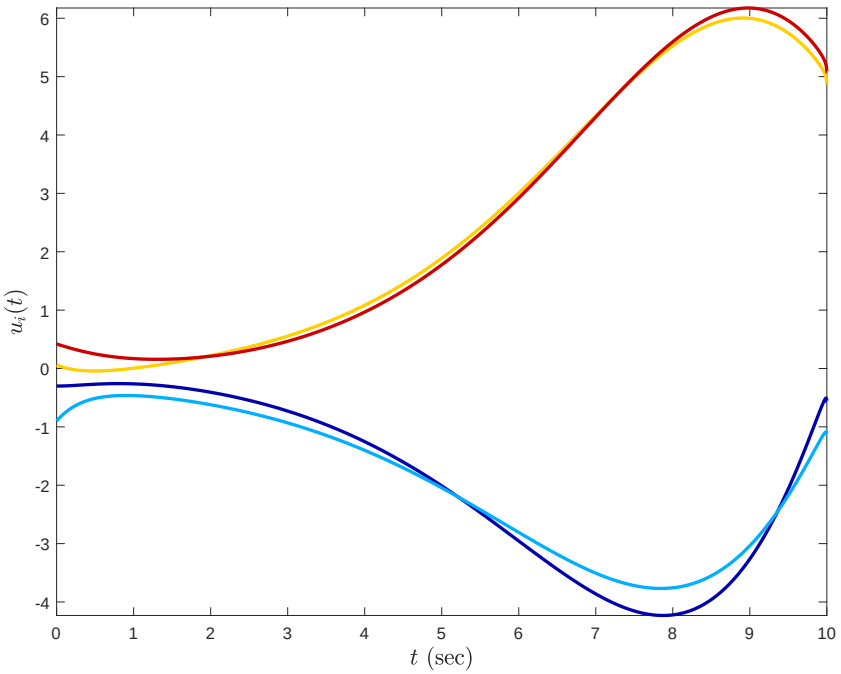

Figure 8.4: Control signals of agents with the finite-time control algorithm in [4] ($T = 10$ and $\alpha = 6$).

in Definition 8.2.2 as $\phi_i(|e_i(t)|) = |e_i(t)|^2/\big(\varepsilon - |e_i(t)|\big)$, $e_i(t) \in \mathcal{D}_\varepsilon$ with $\varepsilon_i = \varepsilon = 0.15,\ i \in \{1,2,\ldots,N\}$ to guarantee $|x_i(t) - x_{ri}(t)| < 0.15,\ i \in \{1,2,\ldots,N\}$.

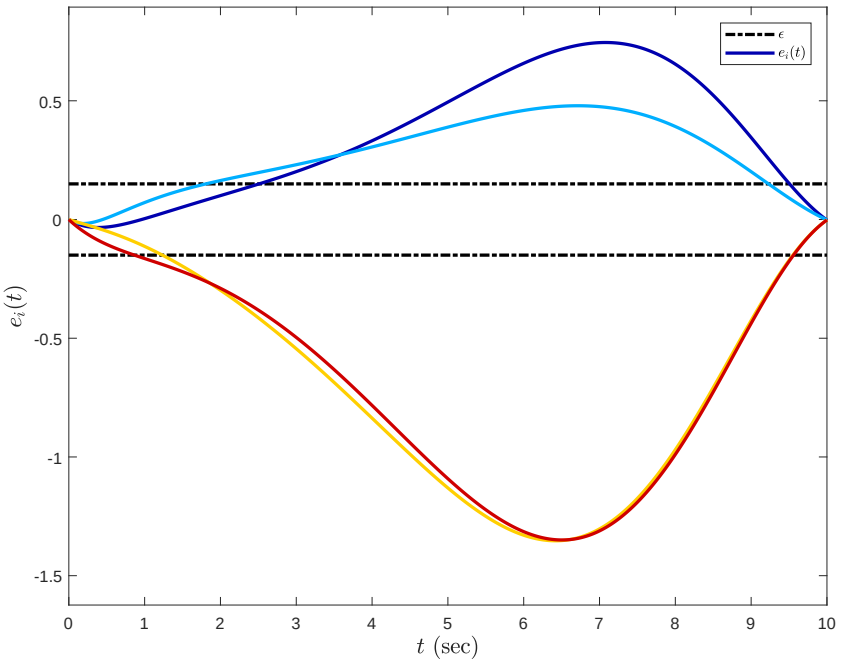

Figure 8.5: The evolution of $e_i(t)$ with the finite-time control algorithm in [4] ($T = 10$ and $\alpha = 6$).

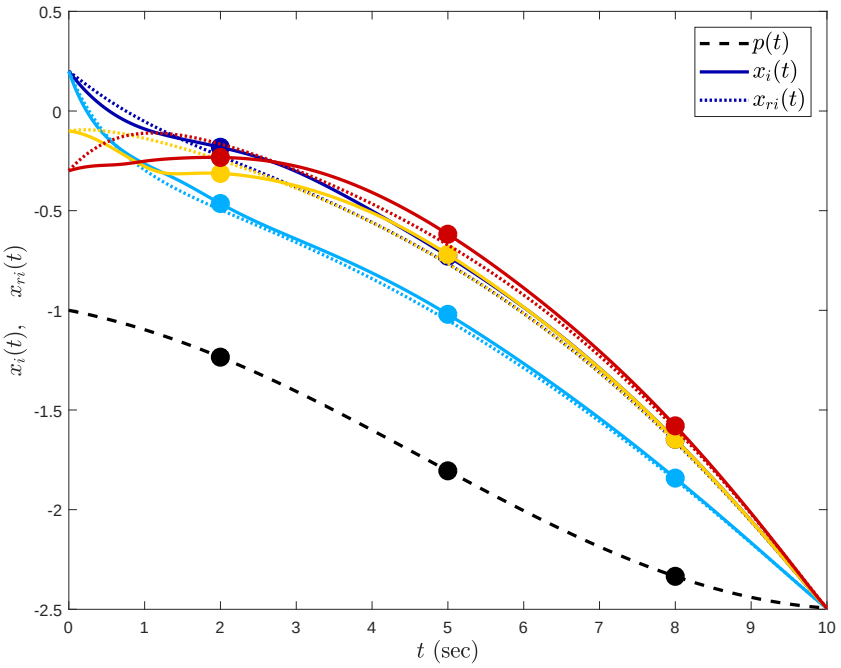

Figure 8.6: Leader-follower performance with the proposed finite-time control algorithm proposed in Theorem 8.4.1 ($T = 10$ and $\alpha = 6$).

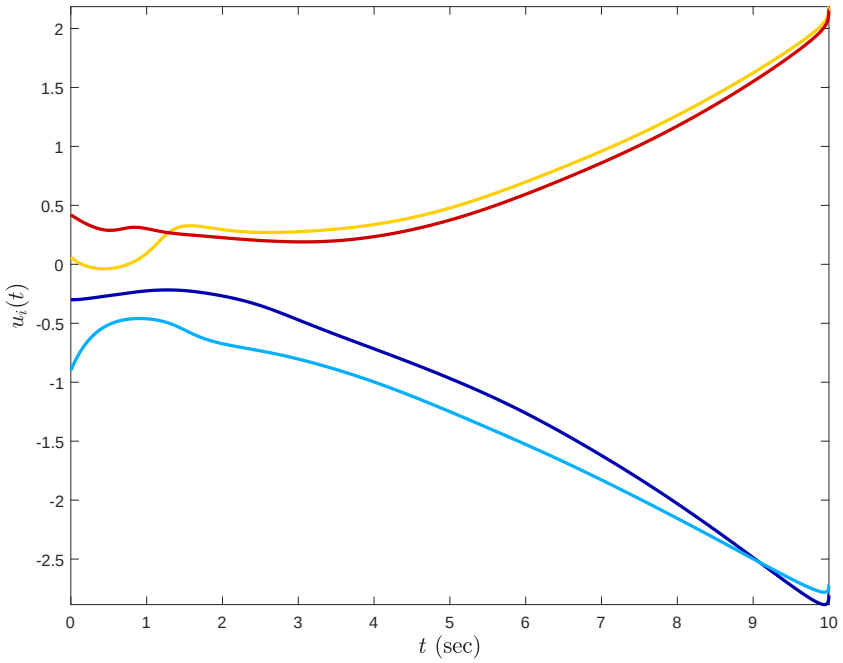

Figure 8.7: Control signals of agents with the proposed finite-time control algorithm in Theorem 8.4.1 ($T = 10$ and $\alpha = 6$).

Figures 8.6 and 8.7 present the performance of the proposed distributed control algorithm for addressing spatial and temporal constraints simultaneously. Specifically, these figures show that the finite-time convergence is obtained at the user-defined finite time of $T = 10$ seconds. In addition, Figure 8.8 shows that the position of each agent is kept within a close neighborhood of the position of their corresponding reference trajectories by guaranteeing user-defined performance bounds $|x_i(t) - x_{ri}(t)| < 0.15,\ i \in \{1,2,\ldots,N\}$. The effective learning rate $\gamma_i \phi_{d_i}(|e_i(t)|),\ i \in \{1,2,\ldots,N\}$ and the estimation of the agentwise system uncertainty $\hat{\omega}_i(t),\ i \in \{1,2,\ldots,N\}$ are also depicted in Figures 8.9 and 8.10, respectively. Finally, comparing Figure 8.7 with Figure 8.4, we note that the proposed distributed control algorithm results in less control effort in accomplishing the considered task.

8.6 Conclusion

To simultaneously guarantee user-defined spatial performance and temporal convergence at a user-defined time for uncertain multiagent systems, we presented a new distributed control algorithm. Specifically, based on a distributed adaptive control law, which utilizes an error-dependent learning rate, the proposed algorithm was shown to enforce user-defined performance bounds on the distance between the uncertain state trajectories of agents and their distributed reference models. Furthermore, based on a

time transformation approach, the proposed algorithm was shown to achieve a user-defined finite-time convergence. These spatiotemporal constraints were addressed regardless of the initial conditions of agents

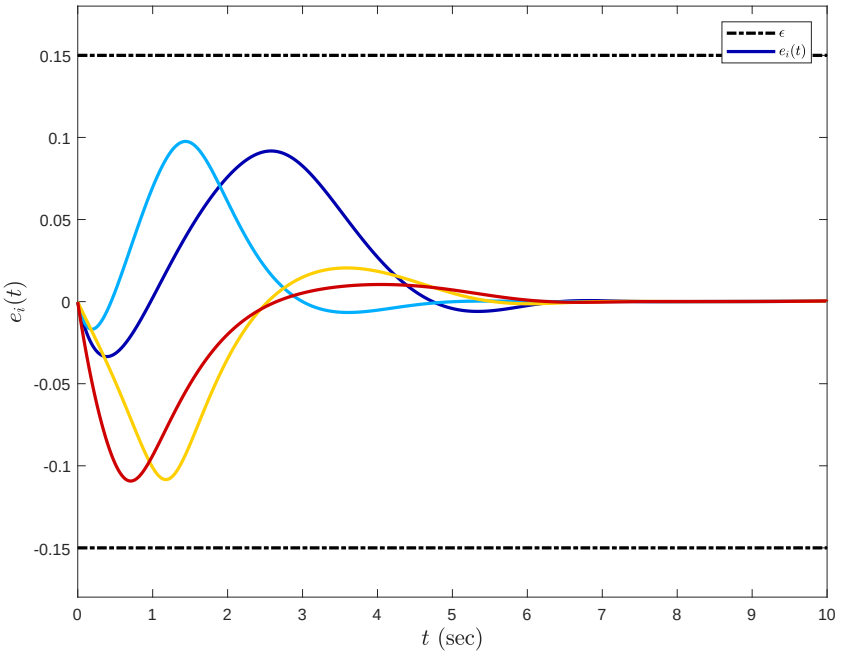

Figure 8.8: The evolution of $e_i(t)$ with the proposed finite-time control algorithm in Theorem 8.4.1 ($T = 10$ and $\alpha = 6$).

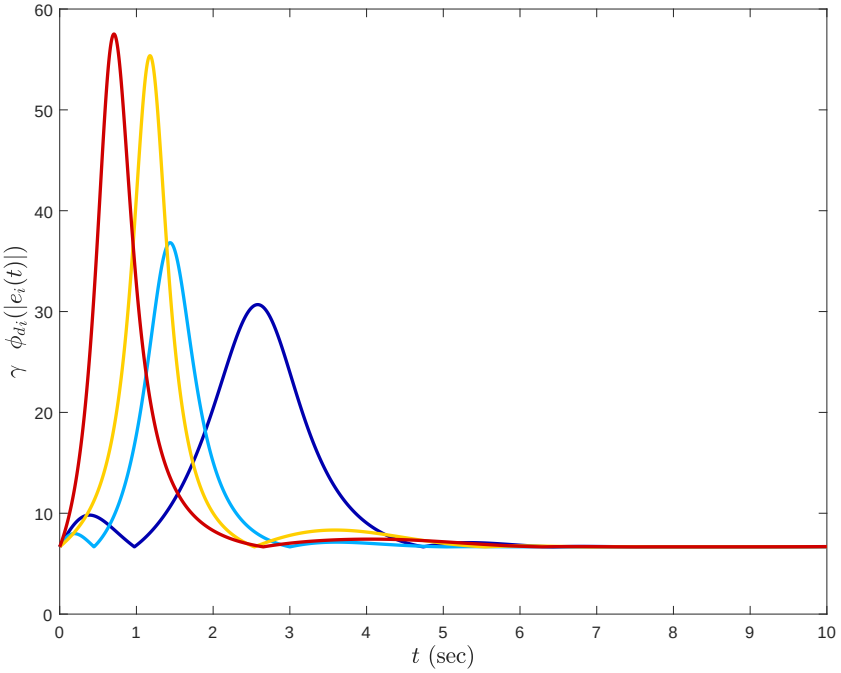

Figure 8.9: The effective learning rate $\gamma_i \phi_{d_i}(|e_i(t)|)$ with the proposed finite-time control algorithm in Theorem 8.4.1 ($T = 10$ and $\alpha = 6$).

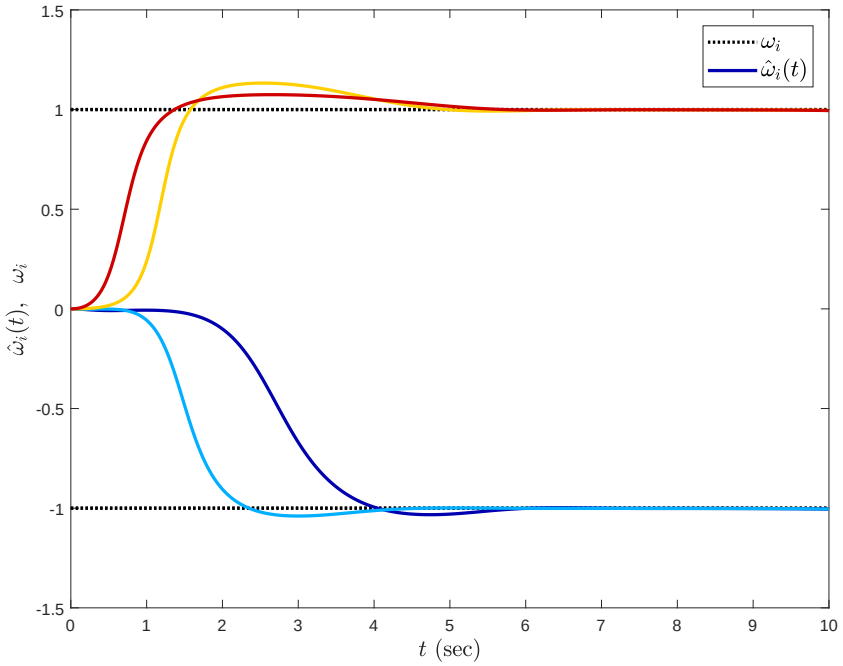

Figure 8.10: The estimation of the system uncertainty $\hat{\omega}_i(t)$ with the proposed finite-time control algorithm in Theorem 8.4.1 ($T = 10$ and $\alpha = 6$).

and without requiring a strict knowledge of the upper bounds of the considered class of system uncertainties. A future research direction can include extensions of the results presented in this paper to high-order multiagent systems as well as application of our theoretical findings to real-world experiments.

CHAPTER 9: CONCLUDING REMARKS AND FUTURE RESEARCH

9.1 Concluding Remarks

The research reported in this dissertation has investigated new model reference adaptive control architectures for uncertain dynamical systems that are subject to spatiotemporal constraints, where the presented control developments were rigorously established through system-theoretic methods to improve the overall system stability, robustness, and performance characteristics.

Specifically, a set-theoretic model reference adaptive control architecture was proposed in Chapter 2 to address the challenge of enforcing user-defined spatial performance constraints. The proposed control architecture was predicated on a generalized restricted potential function to auto-tune the adaptive control design. The key characteristic of this new adaptation mechanism is to increase the effective learning rate when the system error trajectories get close to the boundaries of a prescribed user-defined compact set that represents the spatial constraint. Therefore, the system trajectories were enforced to evolve within this compact set for all time, and importantly, without requiring a strict knowledge of the upper bounds of the system uncertainties. As a byproduct, it was shown that an upper bound for the adaptive control signals can be directly calculated without inducing (excessive) conservatism, which only depends on user-defined design parameters.

The set-theoretic model reference adaptive control architecture for enforcing spatial constraints was then generalized in Chapter 3 for uncertain dynamical systems having unstructured system uncertainties, where these uncertainties are usually estimated by utilizing the universal function approximations within a compact set. It was shown that the proposed controller was capable of keeping the system trajectories within this compact set; hence, the universal function approximation property was always valid and the overall system stability was achieved.

The results obtained for generalizing the set-theoretic model reference adaptive control architecture reported in Chapter 4 provided several essential advances to this control framework. In particular, the proposed control algorithms for enforcing time-varying performance bounds on the system error trajectories,

enable a designer to control the closed-loop system performance as desired on different time intervals, namely, the transient time interval and the steady-state time interval. In addition, for the case where a subset of system states is more critical than the rest (especially when the number of system states is large), a new extension to the set-theoretic model reference adaptive control architecture was proposed, where it allows a control designer to weigh each system error vector elements independently for enforcing componentwise performance guarantees. Moreover, for control of uncertain dynamical systems in the presence of actuator dynamics, the ideal reference model was modified using the hedging method, resulting in separation of the actuator dynamics and the adaptation process. A set-theoretic model reference adaptive control architecture then ensured user-defined performance bounds on the system error, and importantly, it was shown that the deviation of the uncertain dynamical system trajectories from the ideal reference model trajectories can be controlled using this user-defined bound and the actuator bandwidth limit. In addition to the exogenous disturbances and system uncertainties, actuator failures can also significantly deteriorate the closed-loop system performance. To this end, a set-theoretic model reference adaptive control architecture was introduced that not only compensates for these actuator failures but also it preserves user-defined performance guarantees in the presence of finite number of actuator failures.

The efficacy of the proposed set-theoretic model reference adaptive control architecture was then investigated through several applications in Chapter 5. In particular, this framework was applied to the longitudinal and lateral-directional dynamics of the NASA generic transport model. The set-theoretic model reference adaptive control architectures with constant and time-varying performance bounds were then experimentally verified on an aerospace testbed configured as a conventional dual-rotor helicopter. Through several rigorous analyses, our study also concluded that a dead-zone effect can be augmented into the set-theoretic model reference adaptive control architecture to stop the adaptation process when the system errors are small, while guaranteeing a user-defined performance bound. This was motivated by the fact that small system errors generally contain high-frequency residual content of exogenous disturbances and/or measurement noise. In the view of human-in-the-loop control architectures, the set-theoretic model reference adaptive control was implemented at the inner loop system, where its error can propagate to the outer-human loop. As a result, a sufficient stability condition was established for the overall physical system, where this condition does not depend on the system uncertainties and can be assigned with user-defined parameters.

As described in the review of the classical finite-time control literature in Chapter 6, the convergence time of these controllers varies by changing the initial conditions of the system, or a strict knowledge of the upper bounds of the system uncertainties is required for the design. To address these challenges in enforcing temporal constraint, a new distributed control algorithm was proposed for first-order and second-order uncertain multiagent systems. This control architecture utilized a time transformation technique to link a user-defined finite-time interval of interest to a stretched infinite-time interval. As a result, standard system-theoretic tools were used for synthesis and analysis purposes in this infinite horizon, and eventually the convergence guarantee was transferred back to the original finite-time interval. More importantly, deviating from other approaches in the literature, this convergence guarantee was obtained regardless of the initial conditions of the multiagent system and without requiring a knowledge of the upper bounds of the system uncertainties. In addition, another type of system uncertainties known as sensor uncertainties was investigated in the context of multiagent systems in Chapter 7. The proposed distributed control architecture was capable of mitigating the effects of these sensor uncertainties, and achieving a desired leader-follower objective.

Finally, a unified and novel control scheme was presented in Chapter 8 to simultaneously address the spatial and temporal problem. While enforcing user-defined performance bounds on the distance between the state trajectories of agents and the corresponding reference state trajectories, this distributed control algorithm ensured that the agents converge to a time-varying leader within a user-defined finite time of interest. Specifically, the term "user-defined" emphasis on key feature of this control design, that is the achieved spatiotemporal guarantee was independent of the initial conditions of agents, and a strict knowledge of the upper bounds of the considered class of system uncertainties was not required.

9.2 Future Research

As the results of this dissertation have highlighted, the user-defined system performance guarantees incorporated within adaptive control architectures make these controllers unique candidates for control of uncertain physical systems that are subject to spatial and temporal constraints. Yet, other considerations can further improve these control architectures for real-world applications. In this section, some research directions and suggestions for future work are presented to conclude this dissertation.

For the proposed set-theoretic model reference adaptive control, if the user-defined performance bound is not assigned reasonably, the controller may fail due to system structural limits (i.e., the expected

performance characteristics from the user are not practical). To this end, for example, a hybrid performance enforcement technique can be investigated such that it can overrule the user-defined bound (temporarily) to avoid failure of the control architecture in such extreme performance bound assignments. In addition, actuator saturation can be a limiting factor in this framework. Although the actuator rate saturation was indirectly addressed in Section 4.3, actuator amplitude saturation still needs to be investigated thoroughly in this context.

While the results in Chapters 6 and 8 consider first-order and second-order multiagent systems, these control algorithms can be generalized for higher order cases to capture a wider class of uncertain multiagent systems.

Full-state feedback control was considered as a baseline control scheme throughout this dissertation, extending these developments to output feedback control is another possible research direction. Furthermore, other than the presented experimental results, more experimentation can be conducted to further show the efficacy of the proposed control architectures. Specifically, the author is in the process of implementing the set-theoretic model reference adaptive control architecture in human-in-the-loop physical systems that is presented in Section 5.4. Applications of the distributed control architectures presented in Sections 6 and 8 applied to the Khepera IV ground robots are also in progress.

REFERENCES

[1] E. Arabi, B. C. Gruenwald, T. Yucelen, and N. T. Nguyen, "A set-theoretic model reference adaptive control architecture for disturbance rejection and uncertainty suppression with strict performance guarantees," *International Journal of Control*, vol. 91, no. 5, pp. 1195–1208, 2018.

[2] E. Arabi and T. Yucelen, "Set-theoretic model reference adaptive control with time-varying performance bounds," *International Journal of Control*, 2018 (accepted, available online).

[3] *Quanser AERO User Manual*, 2016. Available at https://www.quanser.com/products/quanser-aero/.

[4] E. Arabi, T. Yucelen, and J. R. Singler, "Robustness of finite-time distributed control algorithm with time transformation," in *American Control Conference*, 2019 (submitted).

[5] J. S. Brinker and K. A. Wise, "Flight testing of reconfigurable control law on the x-36 tailless aircraft," *Journal of Guidance, Control, and Dynamics*, vol. 24, no. 5, pp. 903–909, 2001.

[6] S. A. Jacklin, M. R. Lowry, J. M. Schumann, P. P. Gupta, J. T. Bosworth, E. Zavala, J. W. Kelly, K. J. Hayhurst, C. M. Belcastro, and C. Belcastro, "Verification, validation, and certification challenges for adaptive flight-critical control system software," *AIAA Guidance, Navigation, and Control Conference and Exhibit*, 2004.

[7] T. L. Jordan, J. V. Foster, R. M. Bailey, and C. M. Belcastro, "AirSTAR: A UAV platform for flight dynamics and control system testing," *AIAA Aerodynamic Measurement Technology and Ground Testing Conference*, 2006.

[8] M. L. Fravolini and G. Campa, "Design of a neural network adaptive controller via a constrained invariant ellipsoids technique," *IEEE Transactions on Neural Networks*, vol. 22, no. 4, pp. 627–638, 2011.

[9] M. L. Fravolini, T. Yucelen, and G. Campa, "Set theoretic performance verification of low-frequency learning adaptive controllers," *International Journal of Adaptive Control and Signal Processing*, vol. 29, no. 10, pp. 1243–1258, 2015.

[10] S. P. Bhat and D. S. Bernstein, "Continuous finite-time stabilization of the translational and rotational double integrators," *IEEE Transactions on automatic control*, vol. 43, no. 5, pp. 678–682, 1998.

[11] S. P. Bhat and D. S. Bernstein, "Finite-time stability of continuous autonomous systems," *SIAM Journal on Control and Optimization*, vol. 38, no. 3, pp. 751–766, 2000.

[12] M. Basin, Y. Shtessel, and F. Aldukali, "Continuous finite-and fixed-time high-order regulators," *Journal of the Franklin Institute*, vol. 353, no. 18, pp. 5001–5012, 2016.

[13] H. Hong, W. Yu, G. Wen, and X. Yu, "Distributed robust fixed-time consensus for nonlinear and disturbed multiagent systems," *IEEE Transactions on Systems, Man, and Cybernetics: Systems*, 2017.

[14] J. D. Sánchez-Torres, E. N. Sanchez, and A. G. Loukianov, "Predefined-time stability of dynamical systems with sliding modes," in *American Control Conference*, pp. 5842–5846, 2015.

[15] H. M. Becerra, C. R. Vázquez, G. Arechavaleta, and J. Delfin, "Predefined-time convergence control for high-order integrator systems using time base generators," *IEEE Transactions on Control Systems Technology*, 2017.

[16] K. J. Astrom and B. Wittenmark, *Adaptive Control*. Addison-Wesley Longman Publishing Co., Inc., 1994.

[17] N. T. Nguyen, *Model-reference adaptive control*. Springer, 2018.

[18] C. P. Bechlioulis and G. A. Rovithakis, "Robust adaptive control of feedback linearizable mimo nonlinear systems with prescribed performance," *IEEE Transactions on Automatic Control*, vol. 53, no. 9, pp. 2090–2099, 2008.

[19] C. P. Bechlioulis and G. A. Rovithakis, "Adaptive control with guaranteed transient and steady state tracking error bounds for strict feedback systems," *Automatica*, vol. 45, no. 2, pp. 532–538, 2009.

[20] C. P. Bechlioulis and G. A. Rovithakis, "Prescribed performance adaptive control for multi-input multi-output affine in the control nonlinear systems," *IEEE Transactions on Automatic Control*, vol. 55, no. 5, pp. 1220–1226, 2010.

[21] T. Yucelen and J. S. Shamma, "Adaptive architectures for distributed control of modular systems," in *American Control Conference*, pp. 1328–1333, 2014.

[22] K. B. Ngo, R. Mahony, and Z.-P. Jiang, "Integrator backstepping using barrier functions for systems with multiple state constraints," in *IEEE Conference on Decision and Control*, pp. 8306–8312, 2005.

[23] K. P. Tee, S. S. Ge, and E. H. Tay, "Barrier lyapunov functions for the control of output-constrained nonlinear systems," *Automatica*, vol. 45, no. 4, pp. 918–927, 2009.

[24] K. P. Tee, S. S. Ge, and F. E. H. Tay, "Adaptive control of electrostatic microactuators with bidirectional drive," *IEEE Transactions on Control Systems Technology*, vol. 17, no. 2, pp. 340–352, 2009.

[25] B. Ren, S. S. Ge, K. P. Tee, and T. H. Lee, "Adaptive neural control for output feedback nonlinear systems using a barrier lyapunov function," *IEEE Transactions on Neural Networks*, vol. 21, no. 8, pp. 1339–1345, 2010.

[26] A. K. Kostarigka and G. A. Rovithakis, "Adaptive dynamic output feedback neural network control of uncertain mimo nonlinear systems with prescribed performance," *IEEE Transactions on Neural Networks and Learning Systems*, vol. 23, no. 1, pp. 138–149, 2012.

[27] J. Muse, "A method for enforcing state constraints in adaptive control," in *AIAA Guidance, Navigation, and Control Conference*, p. 6205, 2011.

[28] K. S. Narendra and A. M. Annaswamy, *Stable adaptive systems*. Mineola, NY: Courier Corporation, 2012.

[29] P. A. Ioannou and J. Sun, *Robust adaptive control*. Mineola, NY: Courier Corporation, 2012.

[30] E. Lavretsky and K. Wise, *Robust and adaptive control with aerospace applications*. Springer Science & Business Media, 2012.

[31] T. Yucelen and W. M. Haddad, "Low-frequency learning and fast adaptation in model reference adaptive control," *IEEE Transactions on Automatic Control*, vol. 58, no. 4, pp. 1080–1085, 2013.

[32] T. Yucelen, G. De La Torre, and E. N. Johnson, "Improving transient performance of adaptive control architectures using frequency-limited system error dynamics," *International Journal of Control*, vol. 87, no. 11, pp. 2383–2397, 2014.

[33] K. S. Narendra and K. Parthasarathy, "Identification and control of dynamical systems using neural networks," *IEEE Transactions on Neural Networks*, vol. 1, no. 1, pp. 4–27, 1990.

[34] R. M. Sanner and J.-J. E. Slotine, "Gaussian networks for direct adaptive control," *IEEE Transactions on Neural Networks*, vol. 3, no. 6, pp. 837–863, 1992.

[35] F.-C. Chen and H. K. Khalil, "Adaptive control of nonlinear systems using neural networks," *International Journal of Control*, vol. 55, no. 6, pp. 1299–1317, 1992.

[36] A. Yeşildirek and F. L. Lewis, "Feedback linearization using neural networks," *Automatica*, vol. 31, no. 11, pp. 1659–1664, 1995.

[37] E. N. Johnson, *Limited authority adaptive flight control*. PhD thesis, Georgia Institute of Technology, 2000.

[38] E. N. Johnson and A. J. Calise, "Pseudo-control hedging: A new method for adaptive control," in *Advances in Navigation Guidance and Control Technology Workshop*, pp. 1–2, 2000.

[39] E. N. Johnson and A. J. Calise, "Limited authority adaptive flight control for reusable launch vehicles," *Journal of Guidance, Control, and Dynamics*, vol. 26, no. 6, pp. 906–913, 2003.

[40] B. C. Gruenwald, D. Wagner, T. Yucelen, and J. A. Muse, "Computing actuator bandwidth limits for model reference adaptive control," *International Journal of Control*, vol. 89, no. 12, pp. 2434–2452, 2016.

[41] B. C. Gruenwald, J. A. Muse, D. Wagner, and T. Yucelen, "Adaptive architectures for control of uncertain dynamical systems with actuator dynamics," *Advances in Intelligent and Autonomous Aerospace Systems (Editor: John Valasek), Second Edition*, (to appear).

[42] H. G. Kwatny, J.-E. T. Dongmo, B.-C. Chang, G. Bajpai, M. Yasar, and C. Belcastro, "Aircraft accident prevention: Loss-of-control analysis," in *AIAA Guidance, Navigation, and Control Conference and Exhibit*, 2009.

[43] C. M. Belcastro and J. V. Foster, "Aircraft loss-of-control accident analysis," in *Proceedings of AIAA Guidance, Navigation and Control Conference, Toronto, Canada, Paper No. AIAA-2010-8004*, 2010.

[44] C. M. Belcastro, "Loss of control prevention and recovery: Onboard guidance, control, and systems technologies," in *AIAA Conference on Guidance, Navigation and Control*, 2012.

[45] G. Tao, S. M. Joshi, and X. Ma, "Adaptive state feedback and tracking control of systems with actuator failures," *IEEE Transactions on Automatic Control*, vol. 46, no. 1, pp. 78–95, 2001.

[46] G. Tao, S. Chen, and S. M. Joshi, "An adaptive actuator failure compensation controller using output feedback," *IEEE Transactions on Automatic Control*, vol. 47, no. 3, pp. 506–511, 2002.

[47] J. D. Boskovic and R. K. Mehra, "Multiple-model adaptive flight control scheme for accommodation of actuator failures," *Journal of Guidance, Control, and Dynamics*, vol. 25, no. 4, pp. 712–724, 2002.

[48] X. Tang, G. Tao, and S. M. Joshi, "Adaptive actuator failure compensation for parametric strict feedback systems and an aircraft application," *Automatica*, vol. 39, no. 11, pp. 1975–1982, 2003.

[49] M. Schwager, A. M. Annaswamy, and E. Lavretsky, "Adaptation-based reconfiguration in the presence of actuator failures and saturation," in *American Control Conference*, pp. 2640–2645, 2005.

[50] X. Tang, G. Tao, and S. M. Joshi, "Adaptive output feedback actuator failure compensation for a class of non-linear systems," *International Journal of Adaptive Control and Signal Processing*, vol. 19, no. 6, pp. 419–444, 2005.

[51] X. Tang, G. Tao, and S. M. Joshi, "Adaptive actuator failure compensation for nonlinear mimo systems with an aircraft control application," *Automatica*, vol. 43, no. 11, pp. 1869–1883, 2007.

[52] W. Wang and C. Wen, "Adaptive actuator failure compensation control of uncertain nonlinear systems with guaranteed transient performance," *Automatica*, vol. 46, no. 12, pp. 2082–2091, 2010.

[53] J. Cortés, "Finite-time convergent gradient flows with applications to network consensus," *Automatica*, vol. 42, no. 11, pp. 1993–2000, 2006.

[54] F. Xiao, L. Wang, J. Chen, and Y. Gao, "Finite-time formation control for multi-agent systems," *Automatica*, vol. 45, no. 11, pp. 2605–2611, 2009.

[55] F. Jiang and L. Wang, "Finite-time information consensus for multi-agent systems with fixed and switching topologies," *Physica D: Nonlinear Phenomena*, vol. 238, no. 16, pp. 1550–1560, 2009.

[56] L. Wang and F. Xiao, "Finite-time consensus problems for networks of dynamic agents," *IEEE Transactions on Automatic Control*, vol. 55, no. 4, pp. 950–955, 2010.

[57] Z. Meng, W. Ren, and Z. You, "Distributed finite-time attitude containment control for multiple rigid bodies," *Automatica*, vol. 46, no. 12, pp. 2092–2099, 2010.

[58] Y. Shang, "Finite-time consensus for multi-agent systems with fixed topologies," *International Journal of Systems Science*, vol. 43, no. 3, pp. 499–506, 2012.

[59] X. Jin, W. M. Haddad, and T. Yucelen, "An adaptive control architecture for mitigating sensor and actuator attacks in cyber-physical systems," *IEEE Transactions on Automatic Control*, 2017.

[60] X. Jin, "Adaptive decentralized finite-time output tracking control for mimo interconnected nonlinear systems with output constraints and actuator faults," *International Journal of Robust and Nonlinear Control*, vol. 28, no. 5, pp. 1808–1829, 2018.

[61] B. Tian, Z. Zuo, and H. Wang, "Leader–follower fixed-time consensus of multi-agent systems with high-order integrator dynamics," *International Journal of Control*, vol. 90, no. 7, pp. 1420–1427, 2017.

[62] W. Lu, X. Liu, and T. Chen, "A note on finite-time and fixed-time stability," *Neural Networks*, vol. 81, pp. 11–15, 2016.

[63] H. B. Oza, Y. V. Orlov, and S. K. Spurgeon, "Robust finite time stability and stabilisation: A survey of continuous and discontinuous paradigms," in *13th International Workshop on Variable Structure Systems*, pp. 1–7, 2014.

[64] A. Polyakov, "Nonlinear feedback design for fixed-time stabilization of linear control systems," *IEEE Transactions on Automatic Control*, vol. 57, no. 8, pp. 2106–2110, 2012.

[65] H. Ríos and A. R. Teel, "A hybrid observer for fixed-time state estimation of linear systems," in *55th Conference on Decision and Control*, pp. 5408–5413, 2016.

[66] N. Harl and S. Balakrishnan, "Impact time and angle guidance with sliding mode control," *IEEE Transactions on Control Systems Technology*, vol. 20, no. 6, pp. 1436–1449, 2012.

[67] C. Yong, X. Guangming, and L. Huiyang, "Reaching consensus at a preset time: Single-integrator dynamics case," in *Chinese Control Conference*, pp. 6220–6225, 2012.

[68] C. Wang, G. Xie, and M. Cao, "Forming circle formations of anonymous mobile agents with order preservation," *IEEE Transactions on Automatic Control*, vol. 58, no. 12, pp. 3248–3254, 2013.

[69] E. Jiménez-Rodríguez, J. D. Sánchez-Torres, D. Gómez-Gutiérrez, and A. G. Loukianov, "Predefined-time tracking of a class of mechanical systems," in *13th International Conference on Electrical Engineering, Computing Science and Automatic Control*, pp. 1–5, 2016.

[70] E. Jiménez-Rodríguez, J. D. Sánchez-Torres, and A. G. Loukianov, "On optimal predefined-time stabilization," *International Journal of Robust and Nonlinear Control*, 2017.

[71] Y. Wang, Y. Song, D. J. Hill, and M. Krstic, "Prescribed-time consensus and containment control of networked multiagent systems," *IEEE Transactions on Cybernetics*, 2018.

[72] Z. Kan, T. Yucelen, E. Doucette, and E. Pasiliao, "A finite-time consensus framework over time-varying graph topologies with temporal constraints," *Journal of Dynamic Systems, Measurement, and Control*, vol. 139, no. 7, p. 071012, 2017.

[73] T. Yucelen, , Z. Kan, and E. Pasiliao, "Finite-time cooperative engagement," *IEEE Transactions on Automatic Control*, 2018 (under review).

[74] A. T. Vemuri, "Sensor bias fault diagnosis in a class of nonlinear systems," *IEEE Transactions on Automatic Control*, vol. 46, no. 6, pp. 949–954, 2001.

[75] X. Zhang, T. Parisini, and M. M. Polycarpou, "Sensor bias fault isolation in a class of nonlinear systems," *IEEE Transactions on Automatic Control*, vol. 50, no. 3, pp. 370–376, 2005.

[76] D. M. Bevly and B. Parkinson, "Cascaded Kalman filters for accurate estimation of multiple biases, dead-reckoning navigation, and full state feedback control of ground vehicles," *IEEE Transactions on Control Systems Technology*, vol. 15, no. 2, pp. 199–208, 2007.

[77] H. F. Grip, T. Fossen, T. A. Johansen, and A. Saberi, "Attitude estimation using biased gyro and vector measurements with time-varying reference vectors," *IEEE Transactions on Automatic Control*, vol. 57, no. 5, pp. 1332–1338, 2012.

[78] T. Yucelen and A. J. Calise, "Derivative-free model reference adaptive control," *Journal of Guidance, Control, and Dynamics*, vol. 34, no. 4, pp. 933–950, 2011.

[79] T. Yucelen and W. M. Haddad, "A robust adaptive control architecture for disturbance rejection and uncertainty suppression with $\mathcal{L}_\infty$ transient and steady-state performance guarantees," *International Journal of Adaptive Control and Signal Processing*, vol. 26, no. 11, pp. 1024–1055, 2012.

[80] J.-B. Pomet and L. Praly, "Adaptive nonlinear regulation: Estimation from the lyapunov equation," *IEEE Transactions on Automatic Control*, vol. 37, no. 6, pp. 729–740, 1992.

[81] X. Wang and N. Hovakimyan, "$\mathcal{L}_1$ adaptive controller for nonlinear time-varying reference systems," *Systems & Control Letters*, vol. 61, no. 4, pp. 455–463, 2012.

[82] Y. Kawaguchi, H. Eguchi, T. Fukao, and K. Osuka, "Passivity-based adaptive nonlinear control for active steering," *IEEE International Conference on Control Applications*, pp. 214–219, 2007.

[83] S. K. Scarritt, "Nonlinear model reference adaptive control for satellite attitude tracking," *AIAA Guidance, Navigation, and Control Conference*, 2008.

[84] F. Peter, M. Leitao, and F. Holzapfel, "Adaptive augmentation of a new baseline control architecture for tail-controlled missiles using a nonlinear reference model," *AIAA Guidance, Navigation, and Control Conference*, 2012.

[85] T. Yucelen, B. Gruenwald, J. Muse, and G. De La Torre, "Adaptive control with nonlinear reference systems," *American Control Conference*, 2015.

[86] A. E. Bryson, *Control of spacecraft and aircraft*. Princeton University Press, 1994.

[87] B. Gruenwald and T. Yucelen, "On transient performance improvement of adaptive control architectures," *International Journal of Control*, vol. 88, no. 11, pp. 2305–2315, 2015.

[88] B. C. Gruenwald, T. Yucelen, and J. A. Muse, "Direct uncertainty minimization framework for system performance improvement in model reference adaptive control," *Machines*, vol. 5, no. 1, p. 9, 2017.

[89] B. S. Kim and A. J. Calise, "Nonlinear flight control using neural networks," *Journal of Guidance, Control, and Dynamics*, vol. 20, no. 1, pp. 26–33, 1997.

[90] K. Y. Volyanskyy, W. M. Haddad, and A. J. Calise, "A new neuroadaptive control architecture for nonlinear uncertain dynamical systems: Beyond σ-and e-modifications," *IEEE Transactions on Neural Networks*, vol. 20, no. 11, pp. 1707–1723, 2009.

[91] A. J. Calise and T. Yucelen, "Adaptive loop transfer recovery," *Journal of Guidance, Control, and Dynamics*, vol. 35, no. 3, pp. 807–815, 2012.

[92] G. Chowdhary, H. A. Kingravi, J. P. How, and P. A. Vela, "Bayesian nonparametric adaptive control using gaussian processes," *IEEE Transactions on Neural Networks and Learning Systems*, vol. 26, no. 3, pp. 537–550, 2015.

[93] E. Arabi, B. C. Gruenwald, T. Yucelen, M. L. Fravolini, and N. T. Nguyen, "Model reference neuroadaptive control revisited: How to keep the system trajectories on a given compact set," in *AIAA Guidance, Navigation, and Control Conference*, 2017.

[94] M. M. Polycarpou and P. A. Ioannou, "A robust adaptive nonlinear control design," in *American Control Conference*, pp. 1365–1369, 1993.

[95] J. P. Hespanha, *Linear systems theory*. Princeton university press, 2009.

[96] S. A. Campbell, S. Crawford, and K. Morris, "Friction and the inverted pendulum stabilization problem," *Journal of Dynamic Systems, Measurement, and Control*, vol. 130, no. 5, p. 054502, 2008.

[97] R. Siegwart, I. R. Nourbakhsh, and D. Scaramuzza, *Introduction to autonomous mobile robots*. MIT press, 2011.

[98] D. McLean, *Automatic flight control systems*, vol. 16. Prentice Hall New York, 1990.

[99] G. Cybenko, "Approximation by superpositions of a sigmoidal function," *Mathematics of control, signals and systems*, vol. 2, no. 4, pp. 303–314, 1989.

[100] B. L. Stevens, F. L. Lewis, and E. N. Johnson, *Aircraft Control and Simulation: Dynamics, Controls Design, and Autonomous Systems*. John Wiley & Sons, 2015.

[101] E. Arabi, B. C. Gruenwald, T. Yucelen, and J. E. Steck, "Guaranteed model reference adaptive control performance in the presence of actuator failures," in *AIAA Guidance, Navigation, and Control Conference*, 2017.

[102] E. Arabi, T. Yucelen, B. C. Gruenwald, M. L. Fravolini, S. Balakrishnan, and N. T. Nguyen, "A neuroadaptive architecture for model reference control of uncertain dynamical systems with performance guarantees," *Systems & Control Letters*, (submitted).

[103] B. C. Gruenwald, E. Arabi, T. Yucelen, A. Chakravarthy, D. McNeely, and S. N. Balakrishnan, "Decentralized adaptive stabilization of large-scale active-passive modular systems," in *AIAA Guidance, Navigation, and Control Conference*, 2017.

[104] B. C. Gruenwald, E. Arabi, T. Yucelen, A. Chakravarthy, and D. McNeely, "A decentralized adaptive control architecture for large-scale active-passive modular systems," in *American Control Conference*, 2017.

[105] E. Arabi, T. Yucelen, and N. T. Nguyen, "Set-theoretic model reference adaptive control of a generic transport model," in *AIAA Guidance, Navigation, and Control Conference*, 2018.

[106] E. Arabi, S. B. Sarsilmaz, T. Yucelen, M. Maadani, E. A. Butcher, and M. Nazari, "Adaptive control of a rigid body vehicle on exponential coordinates with guaranteed performance," in *AIAA Guidance, Navigation, and Control Conference*, 2018.

[107] K. P. Tee, B. Ren, and S. S. Ge, "Control of nonlinear systems with time-varying output constraints," *Automatica*, vol. 47, no. 11, pp. 2511–2516, 2011.

[108] E. Arabi and T. Yucelen, "A generalization to set-theoretic model reference adaptive control architecture for enforcing user-defined time-varying performance bounds," in *American Control Conference*, pp. 5077–5082, 2017.

[109] W. M. Haddad and V. Chellaboina, *Nonlinear dynamical systems and control: A Lyapunov-based approach*. Princeton, NJ: Princeton University Press, 2008.

[110] M. L. Fravolini, E. Arabi, and T. Yucelen, "A model reference adaptive control approach for uncertain dynamical systems with strict component-wise performance guarantees," in *AIAA Guidance, Navigation, and Control Conference*, p. 1572, 2018.

[111] T. Yucelen, E. Arabi, and S. Balakrishnan, "A structural condition for model reference adaptive control systems to enforce partial performance constraints," in *AIAA Guidance, Navigation, and Control Conference*, 2018.

[112] E. Arabi, T. Yucelen, and S. Balakrishnan, "A set-theoretic model reference adaptive control architecture with partially adjustable strict performance guarantees: A command governor approach," *American Control Conference*, 2018.

[113] V. Stepanyan and K. Krishnakumar, "MRAC revisited: Guaranteed performance with reference model modification," *American Control Conference*, pp. 93–98, 2010.

[114] E. Lavretsky, "Reference dynamics modification in adaptive controllers for improved transient performance," *AIAA Guidance, Navigation, and Control Conference*, pp. 1–13, 2011.

[115] N. Harl, K. Rajagopal, and S. Balakrishnan, "Modified state observer for orbit uncertainty estimation," *AIAA Guidance, Navigation, and Control Conference*, 2011.

[116] T. E. Gibson, A. M. Annaswamy, and E. Lavretsky, "Adaptive systems with closed-loop reference models: Stability, robustness and transient performance," *arXiv preprint arXiv:1201.4897*, 2012.

[117] E. Arabi, T. Yucelen, and B. C. Gruenwald, "Model reference adaptive control for uncertain dynamical systems with unmatched disturbances: A command governor-based approach," in *Robotics and Mechatronics for Agriculture*, pp. 193–202, CRC Press, 2017.

[118] V. Chellaboina, W. M. Haddad, D. S. Bernstein, and D. A. Wilson, "Induced convolution operator norms of linear dynamical systems," *Mathematics of Control, Signals and Systems*, pp. 216–239, 2000.

[119] E. Arabi and T. Yucelen, "On set-theoretic model reference adaptive control of uncertain dynamical systems subject to actuator dynamics," in *2018 AIAA Guidance, Navigation, and Control Conference*, p. 1573, 2018.

[120] S. Bhattacharyya, H. Chapellat, and L. Keel, "Robust control: The parametric approach," *Upper Saddle River*, 1995.

[121] K. Zhou, J. C. Doyle, K. Glover, *et al.*, *Robust and optimal control*, vol. 40. Prentice Hall New Jersey, 1996.

[122] K. Zhou and J. C. Doyle, *Essentials of robust control*, vol. 180. Upper Saddle River, NJ: Prentice Hall, 1998.

[123] J. Ackermann, *Robust control: Systems with uncertain physical parameters*. Springer Science & Business Media, 2012.

[124] T. Yucelen and W. M. Haddad, "Output feedback adaptive stabilization and command following for minimum phase dynamical systems with unmatched uncertainties and disturbances," *International Journal of Control*, vol. 85, no. 6, pp. 706–721, 2012.

[125] K. J. Åström and B. Wittenmark, *Adaptive control*. Mineola, NY: Courier Corporation, 2013.

[126] H. P. Whitaker, J. Yamron, and A. Kezer, *Design of Model Reference Control Systems for Aircraft*. Cambridge, MA: Instrumentation Laboratory, Massachusetts Institute of Technology, 1958.

[127] P. V. Osburn, H. P. Whitaker, and A. Kezer, "New developments in the design of adaptive control systems," *Institute of Aeronautical Sciences*, 1961.

[128] T. Yucelen and E. Johnson, "A new command governor architecture for transient response shaping," *International Journal of Adaptive Control and Signal Processing*, vol. 27, no. 12, pp. 1065–1085, 2013.

[129] J. A. Muse, *An $\mathcal{H}_\infty$ norm minimization approach for adaptive control*. PhD thesis, Georgia Institute of Technology, 2010.

[130] N. Hovakimyan and C. Cao, *$\mathcal{L}_1$ adaptive control theory: Guaranteed robustness with fast adaptation*, vol. 21. Philadelphia, PA: SIAM, 2010.

[131] J. D. Boskovic, S.-H. Yu, and R. K. Mehra, "A stable scheme for automatic control reconfiguration in the presence of actuator failures," in *American Control Conference*, 1998.

[132] G. Tao, S. Chen, X. Tang, and S. M. Joshi, *Adaptive control of systems with actuator failures*. Springer Science & Business Media, 2013.

[133] N. T. Nguyen, K. S. Krishnakumar, J. T. Kaneshige, and P. P. Nespeca, "Flight dynamics and hybrid adaptive control of damaged aircraft," *AIAA Journal of guidance, control, and dynamics*, vol. 31, no. 3, pp. 751–764, 2008.

[134] K. Narendra and B. Peterson, "Bounded error adaptive control," in *Decision and Control including the Symposium on Adaptive Processes, 1980 19th IEEE Conference on*, vol. 19, pp. 605–610, 1980.

[135] J.-J. Slotine and J. Coetsee, "Adaptive sliding controller synthesis for non-linear systems," *International Journal of Control*, vol. 43, no. 6, pp. 1631–1651, 1986.

[136] H. K. Khalil, *Nonlinear Systems*. New Jersey, Prentice Hall, 2002.

[137] E. Arabi and T. Yucelen, "Experimental results with the set-theoretic model reference adaptive control architecture on an aerospace testbed," in *AIAA Guidance, Navigation, and Control Conference*, 2019.

[138] T. Yucelen, Y. Yildiz, R. Sipahi, E. Yousefi, and N. Nguyen, "Stability limit of human-in-the-loop model reference adaptive control architectures," *International Journal of Control*, pp. 1–18, 2017.

[139] D. P. Wiese, *Systematic adaptive control design using sequential loop closure*. PhD thesis, Massachusetts Institute of Technology, 2016.

[140] D. P. Wiese, A. M. Annaswamy, J. A. Muse, M. A. Bolender, and E. Lavretsky, "Sequential loop closure based adaptive autopilot design for a hypersonic vehicle," in *AIAA Guidance, Navigation, and Control Conference*, p. 1379, 2016.

[141] D. T. McRuer and E. S. Krendel, "Mathematical models of human pilot behavior," tech. rep., Advisory Group for Aerospace Research and Development, Paris, France, 1974.

[142] M. Green, "'How Long Does It Take to Stop?' methodological analysis of driver perception-brake times," *Transportation Human Factors*, vol. 2, pp. 195–216, 2000.

[143] D. Helbing, "Traffic and related self-driven many-particle systems," *Reviews of Modern Physics*, vol. 73, pp. 1067–1141, 2001.

[144] M. Treiber, A. Kesting, and D. Helbing, "Delays, inaccuracies and anticipation in microscopic traffic models," *Physica A*, vol. 360, no. 1, pp. 71–88, 2006.

[145] G. Stépán, *Delay effects in brain dynamics*, vol. 367. Philosophical Transactions of The Royal Society A - Mathematical Physical & Engineering Sciences, 2009.

[146] D. Schmidt and B. Bacon, "An optimal control approach to pilot/vehicle analysis and the neal-smith criteria," *Journal of Guidance Control Dynamics*, vol. 6, pp. 339–347, 1983.

[147] A. J. Thurling, "Improving uav handling qualities using time delay compensation," tech. rep., Air Force Inst of Tech Wright-Patterson AFB, 2000.

[148] S. Ryu and D. Andrisani, "Longitudinal flying qualities prediction for nonlinear aircraft," *Journal of Guidance Control and Dynamics*, vol. 26, no. 3, pp. 474–482, 2003.

[149] J. B. Witte, "An investigation relating longitudinal pilot-induced oscillation tendency rating to describing function predictions for rate-limited actuators," tech. rep., Air Force Inst of Tech Wright-Patterson AFB, 2004.

[150] C. J. Miller, "Nonlinear dynamic inversion baseline control law: architecture and performance predictions," in *AIAA Guidance, Navigation, and Control Conference*, p. 6467, 2011.

[151] R. E. Bellman and K. L. Cooke, *Differential-Difference Equations*. Academic Press, 1963.

[152] G. Stépán and T. Insperger, *Semi-Discretization for Time-Delay Systems: Stability and Engineering Applications*. Springer, 2011.

[153] J. K. Hale and S. M. V. Lunel, *Introduction to Functional Differential Equations*. Springer-Verlag, 1993.

[154] R. Datko, "A procedure for determination of the exponential stability of certain differential-difference equations," *Quarterly Applied Mathematics*, vol. 36, pp. 279–292, 1978.

[155] J. Neimark, "D-subdivisions and spaces of quasi-polynomials," *Prikl. Mat Meh.*, vol. 13, pp. 349–380, 1949.

[156] L. E. El'sgol'ts and S. B. Norkin, *Introduction to the Theory and Applications of Differential Equations with Deviating Arguments*. Academic Press, 1973.

[157] R. Sipahi, S.-I. Niculescu, C. T. Abdallah, W. Michiels, and K. Gu, "Stability and stabilization of systems with time delay, limitations and opportunities," *IEEE Control Systems Magazine*, pp. 38–65, 2011.

[158] J. Louisell, "A matrix method for determining the imaginary axis eigenvalues of a delay system," *IEEE Transactions on Automatic Control*, vol. 46, pp. 2008–2012, 2001.

[159] D. Breda, S. Maset, and R. Vermiglio, *Stability of Linear Delay Differential Equations: A Numerical Approach with MATLAB*. SpringerBriefs in Control Automation and Robotics, 2015.

[160] K. Gu, J. Chen, and V. L. Kharitonov, *Stability of time-delay systems*. Springer Science & Business Media, 2003.

[161] R. F. Stengel, *Flight dynamics*. Princeton University Press, 2004.

[162] R. Olfati-Saber, A. Fax, and R. M. Murray, "Consensus and cooperation in networked multi-agent systems," *IEEE Transactions on Automatic Control*, vol. 95, no. 1, pp. 215–233, 2007.

[163] W. Ren, R. W. Beard, and E. M. Atkins, "Information consensus in multivehicle cooperative control," *IEEE Control Systems*, vol. 27, no. 2, pp. 71–82, 2007.

[164] M. Ji, G. Ferrari-Trecate, M. Egerstedt, and A. Buffa, "Containment control in mobile networks," *IEEE Transactions on Automatic Control*, vol. 53, no. 8, pp. 1972–1975, 2008.

[165] Q. Hui and W. M. Haddad, "Distributed nonlinear control algorithms for network consensus," *Automatica*, vol. 44, no. 9, pp. 2375–2381, 2008.

[166] G. Antonelli, "Interconnected dynamic systems: An overview on distributed control," *IEEE Control Systems*, vol. 33, no. 1, pp. 76–88, 2013.

[167] Y. Cao, W. Yu, W. Ren, and G. Chen, "An overview of recent progress in the study of distributed multi-agent coordination," *IEEE Transactions on Industrial informatics*, vol. 9, no. 1, pp. 427–438, 2013.

[168] Q. Hui, W. M. Haddad, and S. P. Bhat, "Finite-time semistability and consensus for nonlinear dynamical networks," *IEEE Transactions on Automatic Control*, vol. 53, no. 8, pp. 1887–1900, 2008.

[169] Y. Cao, W. Ren, and Z. Meng, "Decentralized finite-time sliding mode estimators and their applications in decentralized finite-time formation tracking," *Systems & Control Letters*, vol. 59, no. 9, pp. 522–529, 2010.

[170] Y. Zhao, Z. Duan, G. Wen, and Y. Zhang, "Distributed finite-time tracking control for multi-agent systems: An observer-based approach," *Systems & Control Letters*, vol. 62, no. 1, pp. 22–28, 2013.

[171] E. Arabi, T. Yucelen, and J. R. Singler, "Further results on finite-time distributed control of multiagent systems with time transformation," in *ASME Dynamic Systems and Control Conference*, 2018.

[172] J. Wen, C. Wang, W. Luo, and G. Xie, "Finite-time consensus of networked multiagent systems with time-varying linear control protocols," *Mathematical Problems in Engineering*, 2016.

[173] H. Wang, C. Wang, and G. Xie, "Finite-time containment control of multi-agent systems with static or dynamic leaders," *Neurocomputing*, vol. 226, pp. 1–6, 2017.

[174] C. Yong, X. Guangming, and L. Huiyang, "Reaching consensus at a preset time: Double-integrator dynamics case," in *Chinese Control Conference*, pp. 6309–6314, 2012.

[175] E. A. Coddington and N. Levinson, *Theory of ordinary differential equations*. McGraw-Hill Education, 1955.

[176] M. Mesbahi and M. Egerstedt, *Graph Theoretic Methods in Multiagent Networks*. Princeton University Press, 2010.

[177] C. Godsil and G. F. Royle, *Algebraic Graph Theory*. Springer, 2013.

[178] F. L. Lewis, H. Zhang, K. Hengster-Movric, and A. Das, *Cooperative control of multi-agent systems: optimal and adaptive design approaches*. Springer Science & Business Media, 2013.

[179] P. Benner, R. Findeisen, D. Flockerzi, U. Reichl, K. Sundmacher, and P. Benner, *Large-scale networks in engineering and life sciences*. Springer, 2014.

[180] E. Arabi, T. Yucelen, and W. M. Haddad, "Mitigating the effects of sensor uncertainties in networked multi-agent systems," *Journal of Dynamic Systems, Measurement, and Control*, vol. 139, no. 4, 2017.

[181] J. S. Shamma, *Cooperative Control of Distributed Multi-Agent Systems*. Wiley Online Library, 2007.

[182] W. Ren and Y. Cao, *Distributed Coordination of Multi-Agent Networks: Emergent Problems, Models, and Issues*. Springer Science & Business Media, 2010.

[183] Z.-G. Hou, L. Cheng, and M. Tan, "Decentralized robust adaptive control for the multiagent system consensus problem using neural networks," *IEEE Transactions on Systems, Man, and Cybernetics, Part B: Cybernetics*, vol. 39, no. 3, pp. 636–647, 2009.

[184] A. Das and F. L. Lewis, "Distributed adaptive control for synchronization of unknown nonlinear networked systems," *Automatica*, vol. 46, no. 12, pp. 2014–2021, 2010.

[185] T. Yucelen and M. Egerstedt, "Control of multiagent systems under persistent disturbances," in *Proc. American Control Conference*, pp. 5264–5269, 2012.

[186] H. L. Trentelman, K. Takaba, and N. Monshizadeh, "Robust synchronization of uncertain linear multi-agent systems," *IEEE Transactions on Automatic Control*, vol. 58, no. 6, pp. 1511–1523, 2013.

[187] T. Yucelen and E. N. Johnson, "Control of multivehicle systems in the presence of uncertain dynamics," *International Journal of Control*, vol. 86, no. 9, pp. 1540–1553, 2013.

[188] M.-A. Massoumnia, G. C. Verghese, and A. S. Willsky, "Failure detection and identification," *IEEE Transactions on Automatic Control*, vol. 34, no. 3, pp. 316–321, 1989.

[189] M. Blanke and J. Schröder, *Diagnosis and Fault-Tolerant Control*. Springer, 2006.

[190] F. Pasqualetti, F. Dorfler, and F. Bullo, "Attack detection and identification in cyber-physical systems," *IEEE Transactions on Automatic Control*, vol. 58, no. 11, pp. 2715–2729, 2013.

[191] H. Fawzi, P. Tabuada, and S. Diggavi, "Secure estimation and control for cyber-physical systems under adversarial attacks," *IEEE Transactions on Automatic Control*, vol. 59, no. 6, pp. 1454–1467, 2014.

[192] T. Sadikhov, W. M. Haddad, R. Goebel, and M. Egerstedt, "Set-valued protocols for almost consensus of multiagent systems with uncertain interagent communication," in *Proc. American Control Conference*, pp. 4002–4007, 2014.

[193] E. Arabi, T. Yucelen, and W. M. Haddad, "Mitigating the effects of sensor uncertainties in networked multiagent systems," *American Control Conference*, pp. 5545–5550, 2016.

[194] J. A. Fax and R. M. Murray, "Information flow and cooperative control of vehicle formations," *IEEE Transactions on Automatic Control*, vol. 49, no. 9, pp. 1465–1476, 2004.

[195] C.-Q. Ma and J.-F. Zhang, "Necessary and sufficient conditions for consensusability of linear multi-agent systems," *IEEE Transactions on Automatic Control*, vol. 55, no. 5, pp. 1263–1268, 2010.

[196] Z. Li, X. Liu, P. Lin, and W. Ren, "Consensus of linear multi-agent systems with reduced-order observer-based protocols," *Systems & Control Letters*, vol. 60, no. 7, pp. 510–516, 2011.

[197] S. P. Boyd, L. El Ghaoui, E. Feron, and V. Balakrishnan, *Linear Matrix Inequalities in System and Control Theory*. SIAM, 1994.

[198] G. D. L. Torre and T. Yucelen, "Adaptive architectures for resilient control of networked multiagent systems in the presence of misbehaving agents," *International Journal of Control*, vol. 91, no. 3, pp. 495–507, 2018.

[199] M. M. Zavlanos, A. Jadbabaie, and G. J. Pappas, "Flocking while preserving network connectivity," in *Decision and Control, 2007 46th IEEE Conference on*, pp. 2919–2924, IEEE, 2007.

[200] D. V. Dimarogonas and K. J. Kyriakopoulos, "Connectivity preserving distributed swarm aggregation for multiple kinematic agents," in *Decision and Control, 2007 46th IEEE Conference on*, pp. 2913–2918, IEEE, 2007.

[201] J. Stewart, *Calculus*. Cengage Learning, 8 ed., 2015.

APPENDIX A: PROOF OF THEOREM 3.5.1

To show boundedness of the closed-loop dynamical system given by (3.14), (3.15), and (3.16), consider the energy function $V : \mathcal{D}_\varepsilon \times \mathbb{R}^{(n+n_c+s)\times m} \times \mathbb{R} \to \overline{\mathbb{R}}_+$ given by

$$V(e,\tilde{W},\tilde{q}) = \phi(\|e\|_P) + \gamma_1^{-1}\mathrm{tr}(\tilde{W}\Lambda^{1/2})^{\mathrm{T}}(\tilde{W}\Lambda^{1/2}) + \gamma_2^{-1}\tilde{q}^2\lambda_{\min}(\Lambda), \tag{A.1}$$

where $\mathcal{D}_\varepsilon \triangleq \{e(t) : \|e(t)\|_P < \varepsilon\}$ is chosen as described in Remark 3.3.1, and $P \in \mathbb{R}_+^{n\times n}$ is a solution of the Lyapunov equation in (3.11) with $R \in \mathbb{R}_+^{n\times n}$. Note that $V(0,0,0) = 0$ and $V\left(e,\tilde{W},\tilde{q}\right) > 0$ for all $\left(e,\tilde{W},\tilde{q}\right) \neq (0,0,0)$. Specifically, the time derivative of (A.1) along the closed-loop system trajectories (3.14), (3.15) and (3.16) is given by

$$\begin{aligned}
&\dot{V}\ \left(e(t),\tilde{W}(t),\tilde{q}(t)\right)\\
&= 2\phi_d(\|e(t)\|_P)e^{\mathrm{T}}(t)P\dot{e}(t) + 2\gamma_1^{-1}\mathrm{tr}\tilde{W}^{\mathrm{T}}(t)\Big(\gamma_1\mathrm{Proj}_{\mathrm{m}}\Big(\hat{W}(t),\phi_d(\|e(t)\|_P)\sigma\big(x(t)\big)e^{\mathrm{T}}(t)PB\Big) - \dot{W}(t)\Big)\Lambda\\
&\quad +2\gamma_2^{-1}\tilde{q}(t)\dot{\tilde{q}}(t)\lambda_{\min}(\Lambda)\\
&= 2\phi_d(\|e(t)\|_P)e^{\mathrm{T}}(t)PA_{\mathrm{r}}e(t) - 2\phi_d(\|e(t)\|_P)e^{\mathrm{T}}(t)PB\Lambda\tilde{W}^{\mathrm{T}}(t)\sigma\big(x(t)\big)\\
&\quad +2\mathrm{tr}\tilde{W}^{\mathrm{T}}(t)\mathrm{Proj}_{\mathrm{m}}\Big(\hat{W}(t),\phi_d(\|e(t)\|_P)\sigma\big(x(t)\big)e^{\mathrm{T}}(t)PB\Big)\Lambda - 2\gamma_1^{-1}\mathrm{tr}\tilde{W}^{\mathrm{T}}(t)\dot{W}(t)\Lambda + 2\gamma_2^{-1}\tilde{q}(t)\dot{\tilde{q}}(t)\lambda_{\min}(\Lambda)\\
&\quad +2\phi_d(\|e(t)\|_P)e^{\mathrm{T}}(t)PB\Lambda big(\varepsilon_N(x(t)) - v(t)\big)\\
&= 2\phi_d(\|e(t)\|_P)e^{\mathrm{T}}(t)PA_{\mathrm{r}}e(t) - 2\mathrm{tr}\big(\hat{W}^{\mathrm{T}}(t) - W^{\mathrm{T}}(t)\big)\big(\phi_d(\|e(t)\|_P)\sigma\big(x(t)\big)e^{\mathrm{T}}(t)PB\\
&\quad -\mathrm{Proj}_{\mathrm{m}}\big(\hat{W}(t),\phi_d(\|e(t)\|_P)\sigma\big(x(t)\big)e^{\mathrm{T}}(t)PB\big)\big)\Lambda - 2\gamma_1^{-1}\mathrm{tr}\tilde{W}^{\mathrm{T}}(t)\dot{W}(t)\Lambda\\
&\quad +2\gamma_2^{-1}\tilde{q}(t)\dot{\tilde{q}}(t)\lambda_{\min}(\Lambda) + 2\phi_d(\|e(t)\|_P)e^{\mathrm{T}}(t)PB\Lambda\big(\varepsilon_N(x(t)) - v(t)\big)\\
&\leq -\phi_d(\|e(t)\|_P)e^{\mathrm{T}}(t)Re(t) + d + 2\phi_d(\|e(t)\|_P)e^{\mathrm{T}}(t)PB\Lambda\big(\varepsilon_N(x(t)) - v(t)\big) + 2\gamma_2^{-1}\tilde{q}(t)\dot{\tilde{q}}(t)\lambda_{\min}(\Lambda)\\
&\leq -\phi_d(\|e(t)\|_P)e^{\mathrm{T}}(t)Re(t) + d + 2\phi_d(\|e(t)\|_P)e^{\mathrm{T}}(t)PB\Lambda\varepsilon_N(x(t))\\
&\quad -2\phi_d(\|e(t)\|_P)e^{\mathrm{T}}(t)PB\Lambda v(t) + 2\gamma_2^{-1}\tilde{q}(t)\dot{\tilde{q}}(t)\lambda_{\min}(\Lambda),
\end{aligned} \tag{A.2}$$

where $d \triangleq 2\gamma_1^{-1}\tilde{w}\,\dot{w}\|\Lambda\|_2$ and $\tilde{w} = \hat{W}_{\max} + w$.

Using $v(t)$ from (3.12) and $\lambda_{\min}(\Psi)x^{\mathrm{T}}\tanh(x) \leq x^{\mathrm{T}}\Psi\tanh(x) \leq \lambda_{\max}(\Psi)x^{\mathrm{T}}\cdot\tanh(x)$ for any diagonal matrix $\Psi \in \mathbb{D}^{m\times m}$ and any vector $x \in \mathbb{R}^m$ yields

$$\begin{aligned}\dot{V}\left(e(t),\tilde{W}(t),\tilde{q}(t)\right) \leq\ & -\phi_d(\|e(t)\|_P)e^{\mathrm{T}}(t)Re(t)+d+2\phi_d(\|e(t)\|_P)\|e^{\mathrm{T}}(t)PB\|_2 \\ & \cdot\lambda_{\max}(\Lambda)\varepsilon^* - 2\phi_d(\|e(t)\|_P)e^{\mathrm{T}}(t)PB\tanh\left(\phi_d(\|e(t)\|_P)\right. \\ & \left.\cdot B^{\mathrm{T}}Pe(t)\right)\lambda_{\min}(\Lambda)\hat{q}(t)+2\gamma_2^{-1}\tilde{q}(t)\dot{\tilde{q}}(t)\lambda_{\min}(\Lambda). \end{aligned} \tag{A.3}$$

From the property given in Remark 3.2.2 with $\eta = \phi_d(\|e(t)\|_P)B^{\mathrm{T}}Pe(t)$, (A.3) can be further written as

$$\begin{aligned}&\dot{V}\ \left(e(t),\tilde{W}(t),\tilde{q}(t)\right) \\ &\leq\ -\phi_d(\|e(t)\|_P)e^{\mathrm{T}}(t)Re(t)+d+2\Big(\mathcal{L}+\phi_d(\|e(t)\|_P)e^{\mathrm{T}}(t)PB\tanh\left(\phi_d(\|e(t)\|_P)\right. \\ &\quad \left.\cdot B^{\mathrm{T}}Pe(t)\right)\Big)\lambda_{\max}(\Lambda)\varepsilon^* - 2\phi_d(\|e(t)\|_P)e^{\mathrm{T}}(t)PB\tanh\left(\phi_d(\|e(t)\|_P)B^{\mathrm{T}}Pe(t)\right) \\ &\quad \cdot\lambda_{\min}(\Lambda)\hat{q}(t)+2\gamma_2^{-1}\tilde{q}(t)\dot{\tilde{q}}(t)\lambda_{\min}(\Lambda) \\ &\leq\ -\phi_d(\|e(t)\|_P)e^{\mathrm{T}}(t)Re(t)+d+2\mathcal{L}\lambda_{\max}(\Lambda)\varepsilon^* - 2\phi_d(\|e(t)\|_P)e^{\mathrm{T}}(t)PB \\ &\quad \cdot\tanh\left(\phi_d(\|e(t)\|_P)B^{\mathrm{T}}Pe(t)\right)\tilde{q}(t)\lambda_{\min}(\Lambda)+2\gamma_2^{-1}\tilde{q}(t)\dot{\tilde{q}}(t)\lambda_{\min}(\Lambda) \\ &\leq\ -\phi_d(\|e(t)\|_P)e^{\mathrm{T}}(t)Re(t)+d_2+2\left(\hat{q}(t)-q\right)\left(\mathrm{Proj}\left(\hat{q}(t),\phi_d(\|e(t)\|_P)e^{\mathrm{T}}(t)PB\right.\right. \\ &\quad \cdot\tanh\left(\phi_d(\|e(t)\|_P)B^{\mathrm{T}}Pe(t)\right)-\xi\hat{q}(t)\Big)-\phi_d(\|e(t)\|_P)e^{\mathrm{T}}(t)PB \\ &\quad \cdot\tanh\left(\phi_d(\|e(t)\|_P)B^{\mathrm{T}}Pe(t)\right)+\xi\hat{q}(t)\Big)\lambda_{\min}(\Lambda)-2\xi\hat{q}(t)\tilde{q}(t)\lambda_{\min}(\Lambda) \\ &\leq\ -\phi_d(\|e(t)\|_P)e^{\mathrm{T}}(t)Re(t)+d_2-2\xi\left(\tilde{q}(t)+q\right)\tilde{q}(t)\lambda_{\min}(\Lambda) \\ &\leq\ -\phi_d(\|e(t)\|_P)e^{\mathrm{T}}(t)Re(t)+d_2-2\xi\tilde{q}^2(t)\lambda_{\min}(\Lambda)-2\xi q\tilde{q}(t)\lambda_{\min}(\Lambda) \\ &\leq\ -\phi_d(\|e(t)\|_P)e^{\mathrm{T}}(t)Re(t)+d_2-2\xi\tilde{q}^2(t)\lambda_{\min}(\Lambda)+\xi(q^2+\tilde{q}^2(t))\lambda_{\min}(\Lambda) \\ &\leq\ -\phi_d(\|e(t)\|_P)e^{\mathrm{T}}(t)Re(t)+d_3, \end{aligned} \tag{A.4}$$

where $d_2 \triangleq d+2\mathcal{L}\lambda_{\max}(\Lambda)\varepsilon^*$ and $d_3 \triangleq d_2+\xi q^2\lambda_{\min}(\Lambda)$.

Next, we rewrite (A.4) as

$$\begin{aligned}&\dot{V}\ \left(e(t),\tilde{W}(t),\tilde{q}(t)\right) \\ &\leq\ -\alpha\phi_d(\|e(t)\|_P)e^{\mathrm{T}}(t)Pe(t)+d_3+\frac{1}{2}\alpha\phi(\|e(t)\|_P)-\frac{1}{2}\alpha\phi(\|e(t)\|_P)\end{aligned}$$

$$\leq -\frac{1}{2}\alpha V(e,\tilde{W},\tilde{q}) - \alpha\left[\phi_d(\|e(t)\|_P)e^{\mathrm{T}}(t)Pe(t) - \frac{1}{2}\phi(\|e(t)\|_P)\right] + \mu, \tag{A.5}$$

and it now follows from *vi)* in Definition 3.2.2 that $\dot{V}\big(e(t),\tilde{W}(t),\tilde{q}(t)\big) \leq -\frac{1}{2}\alpha V(e(t),\tilde{W}(t),\tilde{q}(t)) + \mu$, where $\alpha \triangleq \frac{\lambda_{\min}(R)}{\lambda_{\max}(P)}$ and $\mu \triangleq \frac{1}{2}\alpha\big(\gamma_1^{-1}\tilde{w}^2\|\Lambda\|_2 + \gamma_2^{-1}(\hat{q}_{\max}^2 + q^2)\lambda_{\min}(\Lambda)\big) + d_3$. The boundedness of the closed-loop dynamical system given by (3.14), (3.15) and (3.16) as well as the strict performance bound on the system error given by (3.17) is now immediate by applying Lemma 1 of [25] and [23]. ■

APPENDIX B: PROOF OF COROLLARY 3.5.1

From the proof of Theorem 3.5.1, it follows that $V(e,\tilde{W},\tilde{q})$ is upper bounded by $V_{\max} = \max\{V_0, \frac{2\mu}{\alpha}\}$. Now, using (A.1), it follows that $\phi(\|e(t)\|_P) + \gamma_1^{-1}\mathrm{tr}(\tilde{W}(t)\ \Lambda^{1/2})^{\mathrm{T}}(\tilde{W}(t)\Lambda^{1/2}) + \gamma_2^{-1}\tilde{q}^2(t)\lambda_{\min}(\Lambda) \leq V_{\max}$, $t \geq 0$, and hence, $\phi(\|e(t)\|_P) \leq V_{\max}$, $t \geq 0$. Utilizing the structure of the candidate generalized restricted potential function given in the statement of this corollary, one can write $\|e(t)\|_P \in \{\|e(t)\|_P \in \mathbb{R} \ : \ 0 \leq \|e(t)\|_P \leq \bar{e}\}$, $t \geq 0$, and it can be readily shown that $\bar{e} < \varepsilon$, where $\bar{e} = (-V_{\max} + \sqrt{V_{\max}^2 + 4V_{\max}\ \varepsilon})/2$. Using the fact that $\phi_d(\|e(t)\|_P)$, $t \geq 0$, is a strictly increasing function, one can calculate its lower and upper bound as $\phi_d(0) \ \leq \ \phi_d(\|e(t)\|_P) \ \leq \ \phi_d(\bar{e})$, $t \geq 0$, which yields to the result. ■

APPENDIX C: PROOF OF COROLLARY 3.5.2

To show boundedness of the closed-loop dynamical system (3.14) and (3.15), consider the energy function $V : \mathcal{D}_\varepsilon \times \mathbb{R}^{(n+n_c+s)\times m} \to \overline{\mathbb{R}}_+$ given by

$$V(e,\tilde{W}) = \phi(\|e\|_P) + \gamma_1^{-1}\mathrm{tr}(\tilde{W}\Lambda^{1/2})^{\mathrm{T}}(\tilde{W}\Lambda^{1/2}). \tag{C.1}$$

Note that $V(0,0) = 0$ and $V\left(e,\tilde{W}\right) > 0$ for all $\left(e,\tilde{W}\right) \neq (0,0)$. The time derivative of (C.1) along the closed-loop system trajectories (3.14) and (3.15) is

$$\begin{aligned}
&\dot{V}\left(e(t),\tilde{W}(t)\right)\\
&= 2\phi_d(\|e(t)\|_P)e^{\mathrm{T}}(t)P\dot{e}(t) + 2\gamma_1^{-1}\mathrm{tr}\tilde{W}^{\mathrm{T}}(t)\Big(\gamma_1\mathrm{Proj}_{\mathrm{m}}\Big(\hat{W}(t),\phi_d(\|e(t)\|_P)\\
&\quad\cdot\sigma\big(x(t)\big)e^{\mathrm{T}}(t)PB\Big) - \dot{W}(t)\Big)\Lambda\\
&= 2\phi_d(\|e(t)\|_P)e^{\mathrm{T}}(t)PA_{\mathrm{r}}e(t) - 2\mathrm{tr}\big(\hat{W}^{\mathrm{T}}(t) - W^{\mathrm{T}}(t)\big)\big(\phi_d(\|e(t)\|_P)\sigma\big(x(t)\big)e^{\mathrm{T}}(t)\\
&\quad\cdot PB - \mathrm{Proj}_{\mathrm{m}}\big(\hat{W}(t),\phi_d(\|e(t)\|_P)\sigma\big(x(t)\big)e^{\mathrm{T}}(t)PB\big)\big)\Lambda - 2\gamma_1^{-1}\mathrm{tr}\tilde{W}^{\mathrm{T}}(t)\dot{W}(t)\Lambda\\
&\quad+2\phi_d(\|e(t)\|_P)e^{\mathrm{T}}(t)PB\Lambda\big(\varepsilon_N(x(t)) - v(t)\big)\\
&\leq -\phi_d(\|e\|_P)e^{\mathrm{T}}(t)Re(t) + d + 2\phi_d(\|e\|_P)e^{\mathrm{T}}(t)PB\Lambda\big(\varepsilon_N(x(t)) - v(t)\big),
\end{aligned} \tag{C.2}$$

where $d = 2\gamma_1^{-1}\tilde{w}\,\dot{w}\|\Lambda\|_2$ and $\tilde{w} = \hat{W}_{\max} + w$. Now, substituting $v(t)$ from (3.20) and using $\lambda_{\min}(\Psi)x^{\mathrm{T}}\tanh(x)$ $\leq x^{\mathrm{T}}\Psi\tanh(x) \leq \lambda_{\max}(\Psi)x^{\mathrm{T}}\tanh(x)$ for any diagonal matrix $\Psi \in \mathbb{D}^{m\times m}$ and any vector $x \in \mathbb{R}^m$, and the bounds given in (3.18) and (3.19), one can obtain

$$\begin{aligned}
\dot{V}\left(e(t),\tilde{W}(t)\right) \leq &-\phi_d(\|e(t)\|_P)e^{\mathrm{T}}(t)Re(t) + d + 2\phi_d(\|e(t)\|_P)\|e^{\mathrm{T}}(t)PB\|c_1c_3\\
&-2\phi_d(\|e(t)\|_P)e^{\mathrm{T}}(t)PB\tanh\left(\phi_d(\|e(t)\|_P)B^{\mathrm{T}}Pe(t)\right)c_1c_3.
\end{aligned} \tag{C.3}$$

Next, from the property stated in Remark 3.2.2 with $\eta = \phi_d(\|e(t)\|_P)B^{\mathrm{T}}Pe(t)$, one can write

$$\begin{aligned}\dot{V}\left(e(t),\tilde{W}(t)\right) &\leq -\phi_d(\|e(t)\|_P)e^{\mathrm{T}}(t)Re(t)+d+2\Big(\mathcal{L}+\phi_d(\|e(t)\|_P)e^{\mathrm{T}}(t)PB\tanh\left(\phi_d(\|e(t)\|_P)B^{\mathrm{T}}Pe(t)\right)\Big)c_1c_3\\ &\quad -2\phi_d(\|e(t)\|_P)e^{\mathrm{T}}(t)PB\tanh\left(\phi_d(\|e(t)\|_P)B^{\mathrm{T}}Pe(t)\right)c_1c_3\\ &\leq -\phi_d(\|e(t)\|_P)e^{\mathrm{T}}(t)Re(t)+d_c \end{aligned} \tag{C.4}$$

where $d_c \triangleq d+2\mathcal{L}c_1c_3$. Now, (C.4) can be rewritten as

$$\begin{aligned}\dot{V}\left(e(t),\tilde{W}(t)\right) &\leq -\alpha\phi_d(\|e(t)\|_P)e^{\mathrm{T}}(t)Pe(t)+d_c+\frac{1}{2}\alpha\phi(\|e(t)\|_P)-\frac{1}{2}\alpha\phi(\|e(t)\|_P)\\ &\leq -\frac{1}{2}\alpha V(e,\tilde{W})-\alpha\left[\phi_d(\|e\|_P)e^{\mathrm{T}}(t)Pe(t)-\frac{1}{2}\phi(\|e\|_P)\right]+\mu_c, \end{aligned} \tag{C.5}$$

and it follows from *vi)* in Definition 3.2.2 that $\dot{V}\left(e(t),\tilde{W}(t)\right)\leq -\frac{1}{2}\alpha V(e,\tilde{W})+\mu_c$, where $\alpha \triangleq \frac{\lambda_{\min}(R)}{\lambda_{\max}(P)}$ and $\mu_c \triangleq \frac{1}{2}\alpha\gamma_1^{-1}\tilde{w}^2\|\Lambda\|_2+d_c$. Similar to the proof of Theorem 3.5.1, the boundedness of the closed-loop dynamical system given by (3.14) and (3.15) as well as the strict performance bound on the system error given by (3.21) is now immediate by applying Lemma 1 of [25] and [23]. ■

APPENDIX D: OBTAINING (4.2) FROM (4.1)

This appendix summarizes details on how (4.2) is rewritten from (4.1). For this purpose, we first introduce a widely-adopted system uncertainty parameterization [28–30].

Assumption D.1 *The system uncertainty $\delta_{\rm p}(t,x_{\rm p}(t))$ appearing in the uncertain dynamical system given by* (4.1) *is parameterized as*

$$\delta_{\rm p}(t,x_{\rm p}) \quad = \quad W_{\rm p}^{\rm T}(t)\sigma_{\rm p}(x_{\rm p}), \tag{D.1}$$

where $W_{\rm p}(t) \in \mathbb{R}^{s\times m}$, $t \geq 0$, is a bounded unknown weight matrix (i.e., $\|W_{\rm p}(t)\|_{\rm F} \leq w_{\rm p}$, $t \geq 0$) with a bounded time rate of change (i.e., $\|\dot{W}_{\rm p}(t)\|_{\rm F} \leq \dot{w}_{\rm p}$, $t \geq 0$) and $\sigma_{\rm p} : \mathbb{R}^{n_{\rm p}} \to \mathbb{R}^s$ is a known basis function of the form $\sigma_{\rm p}(x_{\rm p}) = [\sigma_{\rm p1}(x_{\rm p}), \sigma_{\rm p2}(x_{\rm p}), \ldots, \sigma_{{\rm p}s}(x_{\rm p})]^{\rm T}$.

Remark D.1 *As it is often done in model reference adaptive control applications (see, for example, [1] and [32]), it is of practice to let the first element of the basis function be a constant (i.e., $\sigma_{\rm p1}(x_{\rm p}) = \eta$, $\eta \in \mathbb{R}$) in order to capture the effects of exogenous disturbances in the parameterization given by* (D.1)*. Thus, this parameterization is sufficient to capture not only system uncertainties but also exogenous disturbances.*

For addressing command following, we next let $c(t) \in \mathbb{R}^{n_{\rm c}}$, $t \geq 0$, be a given command and $x_{\rm c}(t) \in \mathbb{R}^{n_{\rm c}}$, $t \geq 0$, be the integrator state that satisfies

$$\dot{x}_{\rm c}(t) = E_{\rm p}x_{\rm p}(t) - c(t), \quad x_{\rm c}(0) = x_{\rm c0}, \quad t \geq 0. \tag{D.2}$$

In (D.2), $E_{\rm p} \in \mathbb{R}^{n_{\rm c}\times n_{\rm p}}$ allows the selection of a subset of $x_{\rm p}(t)$, $t \geq 0$, to follow $c(t)$, $t \geq 0$. Moreover, as standard, we assume that $c(t)$ is bounded and piecewise continuous. Now, denoting the augmented state vector as $x(t) \triangleq [x_{\rm p}^{\rm T}(t), x_{\rm c}^{\rm T}(t)]^{\rm T} \in \mathbb{R}^n$, $t \geq 0$, and defining

$$A \triangleq \begin{bmatrix} A_{\mathrm{p}} & 0_{n_{\mathrm{p}}\times n_{\mathrm{c}}} \\ E_{\mathrm{p}} & 0_{n_{\mathrm{c}}\times n_{\mathrm{c}}} \end{bmatrix} \in \mathbb{R}^{n\times n}, \tag{D.3}$$

$$B \triangleq \begin{bmatrix} B_{\mathrm{p}}^{\mathrm{T}} & 0_{n_{\mathrm{c}}\times m}^{\mathrm{T}} \end{bmatrix}^{\mathrm{T}} \in \mathbb{R}^{n\times m}, \tag{D.4}$$

$$B_{\mathrm{r}} \triangleq \begin{bmatrix} 0_{n_{\mathrm{p}}\times n_{\mathrm{c}}}^{\mathrm{T}} & -I_{n_{\mathrm{c}}\times n_{\mathrm{c}}} \end{bmatrix}^{\mathrm{T}} \in \mathbb{R}^{n\times n_{\mathrm{c}}}, \tag{D.5}$$

where $n = n_{\mathrm{p}} + n_{\mathrm{c}}$, it follows from (4.1) and (D.2) that

$$\dot{x}(t) = Ax(t) + B\Lambda u(t) + BW_{\mathrm{p}}^{\mathrm{T}}(t)\sigma_{\mathrm{p}}(x_{\mathrm{p}}(t)) + B_{\mathrm{r}}c(t), \quad x(0) = x_0, \quad t \geq 0. \tag{D.6}$$

For the augmented system dynamics given by (D.6), consider the feedback control law given by

$$u(t) = u_{\mathrm{n}}(t) + u_{\mathrm{a}}(t), \quad t \geq 0, \tag{D.7}$$

where $u_{\mathrm{n}}(t) \in \mathbb{R}^m$, $t \geq 0$, is the nominal control signal and $u_{\mathrm{a}}(t) \in \mathbb{R}^m$, $t \geq 0$, is the adaptive control signal.

Now, let the nominal control signal be given by

$$u_{\mathrm{n}}(t) = -Kx(t), \quad t \geq 0, \tag{D.8}$$

such that $A_{\mathrm{r}} \triangleq A - BK$, $K \in \mathbb{R}^{m\times n}$, is Hurwitz. As a consequence, for a given $R \in \mathbb{R}_+^{n\times n}$, there exists $P \in \mathbb{R}_+^{n\times n}$ that satisfies the Lyapunov equation given by

$$0 = A_{\mathrm{r}}^{\mathrm{T}}P + PA_{\mathrm{r}} + R. \tag{D.9}$$

Now using (D.7) and (D.8) in (D.6), one can readily write (4.2).

APPENDIX E: FURTHER REMARKS ON SECTIONS 4.1.3.1 AND 4.1.3.2

We note that Theorem 4.1.1 requires the additional assumption that $\lambda_{\min}(PB\Lambda B^{\mathrm{T}}P)$ is nonzero. However, for the case where $\lambda_{\min}(PB\Lambda B^{\mathrm{T}}P)$ is zero, one can readily show that if $\lambda_{\min}(R) - 2\overline{\varepsilon}\lambda_{\max}(P) > 0$ holds with $\overline{\varepsilon} \triangleq \max_{t\in\overline{\mathbb{R}}_+} \frac{\dot{\varepsilon}(t)}{\varepsilon(t)}$, then the result of Theorem 4.1.1 still holds and the user-defined time-varying system performance bound $\varepsilon(t)$ can be enforced on the system error trajectories (i.e., $\|e(t)\|_{\mathrm{P}} < \varepsilon(t)$). For the case where neither $\lambda_{\min}(PB\Lambda B^{\mathrm{T}}P) \neq 0$ nor $\lambda_{\min}(R) - 2\overline{\varepsilon}\lambda_{\max}(P) > 0$ holds, one can alternatively use Theorem 4.1.2 for enforcing a user-defined time-varying bound without any of the aforementioned assumptions.

APPENDIX F: NECESSARY DEFINITIONS

In this appendix, we state the necessary definitions used in this paper. We start with the definition of the projection operator. For this propose, let $\Omega = \left\{\theta \in \mathbb{R}^n : (\theta_i^{\min} \leq \theta_i \leq \theta_i^{\max})_{i=1,2,\cdots,n}\right\}$ be a convex hypercube in $\mathbb{R}^n$, where $(\theta_i^{\min}, \theta_i^{\max})$ represent the minimum and maximum bounds for the i^{th} component of the n-dimensional parameter vector θ. In addition, define a second hypercube by $\Omega_\nu = \{\theta \in \mathbb{R}^n : (\theta_i^{\min} + \nu \leq \theta_i \leq \theta_i^{\max} - \nu)_{i=1,2,\cdots,n}\}$, for a sufficiently small positive constant ν, such that $\Omega_\nu \subset \Omega$. The projection operator $\text{Proj} : \mathbb{R}^n \times \mathbb{R}^n \to \mathbb{R}^n$ is then componentwise defined by $\text{Proj}(\theta, y) \triangleq \big((\theta_i^{\max} - \theta_i)/\nu\big) y_i$ if $\theta_i > \theta_i^{\max} - \nu$ and $y_i > 0$; $\text{Proj}(\theta, y) \triangleq \big((\theta_i - \theta_i^{\min})/\nu\big) y_i$ if $\theta_i < \theta_i^{\min} + \nu$ and $y_i < 0$; and $\text{Proj}(\theta, y) = y_i$ otherwise; where $y \in \mathbb{R}^n$ [30]. Building on this definition, it follows that

$$(\theta - \theta^*)^{\mathrm{T}} (\text{Proj}\,(\theta, y) - y) \leq 0, \quad \theta^* \in \Omega_\nu, \tag{F.1}$$

holds [30, 80]. Note that the definition of the projection operator can also be extended to matrices as $\text{Proj}_{\text{m}}(\Theta, Y) = \big(\text{Proj}(\text{col}_1(\Theta), \text{col}_1(Y)), \ldots, \text{Proj}(\text{col}_m(\Theta), \text{col}_m(Y))\big)$, where $\Theta \in \mathbb{R}^{n \times m}$, $Y \in \mathbb{R}^{n \times m}$ and $\text{col}_i(\cdot)$ denotes ith column operator. Now, for a given matrix Θ^*, $\text{tr}\left[(\Theta - \Theta^*)^{\mathrm{T}} (\text{Proj}_{\text{m}}(\Theta, Y) - Y)\right] = \sum_{i=1}^{m} \Big[\text{col}_i(\Theta - \Theta^*)^{\mathrm{T}} (\text{Proj}(\text{col}_i(\Theta), \text{col}_i(Y)) - \text{col}_i(Y))\Big] \leq 0$ follows from (F.1).

Next, we state the definition of the generalized restricted potential functions. For a given $z \in \mathbb{R}^p$ and $H \in \mathbb{R}_+^{p \times p}$, let $\|z\|_H = \sqrt{z^{\mathrm{T}} H z}$ be a weighted Euclidean norm. We say $\phi(\|z\|_{\text{H}})$, $\phi : \mathbb{R} \to \mathbb{R}$, is a generalized restricted potential function (generalized barrier Lyapunov function) on the set $\mathcal{D}_\varepsilon \triangleq \left\{z : \|z\|_{\text{H}} \in [0, \varepsilon)\right\}$ with $\varepsilon \in \mathbb{R}_+$ being a user-defined parameter, if the following statements hold:

i) If $\|z\|_{\text{H}} = 0$, then $\phi(\|z\|_{\text{H}}) = 0$.

ii) If $z \in \mathcal{D}_\varepsilon$ and $\|z\|_{\text{H}} \neq 0$, then $\phi(\|z\|_{\text{H}}) > 0$.

iii) If $\|z\|_{\text{H}} \to \varepsilon$, then $\phi(\|z\|_{\text{H}}) \to \infty$.

iv) $\phi(\|z\|_{\text{H}})$ is continuously differentiable on $\mathcal{D}_\varepsilon$.

v) If $z \in \mathcal{D}_\varepsilon$, then $\phi_d(\|z\|_{\mathrm{H}}) > 0$, where

$$\phi_d(\|z\|_{\mathrm{H}}) \triangleq \frac{\mathrm{d}\phi(\|z\|_{\mathrm{H}})}{\mathrm{d}\|z\|_{\mathrm{H}}^2}. \tag{F.2}$$

vi) If $z \in \mathcal{D}_\varepsilon$, then

$$2\phi_d(\|z\|_{\mathrm{H}})\|z\|_{\mathrm{H}}^2 - \phi(\|z\|_{\mathrm{H}}) > 0. \tag{F.3}$$

As noted in [1], this definition generalizes the definition of the restricted potential functions (barrier Lyapunov functions) used by, for example, the authors of [21–26, 107].

APPENDIX G: MATHEMATICAL PRELIMINARIES

The notation used in this paper is fairly standard. Specifically, $\mathbb{R}$ denotes the set of real numbers, $\mathbb{R}^n$ denotes the set of $n \times 1$ real column vectors, $\mathbb{R}^{n\times m}$ denotes the set of $n \times m$ real matrices, $\mathbb{R}_+$ denotes the set of positive real numbers, $\mathbb{R}_+^{n\times n}$ (resp., $\overline{\mathbb{R}}_+^{n\times n}$) denotes the set of $n \times n$ positive-definite (resp., nonnegative-definite) real matrices, $\mathbb{Z}_+$ (resp., $\overline{\mathbb{Z}}_+$) denotes the set of positive (resp., nonnegative) integers, 0_n denotes the $n \times 1$ zero vector, $\mathbf{1}_n$ denotes the $n \times 1$ ones vector, $0_{n\times m}$ denotes the $n \times m$ zero matrix, and "$\triangleq$" denotes equality by definition. In addition, we write $(\cdot)^{\mathrm{T}}$ for the transpose operator, $(\cdot)^{-1}$ for the inverse operator, and $\det(\cdot)$ for the determinant operator, $\|\cdot\|_2$ for the Euclidean norm. Furthermore, we write $\lambda_{\min}(A)$ (resp., $\lambda_{\max}(A)$) for the minimum (resp., maximum) eigenvalue of the square matrix A, $\lambda_i(A)$ for the ith eigenvalue of the square matrix A (with eigenvalues ordered from minimum to maximum value), $[A]_{ij}$ for the (i,j)th entry of the matrix A, and $\underline{x}$ (resp., $\overline{x}$) for the lower bound (resp., upper bound) of a bounded signal $x(t) \in \mathbb{R}^n$, that is, $\underline{x} \leq \|x(t)\|_2$ (resp., $\|x(t)\|_2 \leq \overline{x}$).

Next, we recall some basic notions from graph theory, where we refer the reader to [176, 177] for further details. Specifically, graphs are broadly adopted in the multiagent systems literature to encode interactions between networked systems. An undirected graph $\mathfrak{G}$ is defined by a set $\mathcal{V}_{\mathfrak{G}} = \{1,\ldots,N\}$ of *nodes* and a set $\mathcal{E}_{\mathfrak{G}} \subset \mathcal{V}_{\mathfrak{G}} \times \mathcal{V}_{\mathfrak{G}}$ of *edges*. If $(i,j) \in \mathcal{E}_{\mathfrak{G}}$, then nodes i and j are neighbors and the neighboring relation is indicated by $i \sim j$. The *degree* of a node is given by the number of its neighbors. Letting d_i denote the degree of node i, then the *degree matrix* of a graph $\mathfrak{G}$, denoted by $\mathcal{D}(\mathfrak{G}) \in \mathbb{R}^{N\times N}$, is given by $\mathcal{D}(\mathfrak{G}) \triangleq \operatorname{diag}[d]$, where $d = [d_1,\ldots,d_N]^{\mathrm{T}}$. A *path* $i_0 i_1 \cdots i_L$ of a graph $\mathfrak{G}$ is a finite sequence of nodes such that $i_{k-1} \sim i_k$, $k = 1,\ldots,L$, and if every pair of distinct nodes has a path, then the graph $\mathfrak{G}$ is connected. We write $\mathcal{A}(\mathfrak{G}) \in \mathbb{R}^{N\times N}$ for the *adjacency matrix* of a graph $\mathfrak{G}$ defined by $[\mathcal{A}(\mathfrak{G})]_{ij} \triangleq 1$, if $(i,j) \in \mathcal{E}_{\mathfrak{G}}$, and $[\mathcal{A}(\mathfrak{G})]_{ij} \triangleq 0$, otherwise, and $\mathcal{B}(\mathfrak{G}) \in \mathbb{R}^{N\times M}$ for the (node-edge) *incidence matrix* of a graph $\mathfrak{G}$ defined by $[\mathcal{B}(\mathfrak{G})]_{ij} \triangleq 1$, if node i is the head of edge j, $[\mathcal{B}(\mathfrak{G})]_{ij} \triangleq -1$, if node i is the tail of edge j, and $[\mathcal{B}(\mathfrak{G})]_{ij} \triangleq 0$, otherwise, where M is the number of edges, i is an index for the node set, and j is an index for the edge set.

The *graph Laplacian matrix*, denoted by $\mathcal{L}(\mathfrak{G}) \in \overline{\mathbb{R}}_+^{N\times N}$, is defined by $\mathcal{L}(\mathfrak{G}) \triangleq \mathcal{D}(\mathfrak{G}) - \mathcal{A}(\mathfrak{G})$ or, equivalently, $\mathcal{L}(\mathfrak{G}) = \mathcal{B}(\mathfrak{G})\mathcal{B}(\mathfrak{G})^{\mathrm{T}}$, and the spectrum of the graph Laplacian of a connected, undirected graph $\mathfrak{G}$ can be ordered as $0 = \lambda_1(\mathcal{L}(\mathfrak{G})) < \lambda_2(\mathcal{L}(\mathfrak{G})) \leq \cdots \leq \lambda_N(\mathcal{L}(\mathfrak{G}))$, with 1_N being the eigenvector corresponding to the zero eigenvalue $\lambda_1(\mathcal{L}(\mathfrak{G}))$, and $\mathcal{L}(\mathfrak{G})1_N = 0_N$ and $e^{\mathcal{L}(\mathfrak{G})}1_N = 1_N$.

In this paper, we model a given multiagent system as a connected, undirected graph $\mathfrak{G}$, where nodes and edges respectively represent agents and inter-agent communication links. The following results are needed in this paper.

Remark G.1 *We use the notion from Section 1.1.1.4 of [179]. Specifically, let $\xi(t)$ denote a solution to the dynamical system*

$$\dot{x}(t) = f(t,x(t)), \quad x(0) = x_0. \tag{G.1}$$

In addition, let $t = \theta(s)$ denote a time transformation, where $\theta(s)$ is a strictly increasing and continuously differentiable function, and define $\psi(s) = \xi(t)$. Then,

$$\psi'(s) = \theta'(s)f(\theta(s),\psi(s)), \quad \psi(\theta^{-1}(0)) = x_0, \tag{G.2}$$

where $\psi'(s) \triangleq d\psi(s)/ds$, and $\theta'(s) \triangleq d\theta(s)/ds$.

Remark G.2 *For the sake of simplicity, considering the time transformation $t = \theta(s)$ and any signal $\eta(t)$, we write $\eta_s(s)$ to denote the transformed signal in the infinite interval s; that is $\eta_s(s) \triangleq \eta(\theta(s))$.*

Lemma G.1 (Lemma 3.3, [178]) *Let $K = diag(k), k = [k_1,k_2,\ldots,k_N]^{\mathrm{T}}$, $k_i \in \overline{\mathbb{Z}}_+, i = 1,\ldots,N$, and assume that at least one element of k is nonzero. Then, $\mathcal{F}(\mathfrak{G}) \triangleq \mathcal{L}(\mathfrak{G}) + K \in \mathbb{R}_+^{N\times N}$ and $\det(\mathcal{F}(\mathfrak{G})) \neq 0$ for the Laplacian of a connected and undirected graph*[1].

[1]It follows from Lemma G.1 that $-\mathcal{F}(\mathfrak{G})$ is a symmetric and Hurwitz matrix and it satisfies $R = \mathcal{F}(\mathfrak{G})P + P\mathcal{F}(\mathfrak{G})$, for a given $R \in \mathbb{R}_+^{N\times N}$.

APPENDIX H: COPYRIGHT PERMISSIONS

The permission below is for the use of material in Chapter 2.

Taylor & Francis
Taylor & Francis Group

Our Ref: JB/TCON/P18/1667

30 August 2018

Dear Ehsan Arabi,

Material requested: 'A set-theoretic model reference adaptive control architecture for disturbance rejection and uncertainty suppression with strict performance guarantees' by Ehsan Arabi, Benjamin C. Gruenwald, Tansel Yucelen & Nhan T. Nguyen *International Journal of Control* Vol 91:5 pp. 1195-1208 (2018).

Thank you for your correspondence requesting permission to reproduce the above mentioned material from our Journal in your printed thesis entitled 'Control of Uncertain Dynamical Systems with Spatial and Temporal Constraints' and to be posted in the university's repository - University of South Florida.

We will be pleased to grant permission on the sole condition that you acknowledge the original source of publication and insert a reference to the article on the Journals website: http://www.tandfonline.com

'This is the authors accepted manuscript of an article published as the version of record in International Journal of Control © Taylor & Francis https://doi.org/10.1080/00207179.2017.1312019'

This permission does not cover any third party copyrighted work which may appear in the material requested.

Please note that this license does not allow you to post our content on any third party websites or repositories.

Thank you for your interest in our Journal.

Yours sincerely

Jo Bateman – Permissions Administrator, Journals
Taylor & Francis Group
3 Park Square, Milton Park, Abingdon, Oxon, OX14 4RN, UK.
Tel: +44 (0)20 7017 7617
Fax: +44 (0)20 7017 6336
Web: www.tandfonline.com
e-mail: joanne.bateman@tandf.co.uk

Taylor & Francis Group
an informa business

The permission below is for the use of material in Section 4.1.

Taylor & Francis
Taylor & Francis Group

Our Ref: JB/TCON/P18/1668

30 August 2018

Dear Ehsan Arabi,

Material requested: 'Set-theoretic model reference adaptive control with time-varying performance bounds' by Ehsan Arabi & Tansel Yucelen *International Journal of Control* Vol (2018).

Thank you for your correspondence requesting permission to reproduce the above mentioned material from our Journal in your printed thesis entitled 'Control of Uncertain Dynamical Systems with Spatial and Temporal Constraints' and to be posted in the university's repository - University of South Florida.

We will be pleased to grant permission on the sole condition that you acknowledge the original source of publication and insert a reference to the article on the Journals website: http://www.tandfonline.com

'This is the authors accepted manuscript of an article published as the version of record in International Journal of Control © Taylor & Francis https://doi.org/10.1080/00207179.2018.1442026'

This permission does not cover any third party copyrighted work which may appear in the material requested.

Please note that this license does not allow you to post our content on any third party websites or repositories.

Thank you for your interest in our Journal.

Yours sincerely

Jo Bateman – Permissions Administrator, Journals
Taylor & Francis Group
3 Park Square, Milton Park, Abingdon, Oxon, OX14 4RN, UK.
Tel: +44 (0)20 7017 7617
Fax: +44 (0)20 7017 6336
Web: www.tandfonline.com
e-mail: joanne.bateman@tandf.co.uk

Taylor & Francis Group
an informa business

The permission below is for the use of material in Sections 4.3 and 5.1.

Ehsan Arabi <ehsanarabi@mail.usf.edu>

Republication Permission Request

Heather Brennan <HeatherB@aiaa.org> Thu, Sep 6, 2018 at 2:46 PM
To: Ehsan Arabi <ehsanarabi@mail.usf.edu>
Cc: Lela Durakovic <LelaD@aiaa.org>

Here you go:

Thank you for your request to reprint the following AIAA conference papers in your dissertation:

1_ E. Arabi, T. Yucelen, and N. T. Nguyen, **Set-Theoretic Model Reference Adaptive Control of a Generic Transport Model**, AIAA Guidance, Navigation, and Control Conference, Kissimmee, FL, 2018. (Link)

2_ E. Arabi, and T. Yucelen, **On Set-Theoretic Model Reference Adaptive Control of Uncertain Dynamical Systems Subject to Actuator Dynamics**, AIAA Guidance, Navigation, and Control Conference, Kissimmee, FL, 2018. (Link)

Because you and your coauthors retained copyright to the conference papers cited here, AIAA has no claim to the works, and you do not need to seek permission from AIAA to republish the material in your dissertation. You do need to acknowledge within the main text or in footnotes which sections/chapters of your dissertation are based on your prior publications, and fully cite the original sources in your reference list.

Heather A. Brennan

Director, Publications

NEW FOR 2018: Making changes to a published conference paper?

Read about AIAA's new process using Crossmark.

NEW FOR 2019: AIAA journals go online-only

-

American Institute of Aeronautics and Astronautics www.aiaa.org
12700 Sunrise Valley Drive, Suite 200

Reston, VA 20191-5807

800-639-AIAA (2422)

heatherb@aiaa.org 703.264.7568 (direct)

The permission below is for the use of material in Section 4.4.

Copyright Clearance Center

Confirmation Number: 11740363
Order Date: 08/17/2018

Customer Information

Customer: Ehsan Arabi
Account Number: 3001323479
Organization: Ehsan Arabi
Email: arabi.ehsan@gmail.com
Phone: [redacted]
Payment Method: Invoice

This is not an invoice

Order Details

AIAA Guidance, Navigation, and Control Conference

Billing Status: **N/A**

Order detail ID: 71488841
ISBN: 9781624104503
Publication Type: e-Book
Volume:
Issue:
Start page:
Publisher: AIAA

Permission Status: Granted
Permission type: Republish or display content
Type of use: Republish in a thesis/dissertation
Order License Id: 4411620257886

Requestor type	Academic institution
Format	Print, Electronic
Portion	chapter/article
Number of pages in chapter/article	14
The requesting person/organization	Ehsan Arabi
Title or numeric reference of the portion(s)	AIAA 2017-0669
Title of the article or chapter the portion is from	Guaranteed Model Reference Adaptive Control Performance in the Presence of Actuator Failures
Editor of portion(s)	N/A
Author of portion(s)	Ehsan Arabi
Volume of serial or monograph	N/A
Page range of portion	1-14
Publication date of portion	Jan 2017
Rights for	Main product
Duration of use	Life of current edition
Creation of copies for the disabled	no
With minor editing privileges	no
For distribution to	Worldwide

In the following language(s)	Original language of publication
With incidental promotional use	no
Lifetime unit quantity of new product	Up to 999
Title	Control of Uncertain Dynamical Systems with Spatial and Temporal Constraints
Instructor name	Ehsan Arabi
Institution name	University of South Florida
Expected presentation date	Oct 2018

Note: This item was invoiced separately through our **RightsLink service.** More info **$ 0.00**

Total order items: 1 **Order Total: $0.00**

The permission below is for the use of material in Section 6.2.

Ehsan Arabi <ehsanarabi@mail.usf.edu>

Permission for Reuse in Dissertation

Beth Darchi <DarchiB@asme.org> Thu, Oct 18, 2018 at 2:47 PM
To: Ehsan Arabi <ehsanarabi@mail.usf.edu>

Dear Mr. Arabi,
It is our pleasure to grant you permission to use **all or any part of** the ASME paper "FURTHER RESULTS ON FINITE-TIME DISTRIBUTED CONTROL OF MULTIAGENT SYSTEMS WITH TIME TRANSFORMATION," by Ehsan Arabi, Tansel Yucelen, John R. Singler cited in your le er for inclusion in a disserta on en tled Control of Uncertain Dynamical Systems with Spa al and Temporal Constraints to be published by University of South Florida.

Permission is granted for the specific use as stated herein and does not permit further use of the materials without proper authorization. Proper attribution must be made to the author(s) of the materials. **Please note:** if any or all of the figures and/or Tables are of another source, permission should be granted from that outside source or include the reference of the original source. ASME does not grant permission for outside source material that may be referenced in the ASME works.

As is customary, we request that you ensure full acknowledgment of this material, the author(s), source and ASME as original publisher. Acknowledgment must be retained on all pages where figure is printed and distributed.

Many thanks for your interest in ASME publications.

Sincerely,

Beth Darchi

Publishing Administrator

ASME

2 Park Avenue

New York, NY 10016-5990

Tel 1.212.591.7700

darchib@asme.org

The permission below is for the use of material in Chapter 7.

Account Info Help

Title: Journal of dynamic systems, measurement, and control
Article ID: 0022-0434
Publication: Publication1
Publisher: CCC Republication
Date: Jan 1, 1959

Logged in as:
Ehsan Arabi
Account #:
3001323479

LOGOUT

Order Completed

Thank you for your order.

This Agreement between Ehsan Arabi ("You") and American Society of Mechanical Engineers ASME ("American Society of Mechanical Engineers ASME") consists of your order details and the terms and conditions provided by American Society of Mechanical Engineers ASME and Copyright Clearance Center.

License number	Reference confirmation email for license number
License date	Aug, 27 2018
Licensed content publisher	American Society of Mechanical Engineers ASME
Licensed content title	Journal of dynamic systems, measurement, and control
Licensed content date	Jan 1, 1959
Type of use	Thesis/Dissertation
Requestor type	Academic institution
Format	Print, Electronic
Portion	chapter/article
The requesting person/organization	Ehsan Arabi
Title or numeric reference of the portion(s)	DS-15-1538
Title of the article or chapter the portion is from	Mitigating the Effects of Sensor Uncertainties in Networked Multi-Agent Systems
Editor of portion(s)	N/A
Author of portion(s)	Ehsan Arabi
Volume of serial or monograph	N/A
Page range of portion	
Publication date of portion	Feb 06, 2017
Rights for	Main product
Duration of use	Life of current edition
Creation of copies for the disabled	no
With minor editing privileges	no
For distribution to	Worldwide
In the following language(s)	Original language of publication
With incidental promotional use	no
Lifetime unit quantity of new product	Up to 999
Title	Control of Uncertain Dynamical Systems with Spatial and Temporal Constraints
Instructor name	Ehsan Arabi

Institution name	University of South Florida
Expected presentation date	Oct 2018
Requestor Location	Ehsan Arabi [redacted] [redacted] Attn: Ehsan Arabi
Billing Type	Invoice
Billing address	Ehsan Arabi [redacted] [redacted] Attn: Ehsan Arabi
Total (may include CCC user fee)	0.00 USD
Total	0.00 USD

CLOSE WINDOW